ACTA PHYSICA

ACADEMIAE SCIENTIARUM HUNGARICAE

TOMUS XLII FASCICULUS 1

AKADÉMIAI KIADÓ, BUDAPEST

1977

ACTA PHYS. HUNG. APAHAQ 42 (1) 1–84 (1977)

ACTA PHYSICA

ACADEMIAE SCIENTIARUM HUNGARICAE

SZERKESZTI

KOVÁCS ISTVÁN

Az *Acta Physica* angol, német, francia vagy orosz nyelven közöl értekezéseket. Évente két kötetben, kötetenként 4—4 füzetben jelenik meg. Kéziratok a szerkesztőség címére (1521 Budapest XI., Budafoki út 8.) küldendők.

Megrendelhető a belföld számára az Akadémiai Kiadónál (1363 Budapest Pf. 24. Bankszámla 215-11488), a külföld számára pedig a "Kultúra" Külkereskedelmi Vállalatnál (1389 Budapest 62, P. O. B. 149. Bankszámla 217-10990 sz.), vagy annak külföldi képviseleteinél és bizományosainál.

The *Acta Physica* publish papers on physics in English, German, French or Russian, in issues making up two volumes per year. Subscription price: $32.00 per volume. Distributor: KULTURA Hungarian Trading Co. (1389 Budapest 62, P. O. Box 149) or its representatives abroad.

Die *Acta Physica* veröffentlichen Abhandlungen aus dem Bereich der Physik in deutscher, englischer, französischer oder russischer Sprache, in Heften die jährlich zwei Bände bilden.

Abonnementspreis pro Band: $32.00. Bestellbar bei: KULTURA Außenhandelsunternehmen (1389 Budapest 62, Postfach 149) oder bei seinen Auslandsvertretungen.

Les *Acta Physica* publient des travaux du domaine de la physique, en français, anglais, allemand ou russe, en fascicules qui forment deux volumes par an.

Prix de l'abonnement: $32.00 par volume. On peut s'abonner à l'Entreprise du Commerce Extérieur KULTURA (1389 Budapest 62, P. O. B. 149) ou chez ses représentants à l'étranger.

«*Acta Physica*» публикуют трактаты из области физических наук на русском, немецком, английском и французском языках.

«*Acta Physica*» выходят отдельными выпусками, составляющими два тома в год.

Подписная цена — $32.00 за том. Заказы принимает предприятие по внешней торговле KULTURA (1389 Budapest 62, P. O. B. 149) или его заграничные представительства и уполномоченные.

ACTA PHYSICA

ACADEMIAE SCIENTIARUM HUNGARICAE

TOMUS XLII

AKADÉMIAI KIADÓ, BUDAPEST
1977

INDEX

Tomus 42

ACTA PHYSICA

ACADEMIAE SCIENTIARUM HUNGARICAE

TOMUS XLII FASCICULUS 1

AKADÉMIAI KIADÓ, BUDAPEST

1977

ACTA PHYS. HUNG.

INDEX

Acta Physica Academiae Scientiarum Hungaricae, Tomus 42 (1), pp. 3—19 (1977)

INVESTIGATIONS ON A NEW DEVICE APPLICATION OF THE a. c. JOSEPHSON EFFECT

By

S. DÉSI

TRAINING REACTOR, TECHNICAL UNIVERSITY, BUDAPEST*

(Received in revised form 28. XI. 1976)

After theoretical considerations concerning the properties of the a. c. Josephson effect in case of strip-line type superconducting tunnel junctions, the noise characteristics of these devices are discussed. By making use of the highly nonlinear features together with inherent low-noise a special parametric converter type pulse amplifier has been constructed. The experimental results obtained are presented and suggestions are given for further development.

1. Introduction

The main purpose of the work described below was to investigate some special application possibilities of the Josephson tunnel junctions. The principle of operation could be applied also for the detection and amplification of other types of electromagnetic radiations such as microwave detection, infrared radiation sensor, laser detection and conversion, etc.

We focussed our efforts on the possible device application of the a.c. Josephson effect as a low-noise parametric converter preamplifier in the nuclear radiation detection field.

After theoretical considerations we began our experimental work with developing the manufacturing technology of simple junctions first, then tried to build special devices to check the usefulness of the operational principle.

2. The a. c. Josephson effect

The a.c. Josephson effect, accompanying a d.c. current flow between the ground states of two superconductors when a finite d. c. potential difference exists across the superconducting junction, can be described as an alternating current through a narrow nonsuperconducting gap separating the two superconductors. The gap width should have the same order of magnitude as the range of the superconducting wave function, i.e. about 10—20 Angstroms.

*The experimental part of this work was done during a visit of the author at ORTEC Inc., Oak Ridge, Tenn., U.S.A.

When a small potential difference V is established across the gap photon emission occurs as the tunneling "superfluid" — i.e. paired electrons of opposite spin direction, called "Cooper pairs" — crosses the junction with frequency determined by the following relation [1]

$$\nu = \frac{2eV}{h},$$

where ν is the frequency of the emitted photon, e is the electronic charge, h is Planck's constant and ν is equal to about 483,6 MHz for each microvolt of applied voltage.

The a.c. Josephson current density j inside the gap as a function of the position r and time t is given by

$$j(r,t) = j_1 \sin \varphi\,(r, t),$$

where $\varphi\,(r, t)$ is the relative phase of Cooper pairs in the two superconductors and j_1 is the maximum Josephson current density which can be expressed as[2],

$$j_1 = (\pi/2R_n)\,[\Delta(T)/e]\ \tanh\,[1/2\,\beta\Delta(T)],$$

where R_n = normal state tunneling resistance of 1 cm^2 material; $\Delta(T)$ = superconducting energy gap as a function of temperature $\beta = 1/KT$ and K is Boltzmann's constant.

If we use a junction of crossed superconducting metal strips and the gap is formed in the overlap region of barrier length L and width w (see Fig. 1), then the tunneling supercurrent density across the gap can be regarded as uniform only when L is smaller than λ_j the Josephson penetration depth.

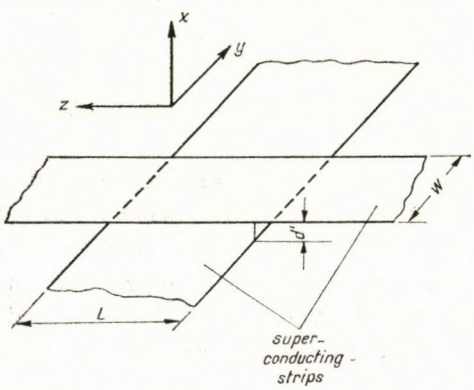

Fig. 1. Arrangement and orientation of the crossed strip-line type superconducting tunnel junctions

The latter is given by [3]

$$\lambda_j = 6.5 \times 10^{-6} \sqrt{\frac{\hbar c^2}{e^2 d j_1}} \text{ cm},$$

where c = speed of light, $d = 2\lambda + d'$, λ = magnetic field penetration depth for ideal superconductor and d' is the gap thickness. This means the junction cannot be made arbitrarily large.

When the junction is connected to a current source, the relative phase φ adjusts itself until $j_1 \sin \varphi$ is equal to the source current. For $\varphi = \pi/2$ the junction carries maximum current without any voltage drop across it. If the current through the junction becomes larger than j_1 a finite voltage appears across the junction as a consequence of quasiparticle (normal) tunneling. If a uniform magnetic field H_0 is applied in the plane of the junction (y-direction), the tunneling current distribution will have the following spatial distribution inside the junction [4]

$$j = j_1 \sin \left(\varphi_0 - \frac{2\, ed}{\hbar c} H_0 z \right),$$

where the z direction is parallel with the junction length L and perpendicular to H_0 .

According to this relation for certain values of H_0 the maximum d.c. Josephson current will be zero. Because, if $\varphi_0 = \pi/2$ then we get the maximum d.c. current $j_{\max}$ by integrating j over the whole junction area

$$j \max = j_1 \left| \frac{\sin \pi \Phi / \Phi_0}{\pi \Phi / \Phi_0} \right|,$$

where $\Phi_0 = hc/2e = 2.07 \times 10^{-7}$ gauss cm^2 is the quantum unit of magnetic flux and $\Phi = (2\lambda + d')\, LH_0$. In this manner $j_{\max}$ vs H_0 gives a typical Fraunhofer pattern.

If we have both a finite voltage V_0 and a finite magnetic field H_0 across the junction, then the current will change both with time and space and will be

$$j = j_1 \sin (\omega_0 t - kz + \varphi_0),$$

where $k = 2\, ed\, H_0/\hbar c$ and $\omega_0 = 2\, eV_0/\hbar = 2\pi\, \nu_0$. This represents a current density wave along the z-direction.

Consider now the case when a junction is irradiated by microwaves of angular frequency ω. In this case current jumps (steps) have been observed on the $I-V$ characteristics of the junction when $2eV_0/\hbar = n\omega$ ($n = 1,2,3,\ldots$),

(see Fig. 2). This phenomenon is the direct consequence of mixing or frequency modulation by the junction between the incident and its own radiations [5,6].

Because, for this case the Josephson current can be expressed as

$$j = j_1 \sin\left[\omega_0 t + \frac{\omega_0 v_0}{\omega V_0} \sin(\omega t + \Theta) + \varphi_0\right],$$

where Θ is the microwave phase relative to φ_0 and v_0 is the induced microwave amplitude. Now, as a result, the frequency modulation by the microwaves gives d. c. sidebands when $n\omega = \omega_0$ and the sideband current $j_{d.c.}$ is given

$$j_{d.c.} = j_1 (-1)^n J_n \left(\frac{n v_0}{V_0}\right) \sin(\varphi_0 - n\Theta),$$

where J_n is the n-th order Bessel function. These d. c. sidebands appear in the $I-V$ characteristics as current steps.

Similarly, without any external electromagnetic field, the a.c. Josephson current generates electromagnetic fields in the junction region and these fields modify the $I-V$ characteristics of the junction which has been also observed as so-called self-induced steps [5,7].

Consider now the junction area as a strip line cavity having a characteristic impedance of Z_j. This is given by the transmission line equations

$$Z_j = \frac{c}{\bar{c}} \left(\frac{d'}{w\varepsilon}\right) Z_0,$$

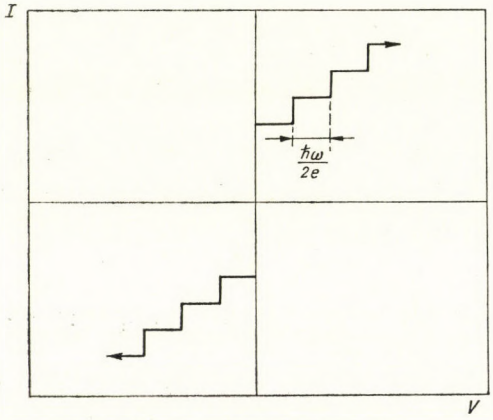

Fig. 2. Current steps on the $I-V$ characteristics of a Josephson tunnel junction irradiated by microwaves of ω angular frequency

where $\bar{c} = c \sqrt{d'/\varepsilon d}$ the phase velocity of the TM wave, ε is the dielectric constant of the gap and Z_0 is the impedance of the free space for TM waves propagating between the strips along the length of the junction (L-direction).

When an external magnetic field H_0 is present, the phase velocity of the Josephson current density wave v_p is given as $v_p = \omega_0/k = V_0 c/H_0 d'$. If $v_p = \bar{c}$ the amplitude of the TM wave will have a maximum and the amplitude distribution results in the $I-V$ characteristics a resonance-peak like structure. In this case, if $v_0/V_0 \ll 1$ solving the transmission line equations, we get for the a.c. voltage across the junction

$$v = v_0 \cos(\omega_0 t - kz + \Theta),$$

where

$$v_0 = \frac{j_1 (4\pi d'/\varepsilon\omega_0)}{\left\{\left[1 - \left(\frac{k\bar{c}}{\omega_0}\right)^2\right]^2 + \left(\frac{1}{Q}\right)^2\right\}^{1/2}};$$

here Q represents the losses of the strip-line cavity and

$$\Theta = \tan^{-1}\left[\frac{1/Q}{1 - (k\bar{c}/\omega_0)^2}\right] + \varphi_0.$$

Since the total voltage across the junction is $v + V_0$, the phase φ will be modified according to $v_0/V_0 \sin(\omega_0 t - kz + \Theta)$ and the current will be

$$j = j_1 \sin\left[\omega_0 t - kz + (v_0/V_0) \sin(\omega_0 t - kz + \Theta) + \varphi_0\right].$$

This a.c. voltage can also result in a d.c. current, which has a resonance shape with a maximum current at

$$V_{\max} = \left(\frac{d'd}{\varepsilon}\right)^{1/2} \cdot H_0.$$

Now let us take into account that the strip line cavity has its allowed voltage modes which vary according to $\cos n\pi z/L$, and have resonant frequencies at $\omega_n = n\pi\bar{c}/L$. Expanding these modes, the spatial average of the direct current density is [8]

$$j_{d.c.} = \frac{4\pi d' j_1^2}{\varepsilon\omega_0 V_0} \sum_{n=0}^{\infty} \frac{1/Q_n}{\left[1 - \left(\frac{n\pi\bar{c}}{\omega_0 L}\right)^2\right]^2 + \left(\frac{1}{Q_n}\right)^2} \cdot \left[\frac{\sin\frac{kL - \pi n}{2}}{\frac{KL - \pi n}{2}}\right]^2 \cdot \frac{1}{\left(1 + \frac{n\pi}{kL}\right)^2} \cdot \begin{cases} 1/2 & \text{for } n = 0 \\ 1 & \text{for } n \neq 0 \end{cases},$$

where $1/Q_n$ is the loss in the n-th mode. Hence, for small n values a step structure can be observed again in the $I-V$ characteristics when the Josephson frequency coincides with one of the characteristic cavity frequencies. The steps appear at equally spaced voltages $V_n = nh\bar{c}/4eL$ (see Fig. 3).

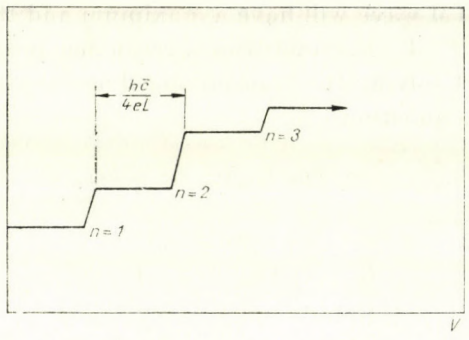

Fig. 3. Current steps on the $I-V$ characteristics of a strip-line cavity type superconducting junction showing the allowed voltage modes

The magnitude of the current step is determined by the applied magnetic field. Generally, as H_0 is increased it decreases the a.c. Josephson current wavelength thus coupling it more strongly to shorter electromagnetic cavity modes. The maximum emitted r. f. radiation occurs at the current steps and numerous observations proved the existence of the a.c. Josephson effect in such cases [9,10,11].

To calculate the intensity or output power of the radiation from the junction we have to take into account the power transmission coefficient T_P at the junction — free space or external waveguide system which is given by

$$T_P = 4 Z_0 Z_j/(Z_0+Z_j)^2 .$$

Here Z_0 is the characteristic impedance of the free space or external cavity in which the junction is located. Typically $Z_j \approx 6\times 10^{-3}\ \Omega$, $Z_0 = 377\ \Omega$ [12] and $T_P = 10^{-4}$. This means that the impedance mismatch makes it rather difficult to couple the junction-free space system effectively.

In this case the radiated output power can be estimated as follows: let the power input to the junction be $P_{d.c.} = V_0 I_0$ at the junction operating point. This power is distributed among a number of simultaneously excited cavity modes because of the nonlinear effects. If we measure the magnitude of the n-th mode current step together with the voltage V_n belonging to it, then the r. f. power in the n-th mode is simply given by $I_n V_n$. As $P_{d.c.}$ lies in the microwatt range or lower, the radiated power in a single mode is only a few picowatts.

Though many experiments have been carried out to detect the junction radiation successfully [11, 13, 14] yet the inherent low-noise properties of the Josephson junctions could not be used because of the rather poor signal-to-noise ratio caused by the very bad impedance mismatch.

Our aim was to attempt finding a new method to detect the junction radiation without loosing appreciably the low-noise properties of the device.

3. Operational principle

The new approach in detecting the Josephson junction radiation was not to get the r.f. power out of the cavity, but using the highly nonlinear properties of the junctions to convert it into a much lower and easy-to-handle frequency instead, and detect this low r. f. by conventional means.

We have seen how an external r.f. power can make a frequency modulation or mixing in the junction. So if we introduce an external r.f. radiation of angular frequency ω then the junction current will contain a series of beat frequencies $\Delta\omega$:

$$\Delta\omega = k\omega_0 \pm l\omega$$

and

$$k,l = 1,2,3,\ldots .$$

The general expression for the normalized Josephson current in the presence of two applied r.f. voltages is [15]

$$\frac{j}{j_1} = \sum_{k=-\infty}^{+\infty} \sum_{l=-\infty}^{+\infty} J_k\left(\frac{2ev_1}{\hbar\omega_1}\right) J_l\left(\frac{2ev_2}{\hbar\omega_2}\right) \sin\left[\omega_0 t + \varphi_0 + \right.$$
$$\left. + k(\omega_1 t + \Theta_1) + l(\omega_2 t + \Theta_2)\right].$$

The phases Θ_1 and Θ_2 are related to an arbitrary zero time and φ_0 is the initial quantum mechanical phase difference across the junction. If the two r.f. frequencies are such that $\omega_1 > \omega_2$ and $\omega_0 = \Delta\omega = \omega_1 - \omega_2$, then the current step amplitude is given by

$$\frac{j_{d.c.}(\Delta\omega)}{j_1} = -J_1(P_1) J_2(P_2) \sin\left[\varphi_0 - (\Theta_1 - \Theta_2)\right] \tag{1}$$

and we have for the beat frequency current

$$\frac{j_{\Delta\omega}(\omega_0 = \Delta\omega)}{j_1} = \left\{J_0^2(P_1) J_0^2((P_2) + J_2^2(P_1) \cdot J_2^2(P_2) - 2J_0(P_1) J_0(P_2) J_2(P_1) J_2(P_2) \cdot \right.$$
$$\left. \cdot \cos 2\left[\varphi_0 - (\Theta_1 - \Theta_2)\right]\right\}^{1/2} \cdot \cos\left[(\omega_1 - \omega_2) t + (\Theta_1 - \Theta_2) - \varphi_{\Delta\omega}\right] \tag{2}$$

where

$$P_1 = \frac{2\,ev_1}{\hbar\omega_1}\,,\quad P_2 = \frac{2\,ev_2}{\hbar\omega_2}$$

and

$$\varphi_{\Delta\omega} = \tan^{-1}\left\{\frac{J_0(P_1)\,J_0(P_2) - J_2(P_1)\,J_2(P_2)}{J_0(P_1)\,J_0(P_2) + J_2(P_1)\,J_2(P_2)} \cdot \cot\left[\varphi_0 - (\Theta_1 - \Theta_2)\right]\right\}.$$

As can be seen, the maximum d.c. current on a given step in the presence of two r.f. powers is determined by the product of two Bessel functions, and the beat frequency in (2) is equal to $\omega_1 - \omega_2$.

4. Noise considerations

If the junction is operated at a bias voltage of V_0 and if in addition there is a modulating noise voltage $V_n(t)$ present, the resulting supercurrent will have the form

$$j = j_1 \sin\left[\omega_0 t + \frac{2e}{\hbar}\int_0^t V_n(t')\,dt'\right],$$

where

$$\omega_0 = \frac{2e}{\hbar}V_0.$$

We can describe the noise voltage V_{rms} in terms of the power spectrum of the voltage fluctuations

$$V_{rms}^2 = \int_0^\infty P_V(\omega)\,d\omega\,.$$

Using the relation between the normalized power spectrum of the emitted radiation $P(\omega - \omega_0)$ and the normalized power spectrum of noise voltage fluctuations [16] which is given by

$$P(\omega - \omega_0) = \frac{j_1^2}{2\pi}\int_0^\infty \cos\,(\omega - \omega_0)\,t \cdot \exp\left[\left(\frac{2e}{\hbar}\right)^2 \int_0^\infty \frac{P_V(\omega)}{\omega^2}\,(\cos\,\omega t - 1)\,d\omega\,dt\right].$$

The linewidth can be calculated by direct integration. If the rms linewidth $2e/hV_{rms}$ is large compared to the bandwidth of the voltage fluctuations, then the power spectrum of the radiation is Gaussian with a half-width of approximately $2e/hV_{rms}$.

When the rms linewidth is small compared to the bandwidth of the voltage fluctuations, the power spectrum is Lorentzian having a full width at the half maximum points of

$$\Delta\nu = \frac{2\pi^2(2e/h)^2 V_{rms}^2}{B}\,,$$

where B is the bandwidth of the voltage fluctuations.

One source of the finite linewidth is the normal or quasi-particle current noise at finite temperature. The power spectrum of this kind of noise is the following [17]

$$P_{V_0}(\omega) = \frac{2eI(V_0)}{2\pi} \coth\left(\frac{\beta e V_0}{2}\right) R_D^2 ,$$

where $\beta = 1/KT$ and R_D is the dynamic resistance of the junction at the bias voltage V_0.

The supercurrent, which actually constitutes the self-induced step, does not contribute to this shot noise. In a typical experiment $\beta e V_0/2 \ll 1$ and $\coth(\beta e V_0/2) \approx 2\ KT/eV_0$.

If B has a sharp cut-off frequency, the rms noise voltage will be

$$V_{rms}^2 = \frac{2\, I_N(V_0)\ KT}{\pi V_0} R_D^2 B = \frac{2KTR_D^2 B}{\pi R_s} ,$$

where R_s is the static resistance, $V_0/I_N(V_0)$ calculated using only the normal current I_N. And because $2e\ V_{rms}/\hbar < B$ the power spectrum of the radiation will be Lorentzian, and the linewidth will be

$$\Delta\nu = 4\pi K(2e/h)^2\, T(R_D^2/R_s) .$$

The other noise source is the Johnson noise of the dynamic resistance at the bias point. The power spectrum of the Johnson noise is given by

$$P_{V_0}(\omega) = \frac{2KTR_D}{\pi}$$

and the rms voltage

$$V_{rms}^2 = \frac{2KTR_D}{\pi} B .$$

The resultant power spectrum will be Lorentzian again and the linewidth

$$\Delta\nu = 4\pi K(2e/h)^2\, TR_D .$$

The total linewidth from the two noise sources will be

$$\Delta\nu = [aR_D + b(R_D^2/R_s)]\ T, \tag{3}$$

where $a = b = 4\pi K(2e/h)^2 \approx 40 \times 10^6$ Hz/KΩ. grad.

Experimental values of a and b show very small linear temperature dependence expected of Johnson noise, but the values of the coefficient b are within a factor of two of the calculated value over a very wide current range. Linewidths in practice can be less than 1 kHz in the 10 GHz frequency range [18].

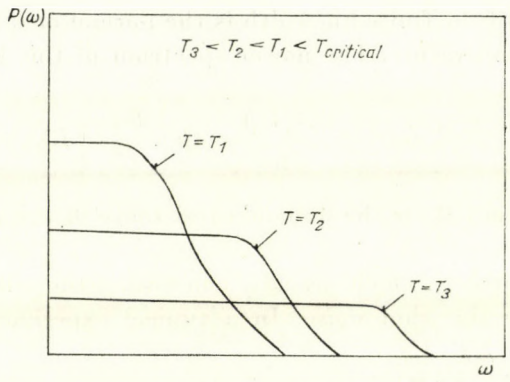

Fig. 4. Noise power spectrum dependence of a superconducting tunnel junction on frequency and temperature

In addition, the power spectrum $P(\omega)$ as a function of temperature qualitatively behaves as is shown in Fig. 4.

Thus, if we decrease the temperature of the junction, it is possible to lower the noise power between two specified frequency limits ω_1 and ω_2 defined by the band-pass filter network in the demodulator and amplifier system. In this manner we hoped to have about one hundred c.p.s. noise linewidth from the junction shot noise. This noise figure would correspond to less than 10 eV noise linewidth for an impedance-matched germanium radiation detector.

5. Experimental

So far it seemed to be very promising to make use of this high spectral purity radiation source combining it with the nonlinear properties and frequency modulation capabilities of the Josephson junctions.

In order to do this, first we planned to operate the Josephson junction as an externally frequency modulated oscillator and mixer at the same time. The mixing frequency in this part of the experiments has been produced by a high stability FM signal generator.

We intended to detect the beat frequency in the usual manner, and regarding the high conversion factor 483,6 KHz/nV, it seemed to be possible to measure very small current or voltage pulses at a high signal-to-noise ratio.

Later we aimed to use two coupled Josephson junctions using one of them as modulated oscillator. If their a.c. frequencies differ slightly the beat frequency should appear across them as a consequence of the mixing action.

At the very beginning of our experimental work we had to develop the manufacturing techniques of reliably good single Josephson junctions.

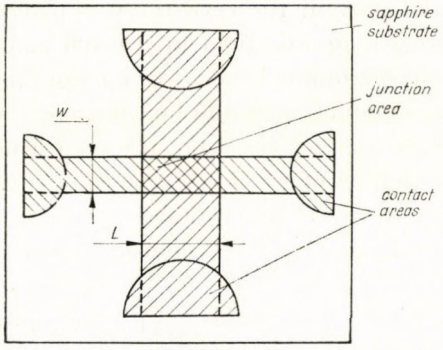

Fig. 5. Layout of the single junctions. The dimensions used during the experiment were: $L = 1$ mm; $w = 0{,}25$ mm

The layout of these devices is shown in Fig. 5.

The superconducting material, tin or lead has been evaporated successively on a 1×1" sapphire substrate of 1/16" thickness.

Between the two evaporations we used Kodak KPR photoresist solution to make the barrier between the two superconductors, dipping a few drops of KPR solution on the surface of the spinning substrate after the first evaporation. Adjusting the r.p.m. value of the spinner we could control the thickness of KPR on the surface. Illuminated with ultraviolet light the KPR polymerizes.

For testing we put the junctions into a double stainless steel cryostat which could be pumped down. The schematic diagram of the cryostat is shown in Fig. 6.

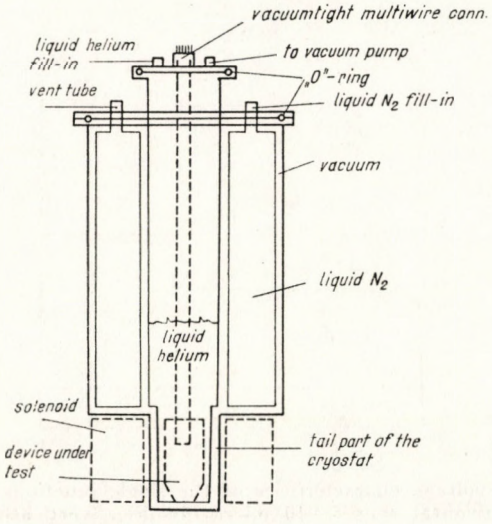

Fig. 6. Schematics of the testing cryostat

Around the tail part of the cryostat was placed a solenoid capable to produce the necessary magnetic field up to 100 gauss. A shield against the earth's magnetic field surrounded the lower part of the cryostat.

The testing of the junctions could be carried out either by manual setting of the voltage and current or, by using a sweep generator and curve tracer we could take photographs of the $I-V$ characteristics of the junction tested. The sweep period lasted less than a minute.

In Fig. 7 several junction $I-V$ characteristics are shown as a function of magnetic field.

As can be seen, it was possible to produce junctions with differential resistance on the current step of less than 0,2 milliohm. The junctions could be recycled several times between the liquid He and room temperature if they had been warmed up under warm He gas.

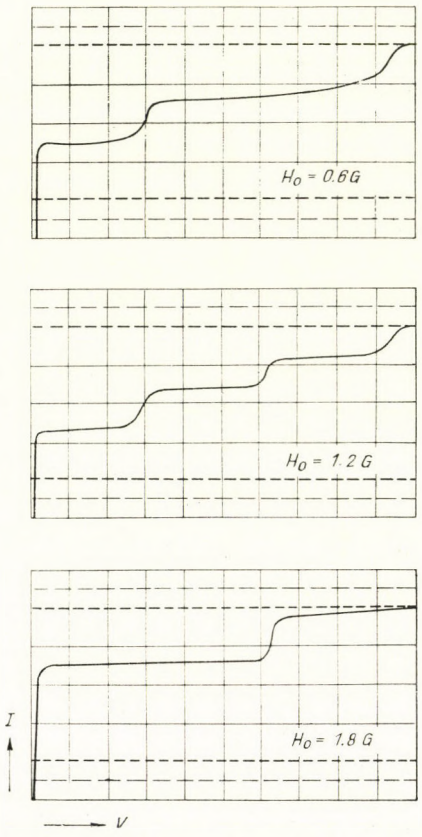

Fig. 7. Typical current-voltage characteristics of the single junctions at different external magnetic field H_0. Horizontal sens. = 10 microvolts/div., vertical sens. = 10 mA/div., $T = 0{,}86$ ° K

6. Results

After having elaborated the manufacturing and testing technology we began to check the operational principle using these junctions. The circuit diagram of the arrangement is shown in Fig. 8.

The junction was part of a resonant r.f. circuit tuned to about 100 megacycles. The circuit once was coupled to a sensitive commercial F.M. receiver, and on the other hand a precision signal generator was coupled to it. The impedance matching to the receiver and generator together with the circuit losses produced a loaded circuit Q-value of about 30. The output of the F.M. receiver was taken out directly from the ratio detector type demodulator and fed into a pulse shaping amplifier whose integrating and differentiating time constants could be varied between 0,1 and 10 μsec independently. At the output of the amplifier the noise value was measured by means of a rms noise meter and we could observe the signal amplitude distribution directly on a precision oscilloscope or to analyze it using a multichannel analyzer.

The junction voltage could be pulse modulated in series with the d.c. power supply. The modulating pulses were taken from a high stability pulse generator. The receiving system noise at 4 °K temperature (without operating the junction) has been checked by tuning the F. M. signal generator, the resonant circuit and the F.M. receiver to the same frequency (about 100 MHz).

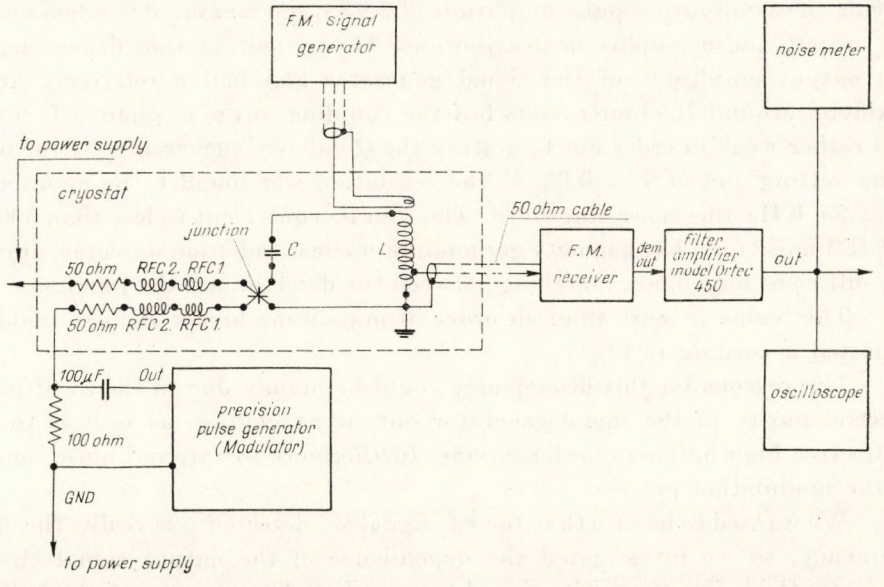

Fig. 8. Electric circuit diagram of the experimental arrangement for single junctions. $C = 15$ pF; $L = 5$ turns, 0,5″ dia. r. f. coil; RFC 1 and RFC 2: superconducting r. f. chokes

With 10 μV output r.f. voltage from the signal generator — which in this case was F. M. modulated from an external pulse generator by pulses of 5μsec exponential decay — the frequency deviation during the modulation period was set to 100 KHz. Using these figures, the output pulse amplitude was 2.9 V and Gaussian in shape. (The Model 450 amplifier has Gaussian filter network to give better noise figures.) The demodulated pulse amplitude dispersion (FWHM) measured on the multichannel analyzer was 0.1%. Without modulation, the overall system noise at the output was 1.25 mV rms. The shaping amplifier time constants were set to 3 μsec.

Finally we switched to operate the junction and set it to the middle of the self-induced current step having the maximum amplitude. At about 1,6 Gauss magnetic field this was the second step.

The dimensions of the junctions we used in this experiment were: $L =$ $= 1$ mm, $w = 0{,}25$ mm and the junction voltage at the second step was about 44 microvolts. The junction current varied from unit to unit between 3 and 30 mA.

Modulating now the junction voltage from the pulse generator with pulses of 5 μsec exponential decay constant we have found the beat frequency, that is the demodulated output pulse at a particular setting of the signal generator. In this case the junction operated as oscillator, frequency modulator and harmonic mixer.

We set the pulse generator output voltage in such a manner that the resulting frequency modulation at the junction was again 100 KHz (i.e. producing the same output pulse amplitude of 2.9 V), and measured the demodulated output pulse amplitude distribution. The resolution was depending on the output amplitude of the signal generator and had a relatively broad optimum around 1000 microvolts but the coupling to the resonant r.f. circuit was rather weak in order not to destroy the Q value of the circuit. At the optimum setting and at $T = 0{,}86$ °K the resolution was found to be about 6%, i.e. 2,55 KHz rms noise linewidth. This can be equivalent to less than 500 eV FWHM noise for a low capacity germanium nuclear radiation detector, providing sufficient impedance matching between the detector and the junction.

This value is more than an order of magnitude higher than it could be expected according to (3).

The reasons for this discrepancy could be mainly due to the insufficient spectral purity of the signal generator output r.f. voltage as well as to the ineffective high harmonic order mixing, furthermore to external noise sources in the modulation process.

We wanted to be sure that the r.f. signal we detected was really the beat frequency, so we investigated the dependence of the output signal on the magnetic field, junction voltage and temperature. The magnetic field dependence was very sharp; a few tenths of a gauss change in the field strength

changed the output signal drastically and so did the changes in the junction voltage. Above the critical temperature we could not find any output signal.

These results led us to the conclusion that we really detected the modulated beat frequency as a result of the harmonic mixing action of the Josephson junction between its own microwave radiation and the external r.f. power source.

Although the measured noise figures could be comparable with those of conventional FET devices we did not investigate this experimental arrangement further, but tried to construct a double and coupled junction ensemble instead. In this case one of the junctions was intended to be used as oscillator and the other as modulator and mixer. We wanted to realize the coupling by a "half strip line" formed by a narrow gap between the junctions as can be seen in Fig. 9 which shows the layout of the device.

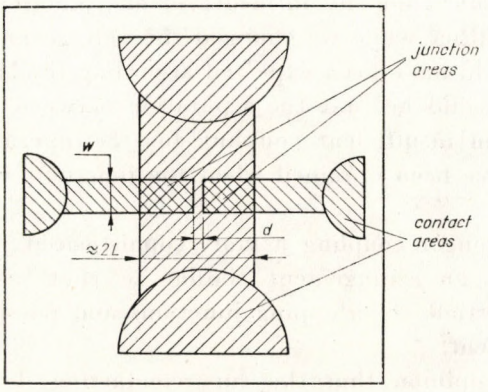

Fig. 9. Layout of the double junctions. The dimensions were the following: $2L = 1{,}6$ mm; $w = 0{,}25$ mm; $d = 10$ microns

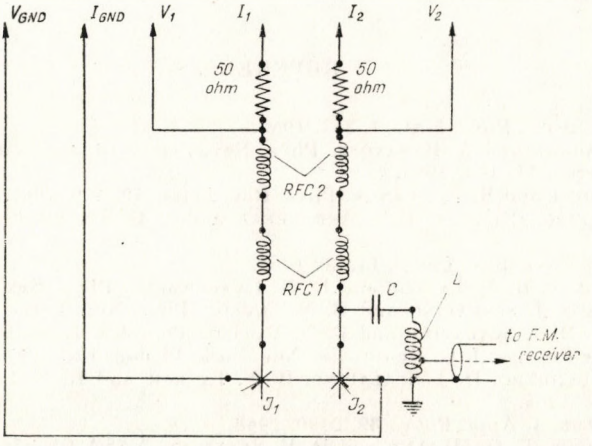

Fig. 10. Electronic circuit diagram of the experimental double junction arrangement. J_1, J_2: superconducting tunnel junctions; RFC 1 and RFC 2: superconducting r.f. chokes; $C = 15$ pF; $L = 5$ turns, 0,5″ dia. r. f. coil

The electronic circuit diagram is shown in Fig. 10. The two junction lengths were identical within 1,5 micron tolerance. The Q of the junctions allowed a detuning by several hundreds of megacycles; changing the voltage across them, the junction remained still on the same step. This was more than enough for resulting about 100 MHz beat frequency. The junctions were operated by the same power source.

After having prepared the double junctions we checked them comparing their $I-V$ characteristics and it was found they were identical within $\pm 50\%$ regarding their zero voltage current.

But we could not find the beat frequency though the operating point of the junctions laid on the same step, and each step "width" was about one microvolt.

We could not find any influence of one junction on the other's $I-V$ characteristics either while we changed the voltage and current across them although it should have been expected according to (1). The only reason for this behaviour could be that the separation between the junctions was too wide resulting in insufficient coupling for the microwave radiations. The same results have been obtained when the junctions were operated at different steps.

To get stronger coupling a more sophisticated junction layout should be realized, e.g. an arrangement similar to that used by GIAEVER [19] consisting of partially overlapping junctions and possibly having adjustable coupling coefficient.

It is our opinion that the superconducting devices described above deserve further investigation because of the promising nature of the Josephson junctions and the encouraging preliminary results obtained.

REFERENCES

1. B. D. JOSEPHSON, Phys. Lett., **1**, 251, 1962.
2. V. AMBEGAOKAR and A. BARATOFF, Phys. Rev. Letts., **10**, 486, 1963; "Erratum", Phys. Rev. Letts., **11**, 104, 1963.
3. R. A. FERRELL and R. E. PRANGE, Phys. Rev. Letts., **10**, 479, 1963.
4. R. C. JAKLEVIC, J. LAMBE, J. E. MERCEREAU and A. H. SILVER, Phys. Rev., **140** A, 1628, 1965.
5. S. SHAPIRO, Phys. Rev. Letts., **11**, 80, 1963.
6. W. H. PARKER, B. N. TAYLOR and D. N. LANGENBERG, Phys. Rev. Letts., **18**, 287, 1967.
7. R. E. ECK, D. J. SCALAPINO and B. N. TAYLOR, Phys. Rev. Letts., **13**, 15, 1964.
8. R. E. ECK, D. J. SCALAPINO and B. N. TAYLOR, Proc. 9th Internat'l Conf. on Low Temperature Physics, J. G. Daunt, Ed. New York, Plenum Press. 1965.
9. D. N. LANGENBERG, D. J. SCALAPINO, B. N. TAYLOR and R. E. ECK, Phys. Rev. Letts., **15**, 294, 1965.
10. B. N. TAYLOR, J. Appl. Phys., **39**, 2490, 1968.
11. R. A. KAMPER, L. O. MULLEN and D. B. SULLIVAN, NASA CR-1565 Report, 1970.
12. S. RAMO and J. R. WHINNERY, Fields and Waves in Modern Radio, John Whiley and Sons Inc., New York, 1945.
13. W. H. HIGA, Proceedings of the Conference on Electron Devices, Montreal, 1967.

14. G. K. GAULÉ, R. L. ROSS, and R. SCHWIDTAL, Proceedings of the Conference on the Physics of Superconducting Devices, Charlottesville, Va., 1967.
15. C. C. GRIMES and S. SHAPIRO, Phys. Rev., **169**, 397, 1968.
16. J. L. STEWART, Proc. IRE, October 1954.
17. D. J. SCALAPINO, Proceedings of the Conference on the Physics of Superconducting Devices, Charlottesville, Va., 1967.
18. W. H. PARKER, Prooeedings of the Conference on Fluctuations in Superconductors, Menlo Park, Cal., 1965.
19. I. GIAEVER, Phys. Rev. Letts., **14**, 904, 1965.

Acta Physica Academiae Scientiarum Hungaricae, Tomus 42 (1), pp. 21—28 (1977)

MHD INSTABILITY OF ROTATING SUPERPOSED FLUIDS THROUGH POROUS MEDIUM

By

R. C. SHARMA

DEPARTMENT OF MATHEMATICS, HIMACHAL PRADESH UNIVERSITY, SIMLA-5, INDIA

(Received 29. XI. 1976)

The present paper is an investigation to study the effect of magnetic field and rotation on the stability of two superposed fluids through porous medium. For the case of no magnetic field, the simultaneous presence of rotation and permeability makes the system unstable. For non-rotating configuration, the magnetic field is found to have stabilizing effect on the system under consideration. The combined effect of rotation and magnetic field on the stability of superposed fluids through porous medium is also discussed.

1. Introduction

A detailed account of the stability of superposed fluids in the presence of rotation or magnetic field through non-porous medium has been given by CHANDRASEKHAR [1]. When a fluid permeates a porous material, the actual path of an individual particle of fluid cannot be followed analytically. The gross effect, as the fluid slowly percolates through the pores of the rock, is represented by a macroscopic law. This is the usual Darcy's law. As a result of this, the usual viscous term in the equations of fluid motion is replaced by the resistance term $(\mu/k_1)\,\mathbf{q}$, where μ is the viscosity of the fluid, k_1 the permeability of the medium and $\mathbf{q}$ the velocity of the fluid, calculated from Darcy's law. LAPWOOD [2] has investigated the stability of convective flow in hydrodynamics in a porous medium using Rayleigh's procedure. The Rayleigh instability of a thermal boundary layer in flow through a porous medium has been considered by WOODING [3].

The effect of magnetic field and rotation in a porous medium may find applications in geophysics. It is therefore the motivation of this study to examine the effect of rotation, magnetic field and permeability on the stability of superposed fluids through porous medium.

2. Perturbation equations

Consider an incompressible and infinitely conducting fluid of variable density which is arranged in horizontal strata in porous medium. The pressure p and the density ϱ are therefore functions of the vertical coordinate z only.

Consider axis Oxyz such that Oz is vertical. Let the system be in a state of uniform rotation $\mathbf{\Omega}$ (0, 0, Ω) about the z-axis and acted on by a magnetic field $\mathbf{H}$(H, 0, 0) and gravity force $\mathbf{g}$(0, 0, $-g$).

Let $\delta\varrho$, δp, $\mathbf{q}$ (u, v, w) and $\mathbf{h}$ (h_x, h_y, h_z) denote respectively the perturbations in density ϱ, pressure p, velocity and magnetic field $\mathbf{H}$. Then the linearized perturbation equations of motion and continuity are

$$\varrho \frac{\partial \mathbf{q}}{\partial t} = - \nabla \delta p + \mathbf{g}\delta\varrho + 2\varrho(\mathbf{q}\times\mathbf{\Omega}) + \frac{\mu_e}{4\pi}(\nabla\times\mathbf{h})\times\mathbf{H} - \frac{\varrho\nu}{k_1}\mathbf{q}, \tag{1}$$

and

$$\nabla \cdot \mathbf{q} = 0\,. \tag{2}$$

Since the density of every particle remains unchanged as we follow it with its motion,

$$\frac{\partial}{\partial t}\delta\varrho + (\mathbf{q}\cdot\nabla)\varrho = 0\,. \tag{3}$$

The Maxwell's equations give

$$\frac{\partial \mathbf{h}}{\partial t} = (\mathbf{H}\cdot\nabla)\mathbf{q}\,, \tag{4}$$

and

$$\nabla \cdot \mathbf{h} = 0. \tag{5}$$

Assuming perturbations of the form

$$(\text{some function of } z)\ \exp(ik_x x + ik_y y + nt), \tag{6}$$

where k_x, k_y are horizontal wave-numbers of the harmonic disturbance, $k(=\sqrt{k_x^2+k_y^2})$ is the resultant wave number and n is, in general, a complex constant.

Eqs. (1)—(5) with the help of expression (6) give

$$\varrho\left(n + \frac{\nu}{k_1}\right)u = - ik_x\,\delta p + 2\varrho\Omega\, v\,, \tag{7}$$

$$\varrho\left(n + \frac{\nu}{k_1}\right)v = - ik_y\,\delta p - 2\varrho\Omega u + \frac{\mu_e H}{4\pi}(ik_x\, h_y - ik_y\, h_x)\,, \tag{8}$$

$$\varrho\left(n + \frac{\nu}{k_1}\right)w = - D\delta p + \frac{g}{n}(D\varrho)\,w - \frac{\mu_e H}{4\pi}(Dh_x - ik_x h_z)\,, \tag{9}$$

$$ik_x\, u + ik_y\, v + Dw = 0\,, \tag{10}$$

$$n\delta\varrho = -\, w\, D\varrho\,, \tag{11}$$

$$nh_x = ik_x\, Hu\,, \tag{12}$$

$$nh_y = ik_x\, Hv\,, \tag{13}$$

$$nh_z = ik_x\, Hw\,, \tag{14}$$

$$ik_x h_x + ik_y h_y + Dh_z = 0\,, \tag{15}$$

where $$D = \frac{d}{dz}\,.$$

μ_e and ν denote the magnetic permeability and the kinematic viscosity, respectively. Eliminating δp between Eqs. (7)—(9) and using Eqs. (10)—(15), we obtain

$$\left(n + \frac{\nu}{k_1}\right)[D\,(\varrho Dw) - k^2\varrho w] + \frac{gk^2}{n}(D\varrho)\,w + \\ + 2\,\Omega D\,(\varrho\zeta) + \frac{\mu_e H^2 k_x^2}{4\pi n}(D^2 - k^2)\,w = 0\,, \tag{16}$$

where $\zeta = ik_x\ v - ik_y\ u$ denotes the z-component of vorticity. Multiplying Eqs. (7) and (8) by $-\ ik_y$ and $+\ ik_x$ respectively and adding, we have

$$\zeta = \frac{2\Omega Dw}{n + \dfrac{\nu}{k_1} + \dfrac{\mu_e H^2 k_x^2}{4\pi\varrho n}}\,. \tag{17}$$

Eliminating ζ between Eqs. (16) and (17), we get

$$\left(n + \frac{\nu}{k_1}\right)[D\,(\varrho Dw) - k^2\varrho w] + \frac{gk^2}{n}(D\varrho)\,w + \frac{\mu_e H^2 k_x^2}{4\pi n}(D^2 - k^2)w + \\ + 4\Omega^2 D\left[\frac{\varrho Dw}{n + \dfrac{\nu}{k_1} + \dfrac{\mu_e H^2 k_x^2}{4\pi\varrho n}}\right] = 0\,. \tag{18}$$

3. Two rotating superposed uniform fluids in the presence of magnetic field separated by a horizontal boundary z=0

Consider the case of two uniform fluids of densities ϱ_1 (lower fluid) and ϱ_2 (upper fluid) separated by a horizontal boundary at $z = 0$. In each of the two regions of constant density, Eq. (18) reduces to

$$(D^2 - \varkappa^2)\,w = 0, \tag{19}$$

where

$$\varkappa = \frac{k}{\sqrt{1 + \dfrac{4\Omega^2}{\left(n + \dfrac{\nu}{k_1} + \dfrac{k_x^2 V^2}{n}\right)^2}}} \,. \tag{20}$$

As w must vanish both when $z \to -\infty$ (in the lower fluid) and $z \to +\infty$ (in the upper fluid), we can write

$$w_1 = A_1 e^{\varkappa z} \, (z < 0), \tag{21}$$

$$w_2 = A_2 e^{-\varkappa z} \, (z > 0), \tag{22}$$

as the solutions appropriate for the two regions. To ensure the continuity of w across the interface at $z = 0$, we must have

$$A_1 = A_2 = A \, (\text{say}).$$

Apart from the condition of continuity of w at $z = 0$, a condition follows from Eq. (18). By integrating it across the interface, we obtain

$$\Delta_0 (\varrho \, Dw) + \frac{\mu_e H^2 k_x^2}{4\pi n \left(n + \dfrac{\nu}{k_1}\right)} \Delta_0 \, (Dw) + \frac{4\Omega^2}{\left(n + \dfrac{\nu}{k_1}\right)^2} \times$$

$$\times \, \Delta_0 \left[\frac{\varrho Dw}{1 + \dfrac{k_x^2 V^2}{n \left(n + \dfrac{\nu}{k_1}\right)}} \right] = - \frac{k^2}{n \left(n + \dfrac{\nu}{k_1}\right)^2} [g \, (\varrho_2 - \varrho_1)] \, w_0 \,, \tag{23}$$

where $\Delta_0 \, (f)$ denotes a jump which a quantity f experiences at the interface $z = 0$, and w_0 is the common value of w at $z = 0$. $V^2 \, (= \mu_e H^2 / 4\pi\varrho)$ denotes the square of Alfvén velocity.

3.a. *The case of no magnetic field* ($\mathbf{H} = 0$)

For the case of no magnetic field, Eq. (19) reduces to

$$(D^2 - \varkappa_1^2) \, w = 0 \,, \tag{24}$$

where

$$\varkappa_1 = \frac{k}{\sqrt{1 + \dfrac{4\Omega^2}{\left(n + \dfrac{\nu}{k_1}\right)^2}}} \,. \tag{25}$$

The solutions appropriate for the two regions can be written as

$$w_1 = Ae^{\varkappa_1 z} \quad (z < 0)\,, \tag{26}$$

$$w_2 = Ae^{-\varkappa_1 z} \quad (z > 0)\,. \tag{27}$$

The condition (23), in the limit of vanishing magnetic field, reduces to

$$\Delta_0 (\varrho Dw) + \frac{4\Omega^2}{\left(n + \frac{\nu}{k_1}\right)^2} \Delta_0 (\varrho Dw) = -\frac{k^2}{n\left(n + \frac{\nu}{k_1}\right)} [g(\varrho_2 - \varrho_1)]\, w_0. \tag{28}$$

Applying the condition (28) to the solutions (26) and (27), we get

$$n\left(n + \frac{\nu}{k_1}\right)\sqrt{1 + \frac{4\Omega^2}{\left(n + \frac{\nu}{k_1}\right)^2}} = \frac{gk\,(\varrho_2 - \varrho_1)}{\varrho_2 + \varrho_1}, \tag{29}$$

which on simplification gives

$$n^4 + \frac{2\nu}{k_1} n^3 + \left\{\left(\frac{\nu}{k_1}\right)^2 + 4\Omega^2\right\} n^2 - \left\{\frac{gk\,(\varrho_2 - \varrho_1)}{\varrho_2 + \varrho_1}\right\}^2 = 0. \tag{30}$$

It follows from Eq. (30) that the constant term in Eq. (30) is negative (whether $\varrho_2 > \varrho_1$ or $\varrho_2 < \varrho_1$) and so there is one change of sign in the quartic equation in n. Hence there exists one positive root of n, meaning thereby instability of the system. We conclude therefore that the simultaneous presence of rotation and permeability on the stability of superposed rotating fluids through porous medium makes the system unstable.

3.b. *The case of no rotation* ($\Omega = 0$)

For non-rotating configuration, Eq. (18) reduces to

$$[D\,(\varrho Dw) - k^2\,\varrho w] + \frac{\mu_e H^2 k_x^2}{4\pi n\left(n + \frac{\nu}{k_1}\right)} (D^2 - k^2)\, w = -\frac{gk^2}{n\left(n + \frac{\nu}{k_1}\right)} (D\varrho) w. \tag{31}$$

For $k_x = 0$, i. e. for disturbances which are independent of the coordinates along the direction of **H**, the presence of magnetic field does not in any way affect the development of Rayleigh–Taylor instability. Thus for $k_x = 0$, there is identity between the hydrodynamic and the hydromagnetic problems. For $k_x \neq 0$, we examine the effect of magnetic field on the Rayleigh–Taylor instability.

The condition (23), for the case of no rotation, reduces to

$$\Delta_0(\varrho Dw) + \frac{\mu_e H^2 k_x^2}{4\pi n\left(n + \frac{\nu}{k_1}\right)} \Delta_0 (Dw) = -\frac{gk^2}{n\left(n + \frac{\nu}{k_1}\right)} (\varrho_2 - \varrho_1) w_0. \quad (32)$$

The solutions appropriate for the two regions can be written as

$$w_1 = A\, e^{kz} \quad (z < 0), \quad (33)$$

$$w_2 = A\, e^{-kz} \quad (z > 0). \quad (34)$$

Applying the condition (32) to the solutions (33) and (34), we get

$$n^2 + \frac{\nu}{k_1} n - gk\left[\frac{\varrho_2 - \varrho_1}{\varrho_2 + \varrho_1} - \frac{\mu_e H^2 k_x^2}{2\pi gk(\varrho_1 + \varrho_2)}\right] = 0. \quad (35)$$

Eq. (35) yields

$$n = -\frac{\nu}{2k_1} \pm \frac{1}{2}\sqrt{\left(\frac{\nu}{k_1}\right)^2 + \frac{4gk}{\varrho_1 + \varrho_2}\left[(\varrho_2 - \varrho_1) - \frac{\mu_e H^2 k_x^2}{2\pi gk}\right]}. \quad (36)$$

(i) *Stable case* ($\varrho_2 < \varrho_1$). It follows from Eq. (36) that if

$$\left|\frac{4gk}{\varrho_1 + \varrho_2}\left[(\varrho_2 - \varrho_1) - \frac{\mu_e H^2 k_x^2}{2\pi gk}\right]\right| > \left(\frac{\nu}{k_1}\right)^2, \quad (37)$$

the two values of n are complex conjugates with negative real parts. This means that the system is stable.

If

$$\left|\frac{4gk}{\varrho_1 + \varrho_2}\left[(\varrho_2 - \varrho_1) - \frac{\mu_e H^2 k_x^2}{2\pi gk}\right]\right| < \left(\frac{\nu}{k_1}\right)^2, \quad (38)$$

the two values of n are real and negative, meaning thereby stability of the system.

Thus the stable case remains stable even in the presence of magnetic field and permeability on the system under consideration.

(ii) *Unstable case* ($\varrho_1 > \varrho_2$). It follows from Eq. (36) that if

$$\varrho_2 - \varrho_1 > \frac{\mu_e H^2 k_x^2}{2\pi gk}, \quad (39)$$

one of the values of n is positive definite, which implies instability of the system.

If

$$\varrho_2 - \varrho_1 < \frac{\mu_e H^2 k_x^2}{2\pi g k}, \tag{40}$$

both the values of n are real and negative or complex conjugates with negative real parts. This means that the system is stable.

Therefore for the unstable case ($\varrho_2 > \varrho_1$), the system is stable or unstable according as $\varrho_2 - \varrho_1$ is less than or greater than $\mu_e H^2 k_x^2/2\pi g k$. The magnetic field thus has got stabilizing effect and completely stabilizes the wave-number band

$$k > \frac{2\pi g (\varrho_2 - \varrho_1)}{\mu_e H^2} \sec^2 \theta, \tag{41}$$

where θ is the inclination of the wave-vector (k_x, k_y) to the direction of **H**.

In the absence of magnetic field, the system is unstable for $\varrho_1 > \varrho_2$, as one of the values of n given by Eq. (36) is positive. But the presence of magnetic field has got stabilizing effect and completely stabilizes the wave-numbers $k > k_*$ where k_* is given by

$$k_* = \frac{2\pi g (\varrho_2 - \varrho_1)}{\mu_e H^2} \sec^2 \theta. \tag{42}$$

3.c. *Simultaneous presence of rotation and magnetic field*

Here we assume that two fluids carry different uniform fields so that they are characterised by the same Alfvén velocities V(i. e. $H_1^2/\varrho_1 = H_2^2/\varrho_2$). Then the equation is rather simpler to interpret.

Applying the condition (23) to the solutions (21) and (22), we get

$$n\left(n + \frac{\nu}{k_1}\right) + k_x^2 V^2 + \frac{4\Omega^2 n^2}{n\left(n + \frac{\nu}{k_1}\right) + k_x^2 V^2} =$$

$$= gk\alpha \sqrt{1 + \frac{4\Omega^2 n^2}{\left\{n\left(n + \frac{\nu}{k_1}\right) + k_x^2 V^2\right\}^2}}, \tag{43}$$

where

$$\alpha = \frac{\varrho_2 - \varrho_1}{\varrho_2 + \varrho_1}.$$

Eq. (43), on simplification, gives

$$n^8 + \frac{4\nu}{k_1} n^7 + 2\left[A + 2\left(\frac{\nu}{k_1}\right)^2\right] n^6 + 2\left[B + 2\left(\frac{\nu}{k_1}\right) A\right] n^5 +$$

$$+\left[A^2 + \frac{4\nu}{k_1} B + (2k_x^4 V^4 - g^2 k^2 \alpha^2)\right] n^4 + 2\left[AB + \left(\frac{\nu}{k_1}\right) \times\right.$$

$$\left.\times \{2 k_x^4 V^4 - g^2 k^2 \alpha^2\}\right] n^3 + \left[4 k_x^4 V^4 \left(\frac{\nu}{k_1}\right)^2 + A (2 k_x^4 V^4 - g^2 k^2 \alpha^2)\right] \times \quad (44)$$

$$\times n^2 + 2 k_x^2 V^2 \left(\frac{\nu}{k_1}\right) [2 k_x^4 V^4 - g^2 k^2 \alpha^2] n + k_x^4 V^4 [k_x^4 V_x^4 - g^2 k^2 \alpha^2] = 0 ,$$

where

$$A = \left(\frac{\nu}{k_1}\right)^2 + 2 k_x^2 V^2 + 4 \Omega^2 \quad \text{and} \quad B = 2 k_x^2 V^2 \left(\frac{\nu}{k_1}\right) . \quad (45)$$

It follows from Eq. (44) that if

$$g^2 k^2 \alpha^2 > k_x^4 V^4 , \quad (46)$$

there is at least one change of sign in the eighth degree equation in n. Hence there exists one positive root of n which means that the system is unstable.

If

$$g^2 k^2 \alpha^2 < k_x^4 V^4, \quad (47)$$

there is no change of sign in Eq. (44). This means that Eq. (44) does not allow any positive root, implying thereby stability of the system. The magnetic field thus has got stabilizing effect and completely stabilizes the wave-numbr band

$$k^2 > \frac{g^2 \alpha^2}{V^4} \sec^4 \theta , \quad (48)$$

θ being the angle between the wave-vector (k_x, k_y) and the direction of **H**.

In the absence of rotation and magnetic field, the system is stable for $\varrho_2 < \varrho_1$ and unstable for $\varrho_2 > \varrho_1$, as can be checked by Eq. (36) after putting $\mathbf{H} = 0$ in it. But in the presence of rotation and magnetic field, the magnetic field has a stabilizing effect and completely stabilizes the wave numbers $k^2 > k_{**}^2$ where k_{**} is given by

$$k_{**}^2 = \frac{g^2 \alpha^2}{V^4} \sec^4 \theta . \quad (49)$$

REFERENCES

1. S. CHANDRASEKHAR, Hydrodynamic and Hydromagnetic Stability, Oxford University Press, London, 1961, Chap. X.
2. E. R. LAPWOOD, Proc. Camb. Phil. Soc., **44**, 508, 1948.
3. R. A. WOODING, J. Fluid Mech., **9**, 183, 1960.

Acta Physica Academiae Scientiarum Hungaricae, Tomus 42 (1), pp. 29—47 (1977)

ZU DER QUANTENMECHANISCHEN THEORIE DES KUGELBLITZES

Von

TH. NEUGEBAUER

INSTITUT FÜR THEORETISCHE PHYSIK, ROLAND EÖTVÖS UNIVERSITÄT, BUDAPEST

(Eingegangen 13. XII. 1976)

Nach einer kritischen Sichtung der sich auf den Kugelblitz beziehenden Beobachtungsresultate und Theorien wird gezeigt, dass die einzige annehmbare Theorie von dieser Erscheinung die ist, dass der Kugelblitz aus einer seifenblasenartig schwebenden und fast ganz ionisierten Plasmakugel besteht, also eine selbstständige Erscheinung ist. Die vollständige Ionisation ensteht jedoch nicht entsprechend der Sahaschen Formel, weil dazu die Temperatur viel zu niedrig wäre, sondern aus der momentanen Ladungstauung beim Einschlagen eines Linienblitzes. Berechnungen beweisen, dass solch eine Gaskugel die quantenmechanischen Austauschkräfte gegen dem thermischen Expansionsbestreben tatsächlich zusammenhalten können. Die sehr wichtige Frage, weshalb der Kugelblitz nicht momentan rekombiniert, wird im vorletzten Paragraphen besprochen. Dort wird gezeigt, dass bezüglich der Verschmiertheit der Elektronen in unserer Plasmakugel teilweise ähnliche Verhältnisse auftreten können, wie in einem Metallgitter und Berechnungen beweisen, dass in diesem Falle der Wert des Rekombinationskoeffizienten so stark herabgedrückt wird, dass unser Plasmatropfen in einer Art metastabilen Zustandes tatsächlich mehrere Sekunden lang existenzfähig ist.

Einleitung

Lange Zeit hindurch hielt sich die Auffassung unter den Physikern, dass es zwei rätselhafte elektrische Erscheinungen gibt, von welchen die Wissenschaft noch immer nicht Rechenschaft geben kann und die sind die Supraleitung und der Kugelblitz. Jetzt kann man schon die Theorie der Supraleitung nach der Ansicht von den meisten Physikern infolge der Theorie von BARDEEN, COOPER und SCHRIEFFER wenigstens in ihren wesentlicheren Zügen als gelöst betrachten. Es ist also als einzige ungelöste Frage noch die Theorie des Kugelblitzes übriggeblieben.

Selbstverständlich ist es eine grosse Schwierigkeit, dass der Kugelblitz eine verhältnismässig seltene Naturerscheinung ist und meistens ist bei dessen zufälliger Erscheinung nicht auch gleich ein geschulter Physiker dabei. Natürlich haben schon viele, die das Glück gehabt haben einen Kugelblitz zu sehen, ihre diesbezüglichen Beobachtungen auch beschrieben. Dieses sehr umfangreiche Material trachteten dann zwei Arbeiten zu ordnen, die eine ist die von BRAND [1], welche zwischen den zwei Weltkriegen erschienen ist und die andere die von STANLEY SINGER [2], die ganz neu, bloss fünf Jahre alt ist.

Nach der kritischen Sichtung des Beobachtungsmaterials enstand nach den genannten Verfassern ungefähr das folgende Bild von dieser Erscheinung:

Die häufigste Erscheinungsform des Kugelblitzes ist der schwebende Kugelblitz. Der ist eine Kugel von ungefähr 10—20 cm Durchmesser, die seifenblasenartig schwebt und dabei auch leuchtet, jedoch nicht besonders intensiv, seine Lichtstärke schätzen die meisten Beobachter mit der einer 5—10 Watt starken Glühlampe gleich. Der Kugelblitz existiert jedenfalls mehrere Sekunden lang, wenn auch vielleicht die von seiner plötzlichen Erscheinung erschrokkenen Beobachter diese Zeitdauer überschätzt haben. Wir müssen noch einige Worte über das Aufhören dieser Erscheinung sagen. Entweder zieht sich der Kugelblitz immer mehr zusammen und verschwindet endlich, oder explodiert er mit einem ziemlich scharfen Knall. Wir wollen nur noch bemerken, dass nach den vorhandenen Beobachtungen diese Art des Kugelblitzes eine nicht besonders heisse und ziemlich harmlose Erscheinung ist.

Die zweite und viel seltenere Art des Kugelblitzes ist der an die Körper aufliegende Kugelblitz. Der leuchtet viel heller, ist bedeutend wärmer und zündet und brennt deshalb, ist also mehr garnicht eine so unschuldige Erscheinung als der schwebende Kugelblitz.

Wir haben noch nicht über die Entstehung des Kugelblitzes gesprochen. Viele Beobachter haben die Erfahrung beschrieben, dass der Kugelblitz scheinbar von der Einschlagstelle eines gewöhnlichen Blitzes abgesprungen ist, aber es gibt auch eine andere interessante Beobachtung. SCHONLAND [3], englischer Blitzforscher, und seine Mitarbeiter haben auf ihren von gewöhlichen Blitzen gemachten photographischen Aufnahmen die Erscheinung beobachtet, dass ein hauptsächlich negative Ladungen führender Entladungskanal, der sich von den Wolken abwerts ausbreitet, oft und in nicht besonders grosser Höhe einen von der Erdoberfläche ausgehenden Entladunsgkanal trifft, der hauptsächlich positive Ladungen befördert und am erwähnten Treffpunkt ein Kugelblitz ensteht, wie darauf besonders ALLIBONE aufmerksam gemacht hat.

Selbstverständlich können wir hier die sehr umfangreiche sich auf den Kugelblitz beziehende Literatur nicht besprechen und möchten deshalb bloss zwei interessante Beobachtungen erwähnen, die bezüglich der Theorie des Kugelblitzes sehr bedeutend sind. Die eine ist die von JENNISON [4], der Berufsphysiker ist, und der auf einem Flugzeug von New York nach Washington reisend es beobachtet hat, dass ein Kugelblitz in die Passagierkabine des Flugzeuges eingedrungen ist. Die andere ist die von WAGNER [5], der es beobachtete, dass in Österreich ins Wirtshaus zu Plöckenhausen ein Kugelblitz eingedrungen ist. Es hielten sich damals dort fünf Personen auf und alle haben die Erscheinung gesehen und hörten auch den Knall mit dem der Kugelblitz explodierte.

Natürlich, wie bei jeder seltenen Erscheinung, ist auch hier die hyperkritische Behauptung entstanden, dass ein Kugelblitz überhaupt nicht existiert, sondern nach der Anschauung von einigen Verfassern nur ein im Auge entstandenes positives Nachbild oder sogar bloss eine Vision ist. Einige sind sogar so

weit gegangen, dass sie angenommen haben, dass die von dem nahen Einschlagen eines Linienblitzes erschrockenen Beobachter einfach runde Milchglastulpen von Lampen als Kugelblitze beobachtet und teilweise auch photographiert haben. Diesbezüglich wollen wir nur bemerken, dass den in einem Wirtshaus eingedrungenen Kugelblitz viele gesehen haben. Visionen hat dagegen nur ein Mensch.

Übrigens tauchten in der Geschichte der Wissenschaft schon oft ähnliche Sachen auf. Es ist z.B. bekannt, dass eine Akademie in einem ihrer Dekrete es für unmöglich erklärte, dass vom Himmel Steine (Meteorite) herunterfallen sollen; die selbe Akademie hielt die Existenz des Riesenpolypen für einen Matrosenaberglauben. Übrigens könnte man noch sehr viele ähnliche Fälle erwähnen. Wir wollen hier nur noch das Beispiel erwähnen, dass noch vor drei Jahren ein Schweizer Blitzforscher [6] in einer vornehmen Fachzeitschrift die tatsächliche Existenz des Kugelblitzes einfach leugnete, weil er noch nicht das Glück gehabt hatte einen Kugelblitz zu sehen. Doch hat er die diesbezügliche ziemlich umfangreiche Literatur garnicht gekannt?

§ 1. Die sich auf den Kugelblitz beziehenden Theorien

Die theoretischen Gedanken bezüglich der Erklärung dieser Erscheinung können wir in zwei Gruppen einteilen. Die in die erste gehörenden haben angenommen, dass der Kugelblitz keine selbstständige Erscheinung ist, sondern bloss der allein leuchtende Teil einer zwischen der Erdoberfläche und den Wolken auftretenden stillen Entladung. Die zweite Gruppe hält dagegen den Kugelblitz für eine selbstständige Erscheinung. Betrachten wir zuerst die in die erste Kategorie gehörenden Theorien. Nach diesen wäre also der Kugelblitz solch eine ähnliche Erscheinung, wie die bei einem gewissen Druck in der Geisslerschen Röhre auftretende geschichtete Entladung. Eine solche Theorie ist die von TOEPLER [7], der eine Gleichstromentladung angenommen hat. Seine Theorie hat dann in neuester Zeit KAPITZA [22] modernisiert, der die Gedanken von TOEPLER nur in der Hinsicht abgeändert hat, dass er eine hochfrequente Entladung annahm. Selbstverständlich haben es schon die erwähnten Verfasser gesehen, dass eine sehr grosse Schwierigkeit ihrer Theorien die Erfahrung ist, dass der Kugelblitz durch offene Fenster oder Türen auch in geschlossene Räume eindringt. Zur Rettung dieser Lage haben sie angenommen, dass in diesen Fällen das Hausdach die Rolle von einer dazwischenliegenden Elektrode spielt. Wenn aber das auch tatsächlich so wäre, so könnte man sich auch dann schwer vorstellen, dass der Kugelblitz bei dem Eindringen in den erwähnten Räumen seine Gestalt oder andere Erscheinungsformen überhaupt nicht ändert. Ganz gegenstandslos machte jedoch diese Theorien die schon erwähnte Beobachtung von JENNISON, dass ein Kugelblitz in die ganz aus

Metall konstruierte Passagierkabine eines Flugzeuges eingedrungen ist. Es bleibt also als die einzig mögliche Erklärung dieser Erscheinung nur die Annahme übrig, dass der Kugelblitz eine selbstständige Erscheinung ist. An phantastischen Theorien war selbstverständlich auch hier kein Mangel. So haben z. B. einige Autoren [8] angenommen, dass der Kugelblitz aus einer aus dem Weltraum auf irgend einem Wege zu uns gelangte Antimaterie, selbstverständlich von sehr geringer Menge, besteht. Doch weshalb wäre das nur im Falle von Gewittern der Fall? Andere Theorien haben dagegen angenommen, dass die Energie des Kugelblitzes von dem radioaktiven Zerfall von ^{15}O und ^{17}F Kernen herrührt [9]. Selbstverständlich ensteht auch hier die Frage, weshalb die eben während Gewitter in einer verhältnismässig so grossen Menge entstehen würden. Ausserdem hat man berechnet, dass wenn das tatsächlich so wäre, dann würden die sich in der Nähe von einem Kugelblitz aufhaltenden Personen eine ernstere radioaktive Strahlungschädigung erleiden, weil ungefähr eine Energie von 10^8 Joule frei werden müsste, doch hat man noch keine Spur von solch einer Erscheinung beobachtet [10].

Es bleibt also als einzige annehmbare Theorie nur die, dass der Kugelblitz irgendeine leuchtende Plasmakugel ist. Selbstverständlich entstehen dann gleich zwei wichtige Fragen. Die eine ist, was für Kräfte diese ionisierte Plasmawolke zusammenhalten und die zweite, weshalb diese Plasmakugel nicht oder nur ganz langsam rekombiniert.

§ 2. Die quantenmechanische Theorie des Kugelblitzes

Der Verfasser der vorliegenden Arbeit hat noch in 1937 eine Theorie publiziert [11], deren springender Punkt ist, dass den Kugelblitz, von dem es angenommen wird, dass er aus einer praktisch vollständig ionisierten Gaswolke besteht, quantenmechanische Austauschkräfte zusammenhalten. Wie wir das aus den folgenden Berechnungen sehen werden, ist es tatsächlich möglich, dass eine sich unter atmosphärischem Druck befindende und praktisch vollständig ionisierte Gaskugel bis zu einer gewissen Temperatur von quantenmechanischen Austauschkräften zusammengehalten werden kann. Selbstverständlich tritt hier gleich das Problem auf, auf welchem Wege die erwähnte Gaskugel zustande kommen kann. Nach der Sahaschen Formel ist über einer gewissen sehr hohen Temperatur ein Gas im praktischen Sinne vollständig ionisiert. Bei einer so hohen Temperatur ist jedoch das thermische Expansionsbestreben so stark, dass im Verhältnis dazu die quantenmechanischen Austauschkräfte absolut unbedeutend sind. In neuerer Zeit haben SPITZER [12] und ECKER [13] zwei Werke über vollständig ionisierte Plasmen geschrieben und aus beiden kann man ersehen, dass man die ganz klassisch behandeln kann. In den in unseren Entladungsröhren auftretenden relative kalten Plas-

men wäre das thermische Expansionsbestreben natürlich sehr gering, die sind jedoch in solch einem kleinen Masse ionisiert, dass in ihnen auch die Austauschkräfte absolut unbedeutend sind. Das sind also die Ursachen von dem, dass man in der Physik der Gasplasmen die Quantenmechanik überhaupt nicht zu berücksichtigen braucht. Selbstverständlich treten diametral entgegengesetzte Verhältnisse in Metallgittern auf, wenn man die als Plasmen auffasst. Solch ein physikalisches System ist eben ein extrem quantenmechanisches Plasma.

Wie könnte also doch, (wenn auch nur temporär) unter atmosphärischem Druck ein praktisch vollständig ionisiertes und dabei doch nicht zu heisses Plasma entstehen? Zur Beantwortung dieser Frage wollen wir zuerst sehen was im Entladungskanal eines gewöhnlichen Blitzes geschieht. Nach den Messungen von POCKELS [14] liegt in dem die Stromintensität um den Wert 10 000 Amp herum, aber nach den neueren Messungsergebnissen von APPLETON und CHAPMAN [15] kann sie bis 250 000 Amp reichen. Der Durchmesser des Entladungskanals beträgt ungefähr 50 cm, die Hauptentladung spielt sich jedoch nur in einer Röhre von einigen cm Durchmesser ab. Die Geschwindigkeit der Elektronen kann man darin auf 10^8 cm sek^{-1} schätzen. Wenn also solch ein Linienblitz an einem nicht besonders gut leitenden Ort einschlägt, so kann momentan tatsächlich eine so grosse Ladungsstauung auftreten, dass ein praktisch vollständig ionisierter "Gastropfen" entsteht. Mit diesem Gedankengange ist in ausgezeichneter Übereinstimmung die schon erwähnte Erfahrung, dass viele Beobachter den Kugelblitz von der Einschlagstelle eines gewöhnlichen Blitzes abzuspringen beobachtet haben. Aber auch mit der schon erwähnten Auffassung von SCHONLAND und seinen Mitarbeitern, dass der Kugelblitz bei dem Zusammentreffen von einer von den Wolken sich abwerts bewegenden und von einer vom Erdboden sich in entgegengesetzter Richtung ausbreitenden und besonders Ladungen von entgegengesetztem Vorzeichen befördernden Entladungröhre entsteht, stimmt der hier erwähnte Gedankengang gut überein.

Jetzt wollen wir nach diesem allgemeinen Gedankengang die dabei auftretenden quantitativen Verhältnisse besprechen. Betrachten wir also zwei auf das Volumen V normierte und ebene Wellen darstellende Eigenfunktionen

$$\psi_m = \frac{1}{V^{1/2}} e^{i(\mathbf{k},\mathbf{r})} \tag{1}$$

und

$$\psi_n = \frac{1}{V^{1/2}} e^{i(\mathbf{k}',\mathbf{r})}, \tag{2}$$

wo

$$\mathbf{k} = 2\pi \frac{1}{\lambda} \tag{3}$$

den Ausbreitungsvektor darstellt und alle übrigen Symbole die gewohnte Bedeutung haben. Das Austauschintegral ist dann

$$J_{mn} = e^2 \iint \psi_m(r_1)\, \bar{\psi}_n(r_1) \frac{1}{r_{12}} \bar{\psi}_m(r_2)\, \psi_n(r_2)\, d\tau_1\, d\tau_2 . \tag{4}$$

Betrachten wir zuerst das folgende Integral

$$U(r_2) = \frac{1}{V} \int e^{i(\mathbf{k},\mathbf{k}',\mathbf{r})} \frac{1}{r_{12}} d\tau_1 . \tag{5}$$

Mit Hilfe des Greenschen Satzes

$$\int (F \Delta G - G \Delta F)\, d\tau = \int \left(F \frac{\partial G}{\partial n} - G \frac{\partial F}{\partial n} \right) df$$

folgt, wenn wir

$$F = \frac{1}{r_{12}} \tag{6}$$

und

$$G = -\frac{1}{(\mathbf{k}-\mathbf{k}')^2} e^{i(\mathbf{k}-\mathbf{k}',\mathbf{r}_1)} . \tag{7}$$

setzen, für (5)

$$U = \frac{1}{V} \frac{4\pi}{(\mathbf{k}-\mathbf{k}')^2} e^{i(\mathbf{k}-\mathbf{k}',\mathbf{r}_2)}, \tag{8}$$

weil das auf der rechten Seite des Greenschen Satzes stehende Flächenintegral verschwindet, wenn wir eine genügend entfernte Fläche annehmen, da ja die Eigenfunktionen in ein Volumen von der Grösse V eingeschlossen sind. Ausserdem hat das auf der linken Seite stehende zweite Glied an der Stelle $r_1 = r_2$ eine Singularität, welche man ausschliessen muss.

Aus (1), (2), (4) und (8) folgt also

$$J_{nm} = \frac{4\pi e^2}{V^2} \int \frac{1}{(\mathbf{k}-\mathbf{k}')^2} d\tau_2 = \frac{4\pi e^2}{V(\mathbf{k}-\mathbf{k}')^2} \tag{9}$$

und damit haben wir das Austauschintegral berechnet.

Wir wollen noch bemerken, dass wir unser Resultat (8) auch auf einem ganz anderen Wege aus (5) erhalten können. Diese Formel können wir nämlich so auffassen, wie das Potential einer durch die Formel $V^{-1} e^{i(\mathbf{k}-\mathbf{k}',\mathbf{r}_1)}$ beschriebenen Ladungsverteilung im Punkt r_2. Also muss in diesem Falle die Poissonsche Differentialgleichung gültig sein, d.h.

$$\Delta U(\mathbf{r}_2) = -4\pi V^{-1} e^{i(\mathbf{k}-\mathbf{k}', \mathbf{r}_2)}.$$

Wenn wir diesen Ausdruck zweimal integrieren, damit wir von der linken Seite den Laplaceschen Operator entfernen, so erhalten wir

$$U(\mathbf{r}_2) = \frac{4\pi}{V(\mathbf{k}-\mathbf{k}')^2} e^{i(\mathbf{k}-\mathbf{k}', \mathbf{r}_2)}$$

und dieses Resultat stimmt gerade mit unserer Formel (8) überein.

Damit wir jetzt $\sum_{mn} J_{mn}$ erhalten, müssen wir über alle in unserem Gasvolumen auftretenden Geschwindigkeiten summieren. Da jedoch hier von einem Gasplasma unter atmosphärischem Druck die Rede ist, so können wir ganz ruhig statt der Fermi—Diracschen Statistik die klassische Boltzmannstatistik benützen, nach der die Geschwindigkeitsverteilungen mit Hilfe der Formel

$$N\left(\frac{m}{2\pi kT}\right)^{3/2} e^{-\frac{mv^2}{2kT}} v^2\, dv \sin\vartheta .\, d\vartheta .\, d\varphi \tag{10}$$

beschrieben werden. In (10) bedeutet k die Boltzmannsche Konstante und alle anderen Symbole haben wieder die gewohnte Bedeutung. Da

$$\lambda = \frac{h}{mv} \tag{11}$$

ist, so folgt aus (3), wenn wir noch zur Vermeidung der Verwechselung mit der Boltzmannschen Konstante jetzt statt $|\mathbf{k}|$ l schreiben

$$|\mathbf{k}| = l = \frac{2\pi mv}{h}. \tag{12}$$

Wenn wir noch, zur Vereinfachung der Schreibweise, die Bezeichnungen

$$B = N\left(\frac{m}{2\pi kT}\right)^{3/2}\left(\frac{h}{2\pi m}\right)^3 \tag{13}$$

und

$$A = \frac{m}{2kT}\left(\frac{h}{2\pi m}\right)^2 \tag{14}$$

einführen, so folgt für (10)

$$Be^{-Al^2} l^2\, dl \sin\vartheta\, d\vartheta\, d\varphi. \tag{15}$$

Endlich haben wir also aus (9) und (15)

$$\sum_m J_{mn} = \frac{4\pi e^2}{V} \cdot B \int_0^\infty \int_0^\pi \int_0^{2\pi} e^{-Al^2} \frac{1}{l^2 + l'^2 - 2ll' \cos\vartheta} l^2 \, dl \sin\vartheta \, d\vartheta \, d\varphi. \quad (16)$$

Nach den Winkelkoordinaten können wir gleich integrieren und erhalten

$$\sum_m J_{mn} = \frac{8\pi^2 e^2}{V} B \frac{1}{2l'} \int_0^\infty e^{-Al^2} \log \frac{l+l'}{|l-l'|} l \, dl. \quad (17)$$

Hier führen wir wieder die folgende Bezeichnung ein:

$$C = \frac{4\pi^2 e^2}{B} V. \quad (18)$$

Weiter benützen wir jetzt (10) gleich in der nach den Winkelkoordinaten integrierten Form, damit wir gleich über n summieren können; wir schreiben also statt (10)

$$4\pi N \left(\frac{m}{2\pi kT}\right)^{3/2} e^{-\frac{mv'^2}{2kT}} v'^2 \, dv. \quad (19)$$

Diesen Ausdruck formen wir wieder mit Hilfe des zu (12) analogen Zusammenhanges

$$|\mathbf{k}'| = l' = \frac{2\pi m v'}{h} \quad (20)$$

um.

Endlich folgt also aus (17), (18), (19) und (20)

$$\sum_{mn} J_{mn} = 4\pi BC \int_0^\infty \int_0^\infty e^{-A(l^2+l'^2)'} \log \frac{l+l'}{|l-l'|} l' \, dl' \, l \, dl. \quad (21)$$

Damit wir das in (21) stehende Doppelintegral berechnen können, führen wir mit Hilfe der Gleichungen

und

$$\left.\begin{aligned} l &= r \cos\varphi \\ l' &= r \sin\varphi \end{aligned}\right\} \quad (22)$$

eine neue Veränderliche ein und auf die Weise erhalten wir

$$\sum_{mn} J_{mn} = 2\pi BC \int_0^\infty \int_0^{\pi/2} e^{-Ar^2} r^3 \, dr \sin 2\varphi \log \frac{\cos\varphi + \sin\varphi}{|\cos\varphi - \sin\varphi|} d\varphi. \quad (23)$$

Aus den Zusammenhängen

$$\left.\begin{aligned} \cos\psi + \sin\psi &= \sqrt{2}\sin\left(\frac{\pi}{4}+\psi\right) \\ \text{und} \\ \cos\psi - \sin\psi &= \sqrt{2}\cos\left(\frac{\pi}{4}+\psi\right) \end{aligned}\right\} \tag{24}$$

erhalten wir mit Hilfe von partieller Integration für das in (23) stehende Winkelintegral

$$\int_0^{\pi/2} \sin 2\psi \log\left|\operatorname{tg}\left(\frac{\pi}{4}+\psi\right)\right| d\psi = \frac{\pi}{2}, \tag{25}$$

so dass endlich das Resultat

$$\sum_{mn} J_{mn} = 2\pi\, BC \frac{1}{2A^2}\frac{\pi}{2} \tag{26}$$

folgt. Aus (13), (14) und (18) erhalten wir also, wenn wir noch die Zahl der in der Volumeneinheit enthaltenen Elektronen mit n bezeichnen

$$\sum_{mn} J_{mn} = N\frac{e^2 n h^2}{4\pi mkT}. \tag{27}$$

Da wir jedoch bei der Summierung alle Elektronenpaare doppelt berücksichtigt haben, so folgt endlich für die ganze Austauschenergie

$$W = -N\frac{e^2 nh^2}{8\pi mkT}. \tag{28}$$

Bei der Herleitung von (28) haben wir angenommen, dass die Spinrichtungen von allen Elektronen zueinander parallel stehen, wenn jedoch Rechts- und Linksspins mit gleicher Wahrscheinlichkeit vorkommen, dann folgt statt (28)

$$W' = -N\frac{e^2 nh^2}{16\,\pi m\,kT}, \tag{29}$$

da ja nur Elektronen mit parallelen Spinrichtungen miteinander in Austauschwechselwirkung treten.

In der Theorie der metallischen Bindung tritt ebenfalls das Problem der Austauschenergie des Elektronengases auf, jedoch in einem extrem entgegengesetzten Fall, weil ja das Elektronengas in Metallen vollständig entartet ist und man deshalb die Fermistatistik für den Fall der vollständigen Entartung

anwenden muss. Diese Berechnung wurde zuerst von BETHE [16] vollführt und es ist interessant sein Ergebnis mit dem unseren zu vergleichen. In den hier benützten Bezeichnungen erhielt BETHE für die erwähnten zwei Fälle

$$W = -\frac{3}{2} e^2 N \left(\frac{3n}{4\pi}\right)^{1/3} \tag{30}$$

und

$$W' = -\frac{3}{2} e^2 N \left(\frac{3n}{8\pi}\right)^{1/3}. \tag{31}$$

Wir sehen, dass in diesen Formeln (entgegen unseren Ausdrücken (28) und (29)) die Temperatur nicht vorkommt, wie ja das auch sein muss.

Aus (28) erhalten wir für die auf ein Elektron fallende Austauschenergie

$$E = -\frac{e^2 nh^2}{8\pi mkT}. \tag{32}$$

Damit also die den Kugelblitz aufbauende Plasmawolke tatsächlich zusammenhalten soll, muss die aus dieser negativen Energie folgende Anziehungskraft dem gaskinetischen Expansionsbestreben widerstehen können.

Da nach der kinetischen Gastheorie

$$\frac{1}{2} m\hat{v}^2 = \frac{3}{2} kT \tag{33}$$

ist, so folgt, wenn wir (32) und (33) einander gleichsetzen

$$T^2 = \frac{e^2 nh^2}{12\ \pi mk^2}, \tag{34}$$

oder wenn nach unserer Annahme die Gaskugel praktisch vollständig ionisiert ist und wir deshalb $n = 27.\ 10^{18}$ setzen können

$$T = 632\ °\text{K}. \tag{35}$$

Dieses Resultat gerechtfertigt einerseits unsere Annahme, dass wir hier in erster Näherung ruhig die Boltzmannstatistik benützen können und zeigt andererseits, dass der schwebende Kugelblitz eine nicht besonders heisse und deshalb ziemlich harmlose Erscheinung ist, wie wir ja das schon in der Einleitung erwähnt haben. Wenn jedoch die Dichte (n) der Elektronen und dementsprechend auch die Zahl der positiven Ionen bedeutend grösser wird, dann können wir aus (34) ersehen, dass solch ein Kugelblitz viel heisser werden

kann. Ein Kugelblitz von dieser Art wird jedoch, da seine Dichte viel grösser ist, als die der umgebenden Luft, nicht mehr schweben, sondern sich auf Körper darauflegen und wegen seiner hohen Temperatur brennen und zünden, wieder in vollständiger Übereinstimmung mit der Erfahrung.

Über das Ende des Kugelblitzes müssen wir noch einige Bemerkungen machen. Aus (28) oder (32) folgt, dass n wegen der Rekombination und T dagegen wegen der Wärmeausstrahlung des Kugelblitzes mit der Zeit abnehmen. Wenn die Abnahme von T die überwiegende ist, so wird sich der Kugelblitz immer mehr zusammenziehen, die grössere Dichte wird auch eine stärkere Rekombinationswahrscheinlichkeit zur Folge haben und zuletzt verschwindet der Kugelblitz. Wenn jedoch die Abnahme von n die vorherrschende ist, dann muss endlich

$$\frac{1}{2} m\hat{v}^2 = \frac{3}{2} kT > \frac{e^2 nh^2}{8\pi mkT} \tag{36}$$

werden, die Austauschkräfte können also die ionisierte Gaswolke nicht mehr zusammenhalten und der Kugelblitz explodiert, wieder in vollständiger Übereinstimmung mit der Erfahrung.

Bis jetzt haben wir bloss mit der Austauschwechselwirkung gerechnet und haben dabei die Umstände, dass zwischen den Ionen und Elektronen selbstverständlich auch elektrostatische Wechselwirkungen auftreten, und ausserdem auch noch Polarisationserscheinungen vorhanden sein müssen, vernachlässigt. Die Berechnung der elektrostatischen Energie in einer ungeordneten Gaswolke wäre ein sehr schwieriges Problem, doch können wir ihre Grössenordnung leicht abschätzen. Wenn wir als Gedankenexperiment für die Anordnung der Ladungen entgegengesetzten Vorzeichens eine steinsalzgitterartige Verteilung annehmen, dann muss

$$\frac{1}{r_0^3} = 2n \tag{37}$$

sein. Die elektrostatische Energie ist dagegen für ein aus einem positiven Ion und einem Elektron bestehenden Paar

$$-\frac{e^2}{r_0}. \tag{38}$$

(In einem streng geordneten Gitter vom Steinsalztyp müsste man diesen Ausdruck noch mit der Madelungschen Konstante 1,74750 multiplizieren, das ändert jedoch an der Grössenordnung mehr nichts.) (38) können wir wegen (37) wie folgt schreiben:

$$-e^2 (2n)^{1/3}. \tag{39}$$

Wenn wir jetzt die aus (39) folgende elektrostatische Energie tatsächlich berechnen und die mit der Austauschenergie vergleichen, so erhalten wir das Resultat, dass beide von der selben Grössenordnung sind. Oder wenn wir die höhere Temperatur des Kugelblitzes berücksichtigen, so würde folgen, dass die elektrostatische Energie sogar auch noch grösser sein könnte. Wir haben jedoch für diese Energie einen extrem günstigen Fall (steinsalzgitterartige Anordnung) angenommen; in einer Gaswolke sind die Ladungen dagegen vollständig ungeordnet und es ist klar, dass deshalb die Energie viel kleiner sein wird. Es ist ja eine bekannte Tatsache, dass wenn wir zwei Ladungen gleicher Grösse, jedoch von entgegengesetztem Vorzeichen in zwei Kugeln vom selben Halbmesser gleichmässig verschmieren und dann diese zwei Kugeln miteinander zur Deckung bringen, dieses elektrostatische System gar kein Potential auf sich selbst besitzt. Dieser Umstand rechtfertigt also unser Verfahren, dass wir die elektrostatische Energie von unserer ionisierten Gaswolke in erster Näherung vernachlässigt haben. Wir wollen noch bemerken, dass weil diese Energie ebenfalls negativ ist, sie die Kohäsion des Kugelblitzes nur noch verstärken könnte.

Die Polarisationsenergie ist zur Austauschenergie weitgehend analog (und ebenfalls negativ), doch wie das besonders die sich auf Kristallgitter beziehenden Berechnungen beweisen, viel kleiner.

Wir haben noch von der sehr wichtigen Frage nicht gesprochen, weshalb der Kugelblitz nicht rekombiniert, oder richtiger ausgedrückt warum das nur so langsam tut. Bevor wir jedoch diese wichtige Frage besprechen, möchten wir noch einige Worte über die anschauliche physikalische Deutung der Austauschkräfte sagen, die ja der springende Punkt unserer ganzen Überlegung ist.

§ 3. Das Wesen der Austauschenergie

Die quantenmechanischen Lehrbücher führen meistens die Austauschkräfte bei der Besprechung des Heitler—London Modells des Wasserstoffmoleküls ein. Dagegen sieht man eben in diesem Fall den physikalischen Inhalt dieser Sache nicht gut. Die Störungsenergie besteht hier aus vier Gliedern, die abwechselnd positiv und negativ sind und sind ausserdem grössenordnungsmässig garnicht kleiner als die Energie in nullter Näherung. Endlich, da das Wasserstoffmolekül dann zustande kommt, wenn die Elektronenspins zueinander antiparallel sind, so hat das den unrichtigen Anschein, dass sich antiparallele Spins anziehen. (Das ist allerdings nur für die sehr geringe magnetische Wechselwirkung richtig.)

Die auftretenden physikalischen Verhältnisse sieht man dagegen viel klarer, wenn wir als Gedankenexperiment zwei Elektronen in einem rechtwinkeligen Parallelepipedon einschliessen. Wenn die Spins dieser Elektronen

antiparallel sind, dann beeinflussen sie sich infolge der Fermistatistik überhaupt nicht und die ganze (positive) elektrostatische Energie wird nur die klassisch berechnete Wechselwirkung der zwei verschmierten Ladungen sein. Wenn jedoch die Spins zueinander parallel gerichtet sind, so dulden sie sich nicht in ihrer unmittelbaren Nähe (infolge der Fermistatistik) und wenn wir jetzt wieder die elektrostatische Energie nach dem erwähnten Verfahren berechnen, so schätzen wir die zu gross, eben deshalb weil bei der Berücksichtigung der verschmierten Ladungen der Fall, dass die beiden Elektronen sich in ihrer unmittelbaren Nähe befinden, nicht vorkommen kann. Der Mangel dieser positiven Energie erscheint deshalb als eine scheinbare negative Energie und der entspricht die Austauschkraft.

Es ist noch interessant das Zustandekommen der Austauschenergie mit der der Polarisationsenergie zu vergleichen. Bei Polarisationserscheinungen verschiebt erstens das elektrische Feld (unabhängig davon ob es sich um Ladungen von gleichem, oder entgegengesetztem Vorzeichen handelt) die Ladungen und zweitens ändert das dann die elektrostatische Energie. Die Polarisationsenergie ist deshalb zu dem Quadrat der Feldintensität proportional und immer negativ. Bei der Austauschenergie entfernt dagegen zuerst die Fermistatistik die Ladungen voneinander und zweitens ändert dann das die elektrostatische Energie. Es ist also auch hier von elektrostatischer Energie die Rede, ebenso wie bei den Polarisationserscheinungen, aber die Verschiebung der Ladungen ist nicht der Feldintensität sondern der Fermistatistik zuzuschreiben. Wir wollen nur noch bemerken, dass infolge des hier besprochenen Gedankenganges Austauschkräfte selbstverständlich nur eine ladungskompensierte Elektronenwolke zusammenhalten können.

§ 4. Das Problem der Rekombination im Kugelblitz

Zuletzt sind wir bei dem verwickeltesten Problem in der Theorie des Kugelblitzes angelangt und zwar zu dem, wie das möglich ist, dass der Kugelblitz in irgend einem metastabilen Zustande doch mehrere Sekunden hindurch existenzfähig ist, andererseits nach den bekannten Gesetzmässigkeiten der Plasmaphysik diese ionisierte Gaswolke schon nach unglaublich kleinen Bruchteilen einer Sekunde, wegen der Rekombination der darin enthaltenen Ladungen, verschwinden müsste.

Damit wir das hierbei auftretende Problem klar sehen, betrachten wir zuerst die bekannte Differentialgleichung der Rekombination. Es bezeichne n_+ die Zahl der in der Volumeneinheit enthaltenen positiven und n_- die der negativen Ionen, dann haben wir

$$\frac{dn_+}{dt} = \frac{dn_-}{dt} = -\alpha n_+ n_-, \tag{40}$$

wo α der Rekombinationskoeffizient ist. Da weiter in unserer Gaswolke die positiven und die negativen Ladungen in gleicher Zahl vorhanden sind, so können wir (40) noch wie folgt schreiben

$$\frac{dn}{dt} = -\alpha n^2 . \tag{41}$$

Für die integrierte Form folgt also

$$\frac{1}{n} - \frac{1}{n_0} = \alpha (t - t_0) . \tag{42}$$

Bei normaler Temperatur und Druck besitzt nach den Messungsergebnissen α die Grössenordnung 10^{-6}, n_0 ist dagegen nach unseren Annahmen von der Grössenordnung 10^{19}. Daraus können wir also ersehen, dass eine wie unglaublich kurze Zeit dazu vergehen müsste, damit n praktisch gleich Null wird. Die Rekombination der Ionen angefangen von einigen mm Druck bis ungefähr 1 Atm beschreibt die Theorie von THOMSON in guter Übereinstimmung mit der Erfahrung, bis mehreren Atmosphären dagegen die Theorie von LANGEVIN. In diesem letzteren Gebiet liegt der Wert des Rekombinationskoeffizienten um die Grössenordnung 10^{-5} herum.

Alle diese Sachen beziehen sich jedoch auf die Rekombination von positiven und negativen Ionen, in unserem Problem handelt es sich dagegen um die Rekombination von positiven Ionen und Elektronen und es ist eine bekannte Tatsache, dass in diesem Fall der Rekombinationskoeffizient viel kleiner ist. Die ausführlichsten Berechnungen über dieses Problem haben BATES, BUCKINGHAM, MASSEY und UNWIN [17] veröffentlicht, die von ihnen hergeleitete Formel lautet

$$Q_n = \frac{64\,\pi^4 \nu^3 e^2}{3\,hc^3 v} \left| \int \bar{\psi}_i \, \mathbf{r} \, \psi_n \, d\tau \right|^2 , \tag{43}$$

wo ν die Frequenz des ausgestrahlten Lichtes, ψ_n die Eigenfunktion des gebundenen Zustandes und ψ_i die des freien Zustandes bedeutet und zwar so normiert, dass sie asymptotisch die Form einer ebenen Welle annimmt. Alle anderen Symbole haben die gewohnte Bedeutung. Daraus folgt für den Rekombinationskoeffizienten

$$\alpha = v \sum_n Q_n . \tag{44}$$

(v ist die Geschwindigkeit des Elektrons.) Die Summation bezieht sich auf alle leeren Zustände des positiven Ions. OPPENHEIMER [18] konnte schon in 1929 die Berechnung von solch einer Summe vereinfachen. Die genannten Verfasser

erhielten das Resultat, dass in diesem Falle die Grössenordnung von α 10^{-12} beträgt, also viel kleiner ist als bei negativen Ionen, doch wie wir das aus (42) ersehen, könnte auch dieser Wert nicht die Tatsache erklären, dass der Kugelblitz mehrere Sekunden hindurch existieren kann. (Wir wollen noch erwähnen, dass in der Ionosphäre $\alpha = 10^{-8}$ der zuverlässigste gemessene Wert ist. In der oberen F_1 Schicht ist α noch kleiner und hat einen Wert um 4.10^{-9} herum und in der F_2 Schicht die Grösse 8.10^{-11}. Alle diese Werte sprechen also dafür, dass dort auch negative Ionen eine gewisse Rolle spielen.)

Ein mit dem hier besprochenen Problem diametral entgegengesetzter Fall tritt in Metallgittern auf. Die können wir auch als ein Plasma auffassen, selbstverständlich entgegen den Gasplasmen als eine extrem quantenmechanische Erscheinung. Nun kann ein Metall deshalb nicht rekombinieren, (die positiven Gitterionen und die quasifreien Elektronen können sich deshalb nicht gegenseitig zu Metallatomen neutralisieren,) weil das einfach energetisch nicht möglich ist. Bei der Entstehung eines Metallgitters wird mehr Energie frei, wie wenn wir die positiven Ionen und die Elektronen zu neutralen Atomen zusammenfügen würden. Ein entgegengesetzter Fall ist der des Wasserstoffs, den man nach seiner Lage im periodischen System als das einfachste Alkaliatom auffassen könnte. Hier ist jedoch die Bildung von neutralen Atomen die energetisch günstigere und tatsächlich beweisen das Berechnungen [19], dass ein "Wasserstoffmetall" nur bei einem Druck von 400 000 Atm entstehen könnte.

Jetzt müssen wir noch die Frage beantworten, wieso das möglich ist, dass der Rekombinationskoeffizient im Kugelblitz so klein werden kann. Nach unserer Annahme ist das Material des Kugelblitzes ein fast vollständig ionisiertes Plasma, aber nicht wegen seiner Temperatur, die nach der Formel von Saha selbstverständlich viel zu niedrig sein würde, sondern deshalb, weil diese Gaswolke infolge der Stauung von Ladungen entstanden ist, entweder an der Einschlagstelle eines Linienblitzes oder am Treffpunkt eines aus den Wolken sich abwerts ausbreitenden Entladungskanales der hauptsächlich negative Ladungen führt und einer von der Erdoberfläche nach oben fortschreitenden Entladungsröhre, in der sich hauptsächlich positive Ionen bewegen. Im Endresultat müssen also im Material des Kugelblitzes teilweise ähnliche Verhältnisse auftreten, wie in einem Metall, selbstverständlich unter Berücksichtigung der viel geringeren Dichte und ausserdem des Umstandes, dass das darin enthaltene Elektronengas nicht entartet ist.

Betrachten wir jetzt nach den gesagten die Eigenfunktion eines Elektrons in einem Kristallgitter. Bis wir das Elektronengas als vollständig frei annehmen, werden diese Eigenfunktionen einfach die folgende Form haben

$$\psi' = A\, e^{ikx}. \tag{45}$$

A ist hier der Normierungsfaktor, also ist

$$|\psi^2| = A^2 = \text{konst} \tag{46}$$

und

$$k = 2\pi\frac{1}{2} = 2\pi\frac{p}{h} \tag{47}$$

ist der Ausbreitungsvektor. $p = mv$ bedeutet den Impuls des Elektrons.

Wenn wir jetzt nach BLOCH berücksichtigen, dass im Inneren des Kristalls ein periodisches Potentialfeld vorhanden ist, das wir mit $V(x)$ bezeichnen, dann muss

$$V(x) = V(x+d) \tag{48}$$

sein, weil das Gitter bezüglich d periodisch ist. BLOCH hat deshalb unter Berücksichtigung dieser Periodizität im Gitter statt (45) die folgende Eigenfunktion eingeführt

$$\psi(x) = u(x)e^{ikx}, \tag{49}$$

wo $u(x)$ ebenso periodisch ist, wie (48), also

$$u(x) = u(x+d) \tag{50}$$

sein muss.

In unserem vollständig ionisierten Kugelblitzmaterial werden die Elektronen jedoch nichteinmal in dem Masse lokalisiert sein als in einem normalen Gasplasma, sondern werden zu dem ganzen Material gehören, ähnlich wie in einem Metall.

Der Verfasser hat es schon in seiner zitierten alten Arbeit erwähnt, dass die im Kugelblitz auftretende sehr langsame Rekombination solch eine Ursache haben kann, dass ein Elektron, weil es infolge seiner Austauschwechselwirkung zu allen übrigen Elektronen gebunden ist, zuerst von dieser Bindung herausgerissen werden muss, damit es sich mit einem positiven Ion vereinigen kann. Wir hätten also mit irgend einer Art ähnlicher Erscheinung zu tun, wie der Übergang über einen Gamowschen Potentialberg. Die Betrachtungen von diesem Typ wollen wir jetzt etwas strenger fassen.

Sehen wir also wie sich die Formeln (43) und (44) von BATES und seine Mitarbeitern ändern werden, wenn wir die im Material des Kugelblitzes auftretenden ganz speziellen Verhältnisse berücksichtigen.

ψ_i gehört dann zu der Umgebung von sehr vielen Ionen, wenn wir also deren Zahl mit einem $\mathfrak{N}$ bezeichnen, so müssen wir in der erwähnten Formel statt ψ_i

$$\frac{\psi_i}{\mathfrak{N}^{1/2}} \tag{51}$$

einsetzen. Ähnliche Verhältnisse werden auftreten, wenn vielleicht wegen der stärkeren Bindung zwar in einem geringeren Masse, auch bei der Eigenfunktion ψ_n.

Es ist zwar selbstverständlich wahr, dass dann alle $\mathfrak{N}$ Elektronen einen ähnlichen Ladungsbeitrag in der Umgebung von allen positiven Ionen liefern werden und man könnte deshalb glauben, dass die erwähnte Erscheinung demzufolge herauskompensiert wird. Das ist jedoch nicht der Fall, weil in der zitierten Formel (43) das Quadrat des Matrixelementes steht, dieses wird jetzt also mit $\mathfrak{N}^2$ dividiert, dagegen multipliziert sich die Formel bei der Summierung über alle Elektronen nur mit $\mathfrak{N}$. Im Endresultat tritt also zum erwähnten Ausdruck der Faktor

$$\mathfrak{N} \frac{1}{\mathfrak{N}^2} = \frac{1}{\mathfrak{N}} \tag{52}$$

hinzu. Da $\mathfrak{N}$ sehr gross ist, so wird das die Grösse des Rekombinationskoeffizienten in einem riesigen Masse herunterdrücken. Selbstverständlich tritt zu dieser Erscheinung auch noch der oben behandelte Effekt des Überganges über den Gamowschen Potentialberg hinzu, doch wird der wahrscheinlich von untergeordneterer Bedeutung sein, oder ist sogar schon in unserem eben besprochenen Gedankengange wenigstens teilweise schon implizit enthalten. Wie gross $\mathfrak{N}$ tatsächlich ist, darüber wäre es sehr schwierig eine konkrete Aussage zu machen, weil diese Frage mit den tiefsten Problemen den Quantenmechanik zusammenhängt. In der Elektronentheorie der Metalle kann man nämlich mit der einfachen Annahme auskommen, dass das Leitungselektron im unendlichen Metallgitter verschmiert ist. Diese Hypothese kann jedoch auch schon bloss aus relativistischen Gründen nicht streng richtig sein. Es wäre jedoch sehr schwer zu sagen, wie weit diese Unlokalisierbarkeit des Elektrons reicht.

Ein ähnlicher Fall tritt übrigens auch in der WIGNER—SEITZschen Theorie der Metallgitter auf. Dort wird ein Alkaliion von einer negativen Ladungskugel umgeben, in der selbstverständich gerade die Ladung von einem Elektron enthalten ist, doch tragen zu der alle Metallelektronen bei und deshalb besitzt diese Ladungskugel ein Potential auf sich selbst, das man als Energie berücksichtigen muss. (Bei Atomen gibt es selbstverständlich so etwas nicht, weil wenn es tatsächlich vorhanden wäre und wir auch dies berücksichtigen müssten, dann würde z.B. die Übereinstimmung mit der Balmerformel und der Erfahrung vollständig verlorengehen.)

Der numerische Wert des Potentials auf sich selbst ist jedoch, wenn wir die Wolke entsprechend den mehreren Elektronen schon aufgeteilt haben, gegenüber dem dass wir diese Zerlegung noch weiter fortsetzen, sehr wenig empfindlich und wir erhalten deshalb in diesem Falle garkein Bild davon,

wie gross $\mathfrak{N}$ sein kann. Ähnliche Verhältnisse treten übrigens auch bei der Berechnung der elektrostatischen Energie von Atomkernen auf.

Wir möchten nur noch erwähnen, dass wenn auch die besprochenen Verhältnisse bezüglich der Zugehörigkeit eines Elektrons zu dem ganzen Plasmamaterial auch nicht so krass wären, als wir das angenommen haben, (und wie das in einem Metallgitter auch tatsächlich ist) und die Verschmiertheit von ψ_n auch geringer wäre, auch dann im Nenner unserer Formel (52) eine sehr grosse Zahl stehen würde, die also den Wert des Rekombinationskoeffizienten noch immer stark herabdrücken würde.

§ 5. Die Energie des Kugelblitzes

Wenn wir die Ionisationsenergie von Stickstoff- und Sauerstoffatomen gleich 14 eV setzen und nach unserer Annahme in einem cm^3 27.10^{18} Elektronen enthalten sind, dann berechnen wir für einen Kugelblitz von 20 cm Durchmesser, dass die Energie von dem rund $2{,}4.10^5$ Joule beträgt, also ebensoviel Energie frei wird, wenn alle darin enthaltenen Elektronen positive Ionen neutralisieren. Wir wollen jedoch noch bemerken, dass weil unser Kugelblitz schwebt und deshalb nahezu im Gleichgewicht mit der umgebenden Luft sein muss, er eigentlich eine doppelte Zahl von Atomen enthält, weil ja jedes Gasmolekül in zwei Atome (bzw. Ionen) dissoziiert. Deshalb müssen wir die angegebene Energie noch mit zwei multiplizieren und müssen ausserdem auch noch die Dissoziationsenergie hinzuaddieren. Weiter ist es möglich, (weil ja im Blitz sehr grosse Spannungen auftreten), dass auch höhere Ionisationsstufen eine Rolle spielen und deshalb in folge von all den erwähnten Umständen die angegebene Energie noch um eine ganze Grössenordnung grösser sein könnte.

Wenn wir das erhaltene numerische Ergebnis mit den sich auf die Energie des Kugelblitzes beziehenden Beobachtungsergebnissen [20], die jedoch von geringer Zahl und oft von problematischem Werte sind, vergleichen, so können wir sehen, dass die grössenordnungsmässige Übereinstimmung auch hier vorhanden ist.

Nach den Messungen von WILSON [21] liegt die Energie eines gewöhnlichen Linienblitzes zwischen 2.10^8 und 2.10^9 Joule. Wir sehen also, dass der beim Einschlagen eventuell entstehende Kugelblitz nur einen verschwindenden Teil dieser Energie enthält.

Man könnte es vielleicht versuchen nach den in dieser Arbeit besprochenen Richtlinien Kugelblitze künstlich herzustellen. Der Verfasser hat dazu hier diese Möglichkeit nicht.

LITERATUR

1. W. BRAND, Der Kugelblitz (Probleme der kosmischen Physik Bd. II/III.) H. Grand, Hamburg, 1923.
2. STANLEY SINGER, The Nature of Ball Lightening, Plenum Press, New York, 1971.
3. B. F. J. SCHONLAND and H. COLLENS, Proc. Roy. Soc. London (A), **143**, 654, 1934.
4. R. C. JENNISON, Nature, **224**, 895, 1969.
5. G. A. WAGNER, Nature, **232**, 187, 1971.
6. K. BERGER, Naturwiss., **60**, 485, 1973.
7. M. TOEPLER, Ann. d. Phys., (4) **2**, 560, 1900 und **7**, 477, 1902; Meteorol. Zeitschr., **17** 1513, 1900 und **34**, 225, 1917.
8. D. E. T. F. ASHBY and O. WHITEHEAD, Nature, **230**, 180, 1971; J. F. CRAWFORD, Nature, **239**, 395, 1972.
9. M. D. ALTSCHULER, L. L. HOUSE and E. HILDNER, Nature, **228**, 545, 1970; C. A. HILL and F. H. SOWBY, Nature, **228**, 1007, 1970.
10. A. A. MILLS, Nature, (Phys.) **233**, 131, 1971.
11. TH. NEUGEBAUER, Zeitschr. f. Phys., **106**, 474, 1937; H. T. FLINT, On the Problem of Ball Lightening, A Note on the Theory Proposed by Th. Neugebauer, Quarterly Journal of the Royal Meteorological Society. Vol. LXV. No. 282. pp. 532—35, October 1939; Nature, **140**, 814, 1937.
12. LYMAN SPITZER, Jr., Physics of Fully Ionized Plasmas, Interscience Publishers Inc., New York 1956 (Interscience Tracts on Physics and Astronomy, No. 3) 2. Aufl. 1968.
13. G. ECKER, Theory of Fully Ionized Plasmas, Academic Press, New York and London, 1972.
14. F. POCKELS, Meteorol. Zeitschr., **15**, 41, 1898 und **18**, 40, 1901.
15. E. V. APPLETON and F. W. CHAPMAN, Proc. Roy. Soc. London, (A), **158**, 1, 1937.
16. GEIGER—SCHEEL, Handb. d. Physik. Bd. XXIV/2, 2. Aufl. Berlin, 1933. Artikel von A. SOMMERFELD und H. BETHE, S. 483.
17. D. R. BATES, R. A. BUCKINGHAM, H. S. W. MASSEY and J. J. UNWIN, Proc. Roy. Soc. A **170**, 322, 1939.
18. J. R. OPPENHEIMER, Zeitschr. f. Phys., **55**, 725, 1929.
19. E. WIGNER and H. B. HUNTINGTON, J. Chem. Phys, **3**, 764, 1935.
20. P. D. ZIMMERMAN, Nature, **226**, 259, 1970.
21. C. T. R. WILSON, Proc. Roy. Soc. London (A), **92**, 555, 1916 und Phil. Trans. (A), **221**, 73, 1921.
22. P. L. KAPITZA, Dokl. Akad. Nauk SSSR, **101**, 245, 1955; Collected Papers of P. L. KAPITZA. Vol. 2. p. 776. Pergamon Press, Oxford, 1965.

Acta Physica Academiae Scientiarum Hungaricae, Tomus 42 (1), pp. 49—57 (1977)

HYDROMAGNETIC NATURAL CONVECTION FLOWS RESULTING FROM THE COMBINED BUOYANCY EFFECTS OF THERMAL AND MASS DIFFUSION

By

P. C. RAM, S. S. SINGH and H. L. AGARWAL

APPLIED MATHEMATICS SECTION, INSTITUTE OF TECHNOLOGY, BANARAS HINDU UNIVERSITY, VARANASI 221 005, INDIA

(Received 14. XII. 1976)

Natural convection of an electrically conducting fluid produced by the interaction of the force of gravity and density differences caused by the simultaneous diffusion of thermal energy and chemical species in the presence of a uniform transverse magnetic field is discussed. On thermal boundary layer thickness, concentration boundary layer thickness X_t and X_c have been calculated for different values of Prandtl number. A direct relation between the film thickness and distance travelled is presented and it is found that the film thickness approaches the uniform film thickness asymptotically.

Nomenclature

u, velocity component in x-direction;
v, velocity component in y-direction;
x, vertical distance along the surface;
y, horizontal distance from the surface;
α, thermal molecular diffusivity;
β, volumetric coefficient of thermal expansion;
β^*, volumetric coefficient of expansion with concentration;
ϱ, fluid density;
$\delta(x)$, boundary layer thickness for velocity;
η, dimensionless distance from the wall $(=y/\delta(x))$;
μ, dynamic viscosity of the fluid;
ν, kinematic viscosity of the fluid;
g, acceleration due to gravity;
$\delta_t(x)$, boundary layer thickness for temperature;
$\delta_c(x)$, boundary layer thickness for concentration;
σ, electric conductivity (assumed to be constant);
q, flow rate per unit width of wall;
C, nondimensional species concentration;
Pr, Prandtl number (ν/α);
Sc, Schmidt number (ν/D);
D, chemical molecular diffusivity;
F_x component of the magnetic body force $(-\sigma u B_0^2)$;
$\mathbf{V}$, the velocity vector with components u and v;
$\mathbf{J}$, the current density;
$\mathbf{F}$, Lorentz body force;
$\mathbf{E}$, electric field;
Gr, Grashof number;
T, fluid temperature;
Δ, $Gr + Gr'$
Le, Lewis number (Sc/Pr);
Δ_m, dimensionless symbol;
X, dimensionless length.

Subscripts

0, at the surface;
∞ in the undisturbed fluid;
p, at the plate surface;
t, based on temperature;
c, based on species concentration.

Introduction

The phenomenon of natural convection arises in a fluid when temperature changes cause density variations leading to buoyancy force acting on the fluid elements. Several papers have appeared in the last few years on magnetohydrodynamic thermal convection. SPARROW et al [1] and BRINDLEY [2] have studied the heat transfer from a vertical flat plate in a variable stream and under the action of gravity. The problem of forced heat transfer from a thin horizontal needle in a uniform stream has been investigated by MARK [3] and TAM [4]. SOMERS [5], has given the combined thermal and species diffusion driven flow that would arise adjacent to a wetted isothermal vertical surface in a non-saturated atmosphere. MATHERS et al [6] formulated the same problem in terms of the boundary layer differential equations resulting from force-momentum, energy, and chemical species conservation, at very low concentration. GEBHART et al [7] considered the stability of vertical natural convection boundary layers and some numerical solutions have been given. GEBHART and PERA [8] formulated the nature of vertical natural convection flows resulting from the combined buoyancy effects of thermal and mass diffusion. GUPTA and SURYAPRAKASHRAO [9] have studied the hydromagnetic free convection past a vertical porous flat plate subjected to suction or injection.

The purpose of the present study is to investigate flows resulting from buoyancy forces which arise from a combination of temperature and species concentration, in the presence of uniform transverse magnetic field. Such types of problem have many important technological applications, e.g., in the cooling of nuclear reactors, providing heat sinks in turbine blades and high speed re-entry vehicles.

Analysis

Consider a two-dimensional steady laminar flow in which the velocity vector **V** and the uniform magnetic field **B** are evrywhere parallel to the $x-y$ plane and the electric field **E** and the current density **J** are normal to the plane. Take the origin at the lower edge of the plate, x-axis along the plate and y-axis normal to the plate. If (i) the electromagnetic body force terms are combined with Navier-Stokes equations, (ii) gravity is absorbed in the hydrostatic pressure, the equations are written in the boundary layer form appropriate when the thickness of the flow region (in y) is small compared to the distance x above the initiation of the natural convection flow. Retaining these effects the equations governing the steady laminar flow in Boussinesq approximation [10] are:

$$\frac{\partial u}{\partial x} + \frac{\partial v}{\partial y} = 0\,, \tag{1}$$

$$u\frac{\partial u}{\partial x}+v\frac{\partial u}{\partial y}=v\frac{\partial^2 u}{\partial y^2}+g\beta(T-T_\infty)+g\beta^*(C-C_\infty)+\frac{F_x}{\varrho}, \quad (2a)$$

$$u\frac{\partial T}{\partial x}+v\frac{\partial T}{\partial y}=\alpha\frac{\partial^2 T}{\partial y^2}, \quad (3)$$

$$u\frac{\partial C}{\partial x}+v\frac{\partial C}{\partial y}=D\frac{\partial^2 C}{\partial y^2}. \quad (4)$$

In this study we neglect stratification, viscous dissipation, electrical dissipation (Joule heating) and other additional effects.

The Lorentz body force **F** in the absence of excess charges may be written as:

$$\mathbf{F}=\mathbf{J}\times\mathbf{B}. \quad (5)$$

If σ is the uniform conductivity and if the induced electrical field is negligible, then Ohm's law gives

$$\mathbf{J}=\sigma(\mathbf{E}+\mathbf{V}\times\mathbf{B}). \quad (6)$$

In steady state **E** must be derivable from a potential. Since it is wholly in the direction normal to the $x-y$ plane, it must be independent of x and y. In the absence of convection the y-component of the magnetic field is uniform and $\mathbf{V}=0=\mathbf{E}$, in the fluid. It may therefore be reasonable to assume that the same is true outside the boundary layer in the presence of convection, i.e. $\mathbf{E}=0$, then

$$\mathbf{J}=\sigma(\mathbf{V}\times\mathbf{B}). \quad (7)$$

If the magnetic Reynolds number is small the induced magnetic field is negligible compared with the applied magnetic field. So that we can write

$$\mathbf{B}=\mathbf{i}y\,B_0, \quad (8)$$

where $\mathbf{i}y$ is the unit normal vector in the normal y-direction, combining Eqs. (5), (7) and (8) the x-component of the body force is found to be equal to

$$F_x=-\sigma u\,B_0^2. \quad (9)$$

The momentum equation can therefore be written as

$$u\frac{\partial u}{\partial x}+v\frac{\partial u}{\partial y}=\nu\frac{\partial^2 u}{\partial y^2}+g\beta(T-T_\infty)+g\beta^*(C-C_\infty)-\frac{\sigma u}{\varrho}B_0^2. \quad (2)$$

We propose to solve the boundary layer equations by an integral method similar to that of Kármán and Pohlhausen.

Integrating (2) with respect to y from 0 to $\delta(x)$ and using (1), we get

$$\frac{\partial}{\partial x}\int_0^{\delta(x)} u^2(x,y)\,dy = \int_0^{\delta(x)} g\beta(T-T_\infty)\,dy + g\beta^*\int_0^{\delta(x)}(C-C_\infty)dy - \\ - \nu\left(\frac{\partial u}{\partial y}\right)_0 - \frac{\sigma B_0^2}{\varrho}\int_0^{\delta(x)} u\,dy\,. \tag{10}$$

We solve (10) by assuming a polynomial of third degree for the velocity function in terms of the dimensionless distance from the wall,

$$\frac{u\delta}{q} = a\eta + b\eta^2 + c\eta^3, \tag{11}$$

where $\eta = \dfrac{y}{\delta(x)}$.

The coefficients a, b and c are evaluated by using the following conditions:

$$\eta = 0,\ u = 0,\ v = 0,$$
$$\eta = 0,\quad \frac{\partial^2 u}{\partial\eta^2} = -\frac{g\beta\delta^2}{\nu}(T_p - T_\infty) - \frac{g\beta^*\delta^2}{\nu}(C - C_\infty), \tag{12}$$
$$\eta = 1,\quad \frac{\partial u}{\partial\eta} = 0\,.$$

The first condition of Eq. (12) is no slip condition at the wall. The second condition has been obtained by using the condition of no slip at the wall. It determines the curvature of the velocity profile. The third condition is at the free surface of the liquid film, and

$$\int_0^{\delta(x)} u dy = q \text{ (constant)}. \tag{13}$$

The coefficients are given by

$$a = \frac{12+\Delta}{5}, \quad b = -\frac{1}{2}\Delta, \quad c = \frac{4\Delta - 12}{15}, \tag{14}$$

where $\Delta = Gr + Gr'$ and

$$Gr = \frac{g\delta^3\beta}{q\nu}(T_p - T_\infty),$$
$$Gr' = \frac{g\beta^*\delta^3}{q\nu}(C_0 - C_\infty)\,.$$

Hence Eq. (11) becomes

$$\frac{u\delta}{q} = \frac{12+\Delta}{5}\eta - \frac{1}{2}\Delta\eta^2 + \frac{4\Delta-12}{15}\eta^3 . \tag{15}$$

Also assuming the polynomial of third degree for temperature, i. e.

$$\frac{T-T_p}{T_\infty - T_p} = E + F\eta + G\eta^2 + H\eta^3 . \tag{16}$$

The coefficients E, F, G and H are evaluated by using the following conditions

$$\begin{aligned} &\eta = 0,\ T = T_p,\quad \eta = 1,\ T = T_\infty , \\ &\eta = 1,\ \frac{\partial T}{\partial \eta} = 0 ,\quad \eta = 0 ,\quad \frac{\partial^2 T}{\partial \eta^2} = 0 . \end{aligned} \tag{17}$$

The coefficients are given by

$$E = 0 , F = 3/2, G = 0 , H = 1/2 .$$

Hence (16) becomes

$$\frac{T-T_p}{T_\infty - T_p} = 1/2\,\eta(3-\eta^2), \tag{18}$$

i.e.

$$(T - T_\infty) = (T_\infty - T_p)\,[1/2\,\eta(3-\eta^2) - 1] . \tag{19}$$

Similarly, we have

$$(C - C_\infty) = (C_\infty - C_0)\,[1/2\,\eta(3-\eta^2) - 1], \tag{20}$$

substituting (11), (13), (14), (19) and (20) in the integrated momentum equation (10), we have

$$\frac{q\delta'}{1575\,\nu}[120\,\Delta^2 - 1968\,\Delta - 78336] - [7\,\Delta - 96 - 40\,\Delta_m] = 0 , \tag{21}$$

where

$$\Delta_m = \frac{\sigma B_0^2 \delta^2(x)}{\varrho\nu},$$

and dash denotes differentiation with respect to x.

Integrating (21) for $\Delta_m = 1$ and $\Delta_m = 2$, we have

$$x = \frac{1}{11025}\,\frac{q}{\nu}\left[\frac{30g}{q\nu}\,\Delta_0\delta^4 + \frac{2544}{7}\,\delta + \frac{3492480}{49}\,\frac{q\nu}{g\Delta_0}\left(\frac{7}{136}\,\frac{g}{q\nu}\,\Delta_0\right)^{2/3}\times\right.$$

$$\times\left\{\frac{1}{6}\log\frac{\delta^2+\left(\frac{136}{7}\,\frac{qv}{g\Delta_0}\right)^{1/3}\delta+\left(\frac{136}{7g}\,\frac{qv}{\Delta_0}\right)^{2/3}}{\left\{\delta-\left(\frac{136}{7g}\,\frac{qv}{\Delta_0}\right)^{1/3}\right\}^2}+\right. \tag{22}$$

$$\left.+\frac{1}{\sqrt{3}}\tan^{-1}\frac{2\delta+\left(\frac{136}{7g}\,\frac{qv}{\Delta_0}\right)^{1/3}}{\sqrt{3}\left(\frac{136}{7g}\,\frac{qv}{\Delta_0}\right)^{1/3}}\right\}\Bigg]$$

and

$$x=\frac{1}{11025}\,\frac{q}{v}\left[\frac{30g}{qv}\,\Delta_0\,\delta^4+\frac{7344}{7}\,\delta+\frac{2534920}{49}\,\frac{qv}{g\Delta_0}\left(\frac{7}{176}\,\frac{g}{qv}\,\Delta_0\right)^{2/3}\times\right.$$

$$\times\left\{\frac{1}{6}\log\frac{\delta^2+\left(\frac{176}{7}\,\frac{qv}{g\Delta_0}\right)^{1/3}\delta+\left(\frac{176}{7}\,\frac{qv}{g\Delta_0}\right)^{2/3}}{\left\{\delta-\left(\frac{176}{7}\,\frac{qv}{g\Delta_0}\right)^{1/3}\right\}^2}+\right. \tag{23}$$

$$\left.\left.+\frac{1}{\sqrt{3}}\tan^{-1}\frac{2\delta+\left(\frac{176}{7}\,\frac{qv}{g\Delta_0}\right)^{1/3}}{\sqrt{3}\left(\frac{176}{7}\,\frac{qv}{g\Delta_0}\right)^{1/3}}\right\}\right],$$

where $$\Delta_0=\beta(T_p-T_\infty)+\beta^*(C_0-C_\infty)\,.$$

Changing Eqs. (22) and (23) into non-dimensional form, we have

$$X=\left[\frac{30\Delta}{11025}+\frac{2544}{77175}+\frac{3492480}{540225}\left(\frac{7}{136}\right)^{2/3}\left(\frac{1}{\Delta}\right)^{1/3}\times\right.$$

$$\times\left\{\frac{1}{6}\log\frac{\Delta^{2/3}+\left(\frac{136}{7}\right)^{1/3}\Delta^{1/3}+\left(\frac{136}{7}\right)^{2/3}}{\left(\frac{136}{7}\right)^{2/3}\left\{1-\left(\frac{7}{136}\,\Delta\right)^{1/3}\right\}^2}+\right. \tag{24}$$

$$\left.\left.+\frac{1}{\sqrt{3}}\tan^{-1}\frac{2\,\Delta^{1/3}+\left(\frac{136}{7}\right)^{1/3}}{\sqrt{3}\left(\frac{136}{7}\right)^{1/3}}\right\}\right]$$

and

$$X = \left[\frac{30}{11025} \Delta + \frac{7344}{77175} + \frac{2545920}{540225} \left(\frac{7}{176}\right)^{2/3} \left(\frac{1}{\Delta}\right)^{1/3} \times \right.$$

$$\times \left(\frac{1}{6} \log \frac{\Delta^{2/3} + \left(\frac{176}{7}\right)^{1/3} (\Delta)^{1/3} + \left(\frac{176}{7}\right)^{2/3}}{\left(\frac{176}{7}\right)^{2/3} \left\{1 - \left(\frac{7}{176}\Delta\right)^{1/3}\right\}^2} \times \right. \tag{25}$$

$$\left. \left. + \frac{1}{\sqrt{3}} \tan^{-1} \frac{2\Delta^{1/3} + \left(\frac{176}{7}\right)^{1/3}}{\sqrt{3}\left(\frac{176}{7}\right)^{1/3}} \right) \right],$$

where

$$X = \frac{xv}{\delta(x) q} . \tag{26}$$

Using Eqs. (11), (13), (14) and (19) in integrated temperature equation,

$$\frac{\partial}{\partial x} \int_0^{\delta_t(x)} (T - T_\infty)\, u dy = -\alpha \left(\frac{\partial T}{\partial y}\right)_{y=0}, \tag{27}$$

we have

$$X_t = \frac{41}{16800} Pr\, \Delta \quad \text{when} \quad \frac{\delta}{\delta t} \propto \frac{1}{\sqrt{Pr}},$$

i.e.

$$X_t - = 0.00244\Delta, \quad \text{when} \quad Pr = 1. \tag{28}$$

For sodium, i.e. when $\frac{\delta}{\delta t} = 0.0258$

$$X_t = 0.03744\, \Delta . \tag{29}$$

For mercury, i.e. when $\frac{\delta}{\delta t} = 0.0074$

$$X_t = 0.08832\, \Delta, \tag{30}$$

where

$$X_t = \frac{xv}{\delta t\, q} . \tag{31}$$

Similarly, we can also find the value of X_c, i. e. for concentration

$$X_c = \frac{xv}{\delta_c q} \quad \text{and} \quad \frac{\delta}{\delta_c} \propto \frac{1}{\sqrt{Sc}}, \tag{32}$$

where Sc is the Schmidt number and is the ratio of the molecular diffusivities of momentum and chemical species, i.e. ν/D.

The values of X_t in terms of Grashof number have been tabulated for different values of Prandtl number.

Table I

Pr	X_t
0.0009	0.32134 Δ
0.0074	0.08832 Δ
0.0100	0.07255 Δ
0.0250	0.03744 Δ
0.2500	0.00144 Δ
1.0000	0.00244 Δ

Conclusions

Analytical solutions between the film thickness and distance travelled have been presented in Eqs. (24) and (25) for different values of Δ_m and it is concluded that the film thickness approaches the uniform film thickness asymptotically. Also the value of Δ for which X is infinite increases as the strength of the magnetic field increases, as shown in Fig. 1. The velocity func-

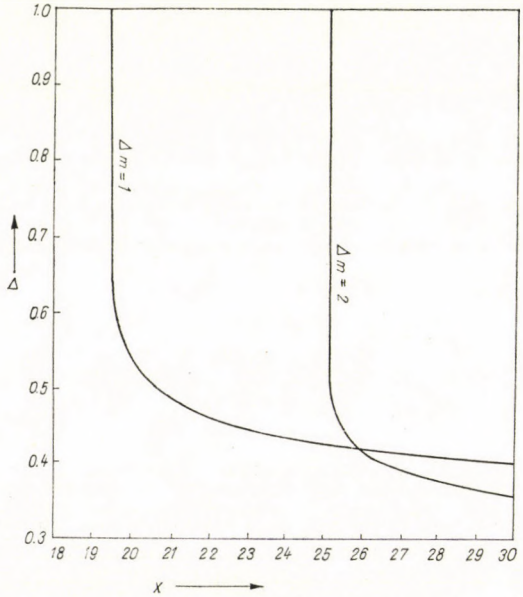

Fig. 1

tion is also obtained as shown in Eq. (15). The value of X_t is also determined for mercury and sodium liquid and it is found that the value of X_t for mercury is greater than the sodium liquid. From Table I it is clear that the values of X_t decrease (in terms of Grashof number) as the value of Prandtl number increases. Similar is the case for X_c.

REFERENCES

1. E. M. Sparrow, R. Eichhorn and J. L. Gregg, Physics Fluids, **2**, 319, 1959.
2. J. Brindley, Int. J. Heat Mass Transfer, **6**, 1035, 1963.
3. R. M. Mark, Guggenheim Aeron. Lab., Memo. No. 21, Cal. Inst. of Tech. (30 July 1954).
4. K. K. Tam, SIAM J. Appl. Maths., **20**, 714, 1971.
5. E. V. Somers, J. Appl. Mech., **23**, 295, 1956.
6. W. G. Mathers, A. J. Madden and E. L. Piret, Ind. Engng. Chem. **49**, 961, 1957.
7. L. Pera and B. Gebhart, Int. J. Heat Mass Transfer, **14**, 975, 1971.
8. B. Gebhart and L. Pera, Int. J. Heat Mass Transfer, **14**, 2025, 1971.
9. A. S. Gupta and U. Suryaprakashrao, J. Phys. Soc. Japan, **20**, No. 10, 1965.
10. B. Gebhart, Heat Transfer, 2nd Ed. McGraw-Hill, New York, 1971.

Acta Physica Academiae Scientiarum Hungaricae, Tomus 42 (1), pp. 59—66 (1977)

FREE CONVECTION EFFECTS ON MHD CHANNEL FLOW WITH VARIABLE VISCOSITY

By

V. M. SOUNDALGEKAR*

INDIAN INSTITUTE OF TECHNOLOGY, BOMBAY-400 076, INDIA

and

D. D. HALDAVNEKAR*

UNIVERSITY DEPARTMENT OF TECHNOLOGY, MATUNGA, BOMBAY-19, INDIA

(Received 4. I. 1977)

An analysis of the influence of buoyancy force and variable viscosity on the horizontal MHD channel flow has been carried out. Approximate solutions to $0(\varepsilon)$ for velocity and temperature are obtained by the method of iteration. Velocity and temperature profiles are shown on graph and numerical values of the skin-friction at lower and upper plates are entered in Tables. During the course of discussion, the effects of different parameters on the stability of flow at the plates, in case of both aiding ($G > 0$) and opposing ($G < 0$) flows have been brought out.

1. Introduction

MHD channel flows have been investigated by a number of research workers in recent years in respect of their practical applications. In all these investigations the flow was assumed horizontal and hence under usual assumptions, the gravitational field was neglected. But SPARROW, EICHHORN and GREGG [1] have shown that the gravitational field is important in horizontal flows of liquids with low Prandtl number. Hence a channel flow without magnetic field was analysed by GILL and CASAL [2] on taking the gravitational field also into account. The corresponding problem in the presence of a transverse magnetic field was recently presented by GUPTA [3] who discussed the open-circuit case of MHD channel flow. GILL and CASAL have also discussed the non-magnetic channel flow problem with variable viscosity .

It is the object of the present paper to discuss GUPTA's problem by also considering the variable viscosity. In Section 2, GUPTA's expressions for velocity and temperature are assumed and the problem is solved by assuming the viscosity to vary linearly with temperature, which is approximately true for liquid sodium. The assumptions of the problem are the same as described by GUPTA. In Section 3, the conclusions are set out.

2. Mathematical analysis

Here the channel is assumed to be bounded by two infinite parallel non-conducting plates. A transverse magnetic field, H_0, is assumed to be applied in the y-direction, where x and y are the axes along and perpendicular

*Department of Mathematics.

to the lower plate. Then assuming the asymptotic solution for the energy equation for fully developed flows and with constant viscosity, the expressions for the velocity and temperature profiles, as derived by GUPTA, are as follows:

$$u_1 = A(1 - \cosh M\eta) + C \sinh M\eta - \frac{G\eta}{M^2} \tag{1}$$

and

$$\begin{aligned} \Phi(\eta) = &\left(\frac{a_1}{M^2} - \frac{2a_7}{M^3}\right) \cosh M\eta + \left(\frac{a_2}{M^2} - \frac{2a_2}{M^3}\right) \sinh M\eta + \\ &+ \frac{a_3}{4M^2} \cosh 2M\eta + \frac{a_4}{4M^2} \sinh 2M\eta + \frac{a_5 \eta^3}{6} + \\ &+ \frac{a_6 \eta^4}{12} + \frac{a_9}{2} \eta^2 + a_{10} \eta + \frac{a_7}{M^2} \eta \sinh M\eta + \\ &+ \frac{a_8}{M^2} \eta \cosh M\eta + a_{11} , \end{aligned} \tag{2}$$

where A, C, a_1, a_2, ... a_{11} are defined in GUPTA's paper.

Variable viscosity

Here on neglecting the axial variation of viscosity and accounting for the viscosity to vary with η only, GUPTA's equation (15), in virtue of (16), reduces to the following

$$\frac{d^2}{d\eta^2}\left(\frac{\mu}{\mu_0} \frac{du_1}{d\eta}\right) - M^2 \frac{du_1}{d\eta} = 0 , \tag{3}$$

where the viscosity used in G is μ_0, the initial value of μ at the lower plate. Introducing the transformation

$$u_1 = \int_0^{\psi} \frac{d\psi}{\mu/\mu_0} \tag{4}$$

in (3), we obtain

$$\frac{d^3\psi}{d\eta^3} - M^2 \frac{d\psi}{d\eta} = G , \tag{5}$$

where ψ represents velocity when viscosity is variable. For electrically conducting liquids, like liquid sodium, the viscosity can be approximated as:

$$\frac{\mu_0}{\mu} = \frac{T + T_a}{T_0 + T_a} = 1 + \frac{T - T_0}{T_0 + T_a} = 1 + \varepsilon\Phi , \tag{6}$$

where $\varepsilon = A_1/(T_0 + T_a)$. Here T_a is assumed to be a reference temperature for the viscosity. In case of variable viscosity, if u' represents the velocity, Eq. (4), in virtue of (6), reduces to

$$u' = \psi + \varepsilon \int_0^\eta \Phi \left(\frac{d\psi}{d\eta}\right) d\eta \,. \tag{7}$$

On neglecting viscous and Joule dissipation terms in the energy equation and denoting Φ' as the temperature in case of variable viscosity, Eq. (31) (from GUPTA [3]) in virtue of (7), reduces to the following:

$$\frac{d^2\Phi'}{d\eta^2} = u' = \psi + \varepsilon \int_0^\eta \Phi \left(\frac{d\psi}{d\eta}\right) d\eta \,. \tag{8}$$

Eqs. (7) and (8) are now solved by the method of iteration. This is accomplished as follows: First Eq. (5) is solved for ψ. This expression for ψ and the one for Φ given by (2), are substituted in (7). On integrating and determining the constants from the boundary conditions (24) and (25) (from GUPTA [3]), the expression for u' is obtained. This expression for u' is again integrated twice to obtain Φ'. In this case the boundary conditions (26) are used.

The shear stress, in non-dimensional form, at the lower and upper plates, is given by

$$\tau = (du'/d\eta)_{\eta=0} \quad \text{or} \quad 1 \tag{9}$$

and hence τ is calculated from the expression for u'.

3. Discussion

Numerical calculations are carried out for the velocity u' and temperature profiles Φ' and they are shown in Figs. 1—5. Also in Tables I and II the numerical values of the skin-friction are entered.

From Fig. 1, we conclude that the velocity increases with increasing ε, but decreases with increasing M. Again in case of variable viscosity, for $G > 0$, which corresponds to aiding flows due to the heating of the plates in the axial direction, the velocity is still observed to be more in the lower half of the channel than that in the upper half, which is evident from Fig. 2. Also opposite is the case for $G < 0$. GUPTA has not shown the effects of the buoyancy force on the temperature distribution in the channel. Hence in Fig. 3, temperature profiles are plotted, which are calculated from equation (32) in GUPTA's paper. For the same value of M, the temperature increases in case of aiding flow i.e. as G increases. Moreover, an increase in M leads to an increase in the temperature when G is constant. The effects of variable viscosity on the tem-

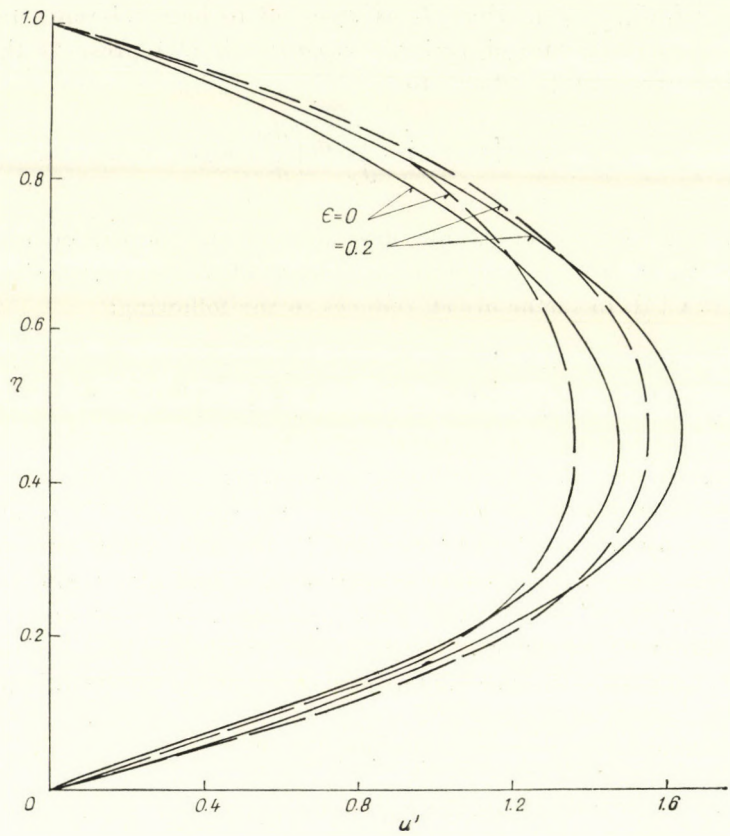

Fig. 1. Velocity profiles $G = 10$, $K = 0{,}05$, $M = 2$ ——, 6 — — —

perature distribution are shown in Figs. 4 and 5. The important effect is that the temperature profiles are reversed in shape which corresponds to cooling of the fluid in a part of the channel. From Fig. 4 one can conclude that there is more cooling effect in aiding flows than that in opposing flows. Also from Fig. 5, for $\varepsilon = 0.1$, we can conclude that in opposing flows the temperature decreases in the lower half of the channel when M increases.

The numerical values of the skin-friction at the lower plate are entered in Table I. In case of constant viscosity, the expression for the skin-friction obtained by GUPTA, is very simple and hence GUPTA concluded that in opposing flows there is more and more cooling of the lower plate which is the main cause of the tendency towards instability for fixed M. In the present case, the expression for the skin friction being complicated, we have calculated the numerical values for τ for $G \gtrless 0$. In case of $G < 0$, a decrease in G leads to a decrease in the value of τ for constant M, ε and K. So in order to describe the

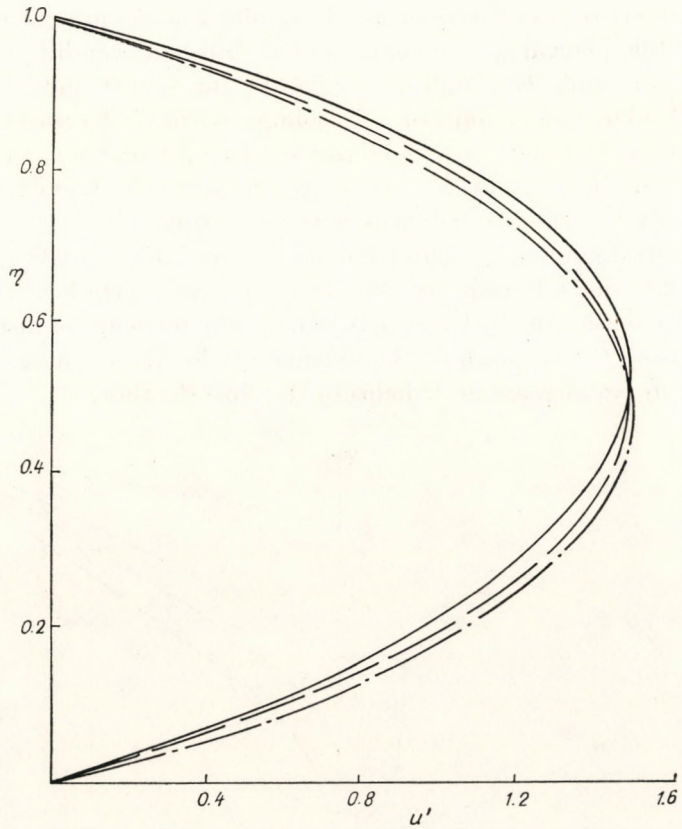

Fig. 2. Velocity profiles, $M = 4$, $\varepsilon = 0.1$, $K = 0{,}025$, $G = -10$ ——, 0 — — —, 10 — · — · —

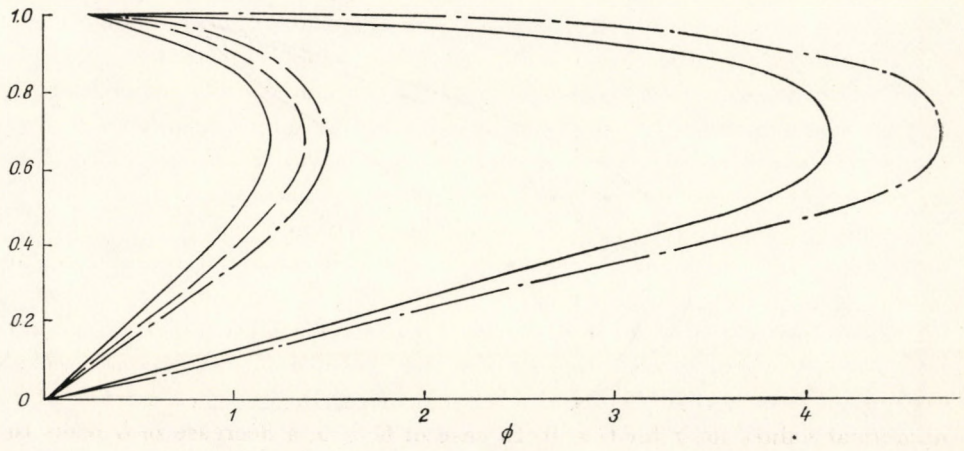

Fig. 3. Temperature profiles, $\varepsilon = 0$, $K = 0{,}025$, $G = -5$ ——, 5 — — —, 10 — · — · —

effects of different parameters on the instability, in the present case, we have calculated the percentage decrease under different conditions. Hence for $M = 4$, $\varepsilon = 0$ and, $K = 0{,}025$, $\tau = 7.4444$ for $G = 0$ and $\tau = 7.1086$ for $G = -5$. Under this condition of cooling, when G decreases by 5 units, τ decreases by 4.51 per cent. Similarly for $\varepsilon = 0.1$ and 0.2, the decrease in percentage for $M = 4$ and $K = 0.025$ are respectively 4.306% and 4.075%. This shows that instability increases with increasing ε.

The corresponding % figures for $M = 6$ are 3.13%, 3.039% and 2.893% for $\varepsilon = 0$, 0.1 and 0.2, respectively. Hence we can conclude that as the magnetic field increases, the% decrease is less, i.e. the tendency of instability is less with increasing the strength of the magnetic field. Hence in case of opposing flows ($G < 0$), an increase in M helps to stabilize the flow.

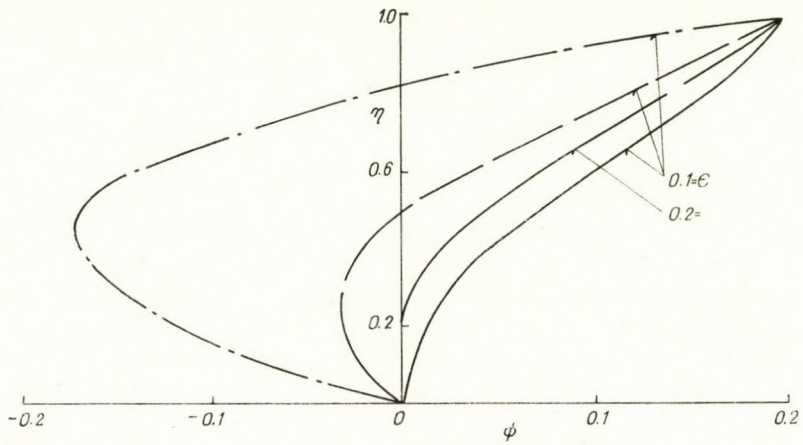

Fig. 4. Temperature profiles, $M = 2$, $K = 0{,}025$, $G = -10$ ——, -5 — — —, 5 —·—·—

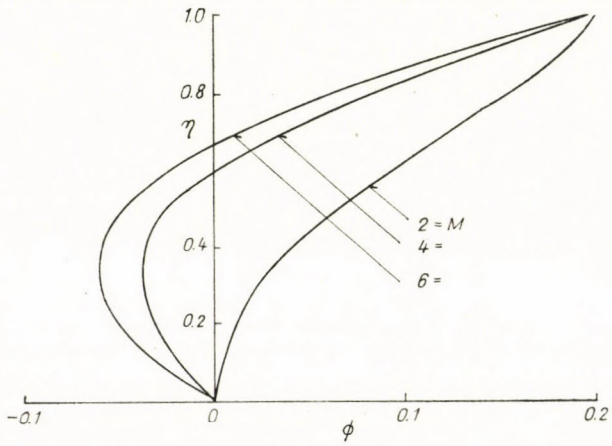

Fig. 5. Temperature profiles, $G = -10$, $\varepsilon = +0{,}1$, $K = +0{,}025$

Table I

Values of $(du/d\eta)_{\eta=0}$

	ε	0	0.1	0.2
M	G \ K	0.025	0.025	0.025
4	− 75	2.4071	2.3089	2.2089
	− 10	6.7728	6.8566	6.9021
	− 5	7.1086	7.1840	7.2149
	0	7.4444	7.5082	7.5214
	5	7.7902	7.8293	7.8218
	10	8.1161	8.1475	8.1162
6	− 75	4.7357	4.7380	4.7012
	− 10	8.3737	8.2712	7.9628
	− 5	8.6535	8.5384	8.2074
	0	8.9334	8.8071	8.4519
	5	9.2132	9.0745	8.6963
	10	9.4931	9.3416	8.9410

Again the numerical values of τ at the upper plate are entered in Table II. As τ is observed to be negative for $G < 0$, the incipient reversed flow does not occur at the upper plate. Hence, the cooling of the upper plate does not

Table II

Values of $(du/d\eta)_{\eta=0}$

	ε	0	0.1	0.2
M	G \ K	0.025	0.025	0.025
4	− 10	− 8.1161	− 8.1267	− 8.1211
	− 5	− 7.7802	− 7.7470	− 8.6974
	0	− 7.4444	− 7.3617	− 7.2634
	5	− 7.1086	− 6.9708	− 6.8197
	10	− 6.7728	− 6.5744	− 6.3660
6	− 10	− 9.4931	− 8.5763	− 7.8208
	− 5	− 9.2132	− 8.1976	− 7.3744
	0	− 8.9334	− 7.8155	− 6.8252
	5	− 8.6536	− 7.4303	− 6.4730
	10	− 8.3737	− 7.0421	− 6.0179

lead to instability. However, as G (> 0) increases, there is a change in the value of τ from negative to positive. Hence in case of aiding flows, there is a tendency of instability at the upper plate for a fixed M. However, the tendency of instability can be minimized by increasing M i.e. by applying the magnetic field of high intensity.

REFERENCES

1. E. M. Sparrow, R. Eichhorn and J. L. Gregg, Phys. Fluids, **2**, 319, 1959.
2. W. N. Gill and A. D. Casal, A. I. Chem. Engg. J., **8**, 513, 1962.
3. A. S. Gupta, ZAMP, **20**, 506, 1969.

Acta Physica Academiae Scientiarum Hungaricae, Tomus 42 (1), pp. 67—79 (1977)

ON THE ANOMALOUS TRIPLET SPLITTING OF THE $C^3\Delta$ TERM OF THE TiO MOLECULE

By

I. KOVÁCS and M. I. M. El AGRAB*

DEPARTMENT OF ATOMIC PHYSICS, TECHNICAL UNIVERSITY, BUDAPEST

(Received 11. I. 1977)

It is shown that the anomalous triplet splitting observed in the $C^3\Delta$ term of the TiO molecule can be interpreted in good agreement with experiment, in addition to the spin-orbit and spin-spin interaction, by taking the centrifugal distortion of the spin-orbit and spin-spin interaction simultaneously into account. The exact values of the coupling constants A and the other correction constants are also given for the $C^3\Delta$ term on the levels $v' = 0$ and $v' = 1$.

1. Introduction

The rotational structure of the (0,0) and (1,0) bands of the α system of the TiO molecule had been analysed first by CHRISTY [1]. In the beginning it was assumed that this system was produced by $C^3\Pi - X^3\Pi$ transition. CHRISTY mentioned that there was some anomaly in the triplet splitting which was thought by PHILLIPS [2] to be due to vibrational perturbation. It was shown by one of the authors (I.K.) [3] that the anomalous triplet splittings observed in the α system can be traced back to the anomalous triplet splittings found on the upper and lower states of the transition which can be interpreted in good agreement with experiment (at least for the lower state) by taking the spin-spin and spin-orbit interactions simultaneously into account. In addition, the exact values of the coupling constants A were determined among others for the upper term on the levels $v' = 0$ by one of the authors (I.K.) [3] and on the level $v' = 1$ by TŐRÖS [4]. The A values for both levels, however, plotted as functions of the rotational quantum number J do not come out to be constant. It was possible to decrease the variation only by means of the supposition of an unusually large spin-rotation interaction but the total elimination was impossible (Figs. 1a and 1b). Later it was established [5] that the transition responsible for the α system is $C^3\Delta - X^3\Delta$ and not $C^3\Pi - X^3\Pi$ as had been formerly assumed. Thus, all the molecular states involved have been reinvestigated and the coupling constants A recalculated [6] but the trend of the variation of A of the upper state with J remained exactly the same as when the upper state was treated as a $^3\Pi$ state (Fig. 2). In addition only one part of the

* On leave from Ain-Shams University, Education College, Cairo, Egypt.

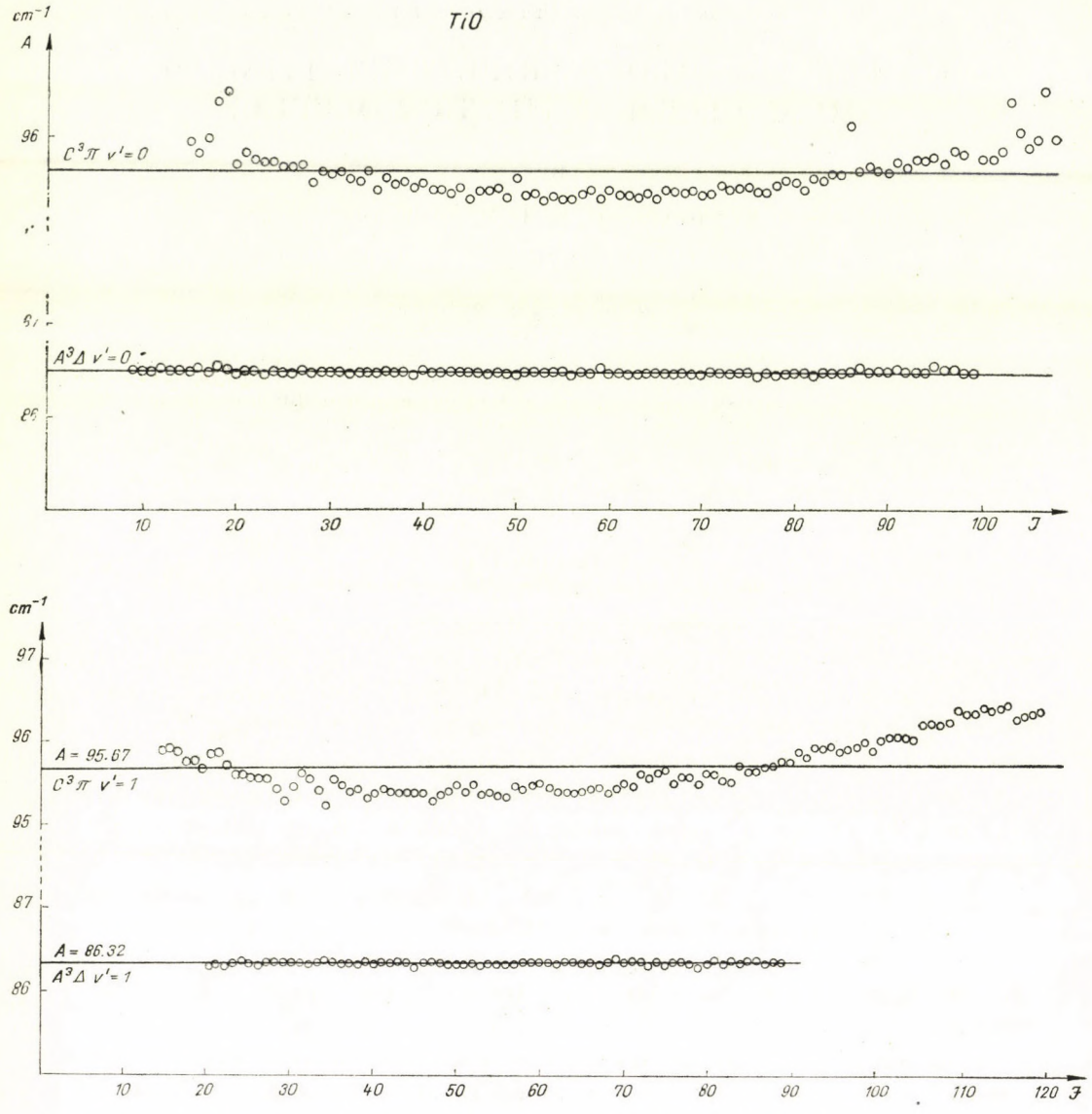

Figs. 1a and *1b*. The variation of the coupling constants A vs the rotational quantum number J taking into account an unusually large spin-rotation interaction for $v' = 0$ and $v' = 1$ levels according to KOVÁCS [3] and TŐRÖS [4], respectively

anomaly of the triplet splitting of the $C^3\Delta$ term could be explained by means of the spin-spin and spin-orbit interactions. Since in the meantime the theory of the centrifugal distortion of the spin-orbit and spin-spin interaction has been worked out we attempt an interpretation of the remaining anomaly of the triplet splitting of the $C^3\Delta$ term by means of the effects mentioned before.

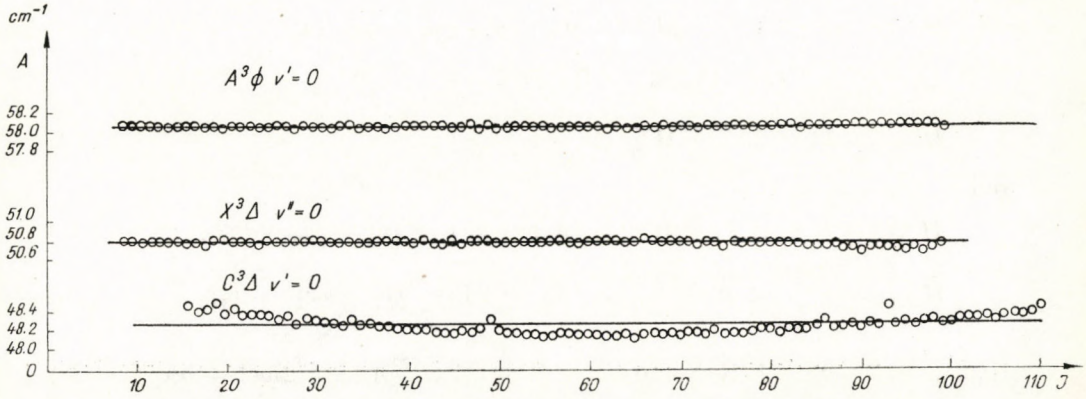

Fig. 2. The variation of the modified coupling constant A vs the rotational quantum number J taking into account an unusually large spin-rotation interaction for $v' = 0$ level according to KOVÁCS and KORWAR [6]

2. Theory of the centrifugal distortion of the spin-orbit and spin-spin interaction

According to KOVÁCS and VUJISIC [7] the form of the spin-orbit and spin spin interaction complemented by the effect of the centrifugal distortion is the following:

$$\left.\begin{aligned} \mathbf{H}^{SO} &= \mathbf{H}_1^{SO} + \mathbf{H}_2^{SO}, \\ \mathbf{H}_1^{SO} &= A_0\,(\mathbf{LS})\,, \\ \mathbf{H}_2^{SO} &= (A_0\,\mathbf{R}^2 + A_2\,\mathbf{R}^4 + A_3\,\mathbf{R}^6)\,(\mathbf{LS})\,, \end{aligned}\right\} \tag{1a}$$

$$\mathbf{H}^{SS} = (\varepsilon + \tau\mathbf{R}^2 + \varrho\mathbf{R}^4 + \sigma\mathbf{R}^6)(3S_Z^2 - \mathbf{S}^2)\,, \tag{1b}$$

where $\mathbf{R}$, $\mathbf{L}$, $\mathbf{S}$ are the angular momentum operators of the rotation of the nuclei, the operators of the resultant of the orbital angular momenta and the spin momenta of the electrons, respectively. The values of the corresponding matrix elements of the $\mathbf{R}^2$, $\mathbf{R}^4$, $\mathbf{LS}$, $3\,\mathbf{S}_Z^2 - \mathbf{S}^2$ and $\mathbf{R}^6$ operators can be found in [8] and in PACHER's paper [12], respectively. Using these values for the calculation of the matrix of (1a) and (1b) due to the non-commutativity of the matrices separated by the brackets the form $1/2(\mathbf{AB}+\mathbf{BA})$ is to be used instead of the multiplication form $\mathbf{AB}$. The explicit form of the (1a) and (1b) matrix elements for triplet terms ($S = 1$, $\Sigma = 0, \pm 1$) is as follows:

$$H^{SO}_{\Lambda\mp1,\Lambda\mp1} = <\Lambda, \mp 1\,|\mathbf{H}^{SO}|\,\Lambda, \mp 1> = \mp\Lambda\,(A_0 + A_1\,u_1^{\pm} + A_2\,u_2^{\pm} + A_3\,u_3^{\pm}), \tag{2a}$$

$$H^{SO}_{\Lambda,\Lambda} = <\Lambda, 0\,|\mathbf{H}^{SO}|\,\Lambda, 0> = 0\,, \tag{2b}$$

$$H^{SO}_{\Lambda\mp1,\Lambda} = <\Lambda, \mp 1\,|\mathbf{H}^{SO}|\,\Lambda, 0> = \mp\frac{\Lambda}{\sqrt{2}}\sqrt{x\pm\Lambda}\times \\ \times (A_1 + 2A_2 w_2^{\pm} + A_3 w_3^{\pm}), \tag{2c}$$

$$H^{SO}_{\Lambda\mp1,\Lambda\pm1} = <\Lambda, \mp 1\,|\mathbf{H}^{SO}|\,\Lambda, \pm 1> = 0 \tag{2d}$$

and

$$H^{SS}_{\Lambda\mp1,\Lambda\mp1} = <\Lambda, \mp 1\,|\mathbf{H}^{SS}|\,\Lambda, \mp 1> = \varepsilon + \tau u_1^{\pm} + \varrho u_2^{\pm} + \sigma u_3^{\pm}, \tag{3a}$$

$$H^{SS}_{\Lambda,\Lambda} = <\Lambda, 0\,|\mathbf{H}^{SS}|\,\Lambda, 0> = -2(\varepsilon + \tau v_1 + \varrho v_2 + \sigma v_3), \tag{3b}$$

$$H^{SS}_{\Lambda\mp1,\Lambda} = <\Lambda, \mp 1\,|\mathbf{H}^{SS}|\,\Lambda, 0> = -\frac{1}{\sqrt{2}}\sqrt{x\pm\Lambda}\,(\tau + 2\varrho w_2^{\pm} + \sigma w_3^{\pm}), \tag{3c}$$

$$H^{SS}_{\Lambda\mp1,\Lambda\pm1} = <\Lambda, \mp 1\,|\mathbf{H}^{SS}|\,\Lambda, \pm 1> = 2\sqrt{x^2-\Lambda^2}\,(\varrho + \sigma(3x+2)). \tag{3d}$$

where

$$\begin{aligned} u_1^{\pm} &= x \pm 2\Lambda, \\ u_2^{\pm} &= x^2 + 2x + 4\Lambda^2 \pm 2\Lambda(2x+1), \\ u_3^{\pm} &= x^3 + 6x^2 + 4x(3\Lambda^2+1) + 8\Lambda^2 \pm 2\Lambda\left(3x^2+7x+2(2\Lambda^2-1)\right), \\ v_1 &= x+2, v_2 = x^2+8x+4, v_3 = x^3+18x^2+28x+8(\Lambda^2+1), \\ w_2^{\pm} &= x \pm \Lambda + 1, w_3^{\pm} = 3x^2 + 2x(2\Lambda+5) + 4(\Lambda+1) \pm 2\Lambda(x+2\Lambda) \end{aligned} \tag{4}$$

and

$$x = J(J+1) - \Lambda^2.$$

The perturbation matrix is now composed of the perturbation matrices of a number of interactions which differ by orders of magnitude. In such cases the most practical method is to select the largest of the interaction terms and to diagonalise the matrix so obtained; the remainder of the weak perturbations can then be taken into account by the perturbation calculation as follows.

Let then $\mathbf{H} = \mathbf{H}' + \bar{\mathbf{H}}^p$, where $\mathbf{H}' = \mathbf{H}_0 + \mathbf{H}^p$ is the energy operator used at the first stage of the calculation; $\mathbf{H}_0$ is the operator of the separable wave equation; $\mathbf{H}^p$ is the operator of the stronger perturbation, namely the terms neglected in the separation of the wave equation and $\mathbf{H}_1^{SO}$, whereas $\bar{\mathbf{H}}^p$ is the weak-perturbation operator, namely $\mathbf{H}_2^{SO}$ and $\mathbf{H}^{SS}$. The eigenvalues $W' = \mathbf{S}\mathbf{H}'\mathbf{S}^{-1}$ of the $\mathbf{H}'$ operator given for triplet terms are the well-known BUDÓ's formulas [9], whereas according to [10]

$$\begin{aligned} \bar{H}^p_N(J) = {} & S^2_{\Lambda-1,N}\,\bar{H}^p_{\Lambda-1,\Lambda-1} + S^2_{\Lambda,N}\,\bar{H}^p_{\Lambda,\Lambda} + S^2_{\Lambda+1,N}\,\bar{H}^p_{\Lambda+1,\Lambda+1} + \\ & + 2S_{\Lambda-1,N}\,S_{\Lambda,N}\,\bar{H}^p_{\Lambda-1,\Lambda} + 2S_{\Lambda,N}\,S_{\Lambda+1,N}\,\bar{H}^p_{\Lambda,\Lambda+1} + \\ & + 2S_{\Lambda-1,N}\,S_{\Lambda+1,N}\,\bar{H}^p_{\Lambda-1,\Lambda+1}; \quad (N = J-1, J+1) \end{aligned} \tag{5}$$

gives the deviations $\mathbf{SHS}^{-1} - \mathbf{W}' = \mathbf{S}\bar{\mathbf{H}}^{p}\mathbf{S}^{-1}$ from the BUDÓ formulas caused by the $\bar{\mathbf{H}}^{p}$ weak perturbations, in the present case by the centrifugal distortion of the spin-orbit interaction if $\bar{\mathbf{H}}^{p} = \mathbf{H}_2^{SO}$ and by the spin-spin interaction including its centrifugal distortions, if $\bar{\mathbf{H}}^{p} = \mathbf{H}^{SS}$. The detailed form of the S transformation matrix elements which transform the $\mathbf{H}'$ energy operator into diagonal form, can be found in [11]. Taken into account in this way the weak interactions contribute additively to the usual term formulas. Hence, they do not modify the formulas already established and the deviations stemming from them can be readily separated from the first stronger perturbation.

3. Application of the theory to the $C^3\Delta$ term

The matrix elements of $\mathbf{H}_2^{SO}$ and $\mathbf{H}^{SS}$ for the $^3\Delta$ term ($\Lambda = 2$) take the following form:

$$H_{11}^{SO} = -2[A_1(x+4)+A_2(x^2+10x+20)+A_3(x^3+18x^2+80x+88)], \quad (6a)$$

$$H_{22}^{SO} = 0, \quad (6b)$$

$$H_{33}^{SO} = 2[A_1(x-4)+A_2(x^2-6x+12)+A_3(x^3-6x^2+24x-24)], \quad (6c)$$

$$H_{11}^{SO} = -\sqrt{2(x+2)}[A_1+2A_2(x+3)+A_3(3x^2+22x+28)], \quad (6d)$$

$$H_{23}^{SO} = \sqrt{2(x-2)}[A_1+2A_2(x-1)+A_3(3x^2+14x-4)], \quad (6e)$$

$$H_{13}^{SO} = 0 \quad (6f)$$

and

$$H_{11}^{SS} = \varepsilon+\tau(x+4)+\varrho(x^2+10x+20)+\sigma(x^3+18x^2+80x+88), \quad (7a)$$

$$H_{22}^{SS} = -2[\varepsilon+\tau(x+2)+\varrho(x^2+8x+4)+\sigma(x^3+18x^2+28x+40)], \quad (7b)$$

$$H_{33}^{SS} = \varepsilon+\tau(x-4)+\varrho(x^2-6x+12)+\sigma(x^3-6x^2+24x-24), \quad (7c)$$

$$H_{12}^{SS} = -\frac{1}{\sqrt{2}}\sqrt{x+2}[\tau+2\varrho(x+3)+\sigma(3x^2+22x+28)], \quad (7d)$$

$$H_{23}^{SS} = -\frac{1}{\sqrt{2}}\sqrt{x-2}[\tau+2\varrho(x-1)+\sigma(3x^2+14x-4)], \quad (7e)$$

$$H_{13}^{SS} = 2\sqrt{x^2-4}[\varrho+\sigma(3x+2)]. \quad (7f)$$

The transformation matrix elements S for the $^3\Delta$ term are given by [11]:

$$S_{1,J-1} = \sqrt{\frac{(J-1)(J+2)}{4C_1(J)}}\, u_1^+(J)\,;$$

$$S_{2,J-1} = -\sqrt{\frac{2(J-2)^2(J+2)^2}{C_1(J)}}\,;\quad S_{3,J-1} = \sqrt{\frac{(J-2)(J+3)}{4C_1(J)}}\, u_1^-(J)\,,$$

$$S_{1,J} = \sqrt{\frac{2(J-1)(J+2)}{C_2(J)}}\,; \tag{8}$$

$$S_{2,J} = \sqrt{\frac{4(Y-2)^2}{C_2(J)}}\,;\quad S_{3,J} = -\sqrt{\frac{2(J-2)(J+3)}{C_2(J)}}\,,$$

$$S_{1,J+1} = \sqrt{\frac{(J-1)(J+2)}{4C_3(J)}}\, u_3^-(J)\,;$$

$$S_{2,J+1} = \sqrt{\frac{2(J-1)^2(J+3)^2}{C_3(J)}}\,;\quad S_{3,J+1} = \sqrt{\frac{(J-2)(J+3)}{4C_3(J)}}\, u_3^+(J)\,,$$

where

$$\begin{aligned} u_1^{\pm}(J) &= 2\left\{[Y(Y-4)+J^2]^{1/2} \pm (Y-2)\right\}; \\ u_3^{\pm}(J) &= 2\left\{[Y(Y-4)+(J+1)^2]^{1/2} \pm (Y-2)\right\} \end{aligned} \tag{9}$$

and

$$\left.\begin{aligned} C_1(J) &= 4Y(Y-4)(J-1)(J+2) + 2(2J+1)(J-2)J(J+2)\,, \\ C_2(J) &= 4Y(Y-4) + 4J(J+1)\,, \\ C_3(J) &= 4Y(Y-4)(J-2)(J+3) + 2(2J+1)(J-1)(J+1)(J+3)\,. \end{aligned}\right\}_{Y=\frac{A_0}{B}} \tag{10}$$

For the determination of the coupling constant A_0 and the coefficients A_1, A_2 A_3 in the first approximation all matrix elements should be neglected with the exception of $\mathbf{H}_1^{SO}$ and (6a), (6c). After the solution of the corresponding secular determinant we obtain in a good approximation for the calculated term differences $F_3'^C - F_1'^C = \Delta F_{31}'^C$ complemented by the centrifugal term

$$\Delta F_{31}'^C(J) = 4B'\sqrt{(\bar{Y}'-2)^2 + x + \frac{1}{3}} + 4D'\,[J^3 + (J+1)^3]\,, \tag{11}$$

where

$$\bar{Y}'B' = \bar{A} = \bar{A}_0 + \bar{A}_1 x + \bar{A}_2 x^2 + \bar{A}_3 x^3 \tag{12}$$

and

$$\begin{aligned} \bar{A}_0 &= A_0 + 16A_2 + 32A_3\,, \\ \bar{A}_1 &= A_1 + 2A_2 + 52A_3\,, \\ \bar{A}_2 &= A_2 + 6A_3\,, \\ \bar{A}_3 &= A_3\,. \end{aligned} \tag{13}$$

In spite of the former statement [3], [4], [6] the interaction of the spin-rotation plays no role here, while the otherwise important spin-spin interaction gives only a negligible contribution for $\Delta F_{31}'^{C}$ (not larger than 0,02 cm^{-1}).

The observed term differences $\Delta F_{31}'^{C}$, owing to the lack of experimental data on satellite branches, cannot be obtained directly but apart from the Λ-type doublet are given by

$$\begin{aligned}\Delta F_{31}'^{0}(J) &= R_3(J-1) - R_1(J-1) + \Delta F_{32}''(J-1) = \\ &= P_3(J+1) - P_1(J+1) + \Delta F_{32}''(J+1)\,,\end{aligned} \tag{14}$$

where $\Delta F_{31}''(J)$ can be calculated theoretically by means of the triplet formulae of the lower state. The data for the lower state for the level $v'' = 0$: $B'' = 0{,}533904$ cm^{-1}, $D'' = -6{,}1.10^{-7}$ cm^{-1}, $Y'' = 95{,}122$ cm^{-1}, $\beta'' = -3{,}320$ cm^{-1} [1], [6].

Comparing (11) with (14) $\bar{A}$ can be expressed as follows,

$$\bar{A} = \bar{Y}'\,B' = \left\{\left[\frac{1}{4}\Delta F_{31}'^{0} - D'\left(J^3 + (J+1)^3\right)\right]^2 - B'^2\left(x + \frac{1}{3}\right)\right\}^{1/2} + 2B', \tag{15}$$

where the values of B' and D' for the levels $v' = 0$ and $v' = 1$ can be found in Table I and the wave numbers of R_3, R_1, P_3, P_1 branches for the (0,0) band (1,0) transition are taken from the paper of CHRISTY [1]. Thus the experimental data given by the right hand side of (15) $\bar{A} - \bar{A}_0$ are plotted vs the rotational quantum number for $v' = 0$ and $v' = 1$ level in Figs. 3a and 3b, respectively. Fitting the curve of (12) (the full line) to the experimental data we obtain the values of the $\bar{A}_0$, $\bar{A}_1$, $\bar{A}_2$ and $\bar{A}_3$, or rather A_0, A_1, A_2 and A_3 constants. These latter are presented in Table I for $v' = 0$ and $v' = 1$ levels.

The experimental data of the triplet splitting can be obtained in a manner similar to (14) in the following way:

$$\begin{aligned}\Delta F_{32}'^{0}(J) &= R_3(J-1) - R_2(J-1) + \Delta F_{32}''(J-1) = \\ &= P_3(J+1) - P_2(J+1) + \Delta F_{32}''(J+1)\,,\end{aligned} \tag{16}$$

$$\begin{aligned}\Delta F_{12}'^{0}(J) &= R_1(J-1) - R_2(J-1) + \Delta F_{12}''(J-1) = \\ &= P_1(J+1) - P_2(J+1) + \Delta F_{12}''(J+1)\,,\end{aligned} \tag{17}$$

where $\Delta F_{32}''$ and $\Delta F_{12}''$ can be calculated theoretically by means of the triplet formula of the lower state with the data given above and the wave numbers of the branches are taken from the paper of CHRISTY [1].

The theoretical values of the triplet splitting can be formed from the BUDÓ's formulas complemented by the centrifugal terms, the $\mathbf{H}_2^{SO}$ centrifugal distortion of the spin-orbit interaction, the $\mathbf{H}^{SS}$ spin-spin interaction including

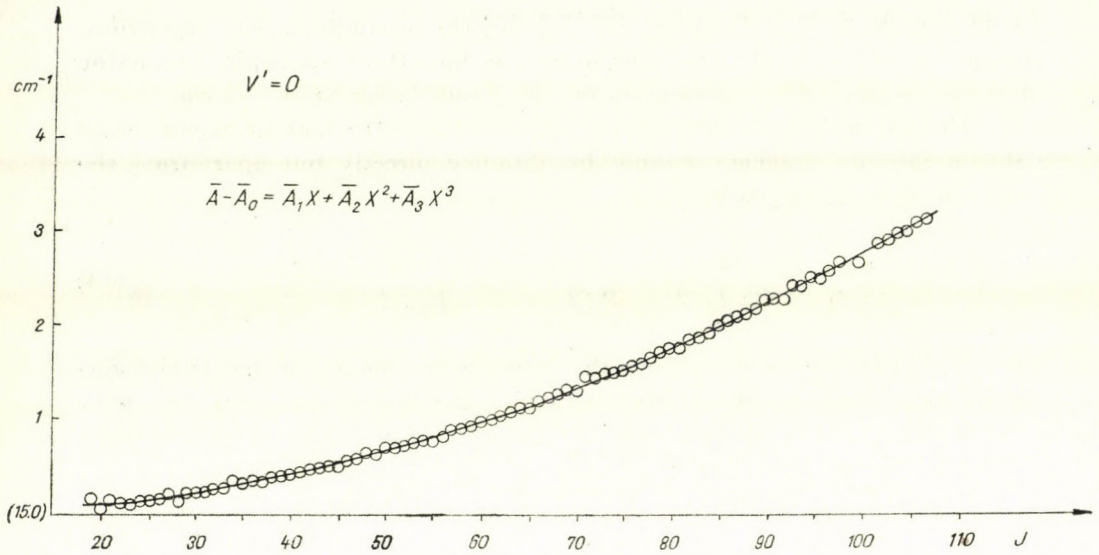

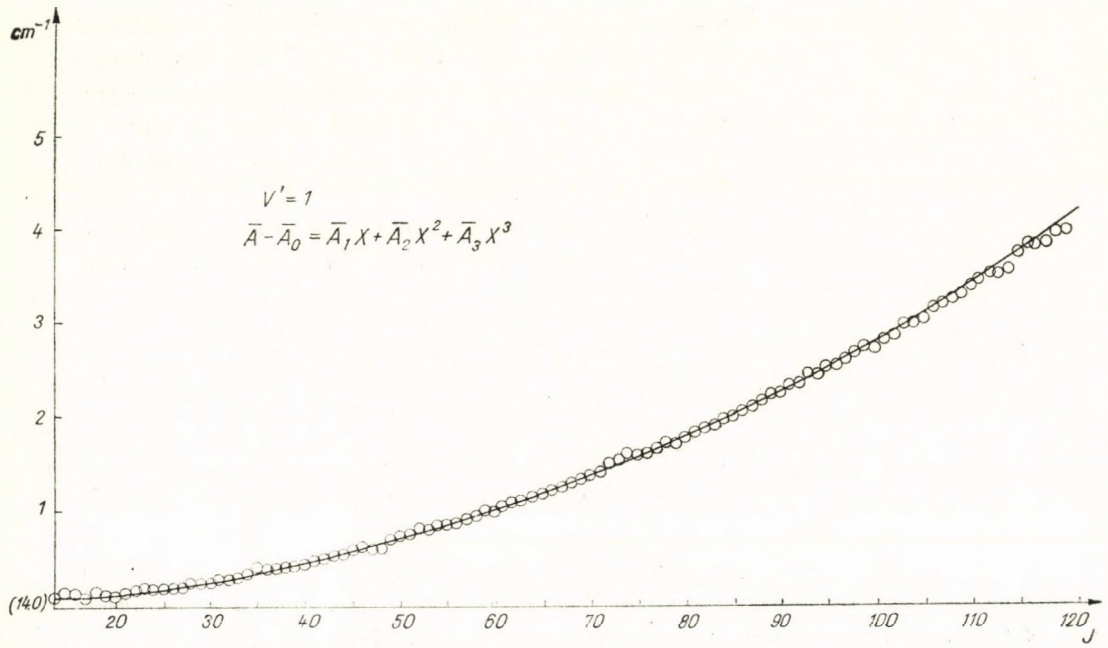

Figs. 3a and *3b*. The experimental variation of the coupling constants $\bar{A}-\bar{A}_0$ ($\bar{A}$ taken from (15))vs the rotational quantum number J without the spin-rotation interaction for $v'=0$ and $v'=1$ levels (indicated by circles). The full lines show the expected theoretical variation taking into account the centrifugal distortion of the spin-orbit interaction

its centrifugal distortion in the following form:

$$\Delta F'^{C}_{32}(J) = 2B'\sqrt{(Y'_0-2)^2+x+\frac{1}{3}} - B'\frac{2\left(Y'_0-\frac{1}{2}\right)^2-x-\frac{85}{18}}{(Y'_0-2)^2+x+\frac{1}{3}} + \\ + 4D'(J+1)^3 + \Delta H^{SS}_{J+1,J} + \Delta H^{SO}_{J+1,J}\,,$$

$$\Delta F'^{C}_{12}(J) = -2B'\sqrt{(Y'_0-2)^2+x+\frac{1}{3}} - B'\frac{2\left(Y'_0-\frac{1}{2}\right)^2-x-\frac{85}{18}}{(Y'_0-2)^2+x+\frac{1}{3}} - \\ - 4D'J^3 + \Delta H^{SS}_{J-1,J} + \Delta H^{SO}_{J-1,J}\,, \tag{18}$$

where

$$\Delta H^{SS}_{J+1,J} = H^{SS}_{J+1} - H^{SS}_{J}\,,\ \Delta H^{SO}_{J+1,J} = H^{SO}_{J+1} - H^{SO}_{J}\,,$$

etc. Here the strong spin-orbit interaction $\mathbf{H}_1^{SO}$ is separated from the weak centrifugal distortion $\mathbf{H}_2^{SO}$ that is to say, $Y'_0 = A_0/B'$ is now constant and $\mathbf{H}_N^{SO}$ was calculated by computer according to (5) using formulas (6a) — (6f) and (8) with the values of A_1, A_2, A_3 given before and with Y'_0 in the elements of S. $\Delta H^{SO}_{J+1,J}$ and $\Delta H^{SO}_{J-1,J}$ are plotted by full lines for $v' = 0$ and $v' = 1$ levels in Figs. 4a and 4b.

Using (5), (7a) — (7f), (8) after omission of some small terms we obtain for $\Delta H^{SS}_{J+1,J}$ and $\Delta H^{SS}_{J-1,J}$ in explicit form

$$\Delta H^{SS}_{J+1,J} = (S^2_{2,J+1} - S^2_{2,J})(\beta_0 - \beta_1 x - \beta_2 x^2 - \beta_3 x^3)\,, \\ \Delta H^{SS}_{J-1,J} = (S^2_{2,J-1} - S^2_{2,J})(\beta_0 - \beta_1 x - \beta_2 x^2 - \beta_3 x^3)\,, \tag{19}$$

where

$$\beta_0 = \alpha - 3\varepsilon,\ \beta_1 = 3\tau, \beta_2 = 3\varrho, \beta_3 = 3\sigma$$

and α is related in a simple way to the perturbation matrix element of the spin-orbit interaction between the $^3\Delta$ and $^1\Delta$ terms [13].

Let us denote the right hand side of (18) apart from ΔH^{SS} and ΔH^{SO} by $\overline{\Delta F'^{C}_{32}(J)}$ and $\overline{\Delta F'^{C}_{12}(J)}$. Then the deviation due to the spin-spin interaction including its centrifugal distortion can be expressed as

$$\Delta F'^{0}_{32}(J) - \overline{\Delta F'^{C}_{32}(J)} - \Delta H^{SO}_{J+1,J} = \Delta H^{SS}_{J+1,J}\,, \\ \Delta F'^{0}_{12}(J) - \overline{\Delta F'^{C}_{12}(J)} - \Delta H^{SO}_{J-1,J} = \Delta H^{SS}_{J-1,J}\,. \tag{20}$$

Using (16) and (17) the left hand side of (20) can be calculated numerically. Fitting the curve of (19) to the experimental data of (20) the values of

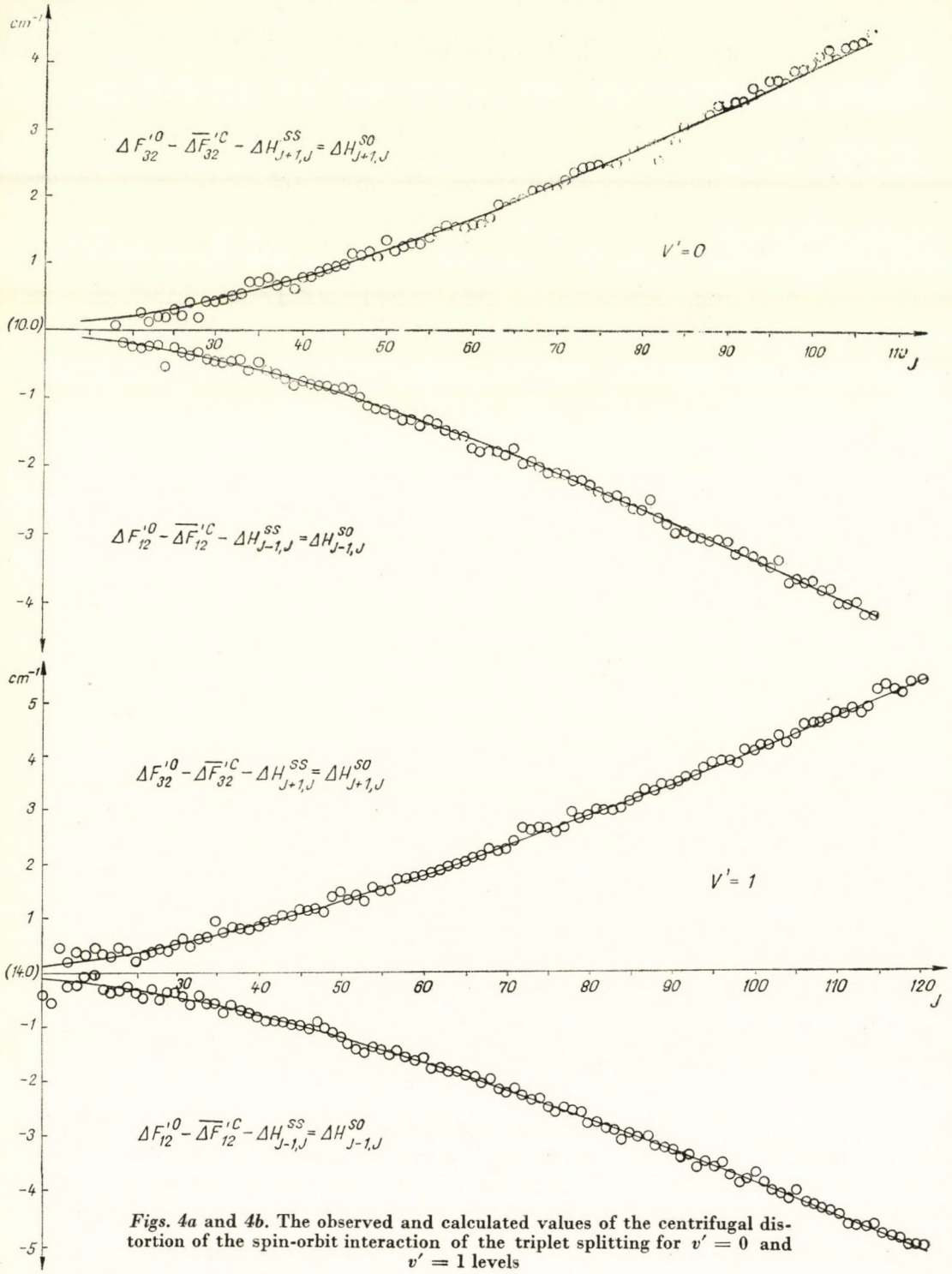

***Figs. 4a* and *4b*.** The observed and calculated values of the centrifugal distortion of the spin-orbit interaction of the triplet splitting for $v' = 0$ and $v' = 1$ levels

β_0, β_1, β_2 and β_3 can be determined. These are presented in Table I for $v' = 0$ and $v' = 1$ levels.

Table I

$v' = 0$		$v' = 1$	
$B^{(0)}$	$= 0{,}488361$*	$B^{(1)}$	$= 0{,}485088$*
$D^{(0)}$	$= -6{,}7092.10^{-7}$*	$D^{(1)}$	$= -6{,}7126.10^{-7}$*
$A_0^{(0)}$	$= 48{,}7974$	$A_0^{(1)}$	$= 48{,}6879$
$A_1^{(0)}$	$= 2{,}5780.10^{-4}$	$A_1^{(1)}$	$= 2{,}7490.10^{-4}$
$A_2^{(0)}$	$= 1{,}9511.10^{-9}$	$A_2^{(1)}$	$= -3{,}3911.10^{-10}$
$A_3^{(0)}$	$= -7{,}2576.10^{-14}$	$A_3^{(1)}$	$= 5{,}5797.10^{-14}$
$Y_0^{(0)}$	$= 99{,}9207$	$Y_0^{(1)}$	$= 100{,}3692$
$\beta_0^{(0)}$	$= 2{,}492$	$\beta_0^{(1)}$	$= 3{,}035$
$\beta_1^{(0)}$	$= 6{,}0992.10^{-5}$	$\beta_1^{(1)}$	$= 8{,}2872.10^{-5}$
$\beta_2^{(0)}$	$= -1{,}5071.10^{-8}$	$\beta_2^{(1)}$	$= -5{,}6305.10^{-9}$
$\beta_3^{(0)}$	$= 0$	$\beta_3^{(1)}$	$= -8{,}8123.10^{-13}$

*According to CHRISTY [1].

With the values of the latter constants we have illustrated the following expressions:

$$\begin{aligned} \Delta F'^{0}_{32}(J) - \overline{\Delta F'^{C}_{32}(J)} - \Delta H^{SS}_{J+1,J} &= \Delta H^{SO}_{J+1,J}\,, \\ \Delta F'^{0}_{12}(J) - \overline{\Delta F'^{C}_{12}(J)} - \Delta H^{SS}_{J-1,J} &= \Delta H^{SO}_{J-1,J}\,, \end{aligned} \tag{21}$$

by circles in Figs. 4a and 4b for the $v' = 0$ and $v' = 1$ levels, respectively. According to (16), (17) and (18) the RMS errors of the differences between the observed and calculated triplet splittings, namely the RMS of the $\Delta F'^{0}_{32} - \Delta F'^{C}_{32}$ and $\Delta F'^{0}_{12} - \Delta F'^{C}_{12}$ differences are 0,083 cm^{-1} for $v' = 0$ and 0,081 cm^{-1} for $v' = 1$ levels (omitting 2 points having larger deviations that 0,3 cm^{-1} for each of the levels $v' = 0$ and $v' = 1$). Owing to the widespread scattering of the experimental data a better agreement with experiment cannot be expected (Figs. 5a and 5b).

Summarizing it can be stated that the observed anomalous triplet splitting of the $C^3\Delta$ term — in accordance with the experimental data — is correctly explained in addition to the spin-orbit and spin-spin interaction by taking the centrifugal distortion of the spin-orbit and spin-spin interaction simultaneously into account.

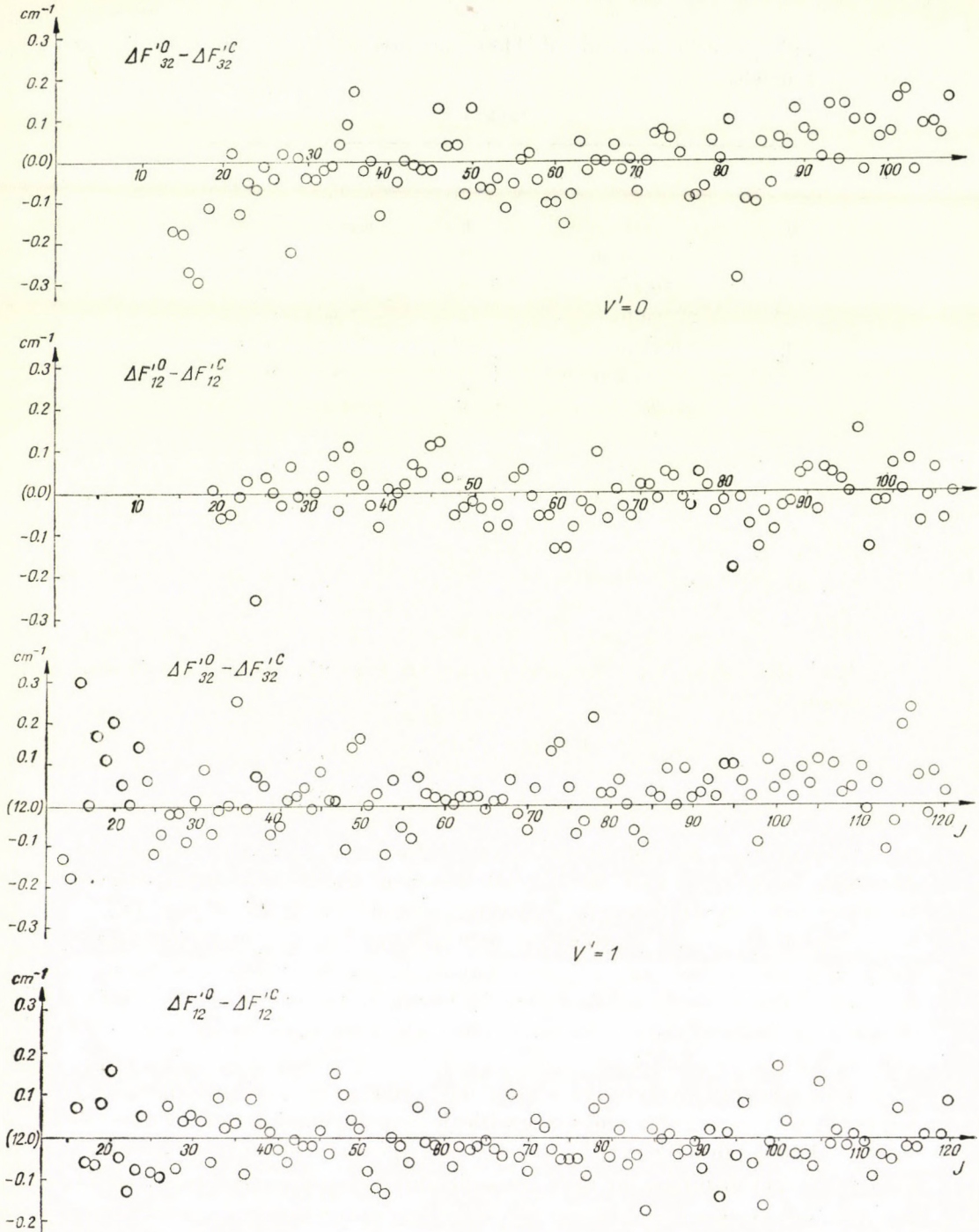

Figs. 5a and *5b*. Deviations between the observed and calculated triplet splitting for $v' = 0$ and $v' = 1$ levels

REFERENCES

1. A. CHRISTY, Phys. Rev., **33**, 701, 1929.
2. J. G. PHILLIPS, Astrophys. J., **114**, 152, 1951.
3. I. KOVÁCS, J. Mol. Spectr., **18**, 229, 1965.
4. R. TŐRÖS, Acta Phys. Hung., **20**, 91, 1966.
5. U. UHLER, Dissertation, Stockholm, 1954.
   K. D. CARLSON and C. MOSER, J. Phys. Chem., **67**, 2644, 1963.
   K. D. CARLSON and R. K. NESBET, J. Chem. Phys., **41**, 1051, 1964.
   J. G. PHILLIPS, Astrophys. J., **157**, 449, 1969.
6. I. KOVÁCS and V. M. KORWAR, Acta Phys. Hung., **29**, 399, 1970.
7. I. KOVÁCS and B. VUJISIC, J. Phys. B, **4**, 1123, 1971.
8. I. KOVÁCS, Rotational Structure in the Spectra of Diatomic Molecules, Akadémiai Kiadó, Budapest and Adam Hilger Ltd. London, 1969, pp. 54—55.
9. ibid. p. 69.
10. ibid. pp. 49—50.
11. ibid. pp. 69—70.
12. P. PACHER, J. Phys. B., **4**, 887, 1971.
13. I. KOVÁCS, Acta Phys. Hung., **12**, 67, 1960; Phys. Rev. **128**, 663, 1962.

RECENSIONES

Atomic Physics and Astrophysics

Edited by M. Chrétien and E. Lipworth
Brandeis University, Summer Institute in Theoretical Physics, 1969, Volume 2,
Gordon and Breach Science Publishers, New-York, 1973. pp. 338

This book is actually a result of the Brandeis University Summer Institute in Theoretical Physics devoted to Atomic Physics and Astrophysics in 1969.

The published notes of Summer Institutes are intended to fill the gap between text books and review articles on the one hand and publications in scientific journals and conference reports on the other.

In this respect a book on the interplay between atomic physics and astrophysics based on 3 lectures is very welcome.

The first part "Some Aspects of the Physics of Gas Lasers" by W. R. BENNETT, Jr. is a successful review of the basic physical processes of gas lasers. It contains two sections. Based on the classical works by FOX and LI as well as on the publications of BOYD and GORDON, BOYD and KOGELNICK the first section on "Properties of Optical Cavity Modes" reviews some very basic considerations on the subject. Hole burning and mode-pulling effects are treated in the second section. This part of the lecture is basically founded upon the investigations of the author. In this part of the book an efficient discussion is given of the dominant physical processes involved in some research done at that time with gas lasers on mode suppression, frequency stabilization, saturable absorption and excited-state spectroscopy. The problems are generally treated by using the hole burning model. This part of the book is a theoretical work, with references to the experimental investigations of the problems in question.

The second part "Experimental X-ray Astronomy" by R. NOVICK deals with a relatively new field of scientific research. In the first two chapters the aims and the techniques of relevant measurements are analysed with great skilfulness. The third chapter gives account of the investigations of the X-ray, optical and infrared continuum flux of Scorpius X-1. Of the possible models for Sco X-1 a simple theoretical model is discussed. The second nonsolar X-ray source analysed is the Crab Nebula. For studying its X-ray spectrum a vast amount of observational data have been referred to. In the next chapter X-ray polarimetry is discussed: after motivation of the problems the physical processes used in the design of polarimeters are analysed. This is followed by the description of ScoX-1 and Crab Nebula observations. Some aspects of the diffuse X-ray background are also treated. In the second part in general a state-of-art report is given on the experimental X-ray astronomy of that time with the analysis of its results, problems and perspectives of development.

The third part "Atomic Processes in Astrophysics" by A. DALGARNO deals with the problems of radiative transitions and collision processes studying these atomic processes in great depth. After a brief summary of the quantum theory of radiation the sections on collision processes start with the definition of these processes, which is followed by the values of collision duration, the rate of allowed transitions and the cross sections of the processes. Most of the collision processes are treated in terms of quantum mechanics.

Considering the volume in its entirety it may be stated that the lectures are well compiled and the authors and the editors defined the object of the book very clearly. The volume as a whole should prove useful to intermediate and advanced graduate as well as postdoctoral students and even to young specialists.

Z. FÜZESSY

C. S. WILLET : An Introduction to Gas Lasers: Population Inversion Mechanism

International Series of Monographs in Natural Philosophy, Volume 67, Pergamon Press, Oxford, 1974, pp 544

In the present stage of development the problems associated purely with the operation of lasers have already been eliminated. In the early stage of the development of lasers there were some working rules for the constructors which as a result of their generality have guaranteed the work of a large variety of gas laser systems with good certainty. Modern laser construction demands not only a knowledge of the atomic processes but also that they are taken into consideration in the design of high stability gas lasers.

During the successful years of gas laser development a number of papers have been published on the problems of gas discharge processes. The few books published till now have given either a pure theoretical consideration of the problems or have treated some special problems of gas laser systems independently. So by the date of publication of the book reviewed here a vast amount of systematic effort had been performed to clarify the details of collision processes involved. The book contains an admirable collection of this work. Up to the present there has been a conspicuous absence of a monography treating in detail gas discharge processes, neutral and ionized gas laser systems, and molecular lasers in a uniform manner from the point of view of population inversion mechanisms.

This book is therefore to be welcomed as it helps to fill a notable gap.

The first brief chapter summarises the historical development and basic principles of gas lasers, where the laws promoting the understanding of the physical principles of laser operation are collected from a peculiar point of view and in adequate depth.

The next two chapters consist of a purposeful treatment of the selective excitation processes in gas discharge and of gas discharge processes. These principal problems in gas laser physics are dealt with thoroughly. In the sections devoted to the different problems one may find some remarks pointing forward on the concrete gas laser system or on the important processes discussed later. The remarks include references to the corresponding figure. The processes involved are dicussed phenomenologically on explicit physical foundation, sometimes with quantum mechanical background.

The subsequent chapters deal with neutral laser systems, ionized laser systems and molecular laser systems. The He-Ne laser system is treated with high accuracy. Among the problems associated with population inversion mechanism the upper level excitation, the operating characteristics and discharge conditions are discussed in the case of different laser systems. The effect of additives is also discussed thoroughly.

Orientation in the field of the atomic characteristics and their usefulness in the numerical calculations related to laser systems is promoted by the tables in the Appendix. The number of references included is over thirteen hundred.

The book is nicely presented and has an extensive set of figures to accompany the text. It will undoubtedly be a useful aid for laser research laboratories and it really is indispensable for university libraries. Experimental laser scientists and graduate students will particularly welcome this careful and thought-provoking study of gas discharge lasers.

Z. FÜZESSY

The Properties of Liquid Metals

Proceedings of the Second International Conference, Tokyo, 1972, Edited by S. Takeuchi

Taylor and Francis Ltd, London, 1973

The volume contains eighty-four papers of the Second International Conference on the Properties of Liquid Metals held in Tokyo, Japan, from 3 to 8 September 1972. The fields represented in the sections covered the following five main subjects: Electronic states and electronic transport properties in liquid metals and alloys; Thermodynamic properties of liquid metals and alloys; Atomic transport properties in liquid metals and alloys and Melting phenomena of metals.

Each section of the conference (each chapter of the book) was introduced by one or two invited reports summarizing the progress in the relevant field, followed by short contributions demonstrating the results of recent research.

The high number of problems encountered in research in this field to-day is well characterised by the title of the opening lecture given by Professor J. M. ZIMAN: "What do we not yet understand about liquid metals?"

G. GROMA

M. KOCSIS: High-Speed Silicon Planar-Epitaxial Switching Diodes

Akadémiai Kiadó, Budapest; Adam Hilger Ltd. London; Halsted Press, New York

The book continues — from the semiconductor devices side — the previous works of the author in the field of semiconductor devices in switching circuits.

The Introduction is a very good and brief summary of the types of semiconductor diodes and their practical applications.

In Chapter 2 the reader obtains a very good survey on the switching behaviour of semiconductor diodes.

Various structures and operation of modern switching diodes are dealt with in Chapter 3.

The development of electronics, however, made it necessary to develop diodes with switching times of a few nanoseconds or less. The gold atoms, diffused into the semiconductor wafer greatly reduced the switching time because of the very high recombination rates brought about by gold. The behaviour of these diodes produced by gold-diffused planar-epitaxial technology and operating in the nanosecond and picosecond ranges is very complicated. In Chapter 4 the calculation of the storage time constant is given for homogeneous and inhomogeneous field distributions.

Chapter 5 is devoted to the relation between the inner structure and some of the important parameters of semiconductor diodes.

In Chapter 7 some methods are suggested for measurements on semiconductor switching diodes.

The style of the book is clear and easy to follow. The problems, given at the beginning of Chapters help the reader to systematize his knowledge.

The results of the theoretical calculations, given in this book are deduced by the author to the concrete devices. He compares them to the parameters of the types of diodes most widely applied and to the results of measurements.

The book is useful for engineers and physicists working in the field of the construction of semiconductor devices and of their application in switching and pulse circuits.

P. B. BARNA

H. KANGRO: Early History of Planck's Radiation Law

Taylor and Francis Ltd., London 1976, pp. 282

The evolution of Planck's radiation law at the turn of the century is generally considered to be a milestone in the history of physics which opened up a completely new field of research.

Such "laws" are not created in a void, and the aim of this book is to explain the historical background to both the experimental techniques and the climate of opinion at the time against which Planck's law was formulated.

Sources of information about Planck's thought-steps towards the radiation equation and its statistical foundation are almost non-existent: the collection of Planck's manuscripts in Berlin was almost completely destroyed in the Second World War. Thus one is limited essentially to a careful study of the publications of Planck and his contemporaries and predecessors. If one also takes into account the writings of the experimenters, including the numerical values they used, one can construct at least a rough picture of the methods and state of physical research in Berlin at the time.

The general subject of Planck's radiation theory (from 1895 onwards) is investigated only to the extent that this book supplements previously published historical works. For example, attention is drawn to those modifications of the theory which Planck undertook several times following discussions with Boltzmann, as well as to his repeated reflections upon the nature of the resonators and to the connection of his radiation work with his early concept of thermodynamic entropy.

Experiment and theory, together and inseparably, determine the genesis of physical knowledge. This book follows both aspects in the development of one of the most important theories of the 20th century, an in so doing it gives a fascinating insight into the birth of such knowledge.

This book is a translation of "Vorgeschichte des Planckschen Strahlungsgesetzes, Messungen und Theorien der spektralen Energieverteilung bis zur Begründung der Quantenhypothese". The opportunity has been taken to revise and supplement the original German version, and to add references to the relevant literature which has since appeared.

I. Kovács
Department of Atomic Physics
Technical University, Budapest

Absorption Spectra in the Infrared Region III.

Edited by L. Láng

This is the third of a series of volumes which presents the infrared spectra of selected organic compounds over a range 400 – 4000 cm^{-1}, together with full details of sample and experimental conditions. The empirical formula, molecular weight and melting point of each substance is also given. The choice of spectra has been made by a panel of experienced spectroscopists, who have given primary consideration to covering compounds which have been isolated or synthesized recently. More familiar materials have also been included, generally because the spectra presented for them are more detailed than those of other published sources, or because they refer to different experimental conditions.

In English · 320 pages · Cloth

A co-edition – distributed on the American Continent by R. E. Krieger Publishing Corp., Huntington; in all other countries by Kultura, Budapest, ISBN 963 05 1181 9

Akadémiai Kiadó
Budapest

R. E. Krieger Publishing Corp.
Huntington

Printed in Hungary

A kiadásért felel az Akadémiai Kiadó igazgatója — Műszaki szerkesztő: Botyánszky Pál

A kézirat nyomdába érkezett: 1977. I. 21. — Terjedelem: 7,5 (A/5) ív, 27 ábra

77.4078 Akadémiai Nyomda, Budapest — Felelős vezető: Bernát György

NOTES TO CONTRIBUTORS

I. PAPERS will be considered for publication in Acta Physica Hungarica only if they have not previously been published or submitted for publication elsewhere. They may be written in English, French, German or Russian.

Papers should be submitted to

Prof. I. Kovács, Editor
Department of Atomic Physics, Polytechnical University
1521 Budapest, Budafoki út 8, Hungary

Papers may be either articles with abstracts or short communications. Both should be as concise as possible, articles in general not exceeding 25 typed pages, short communications 8 typed pages.

II. MANUSCRIPTS

1. Papers should be submitted in five copies.

2. The text of papers must be of high stylistic standard, requiring minor corrections only.

3. Manuscripts should be typed in double spacing on good quality paper, with generous margins.

4. The name of the author(s) and of the institutes where the work was carried out should appear on the first page of the manuscript.

5. Particular care should be taken with mathematical expressions. The following should be clearly distinguished, e.g. by underlining in different colours: special founts (italics, script, bold type, Greek, Gothic, etc); capital and small letters; subscripts and superscripts, e.g. x^3, x_3; small l and 1; zero and capital O; in expressions written by hand: e and i, n and u, v and v, etc.

6. References should be numbered serially and listed at the end of the paper in the following form: J. Ise and W. D. Fretter, Phys. Rev., *76*, 933, 1949.

For books, please give the initials and family name of the author(s), title, name of publisher, place and year of publication, e.g.: J. C. Slater, Quantum Theory of Atomic Structures, I. McGraw-Hill Book Company Inc., New York, 1960.

References should be given in the text in the following forms: Heisenberg [5] or [5]

7. Captions to illustrations should be listed on a separate sheet, not inserted in the text.

III. ILLUSTRATIONS AND TABLES

1. Each paper should be accompanied by five sets of illustrations, one of which must be ready for the blockmaker. The other sets attached to the copies of the manuscript may be rough drawings in pencil or photocopies.

2. Illustrations must not be inserted in the text.

3. All illustrations should be identified in blue pencil by the author's name, abbreviated title of the paper and figure number.

4. Tables should be typed on separate pages and have captions describing their content. Clear wording of column heads is advisable. Tables should be numbered in Roman numerals (I, II, III, etc.).

IV. MANUSCRIPTS not in conformity with the above Notes will immediately be returned to authors for revision. The date of receipt to be shown on the paper will in such cases be that of the receipt of the revised manuscript.

Reviews of the Hungarian Academy of Sciences are obtainable at the following addresses:

AUSTRALIA
C.B.D. LIBRARY AND SUBSCRIPTION SERVICE, Box 4886, G.P.O., *Sydney N.S.W. 2001*
COSMOS BOOKSHOP, 145 Ackland Street, *St. Kilda (Melbourne), Victoria 3182*

AUSTRIA
GLOBUS, Höchstädtplatz 3, *1200 Wien XX*

BELGIUM
OFFICE INTERNATIONAL DE LIBRAIRIE, 30 Avenue Marnix, *1050 Bruxelles*
LIBRAIRIE DU MONDE ENTIER, 162 Rue du Midi, *1000 Bruxelles*

BULGARIA
HEMUS, Bulvar Ruszki 6, *Sofia*

CANADA
PANNONIA BOOKS, P.O. Box 1017, Postal Station "B", *Toronto, Ontario M5T 2T8*

CHINA
CNPICOR, Periodical Department, P.O. Box 50, *Peking*

CZECHOSLOVAKIA
MAD'ARSKÁ KULTURA, Národní třida 22, *115 66 Praha*
PNS DOVOZ TISKU, Vinohradská 46, *Praha 2*
PNS DOVOZ TLAČE, *Bratislava 2*

DENMARK
EJNAR MUNKSGAARD, Norregade 6, *1165 Copenhagen*

FINLAND
AKATEEMINEN KIRJAKAUPPA, P.O. Box 128, *SF-00101 Helsinki 10*

FRANCE
EUROPERIODIQUES S. A., 31 Avenue de Versailles, *78170 La Celle St. Cloud*
LIBRAIRIE LAVOISIER, 11 rue Lavoisier, *75008 Paris*
OFFICE INTERNATIONAL DE DOCUMENTATION ET LIBRAIRIE, 48 rue Gay-Lussac, *75240 Paris Cedex 05*

GERMAN DEMOCRATIC REPUBLIC
HAUS DER UNGARISCHEN KULTUR, Karl-Liebknecht-Strasse 9, *DDR-102 Berlin*
DEUTSCHE POST ZEITUNGSVERTRIEBSAMT, Strasse der Pariser Kommüne 3—4, *DDR-104 Berlin*

GERMAN FEDERAL REPUBLIC
KUNST UND WISSEN ERICH BIEBER, Postfach 46, *7000 Stuttgart 1*

GREAT BRITAIN
BLACKWELL'S PERIODICALS DIVISION, Hythe Bridge Street, *Oxford OX1 2ET*
BUMPUS, HALDANE AND MAXWELL LTD., Cowper Works, *Olney, Bucks MK46 4BN*
COLLET'S HOLDINGS LTD., Denington Estate, *Wellingborough, Northants NN8 2QT*
WM. DAWSON AND SONS LTD., Cannon House, *Folkestone, Kent CT19 5EE*
H. K. LEWIS AND CO., 136 Gower Street, *London WC1E 6BS*

GREECE
KOSTARAKIS BROTHERS, International Booksellers, 2 Hippokratous Street, *Athens-143*

HOLLAND
MEULENHOFF-BRUNA B.V., Beulingstraat 2, *Amsterdam*
MARTINUS NIJHOFF B.V., Lange Voorhout 9—11, *Den Haag*
SWETS SUBSCRIPTION SERVICE, 347b Heereweg, *Lisse*

INDIA
ALLIED PUBLISHING PRIVATE LTD., 13/14 Asaf Ali Road, *New Delhi 110001*
150 B-6 Mount Road, *Madras 600002*
INTERNATIONAL BOOK HOUSE PVT. LTD., Madame Cama Road, *Bombay 400039*
THE STATE TRADING CORPORATION OF INDIA LTS., Books Import Division, Chandralok, 36 Janpath, *New Delhi 110001*

ITALY
EUGENIO CARLUCCI, P.O. Box 252, *70100 Bari*
INTERSCIENTIA, Via Mazzé 28, *10149 Torino*
LIBRERIA COMMISSIONARIA SANSONI, Via Lamarmora 45, *50121 Firenze*
SANTO VANASIA, Via M. Macchi 58, *20124 Milano*
D. E. A., Via Lima 28, *00198 Roma*

JAPAN
KINOKUNIYA BOOK-STORE CO. LTD., 17-7 Shinjuku-ku 3 chome, Shinjuku-ku, *Tokyo 160-91*
MARUZEN COMPANY LTD., Book Department, P.O. Box 5050 Tokyo International, *Tokyo 100-31*
NAUKA LTD. IMPORT DEPARTMENT, 2-30-19 Minami Ikebukuro, Toshima-ku, *Tokyo 171*

KOREA
CHULPANMUL, *Phenjan*

NORWAY
TANUM-CAMMERMEYER, Karl Johansgatan 41—43, *1000 Oslo*

POLAND
WĘGIERSKI INSTYTUT KULTURY, Marszałkowska 80, *Warszawa*
CKP I W ul. Towarowa 28 *00-958 Warsaw*

ROUMANIA
D. E. P., *Bucureşti*
ROMLIBRI, Str. Biserica Amzei 7, *Bucureşti*

SOVIET UNION
SOJUZPETCHATJ — IMPORT, *Moscow*
and the post offices in each town
MEZHDUNARODNAYA KNIGA, *Moscow G-200*

SPAIN
DIAZ DE SANTOS, Lagasca 95, *Madrid 6*

SWEDEN
ALMQVIST AND WIKSELL, Gamla Brogatan 26, *101 20 Stockholm*
GUMPERTS UNIVERSITETSBOKHANDEL AB, Box 346, *401 25 Göteborg 1*

SWITZERLAND
KARGER LIBRI AG, Petersgraben 31, *4011 Basel*

USA
EBSCO SUBSCRIPTION SERVICES, P.O. Box 1943, *Birmingham, Alabama 35201*
F. W. FAXON COMPANY, INC., 15 Southwest Park, *Westwood, Mass, 02090*
THE MOORE-COTTRELL SUBSCRIPTION AGENCIES, *North Cohocton, N. Y. 14868*
READ-MORE PUBLICATIONS, INC., 140 Cedar Street, *New York, N. Y. 10006*
STECHERT-MACMILLAN, INC., 7250 Westfield Avenue, *Pennsauken N. J. 08110*

VIETNAM
XUNHASABA, 32, Hai Ba Trung, *Hanoi*

YUGOSLAVIA
JUGOSLAVENSKA KNJIGA, Terazije 27, *Beograd*
FORUM, Vojvode Mišiča 1, *21000 Novi Sad*

ACTA PHYSICA

ACADEMIAE SCIENTIARUM HUNGARICAE

TOMUS XLII FASCICULUS 2

AKADÉMIAI KIADÓ, BUDAPEST

1977

ACTA PHYS. HUNG. APAHAQ 42 (2) 85—170 (1977)

ACTA PHYSICA

ACADEMIAE SCIENTIARUM HUNGARICAE

SZERKESZTI

KOVÁCS ISTVÁN

Az *Acta Physica* angol, német, francia vagy orosz nyelven közöl értekezéseket. Évente két kötetben, kötetenként 4—4 füzetben jelenik meg. Kéziratok a szerkesztőség címére (1521 Budapest XI., Budafoki út 8.) küldendők.

Megrendelhető a belföld számára az Akadémiai Kiadónál (1363 Budapest Pf. 24. Bankszámla 215-11488), a külföld számára pedig a "Kultúra" Külkereskedelmi Vállalatnál (1389 Budapest 62, P. O. B. 149. Bankszámla 217-10990 sz.), vagy annak külföldi képviseleteinél és bizományosainál.

The *Acta Physica* publish papers on physics in English, German, French or Russian, in issues making up two volumes per year. Subscription price: $32.00 per volume. Distributor: KULTURA Hungarian Trading Co. (1389 Budapest 62, P. O. Box 149) or its representatives abroad.

Die *Acta Physica* veröffentlichen Abhandlungen aus dem Bereich der Physik in deutscher, englischer, französischer oder russischer Sprache, in Heften die jährlich zwei Bände bilden.

Abonnementspreis pro Band: $32.00. Bestellbar bei: KULTURA Außenhandelsunternehmen (1389 Budapest 62, Postfach 149) oder bei seinen Auslandsvertretungen.

Les *Acta Physica* publient des travaux du domaine de la physique, en français, anglais, allemand ou russe, en fascicules qui forment deux volumes par an.

Prix de l'abonnement: $32.00 par volume. On peut s'abonner à l'Entreprise du Commerce Extérieur KULTURA (1389 Budapest 62, P. O. B. 149) ou chez ses représentants à l'étranger.

«*Acta Physica*» публикуют трактаты из области физических наук на русском, немецком, английском и французском языках.

«*Acta Physica*» выходят отдельными выпусками, составляющими два тома в год.

Подписная цена — $32.00 за том. Заказы принимает предприятие по внешней торговле KULTURA (1389 Budapest 62, P. O. B. 149) или его заграничные представительства и уполномоченные.

ACTA PHYSICA

ACADEMIAE SCIENTIARUM HUNGARICAE

TOMUS XLII FASCICULUS 2

AKADÉMIAI KIADÓ, BUDAPEST

1977

ACTA PHYS. HUNG.

INDEX

Acta Physica Academiae Scientiarum Hungaricae, Tomus 42 (2), pp. 85—90 (1977)

RITZ METHOD FOR THE ANHARMONICITY OF THE TYPE λx^{2m}

By

A. K. MITRA

DEPARTMENT OF MATHEMATICS, TEXAS TECH UNIVERSITY, LUBBOCK, TEXAS 79409, USA

(Received 4. XII. 1976)

The generality of the Ritz—Givens—Householder method for finding the first few energy levels of the Schroedinger operator has been emphasized. The anharmonicity of the type λx^{2m} has been considered as an illustration. This method can be extended to a more general class of problems, even possibly to the ones involving the Dirac operator.

I. Introduction

Since the work of BAZLEY and FOX [1], numerous other attempts, based on different techniques, have been made to estimate numerically a first few eigenvalues of the λx^{2m} anharmonic oscillator:

$$Su = -u'' + x^2u + \lambda x^{2m}u = \varepsilon u\,, \tag{1.1}$$

$$-\infty < x < \infty, \quad \lambda > 0 \quad \text{and} \quad u \to 0 \quad \text{as} \quad x \to \pm\infty.$$

Among them, the work of BISWAS et al. [2] is the first attempt to estimate these eigenvalues for higher values of λ and m (≥ 3), whereas the earlier works are mostly confined to the case $m = 2$ (a complete bibliography may be obtained from [2]). The method of BISWAS et al depends on the special choice of the basis $\{U_n\}$ in the domain of S, where $U_n = x^{2n}\exp(-x^2)$. Fortunately, the matrix representation of the Schroedinger operator S in this basis takes the simple tridiagonal form, of course non-symmetric. The approximate eigenvalues are then obtained by using the asymptotic iteration formula for the Hill determinant, to extract the roots of the truncated $N \times N$ determinant of the tridiagonal infinite matrix, for sufficiently large N.

The same problem has been solved here by a more general and attractively simple method, originally due to RITZ [3]. This method essentially finds a representation of the Schroedinger operator, as an infinite *symmetric* matrix, with respect to a chosen basis in the Hilbert space $L_2(-\infty, \infty)$. Thereby the first few eigenvalues are obtained from the corresponding truncated $N \times N$-forms, where the size N depends on the required degree of accuracy. The Ritz theorem tells us that, for a symmetric operator bounded from below (as is

the case for the operator S in (1.1)), it is possible to choose a basis in the Hilbert space such that the kth eigenvalue $\lambda_k^{(n)}$ of the above $N \times N$ form approaches the exact one λ_k from above as $N \to \infty$. With this in mind, one can then use one of the existing algorithms for fast and sufficiently accurate computation of the eigenvalues of finite real symmetric matrices. The Givens—Householder tridiagonalization method has been used in this paper.

All one needs is, therefore, to find a method for computing the matrix elements in a convenient basis. For this purpose, it is natural to choose a complete set of normalized orthogonal polynomials for the basis of the appropriate L_2-space. For our purpose, this will be given in terms of the Hermite polynomials H_n [4]:

$$u_n(x) = \frac{1}{\sqrt{2^n(n!)\sqrt{\pi}}} H_n(x) \exp(-x^2/2), \tag{1.2}$$

which constitute a basis for $L_2(-\infty, \infty)$, endowed with the inner product:

$$\langle f, g \rangle = \int_{-\infty}^{\infty} fg \, dx . \tag{1.3}$$

One of the nicest properties of the orthogonal polynomials is their recurrence relation, which can be used to deduce an iterative procedure to generate a large matrix just from a few elements. This has been done in this paper.

The reason for reconsidering this problem over again is therefore mainly to illustrate one of the several interesting applications of Ritz's variational method in combination with the Givens—Householder [6] algorithm, which has not been used fairly often in quantum mechanics. A similar method has been applied previously by the author to another type of problem [5]. Also more complex types of eigenvalue problems involving interaction of the type $\lambda x^2/(1 + gx^2)$ $(\lambda, g > 0)$ and anharmonicity of the type $\lambda x^{2n} + \mu x^{2m}$ have been studied by the author using a similar method. For all such cases the method proved to be very general and efficient for computation of the eigenvalues. Also the iterative procedure mentioned before becomes almost inevitable for the computation of the matrix elements in several such problems. We hope to present their results in the near future.

In the next section, the iterative procedure to obtain the matrix elements has been described in brief and the first five eigenvalues for $m = 4$ have been presented for illustration, though the results for $m = 2, 3$ have also been obtained, which agree with the earlier works. Also results for higher values of λ, such as $\lambda = 1000$ have been obtained, but not presented here.

II. The analysis

We need to compute the matrix elements of S defined by

$$A_{mn} = \langle u_{m-1}, Su_{n-1} \rangle \,. \qquad (2.1)$$
$$(m, n = 1, 2, 3, \ldots)$$

Using the well-known equation $-u_n'' + x^2 u_n = (2n + 1)u_n$, we obtain, using the orthonormality of u_n's with respect to the inner product (1.3),

$$A_{ij} = (2i - 1)\,\delta_{ij} + \lambda H_{ij}\,, \qquad (2.2)$$

where

$$H_{ij} = \int_{-\infty}^{\infty} x^{2m}\, u_{i-1}(x) u_{j-1}(x)\, dx \,. \qquad (2.3)$$

There are several ways of calculating integral of the type (2.3), but the result can in no case be put in a nice closed form. We, therefore, use an alternative procedure — an iterative procedure, which is extremely efficient for computational purpose. We claim that

$$H_{ij} = 0 \quad \text{unless} \quad i + j \text{ is even} \qquad (2.4)$$

and

$$H_{ij} = 0 \quad \text{unless} \quad j = i + 2m - 2k + 2\,, \qquad (2.5)$$
$$k = 1, 2, \ldots, m + 1 \,.$$

The proof of (2.4) is obvious since $u_n(-x) = (-1)^n u_n(x)$, whereas to prove (2.5) we use the recurrence relation [4]

$$2xH_n = -(H_{n+1} + 2nH_{n-1})$$

repeatedly, to obtain a general relation of the form:

$$(2x)^{2m} H_{i-1} = a_{i+2m} H_{i+2m-1} + a_{i+2m-2} H_{i+2m-3} + \ldots + a_i H_{i-1} \ldots \qquad (2.6)$$

where the coefficients a_i are to be determined from the backward recurrence relation obtained by equating the coefficients of equal powers of x in both sides of (2.6):

$$a_{i+2} = 1$$
$$-a_{i+2m} b_1^{(i+2m-1)} + a_{i+2m-2} b_0^{(i+2m-3)} = -b_1^{(i-1)}$$

and for $k = 2, \ldots, m + 1$

$$a_{i+2m-2k+2} = (-1)^{k-1} b_{k-1}^{(i-1)} \times \theta + \sum_{r=1}^{k-1} (-1)^{k-r+1} b_{k-r}^{(i+2m-2r+1)} a_{i+2m-2r+2}\,,$$

where $q = \left[\frac{i-1}{2}\right]$, the integer part of $(i-1)/2$ and

$$\theta = 1 \text{ if } k \leq q+1$$
$$\theta = 0 \text{ if } k > q+1$$

and $b_l^{(i-1)}$ are the coefficients of x in the Hermite polynomial [4]

$$H_{i-1}(x) = (-1)^{i-1} \sum_{k=1}^{q} (-1)^k b_k^{(i-1)} (2x)^{i-2k-1},$$

$$b_k^{(i)} = \frac{i!}{k!\,(i-2k)!}.$$

Thus substituting the series (2.6) for $(2x)^{2m} H_{i-1}$ in (2.3) and using the orthonormality of the u_n's defined in (1.2), we obtain

$$H_{ij} = \frac{1}{2^{m+k-1}} \left(\frac{(i+2m-2k+1)!}{(i-1)!}\right)^{1/2} a_{i+2m-2k+2}\,, \qquad (2.7)$$

$$j = i + 2m - 2k + 2;\ k = 1, \ldots, m+1$$

$$i = 1, 2, \ldots$$

and

$$H_{ij} = 0 \text{ otherwise.}$$

The backward iteration formula (2.6) has been used to compute numerically the coefficients a_i in (2.7). It takes only a few seconds to generate a 100×100 matrix H_{ij} through this iterative procedure. It is also clear from (2.5) that A_{mn} in (2.2) has the following symmetric band form (shown for $m = 2$; here 'x' represent a non-zero element, whose number is $m + 1$ in each row)

$$A = \begin{bmatrix} x & 0 & x & 0 & x & 0 & . & . & . & . & . & . & . \\ & x & 0 & x & 0 & x & 0 & . & . & . & . & . & . \\ & & x & 0 & x & 0 & x & 0 & . & . & . & . & . \\ & & & x & 0 & x & 0 & x & 0 & . & . & . & . \\ & & & & . & . & . & . & . & . & . & . & . \\ & & & & & . & . & . & . & . & . & . & . \end{bmatrix}.$$

Once these matrix elements are obtained, it is a simple matter to compute a first few eigenvalues by one of the commonly used methods [6, 7]. The Givens—Householder method turns out to be particularly efficient for such a band matrix and has been used in this paper. This method essentially tridia-

gonalizes a given real symmetric matrix by a sequence of orthogonal transformations and then finds the eigenvalues as the roots of the corresponding characteristic equation by Sturm's sequence method (for details see the excellent review by J. ORTEGA [7]).

In the following Table we present the first five eigenvalues ε_i for $m = 4$ rounded to six decimal places. It is clear that the size N of the truncated matrix has to be large enough to obtain enough accuracy. The sizes up to $N = 150$ have been considered. In the extreme right column of the Table, the values of N are given. Also, for the sake of studying the convergence, the eigenvalues (for a given λ) for two distinct, but close values of N have been given. A bar (—) at a certain position means that the number at that position is the same as the one right above it. The results given in [2] are included parentheses for comparison.

We conclude by mentioning once again that the method used in this paper has proved very effective in computing the eigenvalues of the Schroedinger

Table I

The first five eigenvalues for $m = 4$
The dimensions N of the corresponding truncated matrices have been given in the last column

λ	ε_1	ε_2	ε_3	ε_4	ε_5	N
0.1	1.168963	3.939733	7.639991	12.281668	17.762008	45
	—	3.939714	7.639984	12.281255	17.761934	50
	(1.168)		(7.639—40)			
0.5	1.367721	4.839156	9.777363	16.071368	23.540857	100
	—	—	9.777362	16.071364	23.540843	110
	(1.367—8)		(9.776—8)			
1	1.491020	5.368780	10.993742	18.191132	26.743556	100
	—	5.368778	10.993741	18.191106	26.743505	100
	(1.490—1)		(10.993—4)			
10	2.114548	7.929743	16.711159	28.023689	41.497129	120
	—	7.929700	16.711146	28.023000	41.496672	130
	(2.115—22)		(16.707—15)			
20	2.381856	9.000620	19.064608	32.042764	47.504306	130
	2.381848	9.000575	19.064450	32.041671	47.503634	140
	(2.383—91)					
50	2.806129	10.685414	22.748458	38.316075	56.885390	140
	2.806095	10.685376	22.747379	38.315936	56.872607	150
	(2.80—1)					
100	3.188759	12.196253	26.036298	43.918776	65.250858	140
	3.188741	12.195554	26.036230	43.908603	65.244134	150
	(3.18—9)					

operator with varieties of potentials. We hope to carry out a similar treatment for the Dirac operator as well, and expect to present the results in a future publication.

REFERENCES

1. N. Bazley and D. Fox, Phys. Rev., **124**, 483, 1961.
2. S. N. Biswas, K. K. Datta, R. P. Saxena, P. K. Srivastava and V. S. Varma, J. Math. Phys., **14**, 1190, 1973.
3. G. S. Michlin, Variationsmethoden der Mathematischen Physik, Akademie-Verlag, Berlin, 1962.
4. G. Sansone, Orthogonal Functions, Interscience Publishers, Inc., New York, 1959.
5. A. K. Mitra, Z. Naturforsch., **30a**, 256, 1975.
6. H. J. Wilkinson, The Algebraic Eigenvalue Problems, Clarendon Press, Oxford, 1965.
7. T. Ortega, in Mathematical Methods for Digital Computers, Vol. II (A. Ralston, H. S. Wilf, ed.) John Wesley and Sons, Inc., New York/London, 1968.

Acta Physica Academiae Scientiarum Hungaricae, Tomus 42 (2), pp. 91—98 (1977)

MEASUREMENTS OF THE RELAXATION PROCESSES WITH A HIGH TIME CONSTANT

By

T. HEJNAL*

ELECTROTECHNICAL SCHOOL, PRAHA, CZECHOSLOVAKIA**

(Received in revised form 7. XII. 1976)

A new method is proposed which enables the measurements of the magnetic aftereffect in a temperature range where the customary methods are unrealizable owing to the high time constant of relaxation $\tau > 10^4$ sec. Its usefulness in the study of very slow processes is illustrated by the measurement of extremely low diffusion coefficients of carbon in bcc iron. This method can be used in an analogous way also for measurements of anelastic relaxation.

1. Introduction

Orientation magnetic aftereffect originating from the reorientation of anisotropy axis of defects whose symmetry is lower than that of the host lattice is used increasingly as an extremely sensitive technique for investigating point defects [1]. At present it is commonly observed as a disaccommodation by using very sensitive and easy-to-handle ac techniques [2, 3]. The isothermal decrease of the initial susceptibility $\chi(t)$ is measured after demagnetization of the specimen as a function of time. As NÉEL's theory [4] implies, the corresponding increase of the reluctivity $r(t) = 1/\chi(t)$ is described by equation

$$\frac{r(t)}{r(0)} = 1 + \eta[1 - \exp(-t/\tau)] \tag{1}$$

with a single temperature dependent time constant

$$\tau = \tau_0 \exp(E/kT) \tag{2}$$

corresponding to a well-defined diffusion coefficient of defects.

The disaccommodation measurements are usually performed in a temperature range where the time constant is of the order $10^2 - 10^3$ sec and the substantial part of the isotherms can be followed experimentally in a reason-

* On leaving Institute of Physics, Czechosl. Acad. Sci., Prague, Na Slovance 2, 18040 Praha 8, Czechoslovakia.

** Address: Na Bělidle 34, 15000 Praha 5, Czechoslovakia.

able time. In this case either the theoretical curve (1) can be fitted to the experimental points or the isochronal relaxation curves can be constructed by the method outlined in [1]. The evaluation yields in both cases the relaxation strength

$$\eta = \frac{r(\infty) - r(0)}{r(0)}, \tag{3}$$

which is proportional to the concentration of relaxators [4] and the relaxation time constant which is determined by their mobility. At higher temperatures ($\tau = 10^{-4} - 10^{-2}$ sec) the measurements of the loss-factor peak [5, 6], whereas at lower temperatures ($\tau > 10^4$ sec) the method described below can be used.

2. Description of the method

At low temperatures where the time constant of relaxation is high, $\tau > 10^4$ sec, disaccommodation proceeds very slowly and the customary methods mentioned above are unrealizable because only a very small initial part of the isothermal curve (1) can be measured in a reasonable time after the demagnetization of the specimen. Nevertheless, in this case we can determine the relaxation strength directly and the time constant from the measured initial slope of isotherm.

In contrast to the measurements at higher temperatures the bridge can be balanced before perceptible relaxation takes place. After demagnetization of the specimen the unrelaxed value of the reluctivity $r(0)$ is therefore measured directly and by continuing the measurement a small initial part of the isotherm (1) is recorded. From this measurement the initial slope of the isotherm which can be expressed from Eqs. (1) and (3) as

$$\left.\frac{dr(t)}{dt}\right|_{t=0} = \frac{r(\infty) - r(0)}{\tau} \tag{4}$$

is determined. In order to obtain the relaxed value of the reluctivity $r(\infty)$ (which cannot be determined from the isothermal measurement after demagnetization) the sample is heated to a higher temperature where disaccommodation takes place quickly. After complete disaccommodation the sample is cooled again down to the original temperature and the relaxed reluctivity $r(\infty)$ is measured. By the knowledge of $r(0)$, $r(\infty)$ and of the initial slope of the isotherm the relaxation strength and the time constant are calculated from Eq. (3) and (4), respectively.

If the measurements are performed several times at different temperatures it is recommended first to demagnetize the sample at higher tempera-

ture ($\tau \cong 10^2$ sec), to wait up to $t \cong 10\tau$, to cool it down ($\tau > 10^4$ sec) and measure the temperature dependence of $r(\infty)$ without demagnetization ($t \to \infty$ is approximated by $t \cong 10\tau$). Afterwards the sample is gradually demagnetized at different temperatures and $r(0)$ together with initial slopes of isotherms are determined.

The results obtained by the method presented here can be influenced by the presence of other types of relaxators which give rise to disturbing relaxations. In this case the resulting isothermal disaccommodation curve will be a sum of elementary relaxation processes. In the case of several overlapping orientation aftereffects we have [7]

$$\frac{r(t)}{r(0)} = 1 + \sum_i \eta_i \left[1 - \exp\left(-t/\tau_i\right)\right] . \tag{5}$$

The disturbing relaxations can be eliminated by appropriate treatment only if they have substantially shorter $\tau_s \ll \tau$ or substantially longer $\tau_1 \gg \tau$ relaxation time constant. The disturbing relaxation with $\tau_s \ll \tau$ manifests itself by the curvature of the measured initial part of the isotherm in the time interval $t < 5\tau_s \ll \tau$ and can be eliminated by extrapolating $r(0)$ and the initial slope of isotherm from the linear part measured in a time interval $5\tau_s < t < 0.1\tau$. The disturbing relaxation with a long time constant $\tau_1 \gg \tau$ influences the relaxed reluctivity $r(\infty)$ and can be eliminated by approximating $t \to \infty$ with $t \cong 10\tau \ll \tau_1$ as mentioned above.

3. Application of the method

The usefulness of the described method will be now illustrated by the determination of extremely low diffusion coefficients of carbon in *bcc* iron. The cylindrical samples used in this experiment have been prepared from zone-refined Johnson and Matthey spectrographically pure iron. The samples $(5-7) \cdot 10^{-2}$ m long and $(1-2) \cdot 10^{-3}$ m in diameter were purified in dry hydrogen at 1023 K for three days and furnace cooled. Afterwards they were carburized in hydrogen with traces of toluene and water quenched. The resulting concentration of carbon determined on comparable specimen by chemical analysis was 40 ± 20 at.ppm. The disaccommodation of the real part of the initial susceptibility has been measured by the bridge method [2] described in more detail in a previous paper [8]. The bridge operated at a frequency of 1 kHz with a sensitivity better than $5 \cdot 10^{-4}$. The samples were demagnetized by a 50 Hz magnetic field decreasing several times from $H_m = 2.5 \cdot 10^3$ A/m to zero in a few seconds. This procedure has been found to give reproducible results at both customary ($\tau = 10^2 - 10^3$ sec) [9, 10] and low temperature ($\tau > 10^4$ sec) disaccommodation measurements.

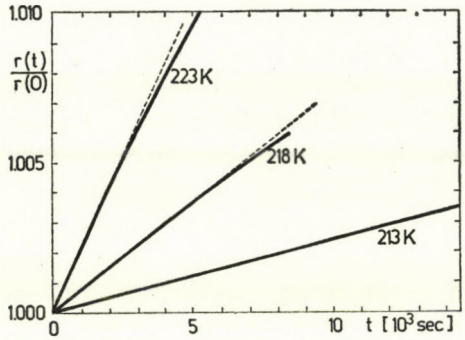

Fig. 1. Determination of the initial slopes of isotherms measured at different temperatures on carburized sample of bcc iron

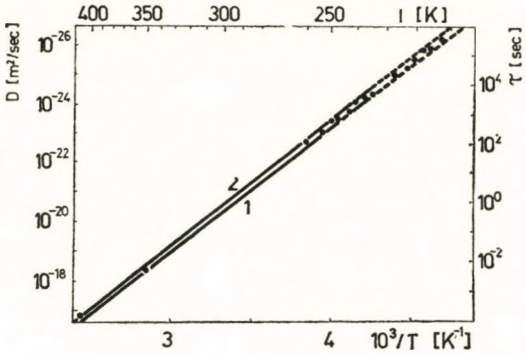

Fig. 2. The diffusion coefficient of carbon in bcc iron: ● — determined by the described method; ○ — determined by customary disaccommodation and loss-factor measurement. Its temperature dependence $D = D_0 \exp(-E/RT)$ as determined by the compilation of available diffusivity data. 1 — $D_0 = 3.94 \cdot 10^{-7}$ m²/sec, $E = 80\,200$ J/mole [11]; 2 — $D_0 = 3.3 \cdot 10^{-7}$ m²/sec, $E = 80\,800$ J/mole [12]

A few measurements of the initial slopes of isotherms performed at different temperatures are shown in Fig. 1. It may be seen that the lower temperature of measurement the longer time interval of measurement is required in order to determine the initial slope of isotherm with a sufficient accuracy. The time constants of relaxation determined by the method outlined in the previous Section are shown in Fig. 2 together with the carbon diffusion coefficients which have been calculated by using equation

$$D = \frac{a^2}{36\,\tau}, \tag{6}$$

where a is the lattice constant and the numerical factor is appropriate for tetragonal defects in bcc lattice [1, 4]. Fig. 2 also includes data on the temperature dependence of the carbon diffusion coefficient found in recent literature

[11, 12] and the values determined from customary disaccommodation and loss-factor measurements. The published data [11, 12] have been obtained by summarizing the results of many authors (available from 234 K to 1136 K [11]) and using the least squares regression. The least squares regression of our data yielded $D_0 = 4.9 \cdot 10^{-7}$ m²/sec and $E = 81300$ J/mole. The concentration of carbon atoms in solid solution is shown in Table I. It has been obtained by correcting the measured relaxation strength for skin effect [1, 13] and using the calibration given in [8].

Table I

The concentration of carbon in solid solution determined by the new method on samples of bcc iron

Sample No.	c [at · ppm]
1	12
2	11
3	16

4. Discussion

A new method which allows the measurements of the relaxation processes with a high time constant is described and its usefulness is illustrated by the determination of extremely low diffusion coefficients of carbon in bcc iron. The method allows the study of extremely slow processes due to elementary jumps of relaxators on interatomic distances with a mean time of stay longer than 10^4 sec. Such extremely slow processes are probably undetectable by any other method. This fact is connected not solely with the proposed experimental procedure but also with the mechanism of the relaxation process itself. The other bulk methods detect namely only a long-range diffusion of defects in contradistinction to the relaxation methods which are sensitive to elementary jumps of relaxators within the crystal cell.

The disaccommodation measurements are based on Eq. (1) obtained from NÉEL's theory of the orientation aftereffect for ballistic measurements [4]. It is also valid for ac measurements if the condition $\omega\tau \gg 1$ (ω being the angular frequency of the magnetic field) is satisfied [6, 14]. It is seen that for $\tau > 10^4$ sec this condition is satisfied very well for any experimentally attainable frequency. The second assumption in deriving Eq. (1) is that the demagnetization is responsible for the isotropic distribution of relaxators at $t = 0$. In nearly all experiments published in literature the single demagnetiza-

tion treatment is used. The distribution of relaxators at $t = 0$ is therefore anisotropic and corresponds to the original structure of Bloch walls. This distribution can be thought to be isotropic only in a statistical sense [15] if many walls are present. True isotropic distribution on dimensions containing only a few relaxators can be obtained by demagnetization repeated many times (duration about 3τ) or by demagnetizing the specimen during its cooling from higher temperature where $\tau \cong 1$ sec. In customary disaccommodation measurements it has been found [9, 10, 15] that for sufficiently high fields used for demagnetization ($H_m > 1{,}2 \cdot 10^2$ A/m) the statistically isotropic distribution of relaxators at $t = 0$ results in the same experimental curve (1) as the true isotropic one. For lower demagnetization fields, however, the single demagnetization treatment is insufficient to produce full disaccommodation [16, 17]. In the proposed method the true isotropic distribution of relaxators at $t = 0$ cannot be obtained by repeated isothermal demagnetization because $\tau > 10^4$ sec. If it has been achieved by demagnetizing the sample during its cooling the same results have been found for the relaxation strength and time constant as for the statistically isotropic distribution (for $H_m = 2.5 \cdot 10^3$ A/m).

The proposed method assumes also a single relaxation process. By overlapping of several relaxation processes it gives uncorrect results. The disturbing relaxations can be eliminated by appropriate treatment as described above only if they have substantially higher or lower time constant. Otherwise the whole isothermal disaccommodation curve must be measured in order to find its decomposition into particular relaxations but it is possible only in conventional measurements.

The precision of the described method is determined not only by the sensitivity of the measuring bridge but also by the precision of the determination of the initial slope of isotherm which depends on the relaxation strength and on the time interval of measurement in respect to the relaxation time constant. At lower temperatures a longer time of measurement must be used. It is believed that the precision of this new method will be better than 10% in the majority of cases. It can be improved by the use of least squares regression in evaluating initial slopes.

It should be further noted that: (a) by combining the proposed method ($\tau > 10^4$ sec) with the customary disaccommodation ($\tau = 10^2 - 10^3$ sec) and loss-factor peak measurements ($\tau = 10^{-4} - 10^{-2}$ sec) the relaxation time constant is determined within ten orders of magnitude by using nearly the same experimental equipment. The values of the activation energy E and τ_0 determined in Eq. (2) are therefore more reliable than those obtained by using only one of these methods. (b) The method can be used in an analogous way also in measurements of anelastic relaxation which is a well-known mechanical counterpart of the magnetic relaxation and which is described by an equation analogous to Eq. (1) [18].

The prepared samples contained only interstitial carbon because the heat treatment given was sufficient to remove any detectable nitrogen impurities [19, 20]. The presence of hydrogen interstitials is possible but improbable because their diffusion coefficient at room temperature is about 10^{-11} m^2/sec [21] and therefore hydrogen was probably removed by storing the prepared samples a few days at room temperature before disaccommodation measurements.

Disturbing relaxations with $\tau_s \ll \tau$ have not been observed in this experiment. On the other hand, the disturbing relaxation with a substantially longer time constant $\tau_1 \gg \tau$ was present. This can be attributed to the fact that carbon interstitials give rise to the combined aftereffect [1, 18, 22] because their reorientation into a new energetically favourable position of the type a/2 ⟨100⟩ cannot take place without any shift of the centre of gravity. The disturbing relaxation which is caused by long-range diffusion of intersitials into Bloch walls [23, 24] progresses with the time constant $\tau_1 \cong 10^5\tau$. The magnetic counterpart [25, 26] of the mechanical KÖSTER's relaxation [27] which is due to the interaction of interstitials with dislocations and the magnetic relaxation due to dislocations [1, 26, 28, 29] are probably also present but they have even longer time constants [26]. All these disturbing relaxations have been eliminated by approximating $t \to \infty$ with $t \cong 10\tau$.

The results on carbon diffusion coefficients obtained by the new method can be compared with other published data [11, 12]. It may be seen from Fig. 2 that: (a) the diffusion coefficients determined by the new method are extremely low. Such low values have not been measured by any other technique up to now. This fact illustrates the usefulness of the proposed method in the study of extremely slow processes as discussed above. (b) The obtained coefficients of diffusion are in good accord with the extrapolation of the temperature dependence of the carbon diffusion coefficient [11, 12] which is based on the compilation of available diffusivity data of many authors.

The results of the new method can also be compared with conventional disaccommodation measurements. The concentrations of carbon in solid solution shown in Table I agreed with that determined from customary disaccommodation measurement within a few percent. The accord of both methods in determining the time constants of relaxation is seen from Fig. 2.

REFERENCES

1. H. KRONMÜLLER, Nachwirkung in Ferromagnetika, Springer-Verlag, Berlin—Heidelberg—New York, 1968.
2. H. WILDE, Arch. el. Übertragung, **6**, 354, 1952.
3. F. WALZ, Phys. stat. sol., **a8**, 125, 1971.
4. L. NÉEL, J. Phys. Radium, **13**, 249, 1952.
5. S. KRUPIČKA and V. ROSKOVEC, Czech. J. Phys., **B16**, 99, 1966.
6. T. HEJNAL, Czech. J. Phys., **B25**, 1251, 1975.

7. J. RASEK, Acta Phys. Polon., **A44,** 85, 1973.
8. T. HEJNAL and J. KUNZE, Czech. J. Phys., **B24,** 951, 1974.
9. J. CHAJA, J. KINEL and J. W. MOROŇ, Physics Papers, Silesian University, Vol. 1, p. 53.
10. T. HEJNAL, Dissertation, University Prague, 1972.
11. A. E. LORD Jr. and D. N. BESHERS, Acta Met., **14,** 1659, 1966.
12. R. B. MCLELLAN, M. L. RUDEE and T. ISCHIBACHI, Trans. AIME, **233,** 1938, 1965.
13. T. HEJNAL, Czech. J. Phys., **B26,** 915, 1976.
14. S. KRUPIČKA, Czech. J. Phys., **B10,** 40, 1960.
15. P. BRISSONNEAU, J. Phys. Chem. Sol., **7,** 22, 1958.
16. A. J. BOSMAN, Dissertation, University Amsterdam, 1960.
17. A. J. BOSMAN, P. E. BROMMER, H. J. VAN DAAL and G. W. RATHENAU, Physica, **23,** 989, 1957.
18. H. KRONMÜLLER, in: Vacancies and Interstitials in Metals, North-Holland, Amsterdam, 1969, p. 667.
19. T. HEJNAL, S. KADEČKOVÁ, V. NOVÁK and B. ŠESTÁK, Czech. J. Phys. B, to be published.
20. H. J. GRABKE, Berichte Bunsenges. physik. Chem., **72,** 533, 1968.
21. E. W. JOHNSON and M. L. HILL, Trans. AIME, **218,** 1104, 1960.
22. M. V. KLEIN, Phys. stat. sol., **2,** 881, 1962.
23. H. D. DIETZE, Techn. Mitt. Krupp, **17,** 67, 1959.
24. H. D. DIETZE, Phys. stat. sol., **3,** 2309, 1963.
25. G. BIORCI, A. FERRO and G. MONTALENTI, J. Appl. Phys., **30,** 1732, 1959.
26. A. KUKE, Diplomarbeit, Universität Stuttgart, 1969.
27. W. KÖSTER, L. BANGERT and R. HAHN, Arch. Eisenhüttenw., **25,** 569, 1954.
28. G. BIORCI, A. FERRO and G. MONTALENTI, Phys. Rev., **119,** 653, 1960.
29. A. KUKE, H. KRONMÜLLER and H. SCHULTZ, Phys. stat. sol., **36,** K161, 1969.

Acta Physica Academiae Scientiarum Hungaricae, Tomus 42 (2), pp. 99—102 (1977)

RKRV FRANCK—CONDON FACTORS AND *r*-CENTROIDS FOR THE ($A^1\Pi - X^1\Sigma^+$) TRANSITION OF GeO MOLECULE

By

V. M. MUMMIGATTI and B. G. JYOTI

DEPARTMENT OF PHYSICS, KARNATAK UNIVERSITY, DHARWAR-3, INDIA

(Received 9. XII. 1976)

Potential Energy (p.e.) curves for $A^1\Pi$ and $X^1\Sigma^+$ states of GeO molecule have been constructed using the RKRV (RYDBERG—KLEIN—REES—VANDERSLICE) potentials. Franck Condon (FC) factors and *r*-centroids are evaluated using wavefunctions appropriate to RKRV p.e. curves. The sequence difference in the computed *r*-centroids remains constant here also. On the basis of the FC-factors the appearance of some of the bands is discussed.

1. Introduction

During the study of GeO molecule under high resolution in the region $\lambda 2200 - \lambda 4200$ Å, it has been shown [1, 2] that the transition involved is ($A^1\Pi - X^1\Sigma^+$) but not ($^1\Sigma - {}^1\Sigma$), as previously reported [3]. It is known that the difference of the observed rotational constant "α_e" from the calculated [4] value is a measure of the deviation of the true p.e. curves from the Morse curve. As already reported [5], this deviation for $X^1\Sigma^+$ state is 46%, whereas for $A^1\Pi$ state it is 3%. Therefore one cannot adopt Morse potential for the computation of FC-factors and *r*-centroids, in such cases.

Hence we report the values of these parameters for the ($A - X$) transition of the astrophysically significant GeO molecule, using wavefunctions appropriate to true (RKRV) p.e. curves. It is also proposed to discuss the appearance of some of the bands in the said transition.

2. Computational methods

2.1. *Potential energy curves*

The semi-classical RKR [6—8] method of calculating the turning points required to construct the p.e. curves of diatomic molecules has been modified [9, 10] and is shown to be highly successful for a large number of molecules. This is essentially a WKB approximation and maximum (r_+) and minimum (r_-) turning points as,

$$r_\pm = (f/g + f^2)^{1/2} \pm f,$$

where

$$f = \left(\frac{8\pi^2 \mu c}{h}\right)^{-1/2} \sum_{i=1}^{n} (\omega x)_i^{-1/2} \ln Z_i ,$$

$$g = \left(\frac{2\pi^2 \mu c}{h}\right)^{1/2} \sum_{i=1}^{n} \{2\alpha_i (\omega x)_i^{-1} [(U_n - U_{n-1})^{1/2} - (U_n - U_1)^{1/2}] + \\ + (\omega x)^{-1/2} [2B_i - \alpha_i (\omega x)_i^{-1} \omega_i] \ln Z_i\}$$

and

$$Z_i = \left| \frac{[\omega_i^2 - 4(\omega x)_i U_i]^{1/2} - 2(\omega x)_i^{1/2} (U_n - U_1)^{1/2}}{[\omega_i^2 - 4(\omega x)_i U_{i-1}]^{1/2} - 2(\omega x)_i^{1/2} (U_n - U_{i-1})^{1/2}} \right| .$$

Using these expressions along with the recently revised [1, 2] molecular data, the turning points for the A and X states of GeO molecule have been computed and are given in Table I.

Table I

RKRV potential energy curves for $X^1\Sigma^+$ and $A^1\Pi$ states of GeO molecule

v	$X^1\Sigma^+$		$A^1\Pi$	
	r_{max}	r_{min}	r_{max}	r_{min}
0	1.6750	1.5721	1.8270	1.7012
1	1.7183	1.5412	1.8819	1.6608
2	1.7512	1.5192	1.9209	1.6357
3	1.7777	1.5039	1.9548	1.6152
4	1.8029	1.4912	1.9657	1.6001
5	1.8261	1.4803	2.0139	1.5862
6	1.8468	1.4699	2.0421	1.5729
7	1.6682	1.4621	2.0662	1.5622
8	1.8881	1.4538	2.0947	1.5504
9	1.9078	1.4473	2.1209	1.5409
10	1.9269	1.4403	2.1417	1.5339
11	1.9449	1.4337		
12	1.9642	1.4279		
13	1.9819	1.4230		
14	2.0012	1.4178		

2.2. *Vibrational wavefunctions*

In the present study, to increase the accuracy, four successive turning points are taken at a time, for each limb on a large scale and the p.e. $U(r)$ are recorded at equal intervals of 0.01 Å for each vibrational level, taking more

than 1000 points. Extension of the p.e. curves beyond the limits covered by the spectroscopic data is achieved by the standard method [11]. The ordinates of the wavefunctions at all these r-values are obtained by inserting these $U(r)$ values in WU's [12] expression.

2.3. *FC-factors and r-centroids*

In terms of the vibrational wavefunctions, the FC-factor and the r-centroid can be defined as

$$q_{v'v''} = \int_0^\infty \psi_{v'}\,\psi_{v''}\,dr\,,$$

$$\bar{r}_{v'v''} = \int_0^\infty \psi_{v'}\,(r)\,\psi_{v''}\,dr \Big/ \int_0^\infty \psi_{v'}\,\psi_{v''}\,dr\,,$$

Table II

Franck–Condon factors and r-centroids for the $(A\text{-}X)$ transition of GeO molecule

$v'v''$	0	1	2	3	4	5	6
0	6.0181-2	1.3121-1	2.9221-1	2.4091-1	1.7011-1	9.9481-2	7.2813-2
	1.6721	1.6981	1.7251	1.7514	1.7788	1.8076	1.8352
	2659.42	2730.02	2804.17	2881.75	2963.04	3048.76	—
1	1.5921-1	1.9873-1	6.7013-2	6.9941-2	7.8232-2	1.6301-1	6.1427-2
	1.6701	1.6833	1.7081	1.7362	1.7634	1.7910	1.8197
	2614.43	2682.98	—	—	2908.1	—	3075.7
2	2.1806-2	7.4319-2	5.1261-2	1.1213-1	8.7401-2	6.1832-2	3.1431-3
	1.6531	1.6713	1.6947	1.7202	1.7483	1.7757	1.8031
	2571.83	—	2702.4	2779.71	2855.42	—	—
3	2.1673-1	5.3421-2	1.0153-1	8.7156-2	3.1421-2	8.1421-3	4.2156-3
	1.6321	1.6682	1.6641	1.7063	1.7324	1.7605	1.7879
	2531.10	—	2662.33	2732.3	—	—	—
4	1.8423-1	1.1784-2	1.0426-1	4.1678-2	1.2422-2	7.4218-3	2.1428-3
	1.6120	1.6444	1.6782	1.6862	1.7173	1.7456	1.7725
	2492.2	—	2619.5	—	—	—	—
5	9.1242-2	8.4216-2	3.1421-2	1.0187-2	8.1471-3	3.1426-3	9.4281-4
	1.5929	1.6240	1.6566	1.6892	1.7025	1.7284	1.7578
	2454.8	2514.88	—	—	—	—	—
6	5.1468-2	6.1871-2	1.0187-2	8.4721-3	5.1231-3	1.0132-3	3.1042-4
	1.5729	1.6052	1.6371	1.6696	1.6999	1.7158	1.7404
	—	2477.8	—	—	—	—	—

First row: FC-factors; Second row: r-centroids; Third row: wavelength. The negative number in each FC-factor entry indicates the power of 10 by which it is multiplied.

where $\psi_{v'}$ and $\psi_{v''}$ are the vibrational wavefunctions for the upper and the lower states, respectively, between which the transition takes place. The FC-factors and r-centroids thus calculated for the said transition are given in Table II along with the wavelength of the corresponding bands.

3. Conclusion

From Table II it is clear that the bands of $\Delta v = 0$ sequence, after $v' = v'' = 3$ are not observed. Similarly, the bands of the v'' progression with $v' = 4$, 5 and 6 after $v'' = 2$ are not observed either. Non-appearance of the said bands is naturally due to the low value of their FC-factors.

Although the bands (1, 2), (1, 3), (2, 1), (3, 2) and (4, 1) are not observed experimentally, their FC-factors calculated have significant values as compared with the values of the said factors for some of the observed bands, as can be seen from the Table II. Therefore, it must be possible to observe these bands under suitable parameter conditions.

REFERENCES

1. A. A. N. Murthy and P. B. V. Haranath, Indian J. Pure and Appl. Phys., **9,** 267, 1971.
2. A. A. N. Murthy and P. B. V. Haranath, Proc. Roy. Irish. Acad., **73A 16,** 1974, 1973.
3. A. K. Sengupta, Proc. Phys. Soc., London **51,** 62, 1939.
4. C. L. Pekeris, Phys. Rev., **45,** 98, 1934.
5. T. Savithry, D. V. K. Rao and P. T. Rao, Curr. Sci., **43,** 329, 1974.
6. R. Rydberg, Z. Phys., **73,** 376, 1931.
7. O. Klein, Z. Phys., **76,** 226, 1932.
8. A. L. G. Rees, Proc. Phys. Soc., **A59,** 998, 1947.
9. J. T. Vanderslice, E. A. Maison, W. G. Maisch and E. R. Lippincott, J. Molec. Spectrosc., **3,** 17, 1959.
10. N. L. Singh and D. C. Jain, Proc. Phys. Soc., **79,** 274, 1962.
11. R. N. Zare, E. O. Larsson and R. A. Berg, J. Molec. Spectrosc., **15,** 117, 1965.
12. Wu Ta You, Proc. Phys. Soc., London, **65,** 965, 1952.

Acta Physica Academiae Scientiarum Hungaricae, Tomus 42 (2), pp. 103—109 (1977)

FINITE LARMOR RADIUS EFFECT ON THERMAL-CONVECTIVE INSTABILITY OF A STELLAR ATMOSPHERE

By

R. C. SHARMA and KIRTI PRAKASH

DEPARTMENT OF MATHEMATICS, HIMACHAL PRADESH UNIVERSITY, SIMLA-171005, INDIA

(Received 16. XII. 1976)

Thermal-convective instability of a stellar atmosphere is considered to include finite Larmor radius effect in the presence of a uniform vertical magnetic field. The effect of a uniform rotation is also included. It is found that the criterion for monotonic instability is the same as in the absence or presence of these two effects. The growth rates are discussed.

1. Introduction

DEFOUW [1] has termed the thermal-convective instability as the convective instability of a thermally unstable atmosphere and has generalized the Schwarzschild criterion for convection to include departures from adiabatic motion.

DEFOUW [1] has given a criterion that a stellar atmosphere will be unstable if

$$D = \frac{1}{C_p}(L_T - \varrho\alpha L_\varrho) + \varkappa k^2 < 0, \tag{1}$$

where L is the energy lost minus the energy gained per gram per second and α, ϱ, $\varkappa$, k, L_T, L_ϱ denote respectively the coefficient of thermal expansion, the density, the coefficient of thermometric conductivity, the wave number of the perturbation, the partial derivative of L with respect to T and the partial derivative of L with respect to ϱ evaluated in the equilibrium state. C_p is the specific heat at constant pressure. In general, the instability due to inequality (1) may be either oscillatory or monotonic.

The criterion for instability (1) has been found to be unchanged by the presence of a uniform rotation and a uniform magnetic field separately by DEFOUW [1] and simultaneously by BHATIA [2].

In the above studies the Larmor radii of the charged particles (electrons and protons) are assumed to be zero. In many astrophysical situations such as the solar corona, interplanetary and interstellar plasmas, it is known that the approximation (zero Larmor radius) is not valid. The effect of the finiteness of the ion Larmor radius, which exhibits itself in the form of a

magnetic viscosity in the fluid equations, on plasma instabilities have been studied by ROSENBLUTH et al. [5] and ROBERTS and TAYLOR [4].

It is, therefore, interesting to study the modification, if any, in the criterion for instability when the effects due to rotation and finite Larmor radius are included in the thermal-convective instability of a stellar atmosphere.

2. Formulation of the problem

Let us consider an infinite horizontal layer which is in a state of uniform rotation $\mathbf{\Omega}(0, 0, \Omega)$, acted on by a vertical magnetic field $\mathbf{H}(0, 0, H)$ and gravity force $\mathbf{g}(0, 0, -g)$. This layer is heated from below such that a steady temperature gradient $\beta(= dT/dz)$ is maintained. Let $\delta\overleftrightarrow{P}$, $\delta\varrho$, $\mathbf{q}(u, v, w)$ and $\mathbf{h}(_x, h_y, h_z)$ denote the perturbations in stress tensor $\overleftrightarrow{P}$, density ϱ, velocity and magnetic field $\mathbf{H}$, respectively; g, ν and η denote respectively the gravitational acceleration, the kinematic viscosity and the resistivity. Then the linearized hydromagnetic perturbation equations are:

$$\varrho \frac{\partial \mathbf{q}}{\partial t} = - \nabla \delta \overleftrightarrow{P} + \varrho \nu \nabla^2 \mathbf{q} + \frac{1}{4\pi} (\nabla \times \mathbf{h}) \times \mathbf{H} + 2\varrho(\mathbf{q} \times \mathbf{\Omega}) + \mathbf{g}\delta\varrho \,, \tag{2}$$

$$\nabla \cdot \mathbf{q} = 0 \,, \quad \nabla \cdot \mathbf{h} = 0 \,. \tag{3}$$

$$\frac{\partial \mathbf{h}}{\partial t} = (\mathbf{H} \cdot \nabla)\, \mathbf{q} + \eta \nabla^2 \mathbf{h} \,. \tag{4}$$

The first law of thermodynamics can be written as

$$C_v \frac{dT}{dt} = - L + \frac{K}{\varrho} \nabla^2 T + \frac{p}{\varrho^2} \frac{d\varrho}{dt} \,, \tag{5}$$

where K, C_v, T, t and p denote the thermal conductivity, the specific heat at constant volume, the temperature, the time and the pressure, respectively.

The linearized perturbation form of Eq. (5), following DEFOUW [1], is

$$\frac{\partial \theta}{\partial t} + \frac{1}{C_p} (L_T - \alpha \varrho L_\varrho)\, \theta - \varkappa \nabla^2 \theta = - \left(\beta + \frac{g}{C_p} \right) w \,, \tag{6}$$

where θ is the perturbation in temperature. In obtaining (6), use has been made of the Boussinesq equation of state

$$\delta\varrho = - \alpha \varrho \theta \,. \tag{7}$$

For the vertical magnetic field $\mathbf{H}(0,0,H)$ the stress tensor components $\delta\overleftrightarrow{P}$, taking into account finite ion gyration, have the components (SHARMA [6]):

$$\left.\begin{aligned}
&\delta P_{xx} = \delta p - \varrho\nu_0\left(\frac{\partial u}{\partial y} + \frac{\partial v}{\partial x}\right), \quad \delta P_{xy} = \delta P_{yx} = \varrho\nu_0\left(\frac{\partial u}{\partial x} - \frac{\partial v}{\partial y}\right),\\
&\delta P_{xz} = \delta P_{zx} = -2\varrho\nu_0\left(\frac{\partial v}{\partial z} + \frac{\partial w}{\partial y}\right),\\
&\delta P_{yy} = \delta p + \varrho\nu_0\left(\frac{\partial u}{\partial y} + \frac{\partial v}{\partial x}\right),\\
&\delta P_{yz} = \delta P_{zy} = 2\varrho\nu_0\left(\frac{\partial w}{\partial x} + \frac{\partial u}{\partial z}\right), \quad \delta P_{zz} = \delta p\,.
\end{aligned}\right\} \tag{8}$$

In Eqs. (8), δp is the perturbation in the scalar part of the pressure and $\varrho\nu_0 = NT/4\omega_H$, where ω_H is the ion-gyration frequency, while N and T denote respectively the number density and temperature of the ions. We consider the case in which both the boundaries are free and the medium adjoining the fluid is nonconducting. The boundary conditions appropriate for the problem are (CHANDRASEKHAR [3])

$$\begin{aligned}
&w = 0\,, \quad \theta = 0\,,\\
&\frac{\partial^2 w}{\partial z^2} = 0\,, \quad \frac{\partial \zeta}{\partial z} = 0\,,
\end{aligned} \tag{9}$$

$\xi = 0$ and $\mathbf{h}$ is continuous with an external vacuum field. Here ζ and ξ denote, respectively, the z-components of vorticity and current density.

3. Dispersion relation and discussion

Analysing in terms of normal modes, we seek solutions whose dependence on the space and time coordinates is of the form,

$$\exp\left[ik_x x + ik_y y + nt\right] \sin k_z z\,, \tag{10}$$

where k_z is an integral multiple of π divided by the thickness of the fluid layer, $(k = \sqrt{k_x^2 + k_y^2 + k_z^2})$ is the wave number of the perturbation and n is the growth rate.

From Eqs. (2)—(4), (6) and (8), we have:

$$\frac{\partial}{\partial t}(\nabla^2 w) = g\alpha\left(\frac{\partial^2\theta}{\partial x^2} + \frac{\partial^2\theta}{\partial y^2}\right) + \nu\nabla^4 w - 2\Omega\frac{\partial\zeta}{\partial z} + \frac{H}{4\pi\varrho}\frac{\partial}{\partial z}\nabla^2 h_z + \\ + \nu_0\left(\nabla^2 - 3\frac{\partial^2}{\partial z^2}\right)\frac{\partial\zeta}{\partial z}, \tag{11}$$

$$\frac{\partial\zeta}{\partial t} = \nu\nabla^2\zeta + 2\Omega\frac{\partial w}{\partial z} + \frac{H}{4\pi\varrho}\frac{\partial\xi}{\partial z} - \nu_0\left(\nabla^2 - 3\frac{\partial^2}{\partial z^2}\right)\frac{\partial w}{\partial z}, \tag{12}$$

$$\frac{\partial h_z}{\partial t} = H\frac{\partial w}{\partial z} + \eta\nabla^2 h_z, \tag{13}$$

$$\frac{\partial\xi}{\partial t} = H\frac{\partial\zeta}{\partial z} + \eta\nabla^2\xi, \tag{14}$$

$$n\theta + \left[\frac{1}{C_p}(L_T - \varrho\alpha L_\varrho) + \varkappa k^2\right]\theta = -\left(\beta + \frac{g}{C_p}\right)w. \tag{15}$$

Eliminating θ, ζ, h_z and ξ from Eqs. (11) — (15) and using (10), we obtain the dispersion relation:

$$n^5 + A_4 n^4 + A_3 n^3 + A_2 n^2 + A_1 n + A_0 = 0, \tag{16}$$

where

$$A_4 = D + 2k^2(\nu + \eta),$$

$$A_3 = 2k^2 D(\nu + \eta) + k^4(\nu^2 + 4\nu\eta + \eta^2) + 2k_z^2 V^2 + \\ + \Gamma\left(\beta + \frac{g}{C_p}\right) + \frac{k_z^2 A^2}{k^2},$$

$$A_2 = k^2(\nu + 2\eta)\Gamma\left(\beta + \frac{g}{C_p}\right) + k^4 D(\nu^2 + 4\nu\eta + \eta^2) + \\ + 2k_z^2 V^2 D + 2k^6\nu\eta(\nu + \eta) + 2k_z^2 k^2 V^2(\nu + \eta) + \\ + \frac{k_z^2}{k^2}A^2(D + 2\eta k^2), \tag{17}$$

$$A_1 = 2k_z^2 k^2 V^2 D(\nu + \eta) + 2k^6 D\nu\eta(\nu + \eta) + \\ + \Gamma\left(\beta + \frac{g}{C_p}\right)\eta k^4(\eta + 2\nu) + \Gamma\left(\beta + \frac{g}{C_p}\right)k_z^2 V^2 + 2\nu\eta k^4 k_z^2 V^2 + \\ + k_z^4 V^4 + \nu^2\eta^2 k^8 + \eta k_z^2 A^2(\eta k^2 + 2D),$$

$$A_0 = (\nu\eta k^4 + k_z^2 V^2)\left[k_z^2 V^2 D + \nu\eta k^4 D + \Gamma\left(\beta + \frac{g}{C_p}\right)\eta k^2\right] + \\ + \eta^2 k^2 k_z^2 D A^2$$

and

$$\Gamma = \frac{g\alpha(k_x^2 + k_y^2)}{k^2}, \quad V^2 = \frac{H^2}{4\pi\varrho}, \quad A = 2\Omega + \nu_0(k^2 - 3k_z^2).$$

Setting $\nu = \eta = 0$ in Eq. (16) as the effects of viscosity and resistivity are negligible in many cases of astrophysical interest, the dispersion relation reduces to:

$$\begin{aligned} n^5 + Dn^4 + \left[2k_z^2 V^2 + \Gamma\left(\beta + \frac{g}{C_p}\right) + \frac{k_z^2}{k^2} A^2\right] n^3 \\ + D\left[2k_z^2 V^2 + \frac{k_z^2}{k^2} A^2\right] n^2 + \\ + \left[\Gamma\left(\beta + \frac{g}{C_p}\right) k_z^2 V^2 + k_z^4 V^4\right] n + k_z^4 V^4 D = 0 . \end{aligned} \tag{18}$$

When $D < 0$, i.e. when inequality (1) is satisfied the constant term in Eq. (18) is negative. This means that the Eq. (18) has a positive real root, leading to monotonic instability. The criterion for instability, therefore, is the same even if the rotation and finite Larmor radius effects are included in thermal-convective instability of a stellar atmosphere. We shall now discuss the dispersion relation (18) in some detail. Let us regard D to be small and solve the dispersion relation in order to study the nature of instability and growth rates in case of instability.

Putting

$$n = n_0 + n_1 D$$

in Eq. (18) and neglecting terms involving powers of D higher than the first, we get the following equations determining n_0 and n_1:

$$n_0\left[n_0^4 + PA^2\left(2f + 1 + \frac{\cos^2\theta}{P}\right) n_0^2 + P^2 A^4 f(1+f)\right] = 0 , \tag{19}$$

$$n_1 = (-)\frac{n_0^4 + PA^2\left(2f + \frac{\cos^2\theta}{P}\right) n_0^2 + P^2 A^4 f^2}{5n_0^4 + 3PA^2\left(2f + 1 + \frac{\cos^2\theta}{P}\right) n_0^2 + P^2 A^4 f(1+f)} . \tag{20}$$

From Eq. (19), we have

$$n_0 = 0 , \tag{21}$$

$$2\left(\frac{n_0}{A}\right)^2 = -\left[(1+2f)P + \cos^2\theta \mp \sqrt{P^2 + 2P(1+2f)\cos^2\theta + \cos^4\theta}\right], \tag{22}$$

where

$$P = \frac{\Gamma\left(\beta + \frac{g}{C_p}\right)}{A^2}, \quad f = \frac{k_z^2 V^2}{PA^2} \quad \text{and} \quad \frac{k_z}{k} = \cos\theta\,, \tag{23}$$

P, f and A^2 are all positive.

Corresponding to

$$n_0 = 0\,,$$

$$n_1 = -\frac{f}{1+f}\,. \tag{24}$$

The modes (21) and (24) correspond to the growing mode with growth rate t_0 given by

$$t_0 = (-D)\frac{f}{1+f} = (-)D\left[1 + \frac{\Gamma\left(\beta + \frac{g}{C_p}\right)}{k_z^2 V^2}\right]^{-1}.$$

Thus when $D < 0$, as k_z and H increase growth rate increases whereas as temperature gradient increases growth rate decreases.

In the Eq. (22), the expression within the square brackets is positive for all f and P which are positive for various values of θ. Therefore all the four values of n_0 are purely imaginary occurring in conjugate pairs so that we have the oscillatory instability when $D = 0$. The frequencies of these oscillations depend on k_z, k, A, f, P, θ i.e. magnetic field, temperature gradient, rotation, finite Larmor radius and wave numbers.

Now

$$n_1 = (-)\frac{1}{2}\frac{P\left[P + \cos^2\theta - \sqrt{P^2 + 2P(1+2f)\cos^2\theta + \cos^4\theta}\right]}{\left[(1-f-2f^2)P^2 + \cos^2\theta\,(2+3f)P + \cos^4\theta - \right.} \\ \left. - \left\{\cos^2\theta + P(f+1)\right\}\sqrt{P^2 + 2P(1+2f)\cos^2\theta + \cos^4\theta}\right], \tag{25}$$

corresponding to the value of n_0^2 given by upper sign in Eq. (22) and

$$n_2 = (-)\frac{1}{2}\frac{P\left[P + \cos^2\theta + \sqrt{P^2 + 2P(1+2f)\cos^2\theta + \cos^4\theta}\right]}{\left[(1-f-2f^2)P^2 + \cos^2\theta(2+3f)P + \cos^4\theta - \right.} \\ \left. - \left\{\cos^2\theta + P(f+1)\right\}\sqrt{P^2 + 2P(1+2f)\cos^2\theta + \cos^4\theta}\right], \tag{26}$$

corresponding to the value of n_0^2 given by lower sign in Eq. (22).

REFERENCES

1. R. J. DEFOUW, Astrophys. J., **160,** 659, 1970.
2. P. K. BHATIA, Publ. Astron. Soc. Japan, **23,** 181, 1971.
3. S. CHANDRASEKHAR, "Hydrodynamic and Hydromagnetic Stability" Clarendon Press, Oxford, 1961, Chap. IV.
4. K. V. ROBERTS and J. B. TAYLOR, Phys. Rev. Letters, **8,** 197, 1962.
5. M. N. ROSENBLUTH, N. KRALL and N. ROSTOKER, Nucl. Fusion Suppl., **1,** 143, 1962.
6. R. C. SHARMA, Phys. Fluids, **15,** 1822, 1972.

Acta Physica Academiae Scientiarum Hungaricae, Tomus 42 (2), pp. 111—125 (1977)

RESONATING GROUP MODEL FOR FEW-NUCLEON PROBLEMS*

By

V. K. SHARMA**

DEPARTMENT OF PHYSICS, DHARMA SAMAJ COLLEGE, ALIGARH-202001, INDIA

(Received in revised form 16. XII. 1976)

A simplified procedure based on the Resonating Group Approximation is proposed to obtain the integral equations for three- and four-nucleon problems. FADDEEV three-nucleon approach has been extended to obtain the FADDEEV—YAKUBOVSKY (FY) model of four nucleons taking into account of their spin and isospin in two-channel resonating group approximation. In this approximation we consider a completely antisymmetric wave function which can be written as the clustering of d + d and n + He^3 (or p + H^3) systems with antisymmetric spin-isospin states. The two nucleon interaction is assumed to be of the separable YAMAGUCHI form in $^3s_1$ and $^1s_0$ states. The equations for the states with quantum numbers $S = 2, 1, 0$; $T = 0$ are obtained. It is shown that the FY equations reduce to a set of one-dimensional coupled integral equations with the kernels containing the functions of two- and three-nucleon problems. By this conjecture one can treat few-body problems involving any number of bound subsystems.

I. Introduction

Few body problems have been studied with rising interest during the last sixteen years. It is now becoming an important tool in studies of nuclear reactions. This is primarily due to the fact that the investigations on few-nucleon problems give valuable information about the nucleon-nucleon interaction which is basic in nuclear physics. The method of the exact integral equations [1] is used almost exclusively at the present time in attempts at carrying out numerical solutions of the three-body problem. Techniques based on FADDEEV equations have been used successfully for studying three-nucleon bound state [2], elastic and inelastic n — d scattering [3].

After the pioneering work of FADDEV on the formulation and solution of the three-body problems, several attempts have been made to obtain FADDEEV-type equations for N-particles. Among these, the YAKUBOVSKY equations are one of the best as their homogeneous equations are free from non-physical solutions [4]. In recent years the FADDEEV—YAKUBOVSKY equations for the four-particle problems with separable pair interactions are widely used to investigate the properties of the bound and scattering states for four-nucleon

* Work supported in part by the University Grants Commission, India.

** Permanent address: 3/221, Adarsh Nagar, Marris Road, Aligarh-202001, India. Present address: Department of Theoretical Physics, University of Manchester, Manchester M139PL, UK.

systems [5, 6]. To obtain the integral equations for four particles, various effective approximation methods [7, 8, 9] have been developed. In particular [9], progress has been achieved in the direction based on the resonating group approximation which reduces the four-particle problem in one dimension.

In this paper we apply the systematic method [10] for the three- and four-nucleon problems, based on using exact integral equations of the FADDEEV-type, in the resonating group approximation to obtain one-dimensional coupled integral equations for various quantum states. As it is clear that the kernels of FADDEEV three-particle equations contain one delta function which can be removed by using nonlocal separable potential to obtain *Equivalent Two Body Problem* as in MITRA's formalism [11]. This formalism provides a concrete concept of WHEELER Resonating Group Substructures [12]. Thus it can be extended to more than three-body problems with nonlocal separable potential. However, in contrast to the three-body problem, the kernels of the FY four body equations contain two delta functions, these delta functions disappear after taking two iterations of the kernels. The exact integral equations for four-body problems with nonlocal separable potential lead to a set of two-dimensional coupled integral equations. In our view, the resonating group structure with nonlocal separable potential removes these delta-functions to obtain a set of one-dimensional coupled integral equations of Fredholm-type.

In Section II, the kinematics is fixed and the separable two-nucleon interactions used in the following are given. The technique to be followed is described in Section III in case of three-nucleon problems, including bound and scattering states. The integral equations for two subsystems of four-nucleon problems are given in Section IV. In Section V, the one-dimensional coupled integral equations for four-nucleon problems (i.e. d + d and n + He^3 or p + H^3 scattering and bound state of four-nucleon systems) with different quantum states are obtained using the method of Section III. Section VI discusses briefly the possibilities of using this framework for applications to few-body problems involving any number of bound subsystems.

II. Kinematics and two-nucleon interactions

It is convenient to use the relative momenta in the normalization of LOVELACE [13] and WEYERS [14]. In the four-nucleon system, we have [9]

$$\mathbf{k}_{ij} = \left[\frac{1}{2(m)^{1/2}}\right](\mathbf{k}_i - \mathbf{k}_j) ,$$

$$\mathbf{p}_{ij,k} = \left[\frac{1}{2(3m)^{1/2}}\right](\mathbf{k}_i + \mathbf{k}_j - 2\mathbf{k}_k) ,$$

$$\mathbf{q}_{ijk,l} = \left[\frac{1}{2(6m)^{1/2}}\right](\mathbf{k}_i + \mathbf{k}_j + \mathbf{k}_k - 3\mathbf{k}_l)\,; \tag{2.1}$$

$$\mathbf{k}_{kl} = \left[\frac{1}{2(m)^{1/2}}\right](\mathbf{k}_k - \mathbf{k}_l)\,,$$

$$\mathbf{S}_{ij,kl} = \left[\frac{1}{2(2m)^{1/2}}\right](\mathbf{k}_i + \mathbf{k}_j - \mathbf{k}_k - \mathbf{k}_l)\,,$$

(m is the nucleon mass).

The normalization is chosen such that the four-nucleon c.m. kinetic energy is given by

$$\mathcal{H}_0 = k_{ij}^2 + k_{kl}^2 + s_{ij,kl}^2 = k_{ij}^2 + p_{ij,k}^2 + q_{ij,kl}^2\,. \tag{2.2}$$

Similarly, the kinematical description of three-nucleon system is identical with the $\mathbf{k}_{ij}$, $\mathbf{p}_{ij,k}$ and the three-nucleon c.m. kinetic energy is given by

$$\mathrm{H}_0 = k_{ij}^2 + p_{ij,k}^2. \tag{2.3}$$

Here, $\mathbf{k}_{ij}$ represents the relative momentum in the two-nucleon subsystem.

Let us consider the s-wave separable potential model which includes neither hard-core nor tensor forces (for simplicity) as,

$$\langle \mathbf{k} \,|V|\, \mathbf{k}' \rangle = -\sum_{t_\alpha=0,1} \lambda_{t_\alpha}\, g_{t_\alpha}(\mathbf{k}) g_{t_\alpha}(\mathbf{k}')\, P_{t_\alpha}\,, \tag{2.4}$$

where P_{t_α}; $t_\alpha = 0, 1$ are the spin-isospin projection operators of deuteron and virtual singlet bound state, respectively. The ansatz (2.4) leads to the following form of the two-nucleon t-matrix as

$$t(\mathbf{k}, \mathbf{k}'\,;\, \mathrm{z}) = \sum_{t_\alpha=0,1} g_{t_\alpha}(\mathbf{k})\, g_{t_\alpha}(\mathbf{k}')\, \tau_{t_\alpha}(\mathrm{z})\, P_{t_\alpha}\,, \tag{2.5}$$

where

$$\tau_{t_\alpha}^{-1}(\mathrm{z}) = -\lambda_{t_\alpha}^{-1} - \int d\mathbf{q}\, \frac{g_{t_\alpha}^2(\mathbf{q})}{(\mathrm{z} - q^2)}\,, \tag{2.6}$$

and YAMAGUCHI [15] form factors as

$$g_{t_\alpha}(\mathbf{k}) = \frac{1}{(k^2 + \mu_{t_\alpha}^2)}\,;\; t_\alpha = 0, 1\,. \tag{2.7}$$

The parameters λ_0, λ_1, μ_0 and μ_1 are determined by the binding energy of the deuteron, the singlet and triplet scattering lengths, and the singlet effective range.

III. Integral equations for three-nucleon system in resonating group approximation

In this Section we describe a new method [9, 10] for solving the FADDEEV [1] equations for three nucleons taking into account their spin and isospin. The FADDEEV equations for three-particle transition operators are given as

$$T^{(ij,k)}(z) = T_{ij}(z) + T_{ij}(z)\, G_0(z)[T^{(jk,i)}(z) + T^{(ki,j)}(z)]\,, \tag{3.1}$$

with $G_0(z) = (z - \mathrm{H}_0)^{-1}$, is the free three-particle Green function and T_α is the two-body transition operator in three-particle space. Here H_0 denotes three-particle kinetic energy (see Eq. (2.3)), and $z = \mathrm{E} + i\varepsilon$ is the energy of the system with a small positive imaginary part. (Later, however, we will reinterpret $\mathcal{Q}_0$, $\mathcal{Z}$, $\mathcal{H}_0$, $\mathcal{T}_\alpha$ and $\mathcal{E}$ as the corresponding four-nucleon quantities.) Using the relation between the operator T and total Green function

$$G(z) = (z - \mathrm{H}_0 - V)^{-1}, \quad G(z) = G_0(z) + G_0(z)T(z)G_0(z);$$

one can obtained the set of equations determining the corresponding Green function as

$$G^{(ij,k)}(z) = G_{ij}(z) - G_0(z) + G_0(z)\, T_{ij}(z)\left[G^{(jk,i)}(z) + G^{(ki,j)}(z)\right], \tag{3.2}$$

where the following notations are used

$$G_{ij}(z) - G_0(z) = G_0(z)T_{ij}(z)G_0(z),\ G^{(ij,k)}(z) = G_0(z)T^{(ij,k)}(z)G_0(z)\,,$$

and

$$G(z) = G_0(z) + \sum_{(ij,k)} G^{(ij,k)}(z)\,. \tag{3.3}$$

The antisymmetric total wave function of three-nucleon system $\Psi^{\sigma\tau}$ is defined by the expression

$$\Psi^{\sigma\tau} \lim_{\varepsilon \to 0}\ i\varepsilon G\,(\mathrm{E} + i\varepsilon)\,\Phi^{\sigma\tau}, \tag{3.4}$$

where $\Phi^{\sigma\tau}$ is an antisymmetric asymptotic function with account of spin σ and isospin τ. Using operator Eqs. (3.2) with Eqs. (3.3) and (3.4), we get a set of equations for three-nucleon wave functions as

$$\Psi^{(ij,k)\sigma\tau} = \Phi_0^{(ij,k)\sigma\tau} + G_0\,(z)\, T_{ij}(z)\left[\Psi^{(jk,i)\sigma\tau} + \Psi^{(ki,j)\sigma\tau}\right], \tag{3.5}$$

where $\Phi_0^{(ij,k)\sigma\tau}$ is the initial wave function.

According to WHEELER's resonating group method [12, 16], the wave function of the system of three-nucleon $\Psi^{\sigma\tau}$, being completely antisymmetric relative to the permutations of the nucleons, can be written as

$$\begin{aligned}\Psi^{\sigma\tau} &= \sum_{(ij,k)} \sum_{\Pi t_{ij}} \Psi^{(ij,k)\sigma\tau}_{\Pi t_{ij}}(\mathbf{k}_{ij}, p_{ij,k}) \mid \zeta^{\sigma\lambda_\sigma \tau\tau_\tau}_{t_{ij}}(ij, k)\rangle; \\ &= \sum_{(ij,k)} \sum_{\Pi t_{ij}} \varphi_{t_{ij}}(\mathbf{k}_{ij})\, F^{\sigma\tau}_{\Pi}(\mathbf{p}_{ij,k}) \mid \zeta^{\sigma\tau\sigma^{\tau}\lambda_\tau}_{t_{ij}}(ij, k)\rangle ,\end{aligned} \tag{3.6}$$

where $\varphi_{t_\alpha}(\mathbf{k})$ is the space part of the normalized wave-function for two-nucleon bound state; $F^{\sigma\tau}_{\Pi}(\mathbf{p})$ is the *Spectator Function* [11] of the corresponding argument with parity quantum number Π; and $\mid \zeta^{\sigma\lambda_\sigma\tau\lambda_\tau}_{t_\alpha}\rangle$ is the antisymmetric spin-isospin states with conserving quantum numbers σ and τ of three-nucleon system.

The invariance of two-nucleon interaction under space inversion and the symmetry of the total wave function of three-nucleon system with antisymmetric spin-isospin states lead to the following parity relations for the functions $\Psi^{\sigma\tau}_{\Pi t_\alpha}(\mathbf{k}, \mathbf{p})$ and $\varphi_{t_\alpha}(\mathbf{k})$ as

$$\begin{aligned}\Psi^{\sigma\tau}_{\Pi t_\alpha}(-\mathbf{k}, \mathbf{p}) &= \Psi^{\sigma\tau}_{\Pi t_\alpha}(\mathbf{k}, \mathbf{p}), \\ \text{and} \qquad \varphi_{t_\alpha}(-\mathbf{k}) &= \varphi_{t_\alpha}(\mathbf{k}) .\end{aligned} \tag{3.7}$$

Substituting the form (3.6) of three-nucleon wave function $\Psi^{\sigma\tau}$ into the FADDEEV equation (3.5), following the resonating group method [9, 10] with account of Section II and parity relations (3.7), we get a set of one-dimensional integral equations as

$$F^{\sigma_a\tau_a}_{\Pi}(\mathbf{p}; z) = F^{\sigma_a\tau_a}_{0\Pi}(\mathbf{p}; z) + \sum_{t_\alpha t_\beta} \int d\mathbf{p}' \, \frac{U^{\sigma_a\tau_a}_{t_\alpha t_\beta}(\mathbf{p}, \mathbf{p}'; p'^2 - b)}{(p^2 - z - b)} \, F^{\sigma_a\tau_a}_{\Pi}(\mathbf{p}'; z), \tag{3.8}$$

where

$$U^{\sigma_a\tau_a}_{t_\alpha t_\beta}(\mathbf{p}, \mathbf{p}'; z) = 2\left(\frac{2}{\sqrt{3}}\right)^3 \frac{g_{t_\alpha}\left(\frac{1}{\sqrt{3}}\mathbf{p} + \frac{2}{\sqrt{3}}\mathbf{p}'\right) g_{t_\alpha}\left(\frac{2}{\sqrt{3}}\mathbf{p} + \frac{1}{\sqrt{3}}\mathbf{p}'\right)}{\frac{4}{3}(p^2 + \mathbf{p}\cdot\mathbf{p}' + p'^2) - z} \, \Lambda^{\sigma_a\tau_a}_{t_\alpha t_\beta} . \tag{3.9}$$

Here the spin-isospin recoupling coefficients $\Lambda^{\sigma_a\tau_a}_{t_\alpha t_\beta}$ are given by the expressions [13]

$$\begin{aligned}\Lambda^{\sigma_a\tau_a}_{t_\alpha t_\beta} = (-1)^{\sigma_a\tau_a} \sqrt{(2s_\alpha + 1)(2t_\alpha + 1)(2s_\beta + 1)(2t_\beta + 1)} \times \\ \times \begin{Bmatrix} \frac{1}{2} & \frac{1}{2} & s_\beta \\ \frac{1}{2} & \sigma_\alpha & s_\alpha \end{Bmatrix} \begin{Bmatrix} \frac{1}{2} & \frac{1}{2} & t_\beta \\ \frac{1}{2} & \tau_\alpha & t_\alpha \end{Bmatrix} .\end{aligned} \tag{3.10}$$

The scattering of a nucleon on two-nucleon bound state

For three-nucleon scattering problem, the inhomogeneous term $F_{0\Pi}^{\sigma_a\tau_a}$ and energy parameter z of Eqs. (3.8) are given by

$$F_{0\Pi}^{\sigma_a\tau_a}(\mathbf{p}; z) = (2\pi)^3\,\delta(\mathbf{p} - \mathbf{p}_0);\; z = p_0^2 - b + i0\,, \tag{3.11}$$

where $\mathbf{p}_0$ is the relative momentum of initial asymptotic motion and b is the binding energy of the two-nucleon system.

In analogy with the two-nucleon problem one should put the outgoing wave boundary condition as

$$F_{\Pi}^{\sigma_a\tau_a}(\mathbf{p}; z) = (2\pi)^3\,\delta(\mathbf{p} - \mathbf{p}_0) + 4\pi\,\frac{A_{\Pi}^{\sigma_a\tau_a}(\mathbf{p}, \mathbf{p}_0)}{[p^2 - p_0^2 - i\varepsilon]}\,, \tag{3.12}$$

where the value of $A_{\Pi}^{\sigma_a\tau_a}(\mathbf{p}, \mathbf{p}_0)$ for $p^2 = p_0^2$ is the exact amplitude for three-nucleon scattering. Substitution of (3.12) with (3.11) in Eqs. (3.8) and partial-wave decomposition leads to the following set of integral equations

$$A_{l\Pi}^{\sigma_a\tau_a}(p, p_0) = 2\pi^2\,K_{l\Pi}^{\sigma_a\tau_a}(p, p_0) + 4\pi\int_0^{\infty} dp'\,p'^2\,\frac{K_{l\Pi}^{\sigma_a\tau_a}(p, p')}{(p'^2 - p_0^2 - i\varepsilon)}\,A_{l\Pi}^{\sigma_a\tau_a}(p', p_0)\,, \tag{3.13}$$

where

$$K_{l\Pi}^{\sigma_a\tau_a}(p, p') =$$

$$\frac{8}{3\sqrt{3}}\sum_{t_\alpha t_\beta} A_{t_\alpha t_\beta}^{\sigma_a\tau_a}\int_{-1}^{+1} dx P_l(x)\,\frac{g_{t_\alpha}\left[\frac{1}{\sqrt{3}}(\mathbf{p} + 2\mathbf{p}')\right] g_{t_\beta}\left[\frac{1}{\sqrt{3}}(2\mathbf{p} + \mathbf{p}')\right]}{\left[\frac{1}{3}(p'^2 + 4\mathbf{p}\cdot\mathbf{p}' + 4p^2) + b\right]}\,,$$

$$x = \frac{\mathbf{p}\cdot\mathbf{p}'}{|\mathbf{p}|\,|\mathbf{p}'|}\,. \tag{3.14}$$

The solution of this equation leads directly to the phase shift δ_l given by

$$A_{l\Pi}^{\sigma\tau}(p, p_0) = \frac{e^{i\delta_l}\sin\delta_l(p_0)}{p_0}\,. \tag{3.15}$$

Since different values of (l, Π) are not coupled, superscript on $A_{l\Pi}^{\sigma\tau}$ and kernels can be dropped for simplicity.

The bound state of three-nucleon system

The homogeneous integral equations (3.8) for $F_{II}^{\sigma_a\tau_a}(\mathbf{p}; z)$ with $F_{0II}^{\sigma\tau} = 0$ and $z = -B + i0$ (B is the binding energy of three-nucleon system) describe the three-nucleon bound state.

IV. Integral equations for two subsystems of four-nucleon problem

Here we consider the systems obtained by switching off all the interactions except those that are internal in the two channels of four-nucleon problem. For the four-particle case, the components of the transition operators of the system of three particles and two non-interacting pairs of particles satisfy FADDEEV-type equations [4] as

$$M_{\alpha,\beta}(\mathbb{Z}) = \mathcal{T}_\alpha(\mathbb{Z})\,\delta_{\alpha\beta} + \mathcal{T}_\alpha(\mathbb{Z})\,\mathcal{G}_{\mathcal{J}0}(\mathbb{Z}) \sum_{\gamma\neq\alpha} M_{\gamma,\beta}(\mathbb{Z})\,; \quad \alpha, \beta, \gamma = ij, jk, ki \tag{4.1a}$$

and

$$N_{\alpha,\beta}(\mathbb{Z}) = \mathcal{T}_\alpha(\mathbb{Z})\,\delta_{\alpha\beta} + \mathcal{T}_\alpha(\mathbb{Z})\,\mathcal{G}_{\mathcal{J}0}(\mathbb{Z}) \sum_{\alpha\neq\gamma} N_{\gamma,\beta}(\mathbb{Z})\,; \quad \alpha, \beta, \gamma = ij, kl, \tag{4.1b}$$

respectively; and other symbols have their usual meaning analogous to the three-nucleon problem (see Section III).

With account of spin and isospin the amplitudes $M_{\alpha,\beta}$, and $N_{\alpha,\beta}$ can be expanded in the spin-isospin space as

$$M_{\alpha,\beta} = \sum_{\substack{ST\sigma_a\tau_a \\ t_\alpha t_\beta}} |\xi_{t_\alpha\sigma_a\tau_a}^{S\lambda_S T\lambda_T}\rangle M_{\alpha,\beta}^{t_\alpha t_\beta\sigma_a\tau_a} \langle \xi_{t_\beta\sigma_a\tau_a}^{S\lambda_S T\lambda_T}| \tag{4.2a}$$

and

$$N_{\alpha,\beta} = \sum_{\substack{ST t_\alpha t_{\bar\alpha} \\ t_\beta t_{\bar\beta}}} |\xi_{t_\alpha t_{\bar\alpha}}^{S\lambda_S T\lambda_T}\rangle N_{\alpha,\beta}^{t_\alpha t_{\bar\alpha} t_\beta t_{\bar\beta}} \langle \xi_{t_\beta t_{\bar\beta}}^{S\lambda_S T\lambda_T}| \begin{cases} 1 & \alpha = \beta \\ (-1)^{S+T}, & \alpha \neq \beta \end{cases} \tag{4.2b}$$

respectively. The amplitudes $M_{\alpha,\beta}$ can have nonphysical singularity in particular, the poles on the negative real axis not responding to the real bound states of the three-nucleon system. These nonphysical singularities cancel out when one proceeds to the following combination as

$$\begin{aligned} M_{t_\alpha t_\beta}^{\sigma_a\tau_a}(\mathbf{k}, \mathbf{p}; \mathbf{k}', \mathbf{p}'; Z) &= M_{ij,ij}^{t_\alpha, t_\beta\sigma_a\tau_a}(\mathbf{k}, \mathbf{p}; \mathbf{k}', \mathbf{p}'\,; Z) + \\ &+ M_{ij,jk}^{t_\alpha t_\beta\sigma_a\tau_a}(\mathbf{k}, \mathbf{p}; \mathbf{k}', \mathbf{p}'; Z) + M_{ij,ki}^{t_\alpha t_\beta\sigma_a\tau_a}(\mathbf{k}, \mathbf{p}; \mathbf{k}', \mathbf{p}'\,; Z)\,. \end{aligned} \tag{4.3a}$$

Similarly, it is more convenient, however, to consider the combinations for the transition operator with the definite parity Π of the state as

$$N^{(\pm)}_{t_\alpha \bar{t}_\alpha t_\beta \bar{t}_\beta}(\mathbf{k}, \mathbf{x}; \mathbf{k}', \mathbf{x}'; Z) = N^{t_\alpha \bar{t}_\alpha t_\beta \bar{t}_\beta}_{ij,ij}(\mathbf{k}, \mathbf{x}; \mathbf{k}', \mathbf{x}'; Z) + \\ + (-1)^{\Pi+S+T} N^{t_\alpha \bar{t}_\alpha t_\beta \bar{t}_\beta}_{ij,kl}(\mathbf{k}, \mathbf{x}; \mathbf{k}', \mathbf{x}'; Z) . \tag{4.3b}$$

With the separable form of pair-interaction (2.4) the amplitudes M and $N^{(\pm)}$ can be represented in the form

$$M^{\sigma_a \tau_a}_{t_\alpha t_a}(\mathbf{k}, \mathbf{p}; \mathbf{k}', \mathbf{p}'; Z) = g_{t_\alpha}(\mathbf{k})\, g_{t_\beta}(\mathbf{k}')\, \tau_{t_\alpha}(Z - p^2)\, \tau_{t_\beta}(Z - p'^2) \times \\ \times \left[\delta_{t_\alpha t_\beta}\, \tau_{t_\beta}^{-1}(Z - p'^2)\, \delta(\mathbf{p} - \mathbf{p}') + X^{\sigma_a \tau_a}_{t_\alpha t_\beta}(\mathbf{p}, \mathbf{p}'; Z)\right] \tag{4.4a}$$

and

$$N^{(\pm)}_{t_\alpha \bar{t}_\alpha t_\beta \bar{t}_\beta}(\mathbf{k}, \mathbf{x}; \mathbf{k}', \mathbf{x}'; Z) = g_{t_\alpha}(\mathbf{k})\, g_{t_\beta}(\mathbf{k}')\, \tau_{t_\alpha}(Z - x^2)\, \tau_{t_\beta}(Z - x'^2) \times \\ \times \left[\delta_{t_\alpha t_\beta}\, \tau_\beta^{-1}(Z - x'^2)\, \delta(\mathbf{x} - \mathbf{x}') + Y^{(\pm)}_{t_\alpha \bar{t}_\alpha t_\beta \bar{t}_\beta}(\mathbf{x}, \mathbf{x}'; Z)\right] ; \tag{4.4b}$$

where the functions $X^{\sigma_a \tau_a}_{t_\alpha t_\beta}$ and $Y^{(\pm)}_{t_\alpha \bar{t}_\alpha t_\beta \bar{t}_\beta}$ satisfy the following integral equations:

$$X^{\sigma_a \tau_a}_{t_\alpha t_\beta}(\mathbf{p}, \mathbf{p}'; Z) = U^{\sigma_a \tau_a}_{t_\alpha t_\beta}(\mathbf{p}, \mathbf{p}'; Z) + \sum_{t_\gamma} \int d\mathbf{p}''\; U^{\sigma_a \tau_a}_{t_\alpha t_\gamma}(\mathbf{p}, \mathbf{p}''; Z) \tau_{t_\gamma}(Z - p''^2) \times \\ \times X^{\sigma_a \tau_a}_{t_\gamma t_\beta}(\mathbf{p}'', \mathbf{p}'; Z) , \tag{4.5a}$$

and

$$Y^{(\pm)}_{t_\alpha \bar{t}_\alpha t_\beta \bar{t}_\beta}(\mathbf{x}, \mathbf{x}'; Z) = (-1)^{\Pi} W_{t_\alpha \bar{t}_\alpha t_\beta \bar{t}_\beta}(\mathbf{x}, \mathbf{x}'; Z) + (-1)^{\Pi+S+T} \sum_{t_\gamma \bar{t}_\gamma} \int d\mathbf{x}'' \times \\ \times W_{t_\alpha \bar{t}_\alpha t_\beta \bar{t}_\beta}(\mathbf{x}, \mathbf{x}''; Z)\, \tau_{t_\gamma}(Z - \mathbf{x}''^2)\, Y^{(\pm)}_{t_\gamma \bar{t}_\gamma t_\beta \bar{t}_\beta}(\mathbf{x}'', \mathbf{x}'; Z) ; \tag{4.5b}$$

with

$$U^{\sigma_a \tau_a}_{t_\alpha t_\beta}(\mathbf{p}, \mathbf{p}'; Z) = 2 \left(\frac{2}{\sqrt{3}}\right)^3 \frac{g_{t_\alpha}\left(\frac{1}{\sqrt{3}}\mathbf{p} + \frac{2}{\sqrt{3}}\mathbf{p}'\right) g_{t_\beta}\left(\frac{2}{\sqrt{3}}\mathbf{p} + \frac{1}{\sqrt{3}}\mathbf{p}'\right)}{\frac{4}{3}(p^2 + \mathbf{p}\cdot\mathbf{p}' + p'^2) - Z}\, \Lambda^{\sigma_a \tau_a}_{t_\alpha t_\beta}, \tag{4.6a}$$

and

$$W_{t_\alpha \bar{t}_\alpha t_\beta \bar{t}_\beta}(\mathbf{x}, \mathbf{x}'; Z) = \frac{g_{t_\alpha}(\mathbf{x})\, g_{t_\beta}(\mathbf{x}')}{x^2 + x'^2 - Z}\, \delta_{t_\alpha \bar{t}_\beta}\, \delta_{\bar{t}_\alpha t_\beta}. \tag{4.6b}$$

V. Integral equations for four-nucleon system in resonating group approximation

In the previous Sections we have discussed what is essentially the problem of the internal motion in the two types of two-body channel (i.e. one nucleon + three-nucleon type, and bound pair + bound pair type), and we have written various integral equations related to the scattering in the corresponding subsystems. It is now necessary to consider the FADDEEV—YAKUBOVSKY (FY) [4] equations so that we can incorporate them into the four-nucleon problem.

The FY equations for four-nucleon wave functions are obtained by following the method of Section III as [4, 7]

$$\begin{aligned}\Psi^{(ijk,l)\,ST} = {} & \Phi_0^{(ijk,l)ST} + \mathcal{G}_{j0}(\mathcal{E})\, M_{ij,ij}(\mathcal{E})[\Psi^{(kjl,i)ST} + \Psi^{(ikl,j)\,ST} + \\ & + \Psi^{(jk,il)\,ST} + \Psi^{(ki,jl)\,ST}] + \mathcal{G}_{j0}(\mathcal{E}) M_{ij,jk}(\mathcal{E})\,[\Psi^{(ikl,j)\,ST} + \\ & + \Psi^{(jil,k)\,ST} + \Psi^{(ki,jl)\,ST} + \Psi^{(ij,kl)\,ST}] + \mathcal{G}_{j0}(\mathcal{E})\, M_{ij,ki}(\mathcal{E}) \times \\ & \times [\Psi^{(jil,k)\,ST} + \Psi^{(kjl,i)\,ST} + \Psi^{(ij,kl)\,ST} + \Psi^{(jk,il)\,ST}]\,,\end{aligned} \tag{5.1a}$$

$$\begin{aligned}\Psi^{(ij,kl)\,ST} = {} & \Phi_0^{(ij,kl)\,ST} + \mathcal{G}_{j0}(\mathcal{E})\, N_{ij,ij}(\mathcal{E})[\Psi^{(lkj,i)\,ST} + \Psi^{(kli,j)\,ST}] + \\ & + \mathcal{G}_{j0}(\mathcal{E})\, N_{ij,kl}(\mathcal{E})\,[\Psi^{(jil,k)\,ST} + \Psi^{(ijk,l)\,ST}]\,;\end{aligned} \tag{5.1b}$$

where $M_{\alpha,\beta}$ and $N_{\alpha,\beta}$ satisfying the Eqs. (4.1a) and (4.1b), respectively, and other symbols have their usual meaning analogous to three-nucleon problem. The free terms $\Phi_0^{(ijk,l)ST}$ and $\Phi_0^{(ij,kl)ST}$ are the appropriate initial asymptotic states for two subsystems of four-nucleon problem.

Using the resonating group method of the three-nucleon case in Section III as a guide, we write the completely antisymmetric wave function of four-nucleon system as*

$$\begin{aligned}\Psi^{ST} = {} & \sum_{(ijk,l)} \sum_{\Pi t_{ij}\sigma_{ijk}\tau_{ijk}} \Psi^{(ijk,l)}_{\Pi t_{ij}\sigma_{ijk}\tau_{ijk}}(\mathbf{k}_{ij}, \mathbf{p}_{ij,k}, \mathbf{q}_{ijk,l})\,|\,\xi^{S\lambda_S T\lambda_T}_{t_{ij}\sigma_{ijk}\tau_{ijk}}(ijk, l)> + \\ & + \sum_{(ij,kl)} \sum_{\Pi t_{ij}t_{kl}} \Psi^{(ij,kl)\,ST}_{\Pi t_{ij}t_{kl}}(\mathbf{k}_{ij}, \mathbf{k}_{kl}, \mathbf{s}_{ij,kl})\,|\,\xi^{S\lambda_S T\lambda_T}_{t_{ij}t_{kl}}(ij, kl)>, \\ = {} & \sum_{(ijk,l)} \sum_{\Pi t_{ij}\sigma_{ijk}\tau_{ijk}} \psi^{\sigma_{ijk}\tau_{ijk}}_{\Pi t_{ij}}(\mathbf{k}_{ij}, \mathbf{p}_{ij,k})\; \mathcal{H}^{ST}_{\Pi}(\mathbf{q}_{ijk.l})\,|\,\xi^{S\lambda_S T\lambda_T}_{t_{ij}\sigma_{ijk}\tau_{ijk}}(ijk, l)> + \\ & + \sum_{(ij,kl)} \sum_{\Pi t_{ij}t_{kl}} \varphi_{t_{ij}}(\mathbf{k}_{ij})\,\varphi_{t_{kl}}(\mathbf{k}_{kl})\; \mathcal{F}^{ST}_{\Pi}(\mathbf{s}_{ij,kl})\,|\,\xi^{S\lambda_S T\lambda_T}_{t_{ij}t_{kl}}(ij, kl)>,\end{aligned} \tag{5.2}$$

where $\psi^{\sigma_\alpha\tau_\alpha}_{\Pi t_\alpha}(\mathbf{k}, \mathbf{p})$ and $\varphi_{t_\alpha}(\mathbf{k})$ are the space parts of the normalized wave functions for three-nucleon and two-nucleon (deuteron) bound states, respectively; $\mathcal{H}^{ST}_{\Pi}(\mathbf{q})$ and $\mathcal{F}^{ST}_{\Pi}(\mathbf{q})$ are the corresponding *Spectator Functions* [17] of two sub-

* Here distortion effect is not taken into account.

systems; $|\,\xi^{S\lambda_S T\lambda_T}_{t_\alpha\sigma_\alpha\tau_\alpha}\rangle$ and $|\,\xi^{S\lambda_S T\lambda_T}_{t_\alpha\bar{t}_{\bar{\alpha}}}\rangle$ are the spin-isospin states defined by*

$$|\,\xi^{S\lambda_S T\lambda_T}_{t_a\sigma_a\tau_a}(ijk,\,l)\,\rangle\,|\,=(\mathbf{s}_i\,\mathbf{s}_j)\,\mathbf{s}_\alpha\,\mathbf{s}_k\,\sigma_\alpha\,\mathbf{s}_l\,S\lambda_S\,\rangle\,|\,(t_i\,t_j)\,t_\alpha\,t_k\,\tau_\alpha\,t_l\,T\lambda_T\,\rangle\,, \tag{5.3a}$$

$$|\,\xi^{S\lambda_S T\lambda_T}_{t_\alpha\bar{t}_{\bar{\alpha}}}(ij,\,kl)\,\rangle\,|\,=(\mathbf{s}_i\,\mathbf{s}_j)\,\mathbf{s}_\alpha,(\mathbf{s}_k\,\mathbf{s}_l)\,\mathbf{s}_{\bar{\alpha}}\,S\lambda_S\rangle|\,(t_i\,t_j)\,t_\alpha,\,(t_k t_l)\,t_{\bar{\alpha}}\,T\lambda_T\rangle\,. \tag{5.3b}$$

Substituting the form (5.2) for Ψ^{ST}, the four-nucleon wave function into the FY equations (5.1a) and (5.1b) and eliminating the spin-isospin functions and further multiplying successively by $\psi^{\sigma\tau *}_{\Pi t_\alpha}$, $\varphi^{*}_{t_\alpha}\,\varphi^{*}_{t_\beta}$ and integrating over the internal variables using symmetric relations, we get a set of the integral equations with nonlocal separable potential as [9, 10]

$$\begin{aligned}\mathcal{H}^{ST}_{\Pi}(\mathbf{q};\,\mathcal{E}) &= \mathcal{H}^{ST}_{0\Pi}(\mathbf{q};\,\mathcal{E}) + \\ &+\left(\frac{3}{2\sqrt{2}}\right)^3 \sum_{t_\beta\sigma_b\tau_b}\int d\mathbf{q}'\,\langle t_\alpha\,\sigma_a\,\tau_a\,|\,K^{t_\alpha t_\beta\sigma_b\tau_b}_{\mathcal{H}\mathcal{H}}(\mathbf{q},\,\mathbf{q};\,\mathcal{E})\,|\,t_\beta\,\sigma_b\,\tau_b\rangle\times \\ &\times\,\mathcal{H}^{ST}_{H}(\mathbf{q};\,\mathcal{E}) + (-1)^{\Pi}\left(\sqrt{\frac{3}{2}}\right)^3 \sum_{t_\beta t_{\bar{\beta}}}\int d\mathbf{q}'\,\langle t_\alpha\,\sigma_a\tau_a\;\times \\ &\times\,|\,K^{t_\alpha t_\beta\sigma_a\tau_a}_{\mathcal{H}\mathcal{F}}(\mathbf{q},\,\mathbf{q}';\,\mathcal{E})\,|\,t_\beta t_{\bar{\beta}}\rangle\;\mathcal{F}^{ST}_{\Pi}(\mathbf{q}';\,\mathcal{E})\,;\end{aligned} \tag{5.4a}$$

$$\mathcal{F}^{ST}_{\Pi}(\mathbf{q};\,\mathcal{E}) = \mathcal{F}^{ST}_{0\Pi}(\mathbf{q};\,\mathcal{E}) + \left(\sqrt{\frac{3}{2}}\right)^3 \sum_{t_\beta\,\sigma_b\tau_b}\int d\mathbf{q}'\times \tag{5.4b}$$
$$\times\,\langle t_\alpha\,t_{\bar{\alpha}}\,|\,K^{t_\alpha t_{\bar{\alpha}} t_\beta t_{\bar{\beta}}}_{\mathcal{F}\mathcal{H}}(\mathbf{q},\,\mathbf{q}';\,\mathcal{E})\,|\,t_\beta\,\sigma_b\,\tau_b\rangle\;\mathcal{H}^{ST}_{\Pi}(\mathbf{q}';\,\mathcal{H})\,;$$

where

$$\begin{aligned}\langle t_\alpha\,\sigma_a\,\tau_a\,|\,K^{t_\alpha t_\beta\sigma_b\tau_b}_{\mathcal{H}\mathcal{H}}(\mathbf{q},\,\mathbf{q}';\,\mathcal{E})\,|\,t_\beta\,\sigma_b\,\tau_b\rangle &= C^{t_\alpha\sigma_a\tau_a}_{t_\beta\,\sigma_b\tau_b}\Bigg[\int d\mathbf{p}\,\frac{U^{\sigma_a\tau_a}_{t_\alpha t_\beta}(\mathbf{p},\,\mathbf{Q}_1;\,Q_1^2-b)}{(p^2+q^2-\mathcal{E}-b)}\times \\ &\times\,F^{\sigma_a\tau_a}_{\Pi}(\mathbf{p};\,B)\;F^{\sigma_b\tau_b}_{\Pi}(\mathbf{Q}_2;\,B) + \\ &+\sum_{t_\gamma}\iint d\mathbf{p}d\mathbf{k}'\,\frac{U^{\sigma_a\tau_a}_{t_\alpha t_\gamma}(\mathbf{k}',\,\mathbf{Q}_1;\,Q_1^2-b)}{(p^2+q^2-\mathcal{E}-b)}\,F^{\sigma_a\tau_a}_{\Pi}(\mathbf{p};\,B)\;F^{\sigma_b\tau_b}_{\Pi}(\mathbf{Q}_2;\,B)\times \\ &\times\,\tau_{t_\gamma}(\mathcal{E}-q^2-k'^2)\,X^{\sigma_a\tau_a}_{t_\gamma t_\beta}(\mathbf{p},\,\mathbf{k}';\,\mathcal{E}-q^2)\Bigg],\end{aligned} \tag{5.5a}$$

$$\begin{aligned}\langle t_\alpha\sigma_a\tau_a\,|\,K^{t_\alpha t_\beta\sigma_a\tau_a}_{\mathcal{H}\mathcal{F}}(\mathbf{q},\,\mathbf{q}';\,\mathcal{E})\,|\,t_\beta t_{\bar{\beta}}\rangle &= D^{t_\alpha\sigma_a\tau_a}_{t_\beta t_{\bar{\beta}} ST}\times \\ &\times\Bigg[\int d\mathbf{p}\,\frac{U^{\sigma_a\tau_a}_{t_\alpha t_\beta}(\mathbf{p},\,\mathbf{R}_1;\,R_1^2-b)}{(p^2+q^2-\mathcal{E}-b)}\times F^{\sigma_a\tau_a}_{\Pi}(\mathbf{p};\,B)\,\varphi_{t_{\bar{\beta}}}(\mathbf{R}_2)\;+ \\ &+\sum_{t_\gamma}\iint d\mathbf{p}d\mathbf{k}'\,\frac{U^{\sigma_a\sigma_a}_{t_\alpha t_\gamma}(\mathbf{k}',\,\mathbf{R}_1;\,R_1^2-b)}{(p^2+q_\sigma^2-\mathcal{E}-b)}\,F^{\sigma_a\tau_a}_{\Pi}(\mathbf{p};\,B)\,\varphi_{t_{\bar{\beta}}}(\mathbf{R}_2)\times \\ &\times\,\tau_{t_\gamma}(\mathcal{E}-q^2-k'^2)\,X^{\sigma_a\tau_a}_{t_\gamma t_\beta}(\mathbf{p},\,\mathbf{k}';\,\mathcal{E}-q^2)\Bigg],\end{aligned} \tag{5.5b}$$

* Here $s_\alpha + t_\alpha = 1$ therefore s_α is omitted in the subscript of $\xi's$.

$$\langle t_\alpha t_{\bar{\alpha}} | K^{t_\alpha t_{\bar{\alpha}} t_\beta t_{\bar{\beta}}}_{\mathcal{SK}}(\mathbf{q}, \mathbf{q}'; \mathcal{E}) | t_\beta \sigma_b \tau_b \rangle = 2 B^{t_\alpha t_{\bar{\alpha}} ST}_{t_\beta \sigma_b \tau_b} \lambda^{-1}_{t_\beta} \times$$

$$\times \left[\frac{\varphi_{t_{\bar{\beta}}}(\mathbf{S}_1) F^{\sigma_b \tau_b}_{\Pi}(\mathbf{S}_2; B)}{(S_1^2 + q^2 - \mathcal{E} - b)} + \int d\mathbf{x} \frac{\varphi_{t_{\bar{\alpha}}}(\mathbf{x}) F^{\sigma_b \tau_b}_{\Pi}(\mathbf{S}_2; B)}{(x^2 + q^2 - \mathcal{E} - b)} \cdot \right. \tag{5.5c}$$

$$\left. \cdot \tau_{t_\beta}(\mathcal{E} - q^2 - S_1^2) Y^{(\pm)}_{t_\alpha t_{\bar{\alpha}} t_\beta t_{\bar{\beta}}}(\mathbf{x}, \mathbf{S}_1; \mathcal{E} - q^2) \right].$$

Here the following notations are used

$$\mathbf{Q}_1 = \frac{3\mathbf{q}' + \mathbf{q}}{2\sqrt{2}}, \qquad \mathbf{Q}_2 = \frac{3\mathbf{q} + \mathbf{q}'}{2\sqrt{2}};$$

$$\mathbf{R}_1 = \frac{\sqrt{3}\,\mathbf{q}' - \mathbf{q}}{\sqrt{2}}, \qquad \mathbf{R}_2 = \frac{\sqrt{3}\,\mathbf{q} - \mathbf{q}'}{\sqrt{2}}; \tag{5.6}$$

$$\mathbf{S}_1 = \frac{\sqrt{3}\,\mathbf{q}' + \mathbf{q}}{\sqrt{2}}, \qquad \mathbf{S}_2 = \frac{-\sqrt{3}\,\mathbf{q} - \mathbf{q}'}{\sqrt{2}};$$

with $B^{t_\alpha t_{\bar{\alpha}} ST}_{t_\beta \sigma_b \tau_b}$, $C^{t_\alpha \sigma_a \tau_a}_{t_\beta \sigma_b \tau_b}$, and $D^{t_\alpha \sigma_a \tau_a}_{t_\beta t_{\bar{\beta}} ST}$ are the spin-isospin recoupling coefficients whose values can be obtained by using the explicit matrix representations of the symmetric group S_4 [8].

The scattering of a nucleon on a system of three nucleons in a bound state

For neutron + He^3 (or p + H^3) scattering the various quantum numbers for spin-isospin states are $S = 1, 0$; $T = 0, t = 0$, $\sigma = 3/2,\ 1/2$, $\tau = 1/2$. The inhomogeneous terms and energy parameters $\mathcal{E}$ of Eqs. (5.4) are given by

$$\mathcal{H}^{10}_{0\Pi} = (2\pi)^3 \delta(\mathbf{q} - \mathbf{q}_0),$$

$$\mathcal{F}^{10}_{0\Pi} = 0, \quad \mathcal{E} = q_0^2 - B + i0; \tag{5.7}$$

where $\mathbf{q}_0$ is the initial relative momentum and B is the binding energy of the He^3 (or H^3).

In analogy with the two- or three-nucleon problem (see Eq. (3.12)) one should put the outgoing wave boundary conditions as

$$\mathcal{H}^{ST}_{\Pi}(\mathbf{q}; q_0^2 - B) = (2\pi)^3 \delta(\mathbf{q} - \mathbf{q}_0) + 4\pi \frac{\mathcal{R}^{ST}_{\Pi}(\mathbf{q}, \mathbf{q}_0)}{[q^2 - q_0^2 - i\varepsilon)}, \tag{5.8a}$$

$$\mathcal{F}^{ST}_{\Pi}(\mathbf{q}; q_0^2 - B) = 4\pi \frac{\mathcal{S}^{ST}_{\Pi}(\mathbf{q}, \mathbf{q}_0)}{[q^2 - q_0^2 - i\varepsilon]}; \tag{5.8b}$$

where the values of $\mathcal{R}^{ST}_{\Pi}(\mathbf{q}, \mathbf{q}_0)$ for $q^2 = q_0^2$ is the exact amplitude for n + He^3

(or p + H^3) scattering. Substitution of Eqs. (5.8) with (5.7) in Eqs. (5.4) and partial-wave decomposition leads to a following set of integral equations

$$\mathcal{A}^{ST}_{II}(q,q_0) = 2\pi^2 K^{\mathcal{HH}}_{II}(q,q_0\,;q_0^2 - B) + 4\pi\int_0^\infty dq'\,q'^2 \frac{K^{\mathcal{HH}}_{II}(q,q';\,q_0^2 - B)}{(q'^2 - q_0^2 - i\varepsilon)} \times$$
$$\times\, \mathcal{A}^{ST}_{II}(q',q_0) + (-1)^{I} 4\pi \int_0^\infty dq'\,q'^2 \frac{K^{\mathcal{SH}}_{II}(q,q';q_0^2 - B)}{(q'^2 - q_0^2 - i\varepsilon)}\, \mathcal{B}^{ST}_{II}(q',q_0), \tag{5.9a}$$

$$\mathcal{B}^{ST}_{II}(q,q_0) = 2\pi^2 K^{\mathcal{SH}}_{II}(q,q_0;q_0^2 - B) + 4\pi\int_0^\infty dq'\,q'^2 \frac{K^{\mathcal{SH}}_{II}(q,q';q_0^2 - B)}{(q'^2 - q_0^2 - i\varepsilon)}\, \mathcal{A}^{ST}_{II}(q',q_0)\,; \tag{5.9b}$$

where

$$K^{\mathcal{HH}}_{II}(q,q';q_0^2 - B) = \frac{27\pi}{8\sqrt{2}} \sum_{t_\beta \sigma_b \tau_b} \int_{-1}^{+1} dx P_l(x)(q^2 - q_0^2 - i\varepsilon) \times$$
$$\times \langle t_\alpha \sigma_a \tau_a \mid K^{t_\alpha t_\beta \sigma_b \tau_b}_{\mathcal{HH}}(\mathbf{q},\mathbf{q}';\,q_0^2 - B) \mid t_\beta \sigma_b \tau_b \rangle\,, \tag{5.10a}$$

$$K^{\mathcal{HS}}_{II}(q,q';q_0^2 - B) = \frac{3\sqrt{3}\pi}{\sqrt{2}} \sum_{t_\beta t_{\bar\beta}} \int_{-1}^{+1} dx P_l(x)(q^2 - q_0^2 - i\varepsilon) \times$$
$$\times \langle t_\alpha \sigma_a \tau_a \mid K^{t_\alpha t_\beta \sigma_a \tau_a}_{\mathcal{HS}}(\mathbf{q},\mathbf{q}';\,q_0^2 - B) \mid t_\beta t_{\bar\beta} \rangle\,, \tag{5.10b}$$

$$K^{\mathcal{SH}}_{II}(q,q';q_0^2 - B) = \frac{3\sqrt{3}\pi}{\sqrt{2}} \sum_{t_\beta \sigma_b \tau_b} \int_{-0}^{+1} dx P_l(x)(q^2 - q_0^2 - i\varepsilon) \times$$
$$\times \langle t_\alpha t_{\bar\alpha} \mid \langle K^{t_\alpha t_{\bar\alpha} t_\beta t_{\bar\beta}}_{\mathcal{SH}}(\mathbf{q},\mathbf{q}';\,q_0^2 - B) \mid t_\beta \sigma_b \tau_b \rangle\,; \tag{5.10c}$$

here $x = \dfrac{\mathbf{q}\cdot\mathbf{q}'}{|\mathbf{q}|\cdot|\mathbf{q}'|}$ and the expressions for kernels are given by Eq. (5.5). The solution of Eqs. (5.9) for amplitude $\mathcal{A}^{ST}_{II}$ leads directly to the phase shifts $\delta^{\mathcal{A}}_l$ for n + He^3 (or p + H^3) scattering given by

$$\mathcal{A}^{ST}_{II}(q,q_0) = \frac{e^{i\delta^{\mathcal{A}}_l} \sin\delta^{\mathcal{A}}_l(q_0)}{q_0}\,. \tag{5.11}$$

The scattering of deuteron by deuteron

For d + d scattering the various quantum numbers for spin-isospin states are $S = 2$, $T = 0$, $t = 0$, $\sigma = 3/2$, $\tau = 1/2$. The inhomogeneous terms and energy parameter $\mathcal{E}$ of Eqs. (5.4) are given by

$$\mathcal{H}^{20}_{0II} = 0\,,\quad \mathcal{E} = q_0^2 - 2b + i0\,,$$
$$\mathcal{F}^{20}_{0II} = (2\pi)^3 \delta(\mathbf{q} - \mathbf{q}_0)\,; \tag{5.12}$$

where $\mathbf{q}_0$ is the initial momentum of relative motion of the centres of mass of deuteron and b is the binding energy of the deuteron. The outgoing wave boundary conditions in this case are as follows (see Eq. (5.8))

$$\mathcal{H}_{II}^{ST}(\mathbf{q}; q_0^2 - 2b) = 4\pi \frac{\mathcal{A}_{II}^{ST}(\mathbf{q}, \mathbf{q}_0)}{[q^2 - q_0^2 - i\varepsilon]}, \tag{5.13a}$$

$$\mathcal{F}_{II}^{ST}(\mathbf{q}; q_0^2 - 2b) = (2\pi)^3 \delta(\mathbf{q} - \mathbf{q}_0) + 4\pi \frac{\mathcal{B}_{II}^{ST}(\mathbf{q}, \mathbf{q}_0)}{[q^2 - q_0^2 - i\varepsilon]}\ ; \tag{5.13b}$$

where the value of $\mathcal{B}_{II}^{ST}(\mathbf{q}, \mathbf{q}_0)$ for $q^2 = q_0^2$ is the exact amplitude for d+d scattering. Substitution of (5.13) with (5.12) in Eqs. (5.4) and partial-wave decomposition leads to a similar set of equations (see Eqs. (5.9)) but with different inhomogeneous terms as

$$\begin{aligned}\mathcal{A}_{III}^{ST}(q, q_0) = {} & 2\pi^2(-1)^{II} K_{III}^{\mathcal{HF}}(q, q_0; q_0^2 - 2b) + \\ & + 4\pi \int_0^\infty dq' q'^2 \frac{K_{III}^{\mathcal{HH}}(q, q'; q_0^2 - 2b)}{(q'^2 - q_0^2 - i\varepsilon)} \mathcal{A}_{III}^{ST}(q', q_0) + \\ & + (-1) 4\pi \int_0^\infty dq' q'^2 \frac{K_{III}^{\mathcal{HF}}(q, q'; q_0^2 - 2b)}{(q'^2 - q_0^2 - i\varepsilon)} \mathcal{B}_{III}^{ST}(q', q_0),\end{aligned} \tag{5.14a}$$

$$\mathcal{B}_{III}^{ST}(q, q_0) = 4\pi \int_0^\infty dq' q'^2 \frac{K_{III}^{\mathcal{FH}}(q, q'; q_0^2 - 2b)}{(q'^2 - q_0^2 - i\varepsilon)} \mathcal{A}_{III}^{ST}(q', q_0)\ ; \tag{5.14b}$$

where

$$\begin{aligned}K_{III}^{\mathcal{HH}}(q, q'; q_0^2 - 2b) = {} & \frac{27\pi}{8\sqrt{2}} \sum_{t_\beta \sigma_b \tau_b} \int_{-1}^{+1} dx P_l(x)(q^2 - q_0^2 - i\varepsilon) \times \\ & \times \langle t_\alpha \sigma_a \tau_a | K_{\mathcal{HH}}^{t_\beta t_\beta \sigma_b \tau_b}(\mathbf{q}, \mathbf{q}'; q_0^2 - 2b) | t_\beta \sigma_b \tau_b \rangle,\end{aligned} \tag{5.15a}$$

$$\begin{aligned}K_{III}^{\mathcal{HF}}(q, q'; q_0^2 - 2b) = {} & \frac{3\sqrt{3}}{\sqrt{2}} \pi \sum_{t_\beta t_{\bar\beta}} \int_{-1}^{+1} dx P_l(x)(q^2 - q_0^2 - i\varepsilon) \times \\ & \times \langle t_\alpha \sigma_a \tau_a | K_{\mathcal{HF}}^{t_\alpha t_\beta \sigma_a \tau_\alpha}(\mathbf{q}, \mathbf{q}'; q_0^2 - 2b) | t_\beta t_{\bar\beta} \rangle,\end{aligned} \tag{5.15b}$$

$$\begin{aligned}K_{III}^{\mathcal{FH}}(q, q'; q_0^2 - 2b) = {} & \frac{3\sqrt{3}}{\sqrt{2}} \pi \sum_{t_\beta \sigma_b \tau_b} \int_{-1}^{+1} dx P_l(x)(q^2 - q_0^2 - i\varepsilon) \times \\ & \times \langle t_\alpha t_{\bar\alpha} | K_{\mathcal{FH}}^{t_\alpha t_{\bar\alpha} t_\beta t_{\bar\beta}}(\mathbf{q}, \mathbf{q}'; q_0^2 - 2b) | t_\beta \sigma_b \tau_b \rangle.\end{aligned} \tag{5.15c}$$

The solution of Eqs. (5.14) for amplitudes $\mathcal{B}_{lII}^{ST}$ leads to the phase shifts $\delta_l^{\mathcal{B}}$ for d + d scattering given by

$$\mathcal{B}_{lII}^{ST}(q, q_0) = \frac{e^{i\delta_l^{\mathcal{B}}} \sin \delta_l^{\mathcal{B}}(q_0)}{q_0} . \tag{5.16}$$

This solution only exists when l is even.

The bound state of four-nucleon system

The energy of the system of four nucleons in a bound state is defined by a homogeneous set of integral equations corresponding to (5.4) with $\mathcal{H}_{0II}^{ST} = \mathcal{F}_{0II}^{ST} = 0$, $\mathcal{Z} = -\mathcal{E} + i0$($\mathcal{E}$ is the binding energy of the four-nucleon system). In this case the energy of the system is negative and does not exceed the total energy of possible subsystems in ground states.

VI. Conclusion and discussion

We have outlined a simple method to obtain one-dimensional integral equations for three- and four-nucleon problems where the main emphasis is on the resonating group structure of the wave function. It is clear that the integral equations (3.8) obtained by the above method are similar to that of MITRA [11]. Therefore, our method could be applied for four- or N-nucleon systems, since the resonating group method, which has been applied successfully in the calculation of scattering data of light nuclei, is closely related to the method of pole approximation by which the exact three-body integral equations can be reduced to effective two-body equations [18]. As regards to the four-nucleon equations obtained by other methods [7, 8, 17], our equations have the following advantages. Firstly, they are superior to the pole approximation because the effect of other channels is also taken into account. Secondly, their inhomogeneous terms have a transparent physical meaning in terms of scattering mechanisms, i.e. inhomogeneous terms are plane waves. And, thirdly, the equations are one-dimensional with the kernels containing the functions of two- and three-nucleon bound and scattering states.

For consideration in principle, therefore, our method can be extended to an N-nucleon system and the problem can be reduced to solve one-dimensional coupled integral equations. But in a more complex system, one encounters practical difficulties since in resonating group calculations one employs a completely antisymmetrical wave function which, from a computational point of view, is feasible only for systems with a relatively small number of nucleons. There-

fore, by this method a practical solution of few-body problems involving any number of bound subsystems is only feasible within the range of modern computers.

Acknowledgement

The author is deeply grateful to Prof. A. N. MITRA for his stimulating interest in the subject of this work.

REFERENCES

1. L. D. FADDEEV, Sov. Phys. JETP, **12,** 1014, 1961.
2. R. A. MALFLIET and J. A. TJON, Ann. Phys., **61,** 425, 1970; Phys. Lett., **35B,** 487, 1971.
3. W. M. KLOET and J. A. TJON, Phys. Lett., **37B,** 460, 1971.
4. O. A. YAKUBOVSKY, Jour. Nucl. Phys. (USSR), **5,** 1312, 1967; L. D. FADDEEV, in Three Body Problem in Nuclear and Particle Physics, edited by J. S. C. McKee and P. M. Rolph, North-Holland, Amsterdam, p. 154, 1970.
5. I. M. NARODETSKY, E. S. GALPERN and V. N. LYAKHOVITSKY, Phys. Lett., **46B,** 51, 1973; I. M. NARODETSKY, Nucl. Phys., **A221,** 191, 1974; J. A. TJON, Phys. Lett., **56B,** 217, 1975.
6. V. F. KHARCHENKO and V. P. LEVASHEV, Phys. Lett., **60B,** 317, 1976.
7. V. F. KHARCHENKO and V. E. KUZMICHEV, Nucl. Phys. **A183,** 606, 1972; Nucl. Phys., **A196,** 636, 1972; Czech. J. Phys., **B24,** 1071, 1974.
8. I. M. NARODETSKY and I. L. GRACH, Preprint, ITEP-**955,** Moscow, 1972; Yad. Fiz., **18,** 667, 1973; V. F. KHARCHENKO and V. P. LEVASHEV, Preprint, ITP-**75-137**E, Kiev, 1975.
9. V. K. SHARMA, Nucl. Phys. and Solid St. Phys. (India), **16B,** 104, 1973; Rev. Roum. Phys., **21,** 641, 1976.
10. V. K. SHARMA, Nucl. Phys. and Solid St. Phys. (India), **17B,** 179, 1974; in Few Body Dynamics, edited by A. N. Mitra et al., North-Holland, Amsterdam—Oxford—New York, p. 120, 1976.
11. A. N. MITRA, Nucl. Phys., **32,** 529, 1962; in Advances in Nuclear Physics, Vol. **3,** edited by M. Baranger and E. Vogt, New York, p. 1, 1969.
12. J. A. WHEELER, Phys. Rev., **52,** 1083, 1937.
13. C. LOVELACE, Phys. Rev., **135, B** 1225, 1964.
14. J. WEYERS, Phys. Rev., **145,** 1236, 1966.
15. Y. YAMAGUCHI, Phys. Rev., **95,** 1628, 1954.
16. R. A. BUCKINGHAM and H. S. W. MASSEY, Proc. Roy. Soc., **A179,** 123, 1941; V. K. SHARMA, Nuovo Cimento, **A23,** 679, 1974.
17. A. N. MITRA and S. ROY, Phys. Rev., **137, B** 982, 1965; N. PANCHAPAKESAN, Phys. Rev., **140, B** 20, 1965.
18. J. SCHWAGER, in Few Body Dynamics, edited by A. N. Mitra et al., North-Holland Pub. Company, Amsterdam—New York—Oxford, p. 113, 1976.

Acta Physica Academiae Scientiarum Hungaricae, Tomus 42 (2), pp. 127—136 (1977)

DEBYE—WALLER FACTORS OF FCC METALS

By

J. P. DIXIT and K. N. MEHROTRA

DEPARTMENT OF PHYSICS, D.A.V. COLLEGE, KANPUR 208001, INDIA

(Received in revised form 30. XII. 1976)

The Debye—Waller exponents for five face centered cubic metals (copper, silver, gold, nickel and aluminium) are calculated at different temperatures from the frequency distribution obtained from a lattice dynamical model in which in addition to the central forces (3 neighbours), the CGW type angular forces (2 neighbours) and the volume forces of the SHARMA—JOSHI type are considered. The results are compared with the available experimental findings in terms of the Debye—Waller factor temperature parameter. Reasonably good agreement is found.

I. Introduction

In the recent past, X-ray diffraction technique has been extensively used in the experimental study of the thermal variation of the Debye—Waller factors $\exp(-2B_T)$ of metals. The usual practice of interpreting the experimental observations in terms of the Debye model for phonon spectrum is found to be inadequate [1—2] because the actual lattice vibration of a solid is different from the Debye theory. The aim of our present work is to make use of a more realistic phonon spectrum in the calculation to obtain Debye—Waller factors. For this purpose a phenomenological model which includes (i) central interaction up to third neighbours, (ii) CGW type angular interaction [3] up to second neighbours and (iii) electron-ion interaction on the lines of the SHARMA—JOSHI model [4] is used.

In the present paper we report the computation of temperature variation of the Debye—Waller exponent in five fcc metals: copper, silver, gold, nickel and aluminium. These metals have been selected because a substantial amount of experimental data for Debye—Waller factors has been accumulated in the literature over a wide range of temperature. The phonon spectrum of nickel resembles closely that of copper. Neutron scattering experiments show that interatomic forces in aluminium are of fairly long range nature. The inclusion of third neighbour central interaction and angular forces may have significant effect on their lattice dynamics and hence on the Debye—Waller factor.

II. Theory

The model

The secular determinant for the phonon frequencies of a cubic crystal can be written as

$$|D_{xy}(\mathbf{q}) - m\omega_{\mathbf{q},i}^2 \delta_{xy}| = 0 . \tag{1}$$

Here $\omega_{\mathbf{q},i}$ is the angular frequency of a phonon of wave vector $\mathbf{q}$ and polarization i, m is the mass of an atom in the lattice. For a fcc lattice the typical elements $D_{xy}(\mathbf{q})$ $[x, y = 1, 2, 3]$ of the dynamical matrix are given by

$$\begin{aligned} D_{xy}(\mathbf{q}) &= 2\alpha_1[2 - C_1(C_2 + C_3)] + 4\alpha_2 S_1^2 + 8\alpha_3\left[1 - \frac{2}{3}C_2C_3(2C_1^2 - 1) - \right. \\ &\left. - \frac{1}{6}C_1C_3(2C_2^2 - 1) - \frac{1}{6}C_1C_2(2C_3^2 - 1)\right] + 4(K_1 + K_2) \times \\ &\times [2 - C_1(C_2 + C_3)] - 2K_1(2C_1^2 - C_2^2 - C_3^2) + 2a^3q_1^2K_eG^2(qr_0), \quad x = y \\ D_{xy}(\mathbf{q}) &= 2\alpha_1 S_1 S_2 + \frac{4}{3}\alpha_3 S_1 S_2[4C_3(C_1 + C_2) + 2C_3^2 - 1] - \\ &- 4K_1 S_1 S_2 + 2a^3 q_1 q_2 K_e G^2(qr_0), \qquad x \neq y \end{aligned} \tag{2}$$

where $C_x = \cos(aq_x)$ and $S_x = \sin(aq_x)$, q_x are the components of the phonon wave vector, $2a$ is the lattice parameter and r_0 is the radius of the Wigner—Seitz sphere. α_1, α_2 and α_3 represent the force constants for central interaction corresponding to the first, second and third neighbours and K_1, K_2 are the nearest and next nearest angular force constants, respectively. K_e is the bulk modulus of the electron gas and

$$G(x) = 3\left\{\frac{\sin x - x\cos x}{x^3}\right\} .$$

SHARMA and JOSHI [4] evaluated in their model three force constants in terms of three elastic constants. The present model contains six disposable parameters (α_1, α_2, α_3, K_1, K_2 and K_e) which are fixed by using the relations obtained from the well known method of long wave ($\mathbf{q} \to 0$) expansion of elements and comparison with the Christoffel's equations [5] of elasticity, the zone boundary longitudinal and transverse frequencies in the [100] direction and the longitudinal frequency at the zone boundary in the [111] direction.

Debye—Waller factor

The exponent $2B_T$ of the Debye—Waller factor at temperature T (in the harmonic approximation) is defined by [6]

$$2B_T = \langle \mathbf{K} \cdot \mathbf{u}(l)^2 \rangle \,, \tag{3}$$

where $\mathbf{K}$ is the difference of the scattered wave vector and incident wave vector of the wave and $\mathbf{u}(l)$ is the displacement of the lth atom. From the well known theory of scattering of waves Eq. (3) can be written as:

$$2B_T = \frac{\hbar}{mN} \sum_{\mathbf{q},i} \frac{(\mathbf{K} \cdot \epsilon_{\mathbf{q},i})^2 \left(n_{\mathbf{q},i} + \frac{1}{2} \right)}{\omega_{\mathbf{q},i}} \,. \tag{4}$$

Here $\epsilon_{\mathbf{q},i}$ is the polarization vector of $\mathbf{q}, i$ is the lattice model, N is the total number of unit cells in the crystal and $n_{\mathbf{q},i}$ is the average occupation number of phonons in the mode $\mathbf{q}, i$. For a monatomic cubic lattice Eq. (4) can be written in the form:

$$2B_T = \frac{8\pi^2 \hbar}{3mN} \frac{\sin^2 \theta}{\lambda^2} \int_0^{\omega_{\max}} \frac{F(\omega)}{\omega} \coth \frac{\hbar\omega}{2k_B T} \, d\omega \,, \tag{5}$$

where $F(\omega)$ is the frequency distribution for the phonons, θ is the glancing angle of incidence, λ is the wavelength of the incident waves, k_B is the Boltzmann constant and $\omega_{\max}$ is the maximum frequency of the vibration spectrum.

III. Numerical computation

The Debye—Waller factor exponent $2B_T$ from Eq. (5) at different temperatures has been calculated by BLACKMAN's root sampling technique [7]. The first Brillouin zone has been divided into a mesh of 8000 equal points. The frequencies have been calculated from Eq. (1) for the nonequivalent points lying within (1/48)th irreducible part of the first Brillouin zone. Proper weight was assigned to each non-equivalent point. The number of frequencies falling in each of the intervals of 0.10×10^{13} rad/sec were collected and a histogram of the vibrational spectrum was determined. Using this histogram $2B_T$ was calculated from Eq. (5). The elastic constants and other parameters needed in the calculations are listed in Table I.

The results of calculations are compared with the experimental data in terms of the temperature parameter Y given as:

$$Y = 0.43 \left(\frac{\lambda^2}{\sin^2 \theta} \right) (2B_0 - 2B_T) \,, \tag{6}$$

Table I

Constants and the parameters used in the calculation

Metal	Atomic mass in a m u*	Elastic constants (10^{11} dyn/cm^2)			Ref.	Temp. (°K)**	Lattice parameter (Å)	Phonon frequencies (THz)			Ref.
		C_{11}	C_{12}	C_{44}				$\nu_L(100)$	$\nu_L(100)$	$\nu_T(\frac{1}{2}\frac{1}{2}\frac{1}{2})$	
Copper	63.54	16.85	12.15	7.55	a	296	3.6147	7.21	5.08	7.4	e
Silver	107.87	12.399	9.367	4.612	b	300	4.080	4.93	3.39	5.07	f
Gold	196.967	19.234	16.314	4.195	b	300	4.070	4.61	2.75	4.70	g
Aluminium	26.9815	10.678	6.074	2.821	c	300	4.049	9.645	5.65	9.533	h
Nickel	58.71	24.60	15.00	12.20	d	296	3.524	8.55	6.27	8.88	i

* AIP Handbook, edited by D. E. Gray (McGraw-Hill, New York, 1972).

** Temperature at which elastic constants are measured.

a. W. C. Overton and J. Gaffney, Phys. Rev., **98,** 969, 1955 (as quoted in Ref. e).

b. J. R. Neighbours and G. A. Alers, Phys. Rev., **111,** 707, 1958.

c. G. N. Kamm and G. Alers, J. Appl. Pnys., **33,** 327, 1964.

d. J. de Klerk, Proc. Phys. Soc. (London), **73,** 337, 1959.

e. A. P. Miller and B. N. Brockhouse, Canad. J. Phys., **49,** 704, 1971.

f. W. A. Kamitakahara and B. N. Brockhouse, Phys. Letters, **29A,** 639, 1969.

g. J. W. Lynn, H. G. Smits and R. M. Nicklow, Phys. Rev., **B8,** 3493, 1973.

h. R. Stedman and G. Nilsson, Phys. Rev., **145,** 492, 1966.

i. R. J. Birgenau, J. Cordes, G. Dolling and A. D. B. Woods, Phys. Rev., **136,** A1359, 1964.

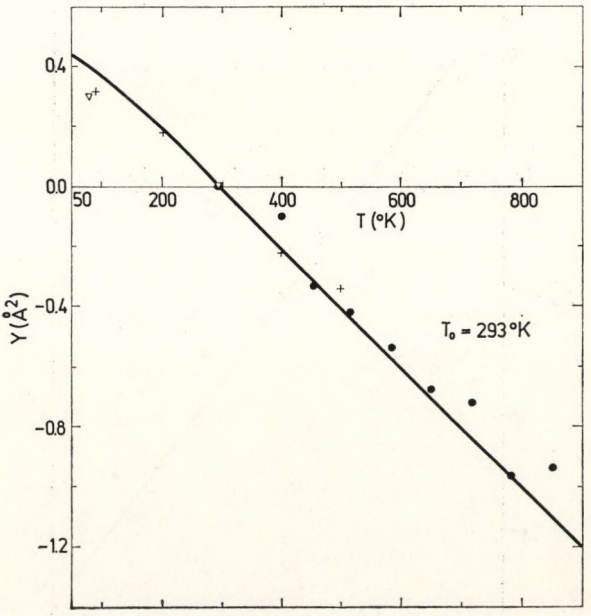

Fig. 1. Variation of Y for copper. Solid line shows the present calculation. Experimental points: ● Owen and Williams; ▽ Chipman and Paskin; + Flinn et al.

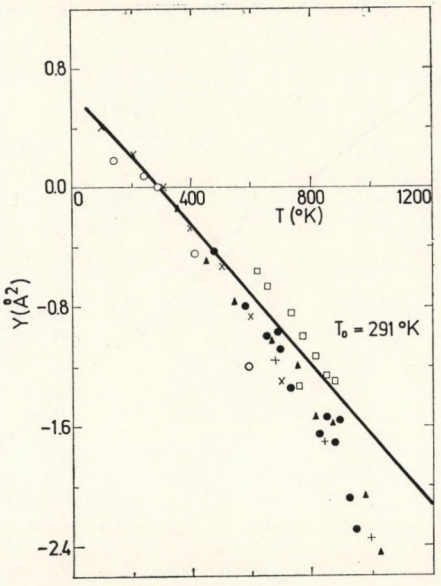

Fig. 2. Variation of Y for silver. Experimental points: ○ Boskovits et al.; □ Andriessen; + Spreadborough and Christian; ● Haworth; ▲ Simerská; × Alexopoulos et al.

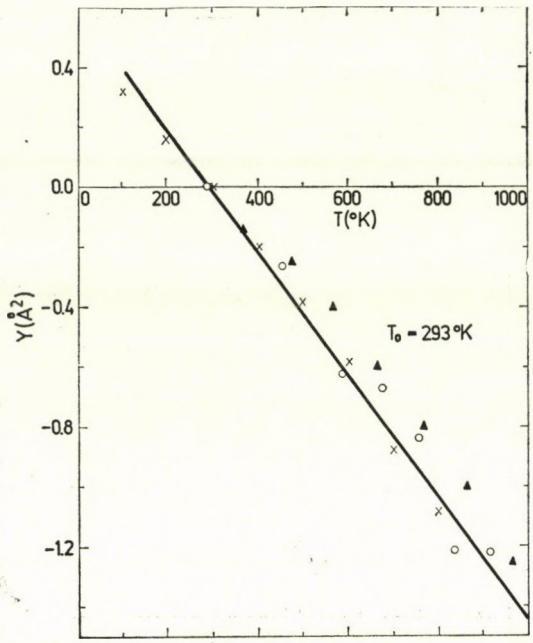

Fig. 3. Variation of Y for gold. Experimental points: ○ OWEN and WILLIAMS; × ALEXOPOULOS et al.; ▲ SYNECEK et al.

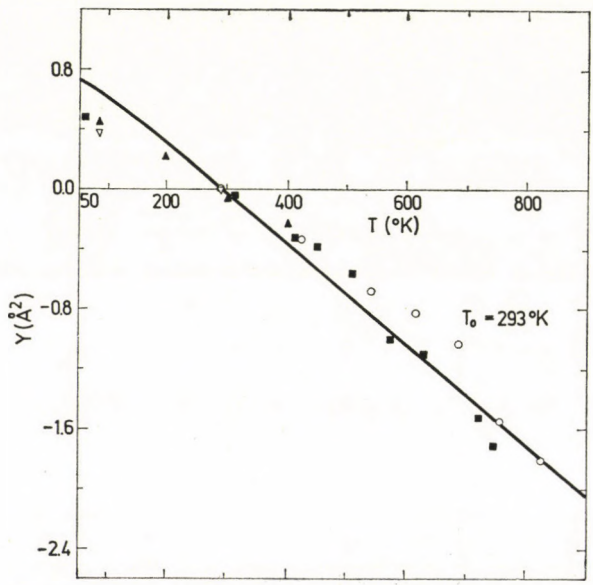

Fig. 4. Variation of Y for aluminium. Experimental points; ○ OWEN and WILLIAMS; ■ CHIPMAN; ▲ FLINN and MCMANUS; ▽ JAMES et al.

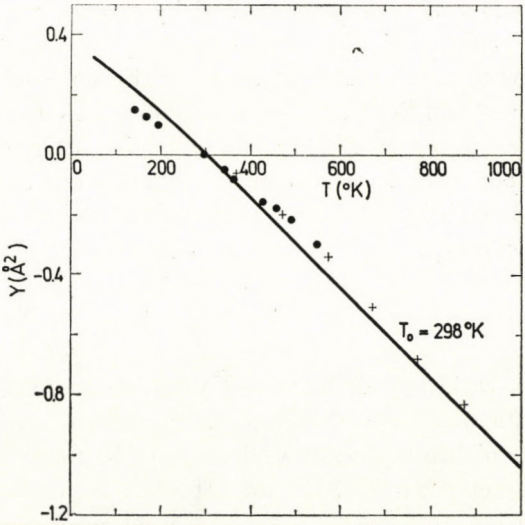

Fig. 5. Variation of Y for nickel. Experimental points: + SIMERSKÁ; ● WILSON et al.

where $2B_0$ is the exponent of Debye—Waller factor at temperature T_0. Y depends only upon the vibration spectrum and is independent of θ and λ. Experimentally determined intensities of Bragg reflections in the X-ray diffraction pattern give us Y directly. If X_T and X_0 are measured intensities of a given reflection at temperature T and T_0, respectively, then

$$\frac{X_T}{X_0} = e^{-2B_T}/e^{-2B_0} .$$

From this we get

$$Y = \frac{\lambda^2}{\sin^2\theta} \log_{10}\left(\frac{X_T}{X_0}\right). \tag{7}$$

Eq. (6) gives the theoretical values of Y while Eq. (7) their experimental values. The computed values of Y for copper, silver, gold, aluminium and nickel along with those obtained by many workers from X-ray intensity measurements are shown in Figs. 1—5.

IV. Results and discussion

(1) *Copper*

The temperature dependence of the intensity of X-ray reflections from a single copper crystal has been studied by FLINN et al [8] in the temperature range 4.2—500 °K. Their results are expressed in terms of the effective Debye temperature. The intensity measurement in the X-ray spectra of powder

specimen from 293 to 900 °K has been studied by OWEN and WILLIAMS [9]. They have given the values of Y at selected temperatures. The results of FLINN et al and OWEN and WILLIAMS agree with those of CHIPMAN and PASKIN [10] at the room and liquid nitrogen temperatures on copper powder. We have deduced the values of Y from the effective Debye temperatures. Fig. 1 shows the experimental results of these authors, taking reference temperature T_0 as 293 °K. The agreement between the theoretical and experimental values is satisfactory.

(2) *Silver*

The temperature variation of Debye—Waller factor of silver from X-ray diffraction experiments has been determined by several authors [11—16]. HAWORTH [11] measured integrated as well as peak intensities of diffraction lines for powder specimen between 286 and 1100 °K. He made correction for the thermal contribution to Bragg peaks and used a specimen repeatedly annealed at 1220 °K. Therefore his results are more reliable than others. His measurements agree with those of SIMERSKÁ [12] and ALEXOPOULOS et al [13] but differ considerably from those of BOSKOVITS [14], ANDRIESSEN [15] and SPREADBOROUGH and CHRISTIAN [16]. The values of all these authors are plotted in Fig. 2. The reference temperature T_0 is 291 °K. An inspection of the Figure shows that the theoretical values of Y agree satisfactorily upto 500 °K with the observations of ALEXOPOULOS et al [13] and thereafter upto 900 °K with the determinations of HAWORTH [11], but beyond that the divergence increases.

(3) *Gold*

The Debye—Waller factor temperature parameter at the selected temperatures in the temperature range 293 to 900 °K has been tabulated by OWEN and WILLIAMS [9]. Their results are in close agreement with the measurements of ALEXOPOULOS et al. [13]. SYNECEK et al [17] have published their experimental results in terms of effective temperatures. The deduced values of Y from these effective temperatures and the work of other authors are plotted in Fig. 3 for comparison with $T_0 = 293$ °K. The theoretical results agree satisfactorily with the observed ones.

(4) *Aluminium*

JAMES et al [18] first reported the reliable measurements of Bragg reflections from a single aluminium crystal at liquid air and room temperatures. Earlier measurements by BACKHURST [19] and COLLINS [20] lack accu-

racy. OWEN and WILLIAMS [9] using powder specimens measured the intensity of X-ray reflections in the temperature range 293—900 °K. CHIPMAN [21] measured the temperature dependence of integrated intensities of X-ray diffraction peaks in the range 60—880 °K. FLINN and MCMANUS [22] measured Debye characteristic temperature in the temperature range 4.2—400 °K. We show in Fig. 4, with $T_0 = 293$ °K, the results of JAMES et al, OWEN and WILLIAMS, CHIPMAN, and FLINN and MCMANUS. The agreement between the computed and experimental values is satisfactory throughout the temperature range studied.

(5) *Nickel*

SIMERSKÁ [23] has published the temperature variation of Debye characteristic temperature of nickel in the range 293—873 °K while WILSON et al [24] reported the experimental results in the temperature range 100—520 °K. Their results in terms of Y are plotted in Fig. 5 with $T_0 = 298$ °K. The experimental values agree reasonably satisfactorily with theory.

The various results of comparison show that the modified SHARMA and JOSHI model provides a reasonable explanation of the experimentally observed temperature variation of the Debye—Waller factor temperature parameter within the framework of approach. A comparison of the present work with those of the earlier workers [25—27] indicates that there is a significant improvement in the case of copper, nickel and aluminium. Discrepancies between the theory and experiment could be the results of neglecting the temperature variation of vibrational frequencies [28] due to thermal expansion and other anharmonic effects [29—33]. In the present calculation the variation of the elastic constants and the lattice parameter with temperature has not been considered. The expansion of lattice at higher temperatures causes a decrease in the vibrational frequencies. Evidently attention has to be paid to this point.

Acknowledgement

One of the authors (J.P.D.) is grateful to the University Grants Commission, New Delhi, for financial assistance.

REFERENCES

1. F. H. HERBSTEIN, Advan. Phys., **10**, 313, 1961.
2. P. DEBRUNNER and R. J. MORRISON, Rev. Mod. Phys., **36**, 463, 1964.
3. P. S. YUEN and Y. P. VARSHNI, Phys. Rev., **164**, 895, 1967.
4. P. K. SHARMA and S. K. JOSHI, J. Chem. Phys., **39**, 2633, 1963; **40**, 662, 1964.
5. A. E. H. LOVE, A Treatise on the Mathematical Theory of Elasticity, Dover Publications, New York, 1944.
6. R. W. JAMES, The Optical Principles of the Diffraction of X-rays, G. Bell and Sons, London, 1954, p. 193.

7. M. Blackman, in Handbuch der Physik, edited by S. Flügge, Springer-Verlag, Berlin, 1955, Vol. 7, p. 325.
8. P. A. Flinn, G. M. McManus and J. A. Rayne, Phys. Rev., **123,** 809, 1961.
9. E. A. Owen and R. W. Williams, Proc. Roy. Soc. (London), **A188,** 509, 1947.
10. D. R. Chipman and A. Paskin, J. Appl. Phys., **30,** 1992, 1959.
11. C. W. Haworth, Phil. Mag., **5,** 1229, 1960.
12. M. Simerská, Acta Cryst., **14,** 1259, 1961.
13. K. Alexopoulos, J. Boskovits, S. Mourikis and M. Roilos, Acta Cryst., **19,** 349, 1965.
14. J. Boskovits, M. Roilos, A. Theodossiou and K. Alexopoulos, Acta Cryst., **11,** 845, 1958.
15. R. Andriessen, Physica, **2,** 417, 1935.
16. J. Spreadborough and J. W. Christian, Proc. Phys. Soc. (London), **74,** 609, 1959.
17. V. Synecek, H. Chessin and M. Simerská, Acta Cryst., **26A,** 108, 1970.
18. R. W. James, G. W. Brindley and R. G. Wood, Proc. Roy. Soc. (London), **A125,** 401, 1929.
19. I. Backhurst, Proc. Roy. Soc. (London), **A102,** 340, 1922.
20. E. H. Collins, Phys. Rev., **24,** 152, 1926.
21. D. R. Chipman, J. Appl. Phys., **31,** 2012, 1960.
22. P. A. Flinn and G. M. McManus, Phys. Rev., **132,** 2458, 1963.
23. M. Simerská, Czech J. Phys., **B12,** 858, 1962.
24. R. H. Wilson, E. F. Skelton and J. L. Katz, Acta Cryst., **21,** 635, 1966.
25. R. P. Gupta and P. K. Sharma, J. Chem. Phys., **46,** 1359, 1967.
26. P. K. Sharma and K. N. Mehrotra, An. Fis., **65,** 189, 1969.
27. J. P. Dixit and K. N. Mehrotra (unpublished; Nickel based on model in Ref. [4]).
28. A. Paskin, Acta Cryst., **10,** 667, 1957.
29. H. Hahn and W. Ludwig, Z. Physik, **161,** 404, 1961.
30. A. A. Maradudin and P. A. Flinn, Phys. Rev., **129,** 2529, 1963.
31. R. A. Cowley, Advan. Phys., **12,** 421, 1963.
32. L. S. Slater, Advan. Phys., **14,** 1, 1965.
33. G. A. Wolfe and B. Goodman, Phys. Rev., **178,** 1171, 1969.

Acta Physica Academiae Scientiarum Hungaricae, Tomus 42 (2), pp. 137—141 (1977)

CALCULATION OF INCOHERENT X-RAY SCATTERING FOR ARGON BY THE STATISTICAL ELECTRON DENSITY DISTRIBUTIONS

By

A. DOBAY-SZEGLETH

INSTITUTE OF PHYSICS, TECHNICAL UNIVERSITY, BUDAPEST

(Received 4. I. 1977)

The paper is concerned with incoherent form factor calculations based on three improved versions of the statistical atom model and the results are illustrated and discussed for Ar.

The formal theory for the scattering of X-ray by bound electrons has been established by WALLER and HARTREE [1]. They use the Born approximation for the calculation of differential cross-section of atoms, which is valid if the X-ray energies are high compared to K-shell binding energies, but small compared to mc^2. In this approximation the differential cross section for incoherent scattering is given by:

$$\sigma(\varkappa) = \sigma_c \int |\psi|^2 \left| \sum_{j=1}^{N} e^{i\bar{\varkappa}\bar{r}_j} \right|^2 \mathrm{d}\bar{\mathbf{x}} = \sigma_c \sum_{i,j} \langle e^{i\bar{\varkappa}(\bar{r}_i - \bar{r}_j)} \rangle, \tag{1}$$

where

$$\sigma_c = \sigma_c(\bar{\varkappa})$$

is the Thomson cross section for scattering by an unbound electron,

$$\psi = \psi(\bar{x}_1, \ldots \bar{x}_N) \tag{2}$$

is the wave function of the ground state of the atom,

$$\bar{x}_j \equiv (\bar{r}_j, \sigma_j) \tag{3}$$

are the electronic space and spin coordinates and $d\bar{x}$ is the product of the $d\bar{x}_j$.

VAN HOVE [2] has shown that the scattering cross section for X-rays by a system of interacting particles can be expressed in terms of density distribution functions for the particles of the system. Following VAN HOVE, D. PARKS and M. ROTENBERG [3] have shown that for systems with large numbers of particles, the incoherent cross section has the form:

$$\sigma_{inc}(\bar{\varkappa}) = \sigma_c \int \mathrm{d}\bar{r}' \int \mathrm{d}\bar{r}\, e^{i\bar{\varkappa}\cdot\bar{r}} \sum_{i,j} [\langle \delta(\bar{r} + \bar{r} - \bar{r}_i)\delta(\bar{r}' - \bar{r}_j)\rangle - \langle \delta(\bar{r} + \bar{r}_i - \bar{r}_j)\rangle\langle \delta(\bar{r}' - \bar{r}_j)\rangle] \tag{4}$$

and in the THOMAS—FERMI approximation the incoherent form factor can be written:

$$F_{inc} \equiv \frac{\sigma_{inc}(\varkappa)}{N\sigma_c} = 1 - \frac{1}{N}\int_0^{R_0} n\,\mathrm{d}\bar{r}' + \frac{\varkappa}{4\pi^2 N}\int_0^{R_0}(3\pi^2 N)^{2/3}\,\mathrm{d}\bar{r}' - \frac{\varkappa^3 R_0^3}{36N}, \quad (5)$$

where

$$n(\bar{r}) = \sum_j \langle \delta(\bar{r} - \bar{r}_j)\rangle \quad (6)$$

is the density distribution and R_0 is defined by

$$n(R_0) = \frac{\varkappa^3}{24\,\pi^2}\,. \quad (7)$$

PARKS and ROTENBERG calculated the incoherent form factor for argon, using THOMAS—FERMI and THOMAS—FERMI—DIRAC densities.

The aim of this paper is to calculate the atomic form factors and the cross sections for X-ray scattering by argon atom using the electron distributions of three more advanced forms of the statistical model of the atom elaborated by GOMBÁS and his co-workers.

First we consider the model, which, besides the exchange correction due to DIRAC [4] contains the WEIZSÄCKER [5] inhomogeneity correction of the kinetic energy. Owing to the effect of the WEIZSÄCKER kinetic energy correction some defects of the statistical atom model disappear. In particular, as a result of this correction, the electron density at the nucleus is finite and falls off exponentially at infinity. The density distribution of this model has been calculated by GOMBÁS [6] for Ar, Ne, Kr and Xe.

It is well-known that the energies of this model, including the WEIZSÄCKER correction, are 20—25% higher than the empirical ones. The origin of this discrepancy has been pointed out by GOMBÁS [7]. The addition of FERMI energy of the electrons and the WEIZSÄCKER correction results in an error, because the two expressions partly overlap, and consequently, a part of the kinetic energy is taken into account twice. The discrepancy can be eliminated by decomposing the kinetic energy to an azymuthal and a radial part and then subtracting the radial self energy of electrons from the radial kinetic energy of the atom. If we add both the DIRAC exchange energy and the GOMBÁS kinetic energy correction to the THOMAS—FERMI model, we arrive at an atom model, which besides its simplicity, describes many features of atoms in a very good approximation.

We shall investigate the X-ray scattering by this second model too.

Our third model is the simplified self-consistent calculation of GOMBÁS and SZONDY [8]. This method will be briefly described below.

The electrons of the atom are grouped into shells corresponding to the principal quantum numbers, i.e. K, L, M, ... shells characterized by the principal quantum numbers $n = 1, 2, 3, \ldots$, respectively. The wave functions of the electrons of the n-th shell are taken to be identical and the radial part of the wave is denoted by $f_n r$. This wave function must, of course, satisfy the usual boundary conditions, so it must vanish for $r = 0$ and $r = \infty$ and it must be a normalized function:

$$\int_0^\infty f_n^2(r)\mathrm{d}r = 1 \,. \tag{8}$$

If there are N_n electrons in the n-th shell, the radial electron density of this shell is

$$D_n(r) = N_n f_n^2(r) \,. \tag{9}$$

The total energy of the atom can be expressed by the functions f_n

$$E = E[f_1, f_2, \ldots] \tag{10}$$

and the wave function f_n are determined from the requirement that E be minimal. GOMBÁS and SZONDY used a Slater-type trial function for f_n

$$f_n(r) = A_n r^{\varkappa_n} e^{-\lambda_n r} \tag{11}$$

and the values of the parameters in the energy minimum are listed in Table I.

Table I

n	$\varkappa_n$	λ_n
1	1.0	18.515
2	2.0	6.560
3	3.0	2.405

The total density of electrons in this model is given by

$$\varrho(r) = \frac{1}{4\pi r^2} \sum_n N_n f_n^2(r) \,. \tag{12}$$

The density distributions of these three models are illustrated in Fig. 1. In this Figure, the radial coordinate r is given in units of a_0 (the Bohr radius) and the abscissa variable $y = rn^{1/2}$ is given in units of $a_0^{-1/2}$.

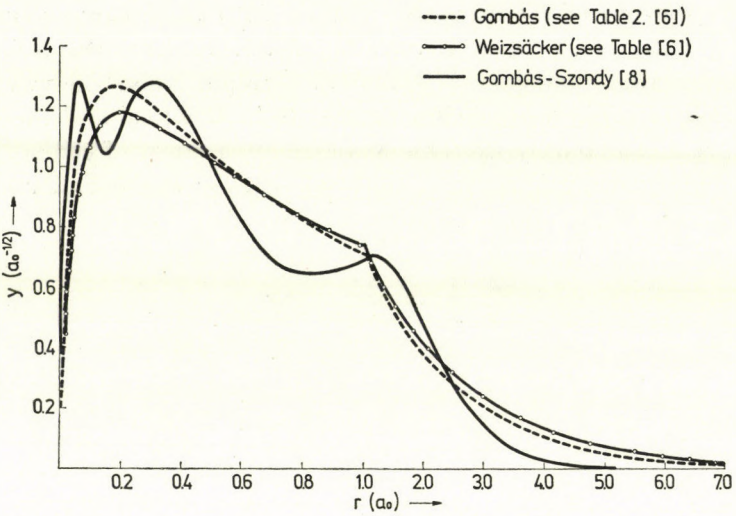

Fig. 1

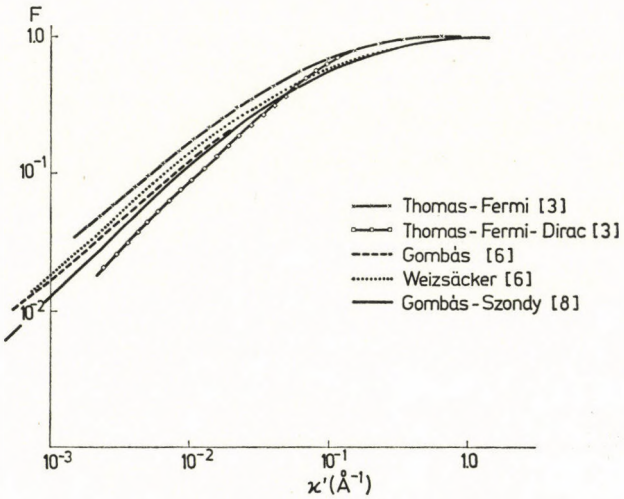

Fig. 2

The results of our calculations concerning F_{inc} for Ar are shown in Fig. 2. The abscissa variable is

$$\varkappa' = \frac{\varkappa}{4\pi Z^{2/3}} = \frac{k}{2\pi Z^{2/3}} \sin\frac{\vartheta}{2}, \tag{13}$$

where k is the wave-number of the incident X-ray, ϑ the angle of the scattering and Z the charge number of the target atom. (In our calculations $Z = 18$.) In Fig. 2 the incoherent form factor of the original THOMAS—FERMI and

THOMAS—FERMI—DIRAC atom models, given by PARKS and ROTENBERG [3] are illustrated by crossed and squared lines, respectively. The results of our calculations are represented by the other characters, the line marked by circles corresponds to the model containing the WEIZSÄCKER correction of the kinetic energy, the dotted line represents the calculation based on the model containing both of the DIRAC's exchange energy and GOMBÁS's kinetic energy correction, and the solid line gives the incoherent form factor for the simplified self-consistent model of GOMBÁS and SZONDY.

Our calculations indicate that the effect on the incoherent form factor of the WEIZSÄCKER correction and the combined correction of DIRAC and GOMBÁS are very similar and the corresponding form factors lie between the THOMAS—FERMI and THOMAS—FERMI—DIRAC models. The simplified self-consistent model due to GOMBÁS and SZONDY results in a form factor, which also remains between the THOMAS—FERMI and THOMAS—FERMI—DIRAC models, but gives somewhat smaller form factors than the above models, especially for small $\varkappa'$-s. Generally, the deviations in the form factors are important in the region of small $\varkappa'$-s ($\varkappa < 10^{-3}$ Å^{-1}) which emphasizes the fact that the outer tail of the electron density distribution has a very important effect on the incoherent form factor. The sharper is the disappearance of the density distribution for $r \to \infty$, the lower is the incoherent form factor for small $\varkappa'$-s. On the other hand, we note that the inner regions of the atomic density distribution have no dramatic effect on F_{inc} and particularly there is no sign of the effect of the shell structure on the incoherent form factor. (See the solid line in Fig. 2.)

Acknowledgment

The author wishes to thank Dr. A. KÓNYA for calling her attention to this topic and his interest in this publication.

REFERENCES

1. I. WALLER and D. R. HARTREE, Proc. Roy. Soc. London, **A124**, 119, 1929.
2. L. VAN HOVE, Phys. Rev., **95**, 249, 1954.
3. D. PARKS and M. ROTENBERG, Phys. Rev., **5**, 521, 1972.
4. L. H. THOMAS, Proc. Cambridge Phil. Soc., **23**, 542, 1926; E. FERMI, Accad. Lincei, **6**, 602, 1927; see also P. GOMBÁS, Die statistische Theorie des Atoms und ihre Anwendungen, Springer, Wien, 1949.
5. P. A. M. DIRAC, Proc. Cambridge Phil. Soc., **26**, 376, 1930.
6. C. F. v. WEIZSÄCKER, Z. Physik, **96**, 431, 1935.
7. P.GOMBÁS, Acta Phys. Hung., **3**, 105, 1953; **3**, 1272, 1953.

Acta Physica Academiae Scientiarum Hungaricae, Tomus 42 (2), pp. 143—149 (1977)

HEAT TRANSFER IN A ROTATING CHANNEL WITH POROUS WALLS

By

V. V. RAMANA RAO and V. BALA PRASAD

DEPARTMENT OF APPLIED MATHEMATICS, ANDHRA UNIVERSITY, WALTAIR 530 003, INDIA

(Received in revised form 4. I. 1977)

An attempt has been made to investigate the effects of uniform suction and injection in the temperature distribution and heat transfer, when a straight channel formed by two parallel porous walls, through which liquid is flowing under a constant pressure gradient, is rotated about an axis perpendicular to the walls. Closed form solutions for temperature θ, Nusselt number Nu are derived. It is found that for a fixed Eckert number E and Prandtl number Pr, the temperature at any point of the fluid decreases in both cases (i) for a fixed Taylor's number α but with an increase in suction Reynolds number β (ii) for a fixed β but with an increase in α. Also for a fixed E and Pr, the Nusselt number Nu is found to decrease in either case. All other parameters remaining fixed, the effect of increasing E is to increase both the temperature at any point of the fluid and the Nusselt number.

1. Introduction

The fundamental difficulty in solving the Navier-Stokes equations either exactly or approximately is the non-linearity introduced by the convection terms in the momentum equations. There exist, however, non-trivial problems in which the convection terms vanish and these provide the simple class of solutions of the equations of motion. One such flow has been considered recently by VIDYANIDHI and NIGAM [1] who have studied the secondary flow when a straight channel formed by two parallel walls, through which liquid is flowing under a constant pressure gradient, is rotated about an axis perpendicular to the walls. This problem was later extended by VIDYANIDHI, BALA PRASAD and RAMANA RAO [2] to include the effects of uniform injection at the lower wall and an equal rate of suction at the upper wall.

However, little effort has been made to determine the effects of uniform injection and an equal rate of suction at the lower and upper walls of a porous channel or vice-versa on the temperature distribution and heat transfer. INMAN [3] has determined the effect of the variation of cross-flow velocity on the temperature distribution and heat transfer for flow in an annular pipe with porous walls under the assumption that the fluid injection rate at one wall is equal to the fluid withdrawal rate at the other wall.

In this paper we have investigated the effects of uniform injection and an equal rate of suction at the lower and upper walls or vice-versa on the

temperature distribution and heat transfer for the fluid flow under a constant pressure gradient through a channel formed by the two walls and when rotated about an axis perpendicular to the walls. The assumptions made in the present study are:

(a) the fluid is incompressible and heat conduction is negligible;
(b) the wall temperatures are constant and
(c) no diffusion takes place.

2. Basic equations and their solution

Following the notation as in our earlier work [2], the equations of motion and energy become in non-dimensional form,

$$\beta \frac{du_x}{dz} - 2\alpha^2 u_y = 2 + \frac{d^2 u_x}{dz^2}, \tag{1}$$

$$\beta \frac{du_y}{dz} + 2\alpha^2 u_x = \frac{d^2 u_y}{dz^2}, \tag{2}$$

$$\frac{d^2\theta}{dz^2} - Pr\beta \frac{d\theta}{dz} = -PrE\left\{\left(\frac{du_x}{dz}\right)^2 + \left(\frac{du_y}{dz}\right)^2\right\}, \tag{3}$$

and are to be solved subject to the boundary conditions

$$u_x = u_y = 0 \quad \text{at} \quad z = \pm 1, \tag{4}$$

$$\theta = 0, 1 \quad \text{at} \quad z = \mp 1, \tag{5}$$

where we have further introduced the non-dimensional quantities

$$Pr = \frac{\mu c_p}{k} \text{ (Prandtl number)}, \quad \theta = \frac{T - T_L}{T_U - T_L}, \tag{6}$$

$$E = \left(\frac{PL^2}{2P_v}\right)^2 \Big/ c_p(T_U - T_L) \text{ (Eckert number)},$$

and it is assumed that

T_U (temperature at the upper wall) $\gg T_L$ (temperature at the lower wall).

The solutions of Eqs. (1, 2) subject to the boundary conditions of Eq. (4) have been provided in Eqs. (2.10), (2.11) of our earlier work [2]. Substituting these expressions in Eq. (3) and solving subject to the boundary conditions of Eq. (5), we obtain

$$\theta = A_1 + B_1 e^{Pr\beta z} - PrEf(z), \tag{7}$$

where

$$A_1 = \frac{1}{2\sinh Pr\beta}\left[-e^{-Pr\beta} + PrE\left\{e^{Pr\beta}f(-1) - e^{-Pr\beta}f(1)\right\}\right], \tag{8}$$

$$B_1 = \frac{1}{2\sinh Pr\beta}\left[1 + PrE\left\{f(1) - f(-1)\right\}\right], \tag{9}$$

$$f(z) = \frac{(k_1 + k_2 + 2k_4)\,e^{(\beta+m)z}}{16\alpha^4(\beta+m)\left\{m+(1-Pr)\beta\right\}} + \frac{(k_1 + k_2 - 2k_4)e^{(\beta-m)z}}{16\alpha^4(\beta-m)\left\{-m+(1-Pr)\beta\right\}} + \\ + \frac{e^{\beta z}\left[(\beta^2 - n^2 - Pr\beta^2)\left\{(k_1 - k_2)\cos nz + 2k_3 \sin nz\right\} + \right.}{\left. + \beta n(2-Pr)\left\{(k_1 - k_2)\sin nz - 2k_3\cos nz\right\}\right]} \\ 8\alpha^4\left\{(\beta^2 - n^2 - Pr\beta^2)^2 + \beta^2 n^2(2-Pr)^2\right\}, \tag{10}$$

$$k_1 = \beta^2 c_1^2 c_2^2 + \beta^2 c_1^2 c_3^2 + m^2 c_4^2 c_5^2 + n^2 c_4^2 c_6^2 + n^2 c_4^2 c_5^2 + m^2 c_4^2 c_6^2 + \\ + 2n\beta c_1 c_2 c_4 c_5 - 2m\beta c_1 c_2 c_4 c_6 - 2m\beta c_1 c_3 c_4 c_5 - 2n\beta c_1 c_3 c_4 c_6, \tag{11}$$

$$k_2 = \beta^2 c_4^2 c_5^2 + \beta^2 c_4^2 c_6^2 + m^2 c_1^2 c_2^2 + n^2 c_1^2 c_3^2 + m^2 c_1^2 c_3^2 + n^2 c_1^2 c_2^2 - \\ - 2m\beta c_1 c_3 c_4 c_5 - 2n\beta c_1 c_2 c_4 c_5 - 2m\beta c_1 c_2 c_4 c_6 + 2n\beta c_1 c_3 c_4 c_6, \tag{12}$$

$$k_3 = \beta^2 c_1 c_2 c_4 c_5 - \beta^2 c_1 c_3 c_4 c_6 + m^2 c_1 c_3 c_4 c_6 - n^2 c_1 c_2 c_4 c_5 + \\ + n^2 c_1 c_3 c_4 c_6 - m^2 c_1 c_2 c_4 c_5 - n\beta c_1^2 c_3^2 - n\beta c_1^2 c_2^2 + n\beta c_4^2 c_5^2 + n\beta c_4^2 c_6^2, \tag{13}$$

$$k_4 = -\beta^2 c_1 c_3 c_4 c_5 - \beta^2 c_1 c_2 c_4 c_6 - m^2 c_1 c_2 c_4 c_6 - n^2 c_1 c_3 c_4 c_5 - \\ - n^2 c_1 c_2 c_4 c_6 - m^2 c_1 c_3 c_4 c_5 + \\ + \beta m c_1^2 c_2^2 + \beta m c_1^2 c_3^2 + \beta m c_4^2 c_5^2 + \beta m c_4^2 c_6^2, \tag{14}$$

$$c_1 = \frac{\cosh(\beta/2)}{\sin h^2 \frac{m}{2} + \cos^2 \frac{n}{2}}, \tag{15}$$

$$c_2 = \sinh \frac{m}{2} \sin \frac{n}{2}, \tag{16}$$

$$c_3 = \cosh \frac{m}{2} \cos \frac{n}{2}, \tag{17}$$

$$c_4 = \frac{\sinh(\beta/2)}{\sinh^2 \frac{m}{2} + \sin^2 \frac{n}{2}}, \tag{18}$$

$$c_5 = \sinh \frac{m}{2} \cos \frac{n}{2}, \tag{19}$$

$$c_6 = \cosh\frac{m}{2}\sin\frac{n}{2}, \tag{20}$$

$$m = \left(\sqrt{\frac{\beta^4 + 64\,\alpha^4} + \beta^2}{2}\right)^{1/2}, \tag{21}$$

$$n = \left(\sqrt{\frac{\beta^4 + 64\,\alpha^4} - \beta^2}{2}\right)^{1/2}, \tag{22}$$

When $\alpha = 0$, $\beta \neq 0$, we get

$$\theta = A_2 + B_2\, e^{Pr\beta z} - \frac{4PrE}{\beta^2 \sinh^2\beta} \times \\ \times \left[\frac{e^{2\beta z}}{2(2 - Pr)} - \frac{z\sinh^2\beta}{Pr\beta} - \frac{2(\sinh\beta)\, e^{\beta z}}{\beta(1 - Pr)}\right], \tag{23}$$

$$A_2 = \frac{4PrE}{\beta^2 \sinh^2\beta}\left[\frac{e^{-2\beta}}{2(2 - Pr)} + \frac{\sinh^2\beta}{Pr\beta} - \frac{2\,(\sinh\beta)e^{-\beta}}{\beta(1 - Pr)}\right] - \\ - \frac{e^{-Pr\beta}}{2\sinh Pr\beta} - \frac{2PrEe^{-Pr\beta}}{\beta^2 \sinh^2\beta \sinh Pr\beta} \times \\ \times \left[\frac{\sinh 2\beta}{2 - Pr} - \frac{2\sinh^2\beta}{Pr\beta} - \frac{4\sinh^2\beta}{\beta(1 - Pr)}\right], \tag{24}$$

$$B_2 = \frac{1}{2\sinh Pr\beta} + \frac{2PrE}{\beta^2 \sinh^2\beta \sinh Pr\beta} \times \\ \times \left[\frac{\sinh 2}{2 - Pr} - \frac{2\sinh^2\beta}{Pr\beta} - \frac{4\sinh^2\beta}{\beta(1 - Pr)}\right]. \tag{25}$$

When $\beta = 0$, $\alpha \neq 0$, we get

$$\theta = \frac{1}{2}\left[1 + z + \frac{PrE(\cosh 2\alpha - \cosh 2\alpha z + \cos 2\alpha - \cos 2\alpha z)}{2\alpha^4(\sin h^2\alpha + \cos^2\alpha)}\right]. \tag{26}$$

When $\beta = 0$, $\alpha = 0$, we get

$$\theta = \frac{1}{2}\left[1 + z + \frac{2PrE}{3}(1 - z^4)\right]. \tag{27}$$

The rate of heat transfer in terms of the Nusselt number is

$$Nu = \frac{L}{T_U - T_L}\left(\frac{dT}{dz'}\right)_{z'=-L} = \left(\frac{d\theta}{dz}\right)_{z=-1}. \tag{28}$$

Hence from Eqs. (7) and (28), we have

$$Nu = Pr\beta B_1 e^{-Pr\beta} - PrEf'(-1)\,. \tag{29}$$

where dash denotes differentiation with respect to z.

When $\alpha = 0$, $\beta \neq 0$, we get

$$Nu = Pr\beta\, B_2\, e^{-Pr\beta} - \frac{4PrE}{\beta^2 \sinh^2 \beta}\left[\frac{\beta e^{-2\beta}}{2-Pr} - \frac{\sinh^2 \beta}{Pr\beta} - \frac{2e^{-\beta}\sinh \beta}{1-Pr}\right]. \tag{30}$$

When $\beta = 0$, $\alpha \neq 0$, we get

$$Nu = \frac{1}{2}\left[1 + \frac{PrE\,(\sinh 2\alpha - \sin 2\alpha)}{a^3(\sinh^2 \alpha + \cos^2 \alpha)}\right]. \tag{31}$$

When $\beta = 0$, $\alpha = 0$, we get

$$Nu = \frac{1}{2}\left[1 + \frac{8PrE}{3}\right]. \tag{32}$$

3. Results and discussion

If we replace the suctions Reynolds number β by their negative values and z by $-z$, the expressions for both the primary and secondary velocity distributions as given by Eqs. (2.10) and (2.11) of our work [2] do not change.

Table I

Temperature profiles for $Pr = 0.7$ and $E = 0$

z	$\beta = 0$	$\beta = 1$
−0.1	0	0
−0.8	0.1	0.049187
−0.6	0.2	0.105765
−0.4	0.3	0.170845
−0.2	0.4	0.245704
0	0.5	0.331813
0.2	0.6	0.430862
0.4	0.7	0.544795
0.6	0.8	0.675850
0.8	0.9	0.826599
1	1	1

This shows that when there is uniform injection at the lower wall, the primary and secondary flow distributions in the lower half are the same as in the upper half for the case of uniform injection at the upper wall and vice-versa. Hence in the numerical computations involved in this problem, we have considered the positive values of the suction Reynolds number.

For $Pr = 0.7$, Tables I—III show the temperature profiles for $\beta = 0,1$, $\alpha = 0, 1$ and $E = 0, 1, 2$. It is inferred that for fixed Eckert number E and the Prandtl number Pr, the temperature at any point of the fluid decreases

Table II

Temperature profiles for $Pr = 0.7$ and $E = 1$

z	$\alpha=0,\ \beta=0$	$\alpha=0,\ \beta=1$	$\alpha=1,\ \beta=0$	$\alpha=1,\ \beta=1$
−1	0	0	0	0
−0.8	0.237760	0.139447	0.183449	0.097345
−0.6	0.403093	0.253919	0.322701	0.184469
−0.4	0.527360	0.351317	0.437227	0.266538
−0.2	0.632960	0.440988	0.540575	0.365985
0	0.733333	0.532700	0.640798	0.453289
0.2	0.832960	0.634982	0.740575	0.536997
0.4	0.927360	0.751827	0.837227	0.674524
0.6	1.003093	0.875569	0.922701	0.799161
0.8	1.037760	0.979636	0.977340	0.919294
1	1	1	1	1

Table III

Temperature profiles for $Pr = 0.7$ and $E = 2$

z	$\alpha=0,\ \beta=0$	$\alpha=0,\ \beta=1$	$\alpha=1,\ \beta=0$	$\alpha=1,\ \beta=1$
−1	0	0	0	0
−0.8	0.375520	0.229706	0.266898	0.145502
−0.6	0.606187	0.402074	0.445402	0.263175
−0.4	0.754720	0.531545	0.574454	0.362233
−0.2	0.865920	0.636270	0.681159	0.486267
0	0.970000	0.733586	0.739756	0.574764
0.2	1.065920	0.839100	0.881159	0.677633
0.4	1.154720	0.958348	0.974454	0.804252
0.6	1.206187	1.075286	1.045402	0.922471
0.8	1.175520	1.132673	1.066898	1.011989
1	1	1	1	1

in both the cases (i) for a fixed Taylor's number α but with an increase in the suction Reynolds number β (ii) for a fixed β but with an increase in α. Also for fixed values of Pr, β and α, the effect of increasing the Eckert number is to increase the temperature at any point of the fluid.

Table IV

Values of the Nusselt number for $Pr = 0.7$

E	β	α:	0	1	2
0	0		0.500000	0.500000	0.500000
	1		0.229118	0.229118	0.229118
1	0		1.433333	1.068520	0.592070
	1		0.770650	0.572602	0.274463
2	0		2.366666	1.637040	0.684140
	1		1.312182	0.916085	0.319807

Table IV shows the calculated values of the Nusselt number for fixed Pr but for different values of E, β and α. For fixed E and Pr, the Nusselt number Nu is found to decrease in both cases (i) for fixed α but with increasing β; (ii) for fixed β but with increasing α. For fixed values of α and β, the effect of increasing the Eckert number is to increase the Nusselt number.

REFERENCES

1. V. VIDYANIDHI and S. D. NIGAM, Jour. Math. Phys. Sci., **1**, 85, 1967.
2. V. VIDYANIDHI, V. BALA PRASAD and V. V. RAMANA RAO, J. Phys. Soc. Japan, **39**, 1077, 1975.
3. R. M. INMAN, J. Aero-Space Sci, **26**, 532, 1959.

Acta Physica Academiae Scientiarum Hungaricae, Tomus 42 (2), pp. 151—157 (1977)

AVERAGE HYDRODYNAMIC BEHAVIOUR OF A NON-LINEAR PION-PION CHIRAL LAGRANGIAN

By

M. LAKSHMANAN*

INSTITUT FÜR THEORETISCHE PHYSIK DER UNIVERSITÄT TÜBINGEN, 7400 TÜBINGEN, W. GERMANY

(Received 10. I. 1977)

In the study of the behaviour of matter at superhigh densities (10^{16} g/cm^3),the properties of e^+e^- and $p - p$ collisions are known to provide conditions which determine the equation of state. In this paper, assuming that a system of pions is a good representation of $p - p$ collisions, we study the hydrodynamic behaviour of an SU(2)×SU(2) chiral Lagrangian in the GASIOROWICZ—GEFFEN coordinates with symmetry-breaking terms included. This model possesses simple classical solutions. By the application of the averaging method of MILEKHIN, we obtain the equation of state and discuss its implications.

I. Introduction

In an attempt to describe the behaviour of matter at densities higher than 10^{16} g/cm^3 and to determine the equation of state $p = c_s^2 E$, CANUTO and LODENQUAI [1] recently made use of the data available on e^+e^- and $p - p$ collisions in the LANDAU hydrodynamic model [2]. The conclusion was that at these superhigh densities $c_s^2 \to 1$, i.e., the pressure p keeps on increasing and approaches E asymptotically and that one does not recover the result of a non-interacting system (i.e. $c_s^2 \to 1/3$). It has been pointed out by HEISENBERG [3] that for a large number of produced particles the meson field is classical in the first approximation and that the system is sufficiently homogeneous to use for its description solutions depending on time only. Later on MILEKHIN [4] has developed a method in which quantum effects are averaged over, a procedure analogous to the method of adiabatic invariants in ordinary mechanics, on account of the large number of particles present and the fact that one is dealing with large quantum numbers.

Assuming now that in the interior of a star at these superhigh densities [1] a system of pions is indeed a good representation of the $p - p$ collision process (and hopefully expecting that the complications due to the presence of the mixture of n, Λ, Σ, etc., alter the equation of state very little), one can study the consequences of the interaction once we know the classical solutions. Realistic interacting systems do not always possess simple solutions even in

* Alexander von Humboldt Research Fellow, on leave of absence from the Department of Theoretical Physics, University of Madras, Madras-600025, India.

the classical case [5]. However, recently [6] we have pointed out that the equation of motion of the system whose classical Lagrangian is

$$L = \frac{1}{2}\left[\dot{\mathbf{q}}^2 - \frac{\lambda(\mathbf{q}\cdot\dot{\mathbf{q}})^2}{(1-\lambda\mathbf{q}^2)} - \frac{m^2\mathbf{q}^2}{(1-\lambda\mathbf{q}^2)}\right] \tag{1}$$

admits simple harmonic periodic bounded solutions [7] and even the corresponding quantum-mechanical version is exactly solvable [8]. We note that the model (1) is just the SU(2)⊗SU(2) chiral Lagrangian (in zero-space dimension) where the triplet field $\boldsymbol{\Phi}(\mathbf{x}, t)$ is replaced by $\mathbf{q}(t)$, with symmetry-breaking non-polynomial term $[m^2\mathbf{q}^2/(1-\lambda\mathbf{q}^2)]$ added to it.

The aim of the present paper is to investigate the average hydrodynamic properties of the pionic system with the aid of the classical solutions and derive the equation of state. The plan of the paper is as follows. In Section II we give a brief account of the formalism of MILEKHIN's hydrodynamic treatment of the pion-pion Lagrangian. In Section III we derive the classical solutions of our model (1) and in Section IV the hydrodynamic properties of our model are obtained. In Section V we briefly discuss the results in lieu of the recent solutions for the LANDAU hydrodynamic model obtained by PERESSUTTI [9].

II. The hydrodynamic formulation for the pion-pion Lagrangian

In the LANDAU hydrodynamic model [2] the run of the thermodynamic and hydrodynamic variables such as temperature and fluid velocity against space and time during the expansion of the hadronic matter are contained in the relativistic Navier—Stokes equation

$$T_{\mu\nu,\nu} = 0\,, \tag{2}$$

where the energy-momentum tensor in Eq. (2) is of the form

$$T_{\mu\nu} = p\delta_{\mu\nu} + (p+E)u_\mu u_\nu + \tau_{\mu\nu}\,. \tag{3}$$

Here $\tau_{\mu\nu}$ is the dissipative term, and u_μ is the usual four velocity in relativistic hydrodynamics. In order to use $T_{\mu\nu}$ in Eq. (2) we need an equation of state $p = p(E)$, where p is the pressure and E is the energy density. The energy-momentum tensor in terms of the Lagrangian

$$\mathfrak{L} = \mathfrak{L}(\Phi^a, \Phi^b_\mu)\,,\ \Phi_\mu = \frac{\partial\Phi}{\partial x_\mu}\,. \tag{4}$$

is of the form

$$T_{\mu\nu} = \mathfrak{L}\delta_{\mu\nu} - 2\frac{\partial\mathfrak{L}}{\partial\Phi_\alpha^2}\Phi_\mu\Phi_\nu\,. \tag{5}$$

As we are interested in the average hydrodynamic behaviour of $\mathfrak{L}$, on comparison of Eqs. (3) we put $\tau_{\mu\nu} = 0$. Then defining the velocity to be

$$u_\mu = \frac{\Phi_\mu}{(-\Phi_\alpha^2)^{1/2}}\,,\quad u_\mu^2 = -1 \tag{6}$$

we identify the Lorentz-invariant proper pressure and energy density of the fluid element to be

$$p = \mathfrak{L},\quad E = 2\frac{\partial\mathfrak{L}}{\partial\Phi_\alpha^2}\Phi_\beta^2 - \mathfrak{L}\,. \tag{7}$$

Now if the supposed system is sufficiently uniform so that the momentum is zero corresponding to the proper frame, i.e. $\Phi_k = 0$, then the energy density in Eq. (7) becomes

$$E = \dot{\phi}\frac{\partial\mathfrak{L}}{\partial\dot{\phi}} - \mathfrak{L}\,. \tag{8}$$

Limiting ourselves to fields that are periodic of period $\tau(E)$, the average pressure over one cycle is given by

$$p = p(E) = \frac{1}{\tau(E)}\oint \mathfrak{L}\,dt\,, \tag{9}$$

which is the desired equation of state. The use of time-averaged quantities is valid only if the system at a given point changes little over the period τ, which means the system should be sufficiently uniform. Similar averaging procedures are common in mechanics which goes in the name of the method of adiabatic invariants [10] and modulation methods in non-linear wave propagation problems [11, 12].

III. The model and its solutions

We now assume that the pionic interaction can be represented by the chiral SU(2)⊗SU(2) Lagrangian in the GASIOROWICZ—GEFFEN coordinates [13] with symmetry breaking terms of the form

$$\mathfrak{L} = \frac{1}{2}\left[-(\partial_\mu\boldsymbol{\Phi})^2 - \frac{\lambda(\boldsymbol{\Phi}\cdot\partial_\mu\boldsymbol{\Phi})^2}{(1-\lambda\boldsymbol{\Phi}^2)} - \frac{m^2\boldsymbol{\Phi}^2}{(1-\lambda\boldsymbol{\Phi}^2)}\right], \tag{10}$$

where Φ is the isotriplet field. Assuming the validity of uniformity condition in accordance with Section II, we have $\Phi_k = 0$, so that $\Phi(\mathbf{x},t) = \Phi(t) = \mathbf{q}(t)$ and

$$\mathfrak{L} = \frac{1}{2}\left[\dot{\mathbf{q}}^2 + \frac{\lambda(\mathbf{q}\cdot\dot{\mathbf{q}})^2}{(1-\lambda\mathbf{q}^2)} - \frac{m^2\mathbf{q}^2}{(1-\lambda\mathbf{q}^2)}\right]. \tag{11}$$

The Euler—Lagrange equation of motion corresponding to the system (11) is given by

$$\ddot{\mathbf{q}}_i + \left[\frac{\lambda(\mathbf{q}\cdot\ddot{\mathbf{q}})}{(1-\lambda\mathbf{q}^2)} + \frac{\lambda\dot{\mathbf{q}}^2}{(1-\lambda\mathbf{q}^2)} + \frac{\lambda^2(\mathbf{q}\cdot\dot{\mathbf{q}})^2}{(1-\lambda\mathbf{q}^2)^2} + \frac{m^2}{(1-\lambda\mathbf{q}^2)^2}\right] q_i = 0\,. \tag{12}$$

With the introduction of the polar coordinates

$$\left.\begin{aligned} q_1 &= q\sin\theta\cos\varphi\,,\\ q_2 &= q\sin\theta\sin\varphi\,,\\ q_3 &= q\cos\theta\,. \end{aligned}\right\} \tag{13}$$

Eq. (12) separates into the following system of differential equations:

$$q^2\sin^2\theta\dot{\phi} = C_1 = \text{const.} \tag{14}$$

$$q^4\dot{\theta}^2 + \frac{C_1^2}{\sin^2\theta} = C_2^2 = \text{const.} \tag{15}$$

and

$$\ddot{q} + \frac{\lambda q(\dot{\mathbf{q}})^2}{(1-\lambda q^2)} + \frac{m^2 q}{(1-\lambda q^2)} = \frac{C_2^2(1-\lambda q^2)}{q^3}\,. \tag{16}$$

Eq. (14) and (15) represent the conservation of the vector current. To obtain the periodic solutions of the system (12) we integrate once Eq. (16) to

$$\frac{\dot{q}^2}{(1-\lambda q^2)} + \frac{m^2}{\lambda}\cdot\frac{1}{(1-\lambda q^2)} + \frac{C_2^2}{q^2} = C_3 = \text{const}\,. \tag{17}$$

For the isoscalar case ($C_2 = 0$) one immediately obtains [7] the solution as

$$q(t) = A\sin(\omega t + \eta) \tag{18a}$$

with

$$\omega^2 = [m^2/(1-\lambda A^2)]\,. \tag{18b}$$

When $C_2 \neq 0$ one can also give the exact solution after some manipulations in the form

$$q(t) = A[1-\beta\sin^2(\omega t+\zeta)]^{1/2}\,, \tag{19}$$

where

$$\omega^2 = \left[\frac{m^2}{(1-\lambda A^2)} + \frac{\lambda C_2^2}{A^2}\right] \tag{20}$$

and

$$\beta = \left[1 - \frac{1}{\lambda A^2}\left\{(1-\lambda A^2) - \frac{(m^2 - \lambda^2 C_2^2)}{\omega^2}\right\}\right]. \tag{21}$$

Here the amplitude A is given in terms of the integration constants C_2 and C_3 by the following expression:

$$A^2 = c + \left(c^2 - \frac{C_2^2}{\lambda C_3}\right)^{1/2}, \tag{22}$$

where

$$c = \frac{1}{2\lambda}\left[1 - \frac{1}{\lambda C_3}(m^2 - \lambda C_3)\right]. \tag{23}$$

One can easily note that when $\lambda > 0$ the range of the periodic solutions is such that $0 \leq A \leq \lambda^{-1/2}$, whereas if $\lambda < 0$ there is no such restriction.

Now the canonically conjugate momenta for the Lagrangian (11) are

$$\mathbf{p} = \dot{\mathbf{q}} + \frac{\lambda(\mathbf{q}\cdot\dot{\mathbf{q}})}{(1-\lambda\mathbf{q}^2)}\mathbf{q}, \tag{24}$$

so that the classical Hamiltonian becomes

$$\begin{aligned} H &= \frac{1}{2}\left[\dot{\mathbf{q}}^2 + \frac{\lambda(\mathbf{q}\cdot\dot{\mathbf{q}})^2}{(1-\lambda\mathbf{q}^2)} + \frac{m^2\mathbf{q}^2}{(1-\lambda\mathbf{q}^2)}\right] = \\ &= \frac{1}{2}\left[\mathbf{p}^2 - \lambda(\mathbf{p}\cdot\mathbf{q})^2 + \frac{m^2\mathbf{q}^2}{(1-\lambda\mathbf{q}^2)}\right]. \end{aligned} \tag{25}$$

On substitution of the periodic solutions (19)—(21) in (25) we obtain the expression for the classical energy as

$$E = \frac{1}{2}\left[\frac{m^2A^2}{(1-\lambda A^2)} + \frac{C_2^2}{A^2}\right] = \frac{1}{2}\left[\frac{\omega^2}{\lambda} - \frac{m^2}{\lambda}\right]. \tag{26}$$

IV. The average hydrodynamical quantities

Following Section II, the proper pressure of the pionic system (10) is given by

$$\begin{aligned} P &= \frac{1}{\tau(A)} \oint \mathfrak{L}\, dt \\ &= \frac{\omega}{\lambda} \oint \left[\frac{(\dot{q}^2 - m^2 q^2)}{(1 - \lambda q^2)} + \frac{C_2^2}{q^2} \right] dt \\ &= \frac{1}{\pi} \int_0^{\pi} \left\{ \frac{\omega^2 A^2 \sin^2 \eta \cos^2 \eta}{(1 - \beta \sin^2 \eta)[1 - \lambda A^2 + \lambda A^2 \beta \sin^2 \beta]} - \right. \\ &\left. - \frac{kA^2(1 - \beta \sin^2 \eta)}{[1 - \lambda A^2 + \lambda A^2 \beta \sin^2 \eta]} + \frac{C_2^2}{A^2} \cdot \frac{1}{(1 - \beta \sin^2 \eta)} \right\} d\eta \,. \end{aligned} \tag{27}$$

The elementary integrals in Eq. (27) may be evaluated without much difficulty. We make use of the following results in this evaluation:

$$\begin{aligned} \int_0^{\pi} \frac{d\eta}{(1 - \beta \sin^2 \eta)} &= \frac{1}{\sqrt{1-\beta}} \cdot \pi, \int_0^{\pi} \frac{d\eta}{[1 - \lambda A^2(1 - \beta \sin^2 \eta)]} = \\ &= \frac{\pi}{\sqrt{1-\lambda A^2}} \cdot \frac{1}{\sqrt{1 - \lambda A^2(1 - \beta)}} \,. \end{aligned} \tag{28}$$

Finally, we obtain the expression for pressure after simplification as

$$p = \frac{1}{2} \left[\frac{\omega^2}{\lambda} + \frac{m^2}{\lambda} - \frac{2\omega m}{\lambda} \right] . \tag{29}$$

On substitution of the classical expression (26) we find that

$$p = \left[\frac{m^2}{\lambda} - (m^2 + 2\lambda E)^{1/2} \frac{m}{\lambda} + E \right] . \tag{30}$$

We thus find that for very low energies the pressure vanishes:

$$p \approx 0 \quad \text{when} \quad E \ll 1 \,. \tag{31a}$$

And at high energy densities the pressure asymptotically approaches E:

$$p \approx E \quad \text{when} \quad E \gg 1 \,. \tag{31b}$$

V. Discussion

We infer from the expression for p at low energies that the pressure is nearly zero corresponding to large multiplicity of produced pions so that POMERANCHUK's statistical model [14] describes the system correctly. At large energies the pressure increases and the multiplicity is slowed down and as a result hydrodynamic acceleration occurs. The LANDAU's hydrodynamical model is valid in such a case. Recent studies of PERESSUTTI [9] also lend credence to these results. He has investigated the LANDAU hydrodynamical model by assuming the generalized equation of state of the form $p = c_0^2 E$, where c_0^2 is a constant parameter bounded in the interval (0, 1) and interpreted as the local velocity of sound in the medium. In the case of an ideal fluid the time t at the moment of disintegration has been shown to be

$$t_k \sim E_{\text{Lab}}^{\frac{1}{2}(1-c_0^2)/(1+c_0^2)},$$

where E_{Lab} is the total lab. energy and the condition on the viscosity ζ to be

$$\zeta \ll \frac{2^{\frac{1}{2}(3c_0^2+1)}\, a^{c_0^2}\, c_0^2}{\sigma} E_{\text{Lab}}^{\frac{1}{2}(1-c_0^2)/(1+c_0^2)}, \quad \sigma = \frac{1}{4}\pi a^2$$

and a is the diameter of the colliding protons. Thus we see that since at high energy densities $c_0^2 \approx 1$ so that ζ is practically zero for all purposes. Thus the LANDAU hydrodynamical model seems to ideally explain the situation.

Acknowledgements

The major part of the work was done, while the author was at the International Center for Theoretical Physics, Trieste. He would like to thank Professor ABDUS SALAM, the International Atomic Energy Agency and UNESCO for hospitality. He would also like to express his gratitude to Professor H. STUMPF for hospitality at Tübingen and the Alexander von Humboldt Foundation for the award of a fellowship.

REFERENCES

1. V. CANUTO and J. LODENQUAI, Phys. Rev., **11D**, 233, 1975.
2. L. LANDAU, Izv. Akad. Nauk SSSR. Ser. Fiz., **17**, 51, 1953; M. CHAICHIAN and E. SUHONEN, Corrections to the Landau Hydrodynamic Model of Multiparticle Production due to Viscosity, University of Helsinki Preprint, 1976.
3. W. HEISENBERG, Zeit. Phys., **126**, 569, 1949.
4. G. A. MILEKHIN, Izv. Akad. Nauk. SSSR. Ser. Fiz., **26**, 625, 1962.
5. A. ANDREEV, Sov. J. Nucl. Phys., **17**, 96, 1973.
6. M. LAKSHMANAN and K. ESWARAN, J. Phys. **A8**, 1658, 1975.
7. P. M. MATHEWS and M. LAKSHMANAN, Quart. Appl. Maths., **32**, 215, 1974.
8. P. M. MATHEWS and M. LAKSHMANAN, Nuov. Cim., **26A**, 299, 1975.
9. G. PERESSUTTI, Nuc.l Phys., **92B**, 58, 1975.
10. L. LANDAU and E. M. LIFSHITZ, Mechanics, Pergamon Press, Addison-Wesley, Reading, Mass. 1960.
11. G. B. WHITHAM, Linear and Non-Linear Waves, John Wiley & Sons, New York, 1974.
12. M. LAKSHMANAN, J. Phys. **A7**, 889, 1974.
13. S. GASIOROWICZ and D. GEFFEN, Rev. Mod. Phys., **43**, 531, 1969; R.-DELBOURGO, ABDUS SALAM and J. STRATHDEE, Phys. Rev., **187**, 1999, 1969.
14. See, e.g., E. L. FEINBERG, Sov. Phys.-Uspekhi, **14**, 455, 1972.

Acta Physica Academiae Scientiarum Hungaricae, Tomus 42 (2), pp. 159—166 (1977)

ПРОЦЕССЫ ФОРМИРОВАНИЯ, СТИМУЛИРОВАННАЯ КРИСТАЛЛИЗАЦИЯ И ЭЛЕКТРОФИЗИЧЕСКИЕ СВОЙСТВА АМОРФНЫХ ПЛЕНОК Cu—Sb—S—I

Ю. Ю. ФИРЦАК, О. В. ЛУКША, Н. И. ДОВГОШЕЙ, А. В. НЕЧИПОРЕНКО и Д. В. ЧЕПУР

УЖГОРОДСКИЙ ГОСУДАРСТВЕННЫЙ УНИВЕРСИТЕТ, УЖГОРОД, СССР

(Поступило 20. I. 1977)

По данным масс-спектрометрического определения состава пара при термоиспарении Cu—Sb—S—I и электронномикроскопического изучения вакуумных конденсатов этого вещества установлено, что при формировании аморфных пленок, наряду с образованием структурных единиц содержащих медь, более предпочтительней процесс образования аморфной структуры, построенной на основе пространственного каркаса пирамид $SbS_{3/2}$, в которой иод локализуется в «пустотах» и на оборванных связях сурьмы. Это обуславливает более высокую кристаллизационную способность пленок Cu—Sb—S—I по сравнению с массивным стеклом. С появлением кристаллической фазы SbSI в пленках при определенных условиях их препарирования или последующей стимулированной кристаллизации связаны сегментоэлектрическая активность конденсатов, обнаруженная по пироэлектрическому эффекту, особенности их электрических свойств и эффекта переключения.

Постановка задачи

Сложные сульфоиодидные стекла систем M—Sb—S—I, где M—Sn, Pd, Cd, Cu, являются перспективными материалами для применения в опто- и микроэлектронике [1]. Стеклообразные сплавы системы Cu—Sb—S—I интересны тем, что введение меди не только увеличивает температуру размягчения стекла, но и способствует образованию сложных структурных единиц $CuSbS_2$, Cu_3SbS_3 и Cu_3SbS_4, способных взаимодействовать с ковалентно увязанной сеткой сульфоиодидного стекла. Они органически входят в его структурное построение, препятствуя тем самы кристаллизации [2]. Поскольку многие из возможных применений халькогалогенидных стекол (элементы записи информации, быстродействуюшие переключатели, защитные покрытия и др.) перспективны в пленочном исполнении, нам представлялось важным провести для пленок Cu—Sb—S—I комплексе физико-технологические, структурные и электрофизические исследования с целью установления особенностей их формирования при вакуумном осаждении, структурного состояния и его изменений в условиях воздействий температуры, облучения электронным и лазерным лучами.

Экспериментальная часть

Исходными материалами для проведения исследований служили синтезированные стекла $Cu_5Sb_{30}S_{45}I_{20}$, $Cu_{10}Sb_{30}S_{40}I_{20}$ и $Cu_{15}Sb_{30}S_{40}I_{15}$. Отдельные исследования проводились на серийном усовершенствованном масс-спектрометре МИ-1305, электронографе ЭГ-100А, электронном микроскопе и рентгеновском микроанализаторе MS-46.

При обычном термическом вакуумном испарении из тигля навески стекла Cu—Sb—S—I в молекулярном пучке в зависимости от температуры нагрева t_e был обнаружены различные частицы (вакуум в масс-спектрометре $\sim 10^{-7}$ тор, энергия ионизующих электронов $\sim$50 эв). Начиная с $t_e \approx 100$ °C и вплоть до $t_e \approx 300$ °C в паре преобладают частицы типа SbI_3^+ и Sb_n^+ ($n=1:4$). Дальнейшее увеличение t_e приводит к обогащению паров комплексами типа Sb_xS_y ($x, y = 1:4$). Ионы Cu^+ регистрировались в пучке при $t_e \lesssim 500$ °C.

Полученные результаты указывают на то, что характер испарения сульфоидидного стекла подобен сильно диссоциативному характеру испарения кристалла SbSI [3]. А значит вследствие большой разницы в парциальных давлениях компонент пара обычное термическое испрение его может привести лишь к фракционной перегонке в вакууме. Конденсируемые при этом пленки будут композиционно и структурно неоднородными по толщине. Это подтверждается изучением структуры тонких конденсатов, осажденных непосредственно в масс-спектрометре, при испарании навески стекла $Cu_{15}Sb_{40}S_{30}I_{15}$ из танталового испарителя ($t_e = 500$ °C), а также при изучении химического состава сравнительно «толстых» пленок, который существенно отличен от химического состава исходного стекла. В частности, сосоставление данных локального рентгеноспектрального анализа пленок и эталона (стекла исходного состава) показало, что наблюдается обогащение пленки иодом по отношению к сере и обеднение серой по отношению к сурьме. Особенно существенно отличается от эталонного отношение $I_{I_{L\alpha}}/I_{S_{L\alpha}}$, так для исходного стекла $Cu_5Sb_{30}S_{45}I_{20}$ оно составляет 0,049, а для пленки, полученной простым термическим испарением, 0,072. Тонкие конденсаты ($d \leqslant 800$ А), имеют микронеоднородную аморфную структуру. Отжиг их при $t = 150$ °C приводит к появлению кристаллической фазы Sb_2S_3. Наблюдения за процессом кристаллизации тонких пленок под действием электронного пучка непосредственно в электронном микроскопе указывает, что этот процесс сопровождается фазовым разделением и селективным плавлением одного из составных компонентов пленки, вероятнее всего, аморфного SbI_3, который в таких условиях легко испаряется. На рис. 1а представлены электронная микрофотография и электронограмма отоженной тонкой пленки.

Однородные по микроструктуре аморфные пленки с химическим составом, близким к составу исходного стекла Cu—Sb—S—I, получались при

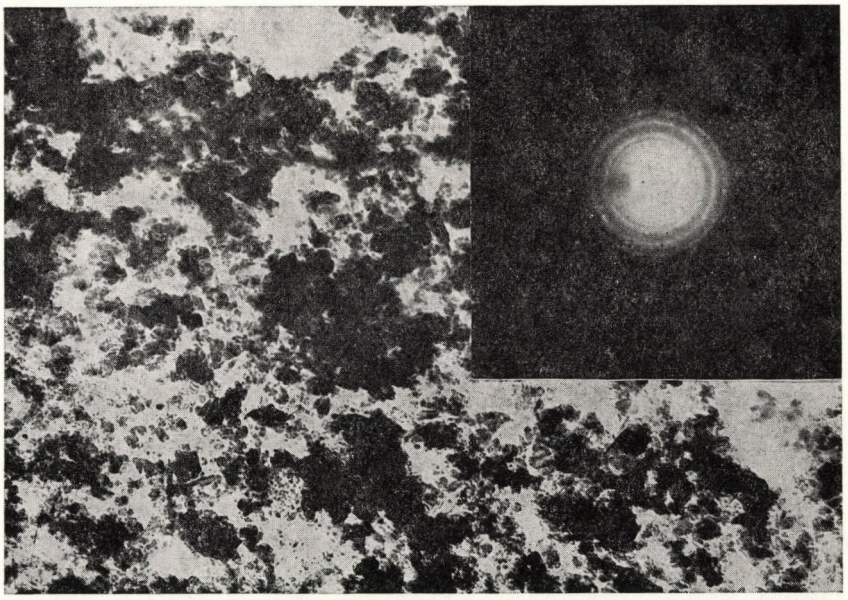

а)

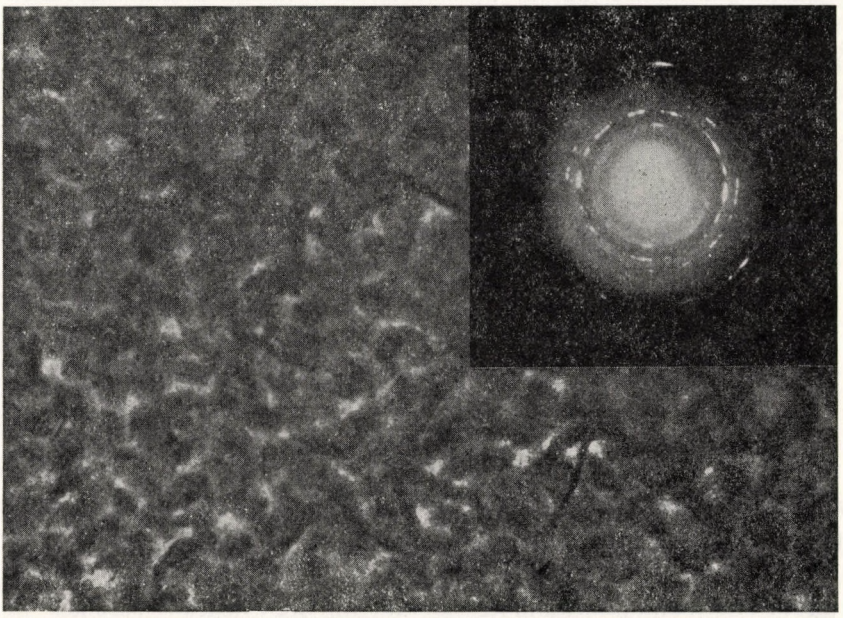

б)

Рис. 1. Электронные микрофотографии и дифракционные картины тонких конденсатов, полученных при обычном термическом (а) и дискретном (б) испарении Cu—Sb—S—I

использовании метода дискретного испарения с конденсацией на охлаждение до 10 °С подложки из очищенного стекла, сколыслюды и NaCl. При нагревании подложек до $t_n = 50$—100 °С для микроструктуры пленок Cu—Sb—S—I характерно появление субмикронных включений кристаллической фазы SbSI, обнаруженной по картинам микродифракции от тонких конденсатов (рис 1*б*). Для аморфных пленок Cu—Sb—S—I осаждаемых на охлаждаемые подложки, частичная кристаллизация (появление включений фазы SbSI) происходит при отжиге их в вакууме при $t = 100$—120 °С. Кристаллизация пленок Cu—Sb—S—I происходит и при облучении их пучком электронов с энергией 60 и 75 кэв, а также лучом CO_2 лазера (мощность падающего излучения $W \sim 20$ вт/см²).

Хотя с помощью метода дискретного испарения удается достичь хорошего воспроизведения в аморфной планке химического состава стекла Cu—Sb—S—I, по-видимому, структура конденсата отличается от структуры массивного стекла. В первую очередь, это обусловлено различными характером достижения аморфного состояния вещества в случае получения стекла из расплава и конденсации пленки из сложного по составу пара, образующегося при взрывообразном испарении Cu—Sb—S—I. Учитывая состав пара при тигельном испарении Cu—Sb—S—I, можно предположить, что при формировании пленок наряду с процессом образования сложных структурных единиц, содержащих медп, входящих в массивном сульфоиодидном стекле в его структурное построение и препятствующих кристаллизации, более предпочтительней процесс образования аморфной структуры на основе пространственного каркаса пирамид $SbS_{3/2}$ (подобно структуре аморфных пленок Sb_2S_3 [4]), в которой иод локализуется в «пустотах» и на оборванных связях сурьмы. Структурное построение такого типа обулавливает сравнительно более высокую кристаллизационную способность пленки (появление фазы SbSI) по сравнению с массивными стеклом Cu—Sb—S—I.

Подтверждением наличия кристаллической фазы сульфоиодида сурьмы в термообработанных пленках Cu—Sb—S—I, а также сконденсированных на нагретой подложке является их сегнетоэлектрическая активность. Вывод о сегнетоэлектрическом поведении конденсатов сделан на основании изучения пироэлектрического эффекта. Пиротоки в пленках Cu—Sb—S—I, как и в поликристаллических пленках SbSI [5], измерялись в квазистационарном режиме на конденсаторах планарного типа в напыленными контактами сурьмы или меди. Положение максимума пиротоков зависело от содержания меди в исходном стекле. Фазовый переход для пленок, полученных при испарении: стекла $Cu_5Sb_{30}S_{45}I_{20}$ происходит при 19 °С; стекла $Cu_{15}Sb_{30}S_{40}I_{15}$ — при 17 °С; поликристаллические пленки SbSI имеют фазовый переход при 24 °С (рис. 2). Смещение положения фазового перехода в сторону низких температур в частичнозакристаллизованных пленках Cu—Sb—S—I по сравнению с конденсатом сульфоиодида сурьмы, свидетельствует о том, что

кристаллическая фаза легирована медью, поскольку подобный результат наблюдали [6] при легировании кристаллов SbSI.

Величина поляризации пленок Cu—Sb—S—I, определяемая из записей кривых пиротоков как $P_0 = \int_{T_1}^{T_n} \partial P/\partial T \, dT$, и степень размытия фазового перехода, характеризуемая T, наклоном зависимости $P_0 = P_0(T)$ в области температуры перехода, зависит от технологических параметров препарирования пленок —

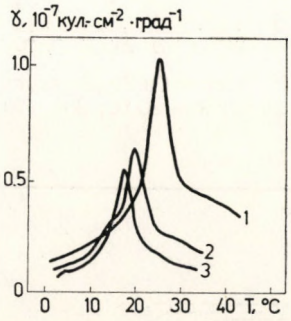

Рис. 2. Записи кривых пиротоков пленок: 1 — SbSI; 2 — $Cu_5Sb_{30}S_{43}I_{20}$; 3 — $Cu_{15}Sb_{30}S_{40}I_{15}$

температуры подложки во время конденсации, термообработки. Повышение t_n от 50 до 120 °C, как и термоотжиг пленок при 120—140 °C, приводят к возрастанию P_0 (рис. 3, кривые 1 и 2), что можно связать с увеличением содержания кристаллической фазы и размеров кристаллитных областей. Пленки Cu—Sb—S—I, сконденсированные при $t_n = 160 \div 200$ °C, имеют более размытый фазовый переход (рис. 3, кривая 3), что вызвано изменением их химического состава при конденсации вследствие реиспарения легколетучего компонента SbI_3.

Электрические измерения проводились на образцах типа «сэндвич», изготовленных на основе пленок Cu—Sb—S—I, различающихя структурным состоянием и содержанием меди. Удельное сопротивление аморфных пленок уменьшается от $\varrho = 5 \cdot 10^8$ ом·см для $Cu_5Sb_{30}S_{45}I_{20}$ до $\varrho = 3 \cdot 10^6$ ом·см для $Cu_{15}Sb_{30}S_{40}I_{15}$. Термическая энергия активации проводимости для пленок этих же составов изменяется, соответственно от 1,45 до 0,85 эв. Измерения при $t > 130 \div 140$ °C приводят к необратимым изменениям электрических параметров пленок Cu—Sb—S—I, что вызвано их кристаллизацией. Спектр термостимулированных токов пленок Sb—S—I при введении меди заметно усложняется.

Изучение вольт-амперных характеристик (ВАХ) аморфных пленок Cu—Sb—S—I показало, что в области малых полей вплоть до $E \approx 5 \cdot 10^3$ в/см имеет место омический характер проводимости. Нелинейный участок ВАХ может быть описан на основании механизма Пула—Франкеля, хотя в

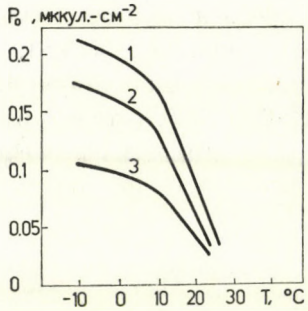

Рис. 3. Зависимость $P_0(T)$ для пленок $Cu_5Sb_{30}S_{45}I_{20}$, сконденсированных при $t_п$: 1 — 120 °C; 2 — 80 °C; 3 — 170 °C

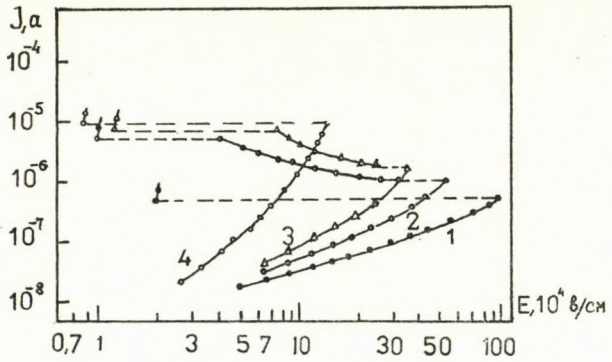

Рис. 4. ВАХ переключателей на основе пленок: 1 — Sb—S—I; 2 — $Cu_5Sb_{30}S_{45}I_{20}$; 3 — $Cu_{15}Sb_{30}S_{40}I_{15}$; 4 — частично закристаллизованной $Cu_{15}Sb_{30}S_{40}I_{15}$

начале этого участка обнаруживается влияние на процесс проводимости токов, ограниченных пространственным зарядом. Переключение происходит при достижении полей $E \approx 10^5$ в/см. При этом сопротивление образца уменьшается на 2—3 порядка с «запоминанием» низкоомного состояния.

В зависимости от содержания меди и структурного состояния пленок наблюдался одно- и двухпороговый ход переключения. Это характерно для некоторых составов халькогалогенидных стекол [7]. Аморфные пленки, не содержащие меди ($Sb_{35}S_{40}I_{25}$), а также частично закристаллизованные пленки Cu—Sb—S—I характеризуются однопороговым переключением (рис. 4, кривые 1 и 4). Аморфные пленки Cu—Sb—S—I обнаруживают двухпороговое переключение, причем более четко это выражено для составов с большим содержанием меди (рис. 4, кривые 2 и 3). Следовательно сложной характер переключения, по-видимому, связан с наличием в аморфных пленках структурных единиц характерных для стекла Sb—S—I, что способствует их кристаллизации, а также структурных образований, содержащих медь. Двухпо-

роговый характер переключения вырождается при увеличении температуры образцов ($t \geqslant 130$ °C) и их толщины ($d \geqslant 10$ мкм).

Сравнение характеристик переключения (u_n — напряжение переключения, I_n — ток переключения) массивных образцов [8] и частично закристаллизованных пленок показывает, что введение одного и того же количества меди приводит в пленках к более значительному изменению u_n, I_n. Поэтому, вероятнее всего, аморфная матрица в таких пленках, обогащена медью. Учитывая, что введение меди приводит к понижению энергии активации проводимости, возрастанию великейности ВАХ в допороговой области, усложению спектра локальных состояний, увеличению концентрации носителей в шнуре тока, т. е. усиливает электронный механизм переключения, проведенные исследования позволяют сделать вывод, что на характер переключения наиболее существенно влияют структурное состояние и кристаллизационные процессы в пленках Cu—Sb—S—I.

Выводы

Таким образом, конденсируемые в вакууме с помощью метода дискретного испарения аморфные пленки Cu—Sb—S—I структурно более неоднородны по сравнению с массивным стеклом, что позволяет легко стимулировать их кристаллизацию.

Сегментоэлектрическая активность структурнонеоднородных пленок Cu—Sb—S—I связана с появлением в них при кристаллизации полярной фазы SbSI, вероятно легированной медью.

Сложный характер и механизм процесса переключения в конденсированных пленках Cu—Sb—S—I определяются соотношением структурных единиц, характерных для стекла Sb—S—I, и структурных образований содержащих медь.

ЛИТЕРАТУРА

1. И. Ф. Копинец, Д. В. Чепур, И. М. Миголинец и И. Д. Туряница, сб. «Полупроводниковая техника и микроэлектроника», изд. «Наукова думка», **18**, 11, 1974.
2. З. У. Борисова, «Химия стеклообразных полупроводников», Изд. ЛГУ, Ленинград, 74, 1970.
3. О. В. Лукша, Н. И. Довгошей, М. Н. Набока и Д. В. Чепур, Депон. в ВИНИТИ, рег. № 1016—76, реферат Изв. вузов, Физика, **6**, 157, 1976.
4. В. П. Захаров, В. С. Герасименко, Ю. Г. Полтавцев и Л. П. Кучеренко, Изв. АН СССР, Неорганические материалы, **10**, 361, 1974.
5. Н. И. Довгошей, О. В. Лукша, Ю. Ю. Фирцак, А. В. Нечипоренко и Д. В. Чепур, Изв. АН СССР, сер. «физическая», **39**, 1084, 1975.
6. И. Д. Туряница, Б. М. Коперлес, Д. Г. Семак, И. П. Михалько и А. А. Кикинеши, УФЖ, **18**, 11, 1918, 1973.
7. С. А. Костылев, В. В. Химинец и В. А. Шкут, сб. «Физика и технология тонких пленок сложных полупроводников» (матер. совещан.), Ужгород, 36, 1975.
8. И. М. Миголинец, Автореферат канд. диссертации, Львов, 1974.

RECENSIONES

Local Properties at Phase Transitions

Proceedings of the International School of Physics "Enrico Fermi", Course LIX; Editors: K. A. Müller and A. Rigamonti. Publisher: Societa Italiana di Fisica — Bologna, Distributor: North-Holland Publishing Company, Amsterdam — New York — Oxford, 1976. pp. xxii + 879

This book is based on the lectures and seminar talks presented at the 1973 Varenna Summer School Course on "Local Properties at Phase Transitions". The central theme of the Course was to demonstrate the usefulness of the various resonance techniques such as NMR, EPR, etc. in providing information, to a large extent complementary to that obtained through scattering experiments, on static and dynamic local properties near phase transitions and to elucidate their relations to collective properties. A good coverage was also given to the applications of these techniques in the field of magnetic and structural transitions and of liquid crystals.

The material in the book is grouped into six chapters, each containing a number of contributions, typically one or two introductory or review-type lectures and a few shorter, more specialized talks.

Chapter I — "General Introductory Topics" contains an introduction to mean field theory by THOMAS, a series of lectures on phase diagrams, universality and scaling by STANLEY and collaborators, an introduction to NMR as a tool for investigating local properties at phase transitions by BORSA, and a talk on double resonance by BLINC.

Chapter II — "Structural Distortive Phase Transitions — Displacive" begins with a review of EPR studies in $SrTiO_3$ and $LaAlO_3$ by MÜLLER and VON WALDKIRCH, followed by a series of shorter lectures on the temperature dependence of the order parameter by BORSA, on dynamical effects as seen by NQR by RIGAMONTI, on birefrigence by COURTENS, on the central mode problem by FEDER, on some lattice-dynamical aspects of anharmonic crystals by MEIER, and on the molecular dynamics investigation of structural phase transitions by SCHNEIDER and STOLL. Also included is in this chapter a short roundtable discussion contribution on the problems of critical dynamics by THOMAS.

Chapter III — "Structural Distortive Phase Transitions — Order-Disorder" contains five shorter talks: on the application of double resonance to order-disorder-type ferroelectrics by BLINC, on NMR and neutron scattering studies in NH_4Cl by MICHEL, on the ferroelectric transition of TSCC by WINDSCH, on the electric field gradient tensors as determined with NQR—NMR in ferro- and antiferroelectrics by KIND, and on the dynamics of the antiferroelectric $NaNO_2$ by HATTA.

Chapter IV "Phase Transitions in Magnetic Systems" begins with a huge lecture by HELLER, reviewing NMR and neutron scattering studies near phase transitions in uniaxial antiferromagnets. This is followd by RICHARDS' review of magnetic resonance in one- and two-dimensional systems and talks on experiments on low dimensional magnets. The chapter ends with THOMAS' lecture on phase transitions in magnetic systems.

Chapter V — "Liquid crystals" starts with a short guide to the physics of mesomorphic phases by DE GENNES. Order parameter fluctuations, spin relaxation and self-diffusion are dealt with by BLINC, different aspects of NMR studies of liquid crystals by LOESCHE and GHOSH, fluorescence by BAUR, and EPR by SCHARA.

Chapter VI — "Scaling and Zero-Dimensional Superconductors" contains a number of theoretical contributions that did not fit either of the previous chapters: the topics discussed here scatter from scaling functions and dynamic scaling to cooperativity in biological systems.

On the whole, despite the three years that elapsed between the Course and the appearence of the book, the volume is an extremely useful source of information on the local aspects of phase transitions and the related experimental techniques. It may serve as an introduction to students entering the field, but it will do a good service as a broad review for specialists as well.

I. KONDOR

Magnetism Letters an International Journal

Gordon and Breach Science Publishers Ltd. London

Papers dealing with magnetism in solids have increased by leaps and bounds over the last 10 years. This is hardly surprising if one considers the outstanding results achieved both in the field of theory — e.g. the application of the renormalization group for the study of critical phenomena — and in the production of magnetic materials of great technical significance, such as memory devices based on the magnetic bubbles, or the permanent magnets of high field energy.

The present new journal, edited by DAVID E. COX, will certainly help in the rapid publication of new achievements in magnetism research. An especially welcome feature is that — in addition to papers dealing with fundamental problems — articles on the results of material and device development are to be offered considerable space.

A number of options is provided for contributors; this, in itself, is likely to accelerate publication. One of these options is that manuscripts can be submitted in a "camera ready" form, i.e. in a version suitable for direct photographic reproduction. My view is that even if this involves more than the usual care in the preparation of papers, so far as Hungarian authors are concerned this additional requirement will cause no particular worry and it is highly likely that they will wish to see their new noteworthy results published in this young but most promising journal.

It gave me particular pleasure to see that the first issue contained a paper written jointly by Hungarian and Czechoslovak authors (I. NAGY, T. TARNÓCZI and Z. FRAIT) on the magnetic anisotropy of Gd-Co amorphous films.

I wish every success to this new venture, both in the name of the community of Hungarian physicists and myself — as one who also has the honour of being a member of the E.A.B.

L. PÁL

Magnetism: Selected Topics

edited by Simon Foner

Gordon and Breach Science Publishers Ltd., London 1976

The increasing interest in the magnetism of solids is reflected by the appearance on the market of a great number of textbooks and manuals. The selection of a good textbook — or even a technical book discussing detailed problems at an adequate level — is thus no simple task these days, especially for a young physicist.

FONER's Magnetism Selected Topics can be recommended to those who wish to gain an insight into specific problems of magnetism by studying a relevant review paper. If, let us suppose, the endeavour is to acquire fundamental knowledge on band magnetism, the reader will certainly benefit from the first chapter of this volume written in a lucid and readable manner by A. BLANDIN, a well-known expert on the subject. The second chapter, by E. P. WOHLFARTH, deals with the applications of band magnetism. Among the problems discussed in this chapter, the sections headed Free Energy-Pressure Effects and Origin of I and Related Effects are of particular interest. Also worthy of mention is G. J. VAN DEN BERG's review in Chapter IV on the experiments performed since 1964 concerning the transport properties of alloys. W. M. STAR, the author of Chapter V expounds in a very pleasant manner the — answered and unanswered — questions on the Kondo effect. Chapter VI is likely to interest

a somewhat narrower circle; however, it is hardly likely that this could be said of Chapters VII and VIII — by P. LEDERER and A. J. HEEGER, respectively. These, together with the following chapter by D. J. KIM provide a brilliant summary of local spin fluctuations and of the problems of magnetic impurities, there is therefore no doubt at all that they will attract a very wide audience. In Chapter X, one can read about hyperfine interactions; Chapters XI and XII survey the efficiency of neutron physical methods in magnetic research. Chapter XIII owes its attraction to the captivating manner in which the authors — primarily, I should think, H. EUGENE STANLEY — correlate the common features of cooperative phenomena observable in magnetic and biological systems while discussing critical phenomena. In this chapter, or possibly in a separate part, a similar survey on the applications of the Wilson renormalization group would also have been of benefit to physicists working in other fields of magnetism. Among the remaining chapters the last — Chapter XVII — deserves mention since this deals with the relation between the exchange interaction and the photoelectron spin polarization and discusses all the experimental results and methods accessible in the field of photoelectron spectroscopy.

To sum up, Magnetism Selected Topics edited by SIMON FONER is an excellent means of gaining fundamental knowledge and an orientation in the surroundings of the most topical problems in magnetism.

L. PÁL

Printed in Hungary

A kiadásért felel az Akadémiai Kiadó igazgatója — Műszaki szerkesztő: Botyánszky Pál

A kézirat nyomdába érkezett: 1977. V. 3. — Terjedelem: 7,5 (A/5) ív, 13 ábra

78.4479 Akadémiai Nyomda, Budapest — Felelős vezető: Bernát György

NOTES TO CONTRIBUTORS

I. PAPERS will be considered for publication in Acta Physica Hungarica only if they have not previously been published or submitted for publication elsewhere. They may be written in English, French, German or Russian.

Papers should be submitted to

Prof. I. Kovács, Editor
Department of Atomic Physics, Polytechnical University
1521 Budapest, Budafoki út 8, Hungary

Papers may be either articles with abstracts or short communications. Both should be as concise as possible, articles in general not exceeding 25 typed pages, short communications 8 typed pages.

II. MANUSCRIPTS

1. Papers should be submitted in five copies.

2. The text of papers must be of high stylistic standard, requiring minor corrections only.

3. Manuscripts should be typed in double spacing on good quality paper, with generous margins.

4. The name of the author(s) and of the institutes where the work was carried out should appear on the first page of the manuscript.

5. Particular care should be taken with mathematical expressions. The following should be clearly distinguished, e.g. by underlining in different colours: special founts (italics, script, bold type, Greek, Gothic, etc); capital and small letters; subscripts and superscripts, e.g. x^3, x_3; small l and 1; zero and capital O; in expressions written by hand: e and i, n and u, v and v, etc.

6. References should be numbered serially and listed at the end of the paper in the following form: J. Ise and W. D. Fretter, Phys. Rev., *76*. 933, 1949.

For books, please give the initials and family name of the author(s), title, name of publisher, place and year of publication, e.g.: J. C. Slater, Quantum Theory of Atomic Structures, I. McGraw-Hill Book Company Inc., New York, 1960.

References should be given in the text in the following forms: Heisenberg [5] or [5].

7. Captions to illustrations should be listed on a separate sheet, not inserted in the text.

III. ILLUSTRATIONS AND TABLES

1. Each paper should be accompanied by five sets of illustrations, one of which must be ready for the blockmaker. The other sets attached to the copies of the manuscript may be rough drawings in pencil or photocopies.

2. Illustrations must not be inserted in the text.

3. All illustrations should be identified in blue pencil by the author's name, abbreviated title of the paper and figure number.

4. Tables should be typed on separate pages and have captions describing their content. Clear wording of column heads is advisable. Tables should be numbered in Roman numerals (I, II, III, etc.).

IV. MANUSCRIPTS not in conformity with the above Notes will immediately be returned to authors for revision. The date of receipt to be shown on the paper will in such cases be that of the receipt of the revised manuscript.

Reviews of the Hungarian Academy of Sciences are obtainable at the following addresses:

AUSTRALIA
C.B.D. LIBRARY AND SUBSCRIPTION SERVICE, Box 4886, G.P.O., *Sydney N.S.W. 2001*
COSMOS BOOKSHOP, 145 Ackland Street, *St. Kilda (Melbourne), Victoria 3182*

AUSTRIA
GLOBUS, Höchstädtplatz 3, *1200 Wien XX*

BELGIUM
OFFICE INTERNATIONAL DE LIBRAIRIE, 30 Avenue Marnix, *1050 Bruxelles*
LIBRAIRIE DU MONDE ENTIER, 162 Rue du Midi, *1000 Bruxelles*

BULGARIA
HEMUS, Bulvar Ruszki 6, *Sofia*

CANADA
PANNONIA BOOKS, P.O. Box 1017, Postal Station "B", *Toronto, Ontario M5T 2T8*

CHINA
CNPICOR, Periodical Department, P.O. Box 50, *Peking*

CZECHOSLOVAKIA
MAD'ARSKÁ KULTURA, Národní třida 22, *115 66 Praha*
PNS DOVOZ TISKU, Vinohradská 46, *Praha 2*
PNS DOVOZ TLAČE, *Bratislava 2*

DENMARK
EJNAR MUNKSGAARD, Norregade 6, *1165 Copenhagen*

FINLAND
AKATEEMINEN KIRJAKAUPPA, P.O. Box 128, *SF-00101 Helsinki 10*

FRANCE
EUROPERIODIQUES S. A., 31 Avenue de Versailles, *78170 La Celle St. Cloud*
LIBRAIRIE LAVOISIER, 11 rue Lavoisier, *75008 Paris*
OFFICE INTERNATIONAL DE DOCUMENTATION ET LIBRAIRIE, 48 rue Gay-Lussac, *75240 Paris Cedex 05*

GERMAN DEMOCRATIC REPUBLIC
HAUS DER UNGARISCHEN KULTUR, Karl-Liebknecht-Strasse 9, *DDR-102 Berlin*
DEUTSCHE POST ZEITUNGSVERTRIEBSAMT, Strasse der Pariser Kommüne 3—4, *DDR-104 Berlin*

GERMAN FEDERAL REPUBLIC
KUNST UND WISSEN ERICH BIEBER, Postfach 46, *7000 Stuttgart 1*

GREAT BRITAIN
BLACKWELL'S PERIODICALS DIVISION, Hythe Bridge Street, *Oxford OX1 2ET*
BUMPUS, HALDANE AND MAXWELL LTD., Cowper Works, *Olney, Bucks MK46 4BN*
COLLET'S HOLDINGS LTD., Denington Estate, *Wellingborough, Northants NN8 2QT*
WM. DAWSON AND SONS LTD., Cannon House, *Folkestone, Kent CT19 5EE*
H. K. LEWIS AND CO., 136 Gower Street, *London WC1E 6BS*

GREECE
KOSTARAKIS BROTHERS, International Booksellers, 2 Hippokratous Street, *Athens-143*

HOLLAND
MEULENHOFF-BRUNA B.V., Beulingstraat 2, *Amsterdam*
MARTINUS NIJHOFF B.V., Lange Voorhout 9—11, *Den Haag*
SWETS SUBSCRIPTION SERVICE, 347b Heereweg, *Lisse*

INDIA
ALLIED PUBLISHING PRIVATE LTD., 13/14 Asaf Ali Road, *New Delhi 110001*
150 B-6 Mount Road, *Madras 600002*
INTERNATIONAL BOOK HOUSE PVT. LTD., Madame Cama Road, *Bombay 400039*
THE STATE TRADING CORPORATION OF INDIA LTS., Books Import Division, Chandralok, 36 Janpath, *New Delhi 110001*

ITALY
EUGENIO CARLUCCI, P.O. Box 252, *70100 Bari*
INTERSCIENTIA, Via Mazzé 28, *10149 Torino*
LIBRERIA COMMISSIONARIA SANSONI, Via Lamarmora 45, *50121 Firenze*
SANTO VANASIA, Via M. Macchi 58, *20124 Milano*
D. E. A., Via Lima 28, *00198 Roma*

JAPAN
KINOKUNIYA BOOK-STORE CO. LTD., 17-7 Shinjuku-ku 3 chome, Shinjuku-ku, *Tokyo 160-91*
MARUZEN COMPANY LTD., Book Department, P.O. Box 5050 Tokyo International, *Tokyo 100-31*
NAUKA LTD. IMPORT DEPARTMENT, 2-30-19 Minami Ikebukuro, Toshima-ku, *Tokyo 171*

KOREA
CHULPANMUL, *Phenjan*

NORWAY
TANUM-CAMMERMEYER, Karl Johansgatan 41—43, *1000 Oslo*

POLAND
WĘGIERSKI INSTYTUT KULTURY, Marszałkowska 80, *Warszawa*
CKP I W ul. Towarowa 28 *00-958 Warsaw*

ROUMANIA
D. E. P., *Bucureşti*
ROMLIBRI, Str. Biserica Amzei 7, *Bucureşti*

SOVIET UNION
SOJUZPETCHATJ — IMPORT, *Moscow*
and the post offices in each town
MEZHDUNARODNAYA KNIGA, *Moscow G-200*

SPAIN
DIAZ DE SANTOS, Lagasca 95, *Madrid 6*

SWEDEN
ALMQVIST AND WIKSELL, Gamla Brogatan 26, *101 20 Stockholm*
GUMPERTS UNIVERSITETSBOKHANDEL AB, Box 346, *401 25 Göteborg 1*

SWITZERLAND
KARGER LIBRI AG, Petersgraben 31, *4011 Basel*

USA
EBSCO SUBSCRIPTION SERVICES, P.O. Box 1943, *Birmingham, Alabama 35201*
F. W. FAXON COMPANY, INC., 15 Southwest Park, *Westwood, Mass, 02090*
THE MOORE-COTTRELL SUBSCRIPTION AGENCIES, *North Cohocton, N. Y. 14868*
READ-MORE PUBLICATIONS, INC., 140 Cedar Street, *New York, N. Y. 10006*
STECHERT-MACMILLAN, INC., 7250 Westfield Avenue, *Pennsauken N. J. 08110*

VIETNAM
XUNHASABA, 32, Hai Ba Trung, *Hanoi*

YUGOSLAVIA
JUGOSLAVENSKA KNJIGA, Terazije 27, *Beograd*
FORUM, Vojvode Mišiča 1, *21000 Novi Sad*

ACTA PHYSICA

ACADEMIAE SCIENTIARUM HUNGARICAE

TOMUS XLII FASCICULUS 3

AKADÉMIAI KIADÓ, BUDAPEST

1977

ACTA PHYS. HUNG. APAHAQ 42 (3) 171–276 (1977)

ACTA PHYSICA

ACADEMIAE SCIENTIARUM HUNGARICAE

SZERKESZTI
KOVÁCS ISTVÁN

Az *Acta Physica* angol, német, francia vagy orosz nyelven közöl értekezéseket. Évente két kötetben, kötetenként 4—4 füzetben jelenik meg. Kéziratok a szerkesztőség címére (1521 Budapest XI., Budafoki út 8.) küldendők.

Megrendelhető a belföld számára az Akadémiai Kiadónál (1363 Budapest Pf. 24. Bankszámla 215-11488), a külföld számára pedig a "Kultúra" Külkereskedelmi Vállalatnál (1389 Budapest 62, P. O. B. 149. Bankszámla 217-10990 sz.), vagy annak külföldi képviseleteinél és bizományosainál.

The *Acta Physica* publish papers on physics in English, German, French or Russian, in issues making up two volumes per year. Subscription price: $32.00 per volume. Distributor: KULTURA Hungarian Trading Co. (1389 Budapest 62, P. O. Box 149) or its representatives abroad.

Die *Acta Physica* veröffentlichen Abhandlungen aus dem Bereich der Physik in deutscher, englischer, französischer oder russischer Sprache, in Heften die jährlich zwei Bände bilden.

Abonnementspreis pro Band: $32.00. Bestellbar bei: KULTURA Außenhandelsunternehmen (1389 Budapest 62, Postfach 149) oder bei seinen Auslandsvertretungen.

Les *Acta Physica* publient des travaux du domaine de la physique, en français, anglais, allemand ou russe, en fascicules qui forment deux volumes par an.

Prix de l'abonnement: $32.00 par volume. On peut s'abonner à l'Entreprise du Commerce Extérieur KULTURA (1389 Budapest 62, P. O. B. 149) ou chez ses représentants à l'étranger.

«*Acta Physica*» публикуют трактаты из области физических наук на русском, немецком, английском и французском языках.

«*Acta Physica*» выходят отдельными выпусками, составляющими два тома в год.

Подписная цена — $32.00 за том. Заказы принимает предприятие по внешней торговле KULTURA (1389 Budapest 62, P. O. B. 149) или его заграничные представительства и уполномоченные.

ACTA PHYSICA

ACADEMIAE SCIENTIARUM HUNGARICAE

TOMUS XLII FASCICULUS 3

AKADÉMIAI KIADÓ, BUDAPEST
1977

ACTA PHYS. HUNG.

INDEX

COMMUNICATIO BREVIS

Acta Physica Academiae Scientiarum Hungaricae, Tomus 42 (3), pp. 171—177 (1977)

A COMMENT ON TRACE CALCULATIONS FOR FERMI SYSTEMS

By

W.-H. STEEB

D—23 KIEL, W. GERMANY*

(Received 8. XII. 1976)

It is shown that the calculation of the partition function for non-interacting fermions can be described within the framework of usual matrix calculation. An extension to interacting fermi systems is given.

From statistical mechanics it is known that all equilibrium thermodynamic quantities of interest for a system of interacting particles can be determined from the grand partition function

$$Z = \mathrm{Tr} \exp\left(-\beta\left(H - \mu N_e\right)\right). \tag{1}$$

Here H is the Hamiltonian describing the system. Throughout, we consider fermi systems in the occupation number formalism. N_e is the total number operator, μ the chemical potential, and β the inverse temperature. In general, the trace cannot be evaluated. However, often, the Hamiltonian consists of two terms, namely $H = H_0 + H_1$, where H_0 is so chosen that the properties described by H_0 alone are well-known. In most cases stated in the literature, the operator $H_0 - \mu N_e$ has the form $H_0 - \mu N_e = \sum_{k\sigma}\left(\varepsilon(k) - \mu\right) c_{k\sigma}^{+} c_{k\sigma}$, where $\varepsilon(k)$ is the one-particle energy, and σ denotes the spin. We investigate a lattice system and therefore k runs over the first Brioullin zone. Here we are able to calculate the trace due to Eq. (1) exactly, and the result can be found in the text-books on this field [1, 2].

Moreover, it should be noted that the Wick's theorem for this case and more complicated ones are well developed [3, 4].

In the present paper it is shown that the trace calculation can easily be performed with the aid of matrix calculation. We shall use the addition, the multiplication, the Kronecker product (denoted by $\otimes$) of matrices and finally the trace of a matrix [5, 6].

First of all, we want to give the rules needed in following. Let A_1, A_2, A_3 and B_1, B_2, B_3 be $n \times n$ matrices and 1 the $n \times n$ identity matrix.

One has

$$(A_1 \otimes A_2)(B_1 \otimes B_2) = (A_1 B_1) \otimes (A_2 B_2) \tag{2}$$

* Address: D—23 Kiel, Reventlouallee 33, W. Germany.

and the extensions

$$(A_1 \otimes A_2 \otimes A_3)(B_1 \otimes B_2 \otimes B_3) = (A_1 B_1) \otimes (A_2 B_2) \otimes (A_3 B_3)$$
$$(A_1 \otimes B_1)(A_2 \otimes B_2)(A_3 \otimes B_3) = (A_1 A_2 A_3) \otimes (B_1 B_2 B_3) . \tag{3}$$

Furthermore, from Eq. (2) follows that

$$[A \otimes 1, 1 \otimes B] \equiv (A \otimes 1)(1 \otimes B) - (1 \otimes B)(A \otimes 1) = 0 . \tag{4}$$

Moreover we need the following rule for a trace of a matrix, namely

$$\mathrm{Tr}\,(A \otimes B) = \mathrm{tr}\,(A)\,\mathrm{tr}\,(B) . \tag{5}$$

Inside the trace on the left-hand side there is an $n^2 \times n^2$ matrix, while inside the traces on the right-hand side there are $n \times n$ matrices. Hence we use the notation "tr" instead of "Tr".

Now let us prove that

$$\mathrm{Tr}\exp(A \otimes 1 + 1 \otimes B) = \mathrm{tr}\exp(A)\,\mathrm{tr}\exp(B) . \tag{6}$$

Due to Eq. (4) we can write

$$\mathrm{Tr}\exp(A \otimes 1 + 1 \otimes B) = \mathrm{Tr}\exp(A \otimes 1)\exp(1 \otimes B).$$

An arbitrary term of the e-functions on the right-hand side takes the form

$$\frac{1}{n!} \cdot \frac{1}{m!}(A \otimes 1)^n (1 \otimes B)^m .$$

Due to Eq. (3) we obtain

$$\frac{1}{n!} \cdot \frac{1}{m!}(A \otimes 1)^n (1 \otimes B)^m = \frac{1}{n!} \cdot \frac{1}{m!}(A^n \otimes 1)(1 \otimes B^m) = \frac{1}{n!} \cdot \frac{1}{m!}(A^n \otimes B^m) .$$

It follows, with the aid of Eq. (5)

$$\mathrm{Tr}\left(\frac{1}{n!} \cdot \frac{1}{m!}(A^n \otimes B^m)\right) = \frac{1}{n!} \cdot \frac{1}{m!}\mathrm{Tr}\,A^n \otimes B^m =$$
$$= \frac{1}{n!} \cdot \frac{1}{m!}\mathrm{tr}\,A^n\,\mathrm{tr}\,B^m = \left(\frac{1}{n!}\,\mathrm{tr}A^n\right)\left(\frac{1}{m!}\,\mathrm{tr}\,B^m\right) .$$

Thus the identity (6) has been proved. The extension to N summands is straightforward.

Hence we obtain

$$\begin{aligned}\operatorname{Tr}\exp\left(A_1\otimes 1\otimes\ldots\otimes 1\right)+\left(1\otimes A_2\otimes 1\ldots\otimes 1\right)+\left(1\otimes 1\otimes\ldots\otimes A_N\right)=\\ =\operatorname{tr}\exp A_1\operatorname{tr}\exp A_2\ldots\operatorname{tr}\exp A_N\,.\end{aligned}\tag{7}$$

This formula is the main result. It remains to show that the Hamiltonian can be brought into the form

$$H=\left(A_1\otimes 1\otimes\ldots\otimes 1\right)+\left(1\otimes A_2\otimes 1\ldots\otimes 1\right)+\ldots+\left(1\otimes 1\otimes\ldots\otimes A_N\right).\tag{8}$$

Therefore the matrix representation for the fermi operators will be given. For the sake of simplicity we consider spinless fermions. The extension to the case described above is straightforward. The requirements of the Pauli principle are satisfied if the fermion operators $\{c_k^+, c_j : k, j = 1, 2, \ldots, N\}$ satisfy the anticommutation relations

$$\begin{aligned}\{c_k^+, c_j\}_+ &= \delta_{kj}\,,\\ \{c_k^+, c_j^+\}_+ &= \{c_k, c_j\}_+ = 0\,,\end{aligned}\tag{9}$$

for all $k, j = 1, 2, \ldots, N$.

Let us now give a faithful matrix representation of the operators. First of all we state the case where $N = 1$. The basis is given by $\{c^+|0\rangle;\ |0\rangle\}$ and the dual one by $\{\langle 0|c;\ \langle 0|$. Thus one has

$$\begin{aligned}c^+ &= \begin{pmatrix}01\\00\end{pmatrix} = \frac{1}{2}\left(\sigma_x + i\sigma_y\right) = \frac{1}{2}\sigma_+\,,\\ c &= \begin{pmatrix}00\\10\end{pmatrix} = \frac{1}{2}\left(\sigma_x - i\sigma_y\right) = \frac{1}{2}\sigma_-\,.\end{aligned}\tag{10}$$

The state vectors are

$$c^+|0\rangle = \begin{pmatrix}1\\0\end{pmatrix};\qquad |0\rangle = \begin{pmatrix}0\\1\end{pmatrix}.\tag{11}$$

Here σ_x, σ_y, σ_z, σ_+, σ_- are the usual Pauli matrices. The number operator $n = c^+c$ becomes

$$n = c^+c = \begin{pmatrix}10\\00\end{pmatrix}.\tag{12}$$

Thus the Hilbert space under consideration is two-dimensional, i.e. $\mathcal{H} = R^2$.

Now the extension to the case where $N > 1$ leads to (compare EMCH[7])

$$c_k^+ = \sigma_z \otimes \sigma_z \otimes \ldots\ldots \otimes \sigma_z \otimes \overbrace{\left(\frac{1}{2}\sigma_+\right)}^{k\text{-th place}} \otimes \underbrace{1 \otimes 1 \otimes \ldots\ldots \otimes 1}_{N \text{ times}},$$

$$c_k = \sigma_z \otimes \sigma_z \otimes \ldots\ldots \otimes \sigma_z \otimes \left(\frac{1}{2}\sigma_-\right) \otimes 1 \otimes 1 \otimes \ldots\ldots \otimes 1 . \tag{13}$$

One can easily calculate, using rule (3), that the anticommutation relations according to Eq. (8) are fulfilled. The number operator $n_k = c_k^+ c_k$ is found, with the aid of Eq. (3), to be

$$n_k = c_k^+ c_k = 1 \otimes 1 \otimes \ldots\ldots \otimes \begin{pmatrix} 1 & 0 \\ 0 & 0 \end{pmatrix} \otimes 1 \otimes 1 \otimes \ldots \otimes 1 . \tag{14}$$

Finally, one has

$$\sum_{k=1}^{N} \lambda_k n_k = \left(\begin{pmatrix} \lambda_1 & 0 \\ 0 & 0 \end{pmatrix} \otimes 1 \otimes 1 \ldots \otimes 1\right) + \left(1 \otimes \begin{pmatrix} \lambda_2 & 0 \\ 0 & 0 \end{pmatrix} \otimes 1 \otimes \ldots \otimes 1\right) + \\ + \ldots\ldots + \left(1 \otimes 1 \otimes \ldots\ldots \otimes \begin{pmatrix} \lambda_N & 0 \\ 0 & 0 \end{pmatrix}\right), \tag{15}$$

where $\lambda_k \in R$. The Hilbert space $\mathcal{H}_N$ obtained in this way is a Kronecker product of N two-dimensional Hilbert spaces

$$\mathcal{H}_N = R^2 \otimes R^2 \otimes \ldots\ldots \otimes R^2 . \tag{16}$$

Thus the determination of the trace

$$Z = \operatorname{Tr} \exp\left(\sum_{k=1}^{N} \lambda_k n_k\right) \tag{17}$$

reduces to the trace calculation in a subspace. In occupation number formalism this subspace is given by the basis $\{c^+|0\rangle; |0\rangle\}$, and in matrix calculation it is given by the basis $\left\{\begin{pmatrix} 1 \\ 0 \end{pmatrix}; \begin{pmatrix} 0 \\ 1 \end{pmatrix}\right\}$.

Here it should be noted that, for the present case, the trace calculation has been known for a long time [8]. However, in modern textbooks [1, 2] this simple representation is not taken into consideration. Moreover, it is also possible with simple matrix calculation to treat interacting systems in an approximative manner. For instance, the BCS-model has been investigated in this fashion by WEHRL [9]. Here we want to give another example. We

consider the HUBBARD model [10]. The Hamiltonian can be written in Bloch representation as

$$H = \sum_{k\sigma} \varepsilon(k)\, c_{k\sigma}^{+} c_{k\sigma} + \sum_{k_1k_2k_3k_4} \delta(k_1 - k_2 + k_3 - k_4) c_{k_1\uparrow}^{+} c_{k_2\uparrow} c_{k_3\downarrow}^{+} c_{k_4\downarrow}\,, \tag{18}$$

where k runs over the first Brioullin zone. As an approximative method we use the following inequality, which is sometimes called Bogolyubov inequality, $\Omega \leq \mathrm{Tr}(H - \mu N_e) W_t + 1/\beta\, \mathrm{Tr}\, W_t \ln W_t$ for the grand potential. W_t is the so-called trial density matrix. Let us consider the case where

$$W_t = \exp\left(-\beta \sum_k E_\uparrow(k) c_{k\uparrow}^{+} c_{k\uparrow} + E_\downarrow(k) c_{k\downarrow}^{+} c_{k\downarrow}\right) / \mathrm{Tr} \exp(\ldots.)\,. \tag{19}$$

Both $E_\uparrow(k)$ and $E_\downarrow(k)$ play the role of real variation parameters.

For example, we have to calculate traces such as

$$\mathrm{Tr}\, c_{k\uparrow}^{+} c_{k\uparrow} W_t\,, \tag{20}$$

$$\sum_{k_1k_2k_3k_4} \delta(k_1 - k_2 + k_3 - k_4)\, \mathrm{Tr}\,(c_{k_1\uparrow}^{+} c_{k_2\uparrow} c_{k_3\downarrow}^{+} c_{k_4\downarrow} W_t)\,. \tag{21}$$

Now we show how, within the framework of the developed calculation, the trace can be evaluated. Since we have included the spin, the representation of the operators $\{c_{k\sigma}^{+}, c_{k\sigma} : k = 1, \ldots, N;\ \sigma = \uparrow, \downarrow\}$ becomes

$$c_{k\uparrow}^{+} = \underbrace{\sigma_z \otimes \ldots \otimes \sigma_z \otimes \overset{k\text{-th place}}{\left(\frac{1}{2}\sigma_+\right)} \otimes 1 \otimes \ldots\ldots \otimes 1}_{2N \text{ times}}\,, \tag{22}$$

$$c_{k\downarrow}^{+} = \sigma_z \otimes \ldots. \otimes \sigma_z \otimes \underset{(k+N)\text{-th place}}{\left(\frac{1}{2}\sigma_+\right)} \otimes 1 \otimes \ldots\ldots \otimes 1\,.$$

Using $\exp\begin{pmatrix}\lambda 0\\ 00\end{pmatrix} = \begin{pmatrix}e^\lambda 0\\ 01\end{pmatrix}$, it follows that

$$\exp\left(\sum_k E_\uparrow(k) c_{k\uparrow}^{+} c_{k\uparrow} + \sum_k E_\downarrow(k) c_{k\downarrow}^{+} c_{k\downarrow}\right) =$$
$$= \begin{pmatrix}e^{E_\uparrow(1)} & 0\\ 0 & 1\end{pmatrix} \otimes \ldots \otimes \begin{pmatrix}e^{E_\uparrow(N)} & 0\\ 0 & 1\end{pmatrix} \otimes \begin{pmatrix}e^{E_\downarrow(N+1)} & 0\\ 0 & 1\end{pmatrix} \otimes \ldots \otimes \begin{pmatrix}e^{E_\downarrow(2N)} & 0\\ 0 & 1\end{pmatrix}. \tag{23}$$

As an abbreviation we have put $-\beta E_\sigma(k) \to E_\sigma(k)$.

Since

$$c_{k\uparrow}^{+}c_{k\uparrow} = 1\otimes 1 \ldots \otimes \underset{\substack{\uparrow \\ k\text{-th place}}}{\begin{pmatrix}1 & 0\\ 0 & 0\end{pmatrix}} \otimes 1 \otimes \ldots \otimes 1\,, \tag{24}$$

we have, applying Eq. (3),

$$\operatorname{Tr}\,(c_{k\uparrow}^{+}c_{k\uparrow}W_t) = \frac{\exp\,(E_{\uparrow}(k))}{\exp\,E_{\uparrow}(k) + 1}\,. \tag{25}$$

In the second case we cast Eq. (21) in a form more convenient for our purpose according to

$$\begin{aligned}\sum_{k_1k_2k_3k_4} \delta(k_1 - k_2 + k_3 - k_4)c_{k_1\uparrow}^{+}c_{k_2\uparrow}c_{k_3\uparrow}^{+}c_{k_4\downarrow} = \\ = \sum_{k_1k_3} c_{k_1\uparrow}^{+}c_{k_1\uparrow}c_{k_3\downarrow}^{+}c_{k_3\downarrow} + \sum_{\substack{k_1k_2k_3k_4\\ k_1\neq k_2}} \delta(k_1 - k_2 + k_3 - k_4)c_{k_1\uparrow}^{+}c_{k_2\uparrow}c_{k_3\downarrow}^{+}c_{k_4\downarrow}\,.\end{aligned} \tag{26}$$

For the first term on the right-hand side of Eq. (26) we find

$$\begin{aligned}c_{k_1\uparrow}^{+}c_{k_1\uparrow}c_{k_3\downarrow}^{+}c_{k_3\downarrow} = \\ = 1\otimes 1\otimes \ldots \otimes \underset{\substack{\uparrow \\ k_1\text{-th place}}}{\begin{pmatrix}1 & 0\\ 0 & 0\end{pmatrix}} \otimes 1 \ldots \otimes 1 \otimes \underset{\substack{\uparrow \\ (k_3+N)\text{ place}}}{\begin{pmatrix}1 & 0\\ 0 & 0\end{pmatrix}} \otimes 1 \ldots \otimes 1\,,\end{aligned} \tag{27}$$

Thus, it follows that

$$\frac{1}{N}\sum_{k_1k_3} \operatorname{Tr}\,(c_{k_1\uparrow}^{+}c_{k_1\uparrow}c_{k_3\downarrow}^{+}c_{k_3\downarrow}W_t) = \frac{1}{N}\sum_{k_1k_3} \frac{e^{E_{\uparrow}(k_1)}}{1 + e^{E_{\uparrow}(k_1)}} \cdot \frac{e^{E_{\downarrow}(k_3)}}{1 + e^{E_{\downarrow}(k_3)}}\,. \tag{28}$$

For the second term on the right hand side of Eq. (26) there is no contribution to the trace since

$$\operatorname{tr}\begin{pmatrix}0 & -1\\ 0 & 0\end{pmatrix}\begin{pmatrix}e^{\lambda} & 0\\ 0 & 1\end{pmatrix} = 0\,, \tag{29}$$

where $1/2\ \sigma_+\sigma_z = \begin{pmatrix}0 & -1\\ 0 & 0\end{pmatrix}$.

Finally, it should be remarked that the described method can be extended in order to obtain better approximations. To this end we make a unitary transformation given by $U = \exp\,(iS)$, with $S = S^{+}$, and then the trace determination (compare [11], for the BCS-theory see [9]). Also, in this case, the trace determination can easily be performed within the framework of usual matrix calculation.

Acknowledgments

Thanks are due to Dr. W. BARRY for a critical reading of the manuscript.

REFERENCES

1. R. D. MATTUK, A Guide to Feynman Diagrams in the Many-Body Problem, Mc Graw Hill, 1967.
2. A. L. FETTER and J. D. WALECKA, Quantum Theory of Many-Particle Systems, Mc Graw Hill, 1971.
3. M. GAUDIN, Nucl. Phys., **15,** 89, 1960
4. W.-H. STEEB, Letters in Mathematical Physics, **1,** 135, 1976.
5. R. BELLMAN, Introduction to Matrix Analysis, Mc Graw Hill, 1960.
6. W. GRÖBNER, Matrizenrechnung, BI Institut Mannheim, 1966.
7. G. EMCH, Algebraic Methods in Statistical Mechanics and Quantum Field Theory, Wiley-Interscience, 1972, pp. 271.
8. A. SOMMERFELD, Z. f. Physik, **47,** 1, 1928.
9. A. WEHRL, Commun. math. Phys., **23,** 319, 1971
10. J. HUBBARD, Proc. Roy. Soc. (London), **A276,** 238, 1963.
11. W.-H. STEEB and E. MARSCH, phys. stat. sol. (b), **65,** 403, 1974.

Acta Physica Academiae Scientiarum Hungaricae, Tomus 42 (3), pp. 179—184 (1977)

EFFECT OF AGGREGATION OF MOLECULES ON THE POLARIZATION OF FLUORESCENCE SPECTRUM OF ERYTHROSIN

By

M. L. PANDYA* and M. K. MACHWE

DEPARTMENT OF PHYSICS & ASTROPHYSICS, DELHI UNIVERSITY, DELHI, INDIA

(Received 20. I. 1977)

The excitation and emission wavelengths for erythrosin in aqueous solution constitute broad bands and the wavelengths corresponding to the maximum intensity in the band are found to shift with the increase of concentration. The excitation and emission peaks are observed at concentrations varying from $\sim 10^{-7}$ g/cc to $\sim 10^{-3}$ g/cc in aqueous solution at room temperature (~ 28 °C). The concentration vs excitation and emission wavelengths plot shows a break in the linearity around $\sim 10^{-5}$ g/cc which can be interpreted as due to the aggregation of molecules. The polarization of fluorescence is measured for concentrations ranging from 3.5×10^{-6} g/cc to 1.4×10^{-4} g/cc. The results indicate that the emission at very low concentration $\sim 3.5\times10^{-6}$ g/cc is essentially due to monomers while at high concentration ($\sim 1.4\times10^{-4}$ g/cc) it is due to dimers. For the concentration 8.7×10^{-6} g/cc, monomers and dimers both exist simultaneously.

Introduction

Most of the fluorescent dyes [1, 2, 3, 4, 5] in solution have been reported to give a broad emission band which has been interpreted as due to the presence of different forms of molecular species like monomers, dimers, polymers etc. In the present investigation erythrosin in aqueous solution is studied for these different forms of molecular aggregation at room temperature (~ 28 °C) by studying (a) the shifts in the excitation and emission peaks at different concentrations varying from 10^{-7} g/cc to 10^{-3} g/cc and also (b) the polarization spectrum for different concentrations at peak excitation wavelengths within the range of broad emission band. It is observed that the polarization spectrum is more useful in distinguishing/identifying the simultaneous existence of different forms of molecular aggregation.

Experimental

The excitation and emission peaks were obtained for each concentration of the dye in aqueous solution at room temperature (~ 28 °C) with an Aminco Bowman Spectro photo fluorometer. The effect of scattering was checked

* Permanent address: Department of Physics, M. M. College, Modinagar (U.P.), 201 204, India.

by using the blank solution in the cuvette and was found to be less than 0.5%. Setting the excitation monochromator to the peak value for each concentration, the emission monochromator was varied to cover the entire emission band from 540 nm to 600 nm. The polarization was calculated using the relation [6]

$$P = \frac{I_{EE} - I_{EB}(I_{BE}/I_{BB})}{I_{EE} + I_{EB}(I_{BE}/I_{BB})}, \tag{1}$$

Table I

Excitation and emission peaks at different concentrations

Concentration (g/cc)	8.8×10^{-7}	2.2×10^{-6}	4.4×10^{-6}	8.8×10^{-6}	1.8×10^{-5}	4.4×10^{-5}	8.8×10^{-5}	2.2×10^{-4}	4.4×10^{-4}	8.8×10^{-4}
λ_{ex}(nm)	520	520	520	520	520	500	484	464	450	434
λ_{ex}(nm)	—	—	—	—	—	532	540	550	556	566
λ_{em}(nm)	556	556	556	556	560	566	568	576	580	584

Table II

Results for polarization measurements

	A	B	C	D	E	F
Conc. / λ_{em} (nm)	3.5×10^{-6} g/cc $\lambda_{ex}\sim 520$ nm P%	8.7×10^{-6} g/cc $\lambda_{ex}\sim 520$ nm P%	2.2×10^{-5} g/cc $\lambda_{ex}\sim 508$ nm P%	4.4×10^{-5} g/cc $\lambda_{ex}\sim 508$ nm P%	1.4×10^{-4} g/cc $\lambda_{ex}\sim 460$ nm P%	1.4×10^{-4} g/cc $\lambda_{ex}\sim 546$ nm P%
540	16.3	17.0	—	—	—	—
544	16.2	17.5	17.5	—	—	—
548	17.0	18.5	18.4	20.2	—	—
552	17.2	18.7	19.1	20.3	—	—
556	19.7	19.4	19.4	20.9	—	—
560	19.7	19.3	20.4	21.3	—	—
564	19.8	19.5	20.5	21.9	—	—
568	19.2	18.8	21.7	22.5	21.1	19.8
572	17.9	17.2	21.9	22.7	21.6	21.4
576	17.5	19.5	22.3	23.4	22.4	22.0
580	17.1	22.7	23.5	23.4	22.5	22.5
584	13.3	22.7	23.5	23.7	23.0	23.3
588	—	23.5	23.5	23.7	23.6	23.6
592	—	22.8	21.2	20.1	23.4	22.8
596	—	—	19.3	18.7	21.4	22.4
600	—	18.6	18.0	17.5	21.2	22.0

where I is the observed intensity, the first and the second subscripts refer to the orientation of the polarizer and analyzer. The results obtained for excitation and emission peaks at different concentrations are given in Table I and shown in Fig. 1 whereas the results for polarization measurements are given in Table II and shown in Figs. 2(A), (B), (C), (D), (E), (F).

Discussion of results

a) Variation of excitation and emission peaks with concentration

The excitation and emission spectra of organic molecules can be discussed in terms of π, π^* and n orbitals. The excited states are essentially obtained by the excitation of the π and n electrons and the states of special interest are those corresponding to lowest singlets $S_1\pi\pi^*$ and $S_1n\pi^*$. Usually the $n\pi^*$ excited states are non fluorescent and generally the molecules fluoresce in solution for which $\pi\pi^*$ is the lowest state. In the present case when the concentration of erythrosin is higher than 1.8×10^{-5} g/cc, it is found that excitation occurs by broad band lying in two different regions. For example in Fig. 1 which is a plot of concentration vs excitation and emission wavelength, one finds that for concentration 4.4×10^{-5} g/cc, the excitation wavelengths are 500 nm and 532 nm. As erythrosin is fluorescent, the lowest excited state must be $S_1\pi\pi^*$ and hence the longest excitation wavelength $\lambda_{ex} = 532$ nm ($\sim$ 2.326 eV) corresponds to this excitation. The second wavelength 500 nm ($\sim$ 2.475 eV) gives an energy difference between the lowest and the next excited state as 0.149 eV. This possibly could be the differecne

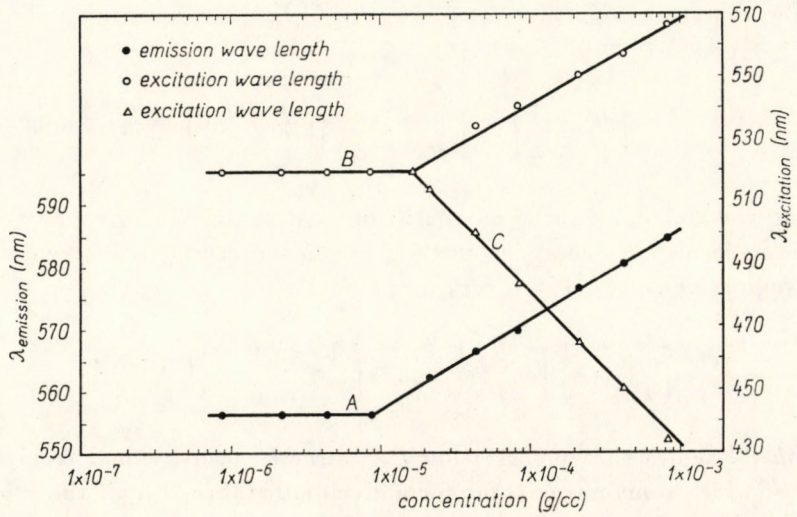

Fig. 1

between the $S_1\pi\pi^*$ and $S_1n\pi^*$ states and so $\lambda = 500$ nm may correspond to the first excited singlet transition $n \rightarrow \pi^*$. Both the excitation wavelengths are found to give only one emission wavelength $\lambda_{em} = 566$ nm. This may be possibly due to the fact that the $S_1n\pi^*$ state degrade to $S_1\pi\pi^*$ by internal conversion and then the emission takes place due to the transition from $S_1\pi\pi^*$ to the ground state [7, 8, 9]. In Fig. 1, as the concentration is decreased from a high value to 1.8×10^{-5} g/cc, all these wavelengths show a linear variation viz. (i) the emission wavelength decreases, (ii) the longest excitation wavelength decreases and (iii) the second excitation wavelength increases. This suggests that with decrease in concentration, the energy of $S_1n\pi^*$ decreases. This change in energy with concentration is similar to the behaviour of these energy levels with the change in solvent polarity and solvation of the absorbing molecule in certain substances [10].

From Fig. 1 it is obvious that the break in the linearity of the concentration vs emission wavelength curve occurs earlier (at conc $\sim 8.8\times10^{-6}$ g/cc) in comparison with the excitation curve where it occurs at conc $\sim 1.8\times$ $\times10^{-5}$ g/cc. This should mean that at the conc $\sim 8.8\times10^{-6}$ g/cc, the probability of excimer formation is higher than that of the ground state dimers. As the concentration further increases, the ground state dimers are formed (conc $\sim 1.8\times10^{-5}$ g/cc) which upon excitation give rise to fluorescence emission. The broad emission band observed can be interpreted as due to the overlapping of the monomer and dimer wavelengths. This point is further analysed with the help of the plot of the percentage polarization with emission wavelength.

b) Variation of percentage polarization with emission wavelength

The polarization of fluorescence has been found to depend upon viscosity, molecular volume, temperature and life time of the excited state and is given by PERRIN's [11] formula:

$$\left(\frac{1}{P}-\frac{1}{3}\right)=\left(\frac{1}{P_0}-\frac{1}{3}\right)\left(1+\frac{RT}{\eta v}\tau\right). \tag{2}$$

Assuming the molecules to be of quasi-spherical shape because many organic aromatic molecules are compact and fused ring structures, the above relation can be approximated to [7]

$$P=\left(\frac{1}{P_0}-\frac{1}{3}\right)^{-1}\frac{V}{10^4+V}=\left(\frac{1}{P_0}-\frac{1}{3}\right)^{-1}V\cdot10^{-4}. \tag{3}$$

Equation (3) shows that polarization P is directly proportional to molecular volume V which remains constant for a given substance. But if the substance in solution exists in more than one form of molecular aggregation, V will be

different and, therefore, polarization may show a change in the overlapping emission band due to these different molecular forms. The fluorescent properties viz. emission, excitation wavelengths, quantum yield and polarization of a solution change with increase in concentration of the dye. These changes may be due to (i) reabsorption of emitted light (ii) formation of ground state dimers and (iii) formation of excited state dimers (excimers). If erythrosin in solution exists in more than one form, then with the increase in concentration of the dye, the possibility of dimer formation increases. Fig. 2(A) corresponds to conc $\sim 3.5\times10^{-6}$ g/cc for which $\lambda_{ex} \sim 520$ nm. For this case, the polariz-

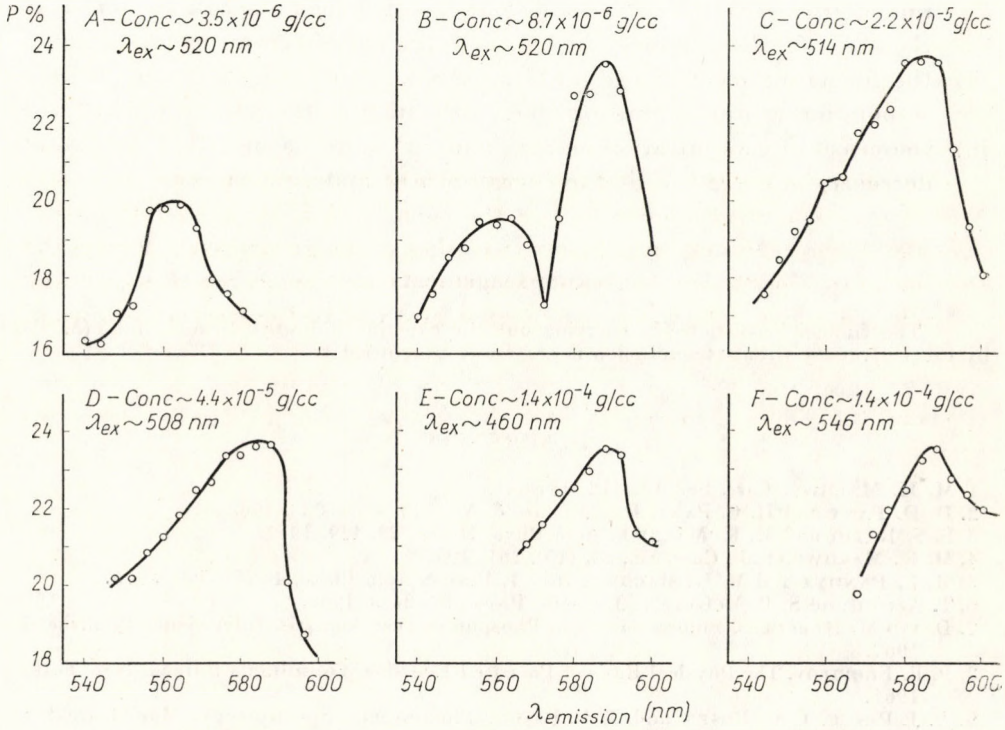

Fig. 2

ation vs emission wavelength curve gives a peak at $\lambda_{em} \sim 564$ nm which agrees with the previous reported value [4] and corresponds to monomer peak. Fig. 2(B) corresponds to conc $\sim 8.7\times10^{-6}$ g/cc for which $\lambda_{ex} \sim 520$ nm. In this case two peaks are observed — one at $\lambda_{em} \sim 564$ nm and the other at $\lambda_{em} \sim 588$ nm thus showing that for this concentration both varieties exist simultaneously. The monomer peak is lower (percentage polarization ~ 19.5) whereas the dimer peak is higher (percentage polarization ~ 23.5). As the concentration is increased, the dimer formation increases and the

monomer contribution decreases. This is obvious from Fig. 2(C) for conc $\sim 2.2\times10^{-5}$ g/cc ($\lambda_{ex} \sim 514$ nm). A very small shoulder is observed at $\lambda_{em} \sim 564$ nm, the dimer peak at $\lambda_{em} \sim 588$ nm. At still higher concentrations 4.4×10^{-5} g/cc and 1.4×10^{-4} g/cc (Figs. 2 D, E and F), the monomer peak completely disappears and the full dimer peak is observed. Figs. 2 (E) and (F) correspond to the $\pi\pi^*$ and $n\pi^*$ excitation wavelengths for conc $\sim 1.4\times10^{-4}$ g/cc showing almost similar behaviour.

Thus the present work indicates that:

i) dimers are formed with increased concentration of erythrosin in solution. The concentration corresponding to the onset of dimerization can be obtained even with a low resolving power instrument like SPF in terms of the shifts in the maxima of excitation and emission wavelength.

ii) the formation of excimers starts at a concentration lower than the corresponding concentration for dimer formation in the ground state.

iii) the effect of concentration on $\pi\pi^*$ and $n\pi^*$ states is such that $\pi\pi^*$ state decreases in energy while the energy of $n\pi^*$ state increases.

Acknowledgements

The financial assistance in carrying out the experimental work to one of us (MLP) by the University Grants Commission is gratefully acknowledged.

REFERENCES

1. M. K. MACHWE, Curr. Sc., **18,** 412, 1970.
2. D. D. PANT and H. C. PANT, Ind. J. Pure & App. Phys., **6,** 238, 1968.
3. S. S. RATHI and M. K. MACHWE, Acta Phys. Hung., **23,** 449, 1967.
4. M. K. MACHWE et al., Curr. Sc., **36,** (10), 261, 1967.
5. M. L. PANDYA and M. K. MACHWE, Ind. J. Pure & App. Phys., **14** (5), 398, 1976.
6. T. AZUMI and S. P. MCGLYNN, J. Chem. Phys., **37,** 2413, 1962.
7. DAVID M. HERCULES, Fluorescence and Phosphorescence Analysis, Interscience Publishers, 1967.
8. P. P. FEOFILOV, The Physical Basis of Polarised Emission, Consultants Bureau, New York, 1961.
9. A. J. PESCE, C. G. ROSEN and T. L. PASBY, Fluorescence Spectroscopy, Marcel Dekker Inc., New York, 1971.
10. H. MCCONNEL, J. Chem. Phys., **20,** 700, 1951.
11. F. PERRIN, Ann. Phys., (Paris) **12,** 169, 1929.

Acta Physica Academiae Scientiarum Hungaricae, Tomus 42 (3), pp. 185—187 (1977)

ADDENDUM TO THE "CORRECTION OF ELECTRON CAPTURE RATIOS MEASURED BY MULTI-WIRE PROPORTIONAL COUNTER" [1]

By

E. VATAI

INSTITUTE OF NUCLEAR RESEARCH OF THE HUNGARIAN ACADEMY OF SCIENCES, DEBRECEN

(Received 28. I. 1977)

The formulas for the calculation of the corrections of multi-wire proportional counters published in [1] are explained, simplified and corrected.

The corrections of the multi-wire proportional counter calculated by us or by using the formulas given in [1] were used in numerous cases in the last 7 years (e.g. [2], [3]). Their use made it possible to increase accuracy and reliability, which was especially important in the measurements of the M/L capture ratios. These corrections are superior to the similar calculations [5] based on the formulas of reactor theory not only because they are calculated for the actual shape of the counter, but because the integrations are performed for all necessary variables without simplification. Such calculations are needed nowadays also [4], therefore the programs have been re-written and the calculations repeated. The results agree with those of previous calculations, nevertheless it became clear that 1) a better explanation of the formulas of [1] is necessary to promote application; 2) in some cases the functions of integration can be simplified; 3) some clerical errors in the formulas should be corrected. These problems are solved below.

Two sections of the counter are given in Fig. 1 to clear the system of coordinates and notations used. The counter is given in cylindrical coordinates (z, r, φ'). The direction of the radiation (X-ray) from a given point of the counter is described by spherical angles φ changing from $-\pi$ to $+\pi$ in the plane perpendicular to the axis of the counter z, and Θ changing from 0 to π in the plane determined by φ and parallel with z. The values of Θ_i in Fig. 1 are given for anticoincidence triggering.

The self absorbtion and emission of X-rays from the counter are given by integrals of the following type:

$$I = \frac{1}{4\pi V}\int_{z_1}^{z_2} \mathrm{d}z \int_{r_1}^{r_2} r\,\mathrm{d}r \int_0^{2\pi} \mathrm{d}\varphi' \int_0^{\pi} \sin\Theta\,\mathrm{d}\Theta \int_{-\pi}^{\pi} \mathrm{d}\varphi f(z, r, \Theta, \varphi)\,,$$

which is valid for homogeneous distribution of activity and when the escape

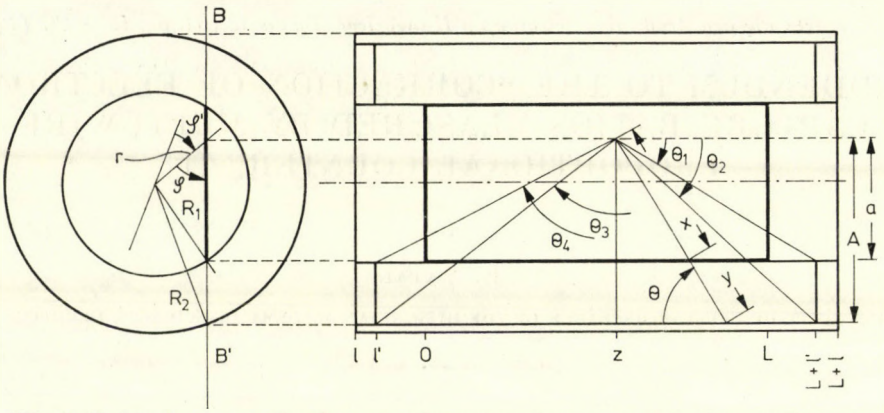

Fig. 1. Multi-wire proportional counter in two sections to explain the notations used

of secondary radiation from the given part of the counter can be neglected. Due to cylindrical symmetry, f is independent of φ', which makes analytical integration feasible for this coordinate.

Below we give the intervals and functions of integration.

Notations

$$a = r\cos\varphi + (R_1^2 - r^2\sin^2\varphi)^{1/2};$$

$$b = r\cos\varphi - (R_1^2 - r^2\sin^2\varphi)^{1/2};$$

and

$$A = r\cos\varphi + (R_2^2 - r^2\sin^2\varphi)^{1/2}$$

are used.

1. *Escape from the central counter* is an integral for $0 \leqq z \leqq L$; $0 \leqq r \leqq R_1$ and $-\pi \leqq \varphi \leqq \pi$. The function $f = \exp(-\mu x)$ where x has different forms for the three intervals of Θ:

$$x = (L - z)/\cos\Theta \quad \text{if } 0 \leqq \operatorname{tg}\Theta \leqq a/(L - z);$$

$$x = a/\sin\Theta \quad \text{if } a/(L - z) \leqq \operatorname{tg}\Theta \leqq a/z;$$

$$x = z/|\cos\Theta| \quad \text{if } a/z \leqq \operatorname{tg}\Theta \leqq \pi.$$

2. *Anticoincidence triggering* can be obtained by subtraction from the radiation unabsorbed in the central counter [$\propto \exp(-\mu x)$] the one unabsorbed both in the central and anticoincidence counters [$\propto \exp(-\mu y)$] i.e. $f = \exp(-\mu x) - \exp(-\mu y)$. Functions of the same form are to be used for all cases below. Integration limits for z, r and φ are the same as in case 1. The value $x = a/\sin\Theta$ is the same for all Θ-s, while

$$y = (L + l' - z)/\cos\Theta \quad \text{if } a/(L + l' - z) \leqq \operatorname{tg}\Theta \leqq A/(L + l' - z) = D_2;$$

$$y = A/\sin\Theta \quad \text{if } D_2 \leqq \operatorname{tg}\Theta \text{ and } \operatorname{tg}(\Theta - \pi/2) \leqq (l' + z)/A = D_3;$$

$$y = (l' + z)/|\cos\Theta| \quad \text{if } D_3 \leqq \operatorname{tg}(\Theta - \pi/2) \leqq (l' + z)/a.$$

3. *Replacement* is the radiation originated outside the central counter but absorbed in it. We divide the corresponding part of the counter into three parts according to the forms of x and y.

3a. *Replacement* from the part of anticoincidence counters, neighbouring with the central counter is an integral for $\sin|\varphi| \leq r/R_1$, because radiation emitted under larger φ does not enter into the central counter. $R_1 \leq r \leq R_3$, R_3 being the radius of the container and $0 \leq z \leq L$; $x = b/\sin\Theta$ for all values of Θ, while

$$y = (L - z)/\cos\Theta \quad \text{if } b/(L - z) \leq \operatorname{tg}\Theta \leq a/(L - z) = D_2 ;$$

$$y = a/\sin\Theta \quad \text{if } D_2 \leq \operatorname{tg}\Theta \text{ and } D_3 = a/z \geq \operatorname{tg}(\Theta - \pi/2) ;$$

$$y = z/|\cos\Theta| \quad \text{if } D_3 \leq \operatorname{tg}(\Theta - \pi/2) \leq b/z .$$

3b. *Replacement* from the ends of the anticoincidence counters is an integral for the same intervals of φ and r as in 3a, and $-l \leq z \leq 0$. The integral for $L \leq z \leq L + l$ is the same. Beside dividing the integral for Θ into three parts, it is necessary to distinguish between the cases when $a/(L - z) \lesseqgtr b/|z|$.

$$x = b/\sin\Theta \; ; \; y = (L - z)/\cos\Theta \quad \text{if } b/(L - z) \leq \operatorname{tg}\Theta \leq a/(L - z) \text{ and } b/|z|$$

$$x = b/\sin\Theta \; ; \; y = a/\sin\Theta \quad \text{if } a/(L - z) \leq \operatorname{tg}\Theta \leq b/|z| .$$

When this condition cannot be fulfilled because $a/(L - z) > b/|z|$, then $x = |z|/\cos\Theta$; $y = (L - z)/\cos\Theta$ for $b/|z| \leq \operatorname{tg}\Theta \leq a/(L - z)$. The functions are the same for both cases in the last interval:

$$x = |z|/\cos\Theta; \; y = a/\sin\Theta \quad \text{if } b/|z| \text{ and } a/(L - z) \leq \operatorname{tg}\Theta \leq a/|z| .$$

3c. *Replacement* from the end of the central counter is integral for the same intervals as in case 1 for r and φ, and as in case 3b for z. The integration for Θ is separated into two parts:

$$x = |z|/\cos\Theta; \; y = (L - z)/\cos\Theta \quad \text{if } 0 \leq \operatorname{tg}\Theta \leq a/(L - z);$$

$$x = |z|/\cos\Theta; \; y = a/\sin\Theta \quad \text{if } a/(L - z) \leq \operatorname{tg}\Theta \leq a/|z| .$$

*

The author is grateful to Prof. D. Berényi, Director of the Institute, for his interest in this work.

REFERENCES

1. E. Vatai, Acta Phys. Hung., **28,** 103, 1970.
2. H. Genz, J. P. Renier, J. G. Pengra and R. W. Fink, Phys. Rev., **C3,** 172, 1971.
3. J. G. Pengra, Second Internat. Conf. on Inner Shell Ionization Phenomena. Abstract of contributed papers, Freiburg, March 29—April 2, 1976. p. 194.
4. K.-W. Hoffmann, private communication, 1976.
5. R. B. Moler and R. W. Fink, Phys. Rev., **131,** 821, 1963.

Acta Physica Academiae Scientiarum Hungaricae, Tomus 42 (3), pp. 189—194 (1977)

ОБ ОЦЕНКЕ ОБЛАСТИ ЛОКАЛИЗАЦИИ ПОЛНОГО УМНОЖЕНИЯ ПРИ ЛАВИННОМ ПРОБОЕ ГЕТЕРОПЕРЕХОДОВ

К. М. ДАТИЕВ

ИНСТИТУТ ЭКСПЕРИМЕНТАЛЬНОЙ ФИЗИКИ, УНИВЕРСИТЕТ ИМ. АТТИЛА ЙОЖЕФА, СЕГЕД, ВЕНГРИЯ*

(Поступило 1. II. 1977)

Рассматриваются методы экспериментальной оценки области локализации полного умножения при лавинном пробое гетеропереходов, основанных на использовании температурного коэффициента напряжения лавинного пробоя и чувствительности слоя умножения $d\Phi_n/dU$.

Получены теоретические зависимости $d\Phi_n/dU$ от напряжения лавинного пробоя для любых гетеропереходов, в которых полное умножение сосредоточено в германиевой части запирающего слоя. Проводится экспериментальная проверка предлагаемых методик и сравнение полученных результатов с теорией.

Введение

Одним из новых перспективных направлений в развитии полупроводниковой электроники в последнее десятилетие является исследование гетеропереходов — контактов двух различных по химическому составу полупроводников, образованных в одном монокристалле. Интерес к гетеропереходам основывается на результатах теоретического анализа в соответствии с которыми гетеропереходы должны быть перспективны как для улучшения параметров существующих полупроводниковых приборов, так и для создания принципиально новых приборов.

Известно, что большие перспективы в направлении значительного повышения к. п. д. лавинно-пролетного диода (ЛПД), а следовательно, и мощности, отдаваемой в нагрузку генератором на ЛПД, открывает идея использования двухслойной структуры запирающего слоя, сотоящей из двух слоев с резко отличающимися значениями пробивных напряженностей электрического поля. Применение двухслойной структуры запирающего слоя, в частности, гетероперехода в ЛПД позволяет сосредоточить слой ударной ионизации в материале с узкой запрещенной зоной (с малой пробивной напряженностью электрического поля), а область пролета носителей — в широкозонном материале (с большой пробивной напряженностью электрического поля).

* Постоянное место работы: Факультет Электронной Техники, Северо-Кавказский Политехнический Институт, г. Орджоникидзе (СССР).

Таким образом, одним из важных моментов при создании ЛПД на основе гетероперехода является выяснение вопроса о локализации полного умножения в области объемного заряда гетероперехода.

Настоящая работа посвящена разработке методики экспериментальной оценки области локализации полного умножения при лавинном пробое гетеропереходов, в частности, гетеропереходов на основе германий-арсенид галлия. Теоретические оценки области локализации полного умножения при лавинном пробое гетеропереходов были рассмотрены в работах [1, 2].

Результаты исследований

Для оценки области локализации полного умножения в одной из частей запирающего слоя гетероперехода предлагается использовать два метода, сущность которых заключается в следующем:

1. проводится измерение температурного коэффициента напряжения (ТКН) пробоя гетероперехода и сравнение его с известными ТКН пробоя гомопереходов, изготовленных из этих же материалов;

2. проводится измерение чувствительности слоя умножения ($d\Phi_n/dU$) гетероперехода и сравнение его с теоретическим значением этой же величины для гомопереходов.

Как известно, температурная зависимость напряжения пробоя p—n переходов описывается выражением

$$U_{пр.}(T) = U_{пр.}(T_0)\,[1 + \beta(T - T_0)]\,, \tag{1}$$

где β — температурный коэффициент напряжения пробоя, знак и величина которого характеризуют как механизм пробоя, так и материал из которого изготовлен p—n переход.

Для p—n переходов, изготовленных из германия, кремния и арсенида галлия температурные коэффициенты напряжения пробоя известны и лежат в пределах $(0{,}7-1{,}5)\cdot 10^{-3}$ град.$^{-1}$ Измеряя температурные коэффициенты напряжения лавинного пробоя гетеропереходов и сравнивая их с известными ТКН пробоя гомопереходов, изготовленных из этих же материалов, можно сделать заключение о локализации полного умножения в одной из областей запирающего слоя гетероперехода. Экспериментальные исследования были проведены на ряде образцов гетеропереходов на основе Ge—GaAs в диапазоне температур 200—400 К.

Методика изготовления экспериментальных образцов гетеропереходов германий-арсенид галлия была описана ранее [5].

Анализ результатов для нескольких образцов гетеродиодов, представленных в Таблице I, показывает, что у ряда приборов ТКН лавинного про-

Таблица I

№ образца	$\beta \cdot 10^3$, град$^{-1}$	Φ_{Ge} [1, 2]	$U_{пр.}$, B	Примечание
A-325	0,9	0,9	23	Полное умножение преобладает в Ge -части запирающего слоя
A-328	0,9	0,9	22	
A-412	1,4	0,1	27,5	... GaAs ...
A-415	0,78	0,95	26,5	... Ge ...
A-512	1,6	0,05	29,3	... GaAs ...
A-553	0,9	0,9	22	... Ge ...
A-654	0,86	0,95	105	... Ge ...
A-659	0,9	0,95	96	... Ge ...
A-662	0,89	0,95	122	... Ge ...

боя лежит в пределах (0,9—0,7) 10^{-3} град.$^{-1}$, характерных для германиевых $p—n$ переходов. Однако, вследствии того, что образцы имели гетероструктуру Ge—GaAs, то можно сделать вывод о локализации полного умножения в германиевой части запирающего слоя. Такой вывод подтверждается теоретическим расчетом доли полного умножения, приходящейся на германиевую часть (Φ_{Ge}) запирающего слоя гетероперехода Ge—GaAs и составляющей величину больше 0,9. Значения доли полного умножения в германиевой области запирающего слоя по данным о профиле распределения концентрации атомов примесей, полученным из вольтфарадных характеристик, определялись по результатам работ [1, 2]. Для гетеродиодов с ТКН лавинного пробоя больше $1{,}4 \cdot 10^{-3}$ град.$^{-1}$ доля полного умножения в германиевой части запирающего слоя составляет величину меньше 0,1 и, следовательно, ударная ионизация происходит в арсенид-галлиевой части запирающего слоя. При промежуточных значениях ТКН лавинного пробоя, очевидно, ударная ионизация будет происходить в обеих частях запирающего слоя.

Таким образом, по величине ТКН лавинного пробоя гетероперехода Ge—GaAs (а равно и любого другого) можно экспериментально оценить область локализации полного умножения в двухслойной структуре запирающего слоя.

Локализацию полного умножения в одной из частей запирающего слоя гетероперехода можно определить также при сопоставлении экспериментально измеренной чувствительности слоя умножения $d\Phi_n/dU$ с теоретическим значением этой же величины для гомопереходов, изготовленных из этих же материалов. Для этого производится теоретический расчет чувствительности слоя умножения для германиевых $p—i—n$ и резкого $p—n$ переходов, т. к. экспериментальные образцы гетеродиодов имели структуру типов: pGe—($n—n^+$)GaAs (с линейным распределением электрического поля в германиевой части запирающего слоя) и ($p^+—p$) Ge—($n—n^+$)GaAs (с относительно однородным распределением электрического поля в германиевой части запирающего слоя) [2].

Как известно, чувствительность слоя умножения по напряжению $d\Phi_n/dU$ представляет собой отношение приращения полного умножения Φ_n к однородному изменению напряжения, действующего на запирающем слое $p—n$ перехода, а полное умножение равно

$$\Phi_n = \int_0^w \alpha(x)dx\,, \tag{2}$$

где $\alpha(x)$ — усредненный в соответствии с [3] коэффициент ударной ионизации носителей; w — толщина запирающего слоя $p—n$ перехода.

Для расчета Φ_n и $d\Phi_n/dU$ германиевых $p—n$ переходов была использована экстраполяционная зависимость коэффициента ударной ионизации от напряженности электрического поля в виде [3]

$$\alpha(E) = AE^n, \tag{3}$$

где $A = 10^{25}$ в$^{-n}$ см$^{n-1}$, $n = 5{,}45$.

Для $p—i—n$ структуры распределение электрического поля в области объемного заряда достаточно однородное и, поскольку

$$U_{пр.} = E_{пр.}\,\delta\,, \tag{4}$$

$$\Phi_n(U_{пр.}) = \int_0^\delta \alpha(E_{пр.})dx = 1\,, \tag{5}$$

то

$$\Phi_n = \left(\frac{U}{U_{пр.}}\right)^n, \tag{6}$$

$$\frac{d\Phi_n}{dU} = n\cdot\frac{1}{U_{пр,}}\,, \tag{7}$$

где $E_{пр}$ — напряженность электрического поля при пробое;
$U_{пр}$ — напряжение лавинного пробоя;
δ — толщина i-слоя;
U — напряжение, при котором полное умножение равно данному значению Φ_n.

Для резкого $p—n$ перехода распределение электрического поля в области объемного заряда имеет вид

$$E(x) = E_m\left(1 - \frac{x}{\delta}\right), \tag{8}$$

тогда

$$\Phi_n = AE_m^n\delta\int_0^1 (1-y)\,dy\,. \tag{9}$$

Учитывая далее связь между напряженностью электрического поля и напряжением $dU = \delta \cdot dE$ окончательно получим

$$\Phi_n = \left(\frac{U}{U_{np}}\right)^{\frac{n+1}{2}}, \tag{10}$$

$$\frac{d\Phi_n}{dU} = \frac{n+1}{2} \cdot \frac{1}{U_{np}}. \tag{11}$$

Экспериментальные значения чувствительности слоя умножения по напряжению для ряда образцов гетеродиодов Ge—GaAs, измеренные по методу умножения теплового тока [3, 4] приведены на рисунке. Там же нанесены теоретические значения $d\Phi_n/dU$ согласно выражениям (7) и (11).

Анализ полученных результатов показывает, что экспериментальные значения чувствительности слоя умножения некоторых гетеродиодов (А-615, А-415, А-325 и др.) близки к аналогичным расчетным величинам германиевых переходов, что является подтверждением сосредоточения полного умножения в германиевой части запирающего слоя гетеропереходов. Сравнение этих данных с результатами полученными по первому методу оценки локализации полного умножения в одной из частей запирающего слоя, показывает достаточно хорошее совпадение результатов обеих методов. Для ряда гетеродиодов (А-642, А-638, А-412, А-512) значения $d\Phi_n/dU$ сильно отличаются от соответствующих теоретических значений для германиевых $p—n$ переходов, что, очевидно, связано с локализацией полного умножения в арсенид-галлиевой части запирающего слоя. Аналогичный вывод следует и из температурных измерений.

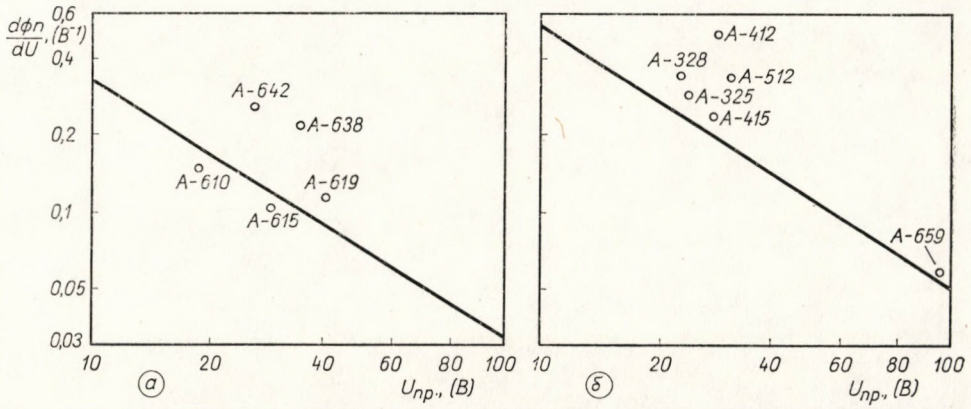

Рис. 1. Теоретические зависимости чувствительности слоя умножения для германиевых резкого $p—n$ (а) и $p—i—n$ переходов (б) (сплошные линии) и экспериментальные значения $d\Phi_n/dU$ гетеропереходов Ge—GaAs

Выводы

1. Предложены два метода, позволяющие оценить область локализации полного умножения при лавинном пробое двухслойных запирающих структур.

2. Получены теоретические зависимости чувствительности слоя умножения от напряжения лавинного пробоя для любых гетеропереходов, в которых полное умножение сосредоточено в германиевой части запирающего слоя.

3. Экспериментальная проверка предложенных методик оценки области локализации полного умножения в двухслойных запирающих структурах находится в достаточно хорошем, для целей практического использования, соответствии с результатами теории.

ЛИТЕРАТУРА

1. К. М. Датиев, И. М. Мартиросов и Я. А. Федотов, Электронная техника, сер. 2, **6**, 35, 1970.
2. Я. А. Федотов и К. М. Датиев, Электронная техника, сер. 2, **6**, 3, 1971.
3. А. П. Шотов, ЖТФ, **28**, 437, 1958.
4. И. М. Мартиросов, ФТП, **3**, 1005, 1969.
5. Я. А. Федотов, И. М. Мартиросов, К. М. Датиев и Ю. А. Кузнецов, ФТП, **5**, 1671, 1971.

Acta Physica Academiae Scientiarum Hungaricae, Tomus 42 (3), pp. 195—200 (1977)

EFFECTS OF IMPURITIES AND TENSILE LOADS ON ELECTRICAL RESISTIVITY BEHAVIOUR OF COPPER DEFORMED BY TORSION

By

G. A. HASSAN

METAL PHYSICS LABORATORY, NATIONAL RESEARCH CENTER, CAIRO, EGYPT

(Received 8. II. 1977)

Changes in the tensile strain and electrical resistivity associated with torsional deformation of copper of varying degrees of purity were investigated at room temperature. The results indicate that the application of tensile loads during torsional deformation of copper increases the tensile strain and decreases the relative changes in electrical resistivity. It was found also that the impurity content of the copper samples affects the shape of the graph of resistivity-strain. The results are explained in terms of the possible interactions of impurities with lattice defects.

Introduction

During the past ten years much attention has been directed to investigate the electrical resistivity changes in metals during simultaneous torsional-tensile deformation [1—9]. Most of them have been carried out on high purity metals and at very low temperatures. For the lack of the data, the present work aims at studying electrical resistivity changes in copper of variable purity and at room temperature.

Experimental

Copper of various purities (99.96% and 99.88%) and spec pure copper were used. The chemical analysis of the copper samples is given in Table I.

Table I

Chemical analysis of copper samples

Purity wt. %	Analysis							
99.96	As 0.00075	Bi 0.0002	Fe 0.001	Rest may be oxygen			P 0.0081	
99.88	Fe	Ni	S	Si	Pb	Mg	Ca	O_2
	<0.10	<0.10	0.002	0.001	0.001	0.0005	0.00001	400 P.P.M.

Wire samples of 0.50 mm in diameter and of 150 mm long were first annealed in a vacuum of 10^{-5} mm Hg at the following temperatures and times:

Spec pure copper: 460 °C, 4 hours

99.96% pure Cu: 900 °C, 4 hours

99.88% pure Cu: 500 °C, 5 hours.

The annealed wire samples were subjected to twisting under various applied tensile loads up to fracture. The level of applied loads did not exceed even one-third of the yield load of the fully annealed samples. The electrical resistance was measured at room temperature. The other experimental details were described in previous publications [10, 11]. In the present investigation N, L_0, D, ϱ_0, ΔL, and $\Delta\varrho$ are the number of turns of twist, initial length of the sample, diameter of the sample, electrical resistivity of annealed samples, change in samples length and change in resistivity, respectively.

Results

Figs 1, 2 and 3 show the relative changes in tensile strain $\Delta L/L_0$ in comparison to electrical resistivity changes $\Delta\varrho/\varrho_0$ accompanying torsional shear strain ND/L_0 at various applied tensile loads, for pure copper and copper of purity 99.96% and 99.88%, respectively. From these Figures it is clear that:

1. The highest applied tensile load produces, in general, the largest changes in tensile strain and the smallest changes in $\Delta\varrho/\varrho_0$ at a given ND/L_0;
2. The tensile strain increases with torsional shear strain and applied loads;
3. The shape of the graphs of $\Delta\varrho/\varrho_0$ versus ND/L_0 depends on the purity of the copper used:
   (a) the increase of $\Delta\varrho/\varrho_0$ of spec pure copper proceeds in two subsequent stages (Fig. 1). $\Delta\varrho/\varrho_0$ increases initially at a relatively rapid rate and then at a much slower rate at high values of ND/L_0. The first stage appears to depend on the magnitude of applied loads. Furthermore, Fig. 1 clearly indicates that $\Delta\varrho/\varrho_0$ of pure copper is highly sensitive to small changes in the magnitude of applied loads.
   (b) From Fig. 2 it is clear that the increase in $\Delta\varrho/\varrho_0$ of 99.96% pure copper occurred in three distinguishable stages. The $\Delta\varrho/\varrho_0$ changes of the present copper are rather similar to that shown by pure copper (Fig. 1), but at large strains further increase appears at the various applied loads used. It is interesting to note that the shape of the graph $\Delta\varrho/\varrho_0$ versus ND/L_0

for 99.98% pure copper (Fig. 2) obtained by unidirectional torsional deformation is similar to that reported by POLAK [12] for 99.99% pure copper cyclically deformed in torsion at room temperature.

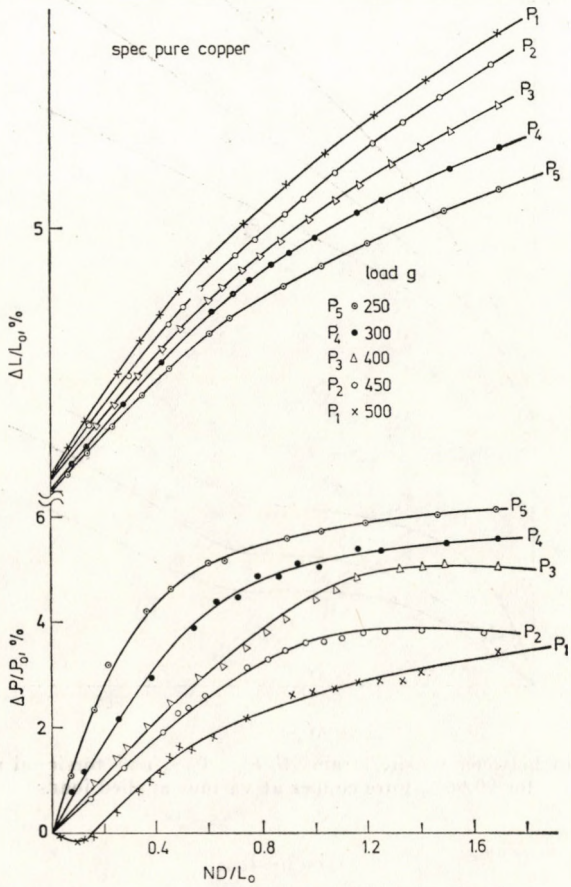

Fig. 1. Relationship between tensile strain $\Delta L/L_0$; $\Delta\varrho/\varrho_0$ and torsional shear strain ND/L_0 for pure copper at various applied loads

(c) Fig. 3 indicates that $\Delta\varrho/\varrho_0$ of 99.88% pure copper increases almost linearly with ND/L_0 at tensile loads 300, 500, and 700 gms. At the highest load used (800 gms) $\Delta\varrho/\varrho_0$ at first increases and attains a value of 2.8% at $ND/L_0 = 0.27$ then drops to a value of 1.5% with a further increase of ND/L_0 followed by an increase up to 2.5% at still higher values of ND/L_0 ($= 0.44$). It may be noted that $\Delta\varrho/\varrho_0$ changes of 99.88% pure copper exhibit lower sensitivity to changes in the level of applied loads as compared to pure copper.

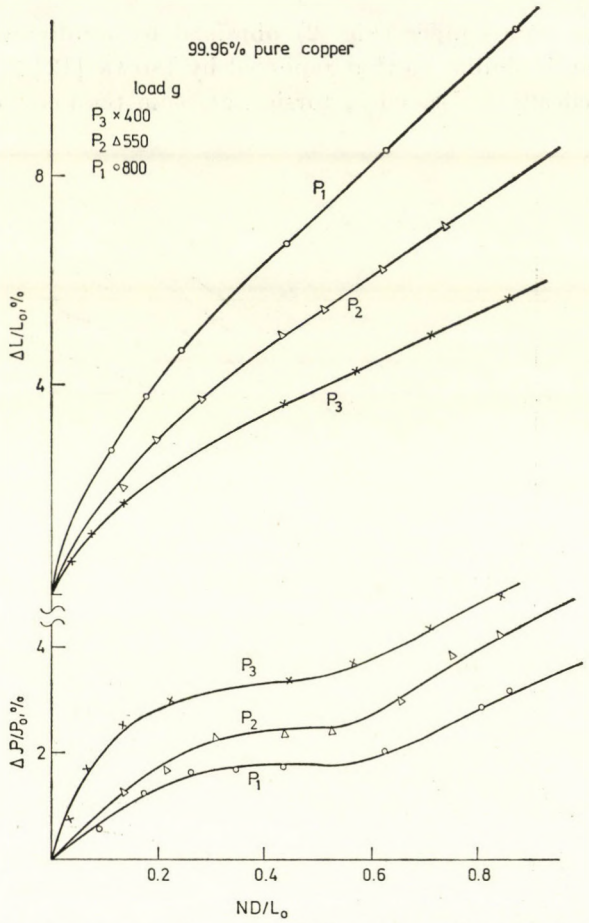

Fig. 2. Relationship between tensile strain $\Delta L/L_0$; $\Delta\varrho/\varrho_0$ and torsional shear strain ND/L_0 for 99.96% pure copper at various applied loads

Discussion

The present results revealed that a given torsional strain, ND/L_0, an increase in tensile strain and a relative decrease in electrical resistivity take place with the increase of magnitude of applied loads. Similar behaviour was noted for aluminium [10, 11] and the results were explained in terms of stress-dependent dynamic recovery processes.

An alternative interpretation is that impurities are acting as dislocation pinning points and an increase in the number of pinning would tend to yield a larger dislocation density and thus a higher resistivity increase for a given strain [13]. The $\Delta\varrho/\varrho_0$ of pure copper showed higher sensitivity to small changes in the magnitude of applied loads which might suggests that dislocation pinning in this material is relatively weak. Thus dislocation segments that

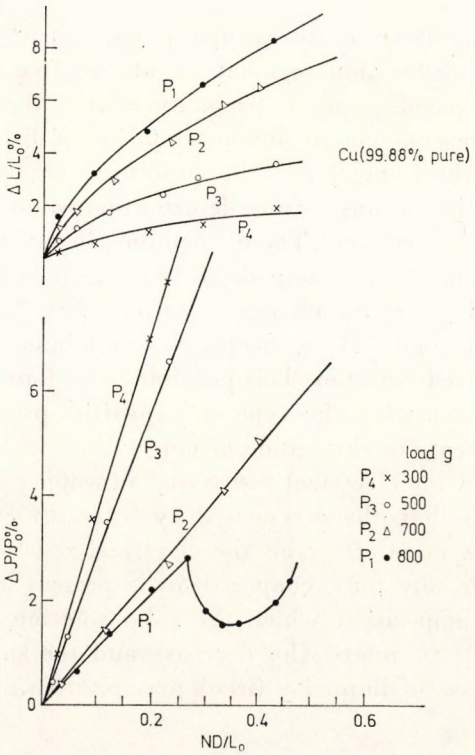

Fig. 3. Relationship between tensile strain $\Delta L/L_0$; $\Delta\varrho/\varrho_0$ and torsional shear strain ND/L_0 for 99.88% pure copper at various applied loads

were loosly pinned could be easily detached from their pinning points by the aid of slightly applied mechanical stress.

The shape of the graph (Fig. 1) which relates $\Delta\varrho/\varrho_0$ of pure copper with ND/L_0 suggests that during deformation two processes occurred which were responsible for the observed increase in $\Delta\varrho/\varrho_0$. The first process may be the continued generation of dislocations and point defects with increasing deformation. The second is believed to be connected with the mutual interaction and annihilation of dislocations and point defects. Although the first process predominated, the second one began to predominate and have a significant influence after a certain amount of ND/L_0 thus producing the decrease at the rate at which $\Delta\varrho/\varrho_0$ increased [14].

In case of 99.96% pure copper the shape of resistivity-strain curves (Fig. 2) might suggests that three processes appear in succession. Due to the presence of impurities (P and As are the major elements in 99.96% pure copper), it is likely that vacancies created by deformation are present in association with solute impurity atoms. Dislocations are favoured sites for the solute-vacancy pairs. The first increase in $\Delta\varrho/\varrho_0$ is possibly due to the pinning of dis-

locations by the migrating solute-vacancy pairs. But as the latter aggregates into fewer clusters, dislocation segments would set free to interact. The consequent increase (second stage) is probably due to the enhancement of rerecovery by some rearrangement and annihilation of dislocations. The further increase in $\Delta\varrho/\varrho_0$ (third stage) may be accounted for by the view [15] that the movement of dislocations during deformation could result in the dissociation of solute-vacancy clusters. The dissociated clusters would form an atmosphere on the dislocations and impede their motion.

The electrical resistivity changes shown in Fig. 3 revealed that at the highest load used (800 gms) $\Delta\varrho/\varrho_0$ decreases to a minimum and then increases with an increase in deformation. This peculiar behaviour of 99.88% pure copper may be connected with the type of impurities present (iron and nickel are the major elements in this grade of copper).

The effects on the electrical resistivity of copper due to the presence of various impurities have been reviewed by GREGORY et al. [16]. It appears that iron has much more effect on the electrical resistivity of copper. Cold working of commercially pure copper (iron is present as a major impurity) accelerates the decomposition which the solid solution undergoes. It seems reasonable [17—20] to relate the decrease and the subsequent increase in $\Delta\varrho/\varrho$ to the processes of impurity (iron) precipitation.

REFERENCES

1. I. KOVÁCS, Acta Phys. Hung., **15,** 65, 1962.
2. I. KOVÁCS and E. NAGY, Phys. Stat. Sol., **3,** 726, 1963.
3. I. KOVÁCS and P. FELTHAM, Phys. Stat. Sol. **3,** 2379, 1963.
4. I. KOVÁCS, E. NAGY and P. FELTHAM, Phil. Mag., **9,** 797, 1964.
5. I. KOVÁCS and E. NAGY, Phys. Stat. Sol., **8,** 795, 1965.
6. I. KOVÁCS, Acta Metall., **15,** 1731, 1967.
7. S. CERESARA and H. EL-KHOLY, Phil. Mag., **2,** 1105, 1965.
8. A. A. IBRAHIM, M. SC. Thesis, 1971, Cairo Univ.
9. F. A. EL-SALAM, Ph. D. Thesis, 1974, Cairo Univ.
10. M. R. SOLIMAN, G. A. HASSAN and F. H. HAMMAD, J. Inst. Metals, TN. 270, 99, 134, 1971.
11. F. H. HAMMAD, G. A. HASSAN and M. R. SOLIMAN, Aluminium, **4,** 49, 275, 1973.
12. J. POLÁK, Czech. J. Phys., **B23,** 322, 1973; **B19,** 315, 1969.
13. M. WINTERBERGER, Acta Metall., **7,** 549, 1959.
14. C. J. BEEVERS, Acta Metall., **11,** 1029, 1963.
15. O. DIMITROV and C. DIMITROV-FROIS, Inter. Conf. on Vacancies and Interstitials in Metals, **1,** 315, 1968 (Kernforschungsanlage Jülich, Germany)
16. P. GREGORY, A. J. BANGAY and T. L. BIRD, Metallurgica, 207, 1965.
17. M. ETO, J. Material Science, **7,** 567, 1972.
18. G. HAUSSLER, Proc. Res. Inst. for Non-Ferrous Metals (Budapest, Hung.), p. 332, 1971.
19. J. REEKLE, T. S. HUTCHISON and F. E. HETHERINGTON, Proc. Phys. Soc., **B66,** 1101, 1953.
20. W. WEYERE, Z. Met., **44,** 51, 1953.

Acta Physica Academiae Scientiarum Hungaricae, Tomus 42 (3), pp. 201—205 (1977)

UNSTEADY FLOW OF A RIVLIN—ERICKSEN LIQUID IN A ROTATING CHANNEL

By

K. S. SHIRKOT and SURJIT SINGH

DEPARTMENT OF MATHEMATICS, HIMACHAL PRADESH UNIVERSITY, SIMLA—171005, INDIA

(Received 22. II. 1977)

The unsteady flow of a Rivlin—Ericksen liquid in a parallel plate channel rotating with an angular velocity Ω is analysed. An exact solution of the governing equations is obtained. The solution in the dimensionless form contains two parameters: the elastic number $\beta_0 = \frac{\Phi_2}{\varrho z_0^2}$ and $K^2 = \frac{\Omega z_0^2}{\nu}$ which is the reciprocal of the Ekman number. The effects of these parameters on the velocity distributions are studied.

1. Introduction

In the present paper we consider the unsteady flow of a Rivlin—Ericksen liquid, confined between two parallel infinite walls, rotating with a uniform angular velocity Ω about an axis perpendicular to their planes. Exact solutions of the governing equations are obtained in closed form. There are two parameters involved, viz. the elastic number, $\beta_0 = \Phi_2/\varrho z_0^2$ and $K_2 = \Omega z_0^2/\nu$ which is the reciprocal of the Ekman number. Velocity profiles for small and large values of the parameter K^2 have been drawn. It is observed that the velocity distribution in the direction of the pressure gradient for small values of K^2 is nearly parabolic with its maximum occurring at the centre. The maximum of this velocity shifts towards the walls for large K^2. On the other hand the velocity of the secondary flow always decreases as K^2 increases and for large K^2 this distribution is oscillatory. The oscillations cause reversal of this velocity near the axis of the channels. Recently DUBE and SHARMA [1] have analysed a similar problem for a dusty viscous liquid.

2. Basic equations and their solution

We choose a cartesian system such that the z-axis is perpendicular to the plates, $z = \pm z_0$. The x-axis is in the direction of the constant pressure gradient. For simplicity the angular velocity Ω is taken to be parallel to the z-axis. Since the plates are infinite in the x and y-directions, the fields set up for the

unsteady state will depend only on z and t. The velocity vector v may reasonably be assumed as

$$\mathbf{v} = (u, v, 0) . \tag{2.1}$$

The equations of motion of a Rivlin—Ericksen liquid in the present case then reduce to

$$\frac{\partial u}{\partial t} - 2\Omega v = -\frac{1}{\varrho}\frac{\partial p}{\partial x} + \alpha\frac{\partial^2 u}{\partial z^2} + \beta\frac{\partial}{\partial t}\left(\frac{\partial^2 u}{\partial z^2}\right), \tag{2.2}$$

$$\frac{\partial v}{\partial t} + 2\Omega u = -\frac{1}{\varrho}\frac{\partial p}{\partial y} + \alpha\frac{\partial^2 v}{\partial z^2} + \beta\frac{\partial}{\partial t}\left(\frac{\partial^2 v}{\partial z^2}\right), \tag{2.3}$$

$$0 = -\frac{1}{\varrho}\frac{\partial p}{\partial z} + (2\beta + \gamma)\left[\frac{\partial}{\partial z}\left\{\left(\frac{\partial u}{\partial z}\right)^2 + \left(\frac{\partial v}{\partial z}\right)^2\right\}\right], \tag{2.4}$$

where Ω is the angular velocity of the system (consisting of the plates and the liquid) parallel to the z-axis referred to a fixed inertial frame and $p = p' - \varrho/2\,|\Omega\hat{k}\times\mathbf{r}|^2$, p' denoting the liquid pressure, $\mathbf{r}$ denoting the position vector from the z-axis, $\alpha = \Phi_1/\varrho$, $\beta = \Phi_2/\varrho$ and $\gamma = \Phi_3/\varrho$ are the kinematical coefficients of viscosity, visco-elasticity and cross-viscosity, respectively. $\hat{k}$ is the unit vector along the z-axis.

Eqs. (2.2) and (2.3) determine the velocities $u(z, t)$ and $v(z, t)$, which show that the coefficient of cross-viscosity does not affect them, as in all two-dimensional flows, but modifies the pressure field. Eq. (2.4) gives the variation of the pressure field along the z-axis, which will not be discussed further in the present investigation.

We now assume that the system is at rest initially and the liquid flows under the action of a constant pressure gradient in the direction of the x-axis between the parallel plates, $z = \pm z_0$. The boundary conditions to be satisfied are

$$\left.\begin{aligned} t = 0 \;:\; u = 0 \;\forall\; z\,\varepsilon[-z_0, z_0] , \\ t > 0 \;:\; u = 0,\; v = 0 \text{ at } z = \pm z_0 . \end{aligned}\right\} \tag{2.5}$$

We now make Eqs. (2.2) and (2.3) dimensionless by introducing the following non-dimensional quantities:

$$\bar{x} = \frac{x}{z_0}, \quad \bar{z} = \frac{z}{z_0}, \quad \bar{u} = \frac{uz_0}{\nu}, \quad \bar{v} = \frac{vz_0}{\nu},$$

$$\bar{p} = \frac{pz_0^2}{\varrho\nu^2}, \quad K^2 = \frac{\Omega z_0^2}{\nu}, \quad \beta_1 = \frac{\beta}{z_0^2}, \quad \bar{t} = \frac{vt}{z_0^2} .$$

After dropping the bars, Eqs. (2.2) and (2.3) become

$$\frac{\partial q}{\partial t} + 2iK^2 q = c + \frac{\partial^2 q}{\partial z^2} + \beta_0\frac{\partial}{\partial t}\left(\frac{\partial^2 q}{\partial z^2}\right), \tag{2.6}$$

where

$$-\frac{\partial p}{\partial x} = c \text{ (constant) for } t > 0 \text{ and } q = u + iv .$$

The boundary conditions then reduce to

$$\left.\begin{aligned} &t = 0 : q = 0 \ \forall \ z\varepsilon[-1, 1] , \\ &t > 0 : q = 0 \text{ at } z = \pm 1 . \end{aligned}\right] \tag{2.7}$$

We define the Laplace transform of q by $\bar{q}$ such that

$$\bar{q} = \int_0^\infty e^{-st} q \, dt . \tag{2.8}$$

The solution of (2.6) in terms of (2.8) [using (2.7)] is

$$\bar{q} = \frac{c}{s(s + 2iK^2)} \left[1 - \frac{\cosh pz}{\cosh p}\right], \tag{2.9}$$

where $p^2(1 - \beta_0 s) = (s + 2ik^2)$.

On inversion we get

$$q = \frac{ic}{2K^2}\left[\frac{\cosh(Kz - iKz)}{\cosh(K + iK)} - 1\right] + \\ + \frac{4c}{\pi} \sum_{n=0}^{\infty} \frac{(-1)^n e^{-a_n t}(\cos b_n t - i \sin b_n t}{(2n + 1)\left[\frac{(2n + 1)^2\pi^2}{4} \beta_0\right]} \cos\left(\frac{2n + 1}{2} \pi z\right),$$

where

$$a_n = \frac{(2n + 1)^2\pi^2}{(2n + 1)^2\pi^2\beta_0 + 4} , \quad b_n = \frac{8K^2}{(2n + 1)^2\pi^2\beta_0 + 4} .$$

Separating real and imaginary parts, we get

$$\frac{u}{c} = \frac{1}{2K^2}\left[\frac{\sin K(1 - z) \sinh K(1 + z) + \sin K(1 + z) \sinh K(1 - z)}{\cosh 2K + \cos 2K}\right] + \\ + \frac{4}{\pi} \sum_{n=0}^{\infty} \frac{4(-1)^n e^{-a_n t} \cos(b_n t)}{(2n + 1)[u + (2n + 1)^2\pi^2\beta_0]} \left(\cos \frac{2n + 1}{2} \pi z\right),$$

$$\frac{v}{c} = \frac{1}{2K^2}\left[\frac{\cosh K(1 + z) \cos K(1 - z) + \cosh K(1 - z) \cos K(1 + z)}{\cosh 2K + \cos 2K} - 1\right] \\ - \frac{u}{\pi} \sum_{n=0}^{\infty} \frac{4(-1)^n e^{-a_n t} \sin(b_n t)}{(2n + 1)[4 + (2n + 1)^2\pi^2\beta_0} \left(\cos \frac{2n + 1}{2} \pi z\right).$$

3. Discussion

The velocity profiles are shown in Figs. 1 to 3 when $t = 1$. Fig. 1 shows the velocity profiles in the direction of the pressure gradient. For small values of K^2, the profiles are nearly parabolic, the maximum of which occurs at the centre. As we increase K^2, the maximum no longer occurs at the centre but is shifted towards the walls and for large K^2, the oscillatory character of the

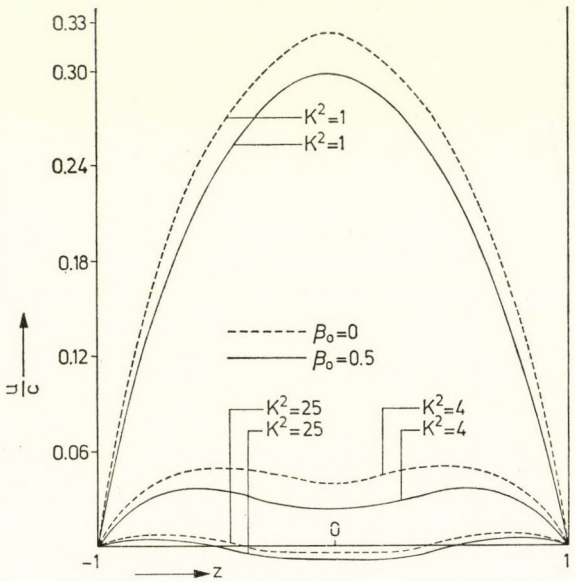

Fig. 1

flow is clearly evident from this Figure. The oscillations cause reversal of the velocity near the axis of the channel. We thus observe an interesting situation in which the Coriolis forces conspire to produce a flow situation against the pressure gradient.

Figs. 2 and 3 show the velocity of the secondary flow. These Figures exhibit that this velocity always decreases as we increase K^2. For large K^2, the profiles are oscillatory, thereby counting the possibility of flow reversal in the y-direction.

From the Figures we also observe that the elastic parameter decreases the speed of flow.

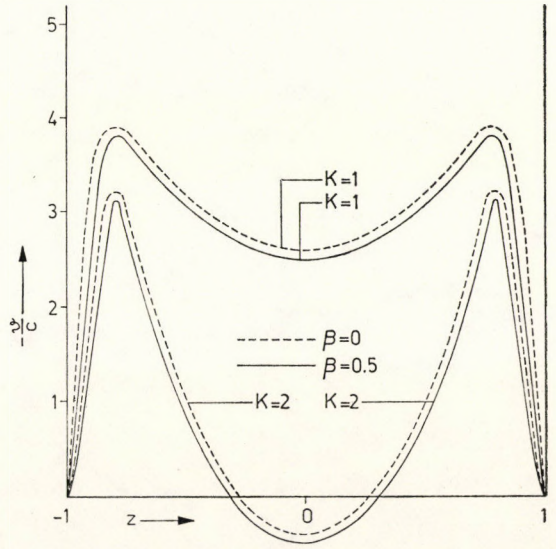

Fig. 2

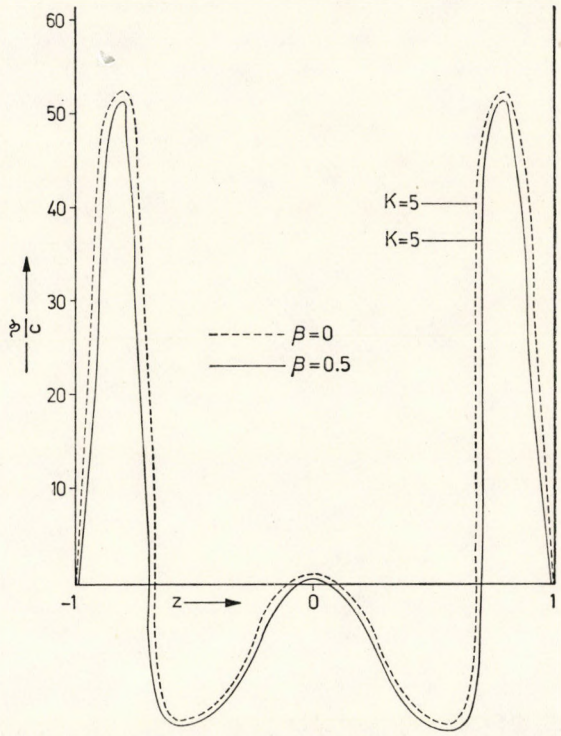

Fig. 3

REFERENCE

1. S. N. Dube and C. L. Sharma, Acta Phys. Hung., **39**, 23, 1975.

Acta Physica Academiae Scientiarum Hungaricae, Tomus 42 (3), pp. 207—214 (1977)

INVESTIGATION OF THE ^{20}Ne(d,p)^{21}Ne REACTION AT LOW BOMBARDING ENERGIES

By

A. VALEK

INSTITUTE OF NUCLEAR RESEARCH OF THE HUNGARIAN ACADEMY OF SCIENCES, DEBRECEN

(Received 22. II. 1977)

The reaction ^{20}Ne(d, p)^{21}Ne was studied in the deuteron energy range 0.5—0.66 MeV. Excitation functions and angular distributions of the proton groups p_0, p_1, p_2 and p_4 were measured. DWBA calculations reproduced the averaged angular distributions of the proton groups p_1 and p_4, indicating the presence of direct processes at low bombarding energies.

1. Introduction

Angular distributions and excitation functions of different proton groups from the ^{20}Ne(d, p)^{21}Ne reaction have been studied in the deuteron energy range 0.75—3.2 MeV [1—6] and 7.8—16.4 MeV [7—9]. The angular distributions displaying stripping patterns were analysed in terms of the BUTLER [2, 3, 5, 7] and DWBA [4, 8, 9] theories. At low bombarding energies the excitation functions of the proton groups leading to the three lowest-lying states of ^{21}Ne showed fluctuations, indicating that compound-nucleus processes play an important role in these transitions [1, 6].

In the present experiment the excitation functions and angular distributions of the proton groups p_0 ($E_x = 0$ MeV), p_1 (0.35 MeV), p_2 (1.75 MeV) and the unresolved $p_3 + p_4$ (2.79 and 2.80 MeV) have been studied in the 0.5—0.66 MeV deuteron energy interval. A DWBA analysis has been performed to investigate the importance of the direct reaction mechanism at the proton groups p_1 and p_4. The ^{20}Ne(d, p)^{21}Ne reaction had not been investigated at $E_d < 0.7$ MeV previously.

2. Experimental apparatus and method

Deuterons were accelerated by the Cockroft—Walton generator of the Institute of Nuclear Research, Debrecen. After passing a 90° magnetic analyser and collimating system, the ion beam crossed a thin-walled gas target cell mounted in the centre of the reaction chamber and was collected in a Faraday cup. The energy of the beam was monitored in the field of the analysing magnet

by a NMR probe calibrated with (p, γ) resonances on ^{7}Li, ^{19}F and ^{27}Al. The energy spread of the beam was less than 1.5 keV.

The target material used in the investigation was Ne gas of natural isotopic composition contained in the gas-cell [10]. Usually, pressures of about 20 mm Hg were used. The thickness of the targets were 2.5 keV when measuring

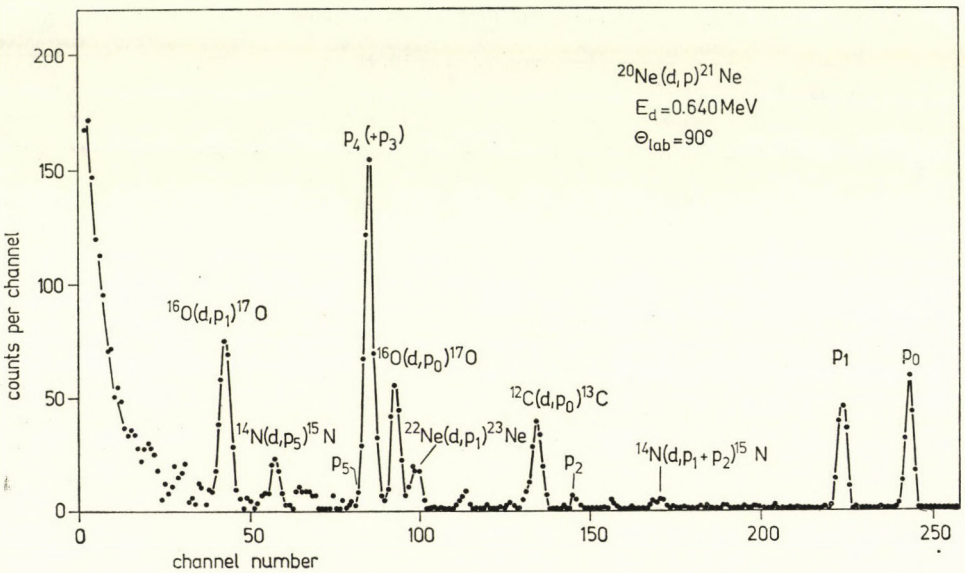

Fig. 1. A typical energy spectrum recorded in this experiment

the excitation function and about 5 keV in the angular distribution measurements. The uncertainty in the effective bombarding energy, primarily due to the changes in the thickness of the entrance window of the targets, was 3 keV in both cases.

The protons produced in the reaction were detected by semiconductor detectors. Fig. 1 shows a typical proton spectrum recorded at $E_d = 0.64$ MeV and $\Theta_{lab} = 90°$. Due to contaminants in the target, levels of ^{13}C, ^{15}N and ^{17}O were also excited. In accordance with the previous works [5, 8, 9] we assumed that in the case of the proton group $p_3 + p_4$ only the upper member ($J_F^{\pi} = 1/2^+$) of the 2.80 MeV doublet was strongly populated. E.g. at $E_d = 4$ MeV the intensity of the groups p_3 and p_5 was less than 1/10 of that of the group p_4 [11]. The proton group p_5 ($E_x = 2.87$ MeV), because of its small intensity, was not observable in this experiment.

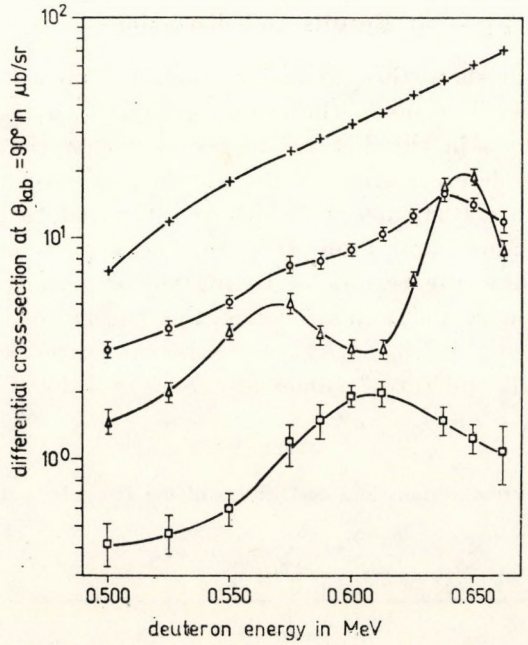

Fig. 2. Excitation functions measured at $\Theta_{lab} = 90°$ for the proton groups p_0 (△), p_1 (○), p_2 (□) and p_4 (+). The statistical error of the data points at the group p_4 is smaller than the size of the cross

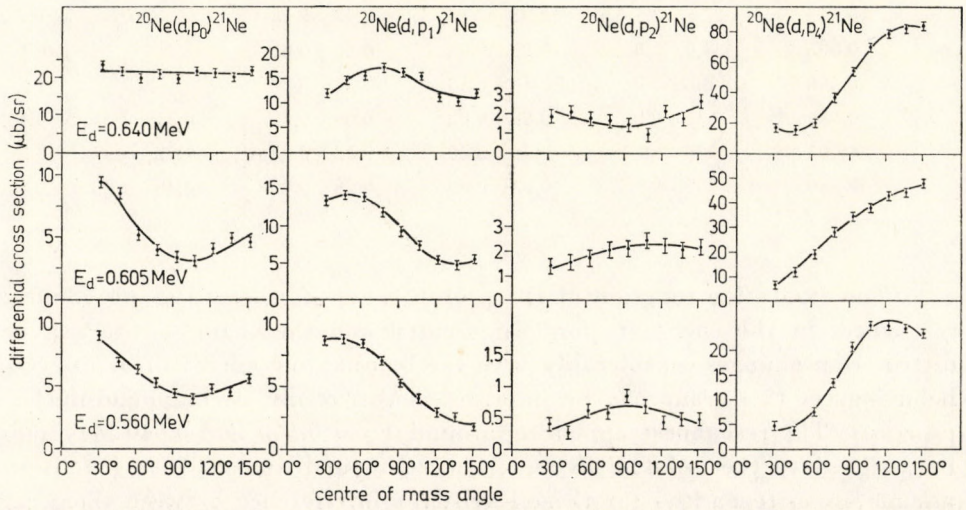

Fig. 3. Angular distributions for the p_0, p_1, p_2 and p_4 proton groups at different bombarding energies

3. Results and discussion

Figs. 2 and 3 show the excitation functions measured at $\Theta_{lab} = 90°$ and the angular distributions of the proton groups p_0, p_1, p_2 and p_4, respectively. The error bars in the Figures represent the statistical errors of the measurement. The determination of the absolute cross-section has an additional error to the statistical one, which is estimated to be about 4% for the excitation functions, and about 10% for the angular distributions. Solid lines in Fig. 3 show the results of fitting the experimental angular distributions by Legendre polynomials using the method of least squares. The expansion coefficients A_1/A_0, A_2/A_0, etc., the integrated cross-sections calculated from the A_0 and the χ^2 values are given in Table I.

Table I

Integrated cross-sections and coefficients of the Legendre polynomials

$$\frac{d\sigma(\Theta)}{d\Omega} = \sum_{l=0}^{n} A_l P_l(\cos\Theta)$$

Proton group	E_d (MeV)	σ_{int} (μb)	A_1/A_0	A_2/A_0	A_3/A_0	χ^2
p_0	0.640	267±27	0.02±0.03			1.1
	0.605	65.7±7.2	0.48±0.07	0.69±0.10		1.9
	0.560	70.2±7.0	0.35±0.04	0.42±0.05		1.4
p_1	0.640	176±19	0.09±0.05	−0.31±0.07	−0.21±0.09	2.4
	0.605	122±12	0.60±0.02	−0.04±0.02	−0.31±0.03	0.2
	0.560	70±7.0	0.77±0.04	−0.06±0.04	−0.21±0.05	0.7
p_2	0.640	22.6±3.1	−0.07±0.13	0.43±0.18		1.4
	0.605	24.9±2.8	−0.25±0.04	−0.20±0.05		0.1
	0.560	6.8±0.9	−0.13±0.13	−0.56±0.20		1.6
p_4	0.640	633±63	−0.88±0.02	0.00±0.02	0.31±0.04	0.4
	0.605	380±38	−0.79±0.02	−0.18±0.03	−0.02±0.04	0.5
	0.560	205±20	−0.83±0.05	−0.28±0.06	0.40±0.08	2.1

The excitation function of the proton group p_0 shows two pronounced resonances in the energy region investigated and the shape of the angular distribution changes considerably with the bombarding energy. The observed behaviour of this group can be interpreted as a result of compound-nucleus processes. The resonances appearing around $E_d = 0.560$ and 0.640 MeV may be assigned to the isolated levels of the compound nucleus ^{22}Na [6]. If we assume opposite parities for these levels, the interference between them can give rise to angular distributions asymmetric around 90°. Detailed calcul-

ations based on this assumption are in progress and will be published elsewhere.

The proton group p_2 measured with large statistical errors due to its small intensity shows similar characteristics. The reaction mechanism of these two transitions is compound one even at larger energies [1, 2, 5—9].

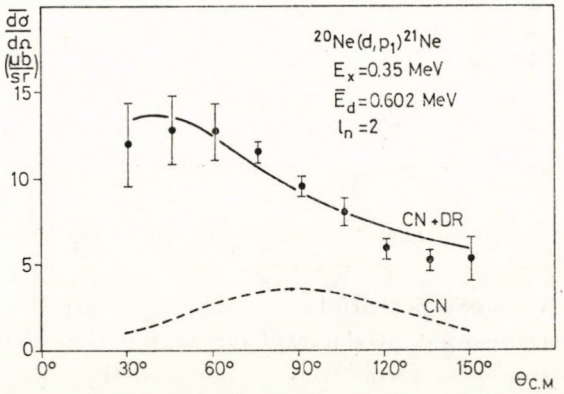

Fig. 4. Energy-averaged angular distribution for the proton group p_1 ($\triangle = 13$)

The proton group p_1 and p_4 showed direct features in the previous investigations [2—5, 7—9]. In our bombarding energy range the contribution of the compound-nucleus processes can also be seen, but its influence on the excitation functions and on the angular distributions is relatively small. The small change in the shape of the angular distributions taken at different bombarding energies is probably due to the interference between the compound-nucleus formation and the direct process. The basic forms of the angular distributions of each proton group do not vary considerably. To reduce the effect arising from the compound-nucleus formation we averaged the angular distributions measured at three deuteron energies by a method suitable for averaging at energies lying far below the Coulomb barrier [12]. The averaged angular distributions for the groups p_1 and p_4 are shown in Figs. 4 and 5, respectively. The error bars in the Figures represent the larger of the standard deviations of the average values and the experimental errors. These averaged angular distributions were compared with calculations based on DWBA theory.

To estimate the direct reaction cross-section we used the zero-range DWBA code DWUCK [13]. The optical potential both in the entrance and the exit channels were of the form:

$$V(r) = V_R f(r_R, a_R) + i\left[W_V f(r_W, a_W) - 4W_D a_W \frac{d}{dr} f(r_W, a_W)\right] + V_C(r)\,,$$

where

$$f(r_i, a_i) = -\left\{1 + \exp\left[(r - r_i A^{1/3})/a_i\right]\right\}^{-1}$$

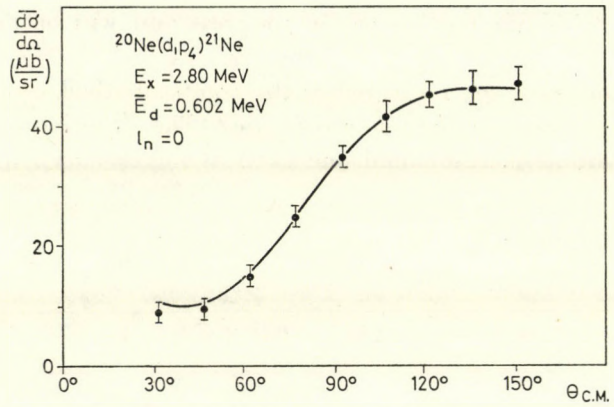

Fig. 5. Energy-averaged angular distribution for the proton group p_4 ($\Delta = 1.5$)

and $V_C(r)$ is the Coulomb potential of a uniformly charged sphere with radius $R_C = r_C A^{1/3}$. The optical-potential parameters used in the calculations are given in Table II. No spin-orbit terms were included in these potentials. The form

Table II

Optical-model parameters used in the DWBA calculations

Particle	V_R (MeV)	W_V (MeV)	W_D (MeV)	r_R (fm)	a_R (fm)	r_W (fm)	a_W (fm)	r_C (fm)	Ref.
deuteron	76	10	—	1.4	0.7	1.4	0.7	1.4	[4]
proton	50	—	10	1.25	0.65	1.25	0.47	1.25	[4, 14]

factor for the transferred neutron was calculated with a Woods—Saxon potential well with $r_0 = 1.25$ fm and $a_0 = 0.65$ fm. The depth of the well was adjusted by the program to give the experimental binding energy of the stripped neutron ($B_n = Q_{d,p} + 2.226$ MeV).

The theoretical cross-section $(d\sigma(\Theta)/d\Omega)_{DR}$ was calculated according to the equation

$$\left(\frac{d\sigma(\Theta)}{d\Omega}\right)_{DR} = 15.3 \frac{(2J_F + 1)S_l}{2j + 1} \left(\frac{d\sigma(\Theta)}{d\Omega}\right)_{DW} \frac{mb}{sr}.$$

Here J_F denotes the spin of the final state, S_l represents the spectroscopic factor, j is the total angular momentum of the transferred neutron and $(d\sigma(\Theta)/d\Omega)_{DW}$ is the cross-section in fm²/sr given by DWUCK. The $(2J_F + 1)S_l$ values obtained in the fitting of the averaged angular distribution of the proton groups p_1 and p_4 and those given by different authors are summarized in

Table III. The accuracy of the fits was measured by the values

$$\Delta = \sum_{i=1}^{9} \left\{ \left[\frac{\overline{d\sigma(\Theta_i)}}{d\Omega} - \left(\frac{d\sigma(\Theta_i)}{d\Omega} \right)_{DR} \right] / \varepsilon_i \right\}^2 ,$$

where $\overline{d\sigma(\Theta_i)/d\Omega}$ and ε_i denote the average cross-section and its error at an angle Θ_i, respectively. The Δ values are given in the figure captions.

Table III

The $(2J_F + 1)S_l$ values for ^{20}Ne(d, p)^{21}Ne reaction

Level (MeV)	J_F^π	l_n	Ref. [15]	Ref. [16]	Ref. [8] 16.4 MeV	Ref. [9] 12 MeV	Ref. [4] 3 MeV	Present work 0.6 MeV
			Theory					
0.35	5/2$^+$	2	3.72	4.0	3.7	4.0	3.1	4.0
2.80	1/2$^+$	0	0.98	0.95	1.6	1.7	0.9	0.95

The contribution of the compound processes to the cross-section of the proton group p_1 has been found to be considerable at low bombarding energies [6]. To estimate the compound nucleus cross-section the Hauser–Feshbach theory is not suitable here, since the levels of the compound nucleus ^{22}Na at an excitation energy of about 12 MeV are not yet overlapping. Therefore the compound part of the cross-section was replaced by an angular distribution of the form $a_0 + a_2 P_2(\cos \Theta)$ (dotted line in Fig. 4) and it was added incoherently to the direct part in fitting the averaged angular distribution. The values of the parameters were found to be $a_0 = 2.4$ and $a_2 = -2.2$, the integrated cross-section calculated from a_0 was in the same order of magnitude as observed for the proton group p_2. The composite curve (solid line) describes fairly well the averaged angular distribution and the value of the spectroscopic factor deduced here is in agreement with both the values extracted at higher energies and with the theoretical results.

The shape of the averaged angular distribution of the proton group p_4 has been successfully described by the DWBA alone (solid line in Fig. 5). This fact and the smooth behaviour of the excitation function encouraged us to suppose that the compound cross-section was not noticeable at this group. Inclusion of a compound contribution comparable with the cross-section of the proton group p_2 or the compound part of that of the group p_1 may decrease the spectroscopic factor by about 10%. At this transition we examined the effect of the optical-potential parameters on the spectroscopic factor. DWBA calculations were carried out with various deuteron and proton optical parameters differing a few MeV in depth from the set given in Table II. Though the goodness of the fit spoiled, the value of the spectroscopic factor was not very sensitive to these changes.

Our DWBA calculation with a potential parameter set used previously in a DWBA analysis of the ^{20}Ne(d, p)^{21}Ne reaction [4] describes quite well the shape of the averaged angular distribution of the proton group p_4 and the spectroscopic factor extracted agrees with the theoretical results and with the value deduced by DWBA analysis at $E_d = 3$ MeV. However, there is a disagreement with the values extracted at $E_d \geq 8$ MeV [8, 9]. It is accepted, that at higher bombarding energies the compound-nucleus processes are negligible and the DWBA analysis may give more reliable values for the spectroscopic factor. On the other hand, in spite of the difficulties arising from the presence of the compound processes the values extracted at low bombarding energies for the spectroscopic factor are in agreement with the values predicted by various nuclear structure calculations. On the basis of the investigations made so far it cannot be determined which of the values is correct. Independently from this uncertainty in the experimental values of the spectroscopic factor, this transition seems to be entirely direct even at very low bombarding energies.

REFERENCES

1. S. Gorodetzky, T. Muller and M. Port, Comp. Rend., **240,** 1704 and 2224, 1955.
2. W. M. Jones and D. G. Waters, Nucl. Phys., **47,** 433, 1963.
3. M. Lambert, G. Dumazet and H. Beaumeveille, Comp. Rend., **263,** 580, 1966.
4. M. Lambert, G. Dumazet, H. Beaumevieille, A. Tellez, C. Meynadier, P. Midy and Nguyen Van Sen, Nucl. Phys., **A112,** 161, 1968.
5. A. J. Howard, J. P. Allen, D. A. Bromley, J. W. Olness and E. K. Warburton, Phys. Rev., **157,** 1022, 1967.
6. M. N. H. Comsan, A. Z. El-Behay and M. A. Farouk, Atomkernenergie, **18,** 317, 1971.
7. R. Middleton and C. T. Tai, Proc. Phys. Soc., **A65,** 752, 1952.
   H. B. Burrows, T. S. Green, S. Hinds and R. Middleton, Proc. Phys. Soc., **A69,** 310, 1956.
8. A. J. Howard, J. G. Pronko and C. A. Whitten, Phys. Rev., **184,** 1094, 1969; Nucl. Phys., **A152,** 317, 1970.
9. D. W. Heikkinen and R. E. Pixley, Phys. Rev., **C3,** 1696, 1971.
10. A. Valek, ATOMKI Közl., **17,** 201, 1975.
11. J. Dubois, J. E. Christiansson, L. Jarneborn, H. Odelius, S. O. Berglund and P. Standzenieks, Physica Scripta, **5,** 169, 1972.
12. A. Valek, T. Vertse, B. Schlenk and I. Hunyadi, Nucl. Phys., **A270,** 200, 1976.
13. P. D. Kunz, University of Colorado, COO-535-606.
14. C. M. Perey and F. G. Perey, Nucl. Data Tables, **10,** 539, 1972.
15. I. P. Johnstone and H. G. Benson, Nucl. Phys., **A134,** 68, 1969.
16. M. Lambert, P. Midy and P. Desgrolard, Phys. Rev., **C8,** 1728, 1973.

Acta Physica Academiae Scientiarum Hungaricae, Tomus 42 (3), pp. 215—219 (1977)

ЛАЗЕР НА КРАСИТЕЛЯХ С РАСПРЕДЕЛЕННОЙ ОБРАТНОЙ СВЯЗЬЮ ВТОРОГО ПОРЯДКА

Т. Ш. ЭФЕНДИЕВ, А. Н. РУБИНОВ и А. Л. КИСЕЛЕВСКИЙ

ИНСТИТУТ ФИЗИКИ АН БССР, Г. МИНСК, СССР

(Поступило 22. II. 1977)

Приведены экспериментальные результаты исследований лазера на красителях с распределенной обратной связью 2-ого порядка. В качестве активной среды использовалась бинарная смесь красителей возбуждаемая излучением основной частоты и второй гармоники рубинового иазера. Описанный эксперимент демонстрирует определяющую роль фазовой решетки, индуцируемой накачкой.

Использование принципа распределенной обратной связи (РОС) в лазерах на красителях позволяет получать узкую линию генерации, перестраиваемую в широкой области спектра без применения внешнего резонатора и селективных элементов. Механизм обратной связи и частотная селекция в лазере с РОС обеспечиваются брэгговским рассеянием на амплитудно-фазовой решетке, образующейся в растворе красителя при взаимодействии когерентных световых пучков.

В лазерах с РОС период пространственной решетки является кратной величиной m половины длины волны генерируемого излучения. Обычно, для получения генерации красителя использовалась РОС 1-го порядка ($m = 1$). В работе [1] получена генерация в лазере на красителях с распределенной обратной связью 2-го и 3-го порядка, т. е. когда m равно, соответственно, 2 и 3. Распределенная обратная связь высокого порядка инициировалась в этанольном растворе родамина 6Ж при накачке излучением второй гармоники рубинового лазера.

В опубликованных до настоящего времени работах по лазерам на красителях с РОС для получения генерации в активной среде формировалась амплитудно-фазовая решетка. В этом случае трудно оценить роль фазовой и амплитудной решеток в отдельности в процессе формирования генерации в лазере с РОС.

Нами получен и исследован режим генерации в лазере на красителях с РОС для случая, когда фазовая решетка и инверсная населенность создавались раздельно в бинарной смеси красителей при накачке раствора излучением различных длин волн. Генерация красителя получена на распределенной обратной связи 2-го порядка.

Схема экспериментальной установки представлена на рисунке 1. В качестве источника накачки использовался моноимпульсный рубиновый лазер

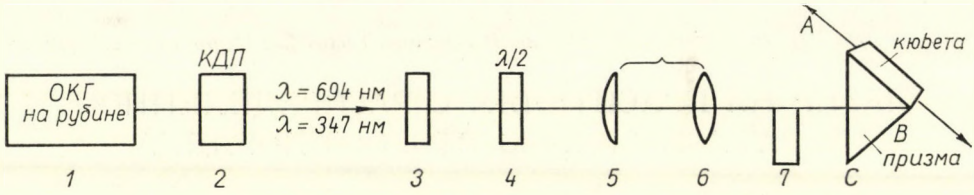

Рис. 1

(1) с удвоением частоты излучения в кристалле КДП (2). Излучение основной частоты и второй гармоники формировалось цилиндрической (5) и сферической (6) линзами в полоску и направлялось на поверхность АС призмы (8) перпендикулярно ее ребру. Раствор заливался в кювету, приставленную к боковой грани призмы [2]. На границе раздела призма — раствор происходит интерференция под углом 2Θ лучей, непосредственно падающих на эту границу, и лучей, отраженных от грани ВС. Размеры накачиваемой зоны в растворе $1{,}5 \times 0{,}1$ см.

Генерация возбуждается на длине волны (в воздухе):

$$\lambda_г = \frac{2dn_p}{m} = \frac{n_p}{n_{пр}} \cdot \frac{\lambda_H}{m \sin \Theta}, \qquad (1)$$

где d — период решетки; n_p — показатель преломления раствора красителя на длине волны генерации $\lambda_г$; $n_{пр}$ — показатель преломления материала призмы на длине волны накачки λ_H (в воздухе); Θ — угол падения накачки на поверхность раздела призма — раствор; m — целое число.

Для того, чтобы электрический вектор основной частоты и второй гармоники имел одинаковое направление, на пути луча накачки помещалась пластинка в полдлины волны (4) для основной частоты, причем вектор **E** колебался в вертикальной плоскости. Этим обеспечивались оптимальные условия для образования РОС и генерации красителя.

Из (1) видно, что для каждого значения угла Θ излучение основной частоты образует в среде решетку вдвое большего периода, чем излучение второй гармоники.

Таким ообразом генерация красителя на пространственных решетках, созданных основной частотой и второй гармоникой при одинаковом значении угла Θ, будет соответственно генерацией на РОС 2-го и 1-го порядка.

В эксперименте использовалась бинарная смесь двух красителей — 7-диэтиламино-4-метилкумарин и 1,3,3; 1′,3′,3′-гексаметил-4,5,4′,5′-дибензоиндодикарбоцианин йодид. Красители растворялись в этаноле. На рисунке 2 приведены спектры поглощения указанных красителей (кривая 1 и 3) и спектр люминесценции кумарина (кривая 2). Из приведенных спектров видно, что полиметиновый краситель почти не поглощает излучение люминесценции

кумарина в области спектра < 500 нм. Коэффициенты поглощения раствора на длинах волн $\lambda = 694$ нм и $\lambda = 347$ нм составляли 40 см$^{-1}$ и 35 см$^{-1}$ соответственно. Перед входной гранью призмы помещался светофильтр (7) (рисунок 1), поглощающий излучение второй гармоники и пропускающий излучение основной частоты рубинового ОКГ. Светофильтр устанавливался таким образом, чтобы перекрывалась половина пучка накачки, состоящего чи основной частоты и второй гармоники. В этом случае излучение основной застоты, поглощаемое полиметиновым красителем, формировало в среде фазовую решетку, а излучение второй гармоники использовалось только для оптического возбуждения кумарина. В этих условиях была получена генерация кумарина в бинарной смеси на фазовой решетке, созданной основной частотой, т. е. на распределенной обратной связи 2-го порядка. Ширина линии второго порядка, измеренная с помощью дифракционного спектрографа, составляла около 1 Å. Осуществлена перестройка длины волны генерации в спектральной области 440—490 нм. Диапазон перестройки с длиноволнового края ограничивается поглощением полиметинового красителя.

На рисунке 3а приведен спектр генерации кумарина в бинарной смеси на РОС 2-го порядка. При возбуждении этого же раствора излучением второй гармоники без формирования в активной среде фазовой решетки (для этого за кристаллом КДП устанавливался светофильтр (3), отсекающий основную частоту) наблюдалась люминесценция кумарина (рисунок 3б).

На рисунке 3в приведена линия генерации кумарина на РОС 1-го порядка. Для этого амплитудно-фазовая решетка с периодом, соответствующим первому порядку, формировалась излучением второй гармоники. (Светофильтр (7) отсутствует; основная частота отсекалась светофильтром (3). Видно различие в длинах волн для РОС 1-го и 2-го порядка (рисунки 3а и 3в) для одного и того же значения угла Θ. Это связано с тем, что показатель преломления призмы различен для длин волн 694 нм и 347 нм.

Измерены пороговые мощности накачки, требуемые для возбуждения генерации кумарина на РОС 1-го и 2-го порядка. При прочих равных условиях пороговое значение мощности накачки для второго порядка было примерно в 8 раз выше, чем для первого порядка, составлявшего ~ 40 kW.

При значительном превышении порога наряду с линией РОС 2-го порядка в спектре наблюдалась еще одна резкая линия с длиной волны равной 452 нм. При изменении угла падения Θ излучения накачки длина волны этой линии не изменялась. Наблюдаемая дополнительная линия есть генерация красителя на амплитудно-фазовой решетке, создаваемой в растворе излучением второй гармоники в результате интерференции лучей, непосредственно падающих на границу раздела AB (рисунок 4), и лучей, претерпевших последовательное отражение на поверхностях BC и AC. При повороте призмы вокруг своей оси угол 2Θ между интерферирующими лучами не изменяется

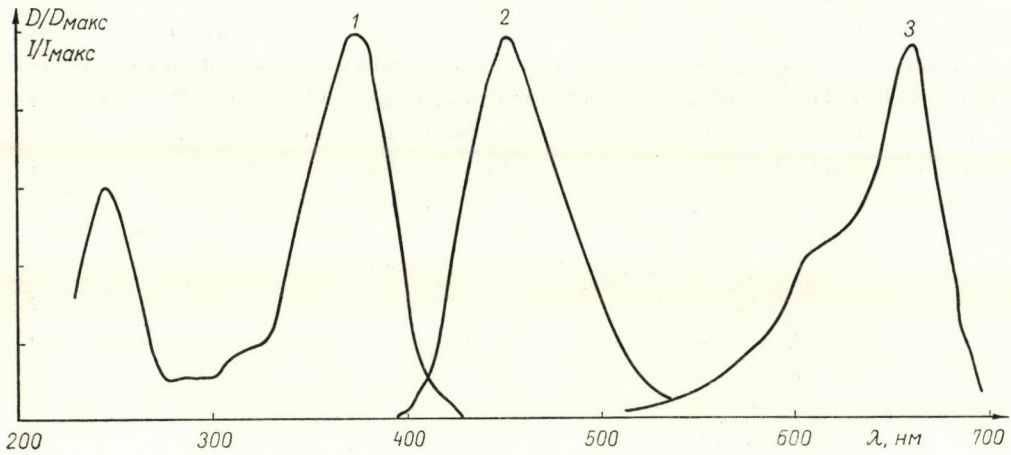

Рис. 2

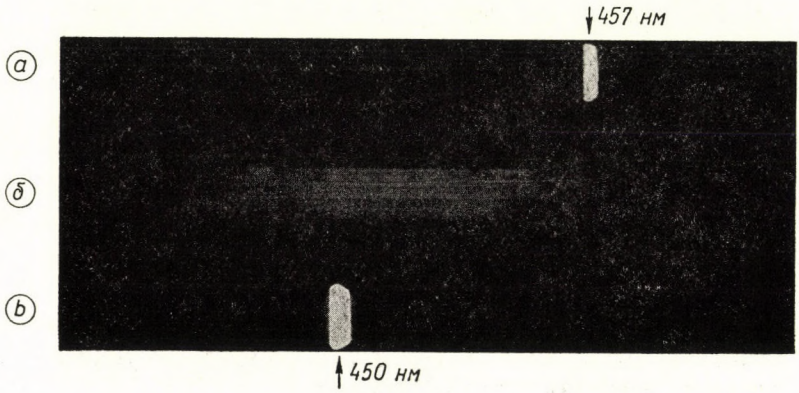

Рис. 3

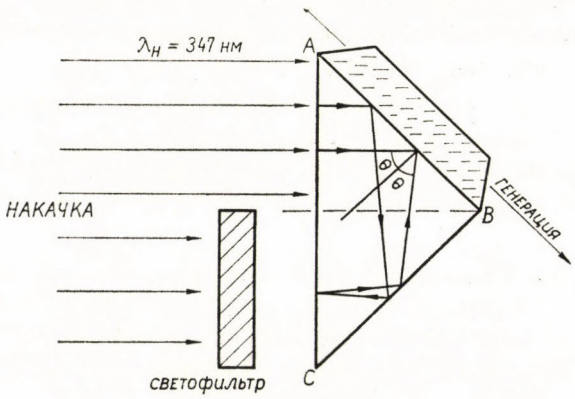

Рис. 4

и равен 90°. Длина волны дополнительной линии соответствует периоду решетки, образованной лучами, интерферирующими под углом 90°.

Плоскости дополнительной пространственной решетки расположены под углом к плоскостям решетки второго порядка. Экспериментально это проявляется в различном направлении распространения излучения генерации на РОС второго порядка и дополнительной линии. Эти направления совпадают лишь в случае нормального падения накачки на входную грань призмы.

Таким образом, настоящий эксперимент непосредственно демонстрирует определяющую роль фазовой решетки индуцируемой накачкой в механизме генерации в лазерах с РОС.

ЛИТЕРАТУРА

1. J. E. Bjorkholm, C. V. Shank, Appl. Phys. Letts., **20**, 306, 1972.
2. S. Chandra, N. Takeuchi, S. R. Hartman, Appl. Phys. Letts., **21**, 144, 1972.

Acta Physica Academiae Scientiarum Hungaricae, Tomus 42 (3), pp. 221—225 (1977)

ЛАЗЕР НА КРАСИТЕЛЯХ С ЛАМПОВОЙ НАКАЧКОЙ, РАБОТАЮЩИЙ В РЕЖИМЕ САМОСИНХРОНИЗАЦИИ МОД

С. С. АНУФРИК, В. А. МОСТОВНИКОВ, В. С. МОТКИН и А. Н. РУБИНОВ

ИНСТИТУТ ФИЗИКИ АН БССР, Г. МИНСК, СССР

(Поступило 22. II. 1977)

Приведены результаты исследования режима самосинхронизации мод в лазере на красителях с ламповой накачкой. Предложен ряд эффективных насыщающихся поглотителей (растворов полиметиновых красителей), обеспечивающих получение пикосекундных импульсов в широкой спектральной области.

Как хорошо известно, оптические квантовые генераторы, работающие в режиме самосинхронизации мод, позволяют получать мощные световые импульсы пикосекундной длительности (10^{-11}—11^{-12} сек). Несмотря на то, что уже имеется ряд работ, посвященных получению и исследованию режима самосинхронизации мод в лазерах на красителях [1—5], накопление экспериментального материала еще необходимо для создания различных типов лазеров на красителях с предельно короткой длительностью импульсов излучения и хорошо воспроизводимыми параметрами. В этом плане, одной из весьма важных задач является создание набора эффективных нелинейных поглотителей для всего спектрального диапазона работы лазеров на красителях. Актуальность таких исследований связана с широкими возможностями практического использования перестраиваемых по спектру пикосекундных световых импульсов. Особенно перспективны пикосекундные лазеры на красителях для создания спектрофотометров сверхвысокого временного разрешения.

В данной работе приведены результаты исследования режима самосинхронизации мод в лазере на красителях с ламповой накачкой, предложен ряд эффективных насыщающихся поглотителей, обеспечивающих получение пикосекундных импульсов в широкой спектральной области.

В лазере использовалась цилиндрическая кварцевая кювета длиной 120 мм и внутренним диаметром 3 мм с брюстеровскими окнами. Осветитель лазерной головки представлял собой эллипсовидный кварцевый циллиндр минимального объема, покрытый снаружи окисью магния.

Возбуждение красителей осуществлялось излучением двух параллельно соединенных импульсных ламп типа ИФП-1200. Длительность импульса накачки составляла $t_{нак} \simeq 5$ мксек при максимальной энергии до 500 дж. Резонатор лазера с базой $L = 100$ см был образован клиновыми зеркалами с

коэффициентами отражения $R_1 \simeq 100\%$ и $R_2 \simeq 70\%$. Кювета с нелинейным поглотителем имела толщину 1 мм и помещалась вблизи глухого или выходного зеркала под небольшим углом к оси резонатора. Временной ход излучения генерации регистрировался с помощью коаксиального фотоэлемента и осциллографа И2—7. При подборе соответствующих нелинейных поглотителей, в основном полиметиновых красителей, и условий возбуждения режим самосинхронизации мод был получен для следующих красителей: эскулина (спектр генерации $\Delta\lambda_г = 470—480$ нм); незамещенного родамина ($\Delta\lambda_г = 550—560$ нм); родамина Ж ($\Delta\lambda_г = 570—590$ нм); родаминов Б и 3Б ($\Delta\lambda_г = 590—630$ нм); родамина 101 ($\Delta\lambda_г = 640—660$ нм); крезил-фиолетового ($\Delta\lambda_г = 686$ нм). Для примера на рис. 1 приведены осциллограммы генерации родаминов Ж и 3Б.

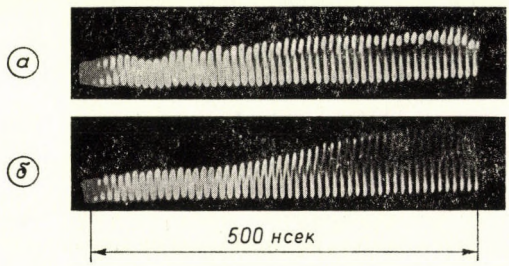

Рис. 1. Осциллограммы генерации: (а) — родамина Ж, насыщающийся поглотитель № 6 в Табл. I; (б) — родамина 3В, насыщающийся поглотитель № 12 в Табл. I

Исследования показали, что глубина модуляции генерируемого излучения в режиме самосинхронизации мод зависит как от свойств нелинейного поглотителя, так и от условий возбуждения. Полная глубина модуляции излучения, как правило, наблюдается в случае малых превышений накачки над пороговой (не более, чем в 1,5—2 раза). Следует также отметить, что для обеспечения устойчивой и надежной модуляции большое значение имеет величина пороговой энергии накачки, зависящая от эффективности активной среды и лазерной головки. Чем ниже пороговое значение энергии накачки, тем меньше термооптические искажения активной среды к моменту начала генерации и тем благоприятнее условия для возникновения режима самосинхронизации мод [2—5]. Существенное влияние на развитие режима самосинхронизации мод оказывает также температура окружающей среды. Так, например, при изменении температуры окружающей среды на несколько градусов (от +23 до +18°С) для родамина Ж (насыщающийся поглотитель — 3,3′-диэтил-9-этокситиаоксадикарбоцианин йодид) режим синхронизации мод полностью срывался (генерировался обычный гладкий импульс). Механизм данного эффекта требует дальнейших исследований. Можно, однако, предположить, что он связан с процессом ориентационной релаксации молекул поглотителя в растворе. Так как в данном лазере генерируется линейно

поляризованное излучение, то просветление красителя носит дихроичный характер. В этих условиях релаксация поглощения определяется двумя процессами — быстрым процессом ориентационной релаксации молекул в растворе, приводящим к исчезновению дихроизма (а следовательно, к увеличению поглощения падающего поляризованного излучения) и более медленным процессом дезактивации возбужденного электронного состояния. Для синхронизации мод основную роль, вероятно, играет менее инерционный процесс ориентационной релаксации молекул поглотителя, скорость которого сильно понижается при понижении температуры среды.

Главная роль в формировании процесса пикосекундной генерации принадлежит нелинейному поглотителю. Поэтому выбор эффективного нелинейного поглотителя является первостепенной задачей при создании лазеров, работающих в режиме самосинхронизации мод. Эффективный насыщающийся поглотитель, как известно, должен обладать малым временем релаксации просветления τ_p (τ_p должно быть значительно меньше времени прохода светом резонатора T); легко просветляться при невысоких интенсивностях излучения и иметь при этом минимальное остаточное поглощение.

С целью выбора наиболее эффективных насыщающихся поглотителей исследовалось большое число различных по структуре полиметиновых красителей. Сведения об их спектральных характеристиках даны в Таблице I. Здесь η — квантовый выход люминесценции; $\lambda_{погл}^{мах}$ длина волны, соответствующая максимуму поглощения; τ_{S_1}-время жизни первого возбужденного синглетного состояния; $B_{S_0-S_1}(\lambda_{погл}^{мах})$ — максимальный коэффициент Эйнштейна для перехода $S_0 \rightarrow S_1$. Среди приведенных в таблице соединений имеются достаточно эффективные, позволившие получить полную модуляцию излучения, генерируемого растворами красителей. К наиболее эффективным насыщающимся поглотителям относятся полиметиновые красители (растворитель этанол) с высоким квантовым выходом люминесценции, для которых максимум поглощения совпадает со спектром генерации, и время жизни уровня S_1 меньше времени прохода светом резонатора ($\tau_{S_1} < T$). Слабая эффективность модуляции, наблюдаемая для ряда красителей, обладающих подобными свойствами, объясняется, по-видимому, накоплением молекул в триплетном состоянии, что приводит к увеличению времени релаксации просветленного состояния (τ_p). Обычно для таких соединений вытеснение кислорода из раствора азотом сопровождается увеличением глубины модуляции генерируемого излучения, что связано с уменьшением вероятности перехода в триплет, стимулируемой до этого кислородом.

В данной работе длительность пикосекундных импульсов не измерялась. Однако, по литературным данным, полученным другими авторами [2—4] для родамина Ж в близких к нашим экспериментальных условиях она составляет 3—10 псек. С учетом этого, оценим мощность отдельного пичка генерации. Так как для применяемого нами лазера общая длительность цуга

Таблица I

Красители, используемые в качестве насыщающихся поглотителей

Растворитель — этанол

№№ п/п	Название красителя	η %	$\lambda^{max}_{погл}$ нм	$\tau_{S_1}\times10^{11}$ сек	$B_{S_0-S_1}\times10^{-6}$ сек	Глубина модуляции	Спектр. область работы нм
1	2	3	4	5	6	7	8
1.	3,3′-диэтилоксакарбоцианин йодид	4	482	—	—	с*	470—480
2.	1,1′,3,3,3′,3′-гексаметилиндокарбоцианин йодид	3	545	—	—	с*	530—560
3.	3,3′-диметил-4,5,4′,5′-дибензо-9--этилтиакарбоцианин хлорид	2	575	6,0	1,4	с*	570—585
4.	3,3′-диэтил-5,5′-дифенилоксадикарбоцианин йодид	53	597	220	4,6	н*	570—600
5.	3,3′-диэтил-9-этокситиаоксадикарбоцианин йодид	16	589	136	3,4		570—600
6.	3,3′-диэтил-5-фенил-9-этоксиоксатиадикарбоцианин йодид	26	593	260	2,8	н*	580—600
7.	3,3′-диэтил-4,5,4′,5′-ди-(2″-фенилтиазоло-4″,5″)-2,2′-тиакарбоцианин-п-толуолсульфонат	10	589	50	3,6	с*	570—600
8.	3,3′-диэтил-6,7,6′,7′-ди-(2″-фенилтиазоло-4″,5″)-2,2′-тиакарбоцианин йодид	8	578	43	3,0	н*	570—600
9.	3,3′-диэтил-10-метилоксадикарбоцианин йодид	13	580	100	4,5	н*	570—600
10.	3,3′-диэтилоксадикарбоцианин йодид	40	585	130	6,2	п	570—620
11.	1,1′-дифенил-3,3′-диэтил-5,5′-ди--(бензоксазол-2″-ил)-2,2′-имидодикарбоцианин йодид	40	633	248	7,0	п	620—650
12.	1,1′-дифенил-3,3′-диэтил-5,5′-диацетил-2,2′-имидодикарбоцианин перхлорат	24	624	156	4,0	п	610—630
13.	3,3′-диэтилтиаоксадикарбоцианин перхлорат	21	620	115	2,6	н	610—630
14.	3,3′-диэтил-10-метилтиаоксадикарбоцианин перхлорат	7	620	54	5,0	н	610—630
15.	3,3′-диэтил-2,2′-тиазолинотрикарбоцианин йодид	30	652	167	4,0	н	640—670
16.	3,3′-диэтил-5,5′-дифенил-2,2′-(1,3,4--тиадиазоло)-дикарбоцианин йодид	37	652	197	4,6	с*	640—660
17.	3,3′-диэтилтиадикарбоцианин йодид	29	650		7,9	н	650—670
18.	1,1′-диэтилхино-4,4′-карбоцианин йодид	2	707	1,5	2,4	н	670—700

Примечание: п — полная, н — неполная, н* — неполная, усиливается при насыщении раствора азотом; с* — слабая, усиливается при насыщении раствора азотом

пикосекундных импульсов равна 2—3 мксек (всего насчитывается 200—300 пичков), а энергия генерации составляет 0,01—0,02 дж, то мощность отдельного пичка генерации имеет величину — 10 Мвт. Следует отметить, что при использовании другой, более эффективной лазерной головки с кюветой,

имеющей внутренний диаметр 6 мм и длину 120 мм (с насыщающимся поглотителем 3,3 — диэтил-9-этокситиаоксадикарбоцианин йодид) была получена энергия генерации —0,2 дж при полной модуляции выходящего излучения. В этих условиях мощность одного пичка генерации достигает —100 Мвт. Таким образом, перспективы практического использования лазеров на красителях с ламповой накачкой, работающих в режиме самосинхронизации мод, связаны не только с чрезвычайно короткой длительностью импульсов, но возможностью получения весьма высоких пиковых мощностей излучения, трудно реализуемых в лазерах на красителях других типов.

ЛИТЕРАТУРА

1. W. Schmidt, F. Schäfer, Phys. Lett., **A26,** 558, 1968.
2. D. J. Bradley, F. O'Neill, Opto-Electron., **1,** 69, 1969.
3. E. Y. Arthyrs, D. J. Bradley, A. Y. Roddie, Appl. Phys. Lett., **19,** 480, 1971.
4. D. J. Bradley, A. J. Purrant, F. O'Neill, B. Sutherland, Phys. Lett., **A30,** 535, 1969.
5. Maeda Mitsuo, Miyazoe Jasushi, Jap. J. Appl. Phys., **13,** 193, 1974.

Acta Physica Academiae Scientiarum Hungaricae, Tomus 42 (3), pp. 227—235 (1977)

NON-EXPONENTIAL WAVE FUNCTIONS IN ELLIPTICAL COORDINATES FOR MOLECULES III

THE $2p\pi$ AND $3d\delta$ EXCITED STATES OF THE HeH^{2+}, LiH^{3+} AND $HeLi^{4+}$ HETERONUCLEAR SYSTEMS

By

I. TAMÁSSY-LENTEI

INSTITUTE OF THEORETICAL PHYSICS, KOSSUTH LAJOS UNIVERSITY, H—4010 DEBRECEN

(Received 22. II. 1977)

The potential energy curves of the two-centre HeH^{2+}, LiH^{3+} and $HeLi^{4+}$ heteronuclear systems in the lowest lying π and δ states, that is in the $2p\pi$ and $3d\delta$ excited states are determined with a simple analytical non-exponential wave function in elliptical coordinates using the variational method. All considered states are repulsive. The energy values calculated in the appropriate approximation agree well with the exact ones, where they are available in the considered range of the internuclear distance ($0.5a_0 \leq R \leq 6a_0$).

Introduction

Many theoretical investigations have been concerned with the ground state of the one-electron two-centre problem, especially with the H_2^+; but much fewer with its excited states.

Therefore in the previous papers of this series [1], [2] simple analytical polynomial (non-exponential) wave functions in elliptical coordinates were proposed to obtain the potential energy curves and wave functions not only for the $1s\sigma_g$ ground state, but for the first $2p\sigma_u$ and some higher excited, namely the $2p\pi_u$, $3d\pi_g$, $3d\delta_g$, $4f\delta_u$ states of the H_2^+.

Now we intend to give a similar treatment of some one-electron two-centre heteronuclear systems, the HeH^{2+}, LiH^{3+}, $HeLi^{4+}$ in the lowest lying π and δ excited states. Earlier the ground states of the later mentioned diatomics having no nuclear symmetry were investigated in a similar manner in [3].

So let the trial wave function of the systems in the n-th approximation be a suitable linear combination, as follows:

$$\psi_{(n)} = \sum_{m=1}^{n} c_m \psi_m , \tag{1}$$

where the form of the one-electron orbitals, ψ_m, is:

$$\psi_m = N_m(1 - \mu/a_m)^{l_m}[(\mu^2 - 1)(1 - \nu^2)]^{\lambda_m/2}\mu^{j_m}\nu^{k_m}e^{i\lambda_m\varphi} , \quad \begin{matrix} 0 \leq \mu \leq a_m , \\ -1 \leq \nu \leq 1 , \\ 0 \leq \varphi \leq 2\pi , \end{matrix} \tag{2}$$

and $\psi_m = 0$, if $\mu > a_m$ · μ, ν, φ are the elliptical coordinates. Regarding the notations we refer e.g. to [1]. Using the variational calculation to determine the energies and wave functions of the systems the orbitals of type (2) make the integration analytically possible. The restrictions for the variational parameters are: $k_m = 0, 1, 2, \ldots$; $l_m = 1, 2, 3, \ldots$; $a_m > 0$. λ_m may be a positive integer or zero. As earlier in [1], [2] for the sake of simplicity during the variation the values of l_m and a_m were kept equal, and the restriction $j_m = 0$ was chosen.

The $2p\pi$ state

For the states having π symmetry the parameters in the basis functions (2) $\lambda_m = 1$; further

$$k_m = m - 1 = 0, 1, 2, \ldots .$$

One can determine the potential curves for the lowest lying states analogously as in [2]. The results in n-th approximations as function of the internuclear distance, R, for the HeH^{2+}, LiH^{3+}, and $HeLi^{4+}$ systems are listed in Tables Ia, IIa and IIIa.

For comparison purposes one can find some approximative theoretical calculations for the $2p\pi$ state of the HeH^{2+}, e.g. [4], [5], [6]. But the numerical results of BATES and CARSON [7] can be considered as exact, determining the energy to five decimal places in the range $0 \leq R \leq 5a_0$.

For the LiH^{3+} and $HeLi^{4+}$ diatomics calculated values are not known.

The $3d\delta$ state

For the states having δ symmetry the parameters in the basis functions (2) $\lambda_m = 2$; further

$$k_m = m - 1 = 0, 1, 2, \ldots .$$

The results concerning the potential curves for the lowest lying $3d\delta$ states in n-th approximations as function of the internuclear distance, R, for the HeH^{2+}, LiH^{3+} and $HeLi^{4+}$ systems are listed in Tables Ib, IIb and IIIb.

Approximate molecular orbital calculation can be found for the $3d\delta$ state of the HeH^{2+} in [8] for comparison purposes, but no exact result exists.

For the further diatomics there are no values available.

Table Ia

The total energy values, $E_{(n)}$, and the parameters of the wave functions, l, a, as a function of the internuclear distance, R, for the HeH^{2+}, in atomic units for the $2p\pi$ state. The best value of a is always in brackets under $E_{(n)}$

R	l	$E_{(1)}$	$E_{(2)}$	$E_{(3)}$	$E_{(4)}$	$E_{(5)}$	$E_{(6)}$	$E_{(7)}$	E^*_{exact}
0.5	230	2.91085 (639)	2.90695 (637)	2.90689 (637)	2.90689 (637)				2.90688
1	100	0.983917 (149)	0.972331 (148)	0.971711 (148)	0.971705 (148)	0.971705 (148)			0.97168
2	80	0.132360 (67.8)	0.105377 (66.2)	0.100569 (65.9)	0.100374 (65.9)	0.100367 (65.9)			0.10035
3	80	−0.083366 (50.0)	−0.123049 (48.0)	−0.136319 (47.4)	−0.137582 (47.4)	−0.137662 (47.4)	−0.137665 (47.4)		−0.13766
4	80	−0.159959 (40.8)	−0.209728 (38.6)	−0.234225 (37.6)	−0.238409 (37.5)	−0.238844 (37.5)	−0.238869 (37.5)		−0.23887
5	90	−0.189649 (39.3)	−0.247174 (36.6)	−0.283339 (35.2)	−0.292654 (34.8)	−0.294086 (34.8)	−0.294212 (34.8)	−0.294219 (34.8)	−0.29422
6	110	−0.200081 (42.2)	−0.263315 (38.8)	−0.309826 (36.8)	−0.325857 (36.1)	−0.329229 (36.0)	−0.329648 (36.0)	−0.329683 (36.0)	

* Ref. [7]

Table Ib

The total energy values, $E_{(n)}$, and the parameters of the wave functions, l, a, as a function of the internuclear distance, R, for the HeH^{2+}, in atomic units for the $3d\delta$ state. The best value of a is always in brackets under $E_{(n)}$

R	l	$E_{(1)}$	$E_{(2)}$	$E_{(3)}$	$E_{(4)}$	$E_{(5)}$	$E_{(6)}$	E^*
0.5	1000	3.50347 (4042)	3.50308 (4039)					3.50308
1	350	1.51285 (725)	1.51145 (723)	1.51143 (723)				1.51143
2	200	0.541343 (220)	0.536942 (218)	0.536713 (218)	0.536709 (218)			0.53678 0.53680
3	110	0.239978 (86.9)	0.232314 (85.6)	0.231473 (85.4)	0.231445 (85.4)	0.231445 (85.4)		0.23173 0.23181
4	90	0.103697 (56.9)	0.092960 (55.6)	0.091015 (55.4)	0.090898 (55.4)	0.090893 (55.4)	0.090893 (55.4)	0.09163 0.09182
5	90	0.031075 (48.0)	0.017573 (46.6)	0.014031 (46.2)	0.013692 (46.2)	0.013670 (46.2)	0.013669 (46.2)	0.01519 0.01552
6	90	−0.011344 (42.0)	−0.027285 (40.5)	−0.032837 (40.0)	−0.033837 (39.9)	−0.033679 (39.9)	−0.033682 (39.9)	−0.03096 −0.03047

* Ref. [8]

Table IIa

The total energy values, $E_{(n)}$, and the parameters of the wave functions, l, a, as a function of the internuclear distance, R, for the LiH^{3+}, in atomic units for the $2p\pi$ state. The best value of a is always in brackets under $E_{(n)}$

R	l	$E_{(1)}$	$E_{(2)}$	$E_{(3)}$	$E_{(4)}$	$E_{(5)}$	$E_{(6)}$	$E_{(7)}$	$E_{(8)}$	$E_{(9)}$
0.5	200	4.10373 (425)	4.07857 (420)	4.07801 (420)	4.07801 (420)					
1	110	1.28610 (128)	1.21922 (124)	1.21375 (124)	1.21361 (124)	1.21361 (124)				
2	100	0.103119 (67.6)	−0.029584 (62.9)	−0.064924 (61.9)	−0.068651 (61.8)	−0.068863 (61.7)	−0.068870 (61.7)			
3	110	−0.173225 (55.4)	−0.343384 (50.0)	−0.421902 (48.0)	−0.439457 (47.6)	−0.441605 (47.5)	−0.441759 (47.5)	−0.441767 (47.5)		
4	140	−0.262522 (57.6)	−0.451082 (50.7)	−0.567489 (47.5)	−0.608174 (46.5)	−0.616572 (46.3)	−0.617612 (46.3)	−0.617697 (46.3)	−0.617702 (46.3)	
5	180	−0.292084 (63.5)	−0.487852 (54.8)	−0.630999 (50.4)	−0.697142 (48.7)	−0.716859 (48.2)	−0.720545 (48.1)	−0.720545 (48.1)	−0.721042 (48.1)	−0.721044 (48.1)
6	230	−0.298463 (71.8)	−0.495165 (61.1)	−0.655315 (55.2)	−0.744267 (52.6)	−0.778696 (51.7)	−0.787536 (51.5)	−0.789062 (51.4)	−0.789249 (51.4)	−0.789267 (51.4)

Acta Physica Academiae Scientiarum Hungaricae 42, 1977

Table IIb

The total energy values, $E_{(n)}$, and the parameters of the wave functions, l, a, as a function of the internuclear distance, R, for the LiH^{+3}, in atomic units for the $3d\delta$ state. The best value of a is always in brackets under $E_{(n)}$

R	l	$E_{(1)}$	$E_{(2)}$	$E_{(3)}$	$E_{(4)}$	$E_{(5)}$	$E_{(6)}$	$E_{(7)}$
0.5	900	5.12184 (2743)	5.11918 (2735)	5.11916 (2735)				
1	290	2.14911 (459)	2.13989 (454)	2.13966 (454)	2.13966 (454)			
2	140	0.722564 (121)	0.696779 (118)	0.694395 (117)	0.694304 (117)	0.694302 (117)		
3	120	0.295475 (75.0)	0.254749 (71.6)	0.246991 (71.0)	0.246325 (70.9)	0.246293 (70.9)	0.246292 (70.9)	
4	120	0.109119 (60.2)	0.056859 (56.5)	0.041099 (55.5)	0.038713 (55.4)	0.038511 (55.4)	0.038500 (55.4)	0.038499 (55.4)
5	120	0.013137 (51.2)	−0.047464 (47.4)	−0.072359 (46.0)	−0.078042 (45.7)	−0.078789 (45.7)	−0.078849 (45.7)	−0.078852 (45.7)
6	140	−0.041058 (52.3)	−0.107438 (47.7)	−0.141219 (45.8)	−0.151641 (45.3)	−0.153578 (45.2)	−0.153800 (45.2)	−0.153818 (45.2)

Table IIIa

The total energy values, $E_{(n)}$, and the parameters of the wave functions, l, a, as a function of the internuclear distance, R, for the $HeLi^{4+}$, in atomic units for the $2p\pi$ state. The best value of a is always in brackets under $E_{(n)}$

R	l	$E_{(1)}$	$E_{(2)}$	$E_{(3)}$	$E_{(4)}$	$E_{(5)}$	$E_{(6)}$	$E_{(7)}$	$E_{(8)}$	$E_{(9)}$
0.5	120	9.10579 (210)	9.09689 (209)	9.09630 (209)	9.09630 (209)					
1	70	3.46067 (68.9)	3.43824 (68.4)	3.43349 (68.3)	3.43342 (68.3)	3.43342 (68.3)				
2	60	1.00728 (35.3)	0.960234 (34.6)	0.933813 (34.3)	0.931985 (34.3)	0.931827 (34.3)	0.931823 (34.3)			
3	70	0.362052 (30.9)	0.291895 (30.0)	0.231309 (29.2)	0.220444 (29.1)	0.218820 (29.0)	0.218712 (29.0)	0.218706 (29.0)		
4	80	0.106039 (29.1)	0.014187 (27.8)	−0.080608 (26.5)	−0.110825 (26.2)	−0.117661 (26.1)	−0.118486 (26.1)	−0.118559 (26.1)	−0.118564 (26.1)	
5	90	−0.016030 (28.3)	−0.125915 (26.6)	−0.246044 (25.0)	−0.299905 (24.3)	−0.316717 (24.2)	−0.319849 (24.1)	−0.320250 (24.1)	−0.320287 (24.1)	
6	110	−0.080299 (30.7)	−0.203214 (28.3)	−0.339708 (26.2)	−0.415517 (25.3)	−0.445704 (24.9)	−0.453472 (24.8)	−0.454836 (24.8)	−0.455006 (24.8)	−0.455023 (24.8)

Acta Physica Academiae Scientiarum Hungaricae 42, 1977

Table IIIb

The total energy values, $E_{(n)}$, and the parameters of the wave functions, l, a, as a function of the internuclear distance, R, for the $HeLi^{4+}$, in atomic units for the $3d\delta$ state. The best value of a is always in brackets under $E_{(n)}$

R	l	$E_{(1)}$	$E_{(2)}$	$E_{(3)}$	$E_{(4)}$	$E_{(5)}$	$E_{(6)}$	$E_{(7)}$
0.5	400	10.6366 (986)	10.6356 (985)	10.6356 (985)				
1	170	4.69729 (221)	4.69395 (220)	4.69377 (220)				
2	100	1.84369 (72.7)	1.83479 (72.3)	1.83315 (72.2)	1.83312 (72.2)			
3	80	0.975204 (42.9)	0.960940 (42.4)	0.955999 (42.3)	0.955724 (42.2)	0.955705 (42.2)		
4	70	0.582991 (30.7)	0.563699 (30.2)	0.553643 (30.0)	0.552557 (29.9)	0.552442 (29.9)	0.552437 (29.9)	
5	70	0.370721 (26.3)	0.346650 (25.8)	0.330049 (25.4)	0.327060 (25.3)	0.326611 (25.3)	0.326578 (25.3)	0.326576 (25.3)
6	80	0.242909 (26.4)	0.214310 (25.7)	0.190491 (25.1)	0.184164 (24.9)	0.182888 (24.9)	0.182749 (24.9)	0.182738 (24.9)

Remarks

According to the above results the lowest lying π and δ excited states of the two-centre problems can be well-treated with simple analytical non-exponential wave functions of type (2) having only two non-linear variational parameters, not only in the homonuclear case, but in the heteronuclear case too, so e.g. for the HeH^{2+}, LiH^{3+} and $HeLi^{4+}$ in the whole considered range of the internuclear distance. Both the investigated states — similarly to the ground states — proved to be repulsive for the considered systems.

The calculated energy values for the HeH^{2+} in fourth-seventh approximation agree to four-five decimal places with the exact ones, where they are available; this agreement is comparable with the accuracy of the exact values.

The results are probably equally good for the LiH^{3+} and $HeLi^{4+}$ systems, for which there are no experimental or theoretical comparative data.

The convergence of the wave functions of type (1) is satisfactory and as expected it is naturally quicker for the small nuclear distances.

*

The author is grateful to Mrs. J. TIBA for her help provided in the course of the numerical calculations.

REFERENCES

1. T. TAMÁSSY-LENTEI, Acta Phys. Hung., **40,** 111, 1976.
2. I. TAMÁSSY-TENTEI, Acta Phys. Hung., **40,** 117, 1976.
3. I. TAMÁSSY-LENTEI and J. SZABÓ, Acta Phys. Hung., **36,** 323, 1974.
4. B. I. MOISEIWITSCH and A. L. STEWART, Proc. Phys. Soc., A **69,** 480, 1956.
5. A. DALGARNO and A. L. STEWART, Proc. Roy. Soc., A **240,** 274, 1957.
6. M. COHEN, R. P. MCEACHRAN and SHEILA D. MCPHEE, Can. J. Phys., **45,** 2231, 1967.
7. D. R. BATES and T. R. CARSON, Proc. Roy. Soc., A **234,** 207, 1956.
8. M. COHEN, R. P. MCEACHRAN and SHEILA D. MCPHEE, Can. J. Phys., **45,** 2749, 1967.

Acta Physica Academiae Scientiarum Hungaricae, Tomus 42 (3), pp. 237—244 (1977)

ON THE MOLECULAR POLARIZABILITIES AND INTERMOLECULAR DISPERSION ENERGIES OF DEUTERATED HYDROCARBONS AND RELATED COMPOUNDS

By

RAMA KAILA, LALJI DIXIT and P. L. GUPTA

ANALYTICAL PHYSICS SECTION, INDIAN INSTITUTE OF PETROLEUM, DEHRA DUN-248005, INDIA

(Received 24. II. 1977)

An effort has been made to discuss the effect of replacing hydrogen by deuterium on electronic polarizabilities and intermolecular dispersion energies of sixteen organic compounds. Standard one-dimensional delta-potential function model of chemical binding has been used. It has been found that the model is capable enough to account for major electronic changes of (C—H) bond region in the form of probability amplitudes of electrons so as to explain H/D isotope effect on the polarizabilities (α_M) and intermolecular dispersion energies (E_d).

Introduction

About four decades have elapsed since BELL [1] examined the effect of replacing hydrogen by deuterium on the polarizabilities of H_2, HCl, HBr and CH_4. He pointed out that because of the anharmonicity of zeropoint-oscillations, the increase in mean internuclear distance relative to the value of the minimum of the potential energy curve is less for the deuterated compounds. The difference in the internuclear distances in deuterated molecules was believed to be an additional cause for the isotope effect on polarizability. The high precision of the modern electron-diffraction measurements and analysis of the vibrational-rotational spectra could successfully explain such effects due to changes in internuclear distances for compounds containing [C—H] bond and its deuterated analogues. CYVIN and coworkers [2] systematically studied the mean vibrational amplitudes of thermal motions and succeeded in explaining H/D effects in numerous hydrocarbons and other molecules. In all such studies, the basic concept has been that the potential energy curve and force constants of bonds remain practically unchanged. The fall in polarizability on replacement of a light isotope by a heavy one was explained by RABINOVICH [3] on the basis of the decrease in zero-point energy (E_0) of the atomic oscillation. In the present communication the same effect has been explained by considering changes in internuclear distances, $R_{(C-H)}$ and $R_{(C-D)}$ using a suitable model potential function where the possibility of considering such changes exists theoretically.

Several investigators had suggested that (C—H)/(C—D) bond lengths in molecules were practically insensitive to the changes in B_0 and C_0 rotational constants, as large changes in the bond lengths could almost exactly be compensated by relatively small alteration in HĈH (DĈD) angles. Later very accurate A_0 values were determined to obtain precise (C—H)/(C—D) bond lengths. Recent studies by DUNCAN et al [4] and MCKEEN et al [5] involve one directly determined constant A_0 along with highly accurate B_0 and C_0 constants to determine molecular geometries within narrow limits assuming that zeropoint energy effects cause a shortening of (C—H) bond length on deuteration. Hence by considering ground state geometries of molecules, an explanation to the undertaken aspects may be sought. The use of one-dimensional delta function potential can be more fruitful to locate coordinates of motions of nuclei as adopted by LIPPINCOTT and DAYHOFF [6] to explain the ground state properties of diatomic molecules and bond properties of polyatomic molecules. Also recently, DIXIT et al [7, 8] have made use of the approach in explaining bond properties of several molecules. The basic concept and theoretical background of the method has been recently discussed in this journal by NAGARAJAN and SINGH [9].

Theoretical considerations

Following the variational treatment of HYLLERAAS [10] and HASSE [11] and making use of Dirac Delta function potential [6], LIPPINCOTT and STUTMAN [12] deduced an expression for molecular polarizability α_M in terms of coordinates of motion of nuclei in the form:

$$\alpha_M = \frac{1}{3}\left\{\sum_{ij}\frac{4nA_{12}\sigma}{a_0}[\langle x^2\rangle]^2 + \sum_j ndfX_j^2\alpha_j \sum_j \alpha_j\right\}, \tag{1}$$

where n is bond order, A_{12} the reduced delta-function strength, σ the covalency factor, α_j the atomic polarizability, X_j the electronegativity of the j-th atoms. The term $\langle x_j^2\rangle$ represents the probability amplitude of electrons expressed in terms of internuclear distance R as

$$\langle X^2\rangle = \frac{R^2}{4} + \frac{1}{2c_{R_{12}}^2}\ . \tag{2}$$

R is the internuclear distance at the equilibrium configuration, and

$$C_{R_{12}}^2 = (n_1 n_2 N_1 N_2)^{1/4}(A_1 A_2)^{1/2}\ ,$$

where A_i, n_i and N_i $(i = 1, 2)$ represent the δ-function strength, the principal quantum number and the number of electrons making contribution to the binding, respectively.

Now for the ground state geometries of parent and deuterated molecules, it may be very well assumed that zero-point energy effects are located within (C—H)/(C—D) bond lengths. Hence taking probability amplitudes of electrons in (C—H)/(C—D) bond region to be $[\langle x^2\rangle]_{C-H} - [\langle x^2\rangle]_{C-D}$ one can very well deduce the expression for change in molecular polarizability on deuteration as

$$\Delta\alpha_M = \frac{1}{3}\sum_i \frac{4nA_{ij}\sigma}{a_0}\left\{[\langle x^2\rangle]^2_{C-H} - [\langle x^2\rangle]^2_{C-D}\right\}. \tag{3}$$

The significant quantity $\Delta\alpha_M$ can be measured by refractometry using Lorentz Equation (4) and refractive index data

$$R_0 = \left[\frac{(n^2-1)}{(n^2+2)}\right]\frac{M}{\varrho} = \frac{4}{3}\Pi N\alpha_0, \tag{4}$$

where R_0 is the molal refraction, M is the molecular weight, ϱ is the density, N is the Avogadro's number and the subscript indicates the static value i.e. the value corresponding to a static electric field.

Further the well-known formula for electronic polarizability in VOLKENSTEIN's [13] notations read

$$\alpha = \frac{2}{h}\sum \frac{\nu_i^e \cdot P_i^2}{(\nu_i^e)^2 - \nu^2}, \tag{5}$$

where P_i^2 represents the probabilities of electronic transitions and ν the frequency of incident light. Since the electron shells of isotope molecules are identical, one can very well assume probability of electronic transition for parent molecule $P_i^2 H$ to be approximately equal to the deuterated molecules, accordingly for the polarizability α_i at the ith level one obtains

$$\frac{\alpha_{iD}}{\alpha_{iH}} = \frac{\nu_{iH}^e - \nu^2/\nu_{iH}^e}{\nu_{iD}^e - \nu^2/\nu_{iD}^e} \tag{6}$$

also since $\nu_{iH}^e < \nu_{iD}^e$([14]—[18]) the above Eq. would give

$$\alpha_{iD} < \alpha_{iH}. \tag{7}$$

These results have been verified for deuterium compounds using data on the dispersion of light [19]. Thus by expanding (6) and omitting the superscript,

e, we obtain

$$\frac{\alpha_{i,D}}{\alpha_{i,H}} = \frac{\nu_{i,H}}{\nu_{i,D}} - \nu^2 \left(\frac{1}{\nu_{i,H}\nu_{i,D}} - \frac{\nu_{i,H}}{\nu_{i,D}^3} \right) -$$

$$- \nu^4 \left(\frac{1}{\nu_{i,H}\nu_{i,D}^3} - \frac{\nu_{i,H}}{\nu_{i,D}^5} \right) - \nu^6 \left(\frac{1}{\nu_{i,H}\nu_{i,D}^5} - \frac{\nu_{i,H}}{\nu_{i,D}^7} \right) \cdots \tag{8}$$

$$\cdots \nu^{2n} \left(\frac{1}{\nu_{i,H}\nu_{i,D}^{2n-1}} - \frac{\nu_{i,H}}{\nu_{i,D}^{2n+1}} \right) \cdots ,$$

where all the coefficients of ν^{2n} have a common form and since $\nu_{i,D} > \nu_{i,H}$ these coefficients are positive. For the static polarizability i.e. $\nu = 0$ we get

$$\frac{\alpha_{iD}}{\alpha_{iH}} = \frac{\nu_{iH}}{\nu_{iD}} . \tag{9}$$

Thus as a result of relation (9), the decrease in intermolecular dispersion energy E_d may be easily estimated through the SLATER—KIRKWOOD formula [20]

$$E_d = \frac{3eh}{8\Pi r^6} \left(\frac{n\alpha_0^3}{m} \right)^{1/2} , \tag{10}$$

where n is the total number of electrons in the outer shells of the atoms forming part of the molecule, m and e are the mass and charge of an electron and r the intermolecular distance. From the computed results for polarizability of heavy and light isotopic molecules from (1) the difference in dispersion energies of the molecules can be easily derived.

Results and discussion

The well known quantum-statistical energy of a harmonic oscillator is given by

$$E = E_0 + E_{\text{therm}},$$

where the zero-point energy $E_0 = 1/2\ \hbar\omega$ and thermal energy

$$E_{\text{therm}} = \left\{ \left[\frac{\hbar\omega}{e^{\hbar\omega/kT} - 1} \right] \right\} .$$

This clearly shows that an increase in frequency will bring an increase in the zero-point energy E_0, but would cause a decrease in the thermal energy (E_{therm}). Thus the total oscillation energy falls with the fall in frequency

more slowly than the zero-point energy and this effect is more marked at higher temperatures. A plot of E vs ν (where $2\pi\nu = \omega$) at different temperatures [3] shows that even at 500 °K, the thermal energy of oscillations is about one third of the total energy (even with $\nu = 800$ cm^{-1}). Thus a change in E_0 plays a dominant role in the change of E at average temperatures. As $\partial E/\partial\omega > 0$ at all values of ω, the energy of intermolecular oscillations for the heavier isotope will be less than that for the lighter isotope. An increase in E, through increase in E_0, will cause an increase in ν_i, which in turn will produce a decrease in α_i. This concept when derived mathematically yielded Eq. (7). HYLLERAAS [10] and HASSÉ [11] variational treatment, as expressed in (1), (2) and (3), when combined with the above result of (7) implies that a decrease in polarizability due to substitution of heavy isotope is directly related to the decrease in internuclear distance R. And it is this effect which we have used to explain the isotope effect in polarizability and intermolecular dispersion energy.

Further, according to the SLATER—KIRKWOOD formula (9), the intermolecular dispersion energy is directly related to polarizability which in turn is related to interatomic forces. Because of the marked dependence of interatomic forces on the interatomic distances, we have been able to estimate the isotope-effect in the intermolecular dispersion energies of molecules.

The computed results for changes in molecular polarizability for some sixteen molecules are given in Table I. In making these calculations it has been assumed that change in polarizability is governed only by changes of internuclear distances. Force constants, bond angles and other characteristics have been assumed not to be affected significantly by deuteration. The molecules comprise (O—H)/(O—D) and (N—H)/(N—D) bonds in addition to (C—H)/(C—D) bonds. The variations in α_M i.e. change in molecular polarizability have been worked out for different ($R_{C-H}-R_{C-D}$), ($R_{O-H}-R_{O-D}$) and ($R_{N-H}-R_{N-D}$) values varying from 0.001 Å to 0.005 Å.

Amongst the calculated values, the one closest to the observed $\Delta\alpha_M$ values, along with the corresponding R_H-R_D value for which the closest value is obtained, are shown (Table I). Due to non-availability of accurate values of all the bond lengths involved for the molecules through gas-diffraction data or neutron-scattering techniques, the absolute values of polarizability of compounds could not be calculated. This limitation has further restricted our calculation of $\left[\frac{E_{d,H}-E_{d,D}}{E_{d,H}}\times 100\right]$ to a few systems only.

Based on extensive studies [21] to [24], it has been established that change in bond length on deuteration i.e. $R_{C-H}-R_{C-D} \approx 0.002$ Å for most of the systems with (C—H) bonds. HERSBACH and LAURIE [22] found that the most reliable parameters can be obtained assuming R_0 (C—H) = R_0 (C—D) + + 0.002 Å. Further, RABINOVICH and VOLOKHOVA [19], on the basis of RI data for deuterium substituted anilines and ethyl acetate, have shown that

Table I

No	System	Observed literature values 10^{-24}cm^3		Calculated $\Delta\alpha_M^{(a)} \times 10^{-24}$ cm^3		$\frac{E_{d,H}-E_{d,D}}{E_{d,H}} \times 100$	
		α_M	$\Delta\alpha_M$			Observed	Calculated
1.	C_6H_6 C_6D_6	9.950 9.896	0.054	0.0227	(0.005)*	0.41	0.37
2.	$C_6H_5CH_3$ $C_6H_5CD_3$	11.861 11.807	0.054	0.0320	(0.005)	0.57	0.45
3.	C_6H_{12} C_6D_{12}	10.745 10.623	0.122	0.0480	(0.005)	1.05	0.63
4.	$CHCl_3$ $CDCl_3$	8.258 8.258	0.00	0.0007	(0.001)	0.30	0.02
5.	$CHBr_2CHBr_2$ $CDBr_2CDBr_2$	16.108 15.991	0.017	0.0079	(0.005)	0.26	—
6.	CH_3NO_2 CD_3NO_2	4.670 2.640	0.030	0.0094	(0.005)	1.00	0.23
7.	$C_6H_5NH_2$ $C_6H_5ND_2$	11.537 11.526	0.009	0.0058	(0.005)	0.40	—
8.	$C_6D_3H_2NH_2$ $C_6D_3H_2ND_2$	11.506 11.495	0.011	0.0058	(0.005)	—	—
9.	CH_3OH CH_3OD	3.191 3.186	0.005	0.0054	(0.003)	0.54	0.08
10.	C_2H_5OH C_2H_5OD	5.010 5.006	0.004	0.0036	(0.003)	0.42	—
11.	$CH_3(CH_2)_2OH$ $CH_3(CH_2)_2OD$	6.805 6.800	0.005	0.0054	(0.003)	0.37	—
12.	$(CH_3)_2CHOH$ $(CH_3)_2CHOD$	6.836 6.834	0.002	0.0018	(0.001)	0.36	—
13.	$CH_2OH \cdot CH_2OH$ $CH_2OD \cdot CH_2OD$	4.474 4.465	0.009	0.0109	(0.003)	0.58	—
14.	$CH_2OH \cdot CHOH \cdot CH_2OH$ $CH_2OD \cdot CHOD \cdot CH_2OD$	7.751 7.730	0.021	0.0216	(0.004)	0.71	—
15.	$(CH_3)_2C(C_6H_5)O-OH$ $(CH_3)_2C(C_6H_5)O-OD$	19.043 19.034	0.009	0.0090	(0.005)	0.08	—
16.	CH_3COOH CH_3COOD	5.038 5.028	0.010	0.009	(0.005)	0.43	0.615

(a) Bond lengths involved have been taken from
(i) D. C. McKean et al., Spectrochim Acta, **29A**, 1037, 1973.
(ii) M. J. S. Dewar, Molecular Orbital Theory for Organic Compounds, McGraw Hill Book Co. Inc. N. Y. 1969.
(iii) Y. Marino, Handbook of Org. Structural Analysis, W. A. Benjamin Inc. Amsterdam, 1965.

* Value in parentheses gives the $(R_{x-H}-R_{x-D})$ value that would yield $\Delta\alpha_M$ closest to the observed value.

differences in the refractive indices of isotopic substances are approximately additive relative to the number of hydrogen atoms replaced by deuterium. This proves the validity of the additivity hypothesis for H/D effect on polarizabilities.

From this, one may expect that $\Delta\alpha_M$ for $C_6H_{12}-C_6D_{12}$ should be approximately twice of $C_6H_6-C_6D_6$ system. This has been observed to be true, as the change brought by 6 (C—D) bonds in benzene is 0.054×10^{-24} cm^3, which is roughly half of 0.122×10^{-24} cm^3, brought by 12(C—D) bonds in n-hexane. Our calculated values (Table I) show that the same is true for other C—H, O—H and N—H bonds as well. The relative difference in $\Delta\alpha_M$ is thus dependent on the number of bonds deuterated. Hence $\Delta\alpha_M$ per (C—D) bond may be easily transferred from one molecule to another under comparable environments. According to the present study $\Delta\alpha_M$ for $CHCl_3/CDCl_3$ systems would be at least 0.001×10^{-24} cm^3 while no change in α_M has been observed experimentally. A study of eight systems with O—H/O—D bonds also shows reasonably good agreement between observed and calculated values of $\Delta\alpha_M$ per O—H/O—D bond. In case of (N—H) bonds, however, the calculated $\Delta\alpha_M$ per (N—H)/(N—D) bond is found to be approximately half of the observed values. Better agreement between our calculated changes in α_M (i.e. $\Delta\alpha_M$) and the observed (literature) values in many cases, however, has been obtained for $(R_{x-H}-R_{x-D})$ values different from 0.002 Å, showing that $(R_{x-H}-R_{x-D}) \approx 0.002$ Å should only be regarded as an approximation.

Above observations prove the validity of the additivity hypothesis for polarizability change per deuterated bond. The expected difference in $\Delta\alpha_M$ in accordance with (7) is justified by the present study. It may be inferred that although the molecular polarizability cannot be resolved into atomic components, the change in α_M due to H/D isotope effect may be safely interpreted considering bond components, a genuine physical ground suggested by DENBIGH [25]. This is also physically reasonable since electrons in the bonding regions are loosely bound relative to electrons close to the nucleus and are therefore more polarizable. Conclusively it may be said that this is a first systematic study in which we have tried to explain H/D isotopic effect and the results may be said to be encouraging.

REFERENCES

1. R. P. BELL, Trans. Faraday Soc., **38,** 422, 1942.
2. S. J. CYVIN, Molecular Structure and Vibrations, Elsevier Publ. Co., Amsterdam, 1972.
3. I. B. RABINOVICH, Influence of Isotopy on the Physico-chemical Properties of Liquids, c/b A special research report translated from Russian, New York, 1970.
4. J. L. DUNCAN, D. C. MCKEAN, P. D. MALLINSON and R. D. MCCULLOCH, J. Mol. Spectrosc., **46,** 232, 1973.
5. D. C. MCKEAN, J. L. DUNCAN and L. BATT, Spectrochim. Acta, **29A,** 1037, 1973.
6. E. R. LIPPINCOTT and M. O. DAYHOFF, Spectrochim. Acta, **16,** 807, 1960.
7. L. DIXIT, S. K. KAPOOR, I. D. SINGH and P. L. GUPTA, Indian J. Pure and Applied Physics, **14,** 648, 1976.
8. N. K. SANYAL, AHMED PARVEZ and L. DIXIT, J. Phys. Chem., **77,** 2552, 1973.
9. G. NAGARAJAN and Z. SINGH, Acta Phys. Hung., **36,** 381, 1974.
10. E. A. HYLLERAAS, Z. Phys., **65,** 209, 1930.
11. H. R. HASSE, Proc. Cambridge Phil. Soc., **26,** 542, 1930; ibid **27,** 66, 1931.
12. E. R. LIPPINCOTT and J. M. STUTMAN, J. Phys. Chem., **68,** 2926, 1964.

13. M. V. VOLKENSTEIN, Structure and Physical Properties of Molecules, Izd. Akad. Nauk. SSSR, Moscow 1955.
14. C. K. INGOLD and C. L. WILSON, J. Chem. Soc., 941, 1936.
15. L. GERÖ and R. SCHMID, Z. Phys., **118**, 210, 1941.
16. J. FRANCK and R. W. WOOD, Phys. Rev., **45**, 667, 1934.
17. R. E. HONIG, J. Chem. Phys., **16**, 105, 1946.
18. H. NEUERT, Z. Naturforsch., **7a**, 293, 1952.
19. I. B. RABINOVICH and Z. V. VOLOKHOVA, Dokl. Akad. Nauk. SSSR, **112**, 844, 1958.
20. J. C. SLATER and J. C. KIRKWOOD, Phys. Rev., **37**, 682, 1931.
21. J. L. DUNCAN and P. D. MALLINSON, J. Mol. Spect., **39**, 471, 1971.
22. D. R. HERSCHBACH and V. W. LAURIE, J. Chem. Phys., **37**, 1687, 1962.
23. A. G. MAKI and R. A. TOTH, J. Mol. Spect., **17**, 136, 1965.
24. D. C. MCKEAN, Chem. Communication, 1373, 1971.
25. K. G. DENBIGH, Trans. Faraday. Soc., **36**, 936, 1940.

Acta Physica Academiae Scientiarum Hungaricae, Tomus 42 (3), pp. 245—250 (1977)

COSMOLOGICAL UNIVERSES WITH SPHERICAL SYMMETRY

By

SHRI RAM* and J. N. S. KASHYAP

DEPARTMENT OF MATHEMATICS, BANARAS HINDU UNIVERSITY, VARANASI—221005, INDIA

(Received 8. III. 1977)

In this paper Einstein's field equations for perfect fluid distribution with a specific equation of state are imposed to the most general spherically symmetric space-time defined by SYNGE in Kruskal coordinates. A functional relationship is obtained which culminates in a prescription for building the most general cosmological solutions. The de Sitter cosmological universe is obtained in a systematic way.

1. Introduction

The most general spherically symmetric metric defined by SYNGE in Kruskal coordinates, is [1]:

$$ds^2 = -2f\,du\,dv + r^2(\mathrm{d}\Theta^2 + \sin^2\Theta\, d\Phi^2)\,, \tag{1.1}$$

where f and r are functions of (u, v). The coordinates $x^1 = u$, $x^4 = v$ are taken on a 2-space U_2. The coordinates $x^2 = \Theta$ and $x^3 = \Phi$ belong to a unit sphere S_2. For this metric SYNGE has explored the solutions of Einstein's field equations in vacuo in terms of suitable coordinates; and obtained Schwarzschild solution in a systematic way. The present authors have imposed Einstein—Maxwell equations to this line-element and obtained a functional relationship between the general functions f and r which enables us to get several solutions under specific coordinate system. The Reissner—Nordström solution is shown to be a special case [2]. The present authors also have obtained an explicit solution of Einstein-Scalar zero-rest-mass field equations [3].

In this paper we have obtained a functional relationship between the functions f and r in (1.1) satisfying the Einstein's field equations for the perfect fluid with the equation of state $\varrho + p = 0$. By using suitable arbitrary functions occurring in the relationship we can create spherically symmetric cosmological universes worthy of study. For justification the de Sitter universe is obtained in a systematic way.

* Applied Mathematics Section, Institute of Technology, Banaras Hindu University, Varanasi — 22 1005, India

2. Field equations

The energy-momentum tensor for a perfect fluid distribution is given by

$$T_{ij} = (\varrho + p)v_i v_j - pg_{ij} \tag{2.1}$$

together with

$$g_{ij}v^i v^j = 1\,,$$

p being the pressure, ϱ the density and $v_i = (v_1, 0, 0, v_4)$ the flow vector which represents the motion of the fluid in the u-direction. The field equations

$$R_{ij} - \frac{1}{2}Rg_{ij} + \Lambda g_{ij} = -8\pi T_{ij} \tag{2.2}$$

for the metric (1.1) are as follows:

$$2r_{14} + 2r_1 r_{4/fr^2} + 1/r^2 + \Lambda = K[-(\varrho + p)\, v_1 v_{4/f} - f]\,, \tag{2.3}$$

$$2r_{14/fr} + (f_{14} - f_1 f_4/f)/f^2 + \Lambda = -Kp\,, \tag{2.4}$$

$$2(r_{11} - r_1 f_1/f)/fr = K(\varrho + p)v_1^2/f\,, \tag{2.5}$$

$$2(r_{44} - r_4 f_4/f)/fr = K(\varrho + p)v_4^2/f\,, \tag{2.6}$$

where Λ is the cosmological constant and $K = -8\pi$. The necessary condition for perfect fluid distribution ensures us the equality of the Einstein tensor components G_1^1, G_2^2, G_3^3 and $G_4^3 (G_i^j = R_i^j - 1/2\delta_i^j R)$. Therefore $\varrho + p = 0$ is the only admissible physical situation for which the Eqs. (2.3)—(2.6) may give solutions. Imposing the condition $\varrho + p = 0$ the above equations reduce to

$$2r_{14}/fr + 2r_1 r_4/fr^2 + 1/r^2 = Kp - \Lambda\,, \tag{2.7}$$

$$2r_{14}/fr + (f_{14} - f_1 f_4/f)/f^2 = Kp - \Lambda\,, \tag{2.8}$$

$$r_{11} - r_1 f_1/f = 0\,, \tag{2.9}$$

$$r_{44} - r_4 f_4/f = 0\,. \tag{2.10}$$

The suffixes 1 and 4 after the symbols f and r denote ordinary differentiation with respect to u and v respectively.

3. Solution of the field equations

The Eqs. (2.9) and (2.10), after integration, provide

$$f = 2B(v)r_1\,,\ f = 2A(u)r_4\,, \tag{3.1}$$

where $A(u)$ and $B(v)$ are arbitrary functions of u and v, respectively. Using (3.1) the Eq. (2.7) can be written in the alternative forms

$$\begin{aligned}(rr_1)_4 &= A(u)(\lambda^2 r^2 - 1)r_4\,,\\ (rr_4)_1 &= B(v)(\lambda^2 r^2 - 1)r_1\,,\end{aligned} \tag{3.2}$$

where $\lambda^2 = Kp - \Lambda$. Integrating Eqs. (3.2) we obtain

$$r_1 = D/r - A(1 - \alpha^2 r^2)\,, \tag{3.3}$$

$$r_4 = E/r - B(1 - \alpha^2 r^2)\,. \tag{3.4}$$

D and E being arbitrary functions of u and v, respectively, and $\alpha^2 = \lambda^2/3$. Differentiating (3.3) and (3.4) with respect to v and u, respectively, and using (3.1) we get

$$D = kA\,, \quad E = kB \qquad k = \text{constant}). \tag{3.5}$$

Substitution of (3.5) in (3.3) and (3.4) provides

$$r_1 = -\,\mathrm{A}(1 - k/r - \alpha^2 r^2)\,, \tag{3.6}$$

$$r_4 = -\,B(1 - k/r - \alpha^2 r^2)\,. \tag{3.7}$$

On account of the Eqs. (3.6) and (3.7) the Eq. (3.1) takes the form

$$f = -\,2AB(1 - k/r - \alpha^2 r^2)\,. \tag{3.8}$$

Making use of the Eqs. (3.6), (3.7) and (3.8) the Eq. (2.8) has been found to be identically satisfied.

In Minkowskian coordinate system the metric (1.1) takes the form

$$\begin{aligned}ds^2 &= 4dudv + r^2(d\Theta^2 + \sin^2\Theta d\Phi^2)\\ u &= (r + t)/2\,, \quad v = (r - t)/2\,.\end{aligned} \tag{3.9}$$

There are no singularities in Minkowskian space-time, and $r = 0$ is merely a time-like geodesic. When $r = u + v$, the Eqs. (3.1) show that f is constant. So in view of the Eqs. (3.2)—(3.9) we must take $k = 0$. Therefore, (3.6) and (3.7) reduce to

$$r_1 = -\,A(1 - \alpha^2 r^2)\,, \tag{3.10}$$

$$r_4 = -\,B(1 - \alpha^2 r^2)\,. \tag{3.11}$$

From $dr = r_1 du + r_4 dv$, we obtain

$$R^2 dr/(R^2 - r^2) = -\,Adu - Bdv\,, \tag{3.12}$$

where $\alpha^2 = 1/R^2$. Thus the problem of finding the functions f and r now reduces to integrate the functional equations (3.10), (3.11) and (3.12).

4. Functional relationship

We now choose a real variable H related to r by the differential equation

$$HdH/(H^2 - R^2) = R^2dr/(r^2 - R^2)\,. \tag{4.1}$$

The solution of this differential equation is

$$(H^2 - R^2) = b\left(\frac{r - R}{r + R}\right)^R \qquad (b = \text{constant})\,. \tag{4.2}$$

From Eqs. (3.12) and (4.1) we have

$$HdH/(H^2 - R^2) = Adu + Bdv\,. \tag{4.3}$$

This equation provides

$$A = HH_1/(H^2 - R^2)\,, \quad B = HH_4/(H^2 - R^2)\,. \tag{4.4}$$

Assuming the solution of (4.3) as

$$H^2 - R^2 = U^2V^2\,, \tag{4.5}$$

where U and V are functions of u and v, respectively, one can obtain

$$A = U_1/U\,, \quad B = V_4/V \tag{4.6}$$

using (4.4). Then from (4.1) we have

$$r_1 = HH_1(r^2/R^2 - 1)/(H^2 - R^2)\,, \tag{4.7}$$

$$r_4 = HH_4(r^2/R^2 - 1)/(H^2 - R^2)\,. \tag{4.8}$$

A simple and straightforward calculation provides the expression for the function f as

$$f = 2H^2H_1H_4(r^2/R^2 - 1)/(H^2 - R^2)^2\,. \tag{4.9}$$

Hence for the metric (1.1) satisfying the Einstein's field equations (2.1), (2.2) and the equation of state $\varrho + p = 0$ the function f is given in terms of r by the functional equation (4.9), where r is determined in terms of H by (4.5) so that r^2 comes out as a function of (u, v). Consequently the function f can be

written in a number of equivalent forms as functions of (u, v). Choosing the suitable forms of the functions U and V we can obtain spherically symmetric cosmological models worthy of study. In the next Section we shall obtain the well-known de Sitter cosmological model for the specific choice of U and V. The constant of integration b, occurring in (4.2), may be taken unity.

5. Particular case

Choosing

$$U = u\,, \quad V = v \tag{5.1}$$

Eq. (4.5) becomes

$$H^2 - R^2 = u^2v^2\,. \tag{5.2}$$

By (5.2)

$$H_1H_4 = u^3v^3/H^2\,. \tag{5.3}$$

Therefore, from (4.9)

$$f = 2(r^2/R^2 - 1)/uv\,. \tag{5.4}$$

Again, since

$$dH = H_1du + H_4dv\,,$$

we obtain

$$HdH/u^2v^2 = du/_u + dv/_v\,. \tag{5.5}$$

From (4.1) and (5.5)

$$du/_u + dv/_v = R^2dr/(r^2 - R^2)\,. \tag{5.6}$$

Define τ by

$$-du/_u + dv/_v = d\tau \quad \text{or} \quad \tau = \log\left(\frac{v}{u}\right) + \text{const}\,. \tag{5.7}$$

The Eqs. (5.6) and (5.7) together give

$$4dudv/uv = dr^2/(1 - r^2/R^2)^{-d\tau^2}\,. \tag{5.8}$$

Combining the Eqs. (5.4) and (5.8) we obtain

$$-2fdudv = [(1 - r^2/R^2)^{-1}dr^2 - (1 - r^2/R^2)d\tau^2]\,. \tag{5.9}$$

Therefore the metric (1.1) reduces to

$$ds^2 = (1 - r^2/R^2)^{-1}dr^2 + r^2(d\Theta^2 + \sin^2\Theta\mathrm{d}\Phi^2) - (1 - r^2/R^2)d\tau^2\,. \tag{5.10}$$

The line-element (5.10) is the de Sitter cosmological universe which is spherically symmetric solution of the Einstein's field equations (2.1) and (2.2) with

the equation of state $\varrho + p = 0$. The expression for the constant R is given by

$$1/R^2 = -(8\Pi p + \Lambda)/3 \tag{5.11}$$

which can be considered as the radius of the universe.

*

The authors are thankful to Dr. K. P. SINGH for valuable suggestions.

REFERENCES

1. J. L. SYNGE, Annali di Matematica pura ed applicata, (VI), **98**, 239, 1974.
2. SHRI RAM and J. N. S. KASHYAP, Acta Phys. Hung., **41**, 87, 1976.
3. SHRI RAM and J. N. S. KASHYAP, communicated.

Acta Physica Academiae Scientiarum Hungaricae, Tomus 42 (3), pp. 251—260 (1977)

ANALOGY BETWEEN DYNAMICS AND STATICS RELATED TO VARIATIONAL MECHANICS

By

P. HORVÁTHY

INSTITUTE OF CHEMICAL SYSTEM ENGINEERING
VESZPRÉM UNIVERSITY OF CHEMICAL ENGINEERING, 8201 VESZPRÉM
and

L. ÚRY

DEPARTMENT OF MATHEMATICS, LORAND EÖTVÖS UNIVERSITY, 1088 BUDAPEST

(Received in revised form 22. III. 1977)

Using modern differential geometry we complete the classical analogy between dynamics and statics in mechanics. For every mechanical system satisfying Maxwell's Principle a local variational principle is valid which in some cases can be extended to a global one. If a further regularity condition holds then we can get a Lagrangian function. There exist mechanical systems in Nature which satisfy Maxwell's Principle but do not have a global variational formalism: such an example is the case of a polarized particle or a particle with spin.

§ 1. Introduction and summary

In classical mechanics the equations of motion of a mechanical system are generally deduced from Hamilton's principle (Euler—Lagrange equations). Conversely, it can be asked under what conditions can this principle be obtained from the equations of motion.

In modern mechanics the equations of motion are expressed in terms of the so-called symplectic structures of differential geometry (SOURIAU [1]; ABRAHAM [2]; GODBILLON [6]). Using these tools we can draw a perfect analogy between dynamics and statics. Our entire investigation is based essentially on this analogy.

First we briefly resume the appropriate notions (§ 2) and formulate the "equational" (type I) and "variational" (type II) formulations:

$$\dot{\tilde{\gamma}} \, \varepsilon \, \mathrm{Ker} \, \sigma_{\tilde{\gamma}(t)} \,, \qquad \text{(type I.)}$$

where γ is a motion of the system, $\tilde{\gamma}$ denotes its "lifted" to the evolution space, σ is the system's Lagrange form ([1]), Ker $\sigma_{\tilde{\gamma}(t)}$ its kernel at the point $\tilde{\gamma}(t) \, \varepsilon E$, a vector space of dimension 1.

$$Y(\vartheta) = 0 \text{ for all } Y_\gamma \varepsilon T_\gamma(\mathcal{S}) \,, \qquad \text{(type II.)}$$

where $T_\gamma(\mathcal{S})$ is the tangent space of the set of all C^∞ curves $(\mathcal{S})$ joining the fixed points a, b; $\gamma \, \varepsilon \, \mathcal{S}$, ϑ is a real valued function defined on $\mathcal{S}$, $Y_\gamma(\vartheta)$ denotes its

directional derivative in the direction of $Y_\gamma \varepsilon T_\sigma(\mathcal{S})$. To condition II we refer as to the "abstract Euler—Lagrange equation" and express its validity as follows:

The actual path is a stationary curve of ϑ. (type II.)

If a Lagrangian function is given, we may define ϑ as $\int_0^T L\,dt$; by introducing the one-form λ called the Cartan form we get ϑ as

$$\vartheta(\gamma)\colon \mathcal{S}\ \varepsilon\gamma \to \int_{\tilde{\gamma}} \lambda = \int_0^T L dt\ \varepsilon\ \mathrm{R}\ .$$

By calculating the directional derivative of this, we arrive at formulation I, deduced from formulation II (usual calculus of variations).

The local variational principle states that there exists — at least locally — a field of 1-forms (λ) such that the Euler—Lagrange equation belonging to λ coincides with the equation given by I with $\sigma = \mathrm{d}\lambda$.

In § 4 we show that the necessary and sufficient condition for a system to satisfy the local variational principle is the validity of Maxwell's principle:

$$d\sigma = 0\ .$$

If a suitable condition is fulfilled, then L can be recovered from λ. (KLEIN [8]).

If the evolution space has some additional topological property, the λ can be extended onto the entire evolution space, that is, we get a global variational principle.

In the conclusion (§ 5) we show that for a particle with spin (THOMAS, 1927, [9]) no global Lagrangian function can exist.

§ 2. Mathematical tools

Our objective is to find the notions denoted by 1, 2, 3 in Table I, that is, to find analogues of finite dimensional tangent space, the principle of virtual work and the directional derivative.

2.1. *Tangent space of $\mathcal{S}$ at a curve $\gamma \varepsilon \mathcal{S}$* [3]

Let M be any differentiable manifold, $a, b \varepsilon M$ fixed points, $\mathcal{S}$ the set of all C^∞ curves which do not intersect and $[0, T]$ an interval of real numbers. We require that $\gamma(0) = a, \gamma(T) = b$ for all $\gamma \varepsilon \mathcal{S}$.

It can be shown [3] that $\mathcal{S}$ can be turned into a locally Banach manifold, i.e. an "infinite dimensional manifold". We need only the following result:

Proposition: a tangent vector of $\mathcal{S}$ at a "point" γ — that is, a curve lying in M — is a differentiable vector field along γ. Throughout this paper it will

Table I

Statics	Dynamics
Q configurational space (n dimensional manifold)	$\mathcal{S}$ the set of all C^∞ paths joining $a, b \in Q$; $\gamma(0) = a$, $\gamma(T) = b$
condition to be realized	
sum of forces $= 0$	equation of motion
I. "equational formulation"	
principle of virtual work $\sigma_q(Y_q) := F_q \cdot Y_q = 0$ for all $Y_q \in T_q(Q)$, the tangent space of Q at q; $\sigma_q : T_q(Q) \to R$ linear function	1. $T_\gamma(\mathcal{S}) = ?$ 2. $\Sigma_\gamma = ?$ $\Sigma_\gamma(Y) = 0$ for all $Y_\gamma \in T_\gamma(\mathcal{S})$ $\Sigma_\gamma : T_\gamma(\mathcal{S}) \to R$ linear function
if $[\mathrm{rot}F](q) = 0$, there exists a function V defined in a neighbourhood of q such that here $\sigma_q(Y_q) = -Y_q(V)$ (the directional derivative of V by Y_q)	4. condition for local solvability 3. directional derivative of a function on $\mathcal{S}$
if Q satisfies certain topological conditions, V is global $V : Q \to R$	5. topological condition for global solution
II. "variational formulation"	
principle of "minimal potential": q is a stationary point of V $Y_q(V) = 0$ for all $Y_q \in T_q(Q)$	Hamilton's principle: the actual path makes the integral $SLdt$ stationary

always be supposed that any such vector field can be extended onto a neighbourhood of γ and generate there a local group of diffeomorphisms.

We can relate this vector field to the classical variational calculus as follows: The local group of diffeomorphisms associated to the above vector field carries γ to a neighbouring curve called classically a "varied curve". As the end points are not changed, our vector field vanishes in a and b.

2.2. *Symplectic mechanics*

This "covariant" form of classical mechanics has been evolving since CARTAN [4]. Modern expositions are due to MACKAY [12], GODBILLON [6] and ABRAHAM [2]. The closest one to our line of thought is that of SOURIAU [1]. We limit ourselves here to a brief review of the basic ideas.

In classical mechanics, states are identified with the points of the set

$$E = T(Q) \times S \times R \tag{2.2.1}$$

called the system's *evolution space*. Here Q is the set of all possible configurations, an n-dimensional C_∞ manifold, $T(Q)$ is its tangent space, S a possible void set if parameters related to inner degrees of freedom; R is time.

Examples:

1. n-body motion: $Q = R^{3n}$, $S = \emptyset$; $E = R^{6n+1}$.

2. In 1927 L. H. THOMAS studied the motion of a polarized particle in electromagnetic field. He discovered that this particle possesses a proper angular and magnetic momentum. Both of these quantities are proportional to a unit vector in three-space, called the *spin* of the particle ([9], or in relativistic description in BARGMANN—MICHEL—TELEGDI [10]). This inner degree of freedom will be represented mathematically by a set S. Hence, in this case $Q = R^3$, $S = S^2$ (unit sphere in three-space) the proper angular momentum will be λs, the proper magnetic momentum μs; $\lambda, \mu \varepsilon R$, $s \varepsilon S^2$.

The equations of motion are given as

$$\begin{aligned} &dq/dt = v\,, \\ &d[mv]/dt = g[E + v \times B] + \partial B/\partial q(\mu s)\,, \\ &d[\lambda s]/dt = \mu s \times B\,, \end{aligned} \tag{2.2.2}$$

(g is the electric charge).

By state we mean that all motions of the system are determined by giving a point in E in the following manner: through every point of E passes exactly one C^∞ curve called evolution curve of the system. The motions can be set into one-to-one correspondence with these evolution curves; they are exactly the projections of the evolution curves onto Q.

The analytical description of these evolution curves is given by a field of antisymmetric 2-forms denoted by σ and called the system's *Lagrange form*. For every $e \varepsilon E$ σ_e is a bilinear antisymmetric function on the tangent space, differentiable in an appropriate sense. In classical terms σ is an antisymmetrical contravariant tensor field. The kernel of σ at a point $e \varepsilon E$ is

$$\operatorname{Ker} \sigma_e = \{X_e \varepsilon T_e(E) : \sigma_e(X_e, Y_e) = 0 \text{ for every } Y_e \varepsilon T_e(E)\}\,. \tag{2.2.3}$$

$\operatorname{Ker} \sigma_e$ is a vector space; it is required that it has the dimension 1 for every $e \varepsilon E$.

The relation between the evolution curves and σ is the following: σ associates a one-dimensional vector space to every point of E; one verifies ([1], [6]) that through every point of E exactly one C^∞ curve passes whose tangent spaces coincide with the vector spaces given by one in the above manner.

In this paper the mechanical systems are characterized by the pair of their evolution spaces and Lagrange forms, (E, σ).

The equations of motion will have the form

$$\tilde{\gamma}(t) \in \operatorname{Ker} \sigma_{\tilde{\gamma}(t)}^{\cdot} ; \tag{2.2.4}$$

here $\tilde{\gamma}$ denotes the "lifted" of the curve γ, : $\tilde{\gamma}(t) = \big(\gamma(t), \dot{\gamma}(t), t\big)$.

Example 1. Let m_i be the mass, $q_i \in R^3$ the space- $v_i \in R^3$ the velocity-coordinate of the i^{th} particle; $F_i \in R^3$ the force applied on it, then

$$\sigma = \sum_{i=1}^{n} (m_i dv_i - F_i dt) \wedge (dq_i - v_i dt) , \tag{2.2.5}$$

where $\wedge$ denotes the exterior product of the vector-valued differential forms. Definition: if α, β are 1-forms with values in R^3, then set

$$(\alpha \wedge \beta)(X, Y) := \langle \alpha(X), \beta(Y) \rangle - \langle \alpha(Y), \beta(X) \rangle \tag{2.2.6}$$

with $\langle \ldots \rangle$ the usual scalar-product, $X, Y \in T_e(E)$. One verifies ([1]) that (2.2.4) now exactly means that γ is a solution of the system of differential equations

$$m_i \frac{dv_i}{dt} = F_i , \quad \frac{dq_i}{dt} = v_i \qquad (i = 1, \ldots, n) \tag{2.2.7}$$

Example 1*. Suppose given n charged particles, let the electric and magnetic forces be characterized by E_i and B_i $(i = 1, \ldots n)$. The corresponding Lagrange-form is then

$$\sigma = \sum_{i=1}^{n} \{(m_i dv_i - E_i dt)(dq_i - v_i dt) + \langle B_i \, dq_i x dq_i \rangle\} ; \tag{2.2.8}$$

here $dq \times dq$ denotes the vector-valued 2-form given by

$$(dq \times dq)(X, Y) := X_q \times Y_q \tag{2.2.9}$$

(a vector $X_e \in T_e(E)$ has the components X_q, X_v, X_t).

Example 2 (particle with spin)

$$\sigma = (mdv - Edt) \wedge (dq - vdt) + \langle B, dqxdq \rangle + \mu d\{\langle s, B \rangle\} - \lambda \langle s, ds \times ds \rangle . \tag{2.2.10}$$

Here d is the operator of exterior derivation ([1], [2], [6], [11]).

According to experience a regularity condition called *Maxwell's principle* by SOURIAU is always valid:

$$\underline{d\sigma = 0}\,. \tag{2.2.11}$$

In local coordinates this means (in case of example 1)

$$\frac{\partial E_j}{\partial v_k} = 0\,;\quad \frac{\partial B_j}{\partial v_k} = 0\,;\quad \overline{\frac{\partial E_k}{\partial q_j}} - \frac{\partial E_j}{\partial q_k} = 0\,;\quad \frac{\partial B_j}{\partial q_k} = 0$$
$$\operatorname{rot} E_k + \frac{\partial B}{\partial t} = 0\,,\quad \operatorname{div} B_k = 0\,. \tag{2.2.12}$$

Here we recognize Maxwell's equations in non-relativistic notation: the terms with $1/c$ are neglected. $\overline{(dE_k/dq_j}$ is the transposed of the matrix $\partial E_k/\partial q_j)$.

In example 2 this condition is automatically satisfied, because the supplementary terms also vanish by exterior differentiation: the first one is itself a total derivative, and $dd = 0$ (Poincaré's lemma); the exterior derivative of the second one is a 3-form on S^2, a two-dimensional manifold, hence it vanishes too.

2.3. *Du Bois Reymond lemma*

In order to formulate the equations of motion in terms of a linear function on $T(\mathcal{S})$ we make use of the proposition called classically Du Bois Reymond lemma.

Just as the lifted of a curve, the lifted of a vector field in Q may be defined as well [1]. Denote it by $\tilde{Y}$; this is a vector field in the evolution space.

Let (a_1, s_1) and (a_2, s_2) be fixed points in $Q \times S$, $\gamma \,\varepsilon\, \mathcal{S}$, Y_γ any differentiable vector field along γ vanishing at the end points. Suppose Y_γ can be extended onto a neighbourhood of γ and it generates there a local group of diffeomorphisms. Then for any σ 2-form with dim Ker $\sigma_e = 1 \vee \varepsilon^{\frac{1}{4}} E$ it holds:

Proposition:

$$\dot{\tilde{\gamma}}(t) \,\varepsilon\, \operatorname{Ker} \sigma_{\tilde{\gamma}(t)} \vee t\varepsilon T \quad \text{if } \int_{\tilde{\gamma}} \sigma(.,\, Y) = 0 \text{ for all } Y_\gamma \,\varepsilon\, T_\varphi(\mathcal{S})\,. \tag{2.3.1}$$

Thus, we arrive at:

Formulation I

Let σ be the Lagrange form of a mechanical system; define Σ as

$$\Sigma_\gamma\colon\ T_\gamma(\mathcal{S}) \,\varepsilon\, Y_\gamma \to \Sigma_\gamma(Y_\gamma)\colon = \int_{\tilde{\gamma}} \sigma(.,\, Y)\,, \tag{2.3.2}$$

then according to Proposition (2.3.1) the equations of motion are equivalent to

$$\underline{\Sigma_\gamma(Y_\gamma) = 0 \text{ all for } Y_\gamma \,\varepsilon\, T_\gamma(\mathcal{S})}\,. \tag{2.3.3}$$

2.4. *Directional derivative of a function on* $\mathcal{S}$

Denote the local group of diffeomorphisms generated by the vector field Y_γ by φ_τ; then for any $\vartheta : \mathcal{S} \to R$ function define V: $\tau \to \vartheta(\varphi_\tau \gamma)$. Then the directional derivative of ϑ at a point γ in the direction of $Y_\gamma \varepsilon T_\gamma(\mathcal{S})$ (denoted by $Y_\gamma(\vartheta)$) will be the simple derivative of V by τ at $\tau = 0$. Suppose this derivative exists and is uniquely determined.

Definition. If $Y_\gamma(\vartheta) = 0$ for all $Y_\gamma \varepsilon T_\gamma(\mathcal{S})$, then we say that γ is a stationary curve of ϑ. We refer to this condition as the *abstract Euler—Lagrange equation.*

In these terms Hamilton's principle can be formulated as follows:

Hamilton's principle: $\vartheta := \int_0^T L\, dt$ — a real valued function on $\mathcal{S}$ — has the actual path as a stationary curve. Hence the formulation of type II:

$$Y_\gamma(\vartheta) = 0 \quad \text{for all} \quad Y_\gamma \varepsilon T_\gamma(\mathcal{S}) . \tag{2.4.1}$$

§ 3. The local variational principle

In order to establish the relation between these two types of descriptions we express Hamilton's principle in terms of geometrical objects. Suppose a Lagrangian function is given (L).

Let the *Cartan form* of the system belonging to L be defined as

$$\lambda := \sum_{i=1}^{n} \left\{ \frac{\partial L}{\partial v_i} (dq_i - v_i dt) \right\} + L dt \tag{3.1}$$

(HERMANN [11]). Then one verifies

$$\int_0^T L dt = \int_{\tilde{\gamma}} \lambda , \quad \gamma \varepsilon \mathcal{S} . \tag{3.2}$$

Calculating the directional derivative, we get:

$$Y_\gamma(\vartheta) = \int_{\tilde{\gamma}} \mathfrak{L}_{\tilde{Y}}(\lambda) , \tag{3.3}$$

where $\mathfrak{L}_{\tilde{Y}}(\lambda)$ is the Lie-derivative of the form λ. Using simple relations we finally have

$$Y_\gamma(\vartheta) = - \int_{\tilde{\gamma}} d\lambda(., \tilde{Y}) . \tag{3.4}$$

Applying the Du Bois Reymond lemma (2.3.1.) gives

$$Y_\gamma(\vartheta) = 0 \quad \text{iff} \quad \operatorname{Ker} (d\lambda)_{\tilde{\gamma}(t)} \varepsilon \dot{\tilde{\gamma}}(t) . \tag{3.5}$$

Using the definition of the Cartan form we can calculate $d\lambda$:

$$d\lambda = \sum_{i=1}^{n} \left\{ \left(d\left[\frac{\partial L}{\partial v_i} \right] - \frac{\partial L}{\partial q_i} dt \right) \wedge (dq_i - v_i dt) \right\}, \tag{3.6}$$

then the condition (3.5.) is equivalent to the system of differential equations

$$\frac{d}{dt}\left[\frac{\partial L}{\partial v_i} \right] - \frac{\partial L}{\partial q_i} = 0\,, \quad \frac{dx_i}{dt} = v_i \quad (i = 1, \ldots n)\,, \tag{3.7}$$

which justifies our terminology.

If we compare (3.5) with the equations of motion given by (2.2.2.) we arrive at:

Definition. A mechanical system given by (E, σ) is told to possess a *variational description* if there exists — at least locally — a λ field of 1-forms for which $d\lambda = \sigma$.

The local variational principle states that every mechanical system has a variational description.

One verifies that $d\lambda = \sigma$ means — at least for sufficiently "short" curves — that $\Sigma(Y) = -Y(\vartheta)$ in perfect analogy with statics.

§ 4. The inverse problem

4.1. *Local solvability*

As we have just seen, the equational description can be deduced from the variational one by derivation. Now we arrive at the problem mentioned in the introduction: under what conditions can we state that the system given by (E, σ) has a variational description and how can we construct a) a Cartan form; b) a Lagrangian function?

Theorem. The necessary and sufficient condition for a system (E, σ) to have a local variational description is $d\sigma = 0$.

The proof is an immediate consequence of Poincaré's lemma ([1], [2], [6], [11]).

In the above theorem we recognize our fundamental assumption (2.2.9) called Maxwell's principle!

Corollary: For every mechanical system satisfying Maxwell's principle a local variational principle holds.

4.2. *Construction of the Cartan form*

In order to have a Cartan form we have to solve the equation $d\lambda = \sigma$ for λ. This leads to partial differential equations. One verifies that if E is connected, then any two solutions differ by a total differential of a function on E.

In case of example 1*, we have the following result (for $n = 1$): there exist two functions

$$\begin{aligned} A&: \quad Q\times R \ni (q, t) \to A(q, t) \in T_q(Q)\,, \\ V&: \quad Q\times R \ni (q, t) \to V(q, t) \in R\,, \end{aligned} \tag{4.2.1}$$

called respectively vector and scalar potential, for which

$$E = -\,\partial V/\partial q - \partial A/\partial t\,; \quad B = \operatorname{rot} A\,. \tag{4.2.2}$$

If we set

$$\begin{aligned} p(q, v, t) &:= mv + A(q, t) + \frac{\partial \varphi}{\partial q}(q, t)\,, \\ H(q, v, t) &:= mv^2/2 + V(q, t) - \frac{\partial \varphi}{\partial t}(q, t) \end{aligned} \tag{4.2.3}$$

where φ is an arbitrary function on $Q\times R$; and set finally

$$\lambda := p\,dq - H\,dt\,, \tag{4.2.4}$$

then one verifies that $d\lambda = \sigma$ and that this is the most general expression for the Cartan form.

4.3. *Construction of the Lagrangian function*

The procedure which gives λ from σ does not yield necessarily a 1-form which corresponds to a Lagrangian function. In a slightly different formulation [8] it is possible to give a condition for σ which assures that one can recover a Lagrangian function. In our example 1* one can calculate directly:

$$L(q, v, t) = \frac{1}{2} mv^2 + \langle A(q, t), q\rangle - V(q) + \left\langle \frac{\partial \varphi}{\partial q}, v \right\rangle + \frac{\partial \varphi}{\partial t}\,. \tag{4.3.1}$$

4.4. *Conditions for a global solution*

Our last goal is to tell when a local principle can be extended to a global one. This depends on the topology of E:

Theorem: If a second cohomology group of E is trivial, i.e. $H^2(E, R) = 0$, then λ can be extended onto E. [7]

§ 5. Conclusion

SOURIAU accepts Maxwell's principle as a new axiom of mechanics. This requirement is mathematically weaker than that accepted by LANDAU [5] who requires the existence of a global Lagrangian function. It is natural

to ask whether this latter condition is actually stronger. The answer is given by Nature: there exist systems which satisfy Maxwell's principle but do not have a global variational description.

Such an example is a particle with spin (2.2.2). If its Lagrange form had the form $d\Theta$ with Θ defined on the entire E, then, according to Stokes' theorem

$$\int_E d\Theta = 0 \,, \tag{5.1}$$

would hold, but an easy calculation shows

$$\int_E \sigma = \int_{S^2} \sigma = 4\pi\lambda \neq 0 \,, \tag{5.2}$$

hence no global variational description can exist.

REFERENCES

1. J.-M. SOURIAU, Structure des Systèmes Dynamiques, Dunod, Paris, 1970.
2. R. ABRAHAM, The Foundations of Mechanics, Benjamin, New York, 1967.
3. J. MILNOR, Morse Theory, Princeton Univ. Press, Princeton, 1963.
4. E. CARTAN, Leçons sur les Invariants Integraux, Hermann, Paris, 1922.
5. L. LANDAU—E. LIFCHITZ, Mécanique, Mir, Moscou, 1969.
6. C. GODBILLON, Géométrie Différentielle et Mécanique Analytique Hermann, Paris, 1969.
7. SULANKE-WINTGEN, Differentialgeometrie und Faserbündel, VEB Deutscher Verlag der Wissenschaften, Berlin, 1972.
8. J. KLEIN, Les Systèmes Dynamiques Abstraits, Ann. Inst. Fourier Grenoble, **13**, 191, 1963.
9. L. H. THOMAS, Phil. Mag., **3**, 1, 1927.
10. V. BARGMANN, L. MICHEL and V. L. TELEGDI, Phys. Rev. Lett., **2**, 435, 1959.
11. R. HERMANN, Differential Geometry and the Calculus of Variations, Benjamin, New York, 1970.
12. G. W. MACKEY, The Mathematical Foundations of Quantum Mechanics, Benjamin, New York, 1963.

Acta Physica Academiae Scientiarum Hungaricae, Tomus 42 (3), pp. 261—264 (1977)

GELL-MANN AND LOW TYPE RENORMALIZATION GROUP AND THE EQUATION OF STATE OF THE HEISENBERG FERROMAGNET

By

G. FORGÁCS

SOLID STATE PHYSICS DEPARTMENT, CENTRAL RESEARCH INSTITUTE FOR PHYSICS
H—1525 BUDAPEST

(Received 22. III. 1977)

It is shown that the Lie differential equation of the modified Gell-Mann and Low renormalization group is a "natural tool" for obtaining the scaled equation of state of the Heisenberg ferromagnet.

As can be seen from the title we are not going to discuss anything new in this short note, since using renormalization group technique, scaled equations of state have already been obtained [1]. The purpose of this work is to demonstrate that using the Lie equations of the modified version of the GELL-MANN and LOW renormalization group (MGLRG), rather than the Callan—Symanzik equations, the equation of state can be obtained in an extremely simple way. By MGLRG we mean a method worked out by SÓLYOM, in which the intuitive picture of the Kadanoff cut-off scaling is combined with the GELL-MANN and LOW renormalization group [2]. The method is based on an assumption the validity of which must be checked order by order in perturbation theory. MGLRG physically is much nearer to Wilson's ideas than the original GELL-MANN and LOW method, on the other hand from the mathematical point of view it uses the same simple Lie differential equations as the traditional formulation. A thorough review of the above method and also applications can be found in the work of FORGÁCS et al. [3].

To get an equation of state for the Heisenberg ferromagnet (near the critical point) we use the φ^4 theory. The assumptions of MGLRG in this case are the following [3]:

$$G(q^2, t, \Lambda, u) = z_1\left(\frac{\tilde{\Lambda}}{\Lambda}, u\right) G(q^2, \tilde{t}, \tilde{\Lambda}, \tilde{u}) , \tag{1}$$

$$\bar{\Gamma}_4(q^2, t, \Lambda, u) = z_2\left(\frac{\tilde{\Lambda}}{\Lambda}, u\right) \bar{\Gamma}_4(q^2, \tilde{t}, \tilde{\Lambda}, \tilde{u}) , \tag{2}$$

$$\tilde{u} = u\left(\frac{\tilde{\Lambda}}{\Lambda}\right)^{-\varepsilon} z_1^2\left(\frac{\tilde{\Lambda}}{\Lambda}, u\right) z_2\left(\frac{\tilde{\Lambda}}{\Lambda}, u\right) , \tag{3}$$

$$\tilde{t} = t z_3\left(\frac{\tilde{\Lambda}}{\Lambda}, u\right) . \tag{4}$$

Here q is the momentum variable, G is the full propagator, $\bar{\Gamma}_4$ is the dimensionless four-point function, with $\bar{\Gamma}_4^{\text{bare}} = 1$ (the momenta of the external lines of $\bar{\Gamma}_4$ are chosen in such a way that $\bar{\Gamma}_4$ depends only on one external momenta variable). t is proportional to $T - T_c$, u is the dimensionless coupling constant, $\varepsilon = 4 - d$ and d is the dimension of space. Λ and $\tilde{\Lambda}$ are the original and the "new" cut-offs in momentum space. The main assumption is that the z factors depend only on $\tilde{\Lambda}/\Lambda$ and u. Eqs. (1—4) determine the z factors and it can be shown that for higher order vertex functions similar equations are valid with z factors not independent of z_1, z_2 and z_3. The z factors as power series in u and ε are given in the Appendix. From the above equations all the critical indices and corrections to scaling have been obtained [3].

In order to get the equation of state we start with

$$F(t, u, \Lambda) = \sum_{n=2}^{\infty} \frac{M^n}{n!} \Gamma_n(t, u, \Lambda) \tag{5}$$

for the free energy [4]. Here Γ_n are the proper n-point functions (not dimensionless). $\Gamma_2 = G^{-1}$. Using dimensional analysis, dimensionless quantities and the transformation properties (1—4) also for higher order vertex functions), it is easy to show that

$$\bar{F}(x, y, u) = \left(\frac{\tilde{\Lambda}}{\Lambda}\right)^d \bar{F}(\tilde{x}, \tilde{y}, \tilde{u}) \,, \tag{6}$$

where $\bar{F}$ is the dimensionless free energy, and

$$x = \frac{M}{\Lambda^{\frac{d-2}{2}}}, \quad y = \frac{t}{\Lambda^2}, \quad \tilde{x} = \frac{M z_1^{-y_2}}{\tilde{\Lambda}^{\frac{d-2}{2}}}, \quad \tilde{y} = \frac{t z_3}{\tilde{\Lambda}^2} \,. \tag{7}$$

It has to be stressed that (5) is only the magnetic part of the free energy. It is only this magnetic part that is multiplicatively renormalizable according to (6). We know that the specific heat is not multiplicatively renormalizable, and since the second derivative of the nonmagnetic free energy is just the specific heat, therefore the nonmagnetic free energy is not multiplicatively renormalizable either.

Differentiating (6) with respect to x and then putting $\varrho = \tilde{\Lambda}^2/\Lambda^2 = yz_3$ ($\tilde{\Lambda}^2/\Lambda^2 = \varrho$), one gets the Lie equation for the free energy.

$$\frac{\partial \bar{F}(x, y, u)}{\partial x} = \frac{\varrho^{d/2}}{z^{1/2} \varrho^{\frac{d-2}{4}}} \frac{\partial}{\partial s} \bar{F}\left(s, 1, u\varrho^{-\varepsilon} z_1^2(\varrho) z_2(\varrho)\right) \Big|_{\substack{s = x z_1^{-1/2} \varrho^{\frac{2-d}{4}} \\ \varrho = y z_3}} \,. \tag{8}$$

Near to the critical point $\tilde{u} = u\varrho^{-\varepsilon} z_1^2 z_2$ can be replaced by its fix point value

u^* and from the definition of the z factors and their value given in the Appendix one can see that

$$z_1(\varrho, u^*) = \varrho^{\sigma(u^*)}, \tag{9}$$

$$z_3(\varrho, u^*) = \varrho^{\varphi(u^*)}, \tag{10}$$

where

$$\sigma(u^*) = \left.\frac{\sigma z_1(\varrho, u^*)}{\sigma \varrho}\right|_{\varrho=1}, \tag{11}$$

$$\varphi(u^*) = \left.\frac{\partial z_3(\varrho, u^*)}{\partial \varrho}\right|_{\varrho=1}. \tag{12}$$

Using (9) and (10) from $\varrho = y z_3(\varrho)$ it follows that

$$\varrho^{1-\varphi(u^*)} = y\,. \tag{13}$$

Putting this value of ϱ into (8), we finally get

$$\frac{\partial \bar{F}(x, y, u)}{\partial x} = y^{\frac{1}{4}\frac{d+2-2\sigma(u^*)}{1-\varphi(u^*)}} \Phi\left(x \cdot y^{-\frac{1}{4}\frac{d-8+3\sigma(u^*)}{1-\varphi(u^*)}}\right). \tag{14}$$

Here

$$\Phi(x) = \frac{\partial}{\partial s} \bar{F}(s, 1, u^*)\bigg|_{s=x} \tag{15}$$

is the generator of the corresponding Lie equation. Calculating φ from perturbation theory $\bar{F}$ can be determined from (14). However, since we are interested in the equation of state, we do not have to calculate $\bar{F}$. As

$$\bar{H} \text{ (dimensionless magnetic field)} = \frac{\partial \bar{F}}{\partial x} \tag{16}$$

we see that the Lie equation (14) is just the equation of state. Comparing(14) with

$$H = M^{\delta} f\left(\frac{t}{M^{1/\beta}}\right) \tag{17}$$

we get

$$\beta = \frac{1}{4}\frac{d - 2 + 2\sigma(u^*)}{1 - \varphi(u^*)}, \tag{18}$$

$$\delta = \frac{d + 2 - 2\sigma(u^*)}{d - 2 + 2\sigma(u^*)}. \tag{19}$$

We would like to stress that in this formalism one does not have to solve any differential equation (unless the aim is to get the scaled equation of state), because the Lie equation for $\bar{F}$ coincides with the equation of state. Comparing this method with others it seems to us that this is the simplest way to get the scaled equation of state. Nothing sophisticated, such as renormalizability of the theory, has been used and therefore all the above is easily digestible for a statistical mechanician. The only thing one has to do is to calculate the z factors. If there are no such z factors which depend only on the ratio of the cut-offs and the dimensionless coupling constants, the method cannot be used. As it has been shown in reference [3] when there is scaling in the theory equations similar to (1—4) can always be satisfied.

*

The author is indebted to Dr. SÓLYOM for stimulating remarks.

Appendix

$$z_1 = 1 + \frac{s^2}{48}\left(1 - \frac{\varepsilon}{4}\right)\ln \varrho + \frac{s^3}{64}\ln^2 \varrho\,, \tag{A.1}$$

$$z^2 = 1 + s\frac{3}{4}\left(\ln \varrho - \frac{\varepsilon}{4}\ln^2 \varrho\right) + s^2\left(-\frac{3}{4}\ln \varrho + \frac{9}{16}\ln^2 \varrho\right), \tag{A.2}$$

$$z_3 = 1 + \frac{s}{4}\left(\ln \varrho - \frac{\varepsilon}{4}\ln^2 \varrho\right) - \frac{s^2}{48}(5\ln \varrho - 6\ln^2 \varrho)\,. \tag{A.3}$$

Here

$$s = uKd,\ Kd = [2^{d-1}\Pi^{d/2}\Gamma(d/2)]^{-1},\ \varrho = \frac{\tilde{\Lambda}^2}{\Lambda^2}\,.$$

REFERENCES

1. E. BREZIN, J. C. LE GUILLON and J. ZINN JUSTIN, Saclay preprint, DPh-T/74/10C.
2. M. GELL-MANN and F. E. LOW, Phys. Rev., **95**, 1300, 1954.
3. G. FORGÁCS, J. SÓLYOM and A. ZAWADOWSKI, preprint of Central Research Institute for Physics, Budapest, KFKI-76-20.
4. G. JONA-LASINIO, Nuovo Cimento, **34**, 1790, 1964.

Acta Physica Academiae Scientiarum Hungaricae, Tomus 42 (3), pp. 265—268 (1977)

ON THE TUNNELLING EFFECT IN THE UNIFIED THEORY OF FERROELECTRICITY

By

S. STAMENKOVIĆ

BORIS KIDRIĆ INSTITUTE FOR NUCLEAR SCIENCES, VINČA, BELGRADE, YUGOSLAVIA*

N. M. PLAKIDA and V. L. AKSIENOV

JOINT INSTITUTE FOR NUCLEAR RESEARCH, DUBNA, USSR**

and

T. SIKLÓS

CENTRAL RESEARCH INSTITUTE FOR PHYSICS, BUDAPEST***

(Received 28. III. 1977)

The unified model Hamiltonian describing both "order-disorder" and "displacive" type ferroelectrics is extended by introducing simultaneously right from the beginning the phonon vibrations, statistical disorder and tunnelling motion of active atoms.

The authors have recently proposed the unified theory of ferroelectrics [1] taking into account both statistical disorder and phonon vibrations of active atoms. Starting from quite a general Hamiltonian

$$H = \sum_i \left\{ \frac{\vec{p}_i^2}{2m} + V(\vec{R}_i) \right\} + \frac{1}{2} \sum_{i \neq j} \varphi(\vec{R}_i - \vec{R}_j) , \tag{1}$$

by representing the atomic coordinate as

$$\vec{R}_i = \vec{l}_i + \sigma_i^+ \vec{S}_i^+ + \sigma_i^- \vec{S}_i^- , \tag{2}$$

and by expressing the potential energy by the first two terms of the Taylor expansion, some kind of a hybridized phonon-Ising Hamiltonian has been obtained

$$H = \sum_{i,\alpha} \sigma_{i\alpha} \left\{ \frac{\vec{p}_{i\alpha}^2}{2m} - \frac{A}{2} \vec{S}_{i\alpha}^2 + \frac{B}{4} S_{i\alpha}^4 \right\} + \frac{1}{4} \sum_{i \neq j, \alpha, \beta} \sigma_{i\alpha} \sigma_{i\beta} \varphi_{ij}'' (\vec{S}_{i\alpha} - \vec{S}_{j\beta})^2 \tag{3}$$

$$(\alpha, \beta = +, -) .$$

In the above expressions $\vec{l}_i$ denotes the atomic site-position; $\vec{S}_{i\alpha} = \vec{b}_{i\alpha} + \vec{u}_{i\alpha}$ is the sum of the off-centre equilibrium displacement ($\vec{b}_{i\alpha}$) and the thermal

* Address: YU—11001 Belgrade, P.O.B. 522, Yugoslavia.
** Address: SU—101000 Moscow, Head Post Office, P.O.B. 79, USSR.
*** Address: H—1525 Budapest, P.O.B. 49, Hungary.

fluctuation ($\vec{u}_{i\alpha}$) of the atom moving in a double well potential $V(\vec{R}_i)$; $\vec{p}_{i\alpha} = m\dot{\vec{S}}_{i\alpha}$ represents the "left" (+) and "right" (−) atomic momentum; $\sigma_{i\alpha} = 1/2(1 + \alpha\sigma_{iz})$ is the projection operator simply expressed by the z-pseudospin component; $\varphi(\vec{R}_i - \vec{R}_j)$ is the familiar interaction between a pair of atoms ($i, j, = 1, 2, \ldots, N$); A and B define, respectively, the height of the potential barrier, $U_0 = A^2/4B$, and the distance between the two potential minima, $d_0 = 2\sqrt{A/B}$.

After the self-consistent pseudospin-phonon procedure a closed system of equations for two order parameters ($\sqrt{B/A}\,\langle b_{i\alpha}\rangle = \eta_\alpha$ and $\langle\sigma_{iz}\rangle = \sigma_z$) as functions of the reduced coupling constant ($f_0 = (1/A)\sum_i' \varphi''_{ij}$) and temperature has been obtained and solved numerically. Further it follows that the ferroelectric phase transition can be either of the order-disorder type or of the displacive type and it can have mixed character also (in all cases the transition of I, II or mixed order is possible) — depending on the ratio of two-particle potential to the single-particle potential.

However, in this model the inherent quantum-mechanical effect, manifested in a single-particle tunnelling motion of active atoms between the two potential minima has not been explicitly taken into account. Such a peculiar motion imposes some kind of the over-Heisenberg uncertainty relation (in the coordinate or pseudospin picture)

$$\langle(\Delta p)^2\rangle\langle\Delta R)^2\rangle \simeq \left\langle\left(\frac{2\Omega m d_0}{\hbar}\,\sigma_y\right)^2\right\rangle\left\langle\left(\frac{d_0\sigma_z}{2}\right)^2\right\rangle \geqslant \frac{\hbar^2}{4}\,, \tag{4}$$

i.e.,

$$d_0(2\Omega m)^{1/2} \geqslant \hbar\,, \tag{5}$$

for which no satisfactory "narrowing" has been obtained so far, even theoretically. In the above relation (5) m is the mass of active atom and $2\Omega \simeq \simeq \int \psi_l(R_i)H_i\psi_r(R_i)dR_i$, $\psi_l(R_i)$ and $\psi_r(R_i)$ being, respectively, the real wave functions* of the "left" and "right" atomic states of the single-particle Hamiltonian, H_i (see also [2], [3]).

As an exact analytic description of dynamics induced by (1) or (3) is rather impossible we propose a novel approximative scheme which takes into account all the intriguing features of the ferroelectric phenomenon, i.e., the tunnelling, statistical disorder and phonon vibrations of active atoms, in the frame of only one universal model.

To realize such a concept we introduce the "left—right" representation of the Hamiltonian (3) using the non-orthogonal pseudospin "basis"

$$|l\rangle = a\begin{pmatrix}1\\0\end{pmatrix} + b\begin{pmatrix}0\\1\end{pmatrix};\quad |r\rangle = a\begin{pmatrix}0\\1\end{pmatrix} + b\begin{pmatrix}1\\0\end{pmatrix};\quad (0 < a \leq 1;\ \ b \ll a)\,. \tag{6}$$

* To explicit these functions, some approximative calculations can be used [4]—[7] provided that the ground state doublet yields a predominant contribution.

It corresponds to the atomic localization in the left (l) or right (r) single-particle potential well in the limit of a non-penetrating barrier ($U_0 \to \infty$). The coefficients a and b are determined from the completeness condition ($a^2 + b^2 = 1$) jointly with the overlap integral ($\varepsilon = 2ab = \int \psi_l(R_i)\psi_r(R_i)dR_i$).

After a straightforward procedure the Hamiltonian (3) is cast in the form we need

$$H = \frac{1}{2}\sum_{i,\alpha}\left\{\frac{\vec{P}_{i\alpha}^2}{2m} - \frac{A}{2}\vec{S}_{i\alpha}^2 + \frac{B}{4}\vec{S}_{i\alpha}^4\right\}\{1 + \varepsilon\sigma_{ix} + \alpha\sqrt{1-\varepsilon^2}\,\sigma_{iz}\} +$$

$$+ \frac{1}{4}\sum_{\substack{i\neq j\\ \alpha,\beta}}\varphi_{ij}''(\vec{S}_{i\alpha} - \vec{S}_{j\beta})^2\left\{\frac{1}{4} + \frac{\varepsilon}{2}\sigma_{ix} + \alpha\frac{\sqrt{1-\varepsilon^2}}{2}\sigma_{iz} + \right. \tag{7}$$

$$\left. + \frac{\varepsilon^2}{4}\sigma_{ix}\sigma_{jx} + \varepsilon\frac{\sqrt{1-\varepsilon^2}}{2}\sigma_{ix}\sigma_{jz} + \alpha\beta\frac{1-\varepsilon^2}{4}\sigma_{iz}\sigma_{jz}\right\}.$$

It is evident that this Hamiltonian takes the previously cited form (3) for $\varepsilon = 0$.

The advantages of such a novel model Hamiltonian are obvious: in addition to the conserved phonon picture (which is missing in earlier approaches [3], [8]) the tunnelling motion is also incorporated as an additional degree of freedom (the displacements and the pseudospins are mutually independent but time-dependent variables). Therefore, our new model can reproduce the pseudospin (diffusive or polarization) waves abreast to all phonon modes in the system as well as the collective motion of atomic clusters.

In conclusion we point out that the present model is favoured by recent computer simulations [9] and, among others [10], should be invoked for reasons of universality (see [10] and cross references). Finally, the model proposed here as analyzed by means of a more accurate self-consistent procedure (including the symmetry point of view at zero temperatures [11], [12]), could give an initial hint for deeper insight into the nature of ferroelectricity in general. Such investigation in addition to the previous analysis will be the subject of our future work.

Acknowledgements

One of the authors (S. S.) would like to thank Drs. H. BECK and S. AUBRY for short but valuable discussions during the EMF—3 in Zürich.

REFERENCES

1. S. STAMENKOVIC, N. M. PLAKIDA, V. L. AKSIENOV and T. SIKLÓS, JINR-Report P 17-9226, Dubna, 1975 (in Russian); Report KFKI-76-1, Budapest, 1976; Ferroelectrics, **14**, 655, 1976; Phys. Rev., **B14**, 5080, 1976.
2. P. G. DE GENNES, Solid State Commun., **1**, 132, 1963.
3. M. TOKUNAGA and T. MATSUBARA, Progr. Theor. Phys., **35**, 581, 1966.
4. S. STAMENKOVIC, Fiz. tverd. tela, **10**, 861, 1968.
5. J. B. COON, N. W. NAUGLE and R. D. MCKENZIE, Journ. Spectr., **20**, 107, 1966.
6. E. MERZBACHER, Quantum Mechanics, Chap. 5, John Wiley, New York, 1970.
7. E. A. PSCHENICHNOV and N. D. SOKOLOV, Opt. Spectr., **11**, 16, 1961; **17**, 343, 1964.
8. V. G. VAKS, Introduction to the Microscopic Theory of Ferroelectrics, Chap. 5, Nauka, Moscow 1973. (in Russian).
9. T. SCHNEIDER and E. STOLL, Phys. Rev. Lett., **31**, 1254, 1973; J. Phys. C: Solid St. Phys., **8**, 283, 1975.
10. H. BECK, J. Phys. C: Solid St. Phys., **9**, 33, 1976.
11. J. VILLAIN and S. AUBRY, phys. stat. sol., **33**, 337, 1969; Proceed. EMF-1, p. 41, Saarbrücken 1969.
12. LJ. NOVAKOVIC, The Pseudo-Spin Method in Magnetism and Ferroelectricity, Chap. 2, Pergamon Press Inc., New York, 1975.

Acta Physica Academiae Scientiarum Hungaricae, Tomus 42 (3), pp. 269—271 (1977)

COMMUNICATIO BREVIS

K-SHELL IONIZATION CROSS SECTIONS OF Pd, Ag, In AND Sn FOR RELATIVISTIC ELECTRONS

By

S. RICZ, B. SCHLENK, D. BERÉNYI, G. HOCK and A. VALEK

INSTITUTE OF NUCLEAR RESEARCH OF THE HUNGARIAN ACADEMY OF SCIENCES (ATOMKI), DEBRECEN

(Received 25. IV. 1977)

There are relatively few measurements for the cross sections of *K*-shell ionization by electron impact in the several hundred keV region of bombarding energy [1—5]. In addition, all of these measurements were performed by using scintillation techniques for the detection of X-rays and partly beta-ray spectrometers for producing monoenergetic electrons. Modern studies at accelerators with semiconductor X-ray detectors were carried out only at lower or higher energies [6, 7]. Of the studies at several hundred keV of bombarding energy, however, none examined the process at closely neighbouring elements.

In the present study we determined the K-shell electron impact ionization cross sections for $_{46}$Pd, $_{47}$Ag, $_{49}$In and $_{50}$Sn in the 300—600 keV region of bombarding energy (for Pd and In no data have been published in this region up till now). The electron beam was obtained from a Cockcroft—Walton accelerator and a Si(Li) detector was used as X-ray spectrometer. All the experimental arrangements were the same here as in our earlier studies [8, 9].

The targets of Ag and Sn were self-supporting, Pd and In were evaporated in vacuum onto a C backing of 2 μg/cm^2 thick. The thickness of the targets was 150—300 μg/cm^2.

The results for *K*-shell ionization cross sections and K_α/K_β ratios together with the corresponding theoretical values are given in Table I. Fig. 1 shows the experimental points and the theoretical curves for one of the bombarding energies. As can be seen in the Figure and in the Table, the experimental values of the cross section are in a fairly good agreement with the BEA theory [11] in the region investigated. At the same time, no dip or irregularities were observed inside the limits of the errors around $Z = 48$ suggested in [7] at 2.04 MeV bombarding energy.

As regards the K_α/K_β ratio, there are rather systematic disagreements with the corresponding theory [12]. It is a general trend for these ratios according to the published literature (e.g. [13]).

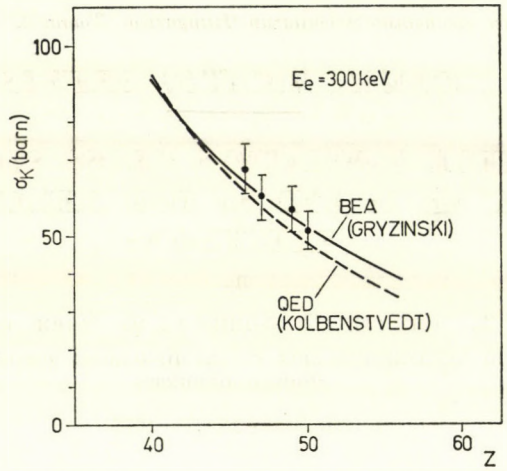

Fig. 1. *K*-shell electron impact ionization cross sections at 300 keV bombarding energy. Full line: calculated according to BEA [11], dashed line: calculated according to QED [10].

Table I

Electron impact *K*-shell ionization cross sections and K_α/K_β ratios

	ω_k	$E_{[\mathrm{keV}]}$	$\sigma_{k_{[\mathrm{barn}]}}$	$\sigma_{k_{[\mathrm{barn}]}}^{\mathrm{Theor.}}$ [11]	K_α/K_β	K_α/K_β Theor [12]
$_{46}$Pd	0.819±0.03	300	67.3±6.0	63.8	3.96±0.20	5.173
		400	64.5±6.0	59.1	3.90±0.20	
		500	64.5±6.0	56.5	3.71±0.19	
		600	64.3±6.0	54.9	3.50±0.18	
$_{47}$Ag	0.830±0.025	300	59.9±5.4	60.4	4.82±0.24	5.092
		400	57.8±5.2	55.9	4.81±0.24	
		500	56.1±5.1	53.5	4.90±0.25	
		600	54.6±5.0	52.0	4.83±0.24	
$_{49}$In	0.850±0.029	300	57.2±5.2	54.2	4.39±0.22	4.933
		400	55.7±5.0	50.3	4.56±0.23	
		500	56.3±5.1	48.1	4.51±0.23	
		600	56.6±5.1	46.8	4.53±0.23	
$_{50}$Sn	0.859±0.028	300	51.0±4.6	51.5	4.41±0.22	4.852
		400	48.9±4.4	47.7	4.53±0.23	
		500	48.8±4.4	45.7	4.37±0.22	
		600	48.5±4.4	44.5	4.35±0.22	

REFERENCES

1. H. HANSEN, H. WEIGMAN and A. FLAMMERSFELD, Nucl. Phys., **58,** 241, 1964.
2. J. W. MOTZ and R. C. PLACIOUS, Phys. Rev., **136A** 663, 1964.
3. H. HANSEN and A. FLAMMERSFELD, Nucl. Phys., **79** 135, 1966.
4. D. H. RESTER and W. E. DANCE, Phys. Rev., **152,** 1, 1966.
5. S. A. H. SEIF EL NASR, D. BERÉNYI and GY. BIBOK, Z. Physik, **267,** 169, 1974.
6. D. V. DAVIES, V. D. MISTRY and C. A. QUARLES, Phys. Lett., **38A,** 169, 1972.
7. ANGELA LI-SCHOLZ, R. COLLÉ, I. L. PREISS and W. SHOLZ, Phys. Rev., **A7,** 1957, 1973.
8. B. SCHLENK, D. BERÉNYI, S. RICZ, A. VALEK and G. HOCK, J. Phys. B., Atomic and Molecular Phys., **10,** 1303, 1977.
9. B. SCHLENK, B. BERÉNYI, S. RICZ, A. VALEK and G. HOCK, Acta Phys. Hung., **41,** 159, 1976.
10. H. KOLBENSTVEDT, J. Appl. Phys., **46,** 2771, 1975.
11. M. GRYZINSKI, Phys. Rev., **138A,** 336, 1965.
12. J. H. SCOFIELD, Atomic Data and Nucl. Data Tables, **14,** 121, 1974.
13. J. S. HANSEN, H. U. FREUND and R. V. FINK, Nucl. Phys., **A142,** 604, 1970.

RECENSIONES

NATHAN W. DEAN:

Introduction to the Strong Interactions

Gordon and Breach Science Publishers Ltd. New York, London 1976, 377 p.

At present, we do have a well-developed high energy phenomenology of the strong interactions which correlates various observations. This phenomenology consists mainly of three components: unitary symmetry, analyticity of S-matrix, Regge theory. The book of Dr. DEAN provides a useful introduction to these three topics in such a way that only the knowledge of courses in quantum mechanics is supposed.

The three parts of the book contain standard results. Thus, in the first part the rotation group, the isospin symmetry and unitary symmetry are surveyed. Both particle classifications and applications (mass relations, electromagnetic properties, three-vertices, two-particle scattering) are treated. The elements of SU(6) and the independent quark model are also included.

In Part II the elements of potential scattering (nature of singularities, Jost function, scattering amplitudes) and relativistic S-matrix (unitarity, analyticity, crossing, dispersion relations, Mandelstam representation) are described.

An introduction to Regge theory can be found in Part III. This Part starts with the complex angular momentum followed by relativistic Regge poles. The problems of ghosts, daughters, conspiracy and evasion are also touched. A separate chapter deals with the applications of Regge poles. Regge cuts and duality are treated in the closing chapters.

The book is written at a level which makes it possible for non-specialists and graduate students, respectively, to follow the topics easily.

G. PÓCSIK

L. H. RYDER: Elementary Particles and Symmetries

(Documents on Modern Physics)

Gordon and Breach Science Publishers Ltd. New York, London, 1975.

This is a valuable introductory book which grew out of lectures given to third year physics undergraduates at the University of Kent. Although quantum electrodynamics and all reference to quantum field theory are omitted, the book provides a great deal of useful information on recent advances in particle physics. Continuous and discrete space-time symmetries, gauge transformations, and the standard internal symmetries (SU (2), SU (3), SU (4)) are clearly and simply explained. These symmetry properties are exploited in many concrete applications which include Cabibbo's theory, CP violation, current algebra and the unified theory of weak and electromagnetic interactions.

One might hope that the second edition of this book will cover some more recent developments such as the interpretation of the charmonium spectrum and the quantitative description of deep inelastic lepton-hadron scattering data.

Contents: 1. Introduction. 2. Symmetries and conservation laws. 3. Isospin. 4. Strangeness. 5. Isospin and strangeness selection rules in weak and electromagnetic interactions. 6. Electromagnetic structure of nucleons. 7. Resonances. 8. Weak interactions and parity violation. 9. K meson decays and CP violation. 10. The conserved vector current theory of unitary symmetry. 11. Unitary symmetry and the quark model. 12. Cabibbo's theory, chiral symmetry and current algebra. 13. Unified weak and electromagnetic interactions and charm.

K. LADÁNYI

A. MÜNSTER: Statistical Thermodynamics

Vols. I., II. Springer Verlag, Berlin—Heidelberg—New York, Academic Press New York—London
Vol. I.: 692 pages, Vol. II.: 841 pages

In 1956 A. MÜNSTER first published "Statistical Thermodynamics" in German with the aim to provide a textbook of level rising considerably above that of an elementary introduction to the subject. A revised and much enlarged version of this book appeared later in English — the two volumes reviewed here — the first volume in 1969, the second one in 1974. By completing this grandiose work the author has filled a serious gap: after thirty years, since the issue of the statistical thermodynamics by FOWLER and GUGGENHEIM, this is the first, up-to-date textbook claiming at completeness. Among its numerous features to be praised rigour and balance should be mentioned in the first place.

The first 416 pages of Vol. I are devoted to the derivation of thermodynamic principles, to the general foundations of thermodynamics and further statements of similarly general character.Of the many problems treated here it is hard to mention only a few. Axiomatic foundations of classical and quantum statistics, ergodic theorem, generalized ensembles, fluctuations etc. are all given full and well-grounded discussions. Part II of Vol. I is concerned with the theory of gases. The treatment of ideal gases is followed by general remarks on the properties of real gases, various theories of the second virial coefficient, general cluster approach, the theory of condensation. Calculations of the molecular distribution functions close the first volume.

Volume II deals with the theory of condensed phases, crystals and liquids. This field has undergone rapid development lately. 1973 is the date up to which this development is traced in the present volume. Moreover, "the statistical theory of condensed phases presents an extraordinarily many-faceted picture. It is not possible in the framework of this book to give even a partially complete presentation from the physical standpoint.". As a consequence severalimportant subjects like the many-body problem, superconductivity, liquid crystals, Kondo effect are not covered here and modern developmental tendencies of critical phenomena are only briefly mentioned. Even without these topics an enormous amount of material is comprised in this volume. The theory of ideal crystals is treated first and numerous results from lattice theory are cited and compared with experiments. Phase transitions in crystals are described in the following chapters. Several theories of superlattice transformations are developed and compared with experimental data. A chapter on the Ising model is followed by the treatment of solid solutions of variable concentration. Critical exponents, homogeneity, scaling laws are introduced and discussed. Further subjects dealt with in Part III are: X-ray scattering by binary alloys, critical scattering in solid solutions, critical phenomena in magnetic systems and rotational transitions. Part IV (470 pages) is devoted to the liquid state, which being intermediate between the gaseous and crystalline state is by far the most difficult for statistical thermodynamics to describe. The treatment starts with pure liquids, giving different model descriptions. Scattering of X-rays by liquids, calculation of the radial distribution function, liquid metal and theory of melting are given detailed analyses. Solutions of non-electrolytes and solutions of strong electrolytes are described in two subsequent chapters. Exact derivation of the asymptotic laws for infinitely dilute solutions, application of the cluster method to finite concentrations, X-ray and light scattering in multicomponent systems, theories based on the use of the lattice model, the Debye—Hückel theory of strong electrolytes are among the topics discussed here.

Sixteen appendices, author and subject indices complete the book.

Statistical Thermodynamics is a basic textbook and can be recommended to all studying or working on this subject.

N. MENYHÁRD

Statistical Physics

Proceedings of the International Conference, Budapest, Hungary, 25—29 August, 1975
Editors: L. Pál and P. Szépfalusy
A joint edition of North-Holland Publishing Co., Amsterdam and Akadémiai Kiadó, Budapest, 1976

This book comprises texts of invited lectures given at the IUPAP International Conference on Statistical Physics, held in Budapest in 1975. Most important tendencies of recent developments in statistical physics are truly reflected by these excellent review papers.

The Opening Address by L. PÁL commemorating L. BOLTZMANN and recalling the 50-year-old paper by Hungarian-born LEO SZILÁRD in which he demonstrated that phenomenological thermodynamics can be extended to the description of fluctuation phenomena is followed by the Boltzmann Medal Address of KENNETH G. WILSON, first recipient of the Boltzmann award. His talk is devoted to the renormalization group and the illustration of its ideas by a simple Kadanoff block spin method. The renormalization group is the central theme of several other talks, too. Thus L. P. KADANOFF's Variational Approximations for Renormalization Group Transformations and B. I. HALPERIN's Theory of Dynamic Critical Phenomena represent some of the most recent advances in renormalization group theory. Probability theory is the basis of the approach to renormalization group in two talks (JA. G. SINAI's and G. JONA-LASENIO's) comprised in this book.

Fluctuations around the macroscopic behaviour in non-linear systems and a systematic approximation to the solution of the master equation are the subjects of N. G. VAN KAMPEN's lecture. Statistical theory of self-organizing structures by H. HAKEN is concerned with the spontaneous formation of structures out of disordered states — a phenomenon common to many physical and non-physical systems. A review of recent theoretical and experimental developments in the problem of turbulent motion of fluids forms the subject matter of the talk by P. C. MARTIN.

Finally, the statistical mechanics of nucleation and phase separation, the kinetic theory of hard spheres and excitonic transitions in strong magnetic fields are also given outstanding accounts in this volume.

N. MENYHÁRD

Printed in Hungary

A kiadásért felelős az Akadémiai Kiadó igazgatója — Műszaki szerkesztő: Botyánszky Pál

A kézirat nyomdába érkezett: 1977. IV. 15. — Terjedelem 9,25 (A/5) ív, 21 ábra

78.4580 Akadémiai Nyomda, Budapest — Felelős vezető: Bernát György

NOTES TO CONTRIBUTORS

I. PAPERS will be considered for publication in Acta Physica Hungarica only if they have not previously been published or submitted for publication elsewhere. They may be written in English, French, German or Russian.

Papers should be submitted to

Prof. I. Kovács, Editor
Department of Atomic Physics, Polytechnical University
1521 Budapest, Budafoki út 8, Hungary

Papers may be either articles with abstracts or short communications. Both should be as concise as possible, articles in general not exceeding 25 typed pages, short communications 8 typed pages.

II. MANUSCRIPTS

1. Papers should be submitted in five copies.

2. The text of papers must be of high stylistic standard, requiring minor corrections only.

3. Manuscripts should be typed in double spacing on good quality paper, with generous margins.

4. The name of the author(s) and of the institutes where the work was carried out should appear on the first page of the manuscript.

5. Particular care should be taken with mathematical expressions. The following should be clearly distinguished, e.g. by underlining in different colours: special fonts (italics, script, bold type, Greek, Gothic, etc); capital and small letters; subscripts and superscripts, e.g. x^3, x_3; small *l* and 1; zero and capital O; in expressions written by hand: *e* and *i*, *n* and *u*, *v* and *v*, etc.

6. References should be numbered serially and listed at the end of the paper in the following form: J. Ise and W. D. Fretter, Phys. Rev., *76*. 933, 1949.

For books, please give the initials and family name of the author(s), title, name of publisher, place and year of publication, e.g.: J. C. Slater. Quantum Theory of Atomic Structures, I. McGraw-Hill Book Company Inc., New York, 1960.

References should be given in the text in the following forms: Heisenberg [5] or [5].

7. Captions to illustrations should be listed on a separate sheet, not inserted in the text.

III. ILLUSTRATIONS AND TABLES

1. Each paper should be accompanied by five sets of illustrations, one of which must be ready for the blockmaker. The other sets attached to the copies of the manuscript may be rough drawings in pencil or photocopies.

2. Illustrations must not be inserted in the text.

3. All illustrations should be identified in blue pencil by the author's name, abbreviated title of the paper and figure number.

4. Tables should be typed on separate pages and have captions describing their content. Clear wording of column heads is advisable. Tables should be numbered in Roman numerals (I, II, III, etc.).

IV. MANUSCRIPTS not in conformity with the above Notes will immediately be returned to authors for revision. The date of receipt to be shown on the paper will in such cases be that of the receipt of the revised manuscript.

Reviews of the Hungarian Academy of Sciences are obtainable at the following addresses:

AUSTRALIA
C.B.D. LIBRARY AND SUBSCRIPTION SERVICE, Box 4886, G.P.O., *Sydney N.S.W. 2001*
COSMOS BOOKSHOP, 145 Ackland Street, *St. Kilda (Melbourne), Victoria 3182*

AUSTRIA
GLOBUS, Höchstädtplatz 3, *1200 Wien XX*

BELGIUM
OFFICE INTERNATIONAL DE LIBRAIRIE, 30 Avenue Marnix, *1050 Bruxelles*
LIBRAIRIE DU MONDE ENTIER, 162 Rue du Midi, *1000 Bruxelles*

BULGARIA
HEMUS, Bulvar Ruszki 6, *Sofia*

CANADA
PANNONIA BOOKS, P.O. Box 1017, Postal Station "B", *Toronto, Ontario M5T 2T8*

CHINA
CNPICOR, Periodical Department, P.O. Box 50, *Peking*

CZECHOSLOVAKIA
MAD'ARSKÁ KULTURA, Národní třida 22, *115 66 Praha*
PNS DOVOZ TISKU, Vinohradská 46, *Praha 2*
PNS DOVOZ TLAČE, *Bratislava 2*

DENMARK
EJNAR MUNKSGAARD, Norregade 6, *1165 Copenhagen*

FINLAND
AKATEEMINEN KIRJAKAUPPA, P.O. Box 128, *SF-00101 Helsinki 10*

FRANCE
EUROPERIODIQUES S. A., 31 Avenue de Versailles, *78170 La Celle St. Cloud*
LIBRAIRIE LAVOISIER, 11 rue Lavoisier, *75008 Paris*
OFFICE INTERNATIONAL DE DOCUMENTATION ET LIBRAIRIE, 48 rue Gay-Lussac, *75240 Paris Cedex 05*

GERMAN DEMOCRATIC REPUBLIC
HAUS DER UNGARISCHEN KULTUR, Karl-Liebknecht-Strasse 9, *DDR-102 Berlin*
DEUTSCHE POST ZEITUNGSVERTRIEBSAMT, Strasse der Pariser Kommüne 3—4, *DDR-104 Berlin*

GERMAN FEDERAL REPUBLIC
KUNST UND WISSEN ERICH BIEBER, Postfach 46, *7000 Stuttgart 1*

GREAT BRITAIN
BLACKWELL'S PERIODICALS DIVISION, Hythe Bridge Street, *Oxford OX1 2ET*
BUMPUS, HALDANE AND MAXWELL LTD., Cowper Works, *Olney, Bucks MK46 4BN*
COLLET'S HOLDINGS LTD., Denington Estate, *Wellingborough, Northants NN8 2QT*
WM. DAWSON AND SONS LTD., Cannon House, *Folkestone, Kent CT19 5EE*
H. K. LEWIS AND CO., 136 Gower Street, *London WC1E 6BS*

GREECE
KOSTARAKIS BROTHERS, International Booksellers, 2 Hippokratous Street, *Athens-143*

HOLLAND
MEULENHOFF-BRUNA B.V., Beulingstraat 2, *Amsterdam*
MARTINUS NIJHOFF B.V., Lange Voorhout 9—11, *Den Haag*
SWETS SUBSCRIPTION SERVICE, 347b Heereweg, *Lisse*

INDIA
ALLIED PUBLISHING PRIVATE LTD., 13/14 Asaf Ali Road, *New Delhi 110001*
150 B-6 Mount Road, *Madras 600002*
INTERNATIONAL BOOK HOUSE PVT. LTD., Madame Cama Road, *Bombay 400039*
THE STATE TRADING CORPORATION OF INDIA LTS., Books Import Division, Chandralok, 36 Janpath, *New Delhi 110001*

ITALY
EUGENIO CARLUCCI, P.O. Box 252, *70100 Bari*
INTERSCIENTIA, Via Mazzé 28, *10149 Torino*
LIBRERIA COMMISSIONARIA SANSONI, Via Lamarmora 45, *50121 Firenze*
SANTO VANASIA, Via M. Macchi 58, *20124 Milano*
D. E. A., Via Lima 28, *00198 Roma*

JAPAN
KINOKUNIYA BOOK-STORE CO. LTD., 17-7 Shinjuku-ku 3 chome, Shinjuku-ku, *Tokyo 160-91*
MARUZEN COMPANY LTD., Book Department, P.O. Box 5050 Tokyo International, *Tokyo 100-31*
NAUKA LTD. IMPORT DEPARTMENT, 2-30-19 Minami Ikebukuro, Toshima-ku, *Tokyo 171*

KOREA
CHULPANMUL, *Phenjan*

NORWAY
TANUM-CAMMERMEYER, Karl Johansgatan 41—43, *1000 Oslo*

POLAND
WĘGIERSKI INSTYTUT KULTURY, Marszałkowska 80, *Warszawa*
CKP I W ul. Towarowa 28 *00-958 Warsaw*

ROUMANIA
D. E. P., *Bucureşti*
ROMLIBRI, Str. Biserica Amzei 7, *Bucureşti*

SOVIET UNION
SOJUZPETCHATJ — IMPORT, *Moscow*
and the post offices in each town
MEZHDUNARODNAYA KNIGA, *Moscow G-200*

SPAIN
DIAZ DE SANTOS, Lagasca 95, *Madrid 6*

SWEDEN
ALMQVIST AND WIKSELL, Gamla Brogatan 26, *101 20 Stockholm*
GUMPERTS UNIVERSITETSBOKHANDEL AB, Box 346, *401 25 Göteborg 1*

SWITZERLAND
KARGER LIBRI AG, Petersgraben 31, *4011 Basel*

USA
EBSCO SUBSCRIPTION SERVICES, P.O. Box 1943, *Birmingham, Alabama 35201*
F. W. FAXON COMPANY, INC., 15 Southwest Park, *Westwood, Mass, 02090*
THE MOORE-COTTRELL SUBSCRIPTION AGENCIES, *North Cohocton, N. Y. 14868*
READ-MORE PUBLICATIONS, INC., 140 Cedar Street, *New York, N. Y. 10006*
STECHERT-MACMILLAN, INC., 7250 Westfield Avenue, *Pennsauken N. J. 08110*

VIETNAM
XUNHASABA, 32, Hai Ba Trung, *Hanoi*

YUGOSLAVIA
JUGOSLAVENSKA KNJIGA, Terazije 27, *Beograd*
FORUM, Vojvode Mišiča 1, *21000 Novi Sad*

ACTA PHYSICA

ACADEMIAE SCIENTIARUM HUNGARICAE

TOMUS XLII FASCICULUS 4

AKADÉMIAI KIADÓ, BUDAPEST
1977

ACTA PHYS. HUNG. APAHAQ 42 (4) 277–380 (1977)

ACTA PHYSICA

ACADEMIAE SCIENTIARUM HUNGARICAE

SZERKESZTI

KOVÁCS ISTVÁN

Az *Acta Physica* angol, német, francia vagy orosz nyelven közöl értekezéseket. Évente két kötetben, kötetenként 4—4 füzetben jelenik meg. Kéziratok a szerkesztőség címére (1521 Budapest XI., Budafoki út 8.) küldendők.

Megrendelhető a belföld számára az Akadémiai Kiadónál (1363 Budapest Pf. 24. Bankszámla 215-11488), a külföld számára pedig a „Kultúra" Külkereskedelmi Vállalatnál (1389 Budapest 62, P. O. B. 149. Bankszámla 217-10990 sz.), vagy annak külföldi képviseleteinél és bizományosainál.

The *Acta Physica* publish papers on physics in English, German, French or Russian, in issues making up two volumes per year. Subscription price: $32.00 per volume. Distributor: KULTURA Hungarian Trading Co. (1389 Budapest 62, P. O. Box 149) or its representatives abroad.

Die *Acta Physica* veröffentlichen Abhandlungen aus dem Bereich der Physik in deutscher, englischer, französischer oder russischer Sprache, in Heften die jährlich zwei Bände bilden.

Abonnementspreis pro Band: $32.00. Bestellbar bei: KULTURA Außenhandelsunternehmen (1389 Budapest 62, Postfach 149) oder bei seinen Auslandsvertretungen.

Les *Acta Physica* publient des travaux du domaine de la physique, en français, anglais, allemand ou russe, en fascicules qui forment deux volumes par an.

Prix de l'abonnement: $32.00 par volume. On peut s'abonner à l'Entreprise du Commerce Extérieur KULTURA (1389 Budapest 62, P. O. B. 149) ou chez ses représentants à l'étranger.

«*Acta Physica*» публикуют трактаты из области физических наук на русском, немецком, английском и французском языках.

«*Acta Physica*» выходят отдельными выпусками, составляющими два тома в год.

Подписная цена — $32.00 за том. Заказы принимает предприятие по внешней торговле KULTURA (1389 Budapest 62, P. O. B. 149) или его заграничные представительства и уполномоченные.

ACTA PHYSICA

ACADEMIAE SCIENTIARUM HUNGARICAE

TOMUS XLII FASCICULUS 4

AKADÉMIAI KIADÓ, BUDAPEST
1977

ACTA PHYS. HUNG.

INDEX

Acta Physica Academiae Scientiarum Hungaricae, Tomus 42 (4), pp. 277—281 (1977)

A CRITICAL STUDY OF GLIDDON'S MODEL OF THE PROTONOSPHERE

By

B. SINGH

DEPARTMENT OF MATHEMATICS, ST. ANDREW'S COLLEGE, GORAKHPUR (UP), INDIA

and

V. B. JOHRI

DEPARTMENT OF MATHEMATICS AND THEORETICAL PHYSICS, GORAKHPUR UNIVERSITY
GORAKHPUR (UP), INDIA

(Received 23. II. 1977)

This work is a theoretical study of GLIDDON's simplified model [7] to establish the feasibility of protonospheric mechanism of heat conduction. GLIDDON's approach has been critically examined and an exact and modified solution to the non-linear heat equation for the protonosphere i.e. static plasma is obtained, the variation of temperature is discussed and it is found to agree with the experimental results. Downward flux of energy has also been calculated.

1. Introduction

There is considerable interest at present in developing a theory for protonospheric observations surrounding the earth. The experimentally observed protonosphere is very complex due to chemical reactions and dynamical motions of internal as well as external origins. GEISLER and BOWHILL [1] proposed that the energy stored in the protonosphere during the day is conducted downward during the night and it is this flux that provides energy necessary to maintain the night time electron temperature above that of the neutrals in the upper F-region. This hypothesis of downward heat condution from the protonosphere was also supported by experimental results [2—6] which explicitly imply that the temperature of the protonosphere falls down to neutral within a time of the order of one second after sunset.

GLIDDON [7] has made theoretical calculations using simplified models to establish the feasibility of the protonospheric mechanism assuming that the electron density is the same at all altitudes. However, his solution fails to express the true nature of the proposed protonospheric model owing to a fallacy in transforming the original heat equation. Further, we do not agree with GLIDDON's observation that standard techniques do not apply to the differential equation governing heat conduction in a homogeneous plasma. In fact, the heat conduction equation is non-linear due to the coefficient of conductivity of the plasma and is amenable to solution by standard techniques as shown in this paper.

2. Remarks on Gliddon's approach

The heat equation for GLIDDON's model protonosphere [7—10] is

$$\frac{\partial}{\partial z}\left(KT^{5/2}\frac{\partial T}{\partial z}\right)=\frac{\partial}{\partial t}(CT)\,. \tag{1}$$

The initial condition is

$$T(z,0)=T_0\,,\quad 0<z<\infty \tag{2}$$

and the boundary condition is

$$T(0,t)=T_1\,,\quad 0<t<\infty\,. \tag{3}$$

Consideration has been made in a homogeneous plasma which occupies the half-space $z \geqslant 0$ and is initially at a uniform temperature T_0. At this time $t \geqslant 0$, the temperature of the boundary $z=0$ is changed to T_1. Effects due to flux of ionization have been ignored. Electromagnetic field effects are not considered either.

Introducing dimensionless variable $t=a\tau$ and $z=b\xi$ GLIDDON has transformed Eq. (1) into the following form:

$$\frac{\partial T}{\partial \tau}=\frac{2Ka}{1Cb}\frac{\partial^2 T^{1/2}}{\partial \xi^2}\,. \tag{4}$$

While attempting to solve Eq. (4) GLIDDON has committed a mistake by making a fallacious transformation $\chi'=\xi/2\tau^{1/2}$ which according to his calculation converts the non-linear partial differential equation (4) into an ordinary differential equation

$$\frac{Ka}{1Cb}\frac{d^2T^{1/2}}{d\chi'^2}=-\chi'\frac{dT}{d\chi'}\,.$$

This transformation is not valid and leads to an inaccurate solution. Therefore, GLIDDON's interpretation of the cooling of protonosphere after sunset and variation temperature, density, flux and the subsequent researches, based on the above solution do not reveal the exact characteristics of Eq. (1) governing the behaviour of the protonospheric model.

3. Exact solution to the heat equation

Considering a solution of (1) in the form[12]

$$T(z,t)=X(t)Y(z) \tag{5}$$

Eq. (1) can be written as

$$\frac{C}{KX^{1/2}}\frac{dX}{dt} = \frac{2}{1Y}\frac{d^2Y^{1/2}}{dz^2} = \lambda \text{ (say)} . \tag{6}$$

Now solving separately two ordinary differential equations which are obtained from (6), we get

$$X = \left(\frac{2C}{5K}\right)^{2/5}(A + \lambda t)^{-2/5} \tag{7}$$

and

$$Y = \left(\frac{5}{6}\right)^{4/5}\lambda^{2/5}(z + \varepsilon)^{4/5} , \tag{8}$$

where A is a constant of integration and ε is any constant. Substituting the value of X and Y from (7) and (8), in (5), we have,

$$T(z, t) = \left(\frac{2C}{5K}\right)^{2/5}\left(\frac{5}{6}\right)^{4/5}\left(\frac{A}{\lambda} + t\right)^{-2/5}(z + \varepsilon)^{4/5} . \tag{9}$$

Eliminating constants λ, A and ε with the help of Eqs. (2) and (3), we get

$$T(z, t) = T_0[1 + tT_0^{5/2}(vt^{1/2} + z\mu^{-1/2})^{-2}]^{-2/5} ,$$

where (10)

$$v = (T_0T_1)^{5/4}(T_0^{5/2} - T_1^{5/2})^{-1/2} \quad \text{and} \quad \mu = \frac{18K}{C}$$

which satisfy the initial and boundary conditions (2) and (3). Using Eq. (10), the flux factor G is given by

$$G = 4K(\mu\varepsilon)^{-1/2}(v + z/\sqrt{\mu t})^{-3}\left\{T_0^{-5/2} + \left(v + \frac{z}{\sqrt{\mu t}}\right)^{-2}\right\}^{-18/5} . \tag{11}$$

4. Discussion

Eq. (10) has great physical significance as shown by Figs. 1 and 2. It is evident from Fig. 1 that at an altitude of 800 km in F-region, the temperature falls down to neutral within a time of the order of one second in conformity with NAGY [11] and WALKER's observations. The graphs corresponding to t = constant are straight lines showing uniformity of the temperature gradient in a static plasma. Fig. 1' shows that temperature falls down within an hour rapidly to the value T_1/T_0. Fig. 2 also deals with the phenomenon of temperature variation at constant altitude with respect to different time scales. As expected, the $\Theta - z$ graphs and $\Theta - t$ graphs of GLIDDON [7] show considerable deviation from the observed data. Flux calculated from (11)

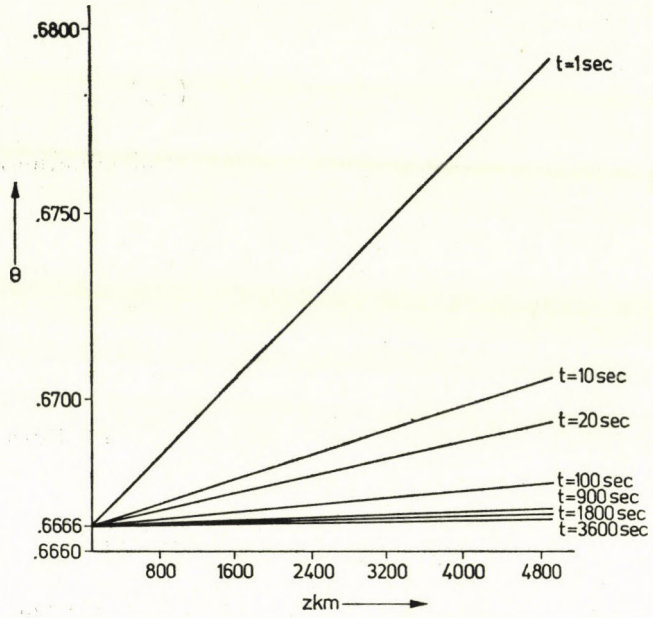

Fig. 1. Normalized temperature distribution along a field line with time as parameter

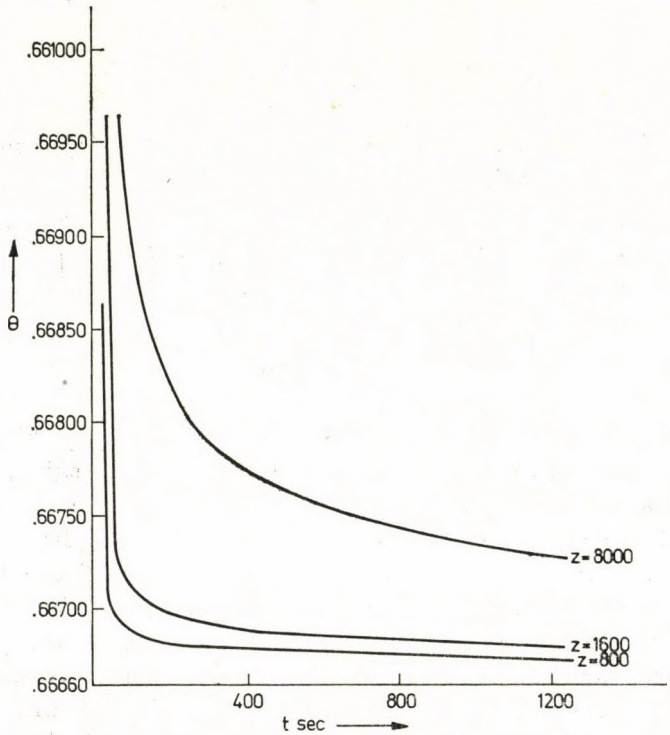

Fig. 2. Same results as Fig. 1 as a function of time with distance as parameter

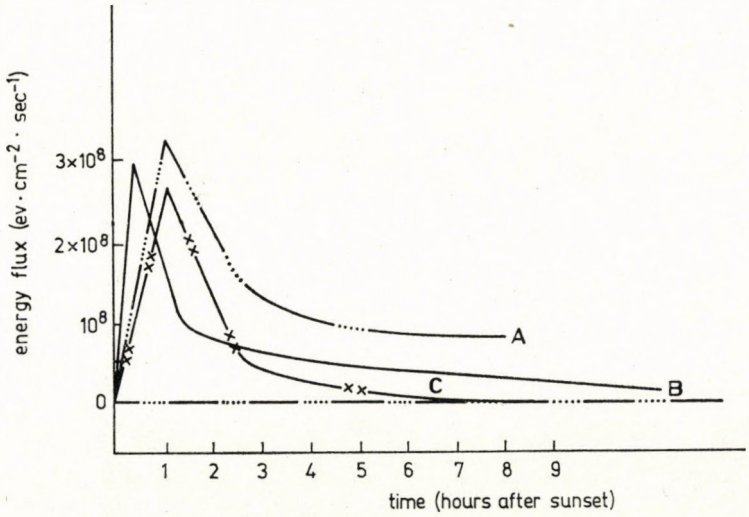

Fig. 3. Calculated night time variation of energy flux (experimental results shown for comparison)
A ——— ··· ——— 6 hours average at 500 km over Millstone (EVANS [6])
B ——— (NAGY—WALKER [2])
C ——— xx ——— our graph

is in close agreement with experimental observations [13, 14] (see Fig. 3 corresponding to (11)). This supports the hypothesis of downward heat conduction from the protonosphere.

Generalisation of the above problem to two-dimensional case has been worked out by the authors and will be reported later.

REFERENCES

1. J. E. GEISLER and S. A. BOWHILL, J. Atmosphere Terrest. Phys., **27**, 119, 1965.
2. A. F. NAGY and J. C. G. WALKER, Planetary Space Sci., **15**, 95, 1967.
3. A. F. NAGY, L. H. BRACE, G. R. CARIGNAN and M. KANAL, J. Geophysics Res., **68**, 6401, 1963.
4. J. V. EVANS, Planetary Space Sci., **13**, 1031, 1965.
5. J. V. EVANS, Planetary Space Sci., **15**, 1887, 1967.
6. J. V. EVANS, Planetary Space Sci., **15**, 1557, 1967.
7. J. E. C. GLIDDON, Theoretical Investigations of the Structure of the Protonosphere and Upper F-region, University of Illinois, Aeronomy Rept. No. 12, June 1966.
8. B. TANENBAUM, Phys. Fluids, **8**, 683, 1965.
9. E. H. HOLT and R. E. HASBALL, Foundations of Plasma Dynamics, pp. 151—166, Macmillan Company, New York, 1965.
10. P. BABER, The Cooling of the Protonosphere, University of Michigan Sci. Report 06 106-10-T, December, 1967.
11. A. F. NAGY, P. BANER and E. G. FONTHEIM, J. Geophysics, Res. Space Phys., Vol. 73, No. 19. October 1, 1968.
12. I. N. SNEDDON, Elements of Partial Differential Equations, McGraw-Hill Book Company, Inc. New York, 1957.
13. B. SINGH and S. N. SHARMA, Accepted for publication in the Indian Journal of Radio and Space Physics.
14. B. SINGH, Downward conducted flux from protonosphere to F-region (unpublished).

Acta Physica Academiae Scientiarum Hungaricae, Tomus 42 (4), pp. 283—287 (1977)

THE CHANGE OF THE LOAD-MICROHARDNESS CURVES OF NaCl SINGLE CRYSTALS DUE TO HEAT TREATMENT AND IMPURITY

By

J. SÁRKÖZI, A. TÓTH and Z. MORLIN*

INSTITUTE OF PHYSICS, DEPARTMENT OF EXPERIMENTAL PHYSICS, TECHNICAL UNIVERSITY, BUDAPEST

(Received 3. III. 1977)

In order to determine the physical meaning of the constants a and n in the equation $H = 1854 \cdot a \cdot d^{n-2}$ describing the microhardness of the alkali halide crystals quenching experiments were carried out on NaCl : Ca systems. By means of combined electrical conductivity and microhardness measurements it was found that values of the constants a and n depend on the concentration and state of impurities in the crystals. The results obtained show that a and n are not defined by the crystal type alone, but also by the type and concentration of impurity centres interacting with the dislocations.

1. Introduction

Experiment shows that the microhardness of alkali halide single crystals is given by the equation

$$H = 1854 \cdot a \cdot d^{n-2} \tag{1}$$

[1, 2]. According to literature the constant n in the exponent of d is the same for all ionic crystals [1], where the value of a changes in accordance with the surface energy. It follows from the constant value of n that instead of the microhardness — which is a quantity depending on the depth of indentation — the a constant may be more profitably utilized to describe the resistance to plastic deformation of the crystals. The aim of the present work is to investigate more closely the physical nature of the constants a and n by means of measuring their dependence on the concentration of Ca impurities and on the heat treatment of NaCl single crystals.

2. Experimental details

The experiments were carried out with specially grown OH^- — free NaCl crystals [3] doped with different amounts (from $2 \cdot 10^{-7}$ to 10^{-3} mol/mol) of Ca^{2+} impurity.

* Present address: Research Laboratory for Crystal Physics of the Hungarian Academy of Sciences, Budapest

The microhardness as a function of the depth of indentation was measured and from the curves obtained the n and a values were determined by Eq. (1).

The ionic conductivity of the crystals was measured in the usual way with a vibrating condenser electrometer.

The annealing and quenching of the crystals were carried out in an inert gas atmosphere. At the cooling rate which was applied in these experiments (100 °C/min) no stresses or plastic deformation were formed, consequently the dislocation density remained unchanged.

3. Results and discussion

The experiments with pure crystals supported the results of G. P. UPIT and S. A. VARCHENYA [1] according to which the n value is the same for every alkali-halide crystal whereas a is a linear function of the surface energy.

If, however, for instance NaCl crystals doped with Ca were investigated the n value showed for various Ca^{2+} concentrations a strong concentration dependence, at the same time a increased at already very small Ca concentration (Fig. 1, Curves 1, 2, 3, 4, 5).

More surprising results were obtained if NaCl crystals containing a certain level of Ca impurity concentration were quenched. After quenching from above 150 °C the "constant" n took the value characteristic for very pure crystals, at the same time the quenching increased the a value (Fig. 1, Curve $\bar{4}$). The microhardness decreased considerably, which shows that the changes in the a and H values are not always simultaneous processes.

Summing up it was found that the a and n values, respectively, change with changing impurity concentration as well as by heat treatment. It is quite clear, however, that any heat treatment and any change of impurity concentration realizes various impurity states in the crystals consequently the changes of the n and a values should be due to the changes of the state of impurities. It follows that in order to obtain a better understanding of the character of n and a, respectively, the state and distribution of the impurity in the sample should be known for given n and a values. On the other hand it also follows that the constant a cannot be used instead of the microhardness which depends on the depth of indentation since apparently the microhardness is determined by two quantities a and n changing independently of each other. Nevertheless, it is feasible that the knowledge of the microscopic beckground of the a and n values yields a better understanding of the physical nature of the microhardness.

Information about the impurity (Ca^{2+}) state in the crystal and its changes due to an increase in concentration or heat treatment can be obtained by electrical conductivity measurements. Curves 1, 2 and 3 of Fig. 2 show that

the impurity is in a dissolved state according to the association range in the form of single ions or impurity-vacancy pairs at room temperature at which the microhardness measurements are carried out. Any increase of the concentration only increases the number of these particles, but no change occurs in the state of the impurity. With these crystals the n value remains unchanged

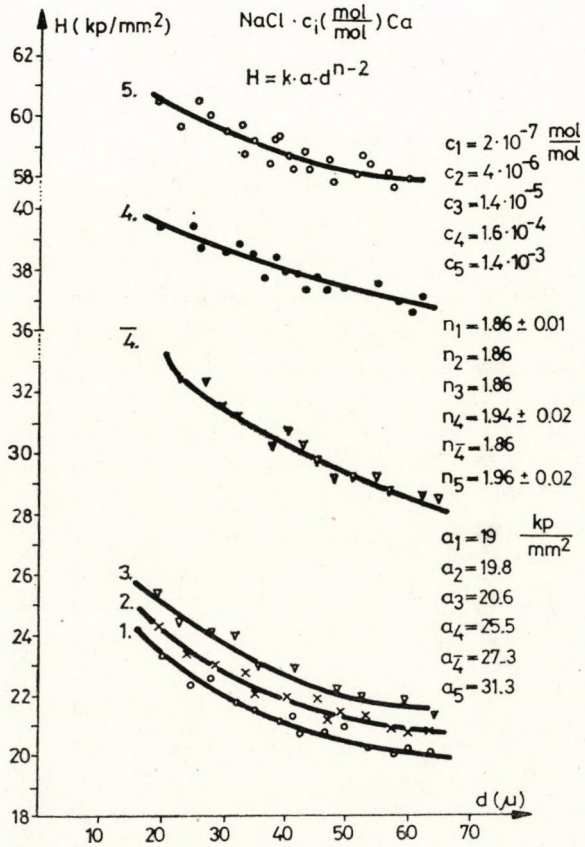

Fig. 1. Indentation diameter dependent change of microhardness for various impurity concentrations in NaCl · Ca^{2+} systems (Curves 1,2,3,4 and 5). The effect of quenching NaCl; 1.6×10^{-4} mol/mol Ca^{2+} systems is demonstrated by curve $\overline{4}$

whereas the a values increase with increasing conductivity values (Fig. 1, Curves 1, 2, 3). With crystals, however, containing an impurity concentration of 1.6×10^{-4} mol/mol Ca^{2+} also the precipitation range appears in the electrical conductivity curves (Fig. 2, Curve 4). The a and n values as measured with these crystals deviate markedly from the corresponding values obtained with less doped crystals. The same applies to crystals containing an even higher impurity concentration (Figs. 1 and 2, Curves 5).

The quenching of the crystals from various annealing temperatures to room temperature leads to the following results. With an impurity content less than 1.6×10^{-4} mol/mol Ca^{2+} the quenching changed neither the conductivity nor the microhardness-indentation diameter curves, thus the constancy of the a and n values is understandable. Quenching carried out with crystals

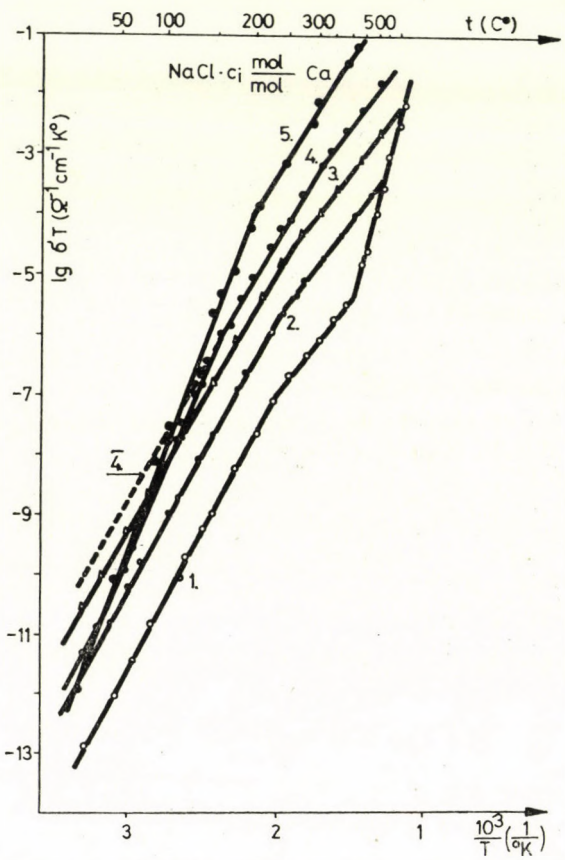

Fig. 2. Electrical conductivity of NaCl · $CaCl_2$ single crystals for various impurity concentrations. (Curves 1,2,3,4 and 5). The effect of quenching for a NaCl, 1.6×10^{-4} mol/mol Ca^{2+} sample is demonstrated by curve 4

of higher impurity concentrations resulted in a considerable change of the electrical conductivity as well as of the a and n values. This is illustrated in Fig. 2 where Curve 4 goes over into curve $\overline{4}$, which means that by quenching the precipitation range is carried over into the association range.

Summarizing the following conclusions regarding the a and n values may be drawn from conductivity and microhardness measurements on doped NaCl crystals.

If the impurity is in a dissolved state, i.e. in the form of single ions and impurity-vacancy pairs, with the increase of impurity concentration n does not change only a. If, however, the impurity becomes precipitated n and a undergo a considerable change. If, by quenching, the precipitation state is terminated and brought over into the association state, n takes the low value belonging to this state whereas a increases further. The quantity n appears to be defined by the state of contamination whereas a may change at the same impurity state if for instance the impurity concentration changes. Consequently an unambiguous relation between a and the microhardness (H) (increasing H with increasing a) exists only if no change occurs in the impurity state.

If the state of impurity does not change one may assume that the character of interaction between the dislocations and point defects does not change either. Consequently in crystals with small impurity content only vacancies and single impurity-vacancy pairs interact with the dislocations. By increasing the impurity concentration only the number of point defects increases. The increase of a thus probably reflects only the increase of the number of damping centres, whereas the constancy of n indicates the constancy of the type of interaction. The appearance of the precipitates apparently leads to new types of interactions. According to the electrical conductivity curves the precipitation forms dipole clusters of impurity-vacancy pairs in crystals with 1.6×10^{-4} mol/mol impurity concentration, whereas with the concentration of 1.4×10^{-3} mol/mol Ca^{2+} clusters become precipitated, i.e. a second phase is formed. Two different n values belong to these two forms of precipitation, whose interaction with dislocations is apparently different. Consequently one may say that the n value is not defined by the crystal type alone, but also by the type of impurity centres interacting with the dislocations. The same applies also to the constant a by adding that a may also change with the same type of the centres if the concentration of these centres changes.

REFERENCES

1. G. P. Upit and S. A. Varchenya, phys. stat. sol., **17**, 831, 1966.
2. Z. Morlin, phys. stat. sol., **8**, K77, 1965.
3. R. Voszka, I. Tarján, L. Berkes and J. Krajsovszky, Kristall und Technik, **1**, 423, 1966

Acta Physica Academiae Scientiarum Hungaricae, Tomus 42 (4), pp. 289—294 (1977)

TORSIONAL OSCILLATIONS OF AN ELASTIC HALF SPACE DUE TO AN ANNULAR DISK

By

M. LATIF PASHA

DEPARTMENT OF PETROLEUM AND NATURAL GAS ENGINEERING, MINERAL INDUSTRIES BUILDING, PENNSYLVANIA STATE UNIVERSITY, UNIVERSITY PARK, PENNSYLVANIA 16802 USA

(Received 23. III. 1977)

The problem of low frequency torsional oscillations of an elastic half space due to a rigid annular disk is solved when the difference between the outer and the inner radii is small. Formulae are presented for the stress distribution, the far field amplitude, and the torque requi red to maintain the oscillations. At the end some related problems in slow viscous flow and MDH are solved.

1. Introduction

The problem of low frequency torsional oscillations of an isotropic, homogeneous elastic half space by a rigid circular disk has been a topic of considerable attention [1]—[6]. The corresponding problem of torsional oscillations by a rigid annular disk of outer and inner radii as a and b such that $b/a \ll 1$ has been considered by JAIN and KANWAL [7] using an integral equation technique. However, the corresponding problem of torsional oscillations of the elastic half space by an annular disk such that the difference between its radii is small in comparison with its either radius, has attracted no attention. Since this problem is of equal importance, it forms the topic of this note.

We begin with the integral equation formulation of this problem, which is then transformed into several Fredholm integral equations of the first kind with invertible kernels. The unknown charge density is approximately calculated as a polynomial of a small parameter. We present the expressions of some physical quantities like the far field amplitude.

Using the solution of the torsional oscillations problem, we consider an annular disk performing rotary oscillations in an infinite mass of viscous fluid which is at rest at infinity and also when an annular disk is rotating with uniform angular velocity about its axis in an incompressible viscous electrically conducting fluid in the presence of a uniform magnetic field applied parallel to its axis. As far as the author is aware even all the results derived in Stokes flow and MDH appear to be new.

2. Mathematical formulation and the solution

It is convenient to introduce cylindrical polar coordinates (ϱ, φ, z) with the elastic medium occupying $z \geqslant 0$ and the disk given by $z = 0$, $b < \varrho < a$, all φ, with a and b as the outer and the inner radii of the annulus, respectively. It is forced to oscillate with period $2\pi/\tilde{\omega}$ about its axis of symmetry thus the rest of the plane $z = 0$ is stress-free. Following [7], let V represent the only non vanishing φ component of the displacement, and let

$$v = Ve^{i\tilde{\omega}t} . \tag{1}$$

Then v satisfies the following boundary value problem:

$$(\nabla^2 + k^2)(v \cos \varphi) = 0, \ (\varrho, \varphi, z) \text{ not on the disk, } z \geq 0 \tag{2}$$

$$v = \varrho\Omega, \ z = 0, \ b < \varrho < a, \tag{3}$$

$$\partial v/\partial z = 0 \text{ on } z = 0 \text{ and } 0 \leqslant \varrho < b, \ a < \varrho < \infty. \tag{4}$$

Further v satisfies the radiation condition at infinity. Here

k^2 = $d\tilde{\omega}^2/\mu$,

d = density of the elastic material,

Ω = amplitude of the oscillation,

μ = shear modulus of the elastic material.

The integral equation formulation of the boundary value problem governed by Eqs. (2)—(4) is [7]

$$\varrho\Omega = \int_b^a t\sigma(t) \int_0^{2\pi} \frac{e^{-ikL(\varrho,t)}}{L(\varrho, t)} \cos \psi d\psi dt, \ b < \varrho < a , \tag{5}$$

with

$$\sigma(t) = -\frac{1}{2\pi} \frac{\partial v(t, z')}{\partial z'}\bigg|_{z'=0}, \ b < t < a , \tag{6}$$

and

$$L(\varrho, t) = (\varrho^2 + t^2 - 2\varrho t \cos \psi)^{1/2} . \tag{7}$$

To solve Eq. (5) for the unknown function $\sigma(t)$, we introduce two new variables α and β as [8]

$$\varrho = R(1 + \varepsilon \cos \alpha), \ t = R(1 + \varepsilon \cos \beta), \quad 0 < \alpha, \quad \beta < \pi , \tag{8}$$

with

$$R = (a + b)/2, \ \varepsilon = (a - b)/(a + b) . \tag{9}$$

Thus by assumption $\varepsilon \ll 1$. We further assume that $k = 0(\varepsilon)$. With these definitions, (5) can be transformed into

$$\Omega R(1 + \varepsilon \cos \alpha) = \int_0^{\pi} u(\beta) R \int_0^{2\pi} \frac{e^{-ikL}}{L} \cos \psi d\psi d\beta \,, \tag{10}$$

with

$$u(\beta) = \sigma(\beta) R\varepsilon \sin \beta(1 + \varepsilon \cos \beta) \,. \tag{11}$$

We first approximate the kernel of the Eq. (10) by neglecting the terms of $0(k^3)$ and more and expand the kernel in powers of ε as [8]

$$R\int_0^{2\pi} \frac{e^{-ikL}}{L} \cos \psi d\psi = \left(K_0 + \frac{4}{3} R^2 k^2\right) + \varepsilon K_1 + \varepsilon^2 K_2 + 0(\varepsilon^3) \,, \tag{12}$$

with

$$K_0 = 2S - 2 \ln 2 \mid \cos \alpha - \cos \beta \mid \,,$$

$$K_1 = -(\cos \alpha + \cos \beta)(K_0 - 2)/2 \,,$$

$$K_2 = K_0[9(\cos^2 \alpha + \cos^2 \beta) - 2 \cos \alpha \cos \beta]/16 - 3[(\cos^2 \alpha + \cos^2 \beta) + 6 \cos \alpha \cos \beta]/8$$

and

$$S = \ln (16/\varepsilon) - 2 \,.$$

We expand $u(\beta)$ in powers of ε as

$$u(\beta) = u_0(\beta) + \varepsilon u_1(\beta) + \varepsilon^2 u_2(\beta) + 0(\varepsilon^3) \,. \tag{13}$$

Substituting the expansions of the kernel in (12) and of $u(\beta)$ in (31), in Eq. (10) and by equating the coefficients of equal powers of ε, we get a set of integral equations involving $u_i(\beta)$. These integral equations can be solved by expanding the functions $u_i(\beta)$ in their Fourier series. Thus we find

$$u(\beta) = b_{0,0} + \varepsilon b_{1,1} \cos \beta + \varepsilon^2 (b_{2,0} + b_{2,2} \cos 2\beta) + 0(\varepsilon^3) \,, \tag{14}$$

with

$$b_{0,0} = \Omega R/[2\pi(S + 4R^2 k^2/3)] \,, \tag{15}$$

$$b_{1,1} = 3\Omega R/4\pi \,, \tag{16}$$

$$b_{2,0} = \Omega R(12S^2 - 9S + 8)/64\pi S^2 \,, \tag{17}$$

and

$$b_{2,2} = \Omega R(18S + 1)/64\pi S \,. \tag{18}$$

In view of Eqs. (14)—(18), and (11) we have determined the approximate value of $\sigma(t)$.

3. Expressions for shear stress, torque and the far field amplitude

The non vanishing components of stress tensor are given by

$$\tau_{\varrho\varphi} = \mu\left(\frac{\partial V}{\partial \varrho} - \frac{V}{\varrho}\right), \quad \tau_{z\varphi} = \mu\frac{\partial V}{\partial z}, \tag{19}$$

so that the shear stress τ is given by

$$\tau = -2\pi\mu\sigma(\varrho)e^{-i\tilde{\omega}t}. \tag{20}$$

Thus its explicit form can be obtained as

$$\begin{aligned}\tau(\beta) = &-2\pi\mu[b_{0,0} + \varepsilon b_{1,1}\cos\beta + \varepsilon^2(b_{2,0} + b_{2,2}\cos 2\beta)] \times \\ &\times [R\varepsilon\sin\beta(1 + \varepsilon\cos\beta)]^{-1}\exp(i\tilde{\omega}t), \quad 0 < \beta < \pi.\end{aligned} \tag{21}$$

When we convert β into t, we find that

$$\sigma(t), \tau(t) = 0(a^2 - t^2)^{-1/2}, \text{ as } t \to a -,$$

and

$$\sigma(t), \tau(t) = 0(t^2 - b^2)^{-1/2} \text{ as } t \to b+,$$

so that σ and τ satisfy the edge conditions.

The value of the torque M needed to maintain the torsional oscillations of the annular disk is

$$M = (2\pi)^2\int_b^a \varrho^2\sigma(\varrho)d\varrho = -4\pi^3R^2\mu[b_{0,0} + \varepsilon^2(b_{2,0} + b_{1,1}/2)]e^{i\tilde{\omega}t} + 0(\varepsilon^3). \tag{22}$$

To find the far field amplitude, we introduce the spherical polar coordinates (r, Θ, φ), with

$$\varrho = r\sin\Theta, \quad z = r\cos\Theta, \tag{23}$$

and we find that [7]

$$v(\varrho, z) = A(\Theta)\exp(-ikr)/r + 0(r^{-2}), \tag{24}$$

with

$$A(\Theta) = i\int_b^a 2\pi t\sigma(t)J_1(kt\sin\Theta)dt. \tag{25}$$

Thus v does satisfy the radiation condition at infinity and the far field amplitude $A(\Theta)$ is given by

$$A(\Theta) = i\pi^3R^2b_{0,0}k\sin\Theta + 0(\varepsilon^3). \tag{26}$$

4. Stokes flow

Let an annular disk be performing torsional oscillations with angular velocity $\Omega e^{i\tilde{\omega}t}$ about its axis of symmetry, the z-axis; in an unbounded viscous fluid which is at rest at infinity. If $ve^{i\tilde{\omega}t}$ is the φ velocity component, it satisfies boundary value problem (2)—(4) with

$$k^2 = -i\tilde{\omega}/\nu\,. \tag{27}$$

Thus in this problem v can be obtained from the previous sections simply by substituting [7]

$$k = \exp(-\pi i/4)R_1^{1/2}/a\,, \tag{28}$$

where

$$R_1 = \tilde{\omega}a^2/\nu \tag{29}$$

is the Reynolds number

Thus the torque T_1 required to maintain the oscillations of the annular disk is

$$T_1 = -8\pi^3 R^2\mu[b_{0,0} + \varepsilon^2(b_{2,0} + b_{1,1}/2)]\exp(i\tilde{\omega}t)\,, \tag{30}$$

where now

$$b_{0,0} = R/[2\pi(S - 4R^2R_1/3a^2)]\,, \tag{31}$$

and $b_{2,0}$ and $b_{1,1}$ are given by (17) and (16).

5. Steady rotation in a conducting fluid

Let the annular disk be rotating about its axis of symmetry with angular velocity Ω in an incompressible viscous and electrically conducting fluid under the influence of a uniform magnetic field B_0 applied parallel to z-axis. If v denotes the only non zero φ component of velocity, and if we write $2v = v_{-1} + v_1$; v_s $(s = +1)$ satisfy the equation

$$\nabla^2(v_s\cos\varphi) + sK\frac{\partial v_s}{\partial z}\cos\varphi = 0\,, \tag{32}$$

where

$$Ka = (\sigma\mu_e)^{1/2}B_0a$$

is the Hartmann number and is assumed to be small, σ and μ_e are respectively the conductivity and the magnetic permeability of the fluid. Further v_s satisfy the boundary condition (2). This problem can be converted to the boundary value problem (2)—(4), if we put

$$v_s = \exp(-sKz/2)v_s'(\varrho, z),\ k^2 = -(K/2)^2\,, \tag{33}$$

and drop the primes [7] and thus v can be determined.

The value of the torque T_2 required to maintain the steady rotation is

$$T_2 = -8\pi^3 R^2 \mu [b_{0,0} + \varepsilon^2 (b_{2,0} + b_{1,1}/2)] , \tag{34}$$

where now

$$b_{0,0} = \Omega R/[2\pi(S - R^2K^2/3)] , \tag{35}$$

and $b_{2,0}$ and $b_{1,1}$ are given as before.

It must be observed that when we take $\tilde{\omega} = 0$ in the previous Sections, we get the corresponding results when the rigid disk is rotating with a constant angular velocity Ω. As far as the author is aware, even all the limiting results thus obtained appear to be new.

Acknowledgements

The author is very grateful to Prof. S. M. Farouq Ali for his kind encouragements throughout the preparation of this note.

REFERENCES

1. E. Reissner and H. F. Sagoci, J. Appl. Phys., **15,** 652, 1944.
2. IA. S. Ufliand, Prikl. Mat. Mekh., **25,** 228, 1961.
3. W. D. Collins, Proc. Lond. Math. Soc., (III) **12,** 226, 1962.
4. A. O. Awojobi and P. Grootehnuis, Proc. R. Soc., **28,** 27 1965.
5. I. A. Robertson, Appl. Sci. Res., **17,** 305, 1967.
6. D. P. Thomas, Int. J. Engg. Sci., **6,** 565, 1968.
7. D. L. Jain and R. P. Kanwal, Int. J. Engg. Sci., **8,** 687, 1970.
8. M. L. Pasha, Jour. Phys. Soc. Japan, **37,** 518, 1974.

Acta Physica Academiae Scientiarum Hungaricae, Tomus 42 (4), pp. 295—317 (1977)

INTERMOLECULAR FORCES AND EQUATION OF STATE FOR SOLID MOLECULAR IN PSEUDOHARMONIC APPROXIMATION

By

C. MALINOWSKA-ADAMSKA

INSTITUTE OF PHYSICS, TECHNICAL UNIVERSITY OF ŁÓDZ, ŁÓDZ, POLAND*

(Received 31. III. 1977)

An analytical and numerical expression for intermolecular potentials appropriate for solid molecular are given in harmonic and pseudoharmonic approximations.

The given potentials are used to compute the internal energy, the specific heat and the coefficient of the linear thermal expansion for atoms crystallize in a face centred cubic lattice and in a body-centred cubic lattice.

I. Introduction

Any adequate theory of chemical binding should allow the derivation of a potential energy function describing the internuclear law of force. In general, it should be possible to obtain such functions from the first principles of quantum theory. However, except for the simplest systems [1—6], these methods have not yielded satisfactory potential energy functions. The reason for this stems from the difficulty in handling polyelectronic problems in quantum theory. Solutions of the differential equations involved are not obtainable in closed form and in order to make the problem tractable, it is necessary to make simplifying assumptions [7, 8] and to use approximate methods. To date these assumptions and approximations have had the effect of removing from quantum theory the possibility of predicting potential energy functions which would quantitatively describe the internuclear law of force and correlate a number of bond properties such as force constant, dissociation energy, bond length, anharmonicity constant etc. Many semi-empirical quantum-mechanical calculations of electronic energies of molecules have been given [9—16]. In general such calculations have been limited to the equilibrium configuration of the molecule or to a limited range of points in the neighbourhood of this point. Because of these difficulties many investigators have proposed empirical potential energy functions. The MORSE function [17] has been the most useful of these, partly because of its simplicity and partly because solutions of the anharmonic oscillator problem are readily obtained when this function is used for the potential energy solving the

* Address: Institute of Physics, Technical University of Łódz, ul. Wólczanska 219, 93-005 Łódz, Poland

Schrödinger wave equation. However, the MORSE function only approximately represents the actual potential energy curve as determined from experimental data for most diatomic molecules. At the expense of simplicity several modified MORSE functions have been proposed [18—21]. Other proposed functions are those of KRATZER [22], RYDBERG [23], MANNING and ROSEN [24], PÖSCHL and TELLER [25], HYLLERAAS [26], LINNET [27], SUTHERLAND [28], FROST [29], LIPPINCOTT [30, 31], VARSHNI [32, 33], WOJTCZAK [34] and TIETZ [7, 8, 35].

In determining the parameters of potential energy function $U(r)$, use is commonly made of the following experimental data: the second virial coefficients, the Joule—Thompson coefficient, the coefficients of viscosity, and properties of crystals [36]. The second virial coefficient is a property for which accurate experimental data are readily available [37]. It is also a property which is easy to calculate theoretically [38—41]. Consequently: the second virial coefficient (and often solely the second virial coefficient) has become the property most used to determine the adjustable parameters of a potential function. It is clear that other properties in addition to the second virial coefficient must be used if the parameters of any potential function are to be physically significant "by themselves" [42, 43].

CORNER [44] has shown how the determination of potential parameters may be improved by the use of crystal data in addition to gas properties data and used this method to determine the potentials of Ne and Ar. This approach was applied by MASON and RICE [45] who used viscosity data as well as crystal and second virial coefficient data to calculate the parameters of the (exp-6) potential. BUCKINGHAM [46] has used both crystal and second virial coefficient data for N_2 and CO_2 to determine the parameters of the (12—6) potential (modified to include the effects of quadrupole-quadrupole interaction), and BARUA [47] has used similar data for Kr and Xe to specify the parameters of the BUCKINGHAM—CORNER (exp-6-8) potential. More recently, KONOWALOW and HIRSCHFELDER [38] have used CORNER's method to determine the MORSE potential parameters for Ne, Ar, Kr, Xe, CH_4 and N_2.

In this paper we use CORNER's method to help to determine the potential parameters appropriate for solid molecular.

II. The determination of potential parameters from properties of crystals at absolute zero

There are three properties [48] of a crystal which can be used in the determination of the intermolecular forces: 1. d_0, the distance between nearest neighbours in the crystal lattice at 0 °K; 2. Θ_D, the energy of sublimation of the crystal at 0 °K; 3. Θ_D, the Debye characteristic temperature determined

at low temperature. In addition the type of crystal lattice sometimes provides a sensitive criterion of the shape of the potential energy function [36].

The total energy of the crystal lattice at absolute zero U_0 is the sum of the potential energy of the lattice Φ_0;and the zero-point energy K_0 associated with the zero point vibrations of the molecules in the lattice:

$$U_0 = \Phi_0 + K_0 \,. \tag{1}$$

If the forces between the molecules in a crystal lattice are pairwise additive, Φ_0 is given by

$$\Phi_0 = \frac{1}{2} N \sum_i n_i \cdot U(d_i) \,, \tag{2}$$

where N is the number of molecules in the lattice, d_i is the distance between a lattice point and i-th shell of lattice points surrounding it, n_i is the number of lattice points in the i-th shell, and $U(d_i)$ is the pair potential function.

The zero-point energy is given approximately in terms of the Debye characteristic temperature Θ_D by

$$K_0 = \frac{9}{8} N k_B \Theta_D \,, \tag{3}$$

where k_B is the Boltzmann constant.

The Debye temperature can be calculated in terms of the increase in potential energy (averaged over all orientations) when one molecule is displaced from its lattice position and the remainder of the molecules are held fixed in their lattice positions. For small vibrations, the square of the fundamental frequency ν^2 is

$$\nu^2 = \frac{1}{12\pi^2 m_a} \sum_i n_i \left[\left(\frac{1}{d_i} \right) U'(d_i) + \frac{1}{2} U''(d_i) \right], \tag{4}$$

where m_a is the mass of the molecule under consideration and the primes indicate differentiation with respect to d_i. If we assume the Debye distribution of frequencies, then the Debye (or maximum) frequency is given by

$$\nu_D = \sqrt{\frac{5}{3}}\, \nu \,. \tag{5}$$

Thus the Debye characteristic temperature is given by

$$\Theta_D = \frac{h \cdot \nu_D}{k_B} \,, \tag{6}$$

where h is Planck's constant. The zero-point energy is then obtained when Eq. (6) is substituted into Eq. (3). The equilibrium separation at absolute zero is found by minimizing the total crystal energy,

$$\frac{dU_0}{d(d_0)} = \frac{d}{d(d_0)}(\Phi_0 + K_0) = 0\,. \tag{7}$$

Since real substances do not have the Debye distribution of frequencies, Eq. (5) is only approximately true. For some molecules considerable error in U_0 may result from neglecting the effects of non-additivity of the intermolecular forces also [49]. However, KIRHARA [50] finds, from comparing the second virial coefficient with crystal data that for Ne, Ar and Kr the corrections for non-additivity are small. It is likely that the uncertainty in our results due to neglecting non-additive effects is no greater than the uncertainty due to the experimental crystal data we have used [51, 52].

The combination of Eqs. (3) to (7) allows to determine 2 parameters of potential function. However, most of the potential energy curves for diatomic molecules contain three, four or more parameters [6—8, 17—35] so that we get them in the following way:

a) From experimental data for U_0, Θ_D and d_0 we determine optimal parameters for the LENNARD-JONES potential ($U_{L\text{-}J}$) widely used to describe the properties of the solid state [53].

b) Then we determine the parameters for any function $U(d_i)$ from equations:

$$U(d_0) = \Phi_0\,, \tag{8a}$$

$$U'(d_0) = 0\,, \tag{8b}$$

$$U''(d_0) = U''_{L-J}(d_0)\,, \tag{8c}$$

$$U^{\mathrm{III}}(d_0) = U^{\mathrm{III}}_{L-J}(d_0)\,, \tag{8d}$$

$$U^{\mathrm{IV}}(d_0) = U^{\mathrm{IV}}_{L-J}(d_0)\,. \tag{8e}$$

For the LENNARD-JONES (t, s) intermolecular potential function $[U(r) = br^{-s} - cr^{-t}]$, the potential energy of the crystal at absolute zero can be expressed in the form [36]:

$$\Phi_0 = U_0 - \frac{9}{8}k_B\Theta_D = \frac{1}{2}\left(\frac{bC_s}{d_0^s} - \frac{cC_t}{d_0^t}\right). \tag{9}$$

From Eqs. (4)—(6) we get directly:

$$\Theta_D^2 = \frac{5}{72}\frac{h^2}{k_B^2\pi^2 m_a}\left[\frac{b(s-1)sC_{s+2}}{d_0^{s+2}} - \frac{c(t-1)tC_{t+2}}{d_0^{t+2}}\right] \tag{10}$$

so that the parameters b and c are given by:

$$b = \frac{d_0^s \left[\frac{\Theta_D^2}{B} C_t d_0^2 - A C_{t+2} t(t-1) \right]}{C_t C_{s+2} s(s-1) - C_s C_{t+2} t(t-1)}, \tag{11}$$

$$c = \frac{d_0^t \left[\frac{\Theta_D^2}{B} C_s d_0^2 - A C_{s+2} s(s-1) \right]}{C_t C_{s+2} s(s-1) - C_s C_{t+2} t(t-1)}, \tag{12}$$

where

$$A = 2U_0 - \frac{9}{4} k_B \Theta_D ,$$

$$B = \frac{5h^2}{72 k_B^2 \pi^2 m_a} . \tag{13}$$

U_0, Θ_D and d_0 are experimental quantities, the constants $C_s = C_{t+6}$ and C_t are given in Table I for two crystal types [36]: a face-centred cubic and a body-centred cubic. For example, the rare gas atoms and the atoms Ag crystallize in a face-centred cubic lattice. The atoms: Cs, Li, K, Rb, Na crystallize in a body-centred cubic lattice.

Table I

The constants for the potential energy of a crystal

t	C_t	
	Face-centred cubic	Body-centred cubic
4	25.33830	22.63872
5	16.9675	14.7585
6	14.45392	12.2533
7	13.35939	11.05424
8	12.80194	10.3550
9	12.49255	9.8945
10	12.31125	9.5640
11	12.2009	9.31326
12	12.13188	9.11418
13	12.08772	8.95180
14	12.05899	8.81670
15	12.04002	8.70298
16	12.02736	8.60625

By applying the method discussed above [Eqs. (8a)—(8e)] we get (Table II) in the following an analytical expression for the parameters of the potential energy functions suggested by different authors [6—8, 17—35].

Table II

An analytical expression for the parameters of the intermolecular potentials appropriate for solid molecular

Position	Potential function	Parameters	Literature
1	LENNARD-JONES $U(r) = 4\varepsilon\left[\left(\frac{\delta}{r}\right)^{12} - \left(\frac{\delta}{r}\right)^{6}\right]$	$\varepsilon = \frac{C(C_{12} - 132\,C_0C_{14})^2}{24(C_6 - 30\,C_0C_8)(22\,C_6C_{14} - 5\,C_8C_{12})}$ $\delta = d_0\left(\frac{C_6 - 30\,C_0C_8}{C_{12} - 132\,C_0C_{14}}\right)^{1/6}$	[36, 53, 58]
2	MECKE—SUTHERLAND $U(r) = \frac{a}{r^m} - \frac{b}{r^n}$	$a = Cd_0^m G_{nm}^{-1}[C_n - n(n-1)C_0C_{n+2}]$ $b = Cd_0^n G_{nm}^{-1}[C_m - m(m-1)C_0C_{m-2}]$	[28, 54—56]
3	RYDBERG $U(r) = -D_e[1 + b(r - r_e)] \cdot \exp[-b(r - r_e)]$	$b = \sqrt{\frac{F - M}{Dd_0^2 - E}}$ $D_e = \frac{Dd_0^2 - E}{G_{ts}}$ $r = d_0\left\{\frac{s[C_t d_0^2 - t(t-1)C_0C_{t+2}]}{t[C_s d_0^2 - s(s-1)C_0C_{s+2}]}\right\}^{1/6}$	[23]
4	MORSE $U(r) = D_e[1 - e^{-a(r-r_e)}]^2$	$a = \sqrt{\frac{F - M}{2(Dd_0^2 - E)}}$	[17]
5	LIPPINCOTT $U(r) = D_e\left[1 - e^{\frac{n(r-r_e)^2}{2r}}\right]^2$	$n = \frac{F - M}{(D - Ed_0^{-2})d_0}$	[30, 31]

6	I VARSHNI $U(r) = D_e[1 - e^{-b(r^2-r_e^2)}]^2$	$\frac{1}{b} = \sqrt{\frac{8d_0^2(Dd_9^2 - E)}{F - M}}$	[32, 33]
7	II VARSHNI $U(r) = D_e\left[1 - \frac{r_e}{r} e^{-\alpha(r-r_e)}\right]^2$	$\frac{1}{\alpha} = \sqrt{\frac{2(Dd_0^2 - E)}{F - M}}$	[33]
8	III VARSHNI $U(r) = D_e\left[1 - \frac{r_e}{r} e^{-\beta(r^2-r_e^2)}\right]^2$	$\beta = \frac{1}{2d_0^2}\left[\sqrt{\frac{F - M}{2(D - Ed_0^{-2})}} - 1\right]$	[33]
9	IV VARSHNI $U(r) = B_1(A_1 + e^{b/r})^2$	$b = d_0(H - 1)$ $A_1 = \exp(H - 1)$ $B_1 = \frac{Dd_0^2 - E}{(A_1 - 1)^2 G_{ts}}$	[33]
10	V VARSHNI $U(r) = D_e\left[1 - \left(\frac{r_e}{r}\right)^n\right]^2$	$n = \sqrt{\frac{F - M}{2(D - Ed_0^{-2})}}$	[33]
11	VI VARSHNI $U(r) = D_e\left[1 - \frac{r}{r_e} e^{-a(r-r_e)}\right]^2$	$a = \frac{1}{d_0}\left[\sqrt{\frac{F - M}{2(D - Ed_0^{-2})}} + 1\right]$	[33]

Table II (continued)

Position	Potential function	Parameters	Literature
12	VII VARSHNI $U(r) = -A_1 r^n e^{-ar}$	$n = \frac{(F-M)d_0^2}{Dd_0^2 - E}$ $a = nd_0^{-1}$ $A_1 = D_e d_0^{-n} - \exp\left[\frac{(F-M)\,d_0^2}{Dd_0^2 - E}\right]$; $D_e = \frac{Dd_0^2 - E}{G_{ls}}$	[33]
13	I TIETZ $U(r) = D_e\left[1 + \frac{(a+b)e^{-2\beta r} - be^{-\beta r}}{(1+ce^{-\beta r})^2}\right]$	$\beta = (2\Delta^{1/2} - \Gamma^{1/2})r_e^{-1}$ $c = \exp[(\beta r_e)/\Delta^{1/2}](\Gamma^{1/2} - \Delta^{1/2})$ $b = 2\left\{\exp(\beta r_e)\left[2 - \left(\frac{\Gamma}{\Delta}\right)^{1/2}\right]\right\}$ $a = -2b\left[2 - \left(\frac{\Gamma}{\Delta}\right)^{1/2}\right]\exp(\beta r_e)$ $r_e = d_0\left\{\frac{s[C_t d_0^2 - t(t-1)C_0 C_{t+2}]}{t[C_s d_0^2 - s(s-1)C_0 C_{s+2}]}\right\}^{1/6}$	[7]
14	II TIETZ $U(r) = D_e \frac{\left(1 - \frac{r}{r_e}\right)^2}{\left(1 + \frac{r}{r_e}\right)^2}\left[1 + \frac{A_1 r_e}{r} + \frac{B_1 r_e^2}{r^2}\right]$	$A_1 = 12\Delta - 4\Delta(\Gamma)^{1/2} - 2$ $B_1 = 1 - 8\Delta + 4\Delta(\Gamma)^{1/2}$	[8]
15	III TIETZ $U(r) = D_e\left[\frac{1 - \frac{r_e}{r}}{1 + a\left(\frac{r}{r_e}\right)}\right]^2\left\{ba^2 + \left[\Delta(1+a)^2 + -a^2(1+b)\right]\left(\frac{r}{r_e}\right)^{\cdot} + \left(a\frac{r}{r_e}\right)^2\right\}$	$a = \frac{[(\Gamma^{1/2} - 3)\Delta}{\Gamma_0} +$ $+ \frac{\{\Delta^2(\Gamma^{1/2} - 3)^2 + \Gamma_0[1 + \Delta(\Gamma^{1/2} - 2)]\}^{1/2}}{\Gamma_0}$ $b = \Delta(\Gamma^{1/2} - 2)\left(\frac{1}{a} + 1\right)^2 + 1 + \Delta\left(\frac{1}{a^2} - 1\right)$	[35]

The symbols used in Table II have the following meaning:

$$C = \Theta_D^2 B^{-1} d_0^2;\ C_0 = d_0^2 A C^{-1};\ D = C d_0^{-2}(C_s - C_t);$$

$$E = A[s(s-1)C_{s+2} - t(t-1)C_{t+2}];$$

$$F = C d_0^{-2}[s(s+1)C_t - t(t+1)C_s];$$

$$M = -A d_0^{-2} s \cdot t[(t-1)(s+1)C_{t+2} - (s-1)(t+1)C_{s+2}];$$

$$G_{ts} = C_t C_{s+2} s(s-1) - C_s C_{t+2} t(t-1);$$

$$H = \frac{C[s(s^2-1)C_t - t(t^2-1)C_s] - As(s-1)t(t-1)[(s+1)C_{t+2} - (t+2)C_{2s+2}]}{3d_0^2(F-M)};$$

$$\Delta = \frac{F-M}{2(D - E d_0^{-2})};\qquad \Gamma^{1/2} = \frac{P-Q}{3d_0^2(F - M d_0^2)};$$

$$\Gamma_0 = \Delta(4 - \Gamma^{1/2}) - 2;$$

$$P = C[s(s+1)(s+2)C_t - t(t+1)(t+2)C_s];$$

$$Q = A.s.t\,[(t-1)(s+1)(s+2)C_{t+2} - (s-1)(t+1)(t+2)C_{s+2}].$$

III. Numerical results for the parameters of the intermolecular potentials

A summary of the results of optimal parameters for intermolecular potentials appropriate for some solid molecular is given in Tables III—VII. In Table VIII we have compared our results with others given in literature [38, 45, 47, 58—62]. From this Table we can see that the results of this paper show good agreement with the MORSE potential parameters determined from the combination of crystal and the transport properties data [38, 59—62]. For comparison the parameters for the LENNARD-JONES (12—6) potential, which have been determined from crystal data [35, 48, 58], are also included in Table VIII.

The comparison of the numerical values of the parameters for the RYDBERG, LIPPINCOTT, VARSHNI and the TIETZ potential models allows us to state that for Ne, Ar, Kr, Xe the three-parametrical functions by RYDBERG, LIPPINCOTT and the I, II, III VARSHNI's functions (Tables IV, V) give nearly the result calculated for the MORSE and for the BUCKINGHAM exp-six potential. (At least, MEISEL and COX [58] found, from analysis of the equation-of-state measurements, that the BUCKINGHAM exp-six potential seems to be most appropriate for solid Ne and Ar). On the contrary, the parameters IV and VI for the VARSHNI's function (Table VI) are comparable with calculation using the TIETZ potentials (Table VII).

The potential constants determined from crystal structure data allow to get the self-consistent potential and to compute solid-phase thermodynamic functions.

IV. Self-consistent potential in pseudoharmonic approximation

The self-consistent potential $\tilde{\Phi}$ (1) in pseudoharmonic approximation can be written as [63]:

$$\tilde{\Phi}(1) = \sum_{s=0}^{\infty} \frac{1}{s!} \left(\frac{\overline{u^2}}{2} \right)^s U^{2s}(1) , \tag{14}$$

where: U (1) is the intermolecular potential,

$$U^{2s}(1) = \frac{d^{2s}(U)}{dl^{2s}} , \quad \overline{u^2} = \frac{1}{Nf} \sum_k \frac{\omega_{0k}}{2\omega_k} \coth \frac{\hbar\omega_k}{2\Theta} , \tag{15}$$

N is the number of molecules in the lattice,

$$\omega_k^2 = \frac{f(\Theta, l_e)}{f} \omega_{0k}^2 , \tag{16}$$

Table III

Summary of parameters for the LENNARD-JONES (t, s) potential function

Substance	Θ_D [°K]	$U_0 \cdot 10^{-21}\left[\frac{\text{J}}{\text{molec}}\right]$	d_0 [nm]	t	$\frac{b}{d_0^s} \cdot 10^{-21}$[J]	$\frac{c}{d_0^t} \cdot 10^{-21}$[J]
1	2	3	4	5	6	7
Ne	64	3.1155	0.320	4	4.28945	2.08900
				5	3.80835	2.73845
				6	3.41265	2.86440
				7	3.08660	2.76280
				8	2.81365	2.65050
Ar	80	12.8655	0.383	4	3.80923	0.85108
				5	3.37413	1.42625
				6	3.12314	1.53779
				7	2.73430	1.47440
				8	2.49302	1.34833
Kr	63	18.6237	0.395	4	5.27100	1.06104
				5	4.66893	1.85731
				6	4.18381	2.01166
				7	3.78412	1.92393
				8	3.44970	1.74949
Xe	55	26.2735	0.434	4	7.60061	1.57293
				5	6.73245	2.72113
				6	6.03291	2.94369
				7	5.45658	2.81720
				8	4.97436	2.56566
Ag	225	47.9643	0.288	4	91.37145	40.63484
				5	80.18832	52.04313
				6	71.04469	53.04068
				7	59.40514	50.24125
				8	55.94183	46.15109
Cs	39.5	132.4854	0.524	4	7.68800	3.24800
				5	6.89600	4.35200
				6	6.24900	4.64800
				7	5.70800	4.62200
				8	5.25000	4.47000
Li	335.0	264.3300	0.303	4	9.65100	4.07700
				5	8.95700	5.46300
				6	7.84500	5.83500
				7	7.16600	5.80300
				8	6.59000	5.61100
K	91.1	150.7482	0.462	4	9.35300	3.95100
				5	8.39000	5.29500
				6	7.60300	5.65500
				7	6.94500	5.62400
				8	6.38700	5.43800
Rb	55.5	137.2914	0.487	4	8.43000	3.56100
				5	7.56200	4.77200
				6	6.85200	5.09700
				7	6.25900	5.06900
				8	5.75600	4.90100
Na	156.0	181.0260	0.371	4	10.39600	4.39200
				5	9.32500	5.88400
				6	8.45000	6.28500
				7	7.71800	6.25000
				8	7.09800	6.04400

Table IV

Summary of parameters for the RYDBERG potential (pos. 3) and the MORSE function (pos. 4 Table II)

Substance	$D_e \cdot 10^{-23}$[J]	r_e [nm]	$b\left[\frac{1}{\text{nm}}\right]$	$a\left[\frac{1}{\text{nm}}\right]$
Ne	54.825	0.31988	25.73647	18.25353
Ar	158.535	0.39483	19.97236	14.16480
Kr	207.215	0.40720	17.18508	12.18802
Xe	308.922	0.44740	17.13890	12.15525
Ag	5457.419	0.33290	139.29676	98.4976
Cs	160.100	0.59741	23.74597	16.79094
Li	201.000	0.34545	13.73135	9.70953
K	194.800	0.52672	20.09371	14.80479
Rb	175.500	0.55523	23.06561	15.60338
Na	216.500	0.42297	16.81290	11,88852

Table V

Summary of parameters for the LIPPINCOTT function (pos. 5) and the VARSHNI functions (pos. 6, 7, 8 Table II)

Substance	Calculated quantities					
	$D_e \cdot 10^{-23}$[J]	r_e [nm]	$n\left[\frac{1}{\text{nm}}\right]$	$b\left[\frac{1}{\text{nm}^2}\right]$	$\alpha\left[\frac{1}{\text{nm}}\right]$	$\beta\left[\frac{1}{\text{nm}}\right]$
Ne	54.825	0.31988	24.21312	18.36360	20.83843	22.38050
Ar	158.535	0.39483	19.10652	12.81920	17.41063	15.62300
Kr	207.215	0.40720	18.61543	12.05240	16.88177	14.68850
He	308.922	0.44740	13.69392	10.98320	15.36470	12.16700
Ag	5457.419	0.33290	55.88231	44.30659	80.23493	165.48574
Cs	160.100	0.59741	10.59487	8.23052	13.05965	12.11135
Li	201.000	0.34545	18.32147	18.59650	22.53938	18.07300
K	194.800	0.52672	12.01579	11.80150	14.81227	13.55802
Rb	175.500	0.55523	11.40358	10.21350	14.05189	14.02150
Na	216.500	0.42297	14.96347	12.42850	18.44552	16.16042

ω_{0k} is the harmonic frequency of vibration,

$$f(\Theta, l_e) = \frac{1}{2} [\tilde{\Phi}''(l)]_{l=l_e} \tag{17}$$

is the renormalization of the strength constant, f is the harmonic strength

Table VI

Summary of optimal parameters for the VARSHNI functions (pos. 9, 10 and 11 Table II)

Substance	Calculated quantities				
	b [nm]	$\ln A_1$	$B_1 \cdot 10^{-23}$ [J]	n	$a\left[\frac{1}{\text{nm}}\right]$
Ne	0.24023	0.75103	0.03800	0.08660	3.99689
Ar	0.48313	1.22365	0.18000	1.10453	5.33022
Kr	0.53750	1.29544	0.23600	1.13578	5.24503
Xe	0.56057	1.25296	0.13900	1.11803	4.73408
Ag	—	—	—	2.83676	10.22642
Cs	1.89063	3.16471	1.20100	1.77763	4.64945
Li	1.09319	3.16454	1.50800	1.77763	8.04061
K	1.66675	3.16441	1.46100	1.77763	5.27344
Rb	1.75774	3.16579	1.31600	1.78044	5.00772
Na	1.38847	3.16447	1.62400	1.77763	6.56696

Table VII

Summary of parameters for the TIETZ potential models (pos. 13, 14 and 15 Table II)

Substance	Calculated quantities							
	βr_e	c	b	a	A_1	B_1	a	b
Ne	5.07737	0.27447	−0.73639	1.94556	−9.23902	10.76510	−2.59560	6.02570
Ar	3.04151	0.17942	−0.26325	1.05300	−13.01563	16.91023		
Kr	2.97901	0.18418	−0.26669	1.06677	−13.66191	17.84367		
Xe	3.01451	0.18218	−0.26579	1.06318	−14.27947	17.29133		
Cs	1.61221	0.38039	−0.36183	1.44732	−29.43765	41.09649	−2.7076	5.0122
Li	1.61221	0.38039	−0.36183	1.44732	−29.46618	41.09434		
K	1.61221	0.38039	−0.36183	1.44732	−12.43505	41.09269		
Rb	1.60658	0.38176	−0.36216	1.44864	−29.44501	41.11017		
Na	1.61221	0.38039	−0.36183	1.44732	−29.43557	41.09345		

constant, $\Theta = k_B T$; k_B is Boltzmann's constant, T is the temperature in degrees Kelvin.

As a model potential $U(1)$ in Eq. (14) we take the RYDBERG potential (Table II). This function, for example, used to describe the properties of C_2 system [64] gave better results than the MORSE [17] or HULBURT—HIRSCHFELDER function [19]. The MORSE potential has been used to determine the

Table VIII

Potential parameters for some solid molecules

Substance	MORSE parameters				LENNARD-JONES (12—6) parameters		
	Source	a^*	r_e[nm]	$D_e \cdot 10^{-23}$ [J]	Source	δ [nm]	$\varepsilon\ 10^{-23}$ [J]
Ne	[38.44]	18.3783	0.3152	60.7281	[38. 45, 58]	0.316	50.1121
	our	18.2535	0.31988	54.8250	our	0.3172	52.4406
Ar	[38, 44] [59, 62]	14.7666	0.3855	199.8964	[38, 45]	0.387	164.6936
	our	14.1648	0.3948	158.5350	our	0.3911	169.2965
Kr	[38, 59]	12.8205	0.4038	252.2173	[38, 45]	0.4040	219.9136
	our	12.1880	0.4072	207.2150			
Xe	[38, 59]	12.6549	0.4420	379.2233	[38, 45]	0.446	314.7540
	our	12.1552	0.4474	308.9220	our	0.4435	315.5908

* In reference [38], different notation was used for the MORSE parameters $\varepsilon = D_e$, $c/\delta = a$, and $r_m = r_e$.

properties of the anharmonic linear chain in the pseudoharmonic approximation and in the dynamic theory of the anharmonic lattice [63, 67].

Applying the expansion of Eq. (14) we get the following expression for the self-consistent potential

$$
\begin{aligned}
\tilde{\Phi}(1) = R_1 \Bigg\{ & C_r \left(l^2 + \frac{2l}{b} + \frac{2}{b^2} \right) - B_r \left(1 + \frac{1}{b} \right) + \\
& + (1 + a^2 b^2) \left[2 C_r a \left(l + \frac{1}{b} \right) - \frac{B_r}{b} \right] + C_r a^2 (3 + a^2 b^2) \Bigg\} + \\
& - \frac{\exp\left(- \dfrac{l^2}{2a^2} \right)}{\sqrt{2\pi}\, l} \Bigg\{ 2 C_r l a \left(1 + \frac{l}{a^2 b} \right) - a B_r \left(1 - \frac{l}{a} - \frac{l}{a^2 b} \right) + \\
& - \exp(-2bl) \left[\frac{C_r l^2}{ab} (1 + ab) - 2 C_r a l + B_r a \left(1 + \frac{l}{a^2 b} \right) \right] \Bigg\} + \\
& - R_2 \left[C_r l a \left(1 - 2ab + a^2 b^2 + \frac{l}{a} \right) - B_r (l - a^2 b) \right] + \\
& + R_3 \left[C_r l a \left(1 + 2ab + a^2 b^2 + \frac{l}{a} \right) + B_r (1 + a^2 b) \right].
\end{aligned}
\tag{18}
$$

where:

$$R_1 = \frac{\exp\left(-\frac{1}{2}a^2b^2 - bl\right)}{2l}\left[\operatorname{erf}\left(\frac{ab}{\sqrt{2}} - \frac{l}{a}\right) - \operatorname{erf}\left(\frac{ab}{\sqrt{2}} + \frac{l}{a}\right)\right], \tag{19}$$

$$R_2 = \frac{\exp\left(-\frac{1}{2}a^2b^2 - bl\right)}{2l}\left[1 - \operatorname{erf}\left(\frac{ab}{\sqrt{2}} + \frac{l}{a}\right)\right], \tag{20}$$

$$R_3 = R_2 \exp(2bl), \tag{21}$$

$$a = \sqrt{\overline{u^2}},$$

$$B_r = D_e(br_e - 1) \cdot \exp(br_e), \tag{22}$$

$$C_r = bD_e \cdot \exp(br_e).$$

The parameters: D_e, b and r_e are given in Table II, position 3.

Taking for example the first VARSHNI's function as a model potential we get the following equation for self-consistent potential:

$$\tilde{\Phi}(l) = D_e\left\{1 - \frac{2\exp\left[b(r_e^2 - B_w \cdot l^2)\right]}{(1 + 2ba^2)^{3/2}} + \frac{\exp\left[2b(r_e^2 - C_w l^2)\right]}{(1 + 4ba^2)^{3/2}}\right\}, \tag{23}$$

where:

$$B_w = \frac{1 + 4ba^2}{1 + 2ba^2}, \quad C_w = \frac{1 + 8ba^2}{1 + 4ba^2}.$$

b is given in Table II, position 6, D_e, r_e and a are the same as those found for the RYDBERG potential function.

The above formulas show that $\tilde{\Phi}$ (1) given by Eq. (23) is much simpler than Eq. (18). However, this self-consistent potential [Eq. (23)] tested by means of investigating the temperature dependence of the pseudoharmonic strength constant gives good results for high temperature only. For this reason, the equation of state and thermodynamic functions will be expressed in terms of the RYDBERG's function [Eq. (18)].

V. Equation of state for solid molecular in pseudoharmonic approximation

The thermal equation of state is given by [53]:

$$p = -\frac{zl_e}{6v}\tilde{\Phi}'(l_e) \tag{24}$$

where: v is the specific volume, z is the number of nearest neighbours,

$$\tilde{\Phi}'(l_e) = \left(\frac{d\tilde{\Phi}(l)}{dl}\right)_{l=l_e} \tag{25}$$

l_e is defined by the condition:

$$\tilde{\Phi}'(l_e) = 0\,.$$

From Eqs. (18), (22) and (24) it follows that we must investigate the case of low and high temperature separately.

a) Low temperature $\Theta \ll \omega_{0L}$

According to Eqs. (24, 25) and (18)—(22) we get:

$$p = \frac{3zf \exp\left(-\frac{3}{4}ba\right)}{64vr_e}\left(\frac{b^2}{r_e}a^6 - P_1 ba^4 + P_2 a^3 - P_3 r_e a^2 - P_2 r_e^2 a\right), \tag{26}$$

where:

$$a^2 = \overline{u^2} = \frac{v_f a_1^3}{\alpha^2 D_e b^2} k_m^4 \left(\frac{3}{4} + \frac{\alpha^2 v_f^2}{6\Theta^2} k_m^2 - \frac{2\alpha v_f}{5\Theta} k_m\right), \tag{27}$$

with $k_m = (18\pi^2)^{1/3}/a_1$ for atoms crystallize in a face-centred cubic lattice and in a body-centred cubic lattice.

$$\alpha^2 = \frac{f(\Theta, l_e)}{f}\,. \quad P_1 = 4 - br_e - \frac{1}{br_e}\,; \quad P_2 = 4\left(\frac{1}{br_e} - 1\right); \quad P_3 = 4r_e b - 1\,.$$

The renormalization of the strength constant $f(\Theta, l_e)$ defined by the condition (17) is given by:

$$f(\Theta, l_e) = \frac{4f^2\Theta^2 S_1^2(\Theta)}{9S^2 S_2^2(\Theta)}\left\{\left[1 + \frac{6S^2 D_1 r_e S_2(\Theta)}{f\Theta^2 S_1^2(\Theta)}\right]^{1/2} - 1\right\}^2, \tag{28}$$

where:

$$\begin{aligned}
S &= \frac{3\pi^2\hbar v_f \sqrt{2\hbar \cdot v_f}}{a_1^3}\,,\\
S_1(\Theta) &= r_e - \frac{1}{2}\frac{S^2 C_1}{\Theta^2 f} + \frac{3}{2}\frac{br_e D_1 S^2}{\Theta^2 f}\,,\\
S_2(\Theta) &= 1 + \frac{bS^2 C_1}{\Theta^2 f}\,,\\
C_1 &= b + \frac{3}{br_e^2} - \frac{3}{r_e}\,,\\
D_1 &= b + \frac{1}{r_e} + \frac{3}{4b^2 r_e^3} - \frac{3}{4br_e^2}\,,
\end{aligned} \tag{29}$$

a_1 is the lattice constant, $\hbar = h/2\pi$, h is Planck's constant, v_f is the velocity of sound, f is the harmonic strength constant. Then the vibrational frequency ω_k at $\Theta \ll \omega_{0L}$ is given by:

$$\omega_k^2 \approx \omega_{0k}^2 \frac{4f\Theta^2 S_1^2(\Theta)}{9S^2 S_2^2(\Theta)} \left\{\left[1 + \frac{6S^2 D_1 r_e S_2(\Theta)}{f\Theta^2 S_1^2(\Theta)}\right]^{1/2} - 1\right\}^2 . \tag{30}$$

b) High temperature $\Theta > \omega_{0L}$

By the above approximations the following results are obtained with the help of (14), (18—22) and (15)—(17):

1. The thermal equation of state:

$$p = \frac{z}{6v}\left\{12C_r b D_k \frac{\Theta}{f(\Theta, l_e)} [D_k(3D_k + 2) + br_e + 1] + \right.$$
$$+ \left(\frac{6\Theta}{f(\Theta, l_e)}\right)^{1/2} C_r \left[D_k(6D_k + 1) + br_e\left(4D_k^2 + \frac{1}{\sqrt{\pi} D_k}\right) - \frac{3}{\sqrt{\pi} D_k}\right] + \tag{31}$$
$$\left. - \frac{C_r D_k}{b} - B_r\left(D_k - \frac{1}{\sqrt{\pi} D_k}\right)\right\},$$

where: $D_k = (3 + br_e)^{1/2}/9.8$;

$$f(\Theta, l_e) = \frac{8\pi\Theta D_k^6 f D_e K^2 \exp(2br_e)}{3Q_1^2} Q_2^{2/3} \tag{32}$$

with

$$Q_1 = 3\sqrt{\pi}\Theta D_k^3 - r_e D_e b \exp(br_e),$$
$$Q_2 = 1 + \frac{9b(2D_k + 1)\eta(\Theta,}{K^2} - \frac{27b^2 D_k \eta^2(\Theta,}{K^3},$$

and

$$K = 4 + 2br_e + \frac{2 + br_e}{\sqrt{\pi} D_k^3},$$
$$\eta(\Theta) = \frac{3\Theta \exp(-br_e)}{D_e \cdot b} - \frac{r_e}{\sqrt{\pi} D_k}.$$

2. The renormalized frequency:

$$\omega_k^2 \approx \frac{8\pi^2\Theta D_k^6 D_e K^2 \exp(2br_e)}{3Q_1^2} Q_2^{2/3} \omega_{0k}^2 . \tag{33}$$

VI. Thermodynamic function for solid molecular in pseudoharmonic approximation

The coefficient of the linear thermal expansion and the specific heat at constant pressure are given by the following formulas [63, 65]:

$$\alpha_T = \frac{k_B}{L}\frac{\partial L}{\partial \Theta}, \tag{34}$$

$$C_p = \frac{k_B}{N}\left[\frac{\partial}{\partial \Theta}(E + p \cdot V)\right]_p, \tag{35}$$

where the internal energy

$$\frac{1}{N}E = \frac{1}{2}\tilde{\Phi}(l_e) + \frac{1}{2}f(\Theta, l_e)\overline{u^2}, \tag{36}$$

and

$$L = Nl_e. \tag{37}$$

Using the above formulas and the expressions (18), (25)—(28) we find in the following an analytical expression for α_T and c_p if $\Theta \ll \omega_{0L}$:

$$\alpha_T \approx \frac{k_B}{\Theta}\left[\frac{1}{1+\frac{3}{2}\frac{S^2 D_1}{\Theta^2 f S_1(\Theta)}}\right]\left\{1 + \frac{3S^2 C_1 b}{4f\Theta^2 S_2(\Theta)} - \frac{4S^2 D_1 r_e S_3(\Theta)}{f\Theta^2 S_1^2(\Theta)} - \frac{9S^4 C_1 b r_e^2 D_1}{f^2\Theta^4 S_1^3(\Theta)}\right\}, \tag{38}$$

where:

$$S_3(\Theta) = r_e + \frac{1}{2}\frac{S^2 C_1}{\Theta^2 f} - \frac{3br_e D_1 S^2}{\Theta^2 f},$$

$$C_p = \frac{3zk_B}{16f\Theta}\, yW\left\{\frac{3b^2}{16r_e^2 f^4}\left(y^6\frac{b}{f} - 8P_7 y^5\right) + \frac{3}{2}\left(\frac{b^2 P_1}{8r_e^2} - \frac{P_0 P_8}{zP_6^2}\right)\frac{y^4}{f^3} + \right.$$
$$+\left[\left(\frac{P_7 P_1}{r_e} + \frac{3}{16}P_2\right)b - \frac{16}{zP_6}\left(P_8 P_7 - \frac{P_0 P_9}{8P_6}\right)\right]\frac{y^3}{f^2} - \left[\frac{3}{4}\left(P_7 P_2 + \frac{1}{4}bP_3\right) + \right.$$
$$+\frac{16}{zP_6}\left(P_9 P_7 - \frac{P_0 P_3}{32P}\right)\Big]\frac{y^2}{f} + \frac{1}{2}\left[\left(P_7 P_3 - \frac{3}{8}br_e P_2\right) - \right. \tag{39}$$
$$\left.\left. - \frac{8}{3P_6 z}\left(P_{10}P_7 - \frac{3P_0 P_4}{8P_6}\right)\right]y + \frac{1}{4}fP_7\left(r_e P_2 - \frac{2P_4}{3zP_6}\right) + \frac{8fP_0 P_5}{zP_6^2}\right\},$$

where:

$$y = \frac{S}{\Theta}\sqrt{f(\Theta, l_e)}\,,$$

$$W = 1 - \frac{S_3(\Theta)}{S_1(\Theta)} + \frac{S^2 C_1 b}{f\Theta^2 S_2(\Theta)} - \frac{\left(6S^2 D_1 r_e \Theta S_3(\Theta) + \dfrac{12S^4 C_1 b r_e^2 D_1}{\Theta f}\right)}{f\Theta^3 S_1^3(\Theta)}\,,$$

$$P_0 = b + \frac{1}{r_e}\,; \quad P_1 = 4 - br_e - \frac{1}{br_e}\,; \quad P_2 = 4\left(\frac{1}{br_e} - 1\right); \quad P_3 = 4r_e b - 1\,;$$

$$P_4 = \frac{1}{4b}\left(12 - \frac{11}{br_e}\right); \quad P_5 = \frac{1}{b^2}\left(1 - \frac{2}{br_e}\right); \quad P_6 = 1 + \frac{3y}{4fr_e}\,;$$

$$P_7 = 1 - \frac{3by}{4f}\,; \quad P_8 = \frac{1}{br_e^3} - \frac{1}{r_e^2}\,; \quad P_9 = b + \frac{1}{r_e} + \frac{3}{4b^2 r_e^3} - \frac{3}{4br_e^2}\,;$$

$$P_{10} = \frac{1}{br_e} - 2\,.$$

High temperature $\Theta > \omega_{0L}$

The application of Eqs. (34—37) and (18), and also (31)—(32) leads to the results:

$$\alpha_T \approx \frac{k_B}{\Theta}(1 - Q_3)\,, \tag{40}$$

$$c_p \approx 3k_B + (1 - Q_3)k_B\left\{\frac{6C_r D_k b[D_k(D_k + 1) + br_e + 1](1 - z)}{f(\Theta, l_e)} + \right.$$
$$\left. + \frac{C_r(z - 1)}{2\sqrt{6\Theta f(\Theta, l_e)}}\left[br_e\left(1 + 2D_k + \frac{1}{\sqrt{\pi}D_k}\right) + (5D_k - 1)D_k - \frac{1}{\sqrt{\pi}D_k}\right]\right\}, \tag{41}$$

where:

$$Q_3 = 1 - \frac{6\pi D_k^3 \Theta}{Q_1} + \left[\frac{6\Theta(2 - Q_2)\exp(-br_e)}{D_e b}\right] \times$$
$$\times \left[\frac{9b(2D_k + 1)}{K^2} + \frac{54b^2 D_k \eta(\Theta)}{K^3}\right]$$

$f(\Theta, l_e)$ is given by Eq. (32).

VII. Comparison of the experimental values for c_p (Θ) with values calculated in pseudoharmonic approximation

In Table IX the numerical values $c_p(\Theta)$ for Ag calculated from Eq. (39) for $\Theta < 1/6\Theta_D$ and Eq. (41) for $\Theta \gg 1/6\,\Theta_D$ in terms of the RYDBERG's renormalized potential function are given and compared with experimental data [53, 66] as well as with those calculated in Debye's approximation [53].

Table IX

Comparison of the experimental data for the specific heat at constant pressure for Ag with the approximations given by Eqs. (39), (41) of the text

Structure	a_1 [nm]	v_l [m/s]	Θ [^oK]	$C_p \cdot 10^{-23}\left[\frac{J}{^\circ K_{molecule}}\right]$		
				experiment	Debye	our results
Face centred cubic	0.428	1794.67	20	0.2778	0.2739	0.275835
			28.56	0.7142	0.7051	0.706278
			190.17	3.8791	3.9013	3.901542
			205.30	3.8978	3.9361	3.9113571

Table IX shows that the values of c_p given by RYDBERG renormalized potential function agree quite well with experimental data. For this reason it seems to be possible to obtain accurate results for other thermodynamic functions.

VIII. Conclusions

The comparative investigations of potential curves for solid molecular show that there are three classes of these curves in fact with respect to their behaviour and numerical values of their parameters. The first one is represented by the LENNARD-JONES potential and the MECKE—SUTHERLAND as well as the VARSHNI (V) function belong to it. The MORSE function as well as the RYDBERG, VARSHNI (I), VARSHNI (II) and TIETZ (I) functions form the second class. The third class contains other functions from Table II and the most representative one is the TIETZ (II) curve. Although the last function in harmonic approximation allows us to find the solution of the Schrödinger equation in its analytic form [68], however, it leads to very complicate calculations in pseudoharmonic approximation. Thus the functions belonging to the third class are not convenient from the point of view of their application to the investigations of thermodynamic properties. The first class represented by the LENNARD-JONES potential is usually discussed in literature also in connection with the pseudoharmonic approximation [69].

On the basis of the analysis presented in this paper we confine our further considerations to the second class of the potential curves which lead to the analytical forms in pseudoharmonic approximation. In particular we consider the RYDBERG potential being more accurate in harmonic approximation than the MORSE function discussed by PLAKIDA and SIKLÓS in pseudoharmonic approximation [63, 67]. The investigation of various functions of the same class is however necessary since the calculations made for the VARSHNI (I) function show that the functions usually applied in harmonic approximation can lead to unphysical results in the case when the pseudoharmonic approach is taken into account. For example, the VARSHNI (I) function tested by means of investigating the temperature dependence of the pseudoharmonic strength constant gives a good result for high temperature only.

If we consider the property of crystal structure we cannot investigate it by help of the potential to isolate from the influence of lattice vibrations. Thus, relative merits of the potential functions must be tested by means of investigating the temperature dependence of self-consistent potential $\tilde{\Phi} = f(\Theta)$. This paper presents a comparative study of renormalised potential curves in pseudoharmonic approximation (in analogy to the comparative tests of the functions for diatomic molecules of gases which have been made by VARSHNI [33]).

From the analysis $\tilde{\Phi} = f(\Theta)$ presented in this paper it follows that only some self-consistent potentials can be used for describing the properties of crystal structure. Among such potentials we find RYDBERG's function. In this paper we have given the equation of state and thermodynamic functions expressed in terms of the RYDBERG's potential. Since the results are quite good (Table IX) this renormalised potential will be used to investigate the spectroscopic properties of crystal structure and to compute the characteristic spectrum as a function of temperature as well as other quantities, for example the electrical conductivity [70].

Acknowledgement

The author wishes to thank Professor T. SIKLÓS for reading the manuscript.

Warm thanks are due to Professor L. WOJTCZAK for his helpful remarks and discussions and also to Professor J. KARNIEWICZ, Head of the Institute of Physics, Technical University of Łódz, for kindly supporting these investigations.

REFERENCES

1. E. TELLER, Z. Physik, **61**, 458, 1930.
2. H. M. JAMES and A. S. COOLIDGE, J. Chem. Phys., **1**, 825, 1933.
3. S. K. CHAKRAVARTY, Phil. Mag., **28**, 423, 1939.
4. E. S. RITTNER, J. Chem. Phys., **19**, 1030, 1951.

5. A. MECKLER, J. Chem. Phys., **21,** 1750, 1953.
6 Y. P. VARSHNI, Trans. Faraday Soc., **53,**, 132, 1957.
7. T. TIETZ, J. Chem. Phys,. **38,** 3036, 1963.
8. T. TIETZ, J. Chem. Phys., **40,** 2418, 1964.
9. G. W. WHELAND, J. Am. Chem. Soc., **63,** 2025, 1941.
10. R. S. MULLIKEN, J. Chem. Phys., **56,** 295, 1952.
11. W. MOFFITT, Proc. Roy. Soc. London, **A210,** 224, 245, 1951.
12. G. G. HALL, Proc. Roy. Soc. London, **A205,** 541, 1951.
13. C. C. J. ROOTHAAN, Revs. Modern Phys., **23,** 69, 1951).
14. J. T. VANDERSLICE, E. A. MASON and W. G. MAISCH, J. Chem. Phys., **33,** 614, 1960.
15. J. T. VANDERSLICE, E. A. MASON and E. R. LIPPINCOTT, J. Chem. Phys., **30,** 129, 1959.
16. D. D. KONORALOW and J. O. HIRSCHFELDER, Phys. Fluids, **4,** 637, 1961.
17. P. M. MORSE, Phys. Rev., **34,** 57, 1929.
18. COOLIDGE, JAMES, VERNON, Phys. Rev., **54,** 726, 1938.
19. H. M. HULBURT and J. O. HIRSCHFELDER, J. Chem. Phys., **9,** 61, 1941.
20. M. L. HUGGINS, J. Chem. Phys., **3,** 473, 1935; **4,** 308, 1936.
21. D. S. ZAKHEIM and D. D. KONOWALOW, J. Chem. Phys., **51,** 5620, 1969.
22. A. KRATZER, Ann. Physik, **67,** 127, 1922.
23. R. RYDBERG, Z. Physik, **73,** 376, 1931.
24. M. F. MANNING and N. ROSEN, Phys. Rev., **44,** 953, 1933.
25. G. PÖSCHL and E. TELLER, Z. Physik, **83,** 143, 1933.
26. E. A. HYLERAAS, Z. Physik, **96,** 661, 1935.
27. J. W. LINNERT, Trans. Faraday Soc., **36,** 1123, 1940; **38,** 1, 1942.
28. G. B. B. M. SUTHERLAND, J. Chem. Phys., **8,** 161, 1940.
29. A. A. FROST and B. MUSULIN, J. Am. Chem. Soc., **76,** 2045, 1954.
30. E. R. LIPPINCOTT, J. Chem. Phys., **21,** 2070, 1953; **23,** 603, 1955.
31. E. R. LIPPINCOTT and R. SCHROEDER, J. Chem. Phys., **23,** 1099, 1955; **23,** 1131, 1955.
32. Y. P. VARSHNI, Trans. Faraday Soc., **53,** 132, 1957; **57,** 537, 196 1.
33. Y. P. VARSHNI, Revs. Modern Phys., **29,** 664, 1957.
34. L. WOJTCZAK, Z. Naturforsch., **19a,** 1338, 1964.
35. T. TIETZ, Acta Phys. Hung., **29,** 391, 1970.
36. J. O. HIRSCHFELDER, C. F. CURTISS and R. B. BIRD, The Molecular Theory of Gases and Liquids, New York, 1954.
37. E. A. MASON and T. H. SPURLING, The Virial Equation of State, Vol. 2, Moscow 1972.
38. D. D. KONOWALOW, M. H. TAYLOR and J. O. HIRSCHFELDER, Phys. Fluids, **4,** 622, 1961; **4,** 629, 1961.
39. A. E. SHERWOOD and J. M. PRAUSNITZ, J. Chem. Phys., **41,** 413, 1964; **41,** 429, 1964.
40. D. S. ZAKHEIM and D. D. KONOWALOW, J. Chem. Phys., **51,** 5620, 1969.
41. C. MALINOWSKA—ADAMSKA, Bull. Soc. Sci. Lettres Lódz, **24,** 5, 1974.
42. J. B. KELLER and B. ZUMINO, J. Chem. Phys., **30,** 1351, 1959.
43. E. WHALLEY and W. G. SCHNEIDER, J. Chem. Phys., **23,** 1644, 1955.
44. J. CORNER, Trans. Faraday Soc., **35,** 711, 1939; **44,** 914, 1948.
45. E. A. MASON and W. E. RICE, J. Chem. Phys., **22,** 843, 1954.
46. A. D. BUCKINGHAM, J. Chem. Phys., **23,** 412, 1955.
47. A. K. BARUA, J. Chem. Phys., **31,** 957, 1959.
48. E. S. CAMPBELL, J. Chem. Phys., **20,** 1411, 1952.
49. R. T. MC GINNIES and L. JANSEN, Phys. Rev., **101,** 1301, 1956. **104,** 961, 1956.
50. T. KIRHARA, Advances in Chem. Phys., **1,** 267, 1958.
51. N. BERNARDES, Phys. Rev., **112,** 1534, 1958.
52. L. H. NOSANOW and G. L. SHAW, Phys. Rev., **128,** 546, 1962.
53. C. KITTEL, Introduction to Solid State Physics, PWN, Warszawa, 1974.
54. R. MECKE, Z. Physik, **42,** 390, 1927.
55. E. GRÜNEISEN, Ann. Physik, **26,** 393, 1908.
56. G. MIE, Ann. Physik, **11,** 657, 1903.
57. E. FUES, Ann. Physik, **80,** 376, 1926.
58. L. V. MEISEL and J. F. COX, Phys. Rev., **B11,** 1762, 1975.
59. D. D. KONOWALOW and S. L. GUBERMAN, Ind. Eng. Chem. Fundamentals, **7,** 622, 1968.
60. D. D. KONOWALOW and S. CARRA, Phys. Fluids, **8,** 1585, 1965.
61. D. D. KONOWALOW, Phys. Fluids, **9,** 23, 1966.
62. D. D. KONOWALOW, J. Chem.hys., **46,** 818, 1967.
63. M. M. PLAKIDA and T. SIKLÓS, Acta Phys. Hung. **25,** 17, 1968; **26,** 387, 1969; Phys. Lett., **26A,** 342, 1968; phys. stat. sol., **33,** 103, 1969; **33,** 113, 1969; **39,** 171, 1970.
64. N. R. TAWDE and K. GOPALKRISHNAN, Indian. J. Phys., **28,** 469, 1954.

65. W. A. HARRISON, Solid State Theory. PWN, Warszawa, 1976.
66. J. G. DAUNT, Progress in Low Temperature Physics, C. J. Gorter North-Holland, Amsterdam, 1955.
67. T. SIKLÓS, Acta Phys. Hung., **30,** 181, 1971; **30,** 301, 1971; **30,** 193, 1971; **34,** 327, 1973.
68. C. MALINOWSKA-ADAMSKA, Zeszyty Naukowe Pł Fizyka (in Polish), **3,** 5, 1976.
69. D. WALLACE, Thermodynamics of Crystals, New York; 1976.
70. L. WOJTCZAK and K. STACHULEC, phys. stat,. sol., (b) **70,** K 165, 1975.

Acta Physica Academiae Scientiarum Hungaricae, Tomus 42 (4), pp. 319—331 (1977)

MANY-HADRON FINAL STATES IN INCLUSIVE e^+e^- ANNIHILATION

By

E. LENDVAI and G. PÓCSIK

INSTITUTE FOR THEORETICAL PHYSICS, ROLAND EÖTVÖS UNIVERSITY, BUDAPEST

(Received 31. III. 1977)

The inclusive e^+e^- annihilation into many spinless hadrons is studied in one-photon and one-neutral Z-meson exchange approximation for arbitrarily polarized incident beams. Polarized e^+e^- beams make the separation of the measurable combinations of the structure functions easier. We discuss also the separations coming from the angular behaviours of the produced hadrons. Several asymmetries are described including three weak ones due to the neutral weak current.

1. Introduction

Recently, the e^+e^- annihilation into hadrons has attracted much attention both theoretically (e.g. [1]—[4] with further references) and experimentally [5]. Since exclusive hadronic final states are expected to be suppressed at high energies, the inclusive channels are of great importance providing considerable cross sections. Up to now, the total cross section and one-particle inclusive cross sections have been measured, leading to important details [5] on the e^+e^- annihilation into hadrons. Further features of the hadron production will follow from measuring n-hadron inclusive final states with $n = 2, 3 \ldots$. Such measurements will shed light on the nature of correlations and restrict the theoretical models.

On the other hand, in the energy range of the next generation of storage rings and at even higher energies, the weak interactions are switched on, producing interference effects with the pure photon exchange (for a review see [6]). In such a way, at high energies, effects of neutral weak currents can be pursued in hadron production. In [3] the effects of neutral weak currents have been investigated in one-particle inclusive e^+e^- annihilation into hadrons, while a discussion of the two-particle inclusive interference is also available [4].

In the present paper the n-hadron inclusive cross section is discussed in e^+e^- annihilation by exchanging one photon and one neutral Z-meson coupled to the neutral weak current. The incident e^+e^- beams are assumed to be arbitrarily polarized. The weak current is a mixture of vector and axial vector currents. Indeed, the total cross section for elastic $\nu_\mu p$ scattering appears to exclude pure S, P from the interaction [7], as well as the existing measure-

ments of electric dipole moment of heavy atoms exclude neutral weak $S-P$, $T-PT$ interactions for the $e^- - N$ system [8].

It turns out that the treatment of the case $n = 3$ is not more complicated than the general case with n hadrons, since for $n = 3$ all the possible types of invariants emerge.

In Section 2 we calculate the n-hadron inclusive cross section. Because of the small number of invariants formed by the products of leptonic variables and polarizations with hadronic four-momenta, the structure functions appear in suitable combinations in the cross section. The measurability of these combinations is discussed in Section 3. It is shown that polarized e^+e^- beams provide a partial separation of hadronic structures. (Usefulness of beam polarizations has been investigated in [9], [6].) In the general case of n hadrons only a small number of hadronic combinations can be separated, since the structure functions depend on too many angles and three-momenta.

For $n \leq 3$ all the combinations of the structure functions appearing in the inclusive cross section can be separated, but for $n > 3$ only partial separations are possible. In particular, this concerns those structure coming from the electromagnetic – weak interference. Stronger results have recently been published in [12].

It is worth emphasizing that even if a limited number of hadronic combinations can be gathered from the cross section with n hadrons, the comparison with detailed theoretical predictions will be of great importance. In particular, parity violating structures can be easily identified. In Section 3 several asymmetries are described including three weak ones coming from the neutral weak current.

2. The cross section

We consider the inclusive processes

$$e^-(k, \vec{n}) + e^+(k', n') \to h_1(p_1) + \ldots + h_n(p_n) + X\,, \tag{1}$$

in which n spinless hadrons are produced, $\vec{n}$ ($\vec{n}'$)means the polarization of $e^-(e^+)$ multiplied by the unit vector representing the spin direction in the rest frame. The cross section is calculated in one-γ and one-Z exchange by means of the interaction Hamiltonian

$$H_1 = -eA_\mu(j_\gamma^\mu + J_\gamma^\mu) - g_z Z_\mu(j_z^\mu + J_z^\mu) \tag{2}$$

with

$$j_\gamma^\mu = \bar{e}\gamma^\mu e, \quad j_z^\mu = \bar{e}\gamma^\mu(g_V + g_A\gamma_5)e \tag{3}$$

the electromagnetic and neutral weak leptonic currents, g_V, g_A, g_z are real, J_γ^μ, J_z^μ denote the corresponding Hermitean hadronic currents.

The differential cross section is

$$d\sigma^{(n)} = \frac{8\pi^2\alpha^2}{e^4q^2} ReT^2 \prod_{i=1}^{n} \frac{d^3p_i}{(2\pi)^3 2p_i^0}\,; \tag{4}$$

here $q^2 = (k + k')^2$, a summation over X is included in ReT^2,

$$ReT^2 = |M_\gamma + M_z|^2\,,$$

$$M_\gamma = -ie^2 \frac{g_{\alpha\beta}}{q^2} \langle h_1(p_1) \ldots h_n(p_n)X|J_\gamma^\alpha|0\rangle \langle 0|j_\gamma^\beta|e^+e^-\rangle\,, \tag{5}$$

$$M_z = -ig_z^2 \frac{g_{\mu\nu} - q_\mu q_\nu/m_z^2}{q^2 - m_z^2} \langle h_1(p_1) \ldots h_n(p_n)X|J_z^\mu|0\rangle \cdot \langle 0|j_z^\nu|e^+e^-\rangle\,.$$

The hadronic matrix elements define hadronic tensors $H_{\mu\nu}$ (J_1J_2) appearing in ReT^2,

$$H_{\mu\nu}(J_1J_2) = \sum_X (2\pi)^4\delta^{(4)}(q - p_1 - \ldots - p_n - p_X) \times$$
$$\langle h_1(p_1) \ldots h_n(p_n)X|J_{1\mu}|0\rangle \langle h_1(p_1) \ldots h_n(p_n)X|J_{2\nu}|0\rangle^*. \tag{6}$$

Introducing the characteristic parameters a, f, t of $d\sigma^{(n)}$,

$$a = \frac{e^4}{q^4}\,, \qquad f = \frac{e^2g_z^2}{q^2(q^2 - m_z^2)}\,, \qquad t = \frac{g_z^4}{(q^2 - m_z^2)^2}\,, \tag{7}$$

as well as

$$\langle 0|j_\gamma^\mu|e^+e^-\rangle = \bar{v}\gamma^\mu u = A^\mu\,,$$
$$\langle 0|j_z^\mu|e^+e^-\rangle = \bar{v}\gamma^\mu(g_V + \gamma_5 g_A)u = A_5^\mu\,, \tag{8}$$

T^2 can be written as

$$T^2 = A^\alpha A^{\beta*}\big(aH_{\alpha\beta}(\gamma\gamma) + 2fg_VH_{\alpha\beta}(\gamma Z) + tg_V^2H_{\alpha\beta}(ZZ)\big) +$$
$$+ 2g_AA^\alpha A_5^{\beta*}\big(fH_{\alpha\beta}(\gamma Z) + tg_VH_{\alpha\beta}(ZZ)\big) + tg_A^2A_5^\alpha A_5^{\beta*}H_{\alpha\beta}(ZZ)\,. \tag{9}$$

Eq. (9) shows clearly parity conserving and parity violating leptonic or/and hadronic pieces. Neglecting the electron mass, for $\vec{k} + \vec{k}' = 0$ the leptonic tensors have the forms

$$\left.\begin{matrix} A_\mu A_\nu^* \\ A_{\mu 5}A_{\nu 5}^* \end{matrix}\right\} = \left(1 + \frac{4}{q^2}\vec{k}\vec{n}\cdot\vec{k}n')(k'_\mu k_\nu + k'_\nu k_\mu - \frac{q^2}{2}g_{\mu\nu}\right) + \frac{2i}{q}\vec{k}(\vec{n} + n')k'^\alpha k^\beta\varepsilon_{\alpha\mu\beta\nu} \pm$$
$$\pm\left[\vec{n}n'(k'_\mu k_\nu + k'_\nu k_\mu - \frac{q^2}{2}g_{\mu\nu}\right) + \frac{4}{q^2}\vec{k}\vec{n}\cdot\vec{k}n'\left(k'_\mu k_\nu + k'_\nu k_\mu +\right.$$
$$\left. + \frac{q^2}{2}g_{\mu\nu}\right) + 2\vec{k}\vec{n}(k_\mu z'_\nu + k_\nu z'_\mu) - 2\vec{k}\vec{n}'(k'_\mu z_\nu + k'_\nu z_\mu) - \frac{q^2}{2}(z_\mu z'_\nu + z_\nu z'_\mu)\Big]\,,$$

$$z_\mu = \left(\frac{2}{q}\vec{k}\vec{n}, \vec{n}\right), \quad z'_\mu = \left(\frac{2}{q}\vec{k}\vec{n}', \vec{n}'\right),$$

$$A_\mu A^*_{\nu 5} = \frac{2}{q}\vec{k}(\vec{n}+\vec{n}')\left(k'_\mu k_\nu + k'_\nu k_\mu - \frac{q^2}{2}g_{\mu\nu}\right) + \tag{10}$$

$$+ i\left(1 + \frac{4}{q^2}\vec{k}\vec{n}\cdot\vec{k}\vec{n}'\right)k'^\alpha k^\beta \varepsilon_{\alpha\mu\beta\nu} - ik'^\alpha z'^\beta(z^\delta k^\nu -$$

$$- k^\delta z^\nu)\varepsilon_{\alpha\beta\delta\mu} + ik^\alpha z^\beta(z'^\delta k'^\mu - k'^\delta z'^\mu)\varepsilon_{\alpha\beta\delta\nu}\,.$$

As can be seen, these leptonic tensors represent divergenceless currents in the absence of electron mass.

To describe the structure of the hadronic tensor $H^{\alpha\beta}$ (12) we first note the elementary tensors and vectors at our disposal[1]

$$\hat{g}_{\mu\nu} = \frac{q_\mu q_\nu}{q^2} - g_{\mu\nu},\ \varepsilon_{\mu\nu\alpha\beta}q^\alpha p_i^\beta,$$

$$\hat{\varepsilon}_{\mu\nu\alpha\beta}p_i^\alpha p_j^\beta = \left(\varepsilon_{\mu\nu\alpha\beta} - \varepsilon_{\varrho\nu\alpha\beta}\frac{q^\varrho q_\mu}{q^2} - \varepsilon_{\mu\varrho\alpha\beta}\frac{q^\varrho q_\nu}{q^2}\right)p_i^\alpha p_j^\beta\,,$$

$$\hat{p}_{i\mu} = \left(p_{i\mu} - \frac{p_i q}{q^2}q_\mu\right),\ \varepsilon_{\mu\alpha\beta\gamma}q^\alpha p_i^\beta p_j^\gamma\,, \tag{11}$$

$$\hat{\varepsilon}_{\mu\alpha\beta\gamma}p_i^\alpha p_j^\beta p_k^\gamma = \left(\varepsilon_{\mu\alpha\beta\gamma} - \varepsilon_{\varrho\alpha\beta\gamma}\frac{q^\varrho q_\mu}{q^2}\right)p_i^\alpha p_j^\beta p_k^\gamma\,,$$

$$i, j, k = 1, \ldots, n\,.$$

These are vanishing by multiplying with q_μ or q_ν. The hadronic structure can be expressed by Lorentz invariant structure functions W, $W_{i,j}$, ... as follows

$$H_{\mu\nu}\,(V_1V_2 \text{ or } A_1A_2) = g^1_{\mu\nu}W + p^1_{i\mu}p^1_{j\nu}W_{i,j}\,,$$

$$H_{\mu\nu}(VA) = \varepsilon_{\mu\nu\alpha\beta}q^\alpha p_i^\beta W_i + \varepsilon^1_{\mu\nu\alpha\beta}p_i^\alpha p_j^\beta W_{ij} + (p_{i\mu}\varepsilon_{\nu\alpha\beta\gamma} + p_{i\nu}\varepsilon_{\mu\alpha\beta\gamma})q^\alpha p_l^\beta p_m^\gamma W_{i,lm} +$$

$$+ (p_{i\mu}\varepsilon^1_{\nu\alpha\beta\gamma} + p_{i\nu}\varepsilon^1_{\mu\alpha\beta\gamma})p_l^\alpha p_m^\beta p_n^\gamma W_{i,lmn}\,. \tag{12}$$

A summation is included over i, etc., Eq. (12) is valid at vanishing electron mass, and even the hats are negligible, so that the remaining terms are correct in order m_e/q. Terms coming from $\varepsilon \times \varepsilon$ are contained in Eq. (12) because of the

[1] Substituting (10) into (9) at $\vec{k} = (0, 0, k)$ it follows that only four combinations of the tensors $H_{\alpha\beta}(J_1J_2)$ are fixed by measuring ReT^2, these are the coefficients of $1 + n_z n'_z$, $n_z + n'_z$, $n_y n'_y - n_x n'_x$, $n_x n'_y + n'_x n_y$. In general, however, in one $H_{\alpha\beta}$ several structure functions may be separated due to various angular behaviours. For each conserved $J_{1,2}$ at most 9 independent elements $H_{\alpha\beta}$ exist with $\alpha, \beta = 1, 2, 3$. In order to keep the hadrons symmetrically, we introduce all the hadronic kinematical forms.

relation

$$\varepsilon_{\alpha\beta\gamma\delta}\,\varepsilon_{\mu\varrho\sigma} = g_{\alpha\mu}\varepsilon^{\varkappa}{}_{\beta\gamma\delta}\,\varepsilon^{\varkappa}{}_{\nu\varrho\sigma} - g_{\alpha\nu}\varepsilon^{\varkappa}{}_{\beta\gamma\delta}\varepsilon_{\varkappa\mu\varrho\sigma} + g_{\alpha\varrho}\varepsilon^{\varkappa}{}_{\beta\gamma\delta}\varepsilon_{\varkappa\mu\nu\sigma} - g_{\alpha\sigma}\varepsilon^{\varkappa}{}_{\beta\gamma\delta}\varepsilon_{\varkappa\mu\nu\varrho}\,, \quad (13)$$

where

$$\begin{aligned}\varepsilon^{\varkappa}{}_{\beta\gamma\delta}\varepsilon_{\varkappa\nu\varrho\sigma} = &-g_{\beta\nu}(g_{\gamma\varrho}g_{\delta\sigma} - g_{\gamma\sigma}g_{\delta\varrho}) + \\ &+ g_{\beta\varrho}(g_{\gamma\nu}g_{\delta\sigma} - g_{\gamma\sigma}g_{\delta\nu}) - g_{\beta\sigma}(g_{\gamma\nu}g_{\delta\varrho} - g_{\gamma\varrho}g_{\delta\nu})\,.\end{aligned} \quad (14)$$

The antisymmetric combinations corresponding to $W_{i,lm}$, $W_{i,lmn}$ can be included in W_i, $W_{i,j}$ due to the relation

$$g_{\alpha\beta}\varepsilon_{\mu\nu\varrho\sigma} - g_{\alpha\mu}\varepsilon_{\beta\nu\varrho\sigma} = g_{\alpha\nu}\varepsilon_{\mu\beta\varrho\sigma} + g_{\alpha\varrho}\varepsilon_{\mu\nu\beta\sigma} + g_{\alpha\sigma}\varepsilon_{\mu\nu\varrho\beta}\,. \quad (15)$$

The structure functions depend on q^2, p_iq, p_ip_j; $i, j = 1, \ldots, n$. (12) obeys the condition $H_{\mu\nu}$ (12) $= H_{\nu\mu}$ (21)*, thus for $J_1 = J_2$ W is real and $W_{i,j} = W^*_{j,i}$. Due to the imaginary, antisymmetric part of $A_\mu A^*_{\nu 5}$, only the imaginary parts of W_i and W_{ij}, contribute to the cross section.

Substituting (10), (12) into (9) we see that the cross section is determined by W and the following combinations

$$\begin{aligned}A_j &= -\,i(qW_j + 2p_l^0 W_{lj})\,,\\ A_{i,l} &= W_{i,l}\,,\\ A_{i,lm} &= 2(qW_{i,lm} + 3p_n^0 W_{i,lmn})\,.\end{aligned} \quad (16)$$

At best these combinations can be separated in $d\sigma^{(n)}$.[2] $d\sigma^{(n)}$ is described most conveniently in a three-vector notation formed by the leptonic terms and polarizations in the order of $\gamma\gamma$, γZ, ZZ-contributions. Therefore, let us introduce

$$\begin{aligned}\tilde{g}_1 &= (1, g_V, g_V^2 - g_A^2),\quad \tilde{g}_3 = (0, g_A, 2g_Vg_A)\,,\\ \tilde{g}_2 &= \left(1 + \frac{4}{q^2}\vec{k}\vec{n}\cdot\vec{k}n'),\ g_V\left(1 + \frac{4}{q^2}\vec{k}\vec{n}\cdot\vec{k}n'\right) + \right.\\ &+ g_A\frac{2}{q}\vec{k}(\vec{n} + \vec{n}'),\quad \left.(g_V^2 + g_A^2)\left(1 + \frac{4}{q^2}\vec{k}\vec{n}\cdot\vec{k}n'\right) + 2g_Vg_A\frac{2}{q}\vec{k}(\vec{n} + \vec{n}')\right)\,,\\ g_4 &= \left(\frac{2}{q}\vec{k}(\vec{n} + \vec{n}'),\ g_V\frac{2}{q}\vec{k}(\vec{n} + \vec{n}') + g_A\left(1 + \frac{4}{q^2}\vec{k}\vec{n}\cdot\vec{k}\vec{n}'\right)\right.,\\ &\left.(g_V^2 + g_A^2)\frac{2}{q}\vec{k}(\vec{n} + \vec{n}') + 2g_Vg_A\left(1 + \frac{4}{q^2}\vec{k}\vec{n}\cdot\vec{k}\vec{n}'\right)\right)\,,\\ \vec{A}_x &= (aA_x(\gamma\gamma), 2fA_x(\gamma Z),\ tA_x(ZZ))\,,\\ B &= \begin{pmatrix} n_yn'_y - n_xn'_x & -(n_xn'_y + n_yn'_x) & 0\\ -(n_xn'_y + n_yn'_x) & n_xn'_x - n_yn'_y & 0\\ 0 & 0 & 0\end{pmatrix},\\ p'_i &= (p_{ix},\ p_{iy},\ 0)\,.\end{aligned} \quad (17)$$

[2] Naturally, this does not mean that all A'_xs are independent. Motivated by (16) one can show that it is perfectly enough to introduce only the terms $W_i \to A_i$, $W_{i,lm} \to A_{i,lm}$ in (12).

where $\vec{k} + \vec{k}' = 0$, $\vec{p}_i'$, B are specialized for $\vec{k} = (0, 0, k)$, A_x is given by Eq. (16). In this notation T^2 has the form

$$T^2 = q^2 \tilde{g}_2 \tilde{W} + 2q\vec{k}\vec{p}_i \tilde{g}_4 \tilde{A}_i + \left[\frac{q^2}{2}(\vec{p}_i'(B\tilde{g}_1 + \tilde{g}_2) - \right.$$

$$\left. - q(\vec{p}_i \times \vec{k})\,(iB\tilde{g}_3 - i\tilde{g}_4)\right]\vec{p}_l \tilde{A}_{i,l} + \left[\frac{q^2}{2}\vec{p}_i'(B\tilde{g}_1 + \right. \tag{18}$$

$$\left. + \tilde{g}_2) - iq(\vec{p}_i \times \vec{k})B\tilde{g}_3\right](\vec{p}_l \times \vec{p}_m)\tilde{A}_{i,lm}\,.$$

A scalar product is included in $\tilde{g}_2\tilde{W}$, etc. while B acts on $\vec{p}_l$, etc.

Cross sections $d\sigma^{(n)}$, $n = 0, 1, \ldots$ corresponding to Eq. (18) are observable in the energy range of PEP as shown by RICHTER's analysis [10] based on the pure photon exchange. Similarly, the γZ-interference seems to be observable in the region $q \approx 30$ GeV (e.g. [4]). Eq. (7) shows that the fundamental parameters a, f, t are proportional to q^{-4} at very high energies, $q^2 \gg m_Z^2$, thus the electromagnetic and weak interactions yield commensurable contributions (see also [6]). At high energies with $q^2 \ll m_Z^2$, however, the relative strength of the weak and electromagnetic terms grows with q^2. The cross section contains polarization independent (dependent) electron-one-(three-) hadron correlations, as well as electron-two-hadron and two-hadron, three-hadron ones, both polarization dependent and independent. In particular, a parity violating weak correlation of type $(\vec{p}_i \times \vec{k})\vec{p}_l$ is present in the term $\tilde{A}_{i,l}$ as first found by PAIS and TREIMAN [11]. In [4] it is emphasized that effects of neutral weak currents in the inclusive cross section differ from those of charmed hadrons and heavy leptons by propagator effects and the form of parity violation which occurs at the hadronic vertex.

3. Separation of structure functions

In general, the separation of the terms $\tilde{W}$, $\tilde{A}_i$, $\tilde{A}_{i,l}$, $\tilde{A}_{i,lm}$ is possible in Eq. (18) due to the different angular behaviours. The separation of the combinations within one class A_x occurs most easily by fixing the structure functions, that is q, $|\vec{p}_i|$, $\vec{p}_i\vec{p}_j$. Therefore, the number of the separable A_x's can be found by rotating all the hadronic momenta in the same way and looking at the transformations of the kinematical factors $K = (1, p_{ix}p_{jx} \pm \pm p_{iy}p_{jy}, p_{ix}p_{jy} \pm p_{iy}p_{jx})$, $p_{lz}K$ (in the centre-of-mass system of the e^+e^- beams $\vec{k}\vec{p}_i = |\vec{k}|p_{iz}$ was taken, etc.). An element of the rotation group can be

parameterized by the Euler angles ϑ, φ_1, φ_2 as follows

$$f(\vartheta, \varphi_1, \varphi_2) =$$

$$= \begin{pmatrix} \cos\varphi_1 \cos\varphi_2 - \cos\vartheta \sin\varphi_1 \sin\varphi_2 & -\cos\varphi_1 \sin\varphi_2 - \cos\vartheta \sin\varphi_1 \cos\varphi_2 & \sin\varphi_1 \sin\vartheta \\ \sin\varphi_1 \cos\varphi_2 + \cos\vartheta \cos\varphi_1 \sin\varphi_2 & -\sin\varphi_1 \sin\varphi_2 + \cos\vartheta \cos\varphi_1 \cos\varphi_2 & -\cos\varphi_1 \sin\vartheta \\ \sin\varphi_2 \sin\vartheta & \cos\varphi_2 \sin\vartheta & \cos\vartheta \end{pmatrix} \tag{19}$$

so that

$$\begin{pmatrix} 0 \\ 0 \\ p_{iz} \end{pmatrix} \to \begin{pmatrix} 0 & 0 & 0 \\ 0 & 0 & 0 \\ \sin\vartheta \sin\varphi_2 & \sin\vartheta \cos\varphi_2 & \cos\vartheta \end{pmatrix} \vec{p}_i ,$$

$$p_{ix}p_{iy} - p_{iy}p_{jx} \to \vec{p}_i \begin{pmatrix} 0 & \cos\vartheta & -\sin\vartheta \cos\varphi_2 \\ -\cos\vartheta & 0 & \sin\vartheta \sin\varphi_2 \\ \sin\vartheta \cos\varphi_2 & -\sin\vartheta \sin\varphi_2 & 0 \end{pmatrix} \vec{p}_j ,$$

$$p_{ix}p_{jx} + p_{iy}p_{jy} \to$$

$$\to \vec{p}_i \begin{pmatrix} \cos^2\varphi_2 + \cos^2\vartheta \sin^2\varphi_2 & -\frac{1}{2}\sin^2\vartheta \sin 2\varphi_2 & \frac{1}{2}\sin 2\vartheta \sin\varphi_2 \\ -\frac{1}{2}\sin^2\vartheta \sin 2\varphi_2 & \sin^2\varphi_2 + \cos^2\vartheta \cos^2\varphi_2 & \frac{1}{2}\sin 2\vartheta \cos\varphi_1 \\ \frac{1}{2}\sin 2\vartheta \sin\varphi_2 & \frac{1}{2}\sin 2\vartheta \cos\varphi_2 & \sin^2\vartheta \end{pmatrix} \vec{p}_j , \tag{20}$$

$$\begin{bmatrix} p_{ix}p_{jx} - p_{iy}p_{jy} \\ p_{ix}p_{jy} + p_{iy}p_{jx} \end{bmatrix} \to$$

$$\to \vec{p}_i \left\{ \begin{bmatrix} -\sin 2\varphi_1 \\ \cos 2\varphi_1 \end{bmatrix} \begin{pmatrix} \cos\vartheta \sin 2\varphi_2 & \cos\vartheta \cos 2\varphi_2 & -\sin\vartheta \cos\varphi_2 \\ \cos\vartheta \cos 2\varphi_2 & -\cos\vartheta \sin 2\varphi_2 & \sin\vartheta \sin\varphi_2 \\ -\sin\vartheta \cos\varphi_2 & \sin\vartheta \sin\varphi_2 & 0 \end{pmatrix} + \right.$$

$$\left. + \begin{bmatrix} \cos 2\varphi_1 \\ \sin 2\varphi_1 \end{bmatrix} \begin{pmatrix} \cos^2\varphi_2 - \cos^2\vartheta \sin^2\varphi_2 & -\frac{1}{2}(1+\cos^2\vartheta)\sin 2\varphi_2 & \frac{1}{2}\sin 2\vartheta \sin\varphi_2 \\ -\frac{1}{2}(1+\cos^2\vartheta)\sin 2\varphi_1 & \sin^2\varphi_2 - \cos^2\vartheta \cos^2\varphi_2 & \frac{1}{2}\sin 2\vartheta \cos\varphi_2 \\ \frac{1}{2}\sin 2\vartheta \sin\varphi_2 & \frac{1}{2}\sin 2\vartheta \cos\varphi_2 & -\sin^2\vartheta \end{pmatrix} \right\} \vec{p}_j .$$

Hence, the numbers of the independent combinations are in turn

$$p_{iz} \to 3, \quad \vec{k}(\vec{p}_i \times \vec{p}_j) \to 3, \quad \vec{p}_i \vec{p}_j \to 6, \quad \vec{p}_i B \vec{p}_j \to 10, \quad (\vec{p}_i \times \vec{k}) B \vec{p}_j \to 10,$$
$$\vec{p}_i(\vec{p}_j \times \vec{p}_l) \to 6, \quad \vec{p} B(\vec{p}_j \times \vec{p}_k) \to 10, \quad (\vec{p}_i \times \vec{k}) B(\vec{p}_j \times \vec{p}_l) \to 10 \tag{21}$$

and the separable hadronic structures are $\tilde{W}$, $\tilde{A}_i : 3$, $\tilde{A}_{i,l} : 29$, $\tilde{A}_{i,lm} : 26$.[3] It follows that $\tilde{W}$ and $\tilde{A}_i$, $\tilde{A}_{i,l}$, $\tilde{A}_{i,lm}$ can be separated always and for $n \leq 3$, $n \leq 5$, $n \leq 4$, respectively. In general, the inclusive cross section is valuable for the possibility of comparing with detailed theoretical predictions.

In what follows we are considering specific asymmetries of $d\sigma^{(n)}$ reflecting various hadronic structures and arising under rotations around the z-axis and/or space reflections. Let us consider the transformations

$$n_z \to \varepsilon n_z, \quad n_z' \to \varepsilon n_z', \qquad \cos\vartheta_i \to \varrho \cos\vartheta_i,$$

		$\varphi_i \to \varphi_i$	$\varphi_i \to -\varphi_i$	$\varphi_i \to \frac{\pi}{2} - \varphi_i$	$\varphi_i \to \frac{\pi}{2} + \varphi_i$
C :	α	$+$	$+$	$-$	$-$
	β	$+$	$-$	$+$	$-$

		$\varphi_i \to \frac{\pi}{4} - \varphi_i$	$\varphi_i \to \frac{\pi}{4} + \varphi_i$	$\varphi_i \to -\frac{\pi}{4} + \varphi_i$	$\varphi_i \to -\frac{\pi}{4} - \varphi_i$
D :	γ	$+$	$-$	$+$	$-$
	δ	$+$	$+$	$-$	$-$

(22)

($\varepsilon, \varrho, \alpha, \beta, \gamma, \delta = \pm 1$)

furthermore, four transformations of B_{ik}

$$\begin{Bmatrix} 1 \\ 2 \\ 3 \\ 4 \end{Bmatrix} \text{ for } C : B_{11} \to \begin{Bmatrix} \alpha \\ -\alpha \\ \beta \\ -\beta \end{Bmatrix} B_{11}, \quad B_{12} \to \begin{Bmatrix} \beta \\ -\beta \\ \alpha \\ -\alpha \end{Bmatrix} B_{12},$$
$$\begin{Bmatrix} 1 \\ 2 \\ 3 \\ 4 \end{Bmatrix} \text{ for } D : B_{11} \to \begin{Bmatrix} \gamma \\ -\gamma \\ -\delta \\ \delta \end{Bmatrix} B_{12}, \quad B_{12} \to \begin{Bmatrix} \delta \\ -\delta \\ -\gamma \\ \gamma \end{Bmatrix} B_{11}. \tag{23}$$

Under these transformations the combinations of the structure functions in T^2 are multiplied by ± 1 as shown in Table I. Table II contains those pieces of the cross section which are transformed in the same manner.

[3] That is, we are leading to separable but not quite independent A_X's.

Table I

Behaviour of structure functions under C_i, D_i, $\tilde{g}^{(1)}_{2,4}$, $\tilde{g}^{(2)}_{2,4}$ mean bilinear and linear parts in the polarization, respectively

	C1	C2	C3	C4	D1	D2	D3	D4
$\tilde{g}^{(1)}_2\tilde{W}$	+	+	+	+	+	+	+	+
$\tilde{g}^{(2)}_2\tilde{W}$	ε	ε	ε	ε	ε	ε	ε	ε
$\tilde{g}^{(2)}_4\vec{k}\vec{p}_i\tilde{A}_i$	$\varepsilon\varrho$	$\varepsilon\varrho$	$\varepsilon\varrho$	$\varepsilon\varrho$	$\varepsilon\varrho$	$\varepsilon\varrho$	$\varepsilon\varrho$	$\varepsilon\varrho$
$\tilde{g}^{(1)}_4\vec{k}\vec{p}_i\tilde{A}_i$	ϱ	ϱ	ϱ	ϱ	ϱ	ϱ	ϱ	ϱ
$\vec{p}'_iB\vec{p}_l\tilde{g}_1\tilde{A}_{i,l}$	+	−	$\alpha\beta$	$-\alpha\beta$	+	−	$-\gamma\delta$	$\gamma\delta$
$\vec{p}'_i\vec{p}_l\tilde{g}^{(1)}_2\tilde{A}_{i,l}$	+	+	+	+	+	+	+	+
$\vec{p}'_i\vec{p}_l\tilde{g}^{(2)}_2\tilde{A}_{i,l}$	ε	ε	ε	ε	ε	ε	ε	ε
$(\vec{p}_i\times\vec{k})B\vec{p}_l\tilde{g}_3\tilde{A}_{i,l}$	$\alpha\beta$	$-\alpha\beta$	+	−	$-\gamma\delta$	$\gamma\delta$	+	−
$(\vec{p}_i\times\vec{k})\vec{p}_l\tilde{g}^{(2)}_4i\tilde{A}_{i,l}$	$\varepsilon\alpha\beta$	$\varepsilon\alpha\beta$	$\varepsilon\alpha\beta$	$\varepsilon\alpha\beta$	$-\varepsilon\alpha\beta$	$-\varepsilon\alpha\beta$	$-\varepsilon\alpha\beta$	$-\varepsilon\alpha\beta$
$(\vec{p}_i\times\vec{k})\vec{p}_l\tilde{g}^{(1)}_4i\tilde{A}_{i,l}$	$\alpha\beta$	$\alpha\beta$	$\alpha\beta$	$\alpha\beta$	$-\gamma\delta$	$-\gamma\delta$	$-\gamma\delta$	$-\gamma\delta$
$\vec{p}'_iB(\vec{p}_l\times\vec{p}_m)\tilde{g}_1\tilde{A}_{i,lm}$	$\varrho\alpha\beta$	$-\varrho\alpha\beta$	ϱ	$-\varrho$	$-\varrho\gamma\delta$	$\varrho\gamma\delta$	ϱ	$-\varrho$
$\vec{p}'_i(\vec{p}_l\times\vec{p}_m)\tilde{g}^{(1)}_2\tilde{A}_{i,lm}$	$\varrho\alpha\beta$	$\varrho\alpha\beta$	$\varrho\alpha\beta$	$\varrho\alpha\beta$	$-\varrho\gamma\delta$	$-\varrho\gamma\delta$	$-\varrho\gamma\delta$	$-\varrho\gamma\delta$
$\vec{p}'_i(\vec{p}_l\times\vec{p}_m)\tilde{g}^{(2)}_2\tilde{A}_{i,lm}$	$\varepsilon\varrho\alpha\beta$	$\varepsilon\varrho\alpha\beta$	$\varepsilon\varrho\alpha\beta$	$\varepsilon\varrho\alpha\beta$	$-\varepsilon\varrho\alpha\beta$	$-\varepsilon\varrho\alpha\beta$	$-\varepsilon\varrho\alpha\beta$	$-\varepsilon\varrho\alpha\beta$
$(\vec{p}_i\times\vec{k})B(\vec{p}_l\times\vec{p}_m)\tilde{g}_3\tilde{A}_{i,lm}$	ϱ	$-\varrho$	$\varrho\alpha\beta$	$-\varrho\alpha\beta$	ϱ	$-\varrho$	$-\varrho\gamma\delta$	$\varrho\gamma\delta$

Table II

Pieces of T^2 transformed in the same manner

$$\Delta_0 = q^2\tilde{g}_2^{(1)}\tilde{W} + \frac{q^2}{2}\vec{p}_i\vec{p}_l\tilde{g}_2^{(1)}\tilde{A}_{i,l},$$

$$\Delta_\varepsilon = q^2\tilde{g}_2^{(2)}\tilde{W} + \frac{q^2}{2}\vec{p}_i'\vec{p}_l\tilde{g}_2^{(2)}\tilde{A}_{i,l},$$

$$\Delta_\varrho = 2q\vec{k}\vec{p}_i\tilde{g}_4^{(1)}\tilde{A}_i,$$

$$\Delta_{\varepsilon\varrho} = 2q\vec{k}\vec{p}_i\tilde{g}_4^{(2)}\tilde{A}_i,$$

$$\Delta_{\alpha\beta} = q(\vec{p}\times\vec{k})\vec{p}_l\tilde{g}_4^{(1)}i\tilde{A}_{l,l},$$

$$\Delta_{\varepsilon\alpha\beta} = q(\vec{p}_i\times\vec{k})\vec{p}_l\tilde{g}_4^{(2)}i\tilde{A}_{i,l},$$

$$\Delta_{\varrho\alpha\beta} = \frac{q^2}{2}\vec{p}_i'(\vec{p}_l\times\vec{p}_m)\tilde{g}_2^{(1)}\tilde{A}_{i,lm},$$

$$\Delta_{\varepsilon\varrho\alpha\beta} = \frac{q^2}{2}\vec{p}_i'(\vec{p}_l\times\vec{p}_m)\tilde{g}_2^{(2)}\tilde{A}_{i,lm},$$

$$\Delta_1 = \frac{q^2}{2}\vec{p}_i'B\vec{p}_l\tilde{g}_1\tilde{A}_{i,l},$$

$$\Delta_2 = -iq(\vec{p}_i\times\vec{k})B\vec{p}_l\tilde{g}_3\tilde{A}_{i,l},$$

$$\Delta_3 = -iq(\vec{p}_i\times\vec{k})B(\vec{p}_l\times\vec{p}_m)\tilde{g}_3\tilde{A}_{i,lm},$$

$$\Delta_4 = \frac{q^2}{2}\vec{p}_i'B(\vec{p}_l\times\vec{p}_m)\tilde{g}_1\tilde{A}_{i,lm},$$

Finally, let us introduce the following transformations from (22), (23)

$$\begin{aligned}
&\Gamma_1: \ C1(\alpha\beta=+), \text{ or } C3(\alpha\beta=+), \text{ or } D1(\gamma\delta=-), \text{ or } D3(\gamma\delta=-),\\
&\Gamma_2: \ C1(\alpha\beta=-), \text{ or } C4(\alpha\beta=-), \text{ or } D1(\gamma\delta=+), \text{ or } D4(\gamma\delta=+),\\
&\Gamma_3: \ C2(\alpha\beta=+), \text{ or } C4(\alpha\beta=+), \text{ or } D2(\gamma\delta=-), \text{ or } D4(\gamma\delta=-),\\
&\Gamma_4: \ C2(\alpha\beta=-), \text{ or } C3(\alpha\beta=-), \text{ or } D2(\gamma\delta=+), \text{ or } D3(\gamma\delta=+),
\end{aligned} \tag{24}$$

and consider the sign changing terms $\Delta(\varepsilon, \varrho, \Gamma_i)$ under the tramsformations ε, ϱ, Γ_i. We list the different asymmetries $\Delta(\varepsilon, \varrho, \Gamma_i)$ in Table III (* means weak asymmetry). These weak asymmetries are coming from the parity transformations of the initial and final states, respectively, and from their combination

$$\begin{aligned}
\Delta_i = \Delta(--\Gamma_2) = q^2\tilde{g}_2^{(2)}\tilde{W} + 2q\tilde{g}_4^{(1)}\vec{k}\vec{p}_i\tilde{A}_i + \\
+\left[\frac{q^2}{2}\vec{p}_i\tilde{g}_2^{(2)} - q(\vec{p}_i\times\vec{k})\,(iB\tilde{g}_3 - i\tilde{g}_4^{(1)})\right]\vec{p}_l\tilde{A}_{i,l} + \\
+\left[\frac{q^2}{2}\vec{p}_i'\tilde{g}_2^{(2)} - q_i i(\vec{p}_i\times\vec{k})B\tilde{g}_3\right](\vec{p}_l\times\vec{p}_m)\tilde{A}_{i,lm},
\end{aligned} \tag{25}$$

$$\Delta_f = \Delta(+-\Gamma_1) = 2q\tilde{g}_4\vec{k}\vec{p}_i\tilde{A}_i + \left[\frac{q^2}{2}\vec{p}_i'(B\tilde{g}_1 + \tilde{g}_2) - \right.$$

$$\left. - qi(\vec{p}_i\times\vec{k})B\tilde{g}_3\right](\vec{p}_l\times\vec{p}_m)\tilde{A}_{i,lm}\,,$$

$$\Delta_P = \Delta(-+\Gamma_2) = q^2\tilde{g}_2^{(2)}\tilde{W} + 2q\vec{k}\vec{p}_i\tilde{A}_i\tilde{g}_4^{(2)} +$$

$$+\left[\frac{q^2}{2}\vec{p}_i'(B\tilde{q}_1 + \tilde{g}_2^{(1)})\right](\vec{p}_l\times\vec{p}_m)\tilde{A}_{i,lm} + \left[\frac{q^2}{2}\vec{p}_i'i\tilde{g}_2^{(2)} - q(\vec{p}_i'\times\vec{k})(iB\tilde{g}_3 - i\tilde{g}_4^{(1)})\right]\vec{p}_l\tilde{A}_{i,l}\,.$$

The terms W, $A_{i,l}$ give rise to parity violations at the leptonic vertex, the others are coming from the hadronic axial vector current. In general, Δ_P occurs in polarization measurements except for the terms with the correlations $(\vec{p}_i\times\vec{k})\vec{p}_l$ and $\vec{p}_i'(\vec{p}_l\times\vec{p}_m)$. The asymmetries in Table III determine those in Table II.

Table III

Various asymmetries under Eq. (24)

$$\Delta(++\Gamma_i) = \begin{cases} 0 \\ \Delta_{\alpha\beta} + \Delta_{\varepsilon\alpha\beta} + \Delta_{\varrho\alpha\beta} + \Delta_{\varepsilon\varrho\alpha\beta} + \Delta_2 + \Delta_4 \\ \Delta_1 + \Delta_2 + \Delta_3 + \Delta_4 \\ \Delta_{\alpha\beta} + \Delta_{\varepsilon\alpha\beta} + \Delta_{\varrho\alpha\beta} + \Delta_{\varepsilon\varrho\alpha\beta} + \Delta_1 + \Delta_3 \end{cases}$$

$$\Delta(+-\Gamma_i) = \Delta_\varrho + \Delta_{\varepsilon\varrho} + \begin{cases} \Delta_{\varrho\alpha\beta} + \Delta_{\varepsilon\varrho\alpha\beta} + \Delta_3 + \Delta_4{}^* \\ \Delta_{\alpha\beta} + \Delta_{\varepsilon\alpha\beta} + \Delta_2 + \Delta_3 \\ \Delta_{\varrho\alpha\beta} + \Delta_{\varepsilon\varrho\alpha\beta} + \Delta_1 + \Delta_2 \\ \Delta_{\alpha\beta} + \Delta_{\varepsilon\alpha\beta} + \Delta_1 + \Delta_4 \end{cases}$$

$$\Delta(-+\Gamma_i) = \Delta_\varepsilon + \Delta_{\varepsilon\varrho} + \begin{cases} \Delta_{\varepsilon\alpha\beta} + \Delta_{\varepsilon\varrho\alpha\beta} \\ \Delta_{\alpha\beta} + \Delta_{\varrho\alpha\beta} + \Delta_2 + \Delta_4{}^* \\ \Delta_{\varepsilon\alpha\beta} + \Delta_{\varepsilon\varrho\alpha\beta} + \Delta_1 + \Delta_2 + \Delta_3 + \Delta_4 \\ \Delta_{\alpha\beta} + \Delta_{\varrho\alpha\beta} + \Delta_1 + \Delta_3 \end{cases}$$

$$\Delta(--\Gamma_i) = \Delta_\varepsilon + \Delta_\varrho + \begin{cases} \Delta_{\varepsilon\alpha\beta} + \Delta_{\varrho\alpha\beta} + \Delta_3 + \Delta_4 \\ \Delta_{\alpha\beta} + \Delta_{\varepsilon\varrho\alpha\beta} + \Delta_2 + \Delta_3{}^* \\ \Delta_{\varepsilon\alpha\beta} + \Delta_{\varrho\alpha\beta} + \Delta_1 + \Delta_2 \\ \Delta_{\alpha\beta} + \Delta_{\varepsilon\varrho\alpha\beta} + \Delta_1 + \Delta_4 \end{cases}$$

We are going to examine the role of the polarization in identifying asymmetries.

1. *Transverse polarizations*, $n_z = n'_z = 0$

In this natural case $\Delta_\varepsilon = \Delta_{\varepsilon\varrho} = \Delta_{\varepsilon\alpha\beta} = \Delta_{\varepsilon\varrho\alpha\beta} = 0$ and

$$\Delta(\pm, +, \Gamma_i) = \begin{cases} 0 & \\ \Delta_{\alpha\beta} + \Delta_{\varrho\alpha\beta} + \Delta_2 + \Delta_4 & * \\ \Delta_1 + \Delta_2 + \Delta_3 + \Delta_4 & \\ \Delta_{\alpha\beta} + \Delta_{\varrho\alpha\beta} + \Delta_1 + \Delta_3\,, & \end{cases}$$

$$\Delta(\pm, -, \Gamma_i) = \begin{cases} \Delta_\varrho + \Delta_{\varrho\alpha\beta} + \Delta_3 + \Delta_4 & * \\ \Delta_\varrho + \Delta_{\alpha\beta} + \Delta_2 + \Delta_3 & * \\ \Delta_\varrho + \Delta_{\varrho\alpha\beta} + \Delta_1 + \Delta_2 & \\ \Delta_\varrho + \Delta_{\alpha\beta} + \Delta_1 + \Delta_4\,. & \end{cases} \tag{26}$$

2. *Longitudinal polarizations*, $B = 0$

Then $\Delta_1 = \Delta_2 = \Delta_3 = \Delta_4 = 0$, $\Gamma_1 = \Gamma_2$, $\Gamma_3 = \Gamma_4$, as well as

$$\Delta(+ + \Gamma_{1,2}) = \begin{cases} 0 & \\ \Delta_{\alpha\beta} + \Delta_{\varepsilon\alpha\beta} + \Delta_{\varrho\alpha\beta} + \Delta_{\varepsilon\varrho\alpha\beta}\,, & \end{cases}$$

$$\Delta(+ - \Gamma_{1,2}) = \Delta_\varrho + \Delta_{\varepsilon\varrho} + \begin{cases} \Delta_{\varrho\alpha\beta} + \Delta_{\varepsilon\varrho\alpha\beta} & * \\ \Delta_{\alpha\beta} + \Delta_{\varepsilon\alpha\beta}\,, & \end{cases}$$

$$\Delta(- + \Gamma_{1,2}) = \Delta_\varepsilon + \Delta_{\varepsilon\varrho} + \begin{cases} \Delta_{\varepsilon\alpha\beta} + \Delta_{\varepsilon\varrho\alpha\beta} & \\ \Delta_{\alpha\beta} + \Delta_{\varrho\alpha\beta}\,, & * \end{cases} \tag{27}$$

$$\Delta(- - \Gamma_{1,2}) = \Delta_\varepsilon + \Delta_\varrho + \begin{cases} \Delta_{\varepsilon\alpha\beta} + \Delta_{\varrho\alpha\beta} & \\ \Delta_{\alpha\beta} + \Delta_{\varepsilon\varrho\alpha\beta}\,. & * \end{cases}$$

3. *Unpolarized beams*, $B = n_z = n'_z = 0$

Here $\Gamma_1 = \Gamma_3$, $\Gamma_2 = \Gamma_4$ and we get completely weak asymmetries

$$\Delta(\pm, +, \Gamma_{1,2}) = \begin{cases} 0 & \\ \Delta_{\alpha\beta} + \Delta_{\varrho\alpha\beta} & * \end{cases}$$

$$\Delta(\pm, -, \Gamma_{1,2}) = \begin{cases} \Delta_{\varrho\alpha\beta} + \Delta_\varrho & * \\ \Delta_{\alpha\beta} + \Delta_\varrho & * \end{cases} \tag{28}$$

For the sake of completeness we note the asymmetries for $n = 0$, $n = 1$ (while for $n = 2$ the general case is valid):

$$n = 0 : \Delta(-, \pm) = \Delta_\varepsilon \qquad *$$

$$n = 1 : \Delta(+ + \Gamma_i) = \Delta(- + \Gamma_i) - \Delta_\varepsilon - \Delta_{\varepsilon\varrho} = \Delta(- - \Gamma_i) - \Delta_\varepsilon - \Delta_\varrho =$$

$$= \Delta(+ - \Gamma_i) - \Delta_\varrho - \Delta_{\varepsilon\varrho} = \begin{cases} 0 & * \\ \Delta_2 & * \\ \Delta_1 + \Delta_2 & \\ \Delta_1\,. & \end{cases} \tag{29}$$

We thank Dr. F. CSIKOR for useful remarks.

REFERENCES

1. M. Greco and Y. Srivastava, Nuovo Cimento, **18A,** 601, 1973.
2. J. D. Bjorken, Proc. VI. Int. Symposium on Electron and Photon Interactions at High Energies, Bonn, 1973 (North-Holland Publ. Co., Amsterdam, 1974) p. 25; J. D. Bjorken and B. L. Ioffe, Talk presented at the Seminar on Quark and Parton Problems, Moscow, 1974 SLAC-PUB-1467, 1974;
R. Gatto and G. Preparata, Nucl. Phys., **B67,** 362, 1973;
F. Elvekjaer and F. Steiner, DESY-preprint, DESY 75/49, 1975;
D. C. Fetzer and H. Schlereth, Aachen preprint (1976).
3. A. McDonald, Nucl. Phys., **B75,** 343, 1974;
R. Gatto and G. Preparata, Lett. Nuovo Cimento, **7,** 89, 1973;
R. Budny and A. McDonald, Physics Letters, **B48,** 423, 1974;
G. V. Dass and G. G. Ross, Physics Letters, **B57,** 173, 1975;
E. Lendvai and L. Palla, ITP-Budapest Rep. No. 354, 1975.
4. G. V. Dass and G. G. Ross, CERN-preprint, Th. 2196-CERN, 1976.
5. R. F. Schwitters, Proc. 1975 Int. Symposium on Lepton and Photon Interactions at High Energies, Stanford, 1975 (SLAC, Stanford, 1975; Ed.: W. T. Kirk) p. 5;
B. H. Wiik, in the above volume, p. 69.
6. G. Pócsik, Ann. Phys. (N. Y.), **105**, 259, 1977.
7. E. Fischbach et al., Physics Rev. Letters, **37,** 582, 1976.
8. C. Bouchiat, Proc. Neutrino Conference, Balatonfüred. 1975 (Ed.: A. Frenkel and G. Marx, Budapest, 1975). Vol. I. p. 241.
9. K. Schilling, Nuovo Cimento, **16A,** 217, 1973.
10. B. Richter, Proc. 1974 PEP Summer Study, (SLAC), Berkeley, 1974; Ed.: J. Kadyk et al., p. 24.
11. A. Pais and S. B. Treiman, Phys. Rev., D**9,** 1459, 1974.
12. E. Lendvai and G. Pócsik, Phys. Lett., **66***B*, 449, 1977.

Acta Physica Academiae Scientiarum Hungaricae, Tomus 42 (4), pp. 333—338 (1977)

INVESTIGATION OF EXCITATION MECHANISMS IN THE He—Cd PLASMA*

By

J. HELDT and L. KOCHANOWSKI

INSTITUTE OF PHYSICS, UNIVERSITY OF GDAŃSK, GDAŃSK, POLAND**

(Received 5. IV. 1977)

The intensity of 5337 and 5378 Å spontaneous emitted lines of Cd II were investigated as a function of helium pressure in the cataphoresis-type He—Cd discharge tube. The number of cadmium metastable atoms in the $^3P_2$ and $^3P_0$ states were determined by means of the absorption method. The intensity changes of the Cd II lines and the variation of cadmium metastable densities with He pressure indicate an existence of collisions between metastable Cd($^3P_{2,0}$) and He(^1S) atoms.

I. Introduction

In the He—Cd^+ laser, in which the cataphoresis-type discharge tube is used, the positive-column of the DC discharge determines the active medium of the laser. In this type of laser only two lines of ionised cadmium, i.e. the 4416 and 3250 Å lines, give lasing action. Now, it is generally accepted that Penning collisions between helium triplet metastable and neutral cadmium ground-state atoms are mainly responsible for the population inversion of the $5s^2\,^2D_{5/2} \rightarrow 5p\,^2P_{3/2}$ (4416 Å) and $5s^2\,^2D_{3/2} \rightarrow 5p\,^2P_{1/2}$ (3250 Å) transitions of the Cd II [1—4].

It follows from many papers [5—8] that in the positive-column of the He-metal plasma, an appreciable population of neutral metastable metal atoms is also observed. The number of helium and cadmium metastable atoms in the discharge plasma is of the order 10^{11} and 10^{12} atoms per cm^3, respectively, for 4 Torr helium pressure and a metal oven temperature of 475 °K [3, 9]. Collisions between these two kinds of metastable atoms can cause a new excitation mechanism to appear responsible for population of higher metal ionic levels. In the case of the He—Cd discharge this excitation process is given by the reaction:

$$Cd(^3P_{0,2}) + He^*(^1S_0) \rightarrow Cd^+(^2F) + He(^1S_0) + e + \Delta E\,. \qquad (1)$$

The yield of this reaction depends on the helium pressure and the discharge current.

* This work was supported by the Institute of Experimental Physics at University of Warszawa within the project 15—1.05

** Address: Institute of Physics, University of Gdańsk ul. Wita Stwosza 57, PL 80-952 Gdańsk, Poland

The existence of the above excitation mechanism can be confirmed, in the case of constant discharge current, by measurements of the relative intensity of ionic cadmium lines and by determining the population of the cadmium metastable atoms ($^3P_{0,2}$) as a function of the helium pressure in the discharge tube.

We report here the experimental results which confirm the presence of the mentioned excitation mechanism (1) in the cataphoresis-type He—Cd discharge tube.

II. Experiment

For relative intensity measurements of the cadmium ion lines the sidelight from the discharge tube was used. This light was focused on a grating spectrograph and detected on ORWO type WT–2 spectrographic plates. The response of the photographic emulsion has been corrected due to the spectral and energetic sensitivity of the plates. The line intensities, at constant discharge current, for various helium pressures were achieved on the same plate. During these measurements the cadmium pressure in the discharge tube was constant. This has been reached by constant temperature of the cadmium reservoir. The temperature of it was controlled by a thermocouple with an accuracy of about ± 0.5 °C.

The number of the cadmium metastable atoms has been determined from the absorption measurements at the centre of the line of the $^3P_2 \rightarrow {}^3S_1$ and $^3P_0 \rightarrow {}^3S_1$ transitions. Fig. 1 shows the scheme of the apparatus. In our experiment two He—Cd discharge tubes were applied. The first tube was used as a light source, the second as an absorbing gas layer. The absorbing length of the excited gas layer amounts to 5 cm. In order to get in the absorption tube a constant cadmium vapour pressure by the cataphoresis effect, the length of the discharge tube was longer than 5 cm, about 50 cm. This was reached

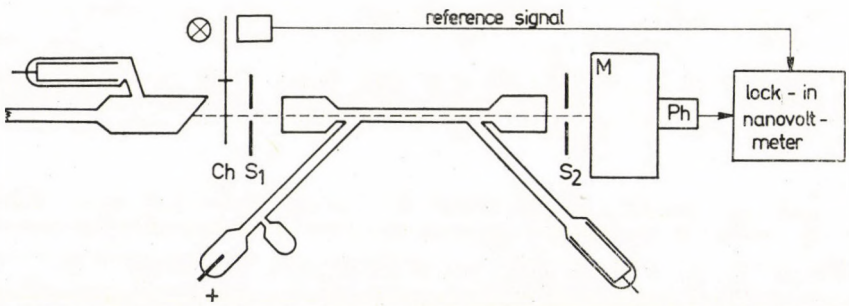

Fig. 1. The experimental set-up in the measurements of the population of the $^3P_2$ and $^3P_0$ metastable levels of Cd I
M — monochromator, S_1, S_2 — lenses, Ch — chopper, Ph — photomultiplier

by a special construction of the absorbing tube which is shown in Fig. 1. The diameter of both discharge tubes was 3 mm. The discharge tubes were supplied from stabilized high voltage suppliers.

In order to determine the number of the cadmium metastable atoms two types of line intensity measurements have been carried out using the lock-in technique. First the radiation from the source tube of a definite line, selected by the monochromator, was detected by the photomultiplier after passing the absorption cell containing pure He discharge. Thus current I_1 gives the intensity of the incident radiation. Next, in the same way, the intensity of this line was measured when the radiation from the source tube passed the absorption cell containing He—Cd discharge. The result of this measurement can be denoted as I_2 which gives the value of transmitted radiation through the absorbing gas layer. From our earlier publication [12] follows, that the Doppler profile of the absorption line is a good approximation for the intensity distribution of spectral lines observed in the DC discharge. Taking this into account, the ratio of the transmitted to the incident radiation $S = I_2/I_1$, can be expressed by [5]:

$$S = \frac{1}{\sqrt{\pi} k_0 l} \int_{-\infty}^{\infty} \left(1 - \exp\left(-k_0 l e^{-\omega^2}\right)\right) d\omega = 1 - \frac{k_0 l}{1! \sqrt{2}} + \ldots (1)^n \frac{(k_0 l)^n}{n! \sqrt{n+1}}, \quad (2)$$

where l is the length of the absorption layer, and the absorption coefficient, k_0, in the centre of the spectral line is defined as

$$\int_0^{\infty} k_\nu d\nu = \frac{1}{4} \sqrt{\frac{\pi}{\ln 2}} k_0 \Delta\nu_D \quad \text{and} \quad \omega = \frac{2(\nu - \nu_0)}{\Delta\nu_D} \sqrt{\ln 2}\,.$$

$\Delta\nu_D$ is the Doppler line width.

Since the population of the $^3S_1$ state of cadmium is considerably smaller than that of the $^3P_{0,2}$ states, the number N of the metastable atoms is given by [5]:

$$N = \frac{mc}{2\pi e^2 f} \sqrt{\frac{\pi}{\ln 2}} \cdot \Delta\nu_D \cdot k_0\,, \quad (3)$$

where f is the oscillator strength of the line, and the other constants have the usual sense. The population of the cadmium atoms in the metastable states $^3P_2$ and $^3P_0$ has been determined ranging helium pressure from 1.5 to 4.0 Torr. The cadmium vapour pressure (estimated from the temperature of the metal reservoir) and the DC current of the absorption cell for the absorption and the emission measurements were constant and equal to $8.15 \cdot 10^{-5}$ Torr and 100 mA, respectively.

III. Results and discussion

Fig. 2 shows a detail of energy level diagram of Cd I and Cd II, where the investigated lines and the energy levels of the He metastable states are also given. As is known from many papers [4, 10] the upper laser levels $4f\,^2F_{5/2,\,7/2}$, $6g\,^2G_{7/2,\,5/2}$ are pumped by charge transfer reactions of the ground state cadmium atom with He^+ ions, cascades from higher levels and by metal atoms and electron collisions. As it follows from Fig. 2 in the case of He—Cd plasma the $^2F_{5/2}$ and $^2F_{7/2}$ levels can also be populated by collisions of Cd and He metastable atoms. This mechanism is possible since the energies of $^2P_{5/2}$ and $^2F_{7/2}$ states are in good coincidence with the sum of energies of the metastable cadmium ($^3P_{2,0}$) and helium ($^1S_0$, $^3S_1$) atoms.

Fig. 3 gives the pressure dependence of the relative intensities of the 5337 and 5378 Å lines of Cd II. From Fig. 3 it follows that the relative intensity of the two lines increases rapidly with increasing He pressure, reaches the

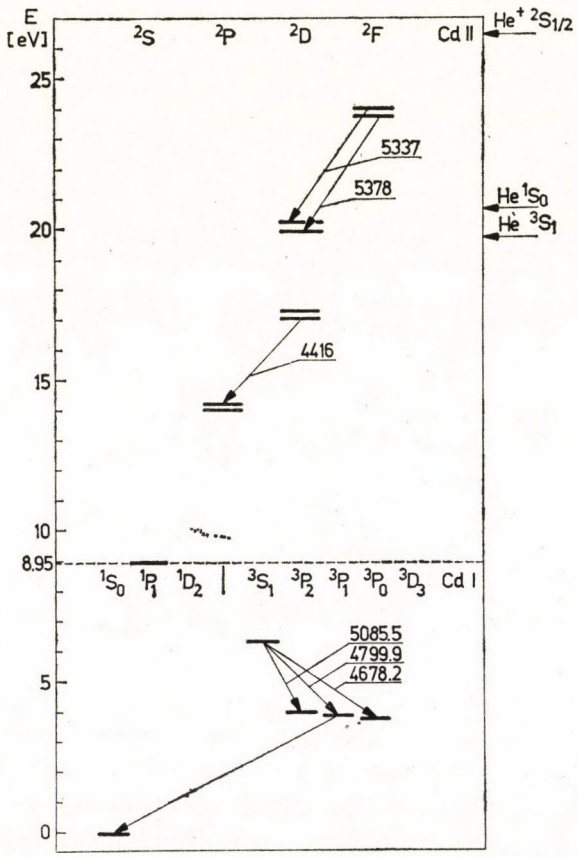

Fig. 2. The energy level diagram of Cd I and Cd II with the indicated lines investigated by us

maximum value at 3 Torr and, for higher He pressures, decreases slowly. This intensity dependence of the two green lines (λ 5337 and 5378 Å), as a function of He pressure, is in agreement with the measurements of GIALLORENZI et al [11]. This behaviour is in agreement with the population dependence of the Cd ($^3P_{2,0}$) metastable atom given in Fig. 4. The maximum of the cadmium metastable atoms population falls on 2.75 Torr which is in good agreement with the pressure dependence of the intensities of λ 5337 and 5378 Å lines. It must be noted that the ratios of the intensities (I_1/I_3) and populations ($N_{1,5}/N_3$) obtained for the pressures 1.5 and 3 Torr are equal and amount to about 40%. This means that the collision process described by Eq. (1) is responsible for the observed increase of the $^2F_{7/2}$ and $^2F_{5/2}$ level population. The participation of the mentioned pumping process of the $^2F_{7/2}$ and $^2F_{5/2}$ levels can be enlarged by using special gas mixtures filling out the cataphoresis-type He—Cd discharge tube. This will cause an increase of the Cd I $^3P_2$ and $^3P_0$ metastable states population as well as the population of the $^2F_{7/2}$, $^2F_{5/2}$ states of Cd II.

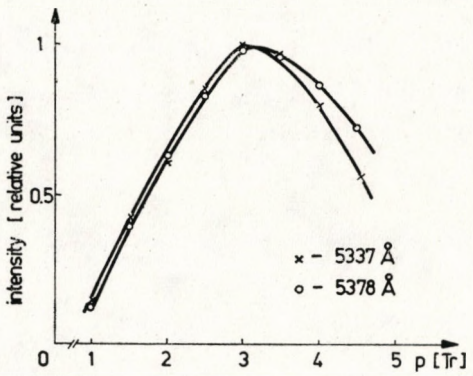

Fig. 3. Variation of the relative intensities the 5337 and 5378 Å lines of Cd II

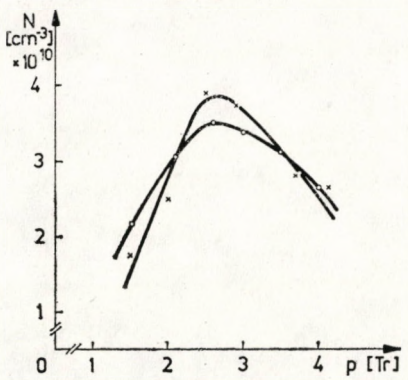

Fig. 4. Variation of cadmium metastable densities with helium pressure at constant discharge current. × — the population of the $^3P_0$ level; ○ — the population of the $^3P_2$ level

REFERENCES

1. W. T. SILFVAST, Phys. Rev. Lett., **27,** 1489, 1971.
2. M. K. DJATLOV, E. P. OSTAPCHENKO and V. A. STAPANOV, Opt. Spectrosc., **29,** 539, 1970.
3. P. G. BROWNE and M. H. DUNN, J. Phys. B, **6,** 1103, 1973.
4. A. R. TURNER-SMITH, J. M. GREEN and C. E. WEBB, J. Phys. B; Atom. molec. Phys., **3L,** 134, 1970.
5. A. C. G. MITCHELL and M. W. ZEMANSKY, Resonance Radiation and Excited Atoms, Cambridge University Press, London, 1961.
6. P. C. DROP and J. POLMAN, J. Phys. D. Appl. Phys., **5,** 562, 1972.
7. J. HELDT, L. KOCHANOWSKI and J. WOJTKOWIAK in VI Konferencja Elektroniki Kwantowej Poznan, 1974, *A*-**15** p. 66—67.
8. Z. LES and H. NIEWODNICZAŃSKI, Acta Phys. Polon., **7,** 365, 1958.
9. K. MIZYAKI, Y. OGATA, T. FUJMOTO and K. FUKUDA, Jap. J. of Appl. Phys., **13,** 1866, 1974.
10. J. A. PIPER and C. E. WEBB, J. Phys. D: Appl. Phys., **6,** 400, 1973.
11. T. G. GIALLORENZI and S. A. AHMED, IEEE J. Quantum Elect,. **7,** 11, 1971.
12. A. SIKORSKA, K. WEREL and J. HELDT, Bull. Acad. Pol. Sci. ser. math., astr. et phys., **24,** 661, 1976.

Acta Physica Academiae Scientiarum Hungaricae, Tomus 42 (4), pp. 339–342 (1977)

VALIDITY OF SPECTROPHOTOMETRIC DETERMINATION OF REFRACTIVE INDICES FOR THIN DIELECTRIC FILMS AND THEIR THICKNESSES

By

A. F. EL-SHAZLY

FACULTY OF EDUCATION, AIN SHAMS UNIVERSITY, CAIRO, EGYPT

T. A. EL-DESSOUKY

FACULTY OF SCIENCE, AIN SHAMS UNIVERSITY, CAIRO, EGYPT

and

H. K. EL-KHOLY

FACULTY OF SCIENCE, SANAA UNIVERSITY, SANAA, YEMEN

(Received in revised form 5. IV. 1977)

One of the familiar methods for determining the refractive index of thin dielectric films and their thicknesses is the spectrophotometric method. In this work it is shown that the applicability of the method requires the thickness investigated to exceed $\lambda/4$. The calculated refractive indices of thin dielectric films of optical thickness $\lambda/4$ were found to be lower than the correct value.

Several authors [1—5] applied spectrophotometric methods in determining the refractive indices of thin nonabsorbing dielectric films and their thicknesses; either by measuring the reflectance R or the transmittance T over a certain region of the spectrum. For ZnS films some authors [1, 2] used films of optical thickness $\lambda/4$. In this case it was observed that only one maximum reflection or one minimum transmission occurred over the visible region of spectrum. The refractive indices of such films for a certain wavelength, at which R_{max} or T_{min} ($T_{min} = 1 - R_{max}$, $A = 0$) were calculated using the well known relation:

$$n_f = \left[\frac{1 + \sqrt{R_{max}}}{1 - \sqrt{R_{max}}} n_0 n_g \right]^{1/2}.$$

where n_0 and n_g are the refractive indices of air and glass, respectively.

Using the value of the refractive index obtained before (n_f), the film thickness can be calculated using the following relation:

$$t = \frac{\lambda}{4 n_f}.$$

where λ is the wavelength at which T_{min} or R_{max} occurs corresponding to the zero order interference pattern at reflection.

Other authors [3—5] prepared thicker films ($t \gg \lambda/4$), the thicknesses of which determined by optical methods. Knowing the thickness of any film and measuring the reflectance or transmittance over a certain region of the spectrum, the refractive index is computed, applying expressions for R or T as shown in [3—5]. The results obtained by the first two authors using film thickness $\lambda/4$, are small as compared to those obtained by others.

To explain the difference between the values of the refractive indices obtained for thin films of zinc sulphide, the values of the refractive indices obtained from the dispersion curve [3—5] of ZnS thin films were used in this work.

The condition of dark interference fringes in transmission is $(m + 1/2)\lambda = 2n_f t$.

Putting $\lambda = 4750$, 5250, 5750, 6250, and 6750 Å for instance, then using the refractive indices corresponding to these wavelengths, taking $m = 1$ and 2, the corresponding thicknesses t_1 and t_2 were calculated. For each thickness the transmittance T was computed over a certain range of spectrum (450—700 nm) using the following relation:

$$T = \frac{16 n_g n_f^2}{(n_f + 1)^2 (n_f + n_g)^2 + (n_f - 1)^2 (n_f - n_g)^2 - 2(n_f^2 - 1)^2 (n_f^2 - n_g^2) \cos 4\pi n_f t/\lambda}.$$

The computed results are shown in Fig. 1, from which an envelope to the transmission minima for the first and second orders of interference was drawn. The curves A and B correspond to the first and second order of interference, respectively.

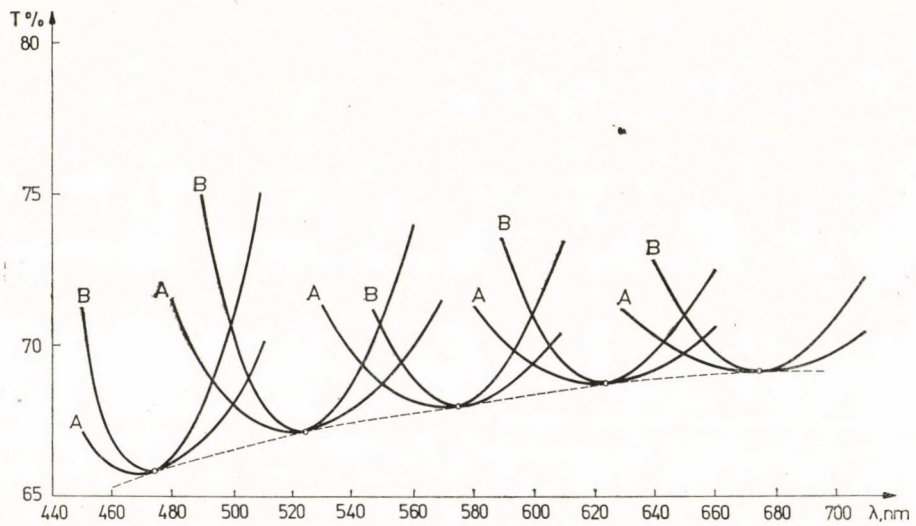

Fig. 1

For $\lambda = 5250$ Å, the refractive index $n_f = 2.366$.

The values of the film thicknesses when $m = 0, 1$ and 2 are 555 Å, 1665 Å and 2775 Å, respectively.

Fig. 2 shows the calculated transmission curves for these thicknesses corresponding to the zero order (curve 1), to the first order (curve 2) and to the second order (curve 3) of interference.

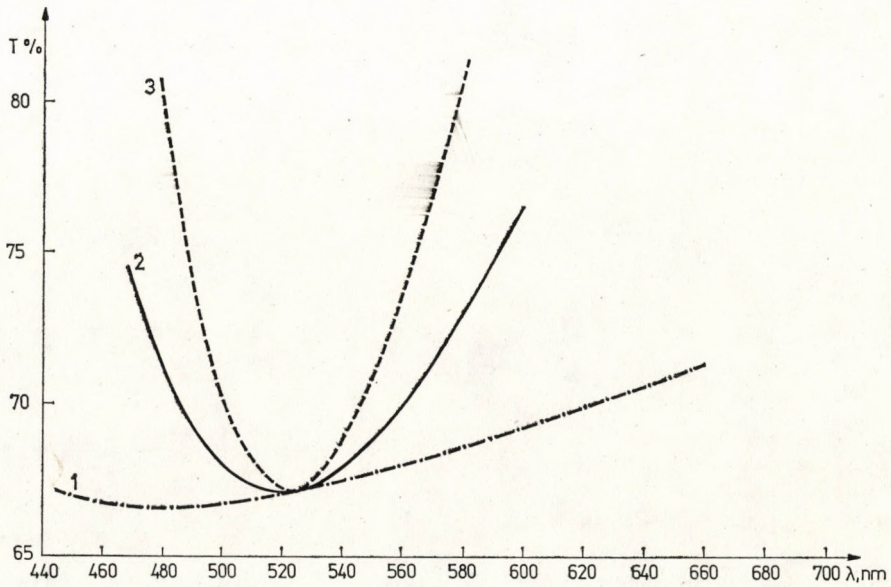

Fig. 2

As is well known, the three minima must coincide, but the minimum of curve (1) seems to be shifted towards shorter wavelengths. In our calculations it seems to be at $\lambda_{min} = 4900$ Å, at which $T = 0.666$. Therefore $(R_{max} = 1 - T_{min}) = 0.334$. Hence, the calculated refractive index $= 2.366$, while the actual value of the refractive index of ZnS thin films at $\lambda = 4900$ Å is 2.40.

The difference between the refractive index calculated here and the real one is due to the difference between the value of the transmittance taken from curve (1) at $\lambda = 4900$ Å and the actual value of T_{min} at the same wavelength which was calculated for higher orders at different positions in the spectral region as shown in Fig. 3.

On the other hand, when the calculated value of the refractive index was used to calculate the thickness of the film ($t = \lambda/4n_f$), the calculated value of the thickness was found to be 518 Å which is less than that in computing T (555 Å).

Conclusion. The optical thicknesses of thin dielectric films to be investigated using spectrophotometric methods must be slightly higher than $\lambda/4$. This conclusion is of considerable importance, because the refractive index and the thickness of such films of optical thickness $\lambda/4$ were found to be less than the correct values.

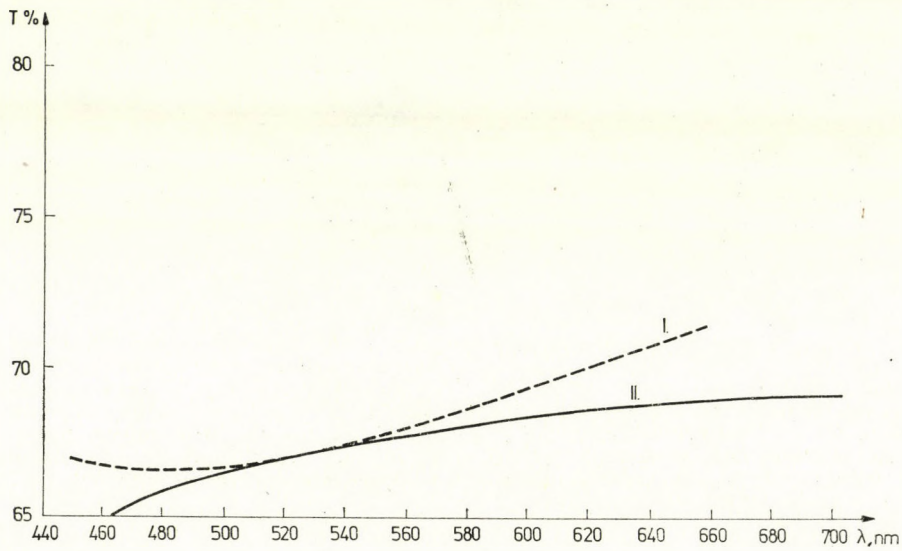

Fig. 3

The authors would like to express their thanks and gratitude to Prof. Dr. N. BARAKAT Dean of the Faculty of Science, Ain Shams University, Cairo, Egypt, for his valuable discussions and comments.

REFERENCES

1. J. L. ROOD, J. Opt. Soc. Am., **41**, 201, 1951.
2. R. I. OMEROV, I. N. SHKLYAREVSKII and G. I. PANOMAREVA, J. Opt. i Spektrosk., **26**, 1027, 1969.
3. J. F. HALL and W. F. FORGUSON, J. Opt. Soc. Am., **45**, 74, 1955
4. C. K. COOGAN, Proc. Phys. Soc. (London), **70**, 845, 1957.
5. I. N. SHKLYAREVSKII, A. F. A. El-SHAZLY and G. V. LESOVA, J. Opt. i Spektrosk., **30**, 1135, 1971.

Acta Physica Academiae Scientiarum Hungaricae, Tomus 42 (4) pp. 343—352 (1977)

CROSS-SECTION FLUCTUATIONS OF THE (d,p) AND (d,α) REACTIONS ON ^{31}P NUCLEUS AT 150°

By

O. E. BADAWY

PHYSICS DEPARTMENT, FACULTY OF SCIENCE, CAIRO UNIVERSITY, CAIRO, GIZA, EGYPT

and

A. A. EL-SOUROGY

PHYSICS DEPARTMENT, ATOMIC ENERGY COMMISSION ARE, CAIRO, EGYPT

(Received 6. IV. 1977)

The yield curves of the (d, p) and (d, α) reactions on ^{31}P nucleus are measured in 10 keV steps from 2.000 up to 2.500 MeV deuteron energy. The analysis of the measured cross-section fluctuations is carried out in terms of the ERICSON theory of statistical fluctuations. The average coherence width Γ obtained amounts to 20 ± 5 keV for the ^{33}S compound nucleus at an energy of excitation of 17.396 MeV, yielding a life time $\tau = 3.0 \times 10^{-20}$ sec. The absence of correlation between the different emitted groups and channels of decay of the ^{33}S compound nucleus is confirmed. Probability distribution of the cross section around their average is found to obey a X^2-distribution with $2N$ degrees of freedom (with N the effective channel number).

I. Introduction

The (d, p) and (d, α) reactions on ^{31}P targets were studied by many authors [1—4], in the deuteron energy range from about 1.0 up to 4.0 MeV, where the angular distributions of the emitted protons and alpha groups were measured, in an attempt to investigate the reaction mechanisms, especially that of the statistical theory. In the deuteron energy range from 7.0 up to 12.0 MeV, the (d, α) reaction on ^{31}P was investigated [5], and the results were analyzed in terms of the ERICSON theory of statistical fluctuation [6].

In the higher energy ranges, these reactions were investigated and analyzed by applying the DWBA theory of direct reactions [7, 8].

In the present work, the excitation functions of the (d, p) and (d, α) reactions on ^{31}P targets are measured in the deuteron energy range from 2.0 up to 2.5 MeV in order to investigate the compound nucleus contribution to the reaction mechanism. The results are analyzed by applying the ERICSON theory of the statistical fluctuations [6].

II. Experimental techniques and data analysis

The 2.5 MeV vertically mounted electrostatic accelerator of the ARE Atomic Energy Establishment served as a source of deuterons (with energy resolution of $\sim 0.25\%$). For the charged particle detection, we used a two

semi-conductor spectrometer which utilizes two solid state semiconductors of $(p - n)$ type for simultaneous recording of the (d, p) and (d, α) reactions on the same target. These two detectors are mounted inside a scattering chamber and adjusted at the desired angles of measurements. The details of the experimental procedures are given in [9]. The spectrometer is schematically shown in Fig. 1.

^{31}P targets were prepared by evaporating Zn_2P_3 onto thin Ag backing. The spectra of elastically scattered deuterons gave a value for the target thickness equivalent to $\sim$ 10 KeV energy loss at 2.0 MeV energy of deuterons.

The data are analyzed according to the ERICSON, BRINK and STEPHEN theories [6]. The two main correlation parameters describing the cross-section

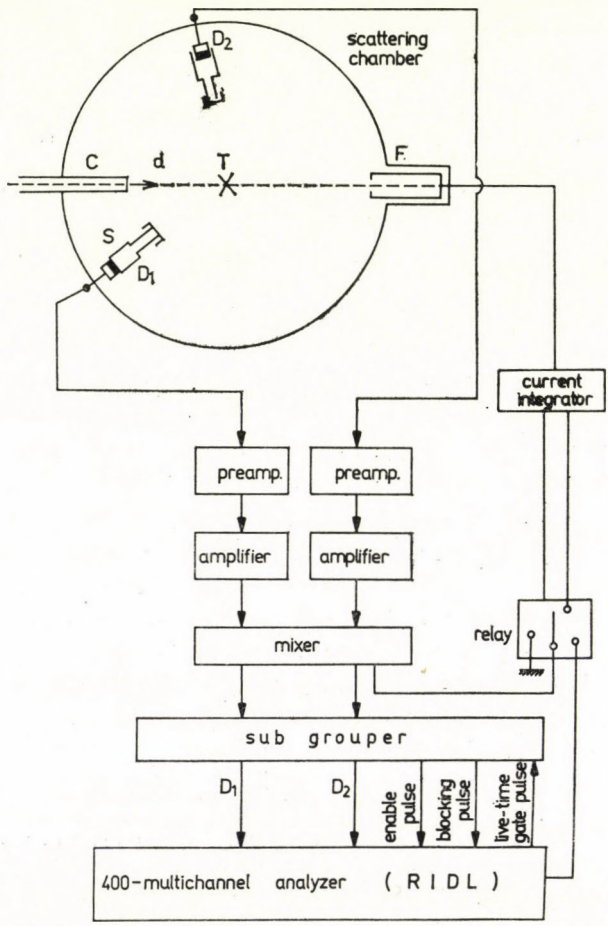

Fig. 1. Two-detector spectrometer. C: collimator, d: deuteron beam, T: target, S: diaphragm, D_1 and D_2: two detectors and F: Faraday cup

fluctuations are the auto-correlation and the group-cross correlation functions, defined by ERICSON [6] as follows:

The auto-correlation function $R(\epsilon)$

$$R(\epsilon) = \left\langle \frac{[\sigma(E) - \langle\sigma(E)\rangle][\sigma(E+\epsilon) - \langle\sigma(E+\epsilon)\rangle]}{\langle\sigma(E)\rangle\langle\sigma(E+\epsilon)\rangle} \right\rangle . \tag{1}$$

The group cross correlation function $R_{a,b}(\epsilon)$

$$R_{a,b}(\epsilon) = \left\langle 1/2 \left[\frac{[\sigma_a(E) - \langle\sigma_a(E)\rangle][\sigma_b(E+\epsilon) - \langle\sigma_b(E+\epsilon)\rangle]}{[\langle\sigma_a(E)\rangle\langle\sigma_b(E+\epsilon)\rangle]} + \right.\right.$$
$$\left.\left. + \frac{[\sigma_a(E+\epsilon) - \langle\sigma_a(E+\epsilon)\rangle][\sigma_b(E) - \langle\sigma_b(E)\rangle]}{[\langle\sigma_a(E+\epsilon)\rangle\langle\sigma_b(E)\rangle]} \right] \right\rangle . \tag{2}$$

The average cross-sections $\langle\sigma(E)\rangle$ at an energy E were represented by a non-periodic Fourier series or with a straight line obtained by a least square fit to the experimental values. Such averaging methods are discussed in detail elsewhere [10].

As predicted by ERICSON [6], the auto correlation function $R(\epsilon)$ is of a Lorentzian shape of half width equal to the level width in such an overlapping region of excitation of the formed compound nuclei. The determination of such level width Γ enabled us then to calculate the lifetime τ. On the other hand, the theory predicts no correlation to be present between the different groups (a and b) given by relation (2).

As stated by ERICSON [6] the cross-section fluctuations will have a X^2 distribution with $2N$ degrees of freedom, i.e. a Thomas—Porter distribution.

$$P(\eta) = \frac{N}{(N-1)!} (N\eta)^{N-1} \exp(-N\eta) , \tag{3}$$

where $\eta = \sigma/\langle\sigma\rangle$ and N is the number of incoherent statistically independent competing channels, i.e. the effective channel number of the reaction.

In all the above functions the average is done over an energy interval $\Delta E \gg \Gamma$. The errors due to the finite range of data (FRD) are calculated according to reference [11]. The analysis of data is carried out with a special program on the 1905E—ICL electronic computer of Cairo University.

III. Results and discussion

1. *Yield curves*

The yield curves for the various studied proton and α-groups (see Table I and Fig. 2a, b for all information), are displayed in Figs 3 and 4. Different runs for parts of the curves were measured for reproducibility. Marked fluctuations of the cross-sections can be easily seen.

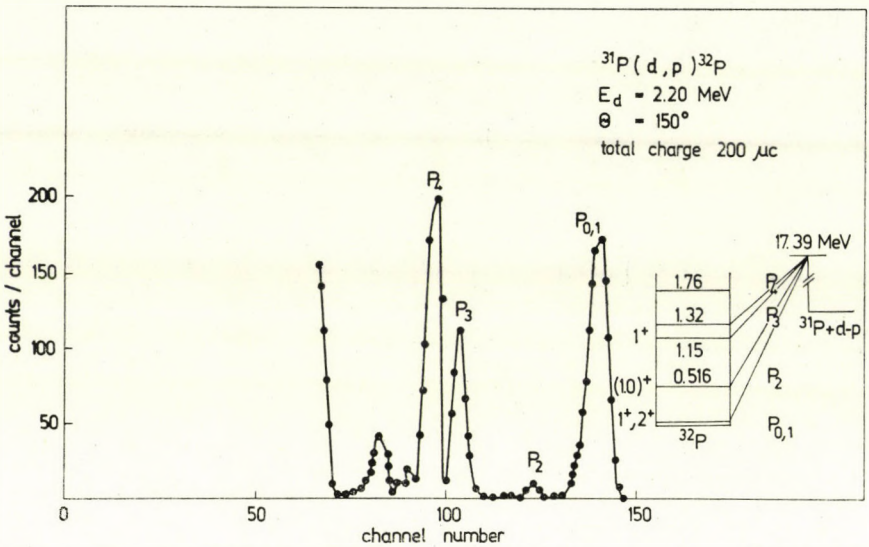

Fig. 2a. Typical spectrum of proton groups emitted from deuteron bombardment of a natural phosphorus target, recorded on the multichannel analyzer. All labelled peaks correspond to single levels in the ^{32}P nucleus

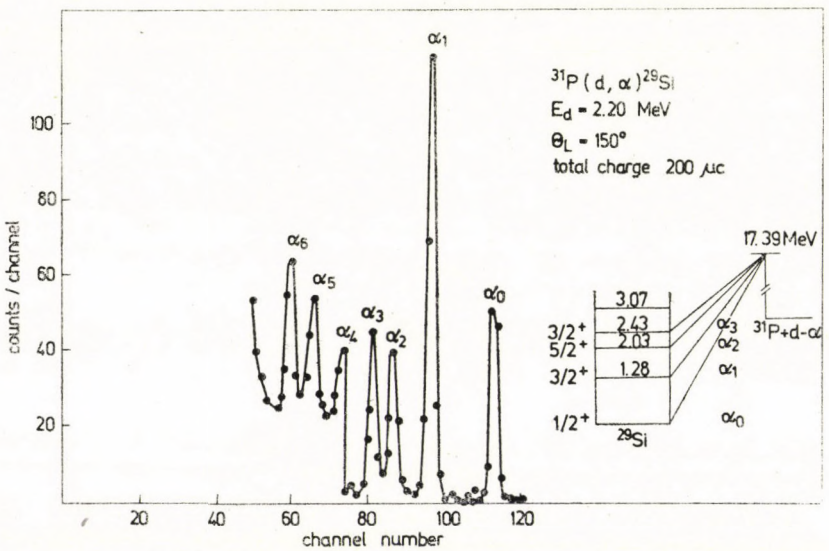

Fig. 2b. Typical spectrum of the α-groups emitted from deuteron bombardment of a natura phosphorus target, recorded on the multichannel analyzer. All labelled peaks correspond to single levels in the ^{29}Si nucleus

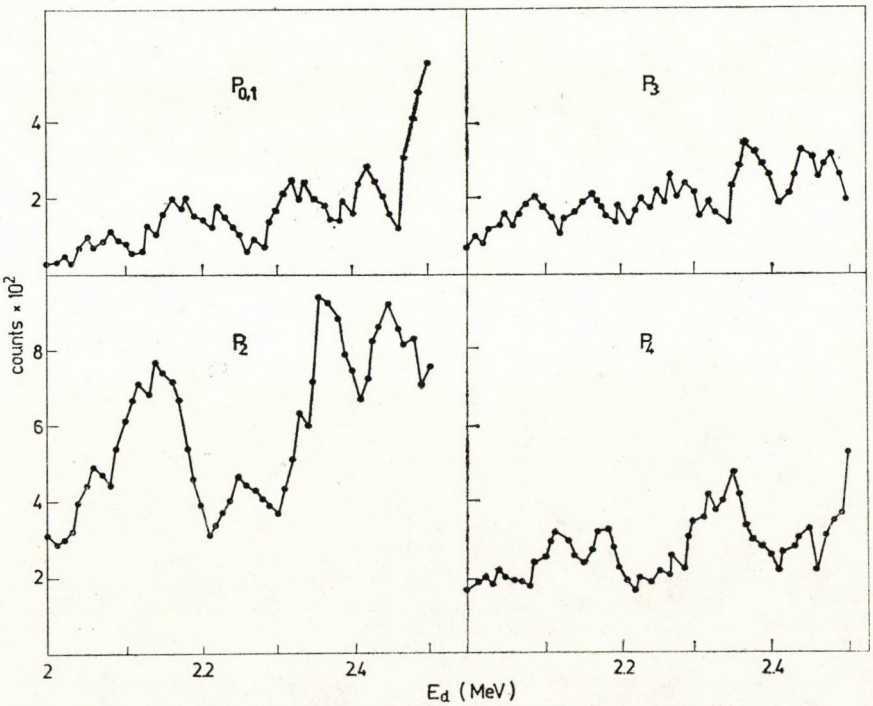

Fig. 3. Excitation functions of the ^{31}P (d,p)^{32}P reactions leading to the first five excited states of the ^{32}P nucleus measured at the scattering angle 150°. The statistical errors are within the dots

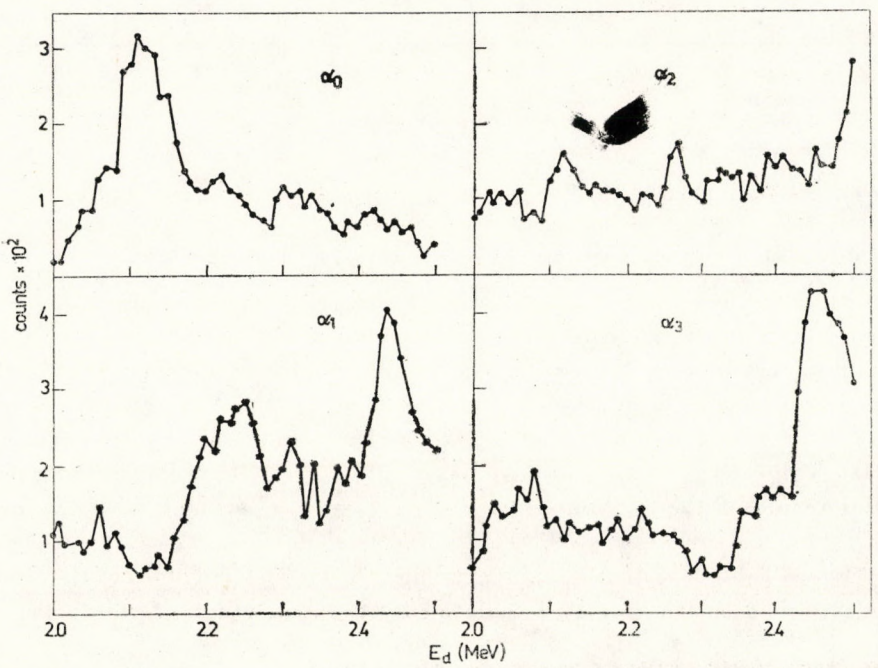

Fig. 4. Excitation functions of the ^{31}P(d,α)^{29}Si reactions leading to the first four excited states of the ^{29}Si nucleus measured at the scattering angle 150°. The statistical errors are within the dots

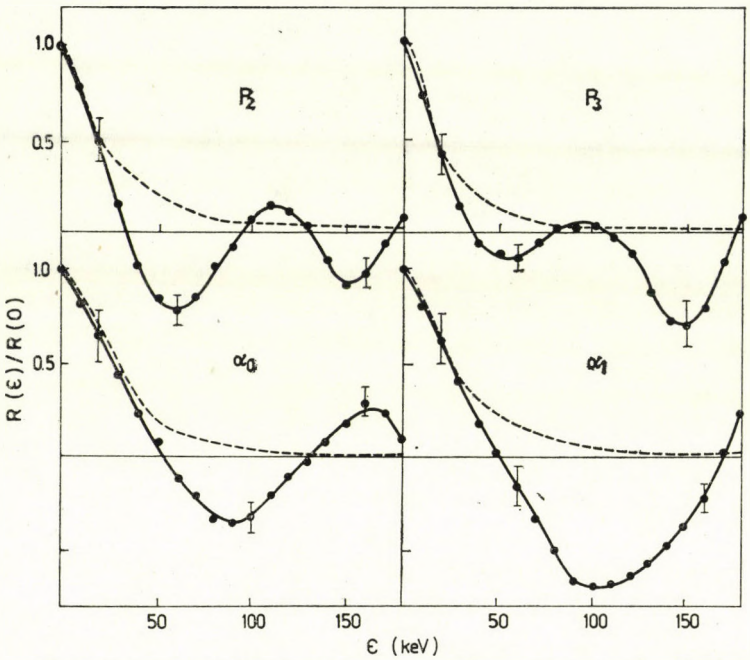

Fig. 5. Normalized auto-correlation functions of the fluctuations in the differential cross-sections for some of the studied proton and α-groups at the scattering angle 150°. The dashed line is the theoretical Lorentzian expression

Table I

Reaction	Groups studied	Compound nucleus	Average excitation energy MeV	Angle of measurement
$^{31}P(d, p)^{32}P$	$P_{0,1}$, P_2, P_3, P_4	^{33}S	17.396	150°
$^{31}P(d, \alpha)^{29}Si$	α_0, α_1, α_2, α_3	^{33}S	17.396	150°

2. *Auto-correlation and probability distributions of cross sections*

Fig. 5 shows an example of the normalized autocorrelation functions for some of the studied proton and α-groups. The Lorentzian expressions calculated for the same value of the coherence width Γ are shown by dashed lines. The marked fluctuations of the auto-correlation function around the ϵ-axis for $\epsilon \gg \Gamma$ reflects the effect of the finite range of experimental data (FRD). Table II gives the results of the auto-correlation analysis. The order of magnitude of the life-time $\tau = 10^{-20}$ sec is in agreement with the order of the slow reaction time of the compound nucleus mechanism.

From Table II we can see the agreement between the values of the fluctuation damping coefficients N calculated by the spin weight formula [6] and

Table II

Results of fluctuation analysis of ^{31}P(d, p)^{32}P and ^{31}P(d, α)^{29}Si reactions at $E_d = 2000-2500$ KeV

Reaction	Group	Residual nucleus level spin	N_{cal}	N_{exp}	Auto Correl.		Four. Tech.		τ sec
					Γ KeV	$\overline{\Gamma}$ KeV	Γ KeV	$\overline{\Gamma}$ KeV	
^{31}P(d, p)^{32}P	$P_{0,1}$	(1$^+$, 2$^+$)	—	8±2	16		13		3.56×10^{-20}
	P_2	1$^+$	18	33±7	20	18.5	22	19.0	
	P_3	1$^+$	10	17±3	17		20		
	P_4	—	—	20±4	21		21		
^{31}P(d, α)^{29}Si	0	1/2$^+$	6	4±1	27		22		3.0×10^{-20}
	1	3/2$^+$	12	10±2	26	22	23.5	20.5	
	2	5/2$^+$	18	21+4	14		16		
	3	3/2$^+$	12	11+2	21		20		

— N_{cal} is the value calculated by the spin weight formula 6.
— N_{exp} is the experimental damping coefficient which is equal to $1/R(0)$.
— Γ refers to the width.
— $\overline{\Gamma}$ the average width.
— Four. Tech. The width obtained by the technique of Fourier analysis.
— τ is the average lifetime of the compound nucleus ^{33}S in this energy range of excitation.
— The FRD error in Γ value is $\simeq 20\%$.
— The values not reported for N are those corresponding to the levels whose spins are not known.

that obtained as $N = 1/R\ (0)$ (neglecting the direct part contribution). The deviations observed in some cases are due to the presence of some contributions from intermediate structures and/or direct mechanisms.

Beside the auto-correlation analysis, the technique of Fourier analysis [10] was used to obtained the coherence width Γ. Thus if an excitation function $\sigma(E)$ is expanded in a Fourier series, then according to [12], a plot of $\log(a_k^2 + b_k^2)$ against k gives the mean width Γ (with a_k and b_k referring to the coefficients of the cosine and sine terms of the expansion of order k, respectively). Fig. 6 shows an example of this analysis, and the results are given in Table II.

The Thomas—Porter distribution was found to describe well the probability distribution of cross-sections around their averages as can be seen from Fig. 7. The deviations in some cases are attributed to the neglection of the structures and mechanisms other than compound nucleus in the calculations. This will be treated in detail in our future work [13].

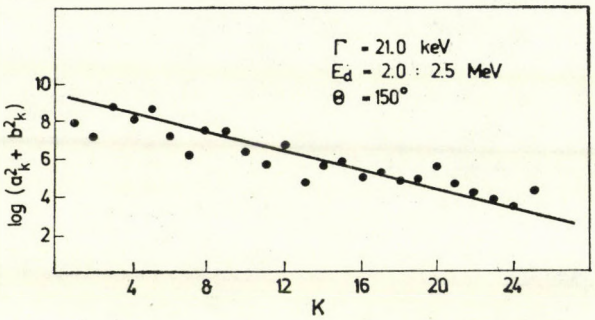

Fig. 6. The determination of the width for p_4 from the reaction ^{31}P (d,p)^{32}P using the technique of Fourier analysis. $\Gamma = 21.0$ KeV which is the same as that obtained from the auto-correlation analysis

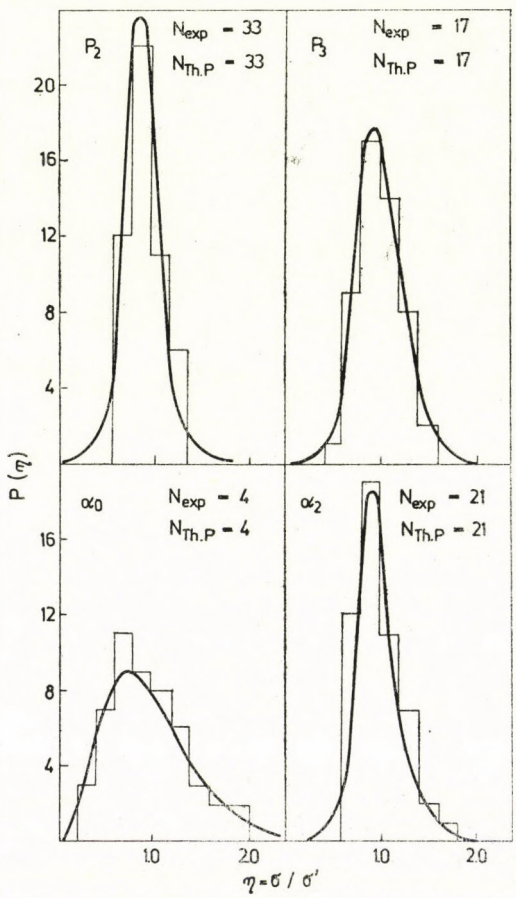

Fig. 7. The cross-section probability distribution histograms for some of the studied proton and α-groups. The experimental histograms are fitted with the theoretical curves assuming no direct interaction contribution

3. *Group-cross correlation*

Fig. 8 presents examples of the group-cross-correlation function between some of the emitted alphas, protons, as well as between the two. It is clear, how the correlation between the different groups and channels of decay is highly suppressed relative to the auto correlation of each of them shown in

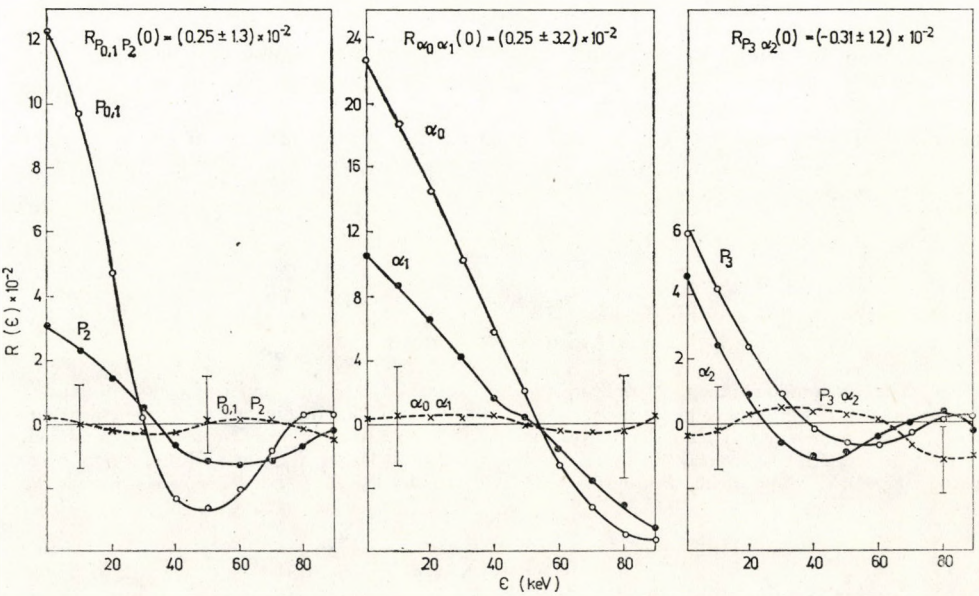

Fig. 8. Absolute auto correlation functions and cross correlation functions in the differential cross sections for some of the studied protons, α-groups, as well as between the two. ($E_d = (2.0 : 2.5)$ MeV, $\Theta = 150°$)

the same Figure. The final results of group cross-correlation analysis gave an overall value of 0.22 ± 1.10, 0.01 ± 0.10, and 0.9 ± 2.0 (for the value of the normalized group cross correlation function i.e. Eq. 2 at $\epsilon = 0$) for the different α, p and α with p groups, respectively. This result is in agreement with the ERICSON predictions as stated in Section II.

IV. Conclusion

Table III summarizes the different properties of the studied reactions, and the results of the analysis of the statistical fluctuations of the differential cross-sections of these reactions at 150°. As is clear, the overlapping conditions $\Gamma/D \gg 1$ are fulfilled in the two reactions. The lifetime $\tau = 3.280 \times 10^{-20}$ sec of the compound nucleus ^{33}S cannot be determined by the conventional methods. The realization of the predictions of the statistical theory indicates

Table III

Reaction	Compound nucleus	Average excitation energy (MeV)	ϱ MeV^{-1}	D KeV	Γ KeV	Γ/D
$^{31}P(d, p)^{32}P$	^{33}S	17.396	10	0.1	18.5	185
$^{31}P(d, \alpha)^{29}Si$	^{33}S	17.396	10	0.1	22.0	220

ϱ is calculated according to [14].
ϱ is the level density of the compound nucleus ^{33}S at the excitation energy stated
D is the level spacing $D = 1/\varrho$

that the interference between direct and compound processes in these studied reactions is small. The determined coherence width Γ being more than the energy resolution of the incident beam rules out the observed fluctuations to be due to energy resolution.

Acknowledgement

The authors are deeply indebted to Professor M. EL-NADI for his valuable scientific discussions and for having generously offered all the facilities in his power to complete this work. Thanks are due to Dr's V. Y. GONCHAR, L. EL-NADI and D. A. E. DARWISH for their help during the experimental measurements. Thanks are due to Dr. M. K. HEGAB for his help in the computer work. The perfect running of the accelerator by the specialized group is appreciated.

REFERENCES

1. G. L. VYSOTSKIJ, I. I. ZALYUBOVSKII, A. V. KUZNICHENKO, A. P. LOBKOVSKII, K. F. USTIMENKOV, V. M. ZABEGAI, A. E. MELENEVSKII, O. F. NEMETS and V. I. NEMYKIN, Izv. Akad. Nauk SSSR, Ser. Fiz., **36,** 2641, 1972.
2. G. L. VYSOTSKIJ, I. I. ZALYUBOVSKII, A. V. KUZNICHENKO, A. P. LOBKOVSKII and K. F. USTIMENKOV, AN SSSR, Moscow, Conf. 1974.
3. A. T. BARANIK, M. A. ABUZEID, M. I. EL-ZAIKI and I. I. ZALYUBOVSKII, Nuclear Physics, **72,** 49, 1965.
4. M. A. ABUZEID, A. T. BARANIK, M. I. EL-ZAIKI, V. Y. GONCHAR, S. M. MORSY and I. I. ZALYUBOVSKII, Nuclear Physics, **62,** 410, 1965.
5. G. A. LOCK, J. R. CURRY, P. J. RILEY and C. G. SHUGERT, Phys. Rev., **176,** 1293, 1968.
6. T. E. ERICSON, Adv. in Physics, **9,** 425, 1960;
   T. E. ERICSON, Annals of Physics, **23,** 390, 1963;
   T. E. ERICSON, Physics Letters, **4,** 258, 1963;
   D. M. BRINK, B. O. STEPHEN and N. W. TANNER, Nuclear Physics, **54,** 577, 1964.
7. J. M. VAN GASTEREN, A. J. L. VERDRAGE and J. F. VAN DER LEEN, Nucl. Phys., **A210,** 29, 1973.
8. J. R. CURRY, W. R. COKER and P. J. RILEY, Phys. Rev., **185,** 1416, 1969.
9. M. A. ABUZEID, A. T. BARANIK, M. I. EL-ZAIKI, V. J. GONCHAR, S. M. MORSY and I. I. ZALYUBOVSKI, Nuclear Instruments and Methods, **30,** 151, 1964.
10. J. O. V. HELLSTROM, Thesis, Canberra, 1970.
11. I. HALL, Physics Letters, **10,** 199, 1964.
12. I. BONDORF and R. B. LEACHMAN, Mat. — Fys. Meddr, **34,** 10, 1965.
13. O. E. BADAWY and A. A. EL-SOUROGY, to be published.
14. A. G. GILBERT and A. G. W. CAMERON, Canadian J. of Physics, **43,** 1446, 1965.

Acta Physica Academiae Scientiarum Hungaricae, Tomus 42 (4), pp. 353—364 (1977)

GELL-MANN AND LOW TYPE RENORMALIZATION GROUP AND THE φ^6 THEORY

By

G. FORGÁCS and A. ZAWADOWSKI

SOLID STATE PHYSICS DEPARTMENT, CENTRAL, RESEARCH INSTITUTE FOR PHYSICS
1525 BUDAPEST

(Received 12. IV. 1977)

The φ^6 theory is investigated using a modified version of the GELL-MANN and LOW renormalization group. Tricritical and critical properties in (or near) three dimensions are discussed.

1. Introduction

Since WILSON's outstanding work [1] renormalization group technique has been widely used in high energy physics and statistical mechanics. This method among others gave new insight into the problems of phase transitions, anomalous dimensions, asymptotic freedom, etc. The term renormalization group is not new in physics and the best would be to speak of the revival of this approach. Renormalization group was successfully used in quantum electrodynamics by GELL—MANN and LOW [2] to describe ultraviolet and infrared properties of different vertex functions. The CALLAN—SYMANZIK equation [3] is also one of the possible formulations of the renormalization group. So, renormalization group is neither new, nor unique. Each of the above mentioned methods applied to the same problems gave the same results. But while the GELL—MANN and LOW theory is tightly connected with perturbation theory (and the same is valid for the CALLAN—SYMANZIK equation) the advantage of the WILSON's method is that in principle it can be formulated independently of the perturbation theory and in special cases concrete calculations can be performed without any reference to perturbation theory. Besides the above mentioned methods there are others which can also deal with the problems of critical phenomena, such as MIGDAL's and POLJAKOV's bootsrap model [4], [5], ABRAHAM's and TSUNETO's skeleton graph expansion [6]. In this paper we would like to further investigate the method first used by SÓLYOM [7]. This method may be called the combination of the GELL—MANN and LOW and the WILSON method. In this context the following fact is very important. In the WILSON's case the underlying physics is quite clear, while in the GELL—MANN and LOW method one cannot say that (at least not if statistical mechanical methods are investigated). On the other hand, in our opinion, from the mathematical point of view the latter method

is much more tractable, since all the mathematics is contained in the Lie equations, characteristic of any continuous group. The advantages of both methods are contained in SÓLYOM's formulation of the renormalization group. More precisely it means that in this variant the cut-off transformation of Kadanoff is explicit, the mathematics is in the Lie equations and the method is applicable to any renormalizable theory. At least the applications so far, such as to the X-ray absorption [8], Kondo-problem [9], one-dimensional electron systems [7], [10], the calculation of anomalous dimensions [11], static critical phenomena [12] and dynamical critical phenomena [13] are consistent with this statement. The results in the case of the above listed applications were equivalent to those obtained by different methods. However all these problems are so-called logarithmic, that is if we let the physical cut-off in momentum space tend to infinity logarithmic divergencies would always appear. The relevant infrared divergencies are also of logarithmic form. It would be good to know the limits of the applicability of this method, since it is extremely simple and physically very clear, so if known exactly to what problems it can be applied, much work could be spared.

It is the aim of this paper to try to give an answer to the above question. For this reason we will very briefly describe the method (an extensive discussion of this method and also comparison of it with the traditional GELL-MANN and LOW theory is given in [12]), then apply it to a renormalizable, but not purely logarithmic problem (the φ^6 theory in 3-ε dimensions). As a result we will obtain correct tricritical indices (correct to the calculated order). Then we will investigate ordinary critical phenomena in $d = 3$ dimensions, and will see how the problem of strong coupling manifests itself in this approach. We will see, when comparing the results obtained by this method with those of the traditional GELL-MANN and LOW theory, that neither method is worse then the other in describing critical phenomena at $d = 3$. Nothing more definite can be said because of the strong coupling region.

2. The modified Gell-Mann and Low renormalization group

Let us assume that the Hamiltonian $\mathcal{H}$ describes a renormalizable theory. Let

$$\mathcal{H} = \mathcal{H}_0 + \mathcal{H}_{\text{int}}, \tag{2.1}$$

where

$$\mathcal{H}_{\text{int}} = \sum_{i=1}^{\infty} \alpha_k O_k . \tag{2.2}$$

Here O_k are operators constructed out of the basic fields of the theory, α_k are the coupling constants. We associate with each O_k a vertex function Γ_k:

$$\Gamma_k = \langle \mid O_k \mid \rangle . \tag{2.3}$$

In the field theory $\langle\ \rangle$ denotes vacuum expectation value, in statistical mechanics it is the statistical average. The Γ_k are defined in such a way that in the zeroeth order of the perturbation theory all are equal to unity. If there are n basic fields in the theory, there will be n propagators $G_1, G_2, \ldots, G_n$. Introducing a cut-off Λ in the momentum space, we assume the following invariance properties to be valid:

$$G_s(p^2, m_i^2, \alpha_k, \Lambda) = z_s G_s(p^2, m_i^2, \tilde{\alpha}_k, \tilde{\Lambda}),\quad s, i = 1, \ldots n;\quad k = 1, \ldots \infty\,. \tag{2.4}$$

$$\Gamma_k(p_1, p_2, \ldots; m_i^2, \alpha_l, \Lambda) = \bar{z}_k^{-1}\Gamma_k(p_1, p_2 \ldots; m_i^2, \tilde{\alpha}_l, \tilde{\Lambda});\quad l = 1, \ldots \infty \tag{2.5}$$

$$\tilde{\alpha}_k = \alpha_k f(z_s, \bar{z}_k)\,. \tag{2.6}$$

Here m_l are the renormalized masses (mass renormalization is performed on mass shell; see below for the specific model), $f(z_s, \bar{z}_k)$ is a product of a certain number of z_s and one $\bar{z}_k$. The explicit form of the f function is constructed in such a way that the following relations hold:

$$\alpha_l\Gamma_l(p_1, \ldots; m_i^2, \alpha_k, \Lambda) \prod_{s=1}^{n} G_s^{l_s}(p^2, m_i^2, \alpha_k, \Lambda) =$$

$$\tilde{\alpha}_l\Gamma_l(p_1, \ldots; m_i^2, \tilde{\alpha}_k, \tilde{\Lambda}) \prod_{s=1}^{n} G_s^{l_s}(p^2, m_i^2, \tilde{\alpha}_k, \tilde{\Lambda});\quad i = 1, \ldots \infty;\ k = 1, \ldots \infty\,, \tag{2.7}$$

where $\sum_{s=1}^{n} l_s = l_p/2$; l_p is the number of the incoming lines in the l-th vertex. Note that the z_s, $\bar{z}_k$ factors can be expressed by Γ_k and G_k from Eqs. (2.4) and (2.5), so the f function can also be written in terms of z_s, $\bar{z}_k$. What do the invariance equations mean? They mean (if they are valid) that for the matrix elements of the S-matrix of the field theory (in statistical mechanics the analogue of the S-matrix is the partition function)

$$\delta S_{\alpha\beta} = \frac{\partial S_{\alpha\beta}}{\partial \Lambda}\,\delta\Lambda + \sum_{i=1}^{\infty} \frac{\partial S_{\alpha\beta}}{\partial \alpha_i}\,\delta\alpha_i = 0\,, \tag{2.8}$$

where the $\delta\alpha_i$ changes are consistent with (2.6). It is assumed that the factors z_i, $\bar{z}_k$ are functions only of α_k and $\tilde{\Lambda}/\Lambda$, but are independent of the momenta and masses. We can prove the validity of these transformations only a posteriori by the help of the perturbation theory. In all the applications so far it turned out that the transformations (2.4)—(2.6) along with (2.7) could be built up explicitly.

Introducing dimensionless coupling constants, and dimensionless functions $d_s = G_s/G_s^0$ (G_s^0 are the bare propagators), after eliminating the z factors, Eqs. (2.4)—(2.6) can be cast into differential form:

$$\frac{\partial}{\partial w} \ln A(x, y_i, u_k, \Lambda) = \frac{1}{w}\left[\frac{\partial}{\partial \xi} \ln A\big(\xi, y_i, u_k^R(w, u_k)\big)\right]_{\xi=1}. \tag{2.9}$$

A can be any of the d_s, Γ_k, u_k^R functions. Here $w = x, y_1, \ldots y_n$; $x = p^2/\Lambda^2$, $y_i = m_i^2/\Lambda^2$; u_k are dimensionless coupling constants, $u_k^R(w, u_l)$ are called invariant coupling constants, (defined later for the specific model), the transformations (2.4)—(2.6) leave them invariant.

$$u_k^R(w, u_l) = \tilde{u}_k^R \mid_{\Lambda \to \tilde{\Lambda},\, a_k \to \tilde{a}_k}. \tag{2.10}$$

The Eqs. (2.9) are the Lie equations of the renormalization group. These equations do not determine uniquely the functions A [13']. In the general solution arbitrary functions of several variables appear. Therefore what one can do is to calculate the right hand sides by the help of perturbation theory and then to solve the equations; in this way improving the results of the perturbational calculations.

3. The φ^6 theory

Let our Hamiltonian be in d dimensional space

$$\mathcal{H} = \int d^9x \left\{ \frac{r_0}{2} \sum_{i=1}^{N} \varphi_i^2(x) + \frac{1}{2} \sum_{i=1}^{N} (\nabla \varphi_i)^2 + \frac{\alpha_4}{4!} \left(\sum_{i=1}^{N} \varphi_i^2 \right)^2 + \frac{\alpha_6}{6!} \left(\sum_{i=1}^{N} \varphi_i^2 \right)^3 \right\}. \tag{3.1}$$

(It is actually the Hamiltonian divided by kT, where k is the Boltzmann constant, T is the temperature.) This corresponds to

$$n = N, \quad O_1 = \frac{1}{4!} \left(\sum_{i=1}^{N} \varphi_i^2 \right)^2, \quad O_2 = \frac{1}{6!} \left(\sum_{i=1}^{N} \varphi_i^2 \right)^3 \tag{3.2}$$

in the previous Section, but actually all the propagators are equal and we call them G. Let us perform mass renormalization in such a way that

$$G^{-1}(k^2, m^2, \alpha_4\, \alpha_6, \Lambda)_{k^2 = -m^2} = 0\,. \tag{3.3}$$

The statistical mechanical analogue of m is the coherence length ξ, namely

$$m = \xi^{-1}\,. \tag{3.4}$$

It means m disappears on the critical line. The equations corresponding to (2.4)—(2.6), expressed via dimensionless quantities, are

$$d\left(\frac{k^2}{\Lambda^2}, \frac{m^2}{\Lambda^2}, u_4, u_6 \right) = z_1 \left(\frac{\tilde{\Lambda}^2}{\Lambda^2}, u_4, u_6 \right) d\left(\frac{k^2}{\tilde{\Lambda}^2}, \frac{m^2}{\tilde{\Lambda}^2}, \tilde{u}_4, \tilde{u}_6 \right), \tag{3.5}$$

$$\Gamma_4\left(\frac{k^2}{\Lambda^2}, \frac{m^2}{\Lambda^2}, u_4, u_6\right) = z_2^{-1}\left(\frac{\tilde{\Lambda}^2}{\Lambda^2}, u_4, u_6\right) \Gamma_4\left(\frac{k^2}{\tilde{\Lambda}^2}, \frac{m^2}{\tilde{\Lambda}^2}, \tilde{u}_4, \tilde{u}_6\right), \tag{3.6}$$

$$\Gamma_6\left(\frac{k^2}{\Lambda^2}, \frac{m^2}{\Lambda^2}, u_4, u_6\right) = z_3^{-1}\left(\frac{\tilde{\Lambda}^2}{\Lambda^2}, u_4, u_6\right) \Gamma_6\left(\frac{k^2}{\tilde{\Lambda}^2}, \frac{m^2}{\tilde{\Lambda}^2}, \tilde{u}_4, \tilde{u}_6\right), \tag{3.7}$$

$$\tilde{u}_4 = u_4\left(\frac{\Lambda}{\tilde{\Lambda}}\right)^{4-d} z_1^2\left(\frac{\tilde{\Lambda}^2}{\Lambda^2}, u_4, u_6\right) z_2^{-1}\left(\frac{\tilde{\Lambda}^2}{\Lambda^2}, u_4, u_6\right), \tag{3.8}$$

$$\tilde{u}_6 = u_6\left(\frac{\Lambda}{\tilde{\Lambda}}\right)^{6-2d} z_1^3\left(\frac{\tilde{\Lambda}^2}{\Lambda^2}, u_4, u_6\right) z_3^{-1}\left(\frac{\tilde{\Lambda}^2}{\Lambda^2}, u_4, u_6\right). \tag{3.9}$$

Here

$$u_4 = \alpha_4 \Lambda^{d-4}, \quad u_6 = \alpha_6 \Lambda^{2d-6} \tag{3.10}$$

are dimensionless coupling constants. For simplicity we choose the external momenta of the vertex functions in such a way that they depend only on a single external momenta variable. We now try to determine the z_i factors to first order in the coupling constants. The invariant coupling constants (u_4^R, u_6^R) are $\tilde{u}_4$ and $\tilde{u}_6$ with $\tilde{\Lambda}^2$ replaced by either k^2 or m^2. Since finally we will be interested in the tricritical (or critical) behaviour of the model we will need the contribution of the perturbational expressions in the limit $k^2 \to 0$ or $m^2 \to 0$. (The relevance of the above model to the tricritical phenomena is described for example in [14]). This corresponds to approaching the tricritical point in the Halperin—Hohenberg space [15] either from the direction parallel to the critical line or from the direction perpendicular to this line. The Halperin—Hohenberg space is now spanned by m, k and v_4. The meaning of v_4 will be given below. In the case of ordinary critical phenomena it was possible to approach the $m^2 = k^2 = 0$ point both from the direction $m^2 = 0$ and also from the direction $k^2 = 0$ in the Halperin—Hohenberg plane (spanned by m and k). The method was symmetrical in the m and k variables and we could start the calculation in any of the two limits. In the present case this symmetry is violated and we will have to work with $k^2 = 0$, $m^2 \neq 0$, that is we cannot approach the $k^2 = m^2 = 0$ point from the direction parallel to $m^2 = 0$. The reason for that is that if $m^2 = 0$ and we have u_4 and u_6 in our Hamiltonian, then in $d = 3$ (d is the dimension of the space) unwanted infrared divergencies would appear and we cannot get rid of them.* To determine the

* This is most easily seen if we consider the graph in Fig. 1. This graph will give contribution to the d function. The analytic expression for this graph is

$$\text{const.} \int \frac{d^3p}{(p-q)^2 p^n}.$$

If q is finite and $n \geq 4$ then this integral is infrared divergent.

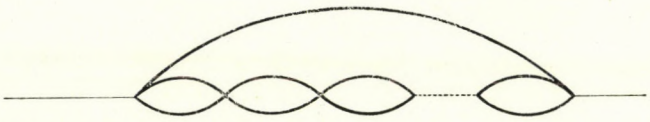

Fig. 1. Infrared divergent graph in the case $m^2 = 0$

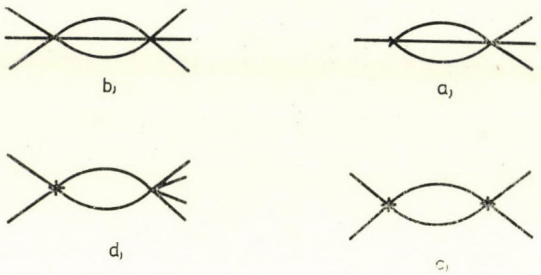

Fig. 2. Graphs giving contributions to the vertex functions

z_i factors up to first order in the coupling constants we need the contribution of the graphs in Fig. 2. (We do not have to calculate the d function, since because of the mass renormalization (3.3) it does not give any contribution in the first order.) Since now $k^2 = 0$, the analytic expressions for the graphs a and b are proportional to $\ln m^2$, and for the graphs c and d to $1/m$. Note that we keep all infrared divergent contributions. The cross in Fig. 2 means that, since in the graph calculation the Γ_4 vertex always appears with the coupling constant $u_4 = u_6 \dfrac{4+N}{10} \cdot \dfrac{1}{2\pi^2}$ (to first order in u_6), therefore instead of u_4 we can introduce this combination as a coupling constant. We call this new coupling constant v_4. The analytic expressions for Γ_4 and Γ_6 are

$$\Gamma_4 = 1 + \frac{4+N}{320\pi^2} u_6 \ln \frac{m^2}{\Lambda^2} - \frac{8+N}{12\pi^2} v_4 \left(\frac{\pi^2}{4} \left(\frac{m}{\Lambda} \right)^{-1} - 1 \right), \tag{3.11}$$

$$\Gamma_6 = 1 + \frac{3N+22}{480\pi^2} u_6 \ln \frac{m^2}{\Lambda^2} - \frac{14+N}{6\pi^2} v_4 \left(\frac{\pi^2}{4} \left(\frac{m}{\Lambda} \right)^{-1} - 1 \right). \tag{3.12}$$

From the point of view of our theory the introduction of v_4 is crucial. If we use the original coupling constants and try to determine the z_i factors in the Eqs. (3.5)—(3.7) it turns out that there are no such z_i (depending only on $\tilde{\Lambda}/\Lambda$ and u_4, u_6) with which we can satisfy these equations. If instead of u_4 we write (3.8) for v_4, the equations can be shown to be valid and the z_i factors

are

$$z_2^{-1} = 1 + \frac{4+N}{320\pi^2} u_6 \ln \frac{\tilde{\Lambda}^2}{\Lambda^2} - \frac{N+8}{12\pi^2} v_4 \left(\left(\frac{\tilde{\Lambda}}{\Lambda} \right)^{-1/2} - 1 \right), \tag{3.13}$$

$$z_3^{-1} = 1 + \frac{3N+22}{480\pi^2} u_6 \ln \frac{\tilde{\Lambda}^2}{\Lambda^2} - \frac{N+14}{6\pi^2} v_4 \left(\left(\frac{\tilde{\Lambda}}{\Lambda} \right)^{-1/2} - 1 \right). \tag{3.14}$$

In the language of RIEDEL [14] it means that the proper scaling field besides m is not u_4 but v_4. After having determined the z_i factors the Lie equations for v_4^R and u_6^R can be set up. They are

$$\frac{dv_4^R(y)}{dy} = \frac{1}{y} v_6^R \left[-\frac{1}{2} + u_6^R \frac{4+N}{320\pi^2} + v_4^R \frac{14+N}{12\pi^2} \right], \tag{3.15}$$

$$\frac{du_6^R(y)}{dy} = \frac{1}{y} u_6^R \left[-\varepsilon + u_6^R \frac{22+3N}{480\pi^2} + v_4^R \frac{8+N}{24\pi^2} \right]. \tag{3.16}$$

Here $y = m^2/\Lambda^2$, $\varepsilon = 3 - d$ (We are performing the calculation in $3 - d$ dimension in order to get a non-trivial fix point for u_6^R).

Before analyzing the above equations let us write down the expressions for Γ_4, Γ_6 and also the equations corresponding to (3.15) and (3.16) in the traditional GELL-MANN and LOW theory. We do not want to describe this method here, since it can be found in many places (see for example [13']; in connection with critical phenomena see also [16] and [12]). Let us mention only that in this approach the exact invariance property of the perturbation series is used to introduce multiplicative factors, which permit a suitable normalization for the Green's functions and vertex functions. Because of this normalization the vertex functions are not those given by (3.11) and (3.12). Denoting the normalized vertex functions by $\tilde{\Gamma}_4$ and $\tilde{\Gamma}_6$, they can be written as

$$\tilde{\Gamma}_4 = 1 + \frac{4+N}{320\pi^2} \tilde{u}_6 \ln \tilde{y} - \frac{8+N}{48} \tilde{v}_4 (\tilde{y}^{-1/2} - 1), \tag{3.17}$$

$$\tilde{\Gamma}_6 = 1 + \frac{22+3N}{480\pi^2} \tilde{u}_6 \ln \tilde{y} - \frac{14+N}{24} \tilde{v}_4 (\tilde{y}^{-1/2} - 1). \tag{3.18}$$

Here $\tilde{y} = m^2/\lambda^2$, $\tilde{v}_4 = \tilde{u}_4 + \frac{4+N}{20\pi^2} \tilde{u}_6$, $\tilde{u}_4 = \alpha_4 \lambda^{d-4}$, $\tilde{u}_6 = \alpha_6 \lambda^{2d-6}$ and λ is connected with the normalization of Γ_4 and Γ_6. In the above we adopted the normalization

$$\tilde{\Gamma}_4(\tilde{y} = 1) = \tilde{\Gamma}_6(\tilde{y} = 1) = 1. \tag{3.19}$$

Details concerning the normalization problem can be found in [12]. Note that the Γ_i and $\tilde{\Gamma}_i (i = 4, 6)$ written in terms of the appropriate variables differ only in the coefficients of the 4-point contributions, but this is true only in first order. In higher order calculation the coefficients in front of the logarithms also may be different [12]. In the case of the GELL-MANN and LOW theory for the Lie equations of the invariant coupling constants one needs $\tilde{\Gamma}_4$ and $\tilde{\Gamma}_6$ (and not z_2 and z_3). The Lie equations now are

$$\frac{d\tilde{v}_4^R(\tilde{y})}{d\tilde{y}} = \frac{1}{\tilde{y}} \tilde{v}_4^R \left[-\frac{1}{2} + \tilde{u}_6^R \frac{4+N}{320\pi^2} + \tilde{v}_4^R \frac{8+N}{96} \right], \tag{3.20}$$

$$\frac{d\tilde{u}_6^R(\tilde{y})}{d\tilde{y}} = \frac{1}{\tilde{y}} \tilde{u}_6^R \left[-\varepsilon + \tilde{u}_6^R \frac{22+3N}{480\pi^2} + \tilde{v}_4^R \frac{8+N}{48} \right]. \tag{3.21}$$

Let us analyze equations (3.15), (3.16) and (3.20), (3.21). See also Fig. 3.

A. The case $v_4(\tilde{v}_4) = 0$

Eqs. (3.15), (3.16) and (3.20), (3.21) have the following fix point

$$v_4^* = 0, \quad u_6^* = \frac{480\pi^2}{22+3N} \varepsilon \tag{3.22}$$

corresponding to $y\,(\tilde{y}) \to 0$. If we solve the above equations around this fix point it turns out that

$$K^R(S) = c_1 s^{\omega_1}, \tag{3.23}$$

$$L^R(S) = c_2 s^{\omega_2} + u_6^*, \tag{3.24}$$

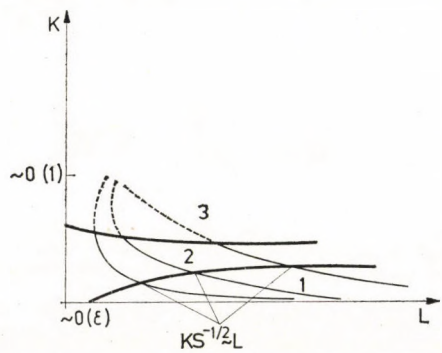

Fig. 3. Trajectories of the Lie equations. Region 1 is the tricritical region. In region 2 perturbation theory can still be used to construct the right hand sides of the Lie equations. Region 3 is the strong coupling region. The dashed trajectories show only the trend of the changes

with

$$\omega_1 = -\frac{1}{2} + \frac{3(4+N)}{3N+22}\varepsilon, \omega_2 = \varepsilon . \tag{3.25}$$

In (3.23) and (3.24) K_R is either v_4^R or $\tilde{v}_4^R$, L^R is either u_6^R or $\tilde{u}_6^R$ and s is either y or $\tilde{y}$. Since $\omega_1 < 0$ the fix point (3.22) can be stable only if $c_1 = 0$. But $K^R(s=1) = K$ (the bare v_4 or $\tilde{v}_4$), therefore $c_1 = K$, so $c_1 = 0$ implies $K = 0$. On the other hand we argued that K is a scaling field, therefore the fix point (3.22), together with $K = 0$ is the tricritical fix point. (The tricritical fix point is the one, where $m^2 = K = 0$).

Let us see how to calculate tricritical indices in this formalism. As an example we will calculate the tricritical index η, the definition of which is

$$d \text{ (at the tricritical point)} \underset{k\to 0}{\sim} k^{\eta} . \tag{3.26}$$

Being at the tricritical point means $K = 0$ and we have a purely logarithmic problem. As it was shown in [12] in such a case

$$\lim_{k\to 0} L^R(m=0, k) = \lim_{m\to 0} L^R(m, k=0) . \tag{3.27}$$

This means we can use the expression (3.22) for u_6^* for the determination of η.

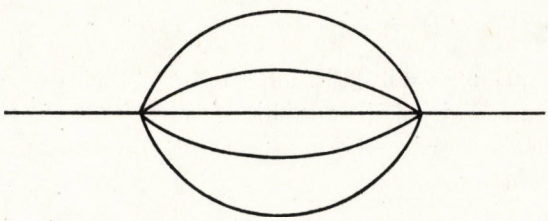

Fig. 4. The graph giving contribution to the tricritical η indices in the lowest order

To find the d function we calculate the right hand side of the corresponding Lie equation to second order in L, that is we calculate the contribution of the graph in Fig. 4. The solution of the Lie equation is

$$d \underset{k\to 0}{\sim} (s)^{\chi(u)_6^*} , \tag{3.28}$$

where

$$\chi(u_6^*) = \frac{\partial}{\partial \xi} \ln d(\xi, u_6^*)\Big|_{\xi=1} . \tag{3.29}$$

From the definition of η and s we finally get

$$\eta = 2\chi(u_6^*) = \frac{1}{12}\frac{(N+2)(N+4)}{(3N+22)^2}\varepsilon^2 . \tag{3.30}$$

This result is in agreement with earlier calculations. Since in the result only s and u_6^* appear it is clear that both the cut-off scaling version of the multiplicative renormalization group and the GELL-MANN and LOW theory give the same result. This is an other confirmation of the equivalence of the two methods in the case of logarithmic problems. Corrections to the above scaling behaviour can be obtained in a way similar to that described in detail in [12].

B. The tricritical region with $K \neq 0$

Let us see what happens if K has a small positive value. In this case the trajectories in Fig. 3 will be nearly parallel to $K = 0$, up to some value of s and then will bend and tend to another fix point. Unless the $K^R (= v_4^R$ or $\tilde{v}_4^R)$ term in Eqs. (3.15), (3.16) and (3.20), (3.21) can be neglected in comparison with the L^R term we will have the same behaviour as before. For that we need (in $d = 3$)

$$K^R \ll L^R , \tag{3.31}$$

For the bare coupling constants K and L the condition (3.31) means that in the lowest order

$$\frac{K}{S^{1/2}} \ll L \ll 1 . \tag{3.32}$$

This is the same relation used in [18], but there (3.32) is the trivial consequence of the Lie equations and we do not have to start with this condition. If $Ks^{-1/2} \sim L$ we get the border line between the tricritical and critical regions (Fig. 2) with the crossover exponent 1/2 [18].

C. Critical phenomena at $d = 3$

When (3.32) is replaced by

$$\frac{K}{S^{1/2}} \ll 1, \; L \ll 1 \tag{3.33}$$

we are out of the critical region, but still may use perturbation theory to construct the right hand sides of the Lie equations. However we loose the logarithmic nature of the problem and simultaneously see that the fix point is now outside of the week coupling region. The right hand sides of the Lie equations calculated to any finite order in perturbation theory can be used only in a very narrow region of the variable s [19]. The dashed trajectories are just qualitative lines and show only the trend of the changes. The same is valid on the $L = 0$ line since in this case also an 0(1) fix point would occur in the

lowest order. So, in the critical domain in the case $d = 3$, the Lie equations are valid only in a very narrow region and we cannot trace the behaviour of the system up to the critical point.

4. Conclusions

We investigated the φ^6 theory near $d = 3$ in the framework of two different formulations of the multiplicative renormalization group. We saw that as in the previous works there is no difference between the two versions provided we deal with a purely logarithmic problem ($K = 0$). What is new in our analysis is that even when the φ^4 coupling is considered and the theory loses its logarithmic character, the invariance equations (3.5)—(3.9) can still be constructed with the z factors depending only on the coupling constants and the ratio $\tilde{\Lambda}/\Lambda$. (Although the z factors have been calculated only up to first order it is not very difficult to show that the above is valid also in higher orders.) While in the case of logarithmic problems we could compare the two theories numerically, it is not the case here, since in order to calculate critical indices in $d = 3$ we have to cross the border line between the weak and strong coupling regions and therefore the numerical values obtained in such a way for critical indices should not be taken too seriously. (They are as bad or as good as the indices obtained by putting $\varepsilon = 1$ in the calculations around four dimensions.) However, we may conjecture that in all cases (that is not only in the case of logarithmic problems) when we have scaling in our theory, with appropriate normalization for the vertex functions in the GELL-MANN and LOW theory the two methods are equivalent. When there is no scaling the cut-off version cannot be used while the original GELL-MANN and LOW theory still works, but does not improve the results of the perturbational calculation. If there is approximate scaling the z factors can be calculated approximately and again there is no difference between the two methods [20].

Acknowledgements

The authors are indebted to Mr. J. SÓLYOM for valuable discussions.

REFERENCES

1. K. G. WILSON and J. KOGUT, Phys. Repts., **12C**, 75, 1974.
2. M. GELL-MANN and F. E. LOW, Phys. Rev., **95**, 1300, 1954.
3. C. C. CALLAN, Phys. Rev., **D2**, 1541, 1970;
   K. SYMANZIK, Comm. Math. Phys., **18**, 227, 1970.
4. A. A. MIGDAL, Zh. E. T. F., **55**, 964, 1968.
5. A. M. POLJAKOV, Zh. E. T. F., **55**, 1025, 1968.
6. E. ABRAHAMS and T. TSUNETO, Phys. Rev. Lett., **30**, 217, 1973.

7. J. SÓLYOM, J. Low Temp. Phys., **12,** 547, 1973.
8. J. SÓLYOM, J. Phys. F., **4,** 2269, 1974.
9. J. SÓLYOM and A. ZAWADOWSKI, J. Phys. F., **4,** 80, 1974.
10. N. MENYHÁRD and J. SÓLYOM, J. Low Temp. Phys., **12,** 529, 1973.
11. G. FORGÁCS, Lett. Nuovo Cim., **12,** 845, 1974.
12. G. FORGÁCS, J. SÓLYOM and A. ZAWADOWSKI, KFKI 76—20.
13. G. GREST and A. ZAWADOWSKI, unpublished.
13'. N. N. BOGOLJUBOV and D. V. SHIRKOV, Introduction to the Theory of Quantized Fields, Interscience Publ. London, 1959.
14. E. K. RIEDEL, Phys. Rev. Lett., **28,** 675, 1972.
15. H. E. STANLEY, Introduction to Phase Transitions and Critical Phenomena, Oxford, 1971.
16. C. DI CASTRO, Lett. Nuovo Cim., **5,** 69, 1972.
17. M. J. STEPHEN, E. ABRAHAMS and J. P. SRALEY, Phys. Rev., **B12,** 256, 1975.
18. D. J. AMIT and C. T. DE DOMINICIS, Phys. Lett., **45A,** 193, 1973.
19. M. WOHRER and E. BREZIN, unpublished.
20. G. ICHE, J. Low Temp. Phys., **11,** 215, 1973.

Acta Physica Academiae Scientiarum Hungaricae, Tomus 42 (4), pp. 365—367 (1977)

МЕХАНИЗМ ПЕРЕНОСА ЗАРЯДА В АМОРФНЫХ ВЕЩЕСТВАХ В ДВУХЦЕНТРОВОЙ МОДЕЛИ (ДЦМ)

В. Т. МАСЛЮК

УЖГОРОДСКИЙ ГОСУДАРСТВЕННЫЙ УНИВЕРСИТЕТ, 294 000 УЖГОРОД, СССР

(Поступило 19. IV. 1977)

Точный расчет $Re\sigma(\omega)$ для ДЦМ в предположении прыжкового механизма переноса заряда приводит к учету многократных перескоков электронов между центрами. Эквивалентная схема проводимости для ДЦМ в этом случае должна включать индуктивность.

Известно [1, 3], что изучение процесса переноса заряда в ДЦМ во многих случаях бывает достаточным для интерпретации наблюдаемой зависимости $Re\sigma(\omega)$ на высокоомных веществах (кристаллах, аморфных телах). В таких веществах всегда имеется достаточно много пар атомов, расстояние между атомами внутри которых много меньше среднего. Уже при сравнительно низких частотах внешнего электрического поля вклад в общий ток от переходов электронов внутри пар близко расположенных атомов может доминировать над выходом от протекания носителей тока по микроскопическим путям, включающим кластеры от 3-х и больше атомов. Поэтому всестороннее изучение модели, в которой один электрон может находиться на одном из двух атомов, причем в разных энергетических состояниях представляет несомненный интерес. В настоящем сообщении применяется метод 2-х временных функций Грина, который ранее не применялся для такого рода задач.

Предположим, что имеется один электрон на два центра, который может находиться в двух состояниях: в основном, с энергией 0, находясь на одном центре, и в возбужденном, с энергией ε на другом. Гамильтониан ДЦМ с учетом взаимодействия электрона с колебаниями решетки можно записать в виде:

$$H = H_{el} + H_{ph} + H_{el-ph}\,, \tag{1}$$

где

$$H_{el} = \varepsilon s^{+}s + \sqrt{2}\,\lambda(\alpha s + s^{+}\alpha), \quad H_{ph} = \sum_{g} \omega_g b_g^{+} b_g, \; H_{el-ph} = \sum_{g} (A_g^{*} b_g^{+} + A_g b_g) s^{+} s\,.$$

Здесь используются обозначения работы [2], $\lambda/\varepsilon < 1, A_g = V_g(1 - e^{iga})$, V_g — константа электрон-фононного взаимодействия.

Будем считать, что электрическое поле включается в момент времени $t = 0$, т. е. $E(t) = \epsilon\Theta(t)$ [1], тогда для плотности тока в ДЦМ можно записать:

$$j(t) = e^2 a^2 \epsilon \frac{d}{dt} \int_0^{\infty} \ll n(t), n(t') \gg dt'\,, \tag{2}$$

$n(t) = s^+(t)\, s(t)$, где $s^+(t)$, $(s(t))$ — операторы рождения (уничтожения) возбуждения в ДЦМ записаны в представлении Гейзенберга, $\ll n(t), n(t')\gg$ — двухвременная функция Грина [4]. Приближения, которые наиболее часто употребляются в теории прыжковой проводимости, можно записать в виде следующих расцеплений:

$$\begin{aligned} \langle s^+(t)\, s(t)\, s^+(t')\, s(t')\rangle &\sim \langle s^+(t)\, s(t')\rangle \langle s(t)\, s^+(t')\rangle\,, \\ \langle s^+(t')\, s(t')\, s^+(t)\, s(t)\rangle &\sim \langle s^+(t')\, s(t)\rangle \langle s(t')\, s^+(t)\rangle\,, \end{aligned} \tag{3}$$

что приводит к зависимости $j(t) \sim \exp(-t/\tau)$ и $Re\,\sigma(\omega) \sim \omega^2\tau/1 + \omega^2 r^2$. Подобные соотношения получены также Поллаком, Джабелом [1] на основании квазиклассических соображений. Однако можно точно решить эту задачу в ДЦМ, используя метод двухвременных функций Грина. В соответствие с теорией линейного отклика [3] можно записать следующее выражение для плотности тока:

$$j(t) = -\frac{e^2a^2\in}{2\pi}\int_{-\infty}^{\infty} e^{i\omega t}\, 2\,\mathrm{Im}\, G_{s^+s}(\omega - i0^+)d\omega\,, \tag{4}$$

где a — расстояние между центрами, $G_{s+s}(\omega)$ — фурье-компонента 2-х частичной функции Грина $G_{s+s}(t-t') = \ll n(t), n(t')\gg$. Без учета электрон-фононного взаимодействия в (1) получаем замкнутую систему уравнений для определения $G_{s+s}(\omega)$, откуда:

$$G_{s^+s}(\omega) = -\frac{\lambda^2}{2\varepsilon}\,\mathrm{th}\,\frac{\varepsilon}{2kT}\,\frac{1}{\omega^2 - \varepsilon^2 - 4\lambda^2}\,.$$

Учет электрон-фононного взаимодействия приводит к сдвигу полюсо в $G_{s+s}(\omega)$ с действительной оси в комплексную плоскость и к конечному времени жизни в ДЦМ.

Окончательное выражение для плотности тока (4) имеет вид:

$$j(t) = \frac{e^2a^2\in}{\varepsilon\tau}\,\mathrm{th}\,\frac{\varepsilon}{2kT}\,e^{-\frac{t}{\tau}}(\cos\varepsilon t + \lambda\tau\sin\varepsilon t)\,,$$

где (5)

$$\frac{1}{\tau} = 4\pi\frac{\lambda^2}{\varepsilon^2}\sum_g V_g^2(1-\cos ga)(n_g+1)\delta(\varepsilon-\omega_g),\; n_g = \frac{1}{e^{\frac{\omega_g}{kT}}+1}\,.$$

Эквивалентная схема, соответствующая временной зависимости плотности тока (5) должна включать индуктивность (рис. 1). Из рис. 1 видно, что расцепление (3) эквивалентно рассмотрению только огибающей для $j(t)$, т. е. постоянной слагаемой, и пренебрежению переменной слагаемой, которая

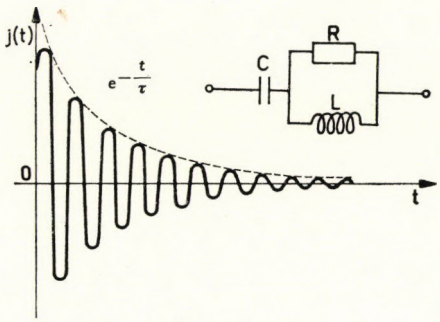

Рис. 1

обусловлена многократными перескоками электронов между двумя центрами. Вычисление $Re\sigma(\omega)$ приводит к зависимости:

$$Re\sigma(\omega) = \frac{e^2a^2\epsilon}{\varepsilon\tau} \operatorname{th} \frac{\varepsilon}{2kT} \left(\frac{\omega^2\tau^2(1 + \omega^2\tau^2 - \varepsilon^2\tau^2) + 2\lambda\tau^4\omega^2\varepsilon}{(1 + \varepsilon^2\tau^2 - \omega^2\tau^2)^2 + (2\omega^2\tau^2)^2} \right) \tag{6}$$

совпадающей с известными результатами [1, 2] при $\varepsilon\tau \ll 1$. Это неравенство и будет критерием справедливости приближения (3).

Отметим также, что эквивалентная схема ДЦМ (рис. 1) предполагает применение аналогичных схем компенсации и на экспериментальных установках, где проводится измерение $Re\sigma(\omega)$.

За обсуждение данной работы и за многочисленные консультации при ее выполнении автор благодарный Плакиде Н. М., Берче Д. М.

ЛИТЕРАТУРА

1. M. Pollak, T. H. Geballe, Phys. Rev., **122,** 1742, 1961.
2. P. Gosar, phys. stat. sol., **10,** 91, 1965.
3. Х. Беттгер, В. В. Брыскин, ФТТ, **18,** 1976.
4. Д. Н. Зубарев, Неравновесная статистическая термодинамика, «Наука», 1971.

Acta Physica Academiae Scientiarum Hungaricae, Tomus 42 (4), pp. 369—376 (1977)

FREE CONVECTION EFFECTS ON FLUCTUATING BOUNDARY LAYER FROM A HORIZONTAL PLATE

By

P. SINGH

DEPARTMENT OF MATHEMATICS, INDIAN INSTITUTE OF TECHNOLOGY, KHARAGPUR, INDIA

(Received 26. IV. 1977)

The paper deals with the combined free and forced convection flows when the free stream and the plate temperature both fluctuate about non-zero mean. The basic flow is nothing but steady state combined free and forced convection flow past a horizontal plate while the oscillations in the free stream and plate temperature cause a time-dependent boundary layer flow and heat transfer. Two separate methods are applied for high and low frequency ranges. It is found that when the frequency of oscillations is extremely low, the boundary layer behaviours can be predicted well with the steady state theory based on instantaneous velocity and temperature distributions. For the very high frequency, the amplitude of the skin friction increases with ω and its phase is ahead of that of the imposed oscillations by 90° while the amplitude of the rate of heat transfer increases as $\sqrt{\omega}$ and its phase has a lead of 45°.

Introduction

The study of laminar boundary layers in oscillatory flow with a non-zero mean was initiated by LIGHTHILL [1], who considered the effect of fluctuations of free stream velocity on the skin friction and heat transfer for plates and cylinders. Since then the various aspects of this problem have been considered by many workers. The specific aim of the present paper is to gain further insight into the effects of buoyancy forces on the oscillatory layer from a horizontal semi-infinite plate. The various aspects of the basic steady flow of this problem were considered by SPARROW and MINKOWYCZ [2] and GILL and CASAL [3].

The unsteady boundary layer equations with buoyancy forces for a semi-infinite horizontal plate are [4]

$$\frac{\partial}{\partial y}\left(\frac{\partial u}{\partial t}+u\frac{\partial u}{\partial x}+v\frac{\partial u}{\partial y}\right)=-g\beta\frac{\partial T}{\partial x}+\nu\frac{\partial^3 u}{\partial y^3}, \tag{1a}$$

$$\frac{\partial u}{\partial x}+\frac{\partial v}{\partial y}=0, \tag{1b}$$

$$\frac{\partial T}{\partial x}+u\frac{\partial T}{\partial x}+v\frac{\partial T}{\partial y}=\alpha\frac{\partial^2 T}{\partial y^2}, \tag{1c}$$

where x, y are the co-ordinates along and normal (measured upward positive) to the plate respectively, g is the acceleration due to gravity, β is the coefficient of thermal expansion and α is the thermal diffusivity of the fluid.

The boundary conditions to be satisfied are

$$\begin{aligned} &y = 0 : \quad u = v = 0, \; T = T_w(x, t) = T_{w0}(x)(1 + \varepsilon e^{i\omega t}), \\ &y \to \infty : \quad u \to U(x, t) = U_0(x)(1 + \epsilon e^{i\omega t}), \frac{\partial u}{\partial y} \to 0, \; T \to T_\infty, \end{aligned} \tag{2}$$

where ω is the frequency of oscillations and $\epsilon \ll 1$.

Following LIGHTHILL [1], we can write u, v and T as the sum of steady and small oscillating components

$$u = u_s + \epsilon u_1 e^{i\omega t}, \; v = v_s + \epsilon v_1 e^{i\omega t}, \; T = T_s + \epsilon T_1 e^{i\omega t}, \tag{3}$$

where u_s, v_s, T_s are the steady components and satisfy

$$\frac{\partial}{\partial y}\left[u_s \frac{\partial u_s}{\partial x} + v_s \frac{\partial u_s}{\partial y}\right] = -g\beta \frac{\partial T_s}{\partial x} + \nu \frac{\partial^3 u_s}{\partial y^3}, \tag{4a}$$

$$\frac{\partial u_s}{\partial x} + \frac{\partial v_s}{\partial y} = 0, \tag{4b}$$

$$u_s \frac{\partial T_s}{\partial x} + v_s \frac{\partial T_s}{\partial y} = \alpha \frac{\partial^2 T_s}{\partial y^2}, \tag{4c}$$

with the boundary conditions

$$\begin{aligned} &y = 0 : \quad u_s = v_s' = 0, \quad T_s = T_{w0}(x); \\ &y \to \infty : \quad u_s \to U_1(x), \quad \frac{\partial u_s}{\partial y} \to 0, \quad T \to T_\infty; \end{aligned} \tag{5}$$

and u_1, v_1, T_1 characterize the oscillatory component of the flow and satisfy the equations

$$\frac{\partial}{\partial y}\left(i\omega u_1 + u_s \frac{\partial u_1}{\partial x} + u_1 \frac{\partial u_s}{\partial x} + v_s \frac{\partial u_1}{\partial y} + v_1 \frac{\partial u_s}{\partial y}\right) = -g\beta \frac{\partial T_1}{\partial x} + \nu \frac{\partial^3 u_1}{\partial y^3}, \tag{6a}$$

$$\frac{\partial u_1}{dx} + \frac{\partial v_1}{\partial y} = 0, \tag{6b}$$

$$i\omega T_1 + u_s \frac{\partial T_1}{\partial x} + u_1 \frac{\partial T_s}{\partial x} + v_s \frac{\partial T_1}{\partial y} + v_1 \frac{\partial T_s}{\partial y} = \alpha \frac{\partial^2 T_1}{\partial y^2}, \tag{6c}$$

with the boundary conditions

$$\begin{aligned} y = 0 &: \; u_1 = v_1 = 0, \quad T_1 = T_{w0}(x); \\ y \to \infty &: \; u_1 \to U_0(x), \quad \frac{\partial u_1}{\partial y} \to 0, \quad T_1 \to 0. \end{aligned} \tag{7}$$

Method of solution

Set (4) and (5) are the boundary layer equations of steady state combined free-forced convection flow past a horizontal plate which can be reduced to the following ordinary differential equations

$$\begin{aligned} &F^{IV} + (m+1)FF'^{III} - (3m-1)F^{I}F^{II} = \frac{N}{2}[(5m-1)\Theta + (m-1)\eta\Theta'], \\ &\Theta^{II} + \sigma[(m+1)F\Theta^{I} - (5m-1)F^{I}\Theta] = 0, \\ &F^{I}(0) = F(0) = F^{II}(\infty) = \Theta(\infty) = 0, \; F^{I}(\infty) = 2, \; \Theta(0) = 1, \end{aligned} \tag{8}$$

by the similarity transformations

$$u_s = \frac{A}{2} x^m F^{I}(\eta), \; T_s - T_\infty = B x^{\frac{5m-1}{2}} \Theta(\eta), \; \eta = \frac{1}{2}\sqrt{\frac{A}{\nu}}\, x^{\frac{m-1}{2}} y,$$

where $U_0(x) = Ax^m$, $\Theta_{w0} = Bx^{\frac{5m-1}{2}}$, $N = 16\sqrt{\nu}\, g\beta B/A^{5/2}$ and $\sigma = \nu/\alpha$ is the Prandtl number and m is a constant. Here primes denote the derivatives with respect to η.

Set (6) and (7) are considered next. In order to take advantage of the simple behaviours of u_s and T_s in (8), the independent variables x and y are transformed into a new co-ordinate system (ξ, η), where ξ is a frequency parameter defined by

$$\xi = \frac{4i\omega}{A} x^{1-m}, \tag{9}$$

in addition, dependent variables u_1 and T_1 in (6) are transformed by

$$u_1 = \frac{A}{2} x^m \frac{\partial}{\partial \eta} f(\xi, \eta), \; T_1 = B x^{\frac{5m-1}{2}} \Phi(\xi, \eta), \tag{10}$$

where the new dependent variables f and Φ are governed by

$$\frac{\partial^4 f}{\partial \eta^4} + \frac{\partial}{\partial \eta}\left[(m+1)F\frac{\partial^2 f}{\partial \eta^2} - 4mF^{\mathrm{I}}\frac{\partial f}{\partial \eta} + (m+1)F^{\mathrm{II}}f + 2(1-m)\xi \times \right.$$
$$\left. \times \left(F^{\mathrm{II}}\frac{\partial f}{\partial \xi} - F^{\mathrm{I}}\frac{\partial^2 f}{\partial \xi \partial \eta}\right)\right] - \xi\frac{\partial^2 f}{\partial \eta^2} - \frac{N}{2}\left[(5m-1)\Phi + 2(1-m)\xi\frac{\partial \Phi}{\partial \xi} + \right. \tag{11}$$
$$\left. + (m-1)\eta\frac{\partial \Phi}{\partial \eta}\right] = 0\,,$$

$$\frac{1}{\sigma}\frac{\partial^2 \Phi}{\partial \eta^2} = \xi\Phi - (m-1)F\frac{\partial \Phi}{\partial \eta} + (5m-1)F^{\mathrm{I}}\Phi + (5m-1)\Theta\frac{\partial f}{\partial \eta} - \tag{12}$$
$$- (m+1)f\Theta^{\mathrm{I}} + 2(1-m)\xi\left(F^{\mathrm{I}}\frac{\partial \Phi}{\partial \xi} - \Theta^{\mathrm{I}}\frac{\partial f}{\partial \xi}\right).$$

The corresponding boundary conditions are

$$\eta = 0 \;:\; \frac{\partial f}{\partial \eta} = 0,\quad f = 0,\quad \Phi = 1\,,$$
$$\eta \to \infty \;:\; \frac{\partial f}{\partial \eta} \to 2,\quad \frac{\partial^2 f}{\partial \eta^2} \to 0,\quad \Phi \to 0\,. \tag{13}$$

When the value of $m = 1$, the independent variable ξ, being now independent of x, reduces to an imaginary constant which essentially depends only on frequency. Consequently, (11) and (12) now reduce to

$$\frac{d^4 f}{d\eta^4} + \frac{d}{d\eta}\left(2F\frac{d^2 f}{d\eta^2} - 4F^{\mathrm{I}}\frac{df}{d\eta} + 2F^{\mathrm{II}}f\right) - \xi\frac{d^2 f}{d\eta^2} - 2N\Phi = 0\,, \tag{14}$$

$$\frac{1}{\varrho}\frac{d^2 \Phi}{d\eta^2} = \xi\Phi - 2F\Phi^{\mathrm{I}} + 4F^{\mathrm{I}}\Phi + 4\Theta f^{\mathrm{I}} - 2\Theta^{\mathrm{I}}f, \tag{15}$$

with $\quad f(0) = f^{\mathrm{I}}(0) = f^{\mathrm{II}}(\infty) = f(\infty) = 0,\quad f^{\mathrm{I}}(\infty) \to \infty,\quad \Phi(0) \to 1;$

which are, for prescribed ξ, two simultaneous complex ordinary differential equations with real independent variable η. The Eqs. (14) and (15) can be integrated numerically over the entire frequency range for any Prandtl number and N. These results will be useful in discussing the possible matching of the low frequency and high frequency solutions.

Low frequency oscillations

For values of $m \neq 1$, Eqs. (11) and (12) remain to be the partial differential ones. However, for low frequency oscillations an asymptotic series in terms of integer powers of ξ

$$f(\xi, \eta) = \sum_{n=0}^{\infty} \xi^n f_n(\eta), \quad \Phi(\xi, \eta) = \sum_{n=0}^{\infty} \xi^n \Phi_n(\eta) \tag{16}$$

may be introduced. Substituting in (11) and (12) and equating like powers of ξ, we obtain the following set of ordinary differential equations for f_n and Φ_n:

$$f_0^{IV} + (m+1) F f_n^{III} - (3m-1) F^I f_0^{II} - (3m-1) F^{II} f_0^I + (m+1) F^{III} f_0 - \\ - \frac{N}{2} [(5m-1) \Phi_0 + (m+1) \eta \Phi_0^I] = 0, \tag{17a}$$

$$\Phi_0^{II} + \sigma[(m+1) F \Phi_0^I - (5m-1)(F^I \Phi_0 + \Theta f_0^I) + (m+1) \Theta^I f_0] = 0; \tag{17b}$$

and

$$f_n^{IV} + (m+1) F f_n^{III} - [2n(1-m) + (3m-1)] F^I f_n^{II} - (3m-1) F^{II} f_n^I + \\ + [(m+1) + 2n(1-m)] F^{III} f_n = f_{n-1}^{II} + \frac{N}{2} [\{(5m-1) + \tag{18a}$$

$$+ 2n(1-m)\} \Phi_n + (m-1) \eta \Phi_x^n],$$

$$\Phi_n^{II} - \sigma[\Phi_{n-1} + (m+1) F \Phi_n^I - \{(5m-1) + 2n(1-m)\} F^I \Phi_n + \\ + (5m-1) \Theta f_n^I - \{(m+1) + 2n(1-m)\} \Theta^I f_n] = 0, \tag{18b}$$

where $n \geq 1$. The boundary conditions are

$$f_0(0) = f_0^I(0) = f_0^{II}(\infty) = \Phi_0(\infty) = 0, \; f_0^I(\infty) = 2, \; \Phi_0(0) = 1; \\ f_n(0) = f_n^I(0) = f_n^{II}(\infty) = f_n^I(\infty) = \Phi_n(0) = \Phi_n(\infty) = 0. \tag{19}$$

Eqs. (17) have exact integrals and are given by

$$f_0 = \frac{1}{2} F + \frac{1}{2} \eta F^I - \frac{3}{2} N \frac{\partial F}{\partial N}, \\ \Phi_0 = \Theta + \frac{1}{2} \eta \Theta^I - \frac{3}{2} N \frac{\partial \Phi}{\partial N}. \tag{20}$$

Physically, when the frequency of oscillations is extremely low, the boundary layer behaviour should be predicted well with the steady state theory based

on instantaneous velocity and temperature distributions. It may be readily shown that the zeroth-order solution (20) is indeed the quasi-steady solution. As the frequency increases, deviations from this solution occur and hence more terms in the asymptotic series (16) must be taken into account. Further investigation of the numerical solutions to Eq. (18) are to be carried out.

High frequency oscillations

When the frequency of oscillations becomes very high, the boundary layer responses should be confined in a very thin region adjacent to the plate. Thus, as the frequency approaches infinity, LIGHTHILL has shown that the oscillatory flow is to a close approximation an ordinary "shear wave" unaffected by the mean flow. In this case, the limiting solution for large frequency is readily obtainable. Here we again seek a series solution in the high frequency range utilizing this limiting solution as the zeroth-order approximation. For this purpose, (11) and (12) are transformed into another co-ordinate system (ξ, z) where z is defined as [5, 6, 7]:

$$z = \sqrt{\frac{i\omega}{\nu}}\, y = \xi^{1/2}\eta\,. \tag{21}$$

The equations take the form

$$\frac{\partial^4 f}{\partial z^4} - \frac{\partial^2 f}{\partial z^2} = \frac{N}{2}\left[2(1-m)\xi^{-1}\frac{\partial \Phi}{\partial \xi} + \xi^{-2}\left\{(5m-1)\Phi + (m-1)z\frac{\partial \Phi}{\partial z}\right\}\right] -$$

$$- \frac{\partial}{\partial z}\left[(m+1)\xi^{-\frac{3}{2}}F^{\mathrm{II}}f - 4m\xi^{-1}F^{\mathrm{I}}\frac{\partial f}{\partial z} + \right. \tag{22a}$$

$$\left. + \xi^{-\frac{1}{2}}\left[(m+1)\,F\frac{\partial^2 f}{\partial z^2} + 2(1-m)F^{\mathrm{II}}\frac{\partial f}{\partial \xi}\right] - 2(1-m)F^{\mathrm{I}}\frac{\partial^2 f}{\partial \xi \partial z}\right],$$

$$\frac{1}{\sigma}\frac{\partial^2 \Phi}{\partial z^2} - \Phi = \xi^{-1}[(5m-1)F^{\mathrm{I}}\Phi - (m+1)\Theta^{\mathrm{I}}f] + \xi^{-\frac{1}{2}}\left[(5m-1)\Phi\frac{\partial f}{\partial z} - \right.$$

$$\left. - (m+1)F\frac{\partial \Phi}{\partial z}\right] + 2(1-m)\left[F^{\mathrm{I}}\frac{\partial \Phi}{\partial \xi} - \Theta'\frac{\partial f}{\partial \xi}\right]. \tag{22b}$$

Since high frequencies are considered here, only the region immediately next to the plate is affected, consequently functions F and Θ in this region can be represented as

$$\begin{aligned} F &= a_2\eta^2 + a_3\eta^3 + a_4\eta^4 + \ldots, \\ &= a_2\xi^{-1}z^2 + a_3\xi^{-3/2}z^3 + a_4\xi^{-2}z^4 + \ldots. \end{aligned} \tag{23}$$

$$\begin{aligned}\Theta &= 1 + b_1\eta + b_2\eta^2 + b_3\eta^3 + \ldots, \\ &= 1 + b_1\xi^{-1/2}z + b_2\xi^{-1}z^2 + b_3\xi^{-3/2}z^3 + \ldots,\end{aligned} \tag{24}$$

where

$$a_2 = F^{II}(0)/2, \quad a_3 = F^{III}(0)/6, \quad a_4 = \frac{5m-1}{48}N,$$

$$b_1 = \Theta^{I}(0), \quad b_2 = 0, \quad b_3 = \frac{\sigma a_2}{3}(5m-3).$$

The following series may be assumed for f and Φ in this case

$$f(\xi, z) = \sum_{m=0}^{\infty} \xi^{-m/2} F_m(z), \tag{25}$$

$$\Phi(\xi, z) = \sum_{m=0}^{\infty} \xi^{-m/2} H_m(z). \tag{26}$$

Substitution of the above series in (22) gives for the first approximation

$$F_0^{IV} - F_0^{II} = 0, \qquad H_0^{II} - \sigma H_0 = 0; \tag{27}$$

subject to the boundary conditions

$$F_0(0) = F_0^{I}(0) = F_0^{II}(\infty) = 0, \quad H_0(\infty) = 0, \quad F_0^{I}(\infty) = 2, \quad H_0(0) = 1. \tag{28}$$

The solution of (27) with (28) gives

$$F_0 = 2\left[e^{-\sqrt{\frac{i\omega}{\nu}}y} + \sqrt{\frac{i\omega}{\nu}}y - 1\right], \tag{29}$$

$$H_0 = e^{-\sqrt{\frac{i\omega}{\alpha}}y}, \tag{30}$$

which is of shear wave type [1]. The oscillating skin friction and the rate of heat transfer are found to be

$$\tau_1 = \mu\left(\frac{\partial u_1}{\partial y}\right)_{y=0} \epsilon e^{i\omega t} = \epsilon\mu\omega x^{\frac{m-1}{2}} \sqrt{\frac{A}{\nu}}\, e^{i(\omega t + \lambda/2)}, \tag{31}$$

$$q_1 = -k\left(\frac{\partial T_1}{\partial y}\right)_{y=0} \epsilon e^{i\omega t} = \epsilon k B \sqrt{\frac{\omega}{\alpha}}\, x^{\frac{5m-1}{2}} e^{i(\omega t + \pi/4)}. \tag{32}$$

The amplitude of the skin friction increases with ω and its phase is ahead

of the imposed oscillations by 90° while the amplitude of the rate of heat transfer increases as $\sqrt{\omega}$ and its phase has a lead of 45°.

It is quite obvious that the higher order terms will become increasingly complex and hence are not considered here.

REFERENCES

1. M. J. LIGHTHILL, Proc. Roy. Soc. A, **224**, 1, 1954.
2. E. M. SPARROW and W. J. MINKOWYCZ, Int. J. Heat Mass Transfer, **5**, 505, 1962.
3. W. N. GILL and E. D. CASAL, A. I. Ch. E. Jl., **8**, 513, 1962.
4. P. SINGH, The laminar viscous flows with body forces: Ph. D. dissertation, Indian Institute of Technology, Kharagpur, India, 1967.
5. M. B. GLAUERT, J. Fluid Mech., **1**, 97, 1956.
6. P. SINGH, Acta Phys. Hung., **40**, 237, 1976.
7. P. SINGH, Acta Phys. Hung., **41**, 263, 1977.

Acta Physica Academiae Scientiarum Hungaricae, Tomus 42 (4), pp. 377—380 (1977)

CONFINEMENT POTENTIAL PRODUCED BY INDEFINITE METRIC MULTIPOLE FIELDS OF INFINITE ORDER

By

K. L. NAGY*

JOINT INSTITUTE FOR NUCLEAR RESEARCH, LABORATORY OF THEORETICAL PHYSICS
DUBNA, USSR

(Received 28. IV. 1977)

The possibility of obtaining some type of confinement of particles is discussed in a field theory with multipole fields of the N-th order. The limiting case $N \to \infty$ yields various forms of static confinement potentials.

1. The data of the charmonium spectrum seem to fit to experiments quite well [1, 2, 3] when a confinement potential between c and $\bar{c}$ is supposed in the form:

$$V(r) = \frac{1}{r}(\alpha + \Delta r + Kr^2) . \tag{1}$$

For example [2] gives the values of α, Δ, K as

$$\alpha = -0{,}2 , \qquad K = -\frac{\alpha}{a^2} , \qquad a = 0,2\ fm .$$

The value of Δ is irrelevant (actually $\Delta = 0$ is taken), it is an additive constant only to the total energy. A great variety of theoretical considerations predicts the form (1). We quote two rather conservative field theoretical approaches only [4, 5] (similar to ours [6]), where other references can be found.

In a previous work [6] we have called the attention to multipole fields as possible sources of some kind of particle confinement. There the free Lagrangian has been proposed to possess the form

$$L_0 = -\frac{1}{2}(\partial_\mu B \partial_\mu B + m^2 B) - (\partial_\mu A \partial_\mu C + m^2 AC) - \lambda AB , \tag{2}$$

and it has been shown that the fields A, B, C interacting via an interaction Lagrangian L_1 in the form

$$L_1 = \bar{c} c \varphi , \quad \varphi = g_1 A + g_2 B + g_3 C ,$$

* On leave of absence from the Institute of Theoretical Physics, Roland Eötvös University, Budapest, Hungary.

give the potential

$$V(r) = \frac{e^{-mr}}{r}(\alpha + \Delta r + Kr^2), \tag{3}$$

where α, Δ, K are given functions of g_i, m and λ. Actually, the propagator

$$\tilde{D}(k) = \frac{1}{m^2 - k^2}\left(\alpha + 2m\left(\Delta - \frac{K}{m}\right)\frac{1}{m^2 - k^2} + 8m^2K\frac{1}{(m^2 - k^2)^2}\right),$$

leads to the form (3). Eq. (1) follows from Eq. (3) in the limit

$$m \to 0, \qquad \frac{\lambda}{m^2} = \text{const}, \qquad g_i^2 \sim \frac{m_c^2}{m^2} \to \infty,$$

where m_c is the quark mass.

2. Multipole fields seem to provide another possibility for obtaining a set of static potentials we want to describe here.

A multipole field of $N+1$ order satisfying the field equations

$$\begin{aligned}(\Box - m^2)\varphi_0 &= 0,\\ (\Box - m^2)\varphi_1 &= \lambda\varphi_0,\\ &\vdots\\ (\Box - m^2)\varphi_N &= \lambda\varphi_{N-1},\end{aligned}$$

gives the Green function for φ

$$\varphi = \sum_{s=0}^{N} g_s\varphi_s \tag{4}$$

in the form [7]:

$$D(x) = \sum_{s=0}^{N} \alpha_s\lambda^s\left(\frac{\partial}{\partial m^2}\right)^s \Delta(x; m^2), \tag{5}$$

where α_s is quadratic in coupling constants g_s. A comparison with the formulae of [7] gives immediately

$$\alpha_s = \frac{\varepsilon}{s!}\sum_{n\geq s}^{N} g_n g_{N+s-n}, \qquad \varepsilon = \pm 1.$$

Introducing

$$A_s = \alpha_s\left(\frac{\lambda}{m^2}\right)^s,$$

$D(x)$ becomes

$$D(x) = \sum_{s=0}^{N} A_s(m^2)^s\left(\frac{\partial}{\partial m^2}\right)^s \Delta(x; m^2). \tag{6}$$

From (6) it is easy to calculate the potential V in an interaction $L_1 = \bar{c}c\varphi$ with the result:

$$V(r) = \frac{1}{r}\sum_{s=0}^{N} A_s \sum_{n=0}^{\infty} \frac{n}{2}\left(\frac{n}{2}-1\right)\cdots\left(\frac{n}{2}-(s-1)\right)\frac{(-mr)^n}{n!} =$$

$$= \frac{1}{r}\sum_n B(n)(-mr)^n, \tag{7}$$

$$B(n) = \sum_{s=0}^{N} \frac{A_s}{s!}\frac{n}{2}\left(\frac{n}{2}-1\right)\cdots\left(\frac{n}{2}-(s-1)\right),$$

i.e.

$$B(0) = A_0,$$

$$B(1) = A_0 + \frac{1}{2}A_1 + \frac{1}{2}\left(\frac{1}{2}-1\right)A_2 + \ldots + \frac{1}{2}\left(\frac{1}{2}-1\right)\ldots\left(\frac{1}{2}-(N-1)\right)A_N,$$

$$B(2) = \frac{1}{2}(A_0 + A_1).$$

$$\vdots$$

If $N \to \infty$ a new possibility opens up. Suppose we wish to reproduce the Coulomb potential, then

$$B(0) = \alpha, \qquad B(n) = 0, \qquad n \geq 1. \tag{8}$$

This gives an infinite number of linear equations for A_i from which it can be calculated to any given order in "mr". (Det $A_i^{(N)} \neq 0$).

It is interesting to compare (8) with the requirement that the Fourier transform $\tilde{D}(k)$ of (6) should be equal to $-k^2$. Eq. (6) gives

$$\tilde{D}(k) = \sum_s A_s (m^2)^s \frac{(-1)^s s!}{(m^2-k^2)^{s+1}} = -\frac{1}{k^2}\sum_n c(n)\left(\frac{m^2}{k^2}\right)^n,$$

$$c(n) = \sum_s A_s \frac{n!}{(n-s)!}.$$

The prescription

$$c(0) = \alpha, \qquad c(n) = 0, \qquad n \geq 1,$$

reproduces (8) for even n. In fact

$$\frac{C(n)}{B(2n)} = \frac{n!}{n(n+1)\ldots 2n}.$$

The confinement potential (1) requires

$$B(0) = \alpha, \quad -mB(1) = \Delta, \quad m^2 B(2) = K, \quad B(n) = 0, \quad n \geq 3,$$

from which A_l can be determined to any given order. The mass m can be chosen arbitrarily, a small value of it may be useful only for practical calculations.

Having obtained the set A_l in such a way, one can substitute that into Eq. (6) and start with $D(x)$ a relativistic calculation.

3. Although we wished to call the attention to multipole fields as a field theoretical explanation of particle confinement, D obtained in such a way can also be considered purely phenomenologically.

To multipole fields Lorentz or inner indices can also be attached.

Since multipole field theories imply a quantization with indefinite metric, a complete field theory as proposed above requires an artificial unitarization [6]. One of the simplest ways is to take the principal value integral in $\tilde{D}(k)$ instead of the usual "$i\varepsilon$" prescription.

REFERENCES

1. B. J. HARRINGTON et al., Phys. Rev. Lett., **34**, 168, 1975.
2. E. EICHTEN et al., Phys. Rev. Lett., **34**, 369, 1975.
3. J. F. GUNION and L. F. LI, Phys. Rev., D**12**, 3583, 1975.
4. S. BLAHA, Phys. Rev., D**10**, 4268, 1974.
5. J. E. KISKIS, Phys. Rev., D**11**, 2978, 1975.
6. K. L. NAGY, Acta Phys. Hung., **39**, 171, 1975.
7. K. YOKOYAMA and R. KUBO, Progr. Theor. Phys., **41**, 542, 1969.

Printed in Hungary

A kiadásért felel az Akadémiai Kiadó igazgatója. Műszaki szerkesztő: Botyánszky Pál

A kézirat nyomdába érkezett: 1977. V. 31. — Terjedelem: 9,25 (A/5) ív, 26 ábra

78.4581 Akadémiai Nyomda, Budapest — Felelős vezető: Bernát György

NOTES TO CONTRIBUTORS

I. PAPERS will be considered for publication in Acta Physica Hungarica only if they have not previously been published or submitted for publication elsewhere. They may be written in English, French, German or Russian.

Papers should be submitted to

Prof. I. Kovács, Editor
Department of Atomic Physics, Polytechnical University
1521 Budapest, Budafoki út 8, Hungary

Papers may be either articles with abstracts or short communications. Both should be as concise as possible, articles in general not exceeding 25 typed pages, short communications 8 typed pages.

II. MANUSCRIPTS

1. Papers should be submitted in five copies.

2. The text of papers must be of high stylistic standard, requiring minor corrections only.

3. Manuscripts should be typed in double spacing on good quality paper, with generous margins.

4. The name of the author(s) and of the institutes where the work was carried out should appear on the first page of the manuscript.

5. Particular care should be taken with mathematical expressions. The following should be clearly distinguished, e.g. by underlining in different colours: special founts (italics, script, bold type, Greek, Gothic, etc); capital and small letters; subscripts and superscripts, e.g. x^3, x_3; small l and 1; zero and capital O; in expressions written by hand: e and l, n and u, v and v, etc.

6. References should be numbered serially and listed at the end of the paper in the following form: J. Ise and W. D. Fretter, Phys. Rev., *76*, 933, 1949.

For books, please give the initials and family name of the author(s), title, name of publisher, place and year of publication, e.g.: J. C. Slater, Quantum Theory of Atomic Structures, I. McGraw-Hill Book Company Inc., New York, 1960.

References should be given in the text in the following forms: Heisenberg [5] or [5].

7. Captions to illustrations should be listed on a separate sheet, not inserted in the text.

III. ILLUSTRATIONS AND TABLES

1. Each paper should be accompanied by five sets of illustrations, one of which must be ready for the blockmaker. The other sets attached to the copies of the manuscript may be rough drawings in pencil or photocopies.

2. Illustrations must not be inserted in the text.

3. All illustrations should be identified in blue pencil by the author's name, abbreviated title of the paper and figure number.

4. Tables should be typed on separate pages and have captions describing their content. Clear wording of column heads is advisable. Tables should be numbered in Roman numerals (I, II, III, etc.).

IV. MANUSCRIPTS not in conformity with the above Notes will immediately be returned to authors for revision. The date of receipt to be shown on the paper will in such cases be that of the receipt of the revised manuscript.

Reviews of the Hungarian Academy of Sciences are obtainable at the following addresses:

AUSTRALIA
C.B.D. LIBRARY AND SUBSCRIPTION SERVICE, Box 4886, G.P.O., *Sydney N.S.W.2001*
COSMOS BOOKSHOP, 145 Ackland Street, *St. Kilda (Melbourne), Victoria 3182*

AUSTRIA
GLOBUS, Höchstädtplatz 3, *1200 Wien XX*

BELGIUM
OFFICE INTERNATIONAL DE LIBRAIRIE, 30 Avenue Marnix, *1050 Bruxelles*
LIBRAIRIE DU MONDE ENTIER, 162 Rue du Midi, *1000 Bruxelles*

BULGARIA
HEMUS, Bulvar Ruszki 6, *Sofia*

CANADA
PANNONIA BOOKS, P.O. Box 1017, Postal Station "B", *Toronto, Ontario M5T 2T8*

CHINA
CNPICOR, Periodical Department, P.O. Box 50, *Peking*

CZECHOSLOVAKIA
MAD'ARSKÁ KULTURA, Národní třida 22, *115 66 Praha*
PNS DOVOZ TISKU, Vinohradská 46, *Praha 2*
PNS DOVOZ TLAČE, *Bratislava 2*

DENMARK
EJNAR MUNKSGAARD, Norregade 6, *1165 Copenhagen*

FINLAND
AKATEEMINEN KIRJAKAUPPA, P.O. Box 128, *SF-00101 Helsinki 10*

FRANCE
EUROPERIODIQUES S. A., 31 Avenue de Versailles, *78170 La Celle St.-Cloud*
LIBRAIRIE LAVOISIER, 11 rue Lavoisier, *75008 Paris*
OFFICE INTERNATIONAL DE DOCUMENTATION ET LIBRAIRIE, 48 rue Gay-Lussac, *75240 Paris Cedex 05*

GERMAN DEMOCRATIC REPUBLIC
HAUS DER UNGARISCHEN KULTUR, Karl-Liebknecht-Strasse 9, *DDR-102 Berlin*
DEUTSCHE POST ZEITUNGSVERTRIEBSAMT, Strasse der Pariser Kommüne 3—4, *DDR-104 Berlin*

GERMAN FEDERAL REPUBLIC
KUNST UND WISSEN ERICH BIEBER, Postfach 46, *7000 Stuttgart 1*

GREAT BRITAIN
BLACKWELL'S PERIODICALS DIVISION, Hythe Bridge Street, *Oxford OX1 2ET*
BUMPUS, HALDANE AND MAXWELL LTD., Cowper Works, *Olney, Bucks MK46 4BN*
COLLET'S HOLDINGS LTD., Denington Estate, *Wellingborough, Northants NN8 2QT*
WM. DAWSON AND SONS LTD., Cannon House, *Folkestone, Kent CT19 5EE*
H. K. LEWIS AND CO., 136 Gower Street, *London WC1E 6BS*

GREECE
KOSTARAKIS BROTHERS, International Booksellers, 2 Hippokratous Street, *Athens-143*

HOLLAND
MEULENHOFF-BRUNA B.V., Beulingstraat 2, *Amsterdam*
MARTINUS NIJHOFF B.V., Lange Voorhout 9—11, *Den Haag*
SWETS SUBSCRIPTION SERVICE, 347b Heereweg, *Lisse*

INDIA
ALLIED PUBLISHING PRIVATE LTD., 13/14 Asaf Ali Road, *New Delhi 110001*
150 B-6 Mount Road, *Madras 600002*
INTERNATIONAL BOOK HOUSE PVT. LTD., Madame Cama Road, *Bombay 400039*
THE STATE TRADING CORPORATION OF INDIA LTS., Books Import Division, Chandralok, 36 Janpath, *New Delhi 110001*

ITALY
EUGENIO CARLUCCI, P.O. Box 252, *70100 Bari*
INTERSCIENTIA, Via Mazzé 28, *10149 Torino*
LIBRERIA COMMISSIONARIA SANSONI, Via Lamarmora 45, *50121 Firenze*
SANTO VANASIA, Via M. Macchi 58, *20124 Milano*
D. E. A., Via Lima 28, *00198 Roma*

JAPAN
KINOKUNIYA BOOK-STORE CO. LTD., 17-7 Shinjuku-ku 3 chome, Shinjuku-ku, *Tokyo 160-91*
MARUZEN COMPANY LTD., Book Department, P.O. Box 5050 Tokyo International, *Tokyo 100-31*
NAUKA LTD. IMPORT DEPARTMENT, 2-30-19 Minami Ikebukuro, Toshima-ku, *Tokyo 171*

KOREA
CHULPANMUL, *Phenjan*

NORWAY
TANUM-CAMMERMEYER, Karl Johansgatan 41—43, *1000 Oslo*

POLAND
WĘGIERSKI INSTYTUT KULTURY, Marszałkowska 80, *Warszawa*
CKP I W ul. Towarowa 28 *00-958 Warsaw*

ROUMANIA
D. E. P., *Bucureşti*
ROMLIBRI, Str. Biserica Amzei 7, *Bucureşti*

SOVIET UNION
SOJUZPETCHATI — IMPORT, *Moscow*
and the post offices in each town
MEZHDUNARODNAYA KNIGA, *Moscow G-200*

SPAIN
DIAZ DE SANTOS, Lagasca 95, *Madrid 6*

SWEDEN
ALMQVIST AND WIKSELL, Gamla Brogatan 26, *101 20 Stockholm*
GUMPERTS UNIVERSITETSBOKHANDEL AB, Box 346, *401 25 Göteborg 1*

SWITZERLAND
KARGER LIBRI AG, Petersgraben 31, *4011 Basel*

USA
EBSCO SUBSCRIPTION SERVICES, P.O. Box 1943, *Birmingham*, Alabama 35201
F. W. FAXON COMPANY, INC., 15 Southwest Park, *Westwood*, Mass. 02090
THE MOORE-COTTRELL SUBSCRIPTION AGENCIES, *North Cohocton, N. Y. 14868*
READ-MORE PUBLICATIONS, INC., 140 Cedar Street, *New York, N. Y. 10006*
STECHERT-MACMILLAN, INC., 7250 Westfield Avenue, *Pennsauken* N. J. 08110

VIETNAM
XUNHASABA, 32, Hai Ba Trung, *Hanoi*

YUGOSLAVIA
JUGOSLAVENSKA KNJIGA, Terazije 27, *Beograd*
FORUM, Vojvode Mišiča 1, *21000 Novi Sad*